

# **STRUCTURAL GEOLOGY**

*by*

**BILLINGS**

# **STRUCTURAL GEOLOGY**

PRENTICE-HALL GEOLOGY SERIES  
EDITED BY NORMAN E. A. HINDS

---

---

---

# STRUCTURAL GEOLOGY

---

*by*

MARLAND P. BILLINGS

*Associate Professor of Geology  
Harvard University*

New York : 1946

PRENTICE-HALL, INC.

---

---

COPYRIGHT, 1942, BY  
PRENTICE-HALL, INC.  
70 Fifth Avenue, New York

ALL RIGHTS RESERVED. NO PART OF THIS BOOK MAY BE REPHO-  
DUCED IN ANY FORM, BY MIMEOGRAPH OR ANY OTHER MEANS,  
WITHOUT PERMISSION IN WRITING FROM THE PUBLISHERS.

First Printing . . . . . April, 1942  
Second Printing . . . . . April, 1946

## Preface

**E**MPHASIS in this book has been placed on principles, methods, and technique. The structure of specific areas is not discussed, except for the purpose of illustrating principles. The writer has intentionally refrained from a treatment of the more speculative phases of geotectonics because he believes that such subjects can be intelligently studied only by geologists with a broad background in many fields of geology.

The indecisiveness of some of the criteria used in structural geology may cause dismay to some students. It is better, however, for the reader to realize the difficulties of structural geology and to understand at the outset that such a subject can never be treated with mathematical precision. The structural geologist must be proficient in weighing and balancing the evidence.

The laboratory exercises—many of which can be done outside the laboratory—included at the end of the book were prepared originally by the writer. They gradually evolved into their present form through the efforts of a succession of able assistants, including Randolph W. Chapman, Jarvis B. Hadley, Robert P. Sharp, and Walter S. White. The author's present assistant, George E. Moore, is largely responsible for the descriptive text that accompanies the laboratory problems.

Some instructors may prefer to make extensive use of the Geologic Folios published by the United States Geological Survey. It seemed inadvisable, however, to base the exercises too directly on such folios, because the folios available differ greatly in different institutions. Four of the laboratory problems may be removed from the book and submitted to the instructor.

The writer is indebted to several colleagues who have read and criticized parts of the original manuscript and have given valuable advice that was utilized in the final revision: Professor

## PREFACE

Francis Birch, Chapters 2 and 19; Professor L. Don Leet, Chapter 19; Professor Robert L. Nichols, Chapter 17. Dr. John Eric read much of the manuscript and made many pertinent suggestions.

The author is indebted to the following for photographs which are reproduced in the book: Dr. Barnum Brown, Dr. W. F. Jenks, Mr. Bradford Washburn, Mr. Herbert Wright, Mr. Douald Everhart, and Dr. Katharine Fowler-Billings. Professor A. K. Lobeck assisted in obtaining some of these pictures. All the figures were drawn by Mr. Edward A. Schmitz.

The following publishers have kindly granted permission to use illustrations, usually modified to some extent: Reinhold Publishing Company, successor to The Chemical Catalog Company, Fig. 1; Geophysics, Fig. 277; McGraw-Hill Book Company, Figs. 107 and 108; American Institute of Mining and Metallurgical Engineers, Fig. 302; American Association of Petroleum Geologists, Figs. 203, 204, 205, 206, 207, 278, 283, 290, 294, and 295.

MARLAND P. BILLINGS

## Table of Contents

CHAPTER		PAGE
PREFACE . . . . .		vii
<b>1. STRUCTURAL GEOLOGY . . . . .</b>	<b>1</b>	
Relation of Structural Geology to Geology. Subdivisions of Structural Geology. Scope of This Book.		
<b>2. MECHANICAL PRINCIPLES . . . . .</b>	<b>7</b>	
Materials of the Outer Shell of the Earth; Atoms; Gases, liquids, and solids. Force: Force and acceleration; Composition and resolution of forces. Stress: Concept of stress; Hydrostatic pressure or confining pressure; Differential forces; Measurement of stress. Strain: Definition; Three stages of deformation; Stress-strain diagram. Factors Controlling Behavior of Material: Confining pressure; Temperature; Time—fatigue and creep; Solutions; Summary. Mechanics of Plastic Deformation: Problem; Intergranular movements; Intragranular movements; Recrystallization. Strain Ellipsoid. Deformation in the Outer Shell of the Earth.		
<b>3. DESCRIPTION OF FOLDS . . . . .</b>	<b>33</b>	
Introduction. Attitude of Beds. Parts of a Fold. Nomenclature of Folds. Plunge of Folds. Fold Systems or Origens. Behavior of Folds with Depth. Calculating the Depth of Folding.		
<b>4. FIELD STUDY AND REPRESENTATION OF FOLDS . . . . .</b>	<b>58</b>	
Recognition of Folds: Direct observation; Plotting attitude of beds; Map pattern; Topography; Drilling; Mining; Geophysical methods. Determination of Top of Beds by Primary Features: Nature of the problem; Paleontological methods; Use of primary features; Ripple-marks; Cross-bedding; Graded bedding; Local unconformities, channeling, and related features; Mud-cracks; Pillow structure; Vesicular or oxidized tops of lavas; Field methods. Determination of Top of Beds by Drag Folds: Relation of drag folds to axes of major folds; Drag folds in cross section; Drag folds in three dimensions; Example of use of drag folds; Minor folds; Limitations of method. Representation of Folds: Photographs and sketches; Maps; Structure sections; Structure contours; Block diagrams; Models.		
<b>5. MECHANICS AND CAUSES OF FOLDING . . . . .</b>	<b>87</b>	
Mechanics of Folding: Flexure folding; Flow folding; Shear folding; Folds due to vertical movements. Causes of Folding: Horizontal		

## TABLE OF CONTENTS

5. MECHANICS AND CAUSES OF FOLDING (*Cont.*)

compression; Horizontal couple; Convection currents; Intrusion of magma, intrusion of salt, and vertical forces of unknown origin; Differential compaction of sediments; Chemical changes; Ice push; Contemporaneous deformation.	
6. FAILURE BY RUPTURE . . . . .	99
Introduction. Tension. Compression. Couples. Torsion. Rupture and the Strain Ellipsoid. Rupture in Rocks.	
7. JOINTS . . . . .	111
General Features. Geometrical Classification. Genetic Classification. Slecting.	
8. DESCRIPTION AND CLASSIFICATION OF FAULTS . . . . .	130
General Characteristics. Nature of Movement along Faults: Translatory and rotational movements; Relative movements; Effects on disrupted strata; Calculation of net slip; Throw and heave; Separation. Geometrical Classifications: Bases of classification; Classification based on pitch of net slip; Classification based on attitude of fault relative to attitude of adjacent beds; Classification based on fault pattern; Classification based on value of dip of fault; Classification based upon apparent movement. Genetic Classification: Ideal classification; Classification based on relative movements; Classification based on absolute movements.	
9. CRITERIA FOR RECOGNITION OF FAULTS . . . . .	155
Introduction. Discontinuity of Structures. Repetition and Omission of Strata. Features Characteristic of Fault Planes. Silicification and Mineralization. Sudden Changes in Sedimentary Facies. Physiographic Criteria. Distinction between Fault Scarps, Fault-line Scarps, and Composite Fault Scarps.	
10. THRUST FAULTS . . . . .	172
Introduction. Terminology. Overthrusts. Mechanics of Thrusting.	
11. GRAVITY OR NORMAL FAULTS . . . . .	192
Introduction. Attitude, Size, and Pattern. <i>En Echelon</i> Gravity Faults. Tilted Fault Blocks. Graben and Horsts. Intermittent Faulting. Origin of Gravity Faults.	
12. SECONDARY FOLIATION AND LINEATION . . . . .	213
Introduction. Types of Cleavage: Flow cleavage; Fracture cleavage; Shear cleavage; Bedding cleavage; Classification; Alternate interpretation of cleavage. Secondary Lineation. Relation of Cleavage to Major Structure: Introduction; Flow cleavage; Fracture cleavage; Shear cleavage; Bedding cleavage; Repeated deformation; Summary. Use and Origin of Lineation.	

## TABLE OF CONTENTS

CHAPTER		PAGE
13. UNCONFORMITIES . . . . .		240
Introduction. Kinds of Unconformities. Recognition of Unconformities: Exposed in one outcrop; Areal mapping; Sharp contrasts in degree of induration; Sharp contrasts in the grade of metamorphism; Sharp contrasts in the intensity of folding; Relation to intrusives. Criteria for Distinguishing Faults from Unconformities.		
14. SALT DOMES . . . . .		251
Introduction. Shape, Size, and Composition. Origin of Salt Domes. Structural Evolution of Salt Domes. Economic Resources.		
15. PLUTONS. . . . .		260
Introduction. Internal Structure. Age Relative to the Adjacent Rocks. Structural Relations to the Surrounding Rocks. Determining the Shape and Size of Plutons. Concordant Plutons: Sills; Laccoliths; Lopoliths; Phacoliths; Other concordant plutons. Discordant Plutons: Dikes; Volcanic vents; Ring-dikes; Batholiths and stocks. Time of Intrusion.		
16. GRANITE TECTONICS. . . . .		298
Introduction. Structures of the Flow Stage: Movement of magma; Platy flow structure; Linear flow structure. Structures of the Transition Stage: Condition of magma; Flexures; Granite-filled shears. Structures of the Solid Stage: Condition of magma; Cross joints; Longitudinal joints; Diagonal joints; Marginal fissures; Primary flat-lying joints; Flat-lying gravity faults; Marginal thrusts. Relation of Structures to Each Other. Distinction between Primary and Secondary Structures: Problem; Planar structures; Lineation. Criticism. Bearing on Mechanics of Intrusion.		
17. EXTRUSIVE IGNEOUS ROCKS . . . . .		313
Introduction. Lava Flows: Characteristics of lava flows; Criteria for distinguishing lava flows from sills. Pyroclastic Beds. Fissure Eruptions. General Character of Central Eruptions. Volcanoes: General features; Classification based on internal structure; Classification based on grouping of volcanoes. Craters, Calderas, and Related Forms: Craters; Calderas. Cryptovolcanic Structures of the United States. Volcanic Pipe.		
18. STRUCTURAL PETROLOGY. . . . .		332
Introduction. Field Technique. Laboratory Technique. Symmetry of Fabric. Symmetry of Movement. Correlation of Fabric Symmetry and Movement Symmetry. Mechanics of Mineral Orientation. Kinds of Tectonites. Field Applications.		

## TABLE OF CONTENTS

CHAPTER		PAGE
19.	<b>GEOPHYSICAL METHODS IN STRUCTURAL GEOLOGY . . .</b>	<b>356</b>
	Introduction. Geophysical Methods. Gravitational Methods: Principles involved; Methods (Pendulum method, Gravimeter method, Corrections applied in pendulum and gravimeter methods, Calculation of gravity anomaly, Torsion balance method); Relation between gravity and structure. Magnetic Methods: Principles; Relation of magnetic intensity to geological structure. Seismic Methods: Principles; Refraction methods; Reflection methods; Geological application of seismic methods. Electrical Methods: Introduction; Natural electrical currents (Spontaneous electric currents, Telluric currents); Artificial currents (Principles, Potential profile and equipotential line methods, Resistivity methods).	
	<b>LABORATORY EXERCISES. . . . .</b>	<b>399</b>
1.	Thickness and Depth of Strata. . . . .	401
2.	Outercap Pattern of Horizontal and Vertical Strata . . . . .	411
3.	Patterns of Dipping Strata; Three-point Problems . . . . .	415
4.	Structure Sections of Folded Strata . . . . .	421
5.	Geometrical Reconstruction of Folds . . . . .	426
6.	Structure Contours and Isopachs . . . . .	430
7.	Trigonometric Solution of Fault Problems . . . . .	434
8.	Projections. . . . .	439
9.	Solution of Three-point Problems and Vertical Fault Problems by Descriptive Geometry . . . . .	444
10.	Solution of Inclined Fault Problems by Descriptive Geometry . . . . .	448
11.	Unconformities, Faults, and Folds. . . . .	454
	<b>INDEX. . . . .</b>	<b>459</b>

## List of Plates

PLATE		FACING PAGE
I.	<i>Flat Strata, Bryce Canyon, Utah.</i>	2
II.	<i>Deformed Strata, Yakataga, Alaska Coast Range</i>	3
III.	<i>Dipping Strata on Mt. Monadnock, New Hampshire.</i>	32
IV.	<i>Vertical Strata, Huasteca Canyon near Monterrey, Mexico.</i>	33
V.	<i>Anticline North of Cerro de Pasco, Peru.</i>	38
VI.	<i>Vertical Isoclinal Syncline West of Cerro de Pasco, Peru.</i>	39
VII.	<i>Small Recumbent Fold, Mt. Monadnock, New Hampshire.</i>	39
VIII.	<i>Plastic Deformation in Ice between Steller Glacier and Bering Glacier, Alaska</i>	76
IX.	<i>Joints and Sheeting, San Diego County, California.</i>	77
X.	<i>Joints in pre-Cambrian Granite, Ozark Mountains</i>	110
XI.	<i>Jointing, Tenaya Canyon, Yosemite National Park, California</i>	111
XII.	<i>Columnar Jointing in Lava at Great Face, Staffa</i>	122
XIII.	<i>Columnar Jointing in Lava at Fingal's Cave, Staffa</i>	123
XIV.	<i>Fault Cutting Santa Fe Formation, Rio Puerco, New Mexico</i>	214
XV.	<i>Flow Cleavage and Fracture Cleavage</i>	215
XVI.	<i>Angular Unconformity, Salina Canyon, Utah</i>	242
XVII.	<i>Volcanic Plug and Dike, Shiprock, New Mexico</i>	243
XVIII.	<i>Cinder Cone near Flagstaff, Arizona</i>	314
XIX.	<i>Obsidian Lava Flow, Paulina Mountains, Oregon.</i>	315

## Structural Geology

### Relation of Structural Geology to Geology

*Structural geology* is the study of the architecture of the earth in so far as it is determined by earth movements. *Tectonics* and *tectonic geology* are terms that are synonymous with structural geology. The movements that affect solid rocks result from forces within the earth, and cause folds, joints, faults, and cleavage. The movement of magma, because it is often intimately associated with the displacement of solid rocks, is also a subject that lies within the domain of structural geology.

Structural geology is closely related to many other branches of geology, and in field work the solution of the structural problems is often only one phase of a broader investigation. It is futile to try to study the structure of folded and faulted sedimentary formations without a knowledge of *stratigraphy*, that phase of geology treating of the sequence in which formations have been deposited. *Paleontology*, which is the study of fossils, is indispensable to the structural geologist who works in rocks containing organic remains. *Petrology*, a subject that includes the systematic description of rocks and the study of their origin, may shed much light on the structural history of igneous, metamorphic, and sedimentary rocks. A knowledge of *physiography*, the study of the surface of the earth, is particularly important to the structural geologist who investigates regions of recent tectonic activity, where the topography is a rather direct expression of the structure. Even in those areas where the tectonic evolution ceased long ago, physiography may furnish important clues to the structural geologist. *Seismology*, the study of earthquakes and the propagation of elastic waves through the earth, gives us our most tangible information about the vast interior of the earth that lies beneath the thin

surface shell visible to the structural geologist. *Geophysics*, the application of physics to problems of the earth, is becoming increasingly important because it not only offers more precise information about the physical properties of rocks, but because it is invaluable to the solution of local structural problems.

It is apparent, therefore, that structural geology is intricately interwoven with other phases of geology and, in some instances, with other sciences. Thus the structural geologist must be familiar with the range and subject matter of these related fields. A systematic treatment of these fields, however, is beyond the scope of this book.

### Subdivisions of Structural Geology

Structural geology may be conveniently partitioned into several subdivisions: (1) the study of relatively local structural units; (2) the study of world-wide structural units; and (3) laboratory studies.

Field work is indispensable to the study of local structural units, and it is this fact that distinguishes most phases of geology from many of the other sciences. The field geologist must be temperamentally attuned to an outdoor life, and many otherwise able men fail because they lack this attribute. Sometimes the field work may be a source of great enjoyment; sometimes it may be a great hardship. At dawn, while climbing some Alpine trail, the geologist may witness the indescribable beauty of sunrise, when the rising mists and snowcapped peaks turn to crimson. But that same afternoon, while he is working on some treacherous cliff, he may feel the fury of the sleet and snow of a summer storm. Another year he may be riding horseback along some Utah trail, or forcing his way through scrub timber on some New England mountain, or plodding across a west Texas desert in the exhausting heat of a summer day.

In all phases of geology, and especially in structural geology, the correct location of outcrops is of the utmost importance to the geologist. Consequently, accurate maps are essential. For many regions topographic maps are available, and by means of topography, drainage, and culture, a precise location is possible. In recent years vertical aerial photographs have



PLATE I. Flat Strata. Sedimentary rocks of the Tertiary age in Bryce Canyon, Utah. (Photo by U. S. Forest Service.)

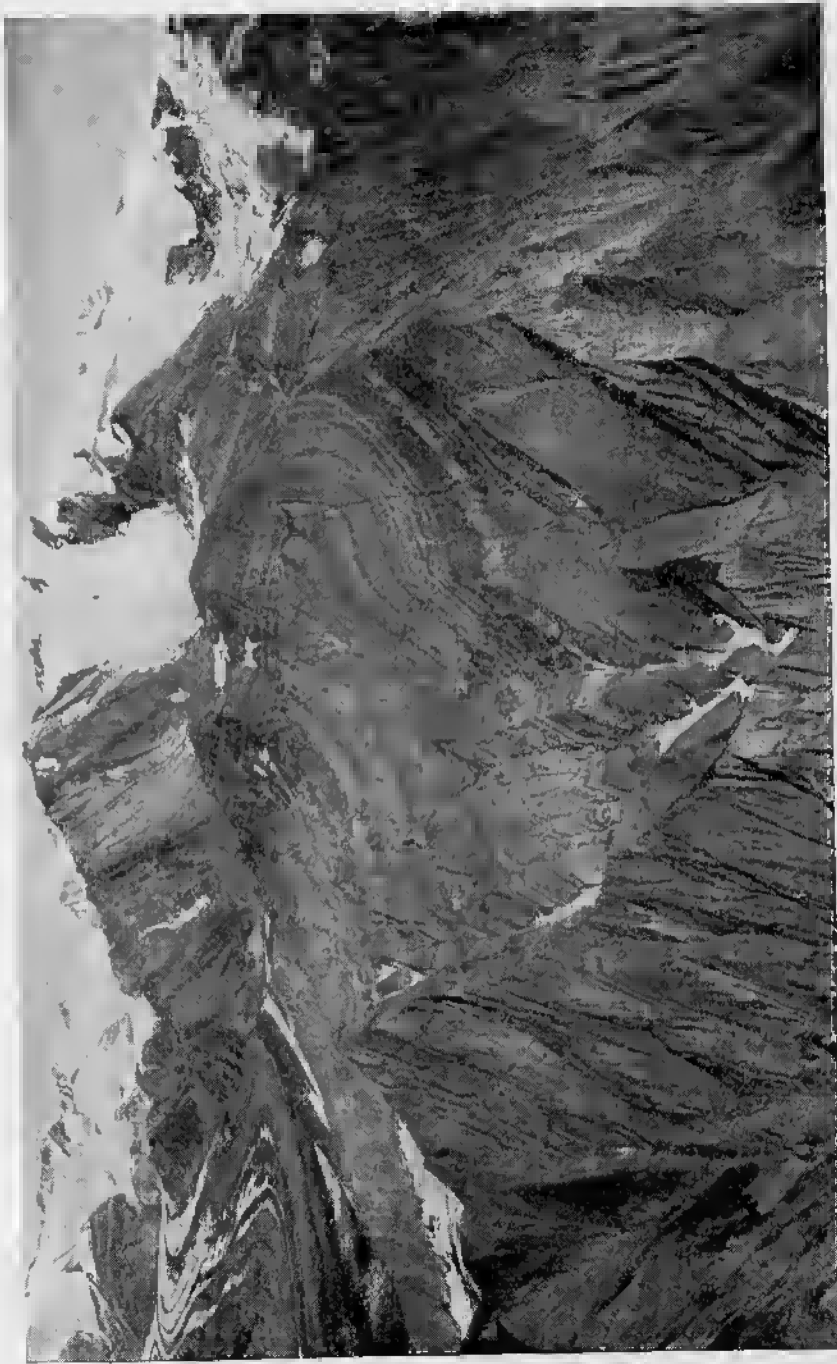


PLATE II. Deformed Strata. Sedimentary rocks of Tertiary age, Yakataga, Alaska Coast Range. In the left background the strata dip away from the observer. In the middle background the strata dip about 60 degrees to the right. In the foreground they are vertical. (Photo by Bradford Washburn.)

become increasingly important in geological field work. These photographs, made from directly above, are essentially maps. In some respects they are superior to topographic maps, because they not only portray all natural and artificial features with great accuracy, but they reveal, too, many features such as trees, forests, open fields, and fences which are not generally indicated on topographic maps. In other respects photographs are inferior to topographic maps because they lack contours; moreover, in mountainous regions, the scale is not constant. In regions for which suitable maps or aerial photographs are not available, it may be necessary for the geologist to prepare his own base map, usually by plane table methods. A discussion of the technique of field methods is beyond the scope of the present book, but this subject is adequately treated in the excellent books by Lahee,<sup>1</sup> Hayes and Paige,<sup>2</sup> and Greenly and Williams.<sup>3</sup>

Successful geological field work consists of the accumulation of significant facts. At each outcrop the geologist records whatever data are pertinent to his problem, and, ideally, he should never have to visit an outcrop a second time. This is especially true in areas that are difficult of access, but even in accessible regions the work should be so planned that a second visit to an outcrop is unnecessary.

Geologic mapping, when properly done, demands skill and judgment. Such mapping requires keen observation and a knowledge of what data are significant. As the field work progresses and the larger geological picture begins to unfold, experience and judgment are essential if the geologist is to evaluate properly the vast number of facts gathered from thousands of outcrops. Above all, the field geologist must use the method of "working multiple hypotheses"<sup>4</sup> to deduce

<sup>1</sup> Lahee, F. H., *Field Geology*, 4th edition. New York: McGraw-Hill Book Company, 1941.

<sup>2</sup> Hayes, C. W., and Paige, S., *Handbook for Field Geologists*, 3rd edition. New York: John Wiley and Sons, 1921.

<sup>3</sup> Greenly, E., and Williams, H., *Methods in Geological Surveying*. New York: D. Van Nostrand Co., 1930.

<sup>4</sup> Chamberlin, T. C., The method of working multiple hypotheses: *Journal of Geology*, Vol. 5, pp. 837-848, 1897; also reprinted in Mather, K. F., and Mason, S. L., *A Source Book in Geology*, pp. 604-612. New York: McGraw-Hill Book Company, 1939.

the geological structure. While the field work progresses, he should conceive as many interpretations as are consistent with the known facts. He should then formulate tests for these interpretations,<sup>5</sup> checking them by data already obtained, or checking them in the future by new data. Many of these interpretations will be abandoned, new ones will develop, and those finally accepted may bear little resemblance to interpretations considered early during the field work.

Nothing is more naïve than for one to believe that a field geologist should gather only "facts," the interpretation of which is to be made at a later date. Because of his numerous tentative interpretations, the field geologist will know how to evaluate the facts; these hypotheses, moreover, will lead him to critical outcrops that might otherwise never have been visited. On the other hand, the field geologist should never let his temporary hypotheses become ruling theories, thus making him incapable of seeing contradictory facts.

A second subdivision of structural geology is the synthesis or weaving together of the many facts, obtained from local areas, into a unified picture of the structure and tectonic history of the outer shell of the whole earth. Such studies are necessarily based in large part upon an intimate knowledge of the literature of structural geology, because it is manifestly impossible for one man to investigate many areas in detail. But, in order that he may more judiciously evaluate the reliability and importance of the published information, such an investigator must have made detailed studies of his own. One of the old classics in this field of synthesis is that by Eduard Suess, published in German and translated into French and English.<sup>6</sup> An excellent modern study of this type is that by Bucher.<sup>7</sup> The strength of the earth has been discussed recently by Daly.<sup>8</sup>

<sup>5</sup> Gilbert, G. K., The inculcation of scientific method, with an illustration drawn from Quaternary geology of Utah: *American Journal of Science*, 3rd series, Vol. 31, pp. 284-299, 1886.

<sup>6</sup> Suess, Eduard, *The Face of the Earth*, 5 Vols. Oxford: Clarendon Press, 1904-1924.

<sup>7</sup> Bucher, W. H., *The Deformation of the Earth's Crust*. Princeton: Princeton University Press, 1933.

<sup>8</sup> Daly, R. A., *The Strength and Structure of the Earth*. New York: Prentice-Hall, Inc., 1940.

A third subdivision of structural geology is the laboratory investigation of structural problems by controlled experiments. In many of these studies the physical properties of rocks have been investigated,<sup>9</sup> but usually it has not been possible to simulate natural conditions. In recent years, however, a few experiments have been performed in which the laboratory conditions closely approximated those found in nature.<sup>10</sup>

In another type of experiment, attempts have been made to reproduce geological structures in small models, or to observe the structures that result from the application of known forces. A classic example is the formation of folds when layers of suitable material are slowly compressed by a moving piston (see also p. 93). But the significance of many of these experiments is questionable, because in many cases the investigator repeatedly changed either the materials or the conditions of the experiment until he obtained the results he desired. It is now possible, however, by the use of sound engineering principles, to construct small scale models that will simulate natural conditions.<sup>11</sup>

### Scope of This Book

Of the three subdivisions of structural geology discussed in the preceding pages, only the first, the study of relatively local structural units, will be considered at any length in this book. The other two subdivisions, synthetic studies of world structure and structural experiments, are, of course, also important, but they are more advanced subjects that can not be understood until the first subdivision is fully mastered. Moreover, an adequate treatment of all the subdivisions of structural geology would occupy far more space than is available in an elementary book on the subject.

A study of geologic structures would be quite barren and fruitless if unaccompanied by a discussion of the forces involved. In the natural course of events, the structural geologist makes

<sup>9</sup> Birch, F., and others, Handbook of physical constants, *Geological Society of America, Special Papers*, No. 36, 1942.

<sup>10</sup> Griggs, D., Experimental flow of rocks under conditions favoring recrystallization; *Bulletin Geological Society of America*, Vol. 51, pp. 1001-1022, 1940.

<sup>11</sup> Hubbert, M. K., Theory of scale models as applied to the study of geologic structures; *Bulletin Geological Society of America*, Vol. 48, pp. 1459-1520, 1937.

his observations first, then deduces the geological structure, and, finally, considers the nature of the causative forces. Normally, observation and description precede interpretation. It might seem logical, therefore, in a book such as this, to reserve a discussion of mechanics until the end. But it is far more satisfactory to treat each structural feature as a unit, describing it first and then considering the forces involved. It is essential, therefore, that a chapter on mechanical principles be given first in order that the origin of the various geological structures may be intelligently discussed.

## 2

### Mechanical Principles

#### Materials of the Outer Shell of the Earth

##### Atoms

Matter is composed of atoms. Although different in size, all atoms are inconceivably small, and average  $2 \times 10^{-7}$  millimeter (0.0000002 mm.) in diameter. Some atoms are much heavier than others; the mass of uranium, the heaviest atom, is about 236 times as great as that of hydrogen, the lightest. An atom of uranium weighs  $392.98 \times 10^{-24}$  gram; an atom of hydrogen weighs only  $1.66 \times 10^{-24}$  gram.

It was formerly believed that atoms were the smallest constituent particles of matter. Modern physical investigations reveal, however, that the atom is made of still smaller particles, such as protons, positrons, neutrons, and electrons. Although a detailed knowledge of atomic structure is essential to the geologist investigating radioactivity and the problem of the heat of the earth, detailed atomic structure is not the direct concern of the structural geologist. For his purpose the atom is the smallest unit of significance.

##### Gases, liquids, and solids

At and near the surface of the earth, the atoms combine to form gases, liquids, and solids. Many substances are found in all three of these states. At atmospheric pressure water is a liquid between 0 and 100 degrees Centigrade, but above 100 degrees it becomes a gas, and below 0 degrees it becomes a solid. At exactly 0 degrees ice and water can exist together in equilibrium, and similarly at exactly 100 degrees water and steam are in equilibrium.

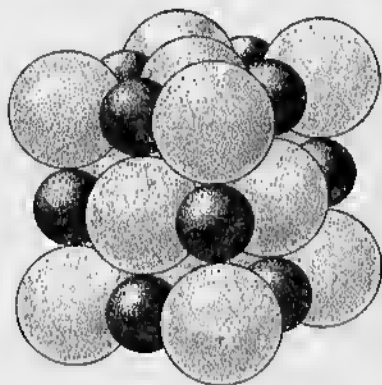
In a *gas* the atoms are in rapid motion, move independently of each other, and have no orderly arrangement. The forces

of mutual attraction are less than the forces of movement. Gases have high mobility.

In a *liquid* the atomic forces are strong enough to keep the atoms together, but there is either no orderly arrangement or only limited orderly arrangement. A liquid is fairly mobile.

*Solids* are characterized by "stiffness" or "rigidity." There are two kinds of solids—the crystalline solid and the noncrystalline solid.

In the *crystalline solid* the atoms have an orderly arrangement. Common salt, for example, is composed of sodium and chlorine, always in the ratio of one to one.



The relation of the atoms to each other is such as to form a cube (Fig. 1), and salt crystals occur as cubes or as some related form. Quartz is another example of a crystalline solid. For every atom of silicon there are two atoms of oxygen; the atoms are associated in such a way as to form an hexagonal pattern.

In the *noncrystalline solids* there is no orderly arrangement of the atoms. The *vitreous solids*, or *glasses*, are liquids that have cooled so rapidly that the atoms

Fig. 1.—Atomic Structure of Common Salt. The large spheres represent chlorine atoms; the small spheres represent sodium atoms. (From R. W. G. Wyckoff's *Structure of Crystals*, 2nd ed. The Chemical Catalog Co., 1931.)

have been unable to organize themselves into a systematic pattern. Technically these vitreous solids are supercooled liquids, and by some they are classified as liquids rather than solids. Window glass is a common example of a vitreous solid. Obsidian, a volcanic glass, is a well-known natural example. *Amorphous solids* do not have a definite arrangement of the atoms. They have not formed from the cooling of a liquid, however, and cannot properly be considered vitreous solids. Organic substances are commonly amorphous, as are, too, certain minerals such as opal.

The outer shell of the earth consists predominantly of solids, but gases and liquids are also present; their importance

varies with time and space. Groundwater and active volcanoes attest to the importance of liquids at the present time, and the igneous rocks of intrusive bodies indicate the abundance of liquids in the past. Gases are present in the outer shell of the earth, and are strikingly manifested in regions where petroleum is found; vast quantities of gas are sometimes expelled by active volcanoes. Never, however, does the gas occupy great underground chambers. The natural gas associated with petroleum occupies small pore spaces and fractures in solid rock and the gas of volcanoes effervesces from magma.

In this section of the book we are concerned primarily with solids. Gases and liquids are important only if their presence in pore spaces modifies the behavior of the solids.

The outer shell of the earth consists of sedimentary, igneous, and metamorphic rocks. The structural geologist, however, is interested primarily in the mechanical properties of the rocks with which he deals, rather than in their origin. Is the rock well-consolidated or not? A poorly cemented sandstone will be weaker than a well-cemented one, and quartzite will have greater strength than lava full of gas bubbles. Is the rock massive or not? Thin-bedded strata are weaker than thick-bedded formations. A thick massive limestone will be stronger than a series of thin lava flows, although in laboratory tests of individual specimens, the lava may be the stronger of the two. A thick, massive sandstone can be stronger than a highly fractured granite. Is the composition such that the fractures may be readily healed? Specimens of quartzite may be stronger than a limestone. But fractures in quartzite heal less readily than those in limestone.

### Force

#### Force and acceleration

*Force* is that which changes or tends to change the motion of a body. The locomotive of a train exerts the force that moves the cars. Force is defined by its magnitude and direction; hence it may be expressed by an arrow, the length of which is proportional to the magnitude of the force, and the direction of which indicates the direction in which the force is acting.

An *unbalanced force* is one that causes a change in the motion of a body. The *acceleration* is the rate of change of velocity. If a train starts from rest and acquires a velocity of 20 miles per hour at the end of 10 minutes, the acceleration

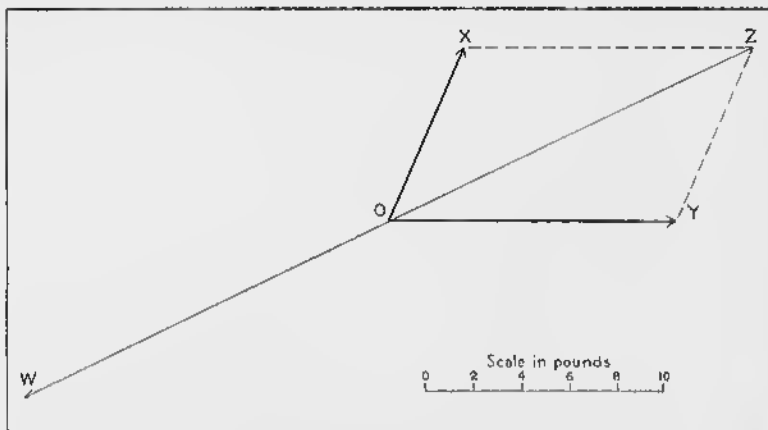


FIG. 2—Composition of Forces.

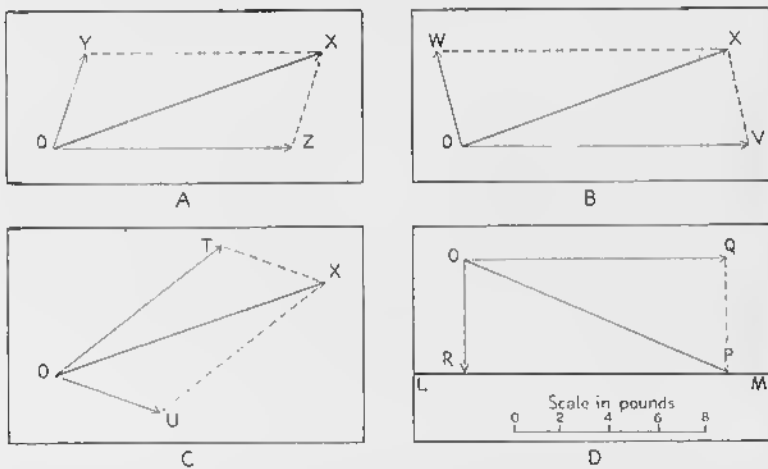


FIG. 3—Resolution of Forces.

is two miles per hour per minute. A body dropped from a high building is subjected to an unbalanced force because of the gravitational pull of the earth, and the body accelerates at the rate of approximately 32 feet per second per second.

*Balanced forces* exist where no change in motion occurs.

If a train is moving at a constant velocity, the frictional resistance of the tracks and the air equals the force exerted by the locomotive. If a man pushes against a wall that he cannot move, the wall is exerting a force equal and opposite to that exerted by the man.

The unit of force in the centimeter-gram-second system, commonly referred to as the c.g.s. system, is the *dyne*; the dyne is that force which, acting upon a mass of one gram, causes an acceleration of one centimeter per second per second.

Most problems confronting the structural geologist may be analyzed by assuming balanced forces, because the velocity of rock bodies is so small that acceleration is negligible. Along faults, however, the motion causing earthquakes may be so rapid that acceleration is important.

### Composition and resolution of forces

Force may be represented by a *vector*—that is, a line oriented in the direction in which the force is operating and proportional in length to the intensity of the force. Two or more forces may act in different directions at a point, as in Fig. 2, where  $OX$  (8 pounds) and  $OY$  (12 pounds) act at  $O$ . The same result would be produced by the force  $OZ$  ( $14\frac{1}{4}$  pounds) acting in the direction indicated;  $OZ$  is the resultant of  $OX$  and  $OY$ . A *resultant* is the single force that produces the same result as two or more forces, and it may be represented by the diagonal of a parallelogram constructed on two arrows that represent the two forces. The *equilibrant* is the force necessary to balance two or more forces. In Fig. 2,  $OW$  is the force necessary to balance  $OX$  and  $OY$ ; it is equal to the resultant of the two forces, but acts in the opposite direction. The process of finding the resultant of two or more forces is called the *composition of forces*.

Conversely, the effect of a single force may be considered in terms of two or more forces that would produce the same result. Thus, in Fig. 3A,  $OY$  and  $OZ$  would produce the same result as  $OX$ ; in Fig. 3B,  $OW$  and  $OV$  would produce the same result as  $OX$ ; in Fig. 3C,  $OT$  and  $OU$  would produce the same result as  $OX$ . A single force may thus be resolved into two *components*, acting in defined directions, by constructing

a parallelogram whose diagonal represents the given force, and whose sides have the directions of the components. The process of finding the components of a single force is called the *resolution of forces*.

In Fig. 3D the force  $OP$  (12 pounds) impinges on the line  $LM$ , and it is necessary to find the value of the component parallel to  $LM$ . This component,  $OQ$ , has a value of about 11 pounds, as can be determined from the scale in the figure.  $OR$ ,

which is the component perpendicular to  $LM$ , has a value of about 5 pounds.

The preceding discussion of the composition and resolution of forces has been confined to two dimensions, but geology is concerned with three dimensions. In Fig. 4 an inclined force,  $OW$ , lies in the vertical plane  $OZVW$ . This force may be resolved into two components, one of which,  $OZ$ , is vertical; the other,  $OV$  lies in the horizontal plane  $OXVY$ .  $OV$  may in turn be resolved into  $OX$  and  $OY$ , which lie in

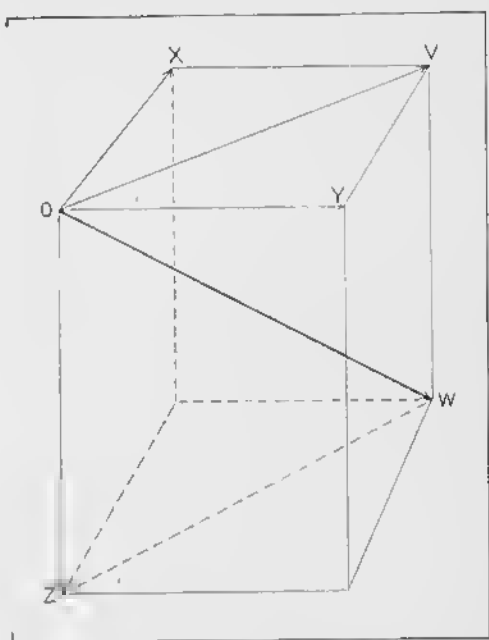


FIG. 4.—Resolution of Forces in Three Dimensions.

the horizontal plane and at right angles to each other. Moreover, any force, regardless of its value and its angle of inclination, may be similarly resolved into three components parallel to the  $X$ ,  $Y$ , and  $Z$  axes of Fig. 4.

### Stress

#### Concept of stress

If two cubes lie one above the other upon a table, the upper cube, because of its weight, pushes downward upon the lower.

Likewise, the lower cube pushes upward with an equal force upon the upper block. This mutual action and reaction along a surface constitutes a stress.<sup>1</sup>

Moreover, along any imaginary plane within either cube, there are similar actions and reactions. The imaginary plane may be horizontal, vertical, or inclined at any angle. The force, due to the weight of that part of the cube that lies above the plane, is directed in a vertical direction. This force would be directed normally to a horizontal plane. Along an inclined plane, however, the vertically directed force would be resolved into a normal component and a tangential component. If Fig. 3D were turned so that  $OP$  were vertical,  $LM$  would represent the inclined plane,  $OR$  the normal component, and  $OQ$  the tangential component.

The normal component is a *compressive stress* if it tends to push together the material on opposite sides of the plane.

The normal component is a *tensile stress* if it tends to pull apart the material on opposite sides of the plane.

The tangential component is generally called a *shearing stress* or *shear*.

The *stress-difference* at any point in a body is the difference between the greatest compressive stress and the least compressive stress at that point.

Physicists measure stress as the force per unit area; it is stated in pounds per square inch, tons per square foot, kilograms per square centimeter, or similar convenient units. Engineers prefer to use *unit stress* for the force per unit area.

Many geologists use stress as synonymous with external force. This usage is unnecessary and is hardly to be commended because it causes misunderstandings between geologists on the one hand and physicists, engineers, and mathematicians on the other. It is desirable to distinguish between the external force that is applied to a body and the resulting internal forces that constitute the stress.

The external forces that cause stress may be of two general types: hydrostatic pressure and differential forces.

---

<sup>1</sup> Love, A. E. H., *A Treatise on the Mathematical Theory of Elasticity*, 4th ed. Cambridge (England): Cambridge University Press, 1934.

### Hydrostatic pressure or confining pressure

The pressure on a small body immersed in a liquid is described as *hydrostatic pressure*. For example, at a depth of a mile in the ocean, the pressure is equal to the weight of a column of salt water one mile high. The pressure is 337,900 pounds per square foot or 2346 pounds per square inch. Every square inch of the surface of a small sphere at this depth would be under a pressure of 2346 pounds per square inch. Such an undirected, all-sided pressure is called hydrostatic pressure.

Rocks in the lithosphere, because of the weight of whatever rocks lie above them, are subjected to a similar but not identical kind of pressure. The weight of a column of rock one mile high will be several times that of an equally high column of water, because rocks have a higher specific gravity. The weight of a column of granite one mile high and one inch square would be 6178 pounds. A small imaginary sphere at a depth of one mile in the granite would be subjected to an all-sided pressure that would simulate hydrostatic pressure. Actually the force exerted on the top and bottom of the sphere would be greater than that exerted on the sides. With increasing depth in the lithosphere, this type of pressure becomes more nearly equal on all sides; below a depth of several tens of miles, the pressure is probably essentially hydrostatic in nature.

Some geologists prefer to call this equal, all-sided pressure on rocks the *confining pressure*, rather than use the term *hydrostatic*, which they believe should be restricted to the equal, all-sided pressure exerted by a liquid.

Obviously, the confining pressure increases with depth in the earth, and reaches tremendous values in the interior. It is equal to the weight of the overlying column of rocks, but near the surface this is only approximately true.

### Differential forces

In many instances the forces acting on a body are not equal on all sides. A body is said to be under *tension* when it is subjected to external forces that tend to pull it apart. Tension may be represented, as in Fig. 5A, by two arrows which are on the same straight line and which are directed away from each

other; the arrows represent the forces, whereas the rectangle represents the body or part of a body upon which the forces act. The rectangle may be omitted. Shearing and tensile stresses may exist in a body under tension.

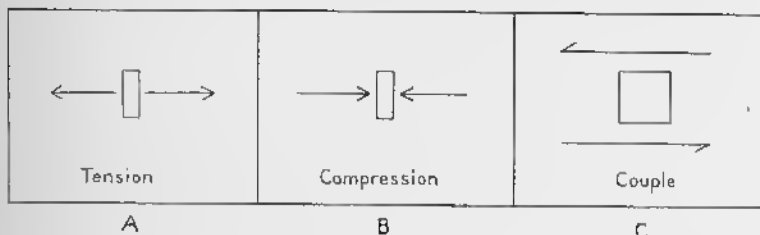


FIG. 5—Arrows Representing Tension, Compression, and a Couple.

A body is said to be under *compression* when it is subjected to external forces that tend to compress it. Compression may be represented, as in Fig. 5B, by two arrows which are on the same straight line and which are directed toward each other; the arrows represent the forces, whereas the rectangle represents the body or part of the body acted upon. The rectangle may be omitted. Shearing and compressive stresses may exist in a body under compression.

A *couple* consists of two equal forces that act in opposite directions in the same plane, but not along the same line. A couple may be represented, as in Fig. 5C, by two parallel arrows which are not on the same straight line and which are directed away from each other. The rectangle, which represents the body or part of the body acted upon, may be omitted. Shearing, tensile, and compressive stresses may exist in a body subjected to a couple. In geology *shear* is often used

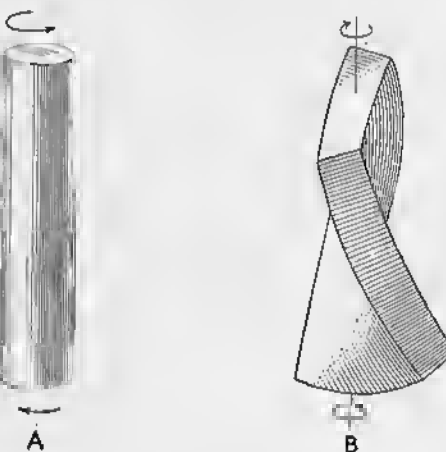


FIG. 6—Torsion. A rod (A) or plate (B) is subjected to torsion when the ends are twisted in opposite directions.

synonymously with *couple*, and may be employed to describe the sliding of rocks past each other along fractures.

Tension, compression, and couple are similar, respectively, to tensile stress, compressive stress, and shearing stress. The first three terms, however, refer to the external forces causing the stress, whereas the last three terms refer to the internal forces within the stressed body.

*Torsion* results from twisting. If the two ends of a rod are turned in opposite directions, the rod is subjected to torsion (Fig. 6A). A plate undergoes torsion, as in Fig. 6B, if two diagonally opposite corners are subjected to forces acting in one direction while the other two corners are subjected to forces acting in the opposite direction.

### Measurement of stress

There is no direct way to measure the internal forces in a body, but they may be calculated if the external forces are known. If a body is compressed or stretched, the stress is referred to a plane perpendicular to the direction in which the external forces are acting. Thus, if a vertical square column 10 inches on a side supports a load of 5000 pounds, every horizontal plane in the column is subjected to a compressive force of 5000 pounds. Each square inch on these horizontal planes supports a load of 50 pounds. The *compressive stress* is said to be 50 pounds per square inch. If a vertical rod with a cross-sectional area of 10 square inches carries a weight of 5000 pounds at its lower end, every horizontal plane in the rod is subjected to a pull of 500 pounds per square inch. The *tensile stress* is said to be 500 pounds per square inch.

### Strain

#### Definition

*Strain* is the deformation caused by stress; strain may be *dilatation*, which is a change in volume, or *distortion*, which is a change in form, or both.

When there is a change in the confining pressure, a body will change in volume, but not in shape. With increasing confining pressure, the volume of the body decreases and the dilatation is

negative. With decreasing confining pressure, the volume of the body increases and the dilatation is positive. Granite has a higher *compressibility* than gabbro and diabase; that is, for unit increase in confining pressure, a granite undergoes a greater decrease in volume than do gabbro and diabase. Under low confining pressure, a unit increase in confining pressure causes a greater decrease in volume than under higher confining pressures.

Under directed forces distortion occurs. For example, a steel rod 10 inches long with a cross section of one square inch is subjected to tension. A pull of 20,000 pounds stretches the rod 0.007 inch. The stress is 20,000 pounds per square inch and the strain is 0.0007 inch per inch.

### Three stages of deformation

If a body is subjected to directed forces, it usually passes through three stages of deformation. At first the deformation is *elastic*; that is, if the stress is withdrawn, the body returns to its original shape and size. There is always a limiting stress, called the *elastic limit*, and, if this is exceeded, the body does not return to its original shape. Below the elastic limit, the deformation obeys *Hooke's law*, which states that strain is proportional to stress.

If the stress exceeds the elastic limit, the deformation is *plastic*; that is, the specimen only partially returns to its original shape even if the stress is removed. Steel rods under tension, for example, begin to get thinner or "neck" in the middle, and, even after the stress is released, the constriction remains in the rod.

When there is a continued increase in the stress, one or more fractures develop, and the specimen eventually fails by *rupture*. The arrangement and form of the fractures depend upon several factors which are fully discussed in Chapter 6.

*Brittle substances* are those that have a small interval between the elastic limit and rupture. In other words, stresses somewhat greater than the elastic limit will cause rupture. *Ductile substances* are those that have a large interval between the elastic limit and rupture. After the elastic limit has been exceeded, ductile substances undergo a long interval of plastic deformation, and in some instances they may never rupture.

**Stress-strain diagram.** In engineering practice the relation existing between stress and strain is commonly expressed in a graph known as the stress-strain diagram (Fig. 7). The stress is commonly plotted on the ordinate (vertical) axis, whereas the strain is commonly plotted on the abscissa (horizontal) axis. Curve A of Fig. 7 is a graph of material under tension. The tensile stress is shown in pounds per square inch. With increasing stress, the specimen becomes longer, and the strain is plotted in terms of the percentage of lengthening of the specimen. Under a stress of

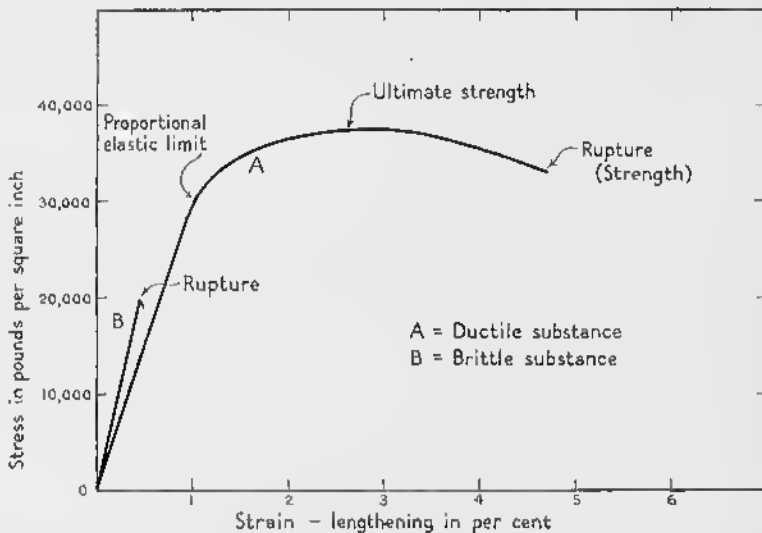


FIG. 7.—Stress-strain Diagrams.

10,000 lb./in.<sup>2</sup>, the specimen has lengthened only a fraction of 1 per cent;<sup>2</sup> at 20,000 lb./in.<sup>2</sup>, the lengthening is 0.7 per cent. When the stress is 30,000 lb./in.<sup>2</sup>, the specimen has been lengthened 1 per cent of its original length. The lengthening increases as the tensile stress is increased and, just before rupture occurs, the specimen is 4.5 per cent longer than it was originally. The point at which the curve departs from a straight line is known as the *proportional elastic limit*; it is usually essentially the same as the elastic limit (p. 17). The proportional elastic limit is 30,000 lb./in.<sup>2</sup>, and the lengthening at this point is one per cent.

<sup>2</sup> lb./in.<sup>2</sup> means "pounds per square inch."

Curve *B* of Fig. 7 is a graph of a brittle substance. The elastic limit is 20,000 lb./in.<sup>2</sup>, and there is no plastic deformation before rupture takes place.

*Strength* may be defined as the force per unit area necessary to cause rupture at room temperature and atmospheric pressure in short-time experiments. Under such conditions most rocks are brittle substances and, consequently, little plastic deformation precedes rupture; the strength is slightly greater than the elastic limit.

Table 1 gives the strength for some common rocks. Data are more complete for some than for others, and such a table is merely indicative of the magnitude of the values. The values are in separate columns for compressive, tensile, and shearing strengths. Some granites, for example, can stand a compressive stress of only 1000 kg./cm.<sup>2</sup> before rupturing;<sup>3</sup> other granites, however, can stand a compressive stress of 2800 kg./cm.<sup>2</sup>. In tension, however, granite ruptures if the stress exceeds a value of 30 to 50 kg./cm.<sup>2</sup>. In other words, granite is 33 times stronger under compression than it is under tension. Under shearing stress granite has a strength of 150 to 300 kg./cm.<sup>2</sup>. Under compression, basalt is the strongest of all the rocks listed in the table.

TABLE 1<sup>4</sup>  
AVERAGE STRENGTH OF ROCKS  
(In kilograms per square centimeter)

<i>Rock</i>	<i>Compressive</i>	<i>Tensile</i>	<i>Shearing</i>
Sandstone.....	500 to 1500	10 to 30	50 to 150
Limestone.....	400 to 1400	30 to 60	100 to 200
Granite.....	1000 to 2800	30 to 50	150 to 300
Diorite.....	1000 to 2500	.....	.....
Gabbro.....	1000 to 1900	.....	.....
Basalt.....	2000 to 3500	.....	.....
Felsite.....	2000 to 2900	.....	.....
Marble.....	800 to 1500	30 to 90	100 to 300
Slate.....	700	250	150 to 250

In ductile materials, shown in curve *A*, Fig. 7, the stress at the time of rupture may be considerably less than the maximum

<sup>3</sup> kg./cm.<sup>2</sup> means kilograms per square centimeter.

<sup>4</sup> Data from *International Critical Tables*, Vol. 2, pp. 47-49. New York: McGraw-Hill Book Company, 1927.

stress that the material has supported. The *ultimate strength* is the highest stress on the stress-strain curve.

*Fundamental strength* is defined on p. 23.

### Factors Controlling Behavior of Material

#### Confining pressure

The engineer is primarily interested in the physical properties of materials under atmospheric pressure and surface tempera-

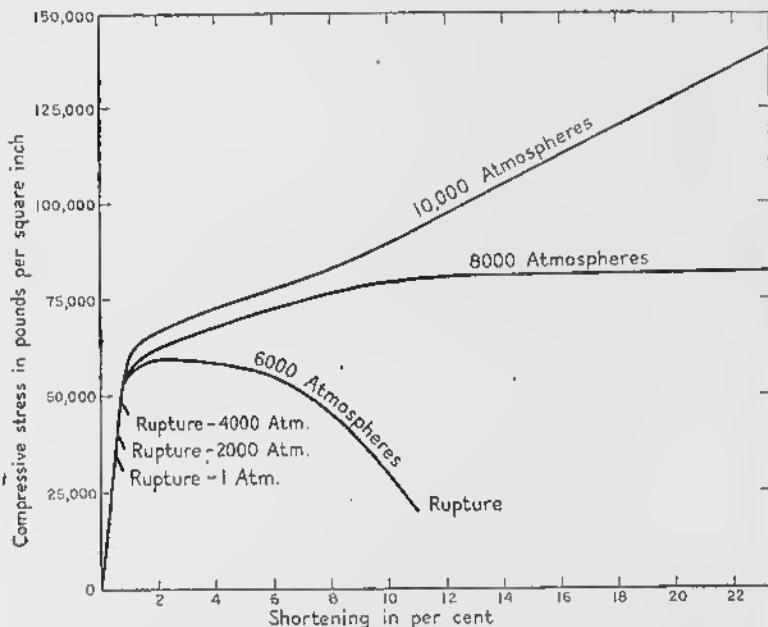


FIG. 8—Effect of Confining Pressure on Behavior of Solenhofen Limestone.  
(After D. T. Griggs.)

tures. Consequently, most of the available experimental data are distinctly limited in their application to geology. Factors that are important to the structural geologist are confining pressure, temperature, time, and solutions.

Griggs<sup>5</sup> has performed a number of experiments showing the effect of confining pressure on the properties of rocks.

<sup>5</sup> Griggs, David T., Deformation of rocks under high confining pressures: *Journal of Geology*, Vol. 44, pp. 541-577, 1936.

Fig. 8 illustrates the behavior of Solenhofen limestone under confining pressure. The compressive stress in pounds per square inch is given on the ordinate, and the per cent of shortening is given on the abscissa. Six separate sets of experiments were run, at confining pressures of 1, 2000, 4000, 6000, 8000, and 10,000 atmospheres. An *atmosphere* is approximately 14.7 pounds per square inch. Separate curves are given for the behavior at each of these confining pressures. Below a compressive stress of 55,000 lb./in<sup>2</sup>., the curves are so similar that they appear as one line on the graph. When the confining pressure was 4000 atmospheres or less, the limestone behaved as brittle material. When the confining pressure was 6000 atmospheres or greater, there was considerable plastic deformation. In one case, a specimen under a confining pressure of 10,000 atmospheres was shortened more than 22 per cent under a compressive stress of 135,000 lb./in<sup>2</sup>., and it did not rupture. Such experiments indicate that rocks exhibiting very little plastic deformation under near-surface conditions may do so readily under high confining pressures. This fact is of the utmost importance to structural geology.

Increase in confining pressure increases the ultimate strength (Fig. 8). Whereas the ultimate strength of Solenhoefen limestone under a confining pressure of one atmosphere is 37,000 lb./in<sup>2</sup>., under 10,000 atmospheres it is over 135,000 lb./in<sup>2</sup>., an increase of more than 360 per cent.

The proportional elastic limit is increased 50 per cent when the confining pressure is increased from 1 atmosphere to 10,000 atmospheres.

#### Temperature

Changes in temperature modify the behavior of materials. Hot steel, for example, undergoes plastic deformation much more readily than does cold steel. Few data are available concerning the mechanical effect of temperature on rocks, but high temperature would increase the field of plastic deformation.

It is apparent that plastic deformation is far less common near the surface of the earth, where the confining pressure and the temperature are low, than it is at greater depths, where

higher temperatures and greater confining pressures increase the possibility of plastic deformation.

### Time: fatigue and creep

Stresses that can be applied a few times without causing failure may, if repeated many times, cause rupture. This subject has been studied particularly in regard to metals. For example, a stress of 35,000 lb./in<sup>2</sup>, repeated 100,000 times may not cause rupture; if the same stress is repeated a million times, however, rupture occurs. If enough experiments are performed, a curve may be prepared, with the stress plotted on the ordinate,

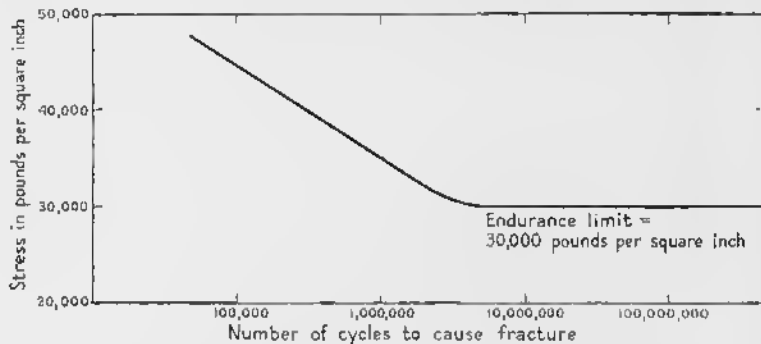


FIG. 9—Fatigue Curve for a Metal.

and the number of cycles of stress necessary to cause fracture plotted on the abscissa (Fig. 9). The curve becomes horizontal toward the right. The *endurance limit*, which is also known as the *fatigue limit*, is defined as the limiting stress below which the specimen can withstand hundreds of millions of repetitions of stress without fracture. In Fig. 9 the endurance limit is 30,000 lb./in<sup>2</sup>.

The endurance limit for many metals is approximately half that of the strength of the metal. For example, wrought iron, with a tensile strength of 46,900 lb./in<sup>2</sup>., has an endurance limit of 23,000 lb./in<sup>2</sup>; nickel steel, with a tensile strength of 111,800 lb./in<sup>2</sup>., has an endurance limit of 67,000 lb./in<sup>2</sup>.

Constantly repeated stresses cause fatigue of the rocks. Tidal stresses are of this nature.

Even more important to geology are those stresses, small though they may be, that act continuously for many years.

*Creep* refers to slow deformation under small stresses acting over long periods of time; ordinarily the term is restricted to deformation resulting from stresses below the elastic limit.<sup>6</sup> But the term is also used to refer to plastic deformation under any long-continued stress, even though the stress exceeds the elastic limit.

Solenhofen limestone under atmospheric pressure and at room temperature has a strength of 2560 kg./cm.<sup>2</sup>. In a long-time experiment, Solenhofen limestone subjected to a compressive stress of 1400 kg./cm.<sup>2</sup>—half the value of the strength—deforms rapidly at first, then more slowly (Fig. 10). At the end of one day, it has been shortened about 0.0006 per cent; after 10 days about 0.011 per cent; after 100 days about 0.016 per cent; and after 400 days a little more than 0.019 per cent.

Creep is the combined effect of "elastic flow" and "pseudoviscous flow." The specimen slowly recovers from that part of the deformation that is due to "elastic flow," which is also called *elastic after-working* and *creep recovery*. That portion of the deformation due to "pseudoviscous flow" is permanent and unrecoverable. The relative importance of these two types of flow during creep depends upon many variables. The creep of Solenhofen limestone illustrated by Fig. 10 is considered to be due exclusively to "elastic flow"; that is, given sufficient time, the specimen would have recovered its original shape. "Pseudoviscous" flow is involved in other experiments, but few precise data are available.

The structural geologist is especially concerned with the time factor. He wants to know what stresses will cause failure if they operate over a long period of time. The *fundamental strength* of any material is defined as the stress which that material is able to withstand, regardless of time, under given physical conditions—temperature, pressure, solutions—without ruptur-

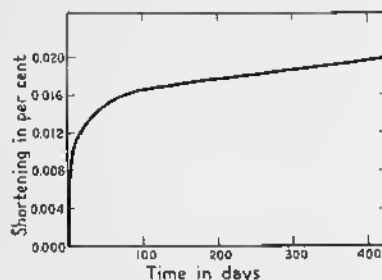


FIG. 10—Creep Curve for Solenhofen Limestone Under a Stress of 1400 kg./cm.<sup>2</sup> (After D. T. Griggs.)

<sup>6</sup> Griggs, David T., Creep of rocks: *Journal of Geology*, Vol. 47, pp. 225-251, 1939.

ing or deforming continuously. The fundamental strength is always less than the strength and the ultimate strength, and is much more significant to the geologist. Unfortunately, at the present time we have few data on the value of the fundamental strength of rocks.

Time is also important in another respect. The amount of plastic deformation before rupture is less if the stress is applied slowly than it is if the stress is applied rapidly. Moreover, the stress necessary to cause rupture is less if the stress is applied slowly. We may cite as specific examples experiments on Solenhofen limestone. In one experiment the confining pressure was 10,000 atmospheres, and a little more than an hour elapsed before the maximum compressive stress was attained. When the stress reached 185,000 lb./in.<sup>2</sup>, the specimen had shortened 30.3 per cent, but rupture had not occurred. In another experiment in which the confining pressure was the same (10,000 atmospheres), but in which 22 hours had elapsed before the maximum stress was attained, the specimen ruptured under a compressive stress of 96,000 lb./in.<sup>2</sup>.

### Solutions

Geologists have for many years realized that much rock deformation takes place while solutions capable of reacting chemically with the rock are present in the pore spaces. This is notably true of metamorphic rocks, in which extensive or complete recrystallization occurs. The solutions dissolve old minerals and precipitate new ones. When rocks are deformed under conditions favoring recrystallization, the mechanical properties of rocks are greatly modified.

Experimental data corroborate these deductions.<sup>7</sup> Dry alabaster, for example, under a compressive stress of 205 kg./cm.<sup>2</sup>, in an ordinary short-time experiment, will shorten 0.15 per cent. Even in experiments extending for more than 40 days, little difference is noted. If the alabaster is subjected to a similar stress, but in the presence of water, it will, within 36 days, have been shortened 1.8 per cent. In a similar experi-

<sup>7</sup> Griggs, David T., Experimental flow of rocks under conditions favoring recrystallization: *Bulletin Geological Society of America*, Vol. 51, pp. 1001-1022, 1940.

ment in the presence of dilute hydrochloric acid, the alabaster has shortened 23 per cent within 20 days. Whereas the strength of the dry alabaster under room temperature and a confining pressure of 1 atmosphere is 480 kg./cm.<sup>2</sup>, and the ultimate strength is 520 kg./cm.<sup>2</sup>, the fundamental strength under similar conditions, but with the specimen free to react with water, is estimated to be only 92 kg./cm.<sup>2</sup>. In this particular case, in other words, the fundamental strength is less than 20 per cent of the strength and ultimate strength.

### Summary

It is clear that the mechanical properties of rocks are profoundly modified by confining pressure, temperature, the time factor, and the presence of reacting solutions. The combined effect of these factors is so great that it is impossible in the present state of our knowledge to treat rock deformation in a quantitative way. Increase in confining pressure increases the elastic limit and the ultimate strength. Increase in the temperature presumably weakens the rocks, although data are lacking. After long continued stress the rocks become much weaker. The fundamental strength is of more interest to the structural geologist than is the strength or ultimate strength. Reacting solutions lower the strength, the ultimate strength, and the fundamental strength of rocks.

## Mechanics of Plastic Deformation

### Problem

The plastic deformation of solids is a subject of utmost importance to structural geology. How can solid rocks change their shape without the appearance of any visible fractures? Just what happens within the rocks to permit such a change in form? The processes may be classified into intergranular movements, intragranular movements, and recrystallization.

### Intergranular movements

Intergranular movements involve displacements between individual grains. Intrusive igneous rocks are usually composed of such minerals as quartz, feldspar, mica, and hornblende. Sandstones consist of rounded grains, usually quartz,

cemented together. Limestones are composed of small interlocking crystals of calcite. If such rocks are subjected to stress, the individual crystals and grains may move independently. All the displacements, because they are between grains, may be described as intergranular. The individual grains maintain their shape and size. The deformation of such a body might be compared to the change in shape undergone by a moving mass of B-B shot. Each grain can move and rotate relative to its neighbors.

In the plastic deformation of metals, such intergranular movements seem to be of subordinate importance. In rocks, particularly those of granitoid character, in which the crystals tend to interlock, more or less *granulation* takes place first; that is, the larger crystals are broken into smaller spherical grains that may rotate relative to each other.

### Intragranular movements

Intragranular movements are very important in the plastic deformation of metals. Displacements take place entirely within the individual crystals, and slipping takes place along what are known as *glide planes*. Some minerals have no glide planes. In others there is one glide plane—that is, one plane parallel to which there are a vast number of additional planes along which gliding can take place. In still other minerals there are several glide planes—that is, several planes, parallel to each of which there are a vast number of additional planes. The atomic structure controls the position and number of glide planes. Hence the glide planes are related to the symmetry of the mineral. Gliding is of two types, translation-gliding and twin-gliding.

*Translation-gliding* is illustrated very diagrammatically by Fig. 11. The centers of the atoms are represented by dots, and the glide planes by heavy horizontal lines labeled  $g_1g_1$  and  $g_2g_2$ . Diagram A shows the distribution of atoms before gliding takes place. The crystal lattice—that is, the spacing of the atoms relative to one another—is such as to give a characteristic pattern. Diagram B shows the arrangement of the atoms after gliding. Layers of atoms have slid to the right one interatomic distance relative to the layers beneath. The shape of the

figure as a whole has been changed. The lattice, however, is unchanged; the same diamond-shaped pattern is maintained as before. The distance between planes of gliding differs with the substance. In gold the distance is 0.00045 millimeter, in zinc 0.00080 millimeter.

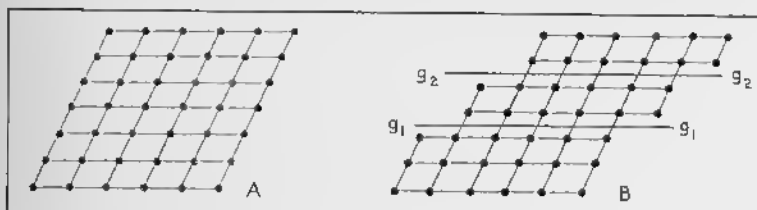


FIG. 11—Translation-Gliding. A. Arrangement of atoms before gliding. B. Arrangement of atoms after gliding along glide planes  $g_1g_1$  and  $g_2g_2$ .

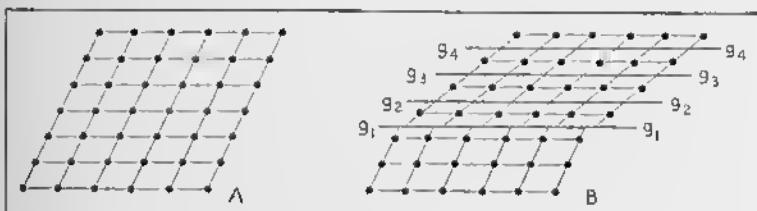


FIG. 12—Twin-Gliding. A. Arrangement of atoms before gliding. B. Arrangement of atoms after gliding on glide planes  $g_1g_1$ ,  $g_2g_2$ ,  $g_3g_3$ , and  $g_4g_4$ .

*Twin-gliding* is essentially the same as translation-gliding, except that in twin-gliding the layers of atoms slide a fraction of an interatomic distance relative to the layers beneath (Fig. 12). Fig. 12A shows the distribution of the atoms prior to deformation and Fig. 12B shows the distribution of the atoms after deformation. In this way the lattice of the displaced part of the crystal is symmetrically altered with respect to the lower, undisplaced part. In the terminology of mineralogy, the displaced part bears a twinned relation to the undisplaced part.

The sheets of atoms cannot slip along the glide planes in any direction. There are a limited number of lines parallel to which the movement can take place, and these lines are known as the *glide directions*. It is apparent, therefore, that the number and position of the glide planes and the glide direction depends upon the mineral. Aluminum, for example, has four glide planes and

three glide directions; altogether, therefore, there are twelve possible movements in this mineral.

A rock is an aggregate of minerals. Because the individual grains comprising the rock can be permanently deformed through gliding, the shape of the entire body of rock can be changed.

Fig. 13 illustrates in a two-dimensional model the deformation of a circle into an ellipse by gliding. One set of horizontal glide planes is present, and along these each successively higher sheet has moved toward the right. In the diagram the resulting

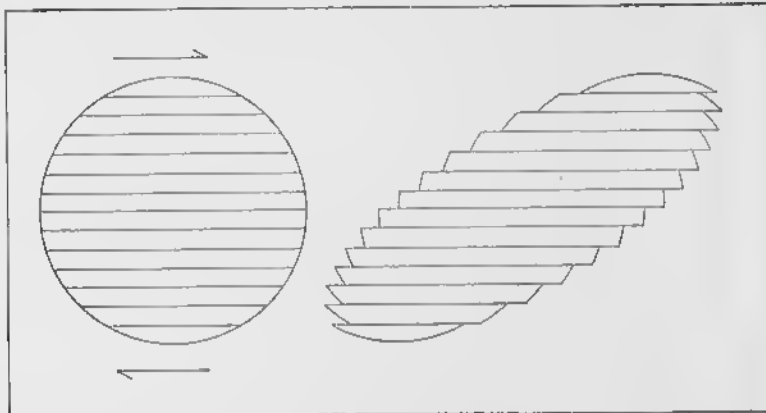


FIG. 13—Circle Changed into Ellipse by Movement Along Glide Planes.

ellipse is characterized by jagged edges, but in minerals the glide planes are so close that such irregularities are not detectable.

### Recrystallization

Recrystallization is another mechanism aiding plastic deformation. Rocks can crystallize without any change in shape, as is shown by limestone altered to marble near igneous intrusions. The number of crystals per unit volume decreases, but the size of the individual crystals increases. The rock mass as a whole need not change its shape.

Under conditions of differential pressure, however, solution and recrystallization may proceed in such a way that the rock is shortened in one direction and lengthened in another. The process may be explained by the so-called *Riecke principle*.

This principle supposes that solutions are present in the pore spaces of the rock, and that the portion of a crystal under greatest stress is dissolved. At the same time there is precipitation on that portion of the crystal subjected to the least stress. In this way the grain changes shape. If all the crystals in a body of rock are similarly affected, the mass as a whole changes shape.

It is obvious from observations in the field that plastic deformation and recrystallization have often been simultaneous, and we must accept the principle that recrystallization greatly facilitates plastic deformation.

### Strain Ellipsoid

A convenient way of visualizing deformation is to imagine a sphere under stress. Under simple compression, a sphere would change into an *oblate spheroid*, which is a solid geometrical figure generated by the rotation of an ellipse about its short axis. If the sphere shown in Fig. 14A were compressed along the vertical axis, the vertical axis of the resulting oblate spheroid would be shorter than the diameter of the original sphere, but the horizontal axes would be equal to each other and would be longer than the diameter of the original sphere. Under simple tension, a sphere would change into a *prolate spheroid*, which is the solid generated by the rotation of an ellipse about its long axis. If the sphere shown in Fig. 14A were stretched along the vertical axis, the vertical axis of the resulting prolate spheroid would be longer than the diameter of the original sphere, but the horizontal axes would be equal to each other and would be shorter than the diameter of the original sphere.

The most general solid resulting from the deformation of a sphere is an ellipsoid (Fig. 14B), which has three mutually perpendicular, unequal axes. Such an ellipsoid would form if a sphere, compressed along the vertical axis, were constrained on two sides, but were free to move on the opposite sides.

An oblate spheroid may be considered an ellipsoid in which two of the axes are equal and in which the third axis is shorter than the other two. A prolate spheroid may be considered an ellipsoid in which two of the axes are equal and in which the third axis is longer than the other two. Otherwise the sphere is

deformed into an ellipsoid. This imaginary figure may be called the *strain ellipsoid* or the *deformation ellipsoid*.

A strain ellipsoid has three unequal axes at right angles to one another (Fig. 14B). The largest axis of the ellipsoid may be called the *greatest strain axis*; the intermediate axis is the *intermediate strain axis*, and the shortest axis is the *least strain axis*. With two exceptions, all sections through an ellipsoid are ellipses. Two of the sections, which pass through the intermediate axis, are circles (Fig. 14C). The possible significance of these two circular sections in the strain ellipsoid will be discussed in Chapter 6.

Engineers have long utilized the strain ellipsoid in order to consider deformation below the elastic limit. The concept of the strain ellipsoid is useful to geologists in several ways. A point of fundamental importance is that the strain gives us no direct evidence of the external forces that caused the deformation. An ellipsoid may be formed from a sphere by simple compression, by tension, or by a couple. This fact is illustrated in two dimensions by Fig. 15. The three ellipses are identical. The ellipse in Fig. 15A, however, is the result of compression; that in Fig. 15B is the result of tension; and that in Fig. 15C is the result of a couple, as is shown by the solid arrows. The dotted arrows would give the same result. Thus, even though the field geologist may accurately describe the strain, he cannot directly deduce the external forces without some additional evidence. Further uses of the strain ellipsoid concept will be discussed in the chapter dealing with folding, rupture, and secondary foliation.

For convenience in making illustrations in two dimensions, we may consider the deformation of a circle into an ellipse. In such cases the long axis of the ellipse represents the long axis of the ellipsoid, and the short axis of the ellipse represents the short axis of the ellipsoid. The intermediate axis of the ellipsoid is perpendicular to the paper on which the diagram is drawn. In the ultimate analysis, however, the deformation should be considered in three dimensions; if the deformation is not so considered, mistakes of interpretation may be made.

A distinction is often made between *non-rotational* and *rotational* strain. Figs. 15A and 15B are examples of non-rotational

strain, because the external forces bear the same relation to the strain axes throughout the deformation. Under a couple, however, such as is illustrated in Fig. 15C, the strain axes rotate in a clockwise direction with continued application of the external forces.

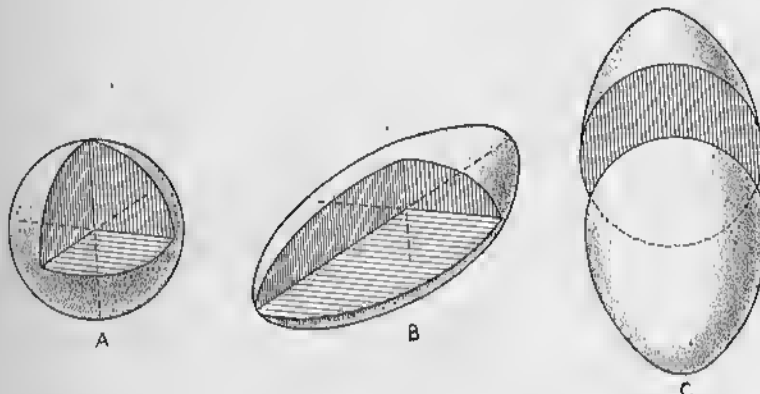


FIG. 14—Sphere and Ellipsoid. A. Sphere: has three mutually perpendicular axes that are equal. B. Ellipsoid: has three mutually perpendicular axes that are not equal. C. Circular section through an ellipsoid. This section includes the intermediate axis. There are two circular sections in every ellipsoid.

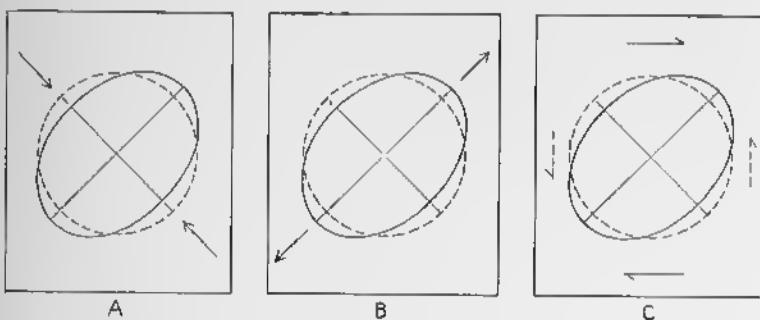


FIG. 15—Deformation of Circle into an Ellipse. A. Compression. B. Tension. C. Couple.

### Deformation in the Outer Shell of the Earth

The rocks in the outer shell of the earth are affected by all three of the major types of deformation: elastic, plastic, and rupture.

Tidal stresses and the passage of earthquake waves cause elastic strain, but no permanent effect is recorded, and hence it cannot be observed by the structural geologist.

Plastic deformation is involved in folding, in the development of flow cleavage, and in mass changes in the shape of rock bodies. Horizontal strata are permanently deformed by folding; although folding involves the sliding of beds past one another, each stratum undergoes plastic deformation. The origin of cleavage is a controversial subject, but that variety known as flow cleavage is generally considered to be the result of plastic deformation. As will be manifested later, solid rocks may flow from the limbs of folds, and may concentrate near the axes. Even large bodies of solid granite, if subjected to sufficient stress, may change shape through plastic deformation. Rock salt, under the influence of gravity or tectonic forces, may move as a plastic body to form salt domes.

Rupture is involved in the formation of joints, faults, and some varieties of cleavage. In some instances the walls visibly slide past each other to produce faults, but if there is no obvious differential movement, the fractures are called joints or cleavage.

Although it might seem most logical to consider the results of plastic deformation first, and to follow this by a consideration of the results of rupture, such a treatment is not feasible because some types of cleavage are plastic in origin and others are due to rupture. It seems better, therefore, to utilize a geological classification and consider folds, joints, faults, and cleavage in that sequence. The subsequent chapters are therefore organized accordingly.



PLATE III. Dipping Strata on Mt. Monadnock, New Hampshire. Interbedded quartzite (light gray) and mica schist (dark gray), dipping 50 degrees to the right. The long edge of the compass is parallel to the dip. In measuring dip, one ordinarily stands at a distance from the outcrop in order to eliminate the effect of small, local irregularities. (Photo by K. Fowler-Billings.)



PLATE IV. Vertical Strata. Middle Cretaceous limestone, Huasteca Canyon, near Monterrey, Mexico. (Photo by M. P. Billings.)

## 3

## Description of Folds

### Introduction

Folds are undulations or waves in the rocks of the earth. They are best displayed by stratified formations, such as sedimentary and volcanic rocks, or their metamorphosed equivalents. But any layered or foliated rock, such as banded gabbro or granite gneiss, may display folds.

Some folds are a few miles across; the width of others is to be measured in feet or inches—or even in fractions of an inch. Folds of continental proportions are hundreds of miles wide.

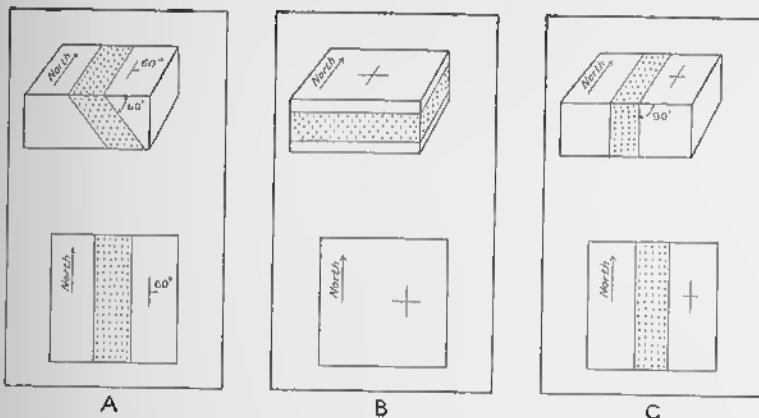


FIG. 16—Dip-Strike Symbols Used for Inclined, Horizontal, and Vertical Strata. Block diagram above, map below. A. Inclined strata. B. Horizontal strata. C. Vertical strata.

Some geologists prefer to use a special term for these larger folds, such as *flexures* or *broad warps*. Because the larger folds differ from the smaller folds only in size, it seems best to consider these broad warps or flexures merely as a variety of fold.

### Attitude of Beds

The *strike* of a bed is its trend measured on a horizontal surface. More precisely, strike may be defined as the direction

## DESCRIPTION OF FOLDS

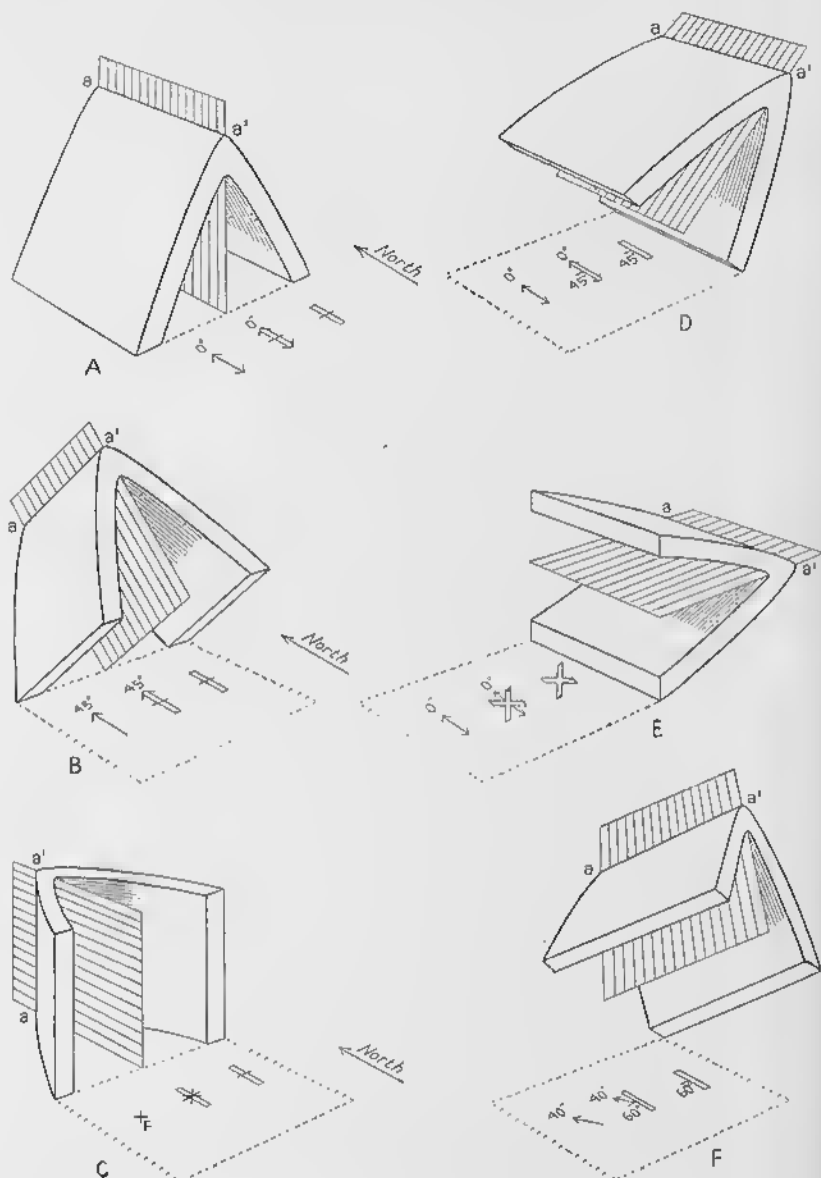


FIG. 17—Different Attitudes Assumed by Axial Plane of Folds. The axial plane is shaded in each diagram;  $aa'$  is axis of fold. The symbols below each fold refer to the attitude of the axial plane and the axis; the symbols are described on p. 60; see also Fig. 48.

of a line formed by the intersection of the bedding and a horizontal plane. In Fig. 16A the strike is north; the upper part of the figure is a block diagram, the lower part a map or plan.

The *dip* of a stratum is the angle between the bedding and a horizontal plane; it is measured in a vertical plane that strikes at right angles to the strike of the bedding. In Fig. 16A the dip is 60 degrees to the east. (See also Pl. III.)

A special *dip-strike symbol* is employed on geological maps to show the attitude of beds. It is shaped somewhat like the capital letter *T*, but the relative lengths of the two parts are reversed (Fig. 16A). The longer line is parallel to the strike of the bedding, whereas the shorter line points in the direction of the dip, and a figure gives the value of the dip. For horizontal strata (Pl. I), a special symbol,  $\perp$ , may be used (Fig. 16B). For vertical strata (Pl. IV) a long line gives the strike, and a short cross-bar extends on either side of the long line (Fig. 16C). Although most geological maps use symbols similar to these to give dip and strike of the bedding, the system is not standardized, and it is necessary to look at the legend accompanying the map in order to ascertain the meaning of the symbols employed.

### Parts of a Fold

The *axial plane* or *axial surface* of a fold is the plane or surface that divides the fold as symmetrically as possible. In a two-dimensional diagram, the axial plane is represented by a line.

In some folds the axial plane is vertical (Fig. 17A, B, and C), in others it is inclined (Fig. 17D and F), and in still others it is horizontal (Fig. 17E). Although, in many folds, the axial surface is a relatively smooth plane, it may be curved. The attitude of the axial plane is defined by its strike and dip, just as the attitude of a bed is defined. In Fig. 17, north is toward the upper left-hand corner. In Fig. 17A, B, and C, the axial plane strikes north and has a vertical dip. In Fig. 17D, the strike is north, the dip 45 degrees to the west. In Fig. 17F, the axial plane strikes north and dips 60 degrees to the west; in Fig. 17E, the axial plane is horizontal. If the axial plane is curved, the dip or strike—or both—may differ from place to place, as in the case of a curved bedding plane.

The meaning of the symbols beneath each fold in Fig. 17 is discussed on p. 60.

An *axis* of a fold is the intersection of the axial surface with a particular bed. Such an intersection is a line, and in Fig. 17 it is lettered  $aa'$ . Actually, of course, there is an axis for every bed, and every fold has countless axes. Inasmuch as these axes

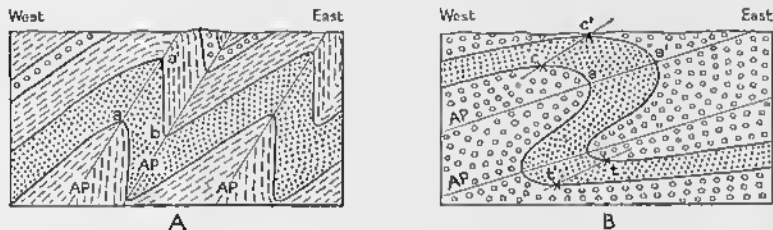


FIG. 18—Parts of a Fold.  $AP$  = axial plane;  $ab$  = limb of a fold;  $c$  = crest on one bed,  $c'$  = crest on another bed,  $cc'$  = crestal plane;  $t$  = trough on one bed,  $t'$  = trough on another bed,  $tt'$  = trough plane.

are generally parallel, one axis is sufficient to indicate the attitude of the fold. In some folds the axes of the fold are horizontal (Fig. 17A, D, E); in others, the axes are inclined (Fig. 17B, F); and in still others, the axes are vertical (Fig. 17C).

The sides of a fold are called the *limbs* or *flanks*. Terms used in the past, but now obsolete, were *legs*, *shanks*, *branches*, and

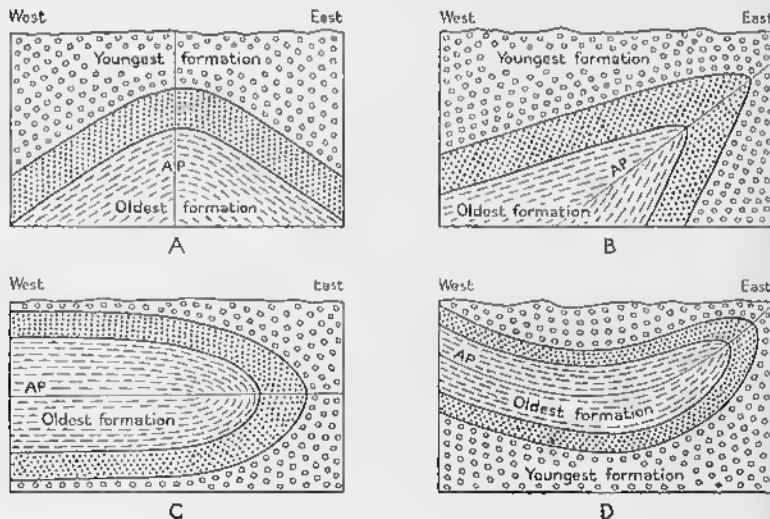


FIG. 19—Some Varieties of Anticlines.  $AP$  = axial plane.

*slopes.* A limb extends from the axial plane in one fold to the axial plane in the next. For example, in Fig. 18A,  $a'b$  is the limb of a fold. It may be considered either the east limb of the upfold or the west limb of the adjacent downfold. In other words, every limb is mutually shared by two adjacent folds.

Although in many instances the axis is at the highest part of the fold, as in Fig. 18A, this is not necessarily the case. In Fig. 18B, for example,  $a$  and  $a'$  are axes, or, to be more precise, the intersection of axes with the plane of the paper;  $c$  and  $c'$  are the highest points on the folds. The *crest* is a line along the highest part of the fold, or, more precisely, the line connecting the highest points on the same bed in an infinite number of cross sections. There is a separate crest for each bed. The plane or surface formed by all the crests is called the *crestral plane* ( $cc'$  of Fig. 18B).

In many phases of geology, the distinction between the crest and axis is not important, either because the two correspond or, if there is a difference, because the distinction is of academic interest only. The same is true of the distinction between crestral plane and axial plane. In the accumulation of gas and petroleum, however, the difference is significant. The trapping of such materials is controlled by the crest and crestral plane rather than by the axis and axial plane. In American oil fields, however, the crestral plane and axial plane are usually identical.

The *trough* is the line occupying the lowest part of the fold, or, more precisely, the line connecting the lowest parts on the same bed in an infinite number of cross sections. In Fig. 18B,  $t$  and  $t'$  are troughs. The plane connecting such lines may be called the *trough plane*.

### Nomenclature of Folds

During the last one hundred years, a rather elaborate terminology has been evolved to describe the geometrical aspect of folds. Many of the terms refer to the appearance of folds in vertical cross sections perpendicular to the strike of the axial planes of the folds. Other terms refer to the attitude of the axes. The nomenclature based on the appearance of folds in cross sections may be considered first. As is to be expected,

these terms refer primarily to the attitude of the axial plane and the attitude of the limbs.

An *anticline* is a fold that is convex upward or, in more complicated folds, is inferred to have had such an attitude at some stage in its development (Pl. V). The word is from the Greek, and means "opposite inclined." It refers to the fact that in the simplest anticlines, the two limbs dip away from each other (Fig. 19A). In some anticlines, however, the two limbs dip in the same direction (Fig. 19B), or are horizontal (Fig. 19C). Still other anticlines have attained such a complicated form (Fig. 19D) that no simple definition may be given. An anticline may also be defined as a fold with older rocks toward the center of curvature. This is correct, unless the structural history has been unusually complex.

A *syncline* is a fold that is concave upward, or, in more complicated folds, is inferred to have had such an attitude at some

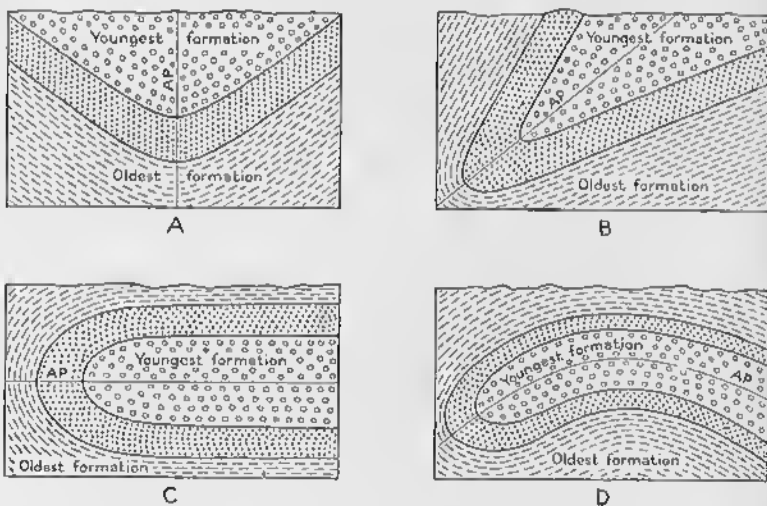


FIG. 20—Some Varieties of Synclines. *AP* = axial plane.

stage in its development. The word is from the Greek, meaning "together inclined," and refers to the fact that in the simplest synclines, the two limbs dip toward each other (Fig. 20A). But the limbs may dip in the same direction, be horizontal, or be complexly folded (Fig. 20B, C, and D). A syncline is generally a fold with younger rocks toward the center of curvature.

PLATE V. Anticline about 20 Miles North of Cerro de Pasco, Peru. Strata are Mesozoic and Tertiary. (Photo by W. F. Jenks.)





PLATE VI. Vertical Isoclinal Syncline about 3 Miles West of Cerro de Pasco, Peru. Strata are of Tertiary age. View looking S.  $20^{\circ}$  E. along axis of fold.  
(Photo by W. F. Jenks.)



PLATE VII. Small Recumbent Fold, Mt. Monadnock, New Hampshire. (Photo by K. Fowler-Billings.)

Another set of terms refers to the attitude of the axial plane. A *symmetrical fold* is one in which the axial plane is essentially vertical. In other words, the two limbs have the same angle of dip (Fig. 21A).

In the *asymmetrical fold* the axial plane is inclined; the two limbs dip in opposite directions, but at different angles (Fig. 21B).

In the *overturned fold* or *overfold* the axial plane is inclined, and both limbs dip in the same direction, usually at different angles (Fig. 21C). The *overturned, inverted, or reversed limb* is the one that has been rotated through more than ninety degrees

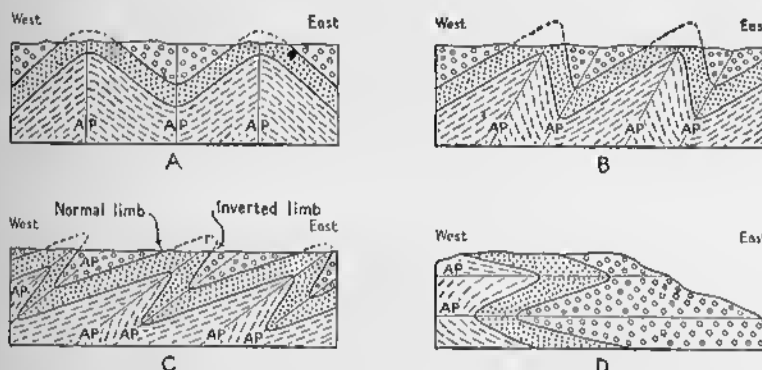


FIG. 21—Some Varieties of Folds. AP = axial planes. A. Symmetrical folds. B. Asymmetrical folds. C. Overturned folds (overfolds). D. Recumbent folds.

to attain its present attitude. A special dip-strike symbol is commonly used on modern maps to indicate overturned strata (Fig. 22). The *normal limb* is the one that is right-side-up.

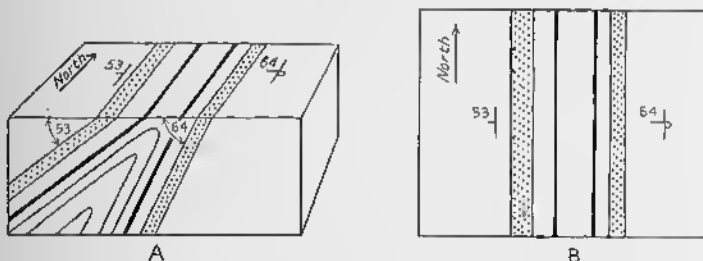


FIG. 22—Dip-Strike Symbol for Overturned Strata. A. Block diagram. B. Map. The dip-strike symbol with 53 side of it indicates beds that dip 53 degrees to the west (left) and are not overturned. The dip-strike symbol with 64 side of it indicates beds that dip 64 degrees to the west (left), but are overturned.

A *recumbent fold* is one in which the axial plane is essentially horizontal (Fig. 21D; Pl. VII). Large-scale folds of this type are rare in North America, but they are common in the Alps. Consequently, a rather elaborate terminology has been evolved by European geologists to describe such folds (Fig. 23). The strata in the inverted limb are usually much thinner than the corresponding beds in the normal limb. Many of the recumbent folds in the Alps have Paleozoic crystalline rocks in the center and Mesozoic sedimentary rocks in the outer covering. Thus there is a distinct core of crystalline rocks within a shell of sedimentary rocks. Even in a recumbent fold composed entirely of one kind of rock, the terms *core* and *shell* may be used to refer, respectively, to the inner and outer parts of the fold. Many recumbent folds have subsidiary recumbent

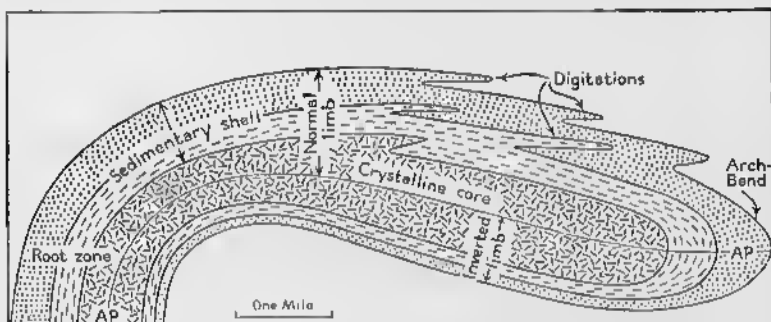


FIG. 23—Recumbent Anticline with Names of Various Parts.

anticlines attached to them; these subsidiary folds may be called *digitations*, because they look like great fingers extending from a hand. All recumbent folds, if satisfactory exposures are available, may be traced back to the *root* or *root-zone*—that is, to the place on the surface of the earth from which they arise; in other words, recumbent folds may be traced to the place where the axial plane becomes much steeper.

An *isoclinal fold*, from the Greek meaning “equally inclined,” refers to folds in which the two limbs dip at equal angles in the same direction (Fig. 24). A vertical or symmetrical isoclinal fold (Fig. 24A) is one in which the axial plane is vertical (Pl. VI); an inclined or overturned isoclinal fold is one in which the axial

plane is inclined. A recumbent isoclinal fold is one in which the axial plane is horizontal. Many recumbent folds are isoclinal.

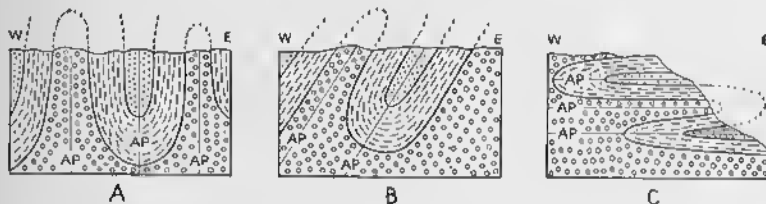


FIG. 24—Isoclinal Folds.  $AP$  = Axial planes. A. Vertical isoclinal folds. B. Inclined isoclinal folds. C. Recumbent isoclinal folds.

Although most folds are relatively well-rounded at the anticlinal and synclinal axes, some are sharp and angular. Such folds are called *chevron folds* (Fig. 25A).

A *fan fold* is one in which both limbs are overturned (Fig. 25B). In the anticlinal fan fold, the two limbs dip toward each other; in the synclinal fan fold, the two limbs dip away from each other. Fan folds are not as common as was formerly

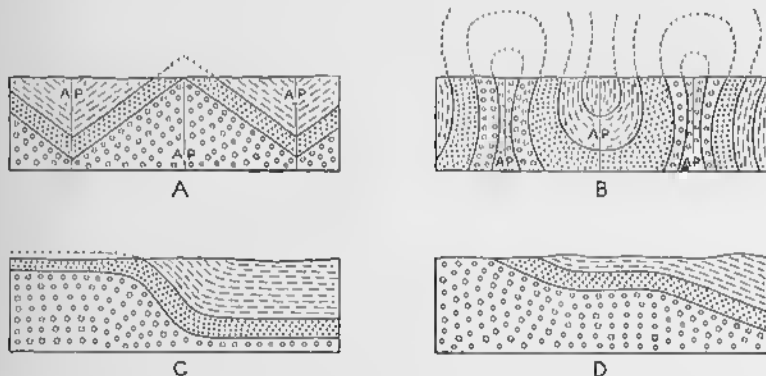


FIG. 25—Some Varieties of Folds.  $AP$  = Axial planes. A. Chevron fold. B. Fan fold. C. Monocline. D. Structural terraces.

supposed; fifty years ago they were thought to be abundant in the Alps.

In plateau areas, where the bedding is relatively flat, the strata may locally assume a steeper dip (Fig. 25C). Such a fold is a *monocline*. The beds in a monocline may dip at angles ranging from a few degrees to ninety degrees, and the elevation

of the same bed on opposite sides of the monocline may differ by hundreds or even thousands of feet.

In areas where dipping strata locally assume a horizontal attitude, a *structural terrace* is formed (Fig. 25D). This usage should not be confused with that of the physiographer, who employs the term to refer to terraces that are structurally controlled.

The term *homoclinal*, from the Greek meaning "one inclination," may be applied to strata that dip in one direction at a uniform angle. Although many homoclines are, if large areas are considered, limbs of folds, the term is useful to refer to the structure within the limits of a small area.

A *closed* or *tight fold* is one in which the deformation has been sufficiently intense to cause flowage of the more mobile beds, so that these beds thicken and thin (Fig. 26B). Conversely an *open fold* is one in which this flowage has not taken

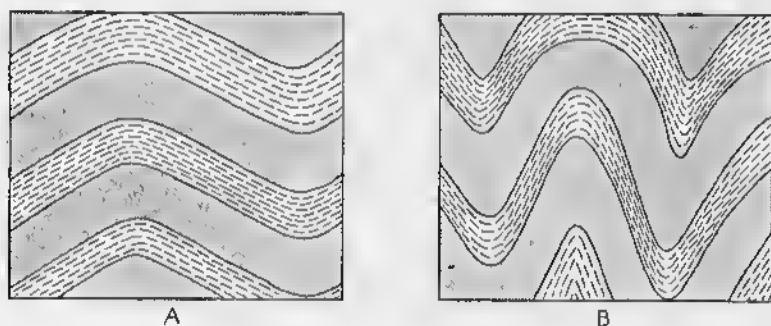


FIG. 26—Open and Closed Folds. A. Open folds. B. Closed folds.

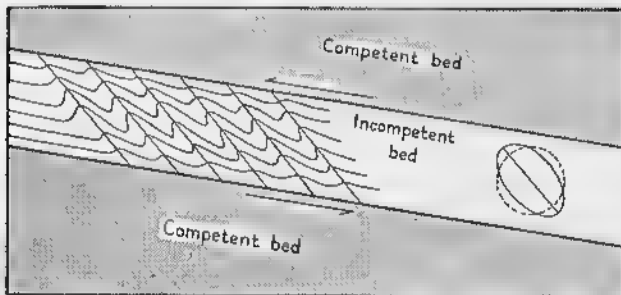


FIG. 27—Drag Folds Resulting from Shearing of Beds Past Each Other.

place (Fig. 26A). Although the more extreme cases of these two types may be readily distinguished from each other, there are intermediate examples that are difficult to classify.

*Drag folds* form when a competent ("strong") bed slides past an incompetent ("weak") bed (Fig. 27). Such folds may form on the limbs of folds, because of the slipping of beds past each other, or they may develop beneath overthrust blocks (Chapter 10). The axial planes of the drag folds are not perpendicular to the bedding of the competent strata, but are inclined at an angle. Under a couple, of the type illustrated in Fig. 27, an imaginary circle in the incompetent bed would be deformed into an ellipse. The traces of the axial planes of the folds are parallel to the long axis of this ellipse. The acute angles between the axial planes and the main bedding plane point in the direction of the differential movement.

The use of drag folds in solving structural problems will be discussed on pp. 76-81.

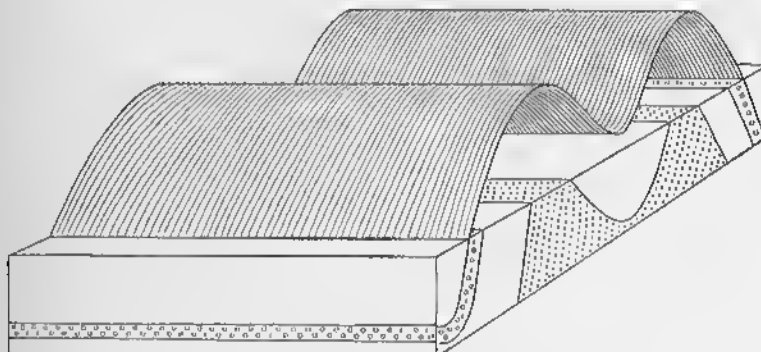


FIG. 28—Non-Plunging Folds.

### Plunge of Folds

In the preceding section, emphasis has been placed upon the appearance of folds in cross sections. But folds, like any geological structure, must be considered in three dimensions. The attitude of the axis is of the greatest importance in describing the third dimension.

In some folds the axis is horizontal (Fig. 17A, D, and E); in other folds the axis is inclined (Fig. 17B, C, and F). The attitude of the axis of a fold is defined by two measurements:

the *strike* of its horizontal projection and the *plunge*. It must be remembered that an axis is a line, such as  $FD$  in Fig. 29. Of all the possible vertical planes in the figure, only one,  $ADFG$ , contains the line  $FD$ . The intersection of this plane with the horizontal plane  $ABCD$ , is the line  $AD$ .  $AD$  is the horizontal projection of  $FD$ . In Fig. 2, the line  $AD$  strikes northwest, and this is therefore the strike of the horizontal projection of  $FD$ . The plunge of  $FD$  is the angle  $P$ , which is the angle between  $AD$  and  $FD$  measured in the vertical plane  $ADFG$ .

Although the larger plunging folds cannot be directly observed, they are easily recognized from their outcrop pattern. Fig. 28 is a block diagram of a fold that does not plunge. On the map, the beds on the opposite limbs strike parallel to each other; they do not converge. Fig. 30 is a geological map of a non-plunging syncline. Fig. 31 is a block diagram of plunging

folds, and shows that the beds converge; the formations have a zig-zag pattern. Figs. 32 and 33 are geological maps of plunging folds; the beds on the opposite limbs strike toward each other and the formations converge. Fig. 32 shows a plunging anticline; Fig. 33 shows a plunging syncline. The place on the map where a bed shows the maximum curvature is known as the *nose* of the fold; there is a nose

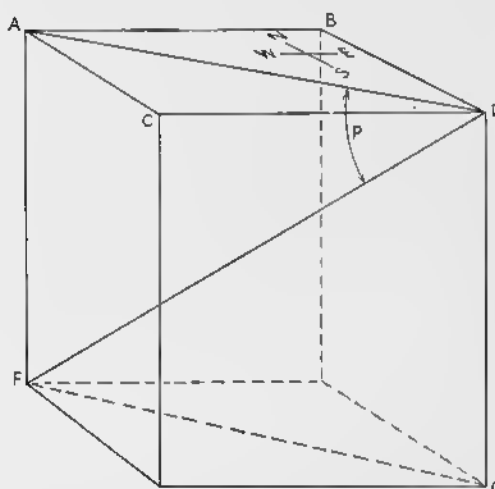


FIG. 29—Attitude of Axis of a Fold. If  $FD$  is the axis;  $AD$  is the strike of the horizontal projection of the axis; the angle of plunge is  $P$ .

for each stratum. The *axial trace* of a fold connects the points where, on the map, each bed shows the maximum curvature (Figs. 32 and 33). On most published geological maps this is called the axis, but this term is preferably used in a different sense, as defined on p. 36. For symmetrical folds or non-plunging folds, the axial trace and the horizontal projection of

## DESCRIPTION OF FOLDS

45

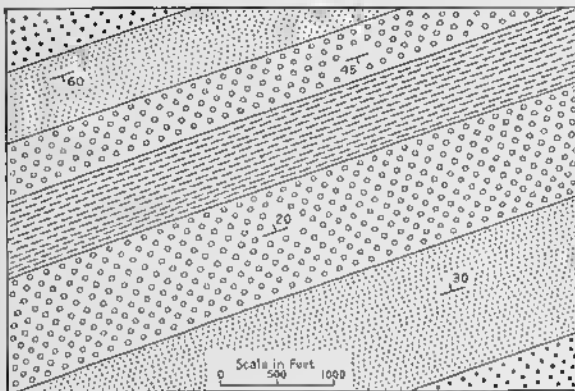


FIG. 30—Geological Map of Non-Plunging Fold.

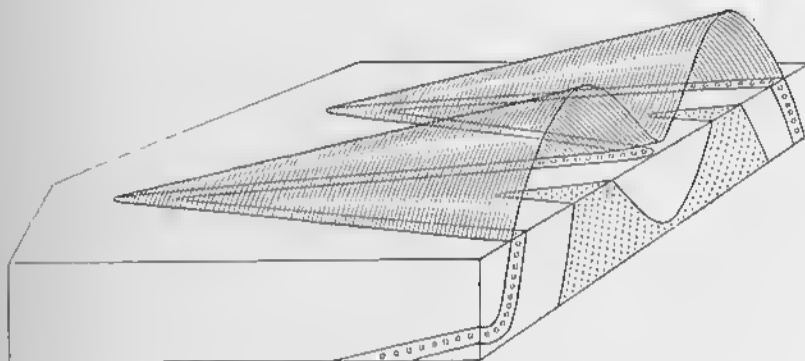


FIG. 31—Plunging Folds. Plunge is 10 degrees to the left.

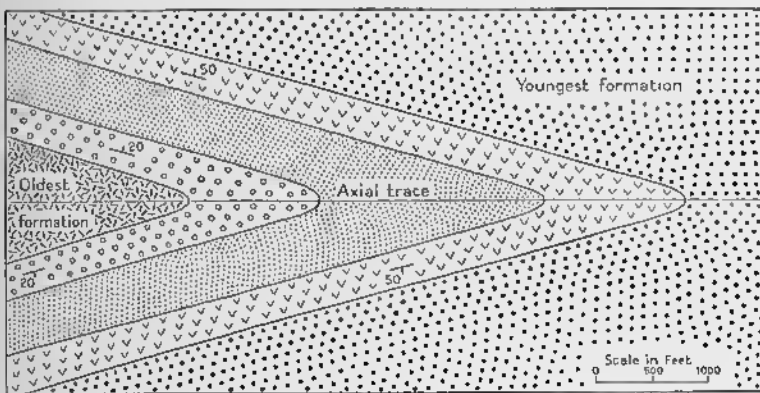


FIG. 32—Geological Map of an Antioline Plunging East (to the right).

the axis coincide, but this is not true if the axial plane is inclined and the fold plunges.

In the preceding paragraphs it has been tacitly assumed that the plunge is constant. In most instances, however, the value of the plunge changes along the strike, and the direction of plunge may even be reversed. Fig. 34A is a geological map of a symmetrical anticline, the axial trace of which trends northeast. In the northeast corner of the map, the fold plunges 10 degrees to the northeast, and the strata converge northeastward. Toward the southwest, the value of the plunge decreases, and in the center of the map it is zero, because the strata on opposite limbs are parallel in strike. In the southwest corner, the anticline plunges 15 degrees to the southwest. Fig. 34B shows a syncline that plunges southwest at the northeast corner of the map, and northeast at the southwest corner.

A *doubly plunging* fold is one that reverses its direction of plunge within the limits of the area under discussion. Most folds, if followed far enough, are doubly plunging.

A *dome* is an anticlinal uplift that has no distinct trend (Fig. 34C). A *basin* is a synclinal depression that has no distinct trend (Fig. 34D).

The angle of plunge is commonly not great, but in some regions, particularly those composed of metamorphic rocks, the angle of plunge may approach 90 degrees. In some localities the folds may even have inverted plunges.

### Fold Systems or Orogens

The preceding discussion has been concerned primarily with single folds. Folds, however, are seldom found alone, but commonly belong to a system composed of many folds. In some regions the axial traces ("axes") of the folds are parallel and straight; whereas in other regions the axial traces are parallel and curved. Most characteristically, however, they are neither parallel nor straight.

Fig. 35 is a geological map of an area in which the axial traces are curved. Along the line  $cc'$  they are convex toward the north, and they diverge toward the east and west.

In some localities individual folds do not extend any great distance, but overlap one another, *en échelon*, as is shown in Fig. 36.

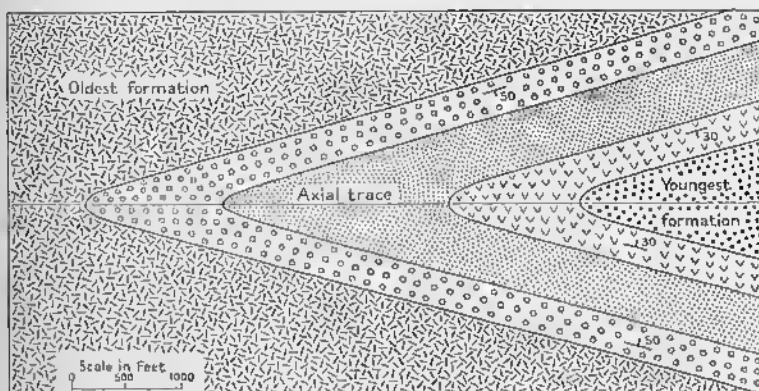


FIG. 33—Geological Map of a Syncline Plunging East (to the right).

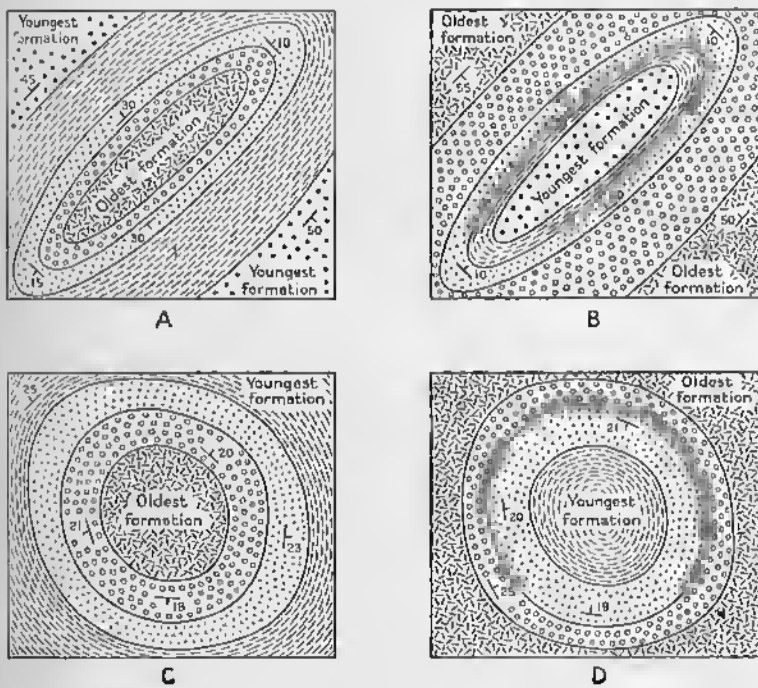


FIG. 34—Plunging Folds. A. Doubly plunging anticline. B. Doubly plunging syncline. C. Dome. D. Basin.

A system of folds is called an *orogen*. Most orogens are hundreds or thousands of miles long and scores or hundreds

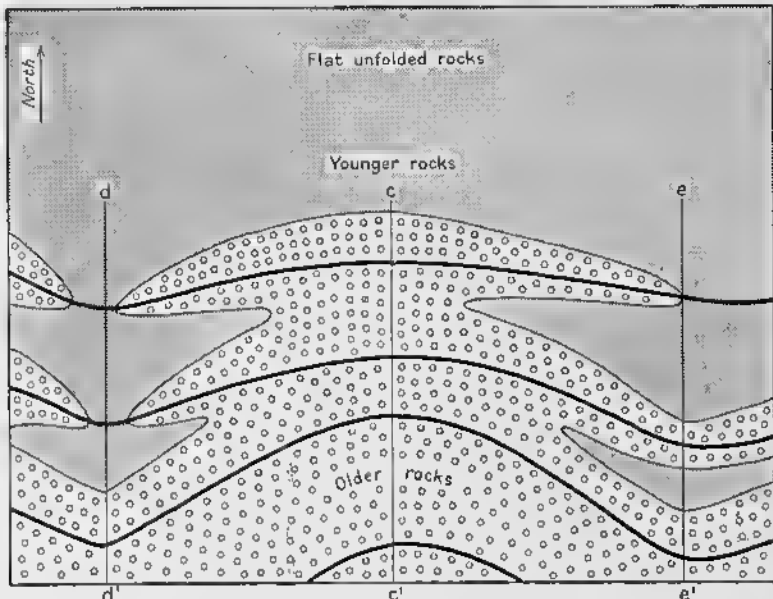


FIG. 35—Convergence and Divergence of Axial Traces of Folds. The axial traces ("axes") are shown as heavy black lines. These lines diverge from one another on either side of  $cc'$ , and converge toward  $cc'$  if approached from  $dd'$  or  $ee'$ .

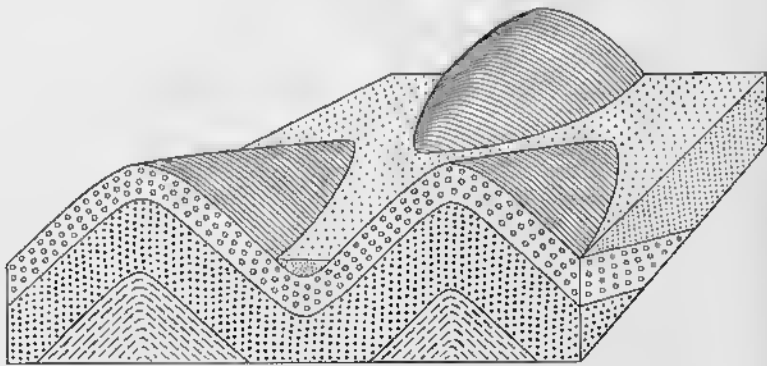


FIG. 36—*En échelon* Folds. The anticlines hold up antielinal mountains rising above a flat plain. The axial trace of the fold in the background is *en échelon* relative to the folds in the foreground.

of miles wide. A complete orogen is usually bounded on both sides by horizontal strata that were deposited contempor-

neously with the rocks in the orogen. Many orogens, however, are partially buried by younger sediments.

In a *salient* the axial traces of the folds are convex toward the outer edge of the orogen. The lines labeled  $cc'$  in Figs. 35 and 37 are located on a salient. In a *recess* the axial traces are concave toward the outer edge of the orogen. In Figs. 35 and 37, the lines  $dd'$  and  $ee'$  are located on recesses.

Over large parts of an orogen the axial planes of many of the folds dip in the same direction. In the Valley and Ridge Province of the Appalachian Highlands, for example, the axial

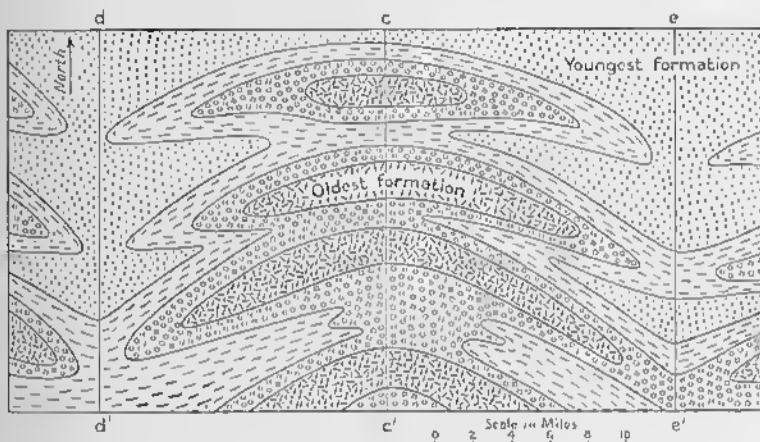


FIG. 37—Culmination and Depression. The line  $cc'$  is on a culmination, away from which the folds plunge;  $dd'$  and  $ee'$  are depressions, toward which the folds plunge.

planes dip toward the southeast. Most of the thrust faults, as well as the cleavage, dip in the same direction in this region.

In many areas all the folds plunge in the same direction. In Fig. 37, the folds between  $cc'$  and  $ee'$  plunge toward the east. East of  $ee'$  the folds plunge to the west. West of  $cc'$ , but east of  $dd'$ , the folds plunge to the west. West of  $dd'$  the folds plunge to the east. The line  $cc'$  represents a culmination;  $dd'$  and  $ee'$  represent depressions. *Culminations* and *depressions* trend essentially at right angles to the trend of the folds; the folds plunge away from culminations toward depressions. The concept of culminations and depressions has proved of great importance in understanding the structure of the Alps.

## DESCRIPTION OF FOLDS

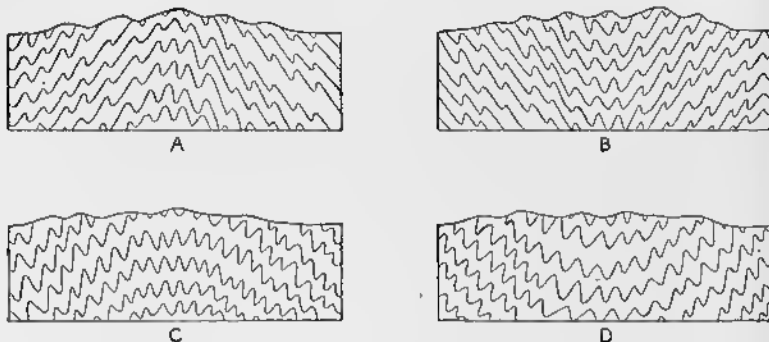


FIG. 38—Anticlinoria and Synclinoria. A. Abnormal anticlinorium. B. Abnormal synclinorium. C. Normal anticlinorium. D. Normal synclinorium.

Many folds have minor folds on their flanks. Extreme examples are found in highly deformed rocks. In western New Hampshire, for example, the distance between the crests of major anticlines is several miles. Superimposed on these major folds are subsidiary folds, the axes of which are thousands of feet apart. On these subsidiary folds are lesser folds, the axes

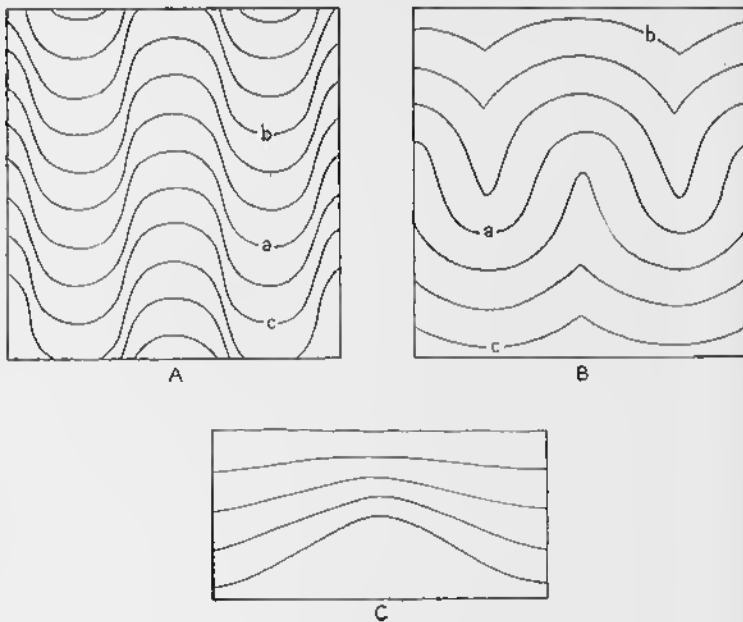


FIG. 39—Types of Folding. A. Similar folding. B. Parallel folding. C. Supratenuous folding.

of which are hundreds of feet apart. On these lesser folds are minor folds which may be observed in single outcrops; the distance between the crests of the minor folds is measured in feet. On the limbs of the minor folds are small crenulations, less than an inch apart. Microscopic study shows still smaller folds, too minute for the unaided eye to detect.

A major anticline that is composed of many smaller folds is called an *anticlinorium* (Figs. 38A and 38C). An anticlinorium must be a large fold, of the magnitude of a mountain or a mountain range; that is, it must be at least several miles across. A *synclinorium* is a large syncline that is composed of many smaller folds (Figs. 38B and 38D).

In a *normal anticlinorium* (Fig. 38C), the axial planes of the minor folds converge downward; in a *normal synclinorium* (Fig. 38D), the axial planes converge upward. In an *abnormal anticlinorium* (Fig. 38A), the axial planes of the minor folds converge upward; in an *abnormal synclinorium* (Fig. 38B), the axial planes converge downward.

Two terms that are frequently misused are *geosyncline* and *geanticline*. *Geosyncline* literally means an "earth syncline." The term should not be used, however, for every large syncline. A *geosyncline* is a basin in which many thousands of feet of sediments accumulate. Although the sediments deposited in the Appalachian geosyncline during the Paleozoic Era were 40,000 feet thick in places, the water was never very deep. In fact, many of the sediments were deposited above sea level on the surface of deltas. The floor of the basin sank while the sediments accumulated. European geologists believe that the Alpine geosyncline, on the other hand, was at times very deep. Recent studies show that a modern geosyncline exists along the coast of the Gulf of Mexico; the Cenozoic sediments here are many tens of thousands of feet thick.

A *geanticline*, the counterpart of a geosyncline, is an area from which the sediments are derived. The geanticline that lay southeast of the Appalachian geosyncline is known as Appalachia.

### Behavior of Folds with Depth

What happens to folds at depth? Do they continue downward indefinitely, or do they gradually or suddenly disappear?

## DESCRIPTION OF FOLDS

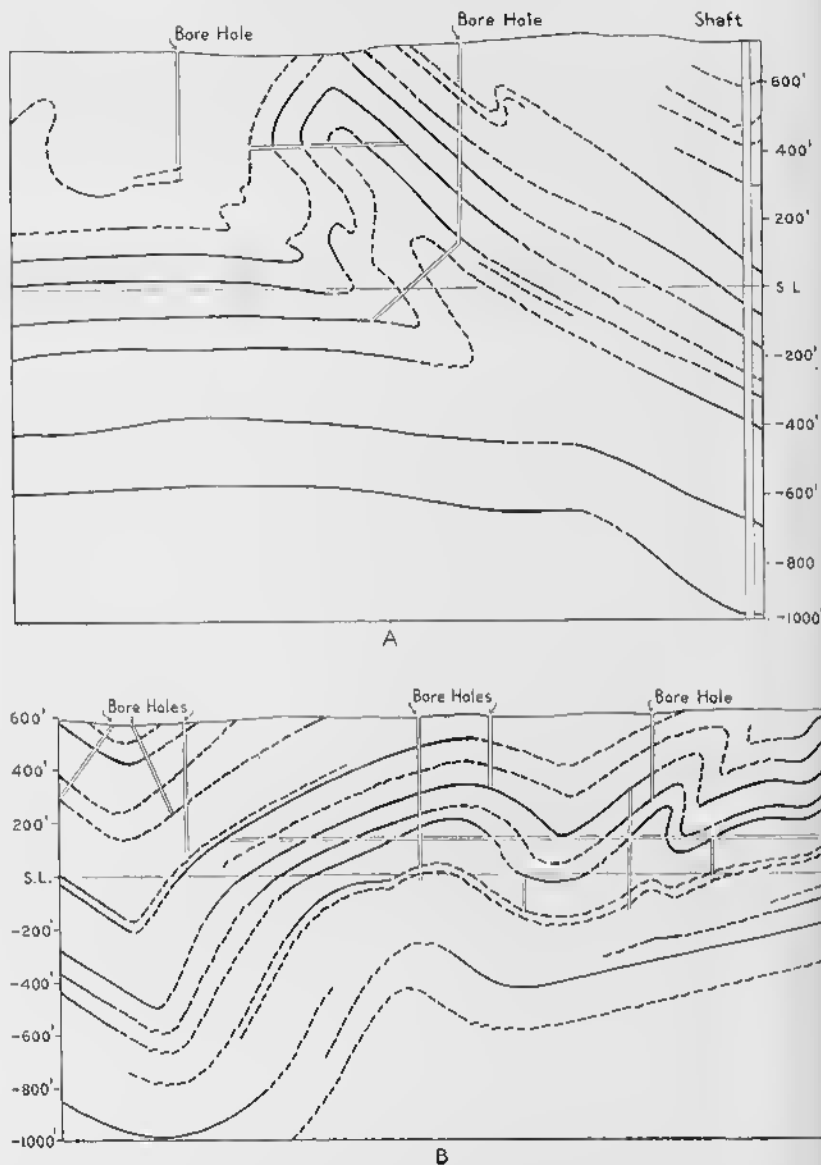


FIG. 40—Cross Sections of Disharmonic Folds in the Northern Anthracite Basin of Pennsylvania. Solid lines: beds of coal that have been mined out; broken lines: beds of coal based on drill records. (After N. H. Darton.)

Most structure sections show the folds as continuing downward without change, but this is merely a convention because, without precise information, little else can be done.

A theoretical approach sheds some light on the problem. Fig. 39A illustrates *similar folding*. The line *a* is taken as the form of the fold shown by one bedding plane. The other lines have been drawn on the assumption that they have the same form as the line *a*. In this way the form of the fold is propagated indefinitely upward and downward. Moreover, the lines *b* and *c* have the same length as *a*. In this type of folding every bed is thinner on the limbs and thicker near the axes. To produce folds of this type there must be considerable plastic movement of material away from the limbs and toward the axes. In natural folds the stronger or more competent beds preserve a relatively uniform thickness, but the weaker, less competent beds adjust themselves by flowage and drag folding.

Fig. 39B illustrates *parallel folding*. The line *a* is taken as the form of the fold shown by one bedding plane. The rest of the figure has been constructed on the assumption that the thickness of the beds has not changed during the folding. It is apparent that, under such conditions, the form of the fold must change upward and downward. The anticlines become sharper with depth, but broader and more open upward. Conversely, the synclines become broader with depth, but sharper upward. The folds die out downward and upward. In regions of gentle folding, where the dips do not exceed 10 or 20 degrees, the folding may well approach the parallel type. In Fig. 39B, the lines *b* and *c* are shorter than *a*, but in the original basin of deposition, they must have had the same length as *a*.

Where unusually good data are available, it is clear that most folding is *disharmonic*; that is, the form of the fold is not uniform throughout the stratigraphic column. Fig. 40 shows structure sections in the Northern Anthracite Basin of Pennsylvania, based on data obtained from mines and drill holes.<sup>1</sup> In Fig. 40A, a symmetrical anticline between two bore

<sup>1</sup> Darton, N. H., Some structural features of the Northern Anthracite Coal Basin, Pennsylvania: U. S. Geological Survey Professional Paper 193, pp. 69-81, 1940.

holes passes downward into an overturned anticline at 400 feet above sea level. At 400 feet below sea level the fold has disappeared. Similar changes are illustrated by Fig. 40B. Dis-harmonic folding is well displayed on some of the great cliffs in the Alps. Fig. 41 is one example, but inasmuch as the folds are recumbent, the change of form takes place in the horizontal direction rather than with depth. The formation labeled *Jd* shows four recumbent anticlines approximately equal to each

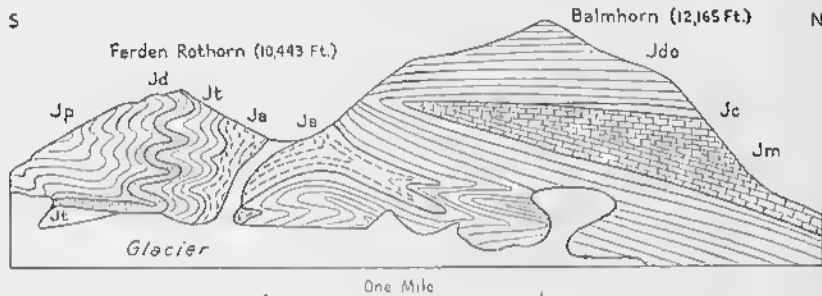


FIG. 41—Folds in the Ferden Rothorn and Balmhorn, Switzerland. Sketched by author from the Hockenhorn. The cliff on the east slope of the Balmhorn is about 4000 feet high; that on the east face of the Ferden Rothorn is about 1600 feet high. *Jp* = Plünsbachian limestone; *Jd* = Domerian quartzite; *Jt* = Toarcian formation; *Ja* = Aalenian shale; *Jdo* = Dogger shale; *Jc* = Callovian shale; *Jm* = Malm limestone.

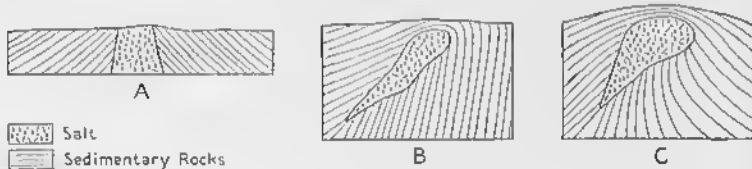


FIG. 42—Dimpir Folds. (After M. L. Mrazec.)

other in size; the top (north) of formation *Ja* shows folds of very different form.

*Piercing* or *diapir* folds are anticlines in which a mobile core has been able to break through the more brittle overlying rocks. Fig. 42 illustrates such folds in Rumania, where mobile salt beds have penetrated the overlying rocks.<sup>2</sup>

*Supratenuous* folds develop if folding and sedimentation are contemporaneous. In Fig. 39C, the strata are thinnest on the

<sup>2</sup> Mrazec, M. L., "Les plis diapirs et le diapirisme en général," *Comptes rendus, Institut géologique de Roumanie*, Vol. 6, pp. 226-272, 1927.

crest of the anticline, and are thickest in the trough of the syncline. The beds are thinnest on top of the anticline because it was rising during sedimentation; conversely, the beds are thickest in the syncline because it was sinking during sedimentation.

A sheet of sedimentary rocks may break loose from the underlying formations and fold independently. This is called a *décollement*, that is, a shearing-off. In the Jura Mountains, as is shown by Fig. 43, the Mesozoic and Tertiary strata are thrown into a series of anticlines and synclines that do not affect the

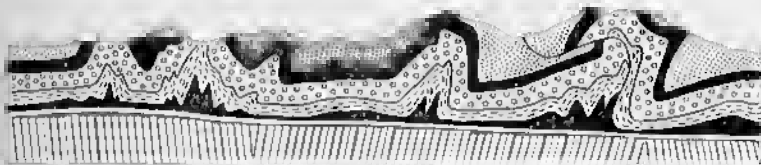


FIG. 43.—*Décollement* of the Jura Mountains. The lowest formation, with nearly vertical structure, consists of Paleozoic crystalline rocks. Directly above these is a thin bed of flat lying Triassic quartzite, left blank. The lower, solid black formation consists of anhydrite, shale, and salt, which is very incompetent. The higher beds are Triassic, Jurassic, Cretaceous, and Tertiary sedimentary rocks. (After A. Buxtorf.)

underlying Paleozoic crystalline rocks. The weak shales and salt beds near the base of the Mesozoic served as a lubricant over which the higher stratigraphic units slid.

### Calculating the Depth of Folding

The depth of folding can be calculated under certain conditions.<sup>3</sup> In Fig. 44A it is assumed that the vertical rectangle  $dl$  is changed into the rectangle  $b(d + h)$ , with no change in area. Then:

$$dl = b(d + h).$$

With certain modifications, the same concept may be extended to folded belts. It is assumed that there is no lengthening or shortening parallel to the axes of the folds, and that the rocks do not change in volume. The term  $b$  is the present breadth of the folded area;  $l$ , which is the original width before folding, is measured along some convenient bed in the folded belt. The term  $h$  is the amount of uplift due to folding.

<sup>3</sup> Chamberlin, R. T., The Appalachian folds of central Pennsylvania: *Journal of Geology*, Vol. 18, pp. 228-251, 1910.

In Fig. 44B the heavy black line represents a single bed. At the left end of the section it is flat and has not been affected by the folding. In the folded area it has been uplifted from the position of the broken line to the position shown by the heavy solid line. The average uplift,  $h$ , can be determined in several ways. The simplest is to measure the actual uplift at stated intervals—such as at every millimeter in the figure shown—and to compute the average. All the factors in the

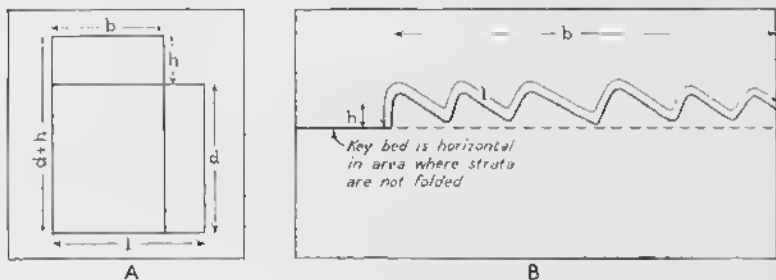


FIG. 44—Method of Calculating Depth of Folding.  $b$  = present breadth of folded belt;  $h$  = average uplift due to folding;  $l$  = original breadth of folded belt;  $d$  = depth of folding. A. Square deformed into a rectangle, no change in area. B. Folded strata. (After R. T. Chamberlin.)

equation given above, except  $d$ , are known. For convenience in computation, the equation can be rewritten:

$$d = \frac{bh}{l - b}.$$

The answer,  $d$ , gives the depth of folding, measured from the key bed where it is horizontal.

Several assumptions are made in applying this method. One assumption is that there is a sharp break between the folded rocks and the unfolded rocks below; in other words, a *décollement* is assumed. If the folds gradually disappear downward, the calculations would be incorrect, and the depth of folding would be greater than the calculations indicate. Secondly, the method assumes that the base of the strata is not depressed by the folding. There are reasons for believing, however, that in many orogens the basement is down-folded by horizontal compression. If this is so, the method employed for determining  $h$  gives too low a value, and the depth of the folded zone would be much greater than the calculated value.

Bucher<sup>4</sup> has calculated the depth of folding in the Jura Mountains. In this case the method is applicable, because a relatively thin column of sedimentary rock is separated from a crystalline basement by a *décollement*. The calculated depth is comparable to that deduced by the Europeans by other means.

---

<sup>4</sup> Bucher, W. H., *Deformation of the Earth's Crust*, pp. 155-156. Princeton: Princeton University Press, 1933.

## Field Study and Representation of Folds

### Recognition of Folds

#### Direct observation

Folds may be discovered in many ways. The easiest and most satisfactory method is to observe the fold, but this can be

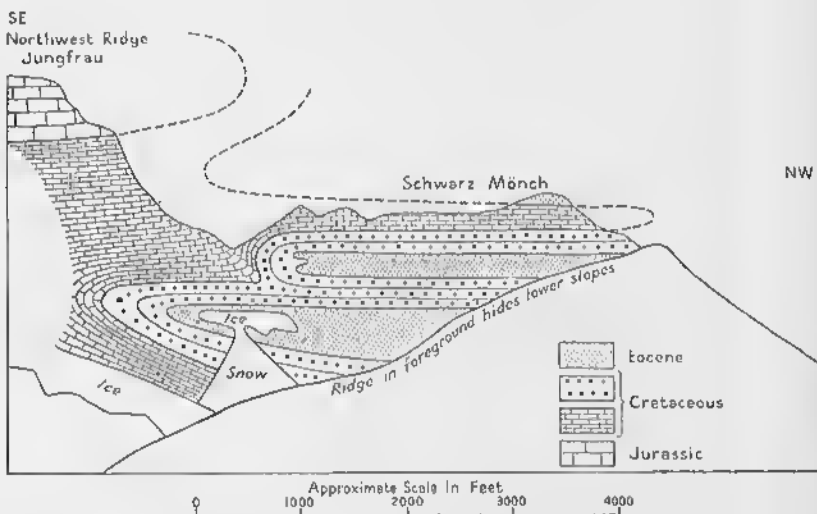


FIG. 45—Recumbent Folds on the Schwarz Mönch, Switzerland. The Eocene strata are exposed in two recumbent synclines. Cliff on southeast face of Schwarz Mönch is about 1800 feet high. View from Kleine Scheidegg, sketched by author.

done in comparatively few regions. Folds may be readily seen on some of the great cliffs in the Alps (Figs. 41 and 45). Folds are exposed in some parts of the Appalachian Mountains in large highway cuts (Fig. 46), railroad cuts, or in natural exposures (Fig. 47). Folds may be observed also in the Rocky Mountains and in other parts of the North American Cordillera, as well as in many other places in the world. Far more com-

monly, however, folds must be deduced from other data, and detailed studies show that most visible folds, even in such places as the Alps, are minor features associated with much larger folds.

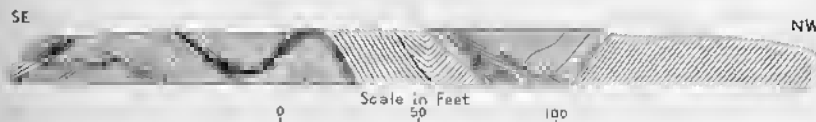


FIG. 46—Folds in Highway Cut One Mile South of Alexandria, Pennsylvania. Strata belong to the Wills Creek formation, which is of upper Silurian age. The bed represented by solid black is actually red in the field.

Wherever small folds are observed in single outcrops, it is desirable to record their attitude. To do this one must measure the attitude of the axial plane and the attitude of the axis.

A notebook or a sheet of paper may be held parallel to the axial plane of the fold. A second person then measures the strike and dip of the notebook, just as the attitude of a bedding

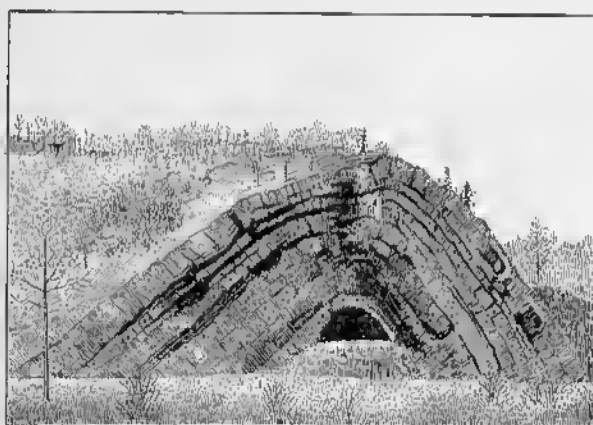


FIG. 47—Anticline One-quarter mile East of Roundtop, Maryland. View looking across Potomac River from West Virginia. Strata belong to upper Silurian Bloomsburg formation.

plane is measured. An experienced field geologist can measure the attitude of the axial plane without the help of a second person. In recording such information on a map, a symbol similar to that utilized for bedding may be employed, except that a double line is used for the strike of the axial plane.

Symbol *a* in Fig. 48 means that the axial plane strikes north and dips 25 degrees to the west. Symbol *b* refers to a vertical axial plane that strikes northwest. Symbol *c* refers to a horizontal axial plane.

The attitude of the axis of the fold may be readily measured if it is possible to look down on the fold. One edge of the compass is held in such a way as to cover the axis of the fold.

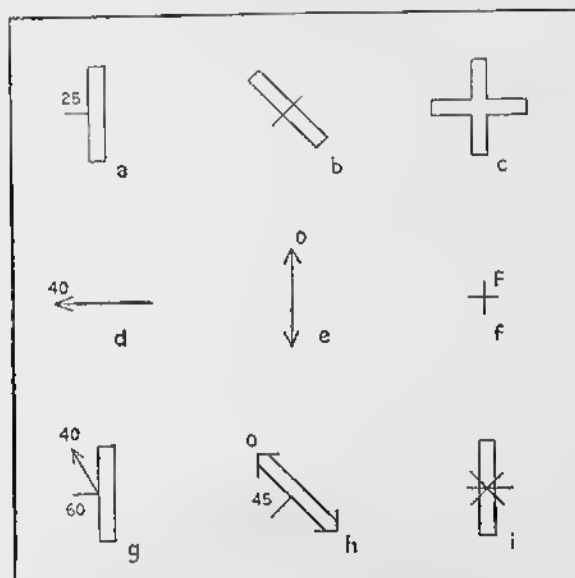


FIG. 48—Symbols to Represent Attitude of Folds.  
Top group are for axial plane, middle group for axis, and  
bottom group for axial plane and axis combined. (See  
text.)

In this way the strike of the horizontal projection of the axis is obtained (see also Fig. 29). The plunge is measured by means of the clinometer attached to the compass. The attitude of the axis can then be recorded by an arrow (Fig. 48). Symbol *d* means that the axis plunges 40 degrees due west. Symbol *e* refers to a horizontal axis that strikes north. Symbol *f* is used for a vertical axis; a capital *F* is placed at the side of this symbol to distinguish it from that used for horizontal bedding.

Ordinarily, the symbols indicating the attitudes of the axial plane and axis are combined into one. Thus, symbol *g* of

Fig. 48 means that the axial plane strikes north and dips 60 degrees to the west; the axis plunges 40 degrees in a direction 30 degrees west of north. Symbol *h* means that the axial plane strikes northwest and dips 45 degrees to the southwest; the axis strikes northwest and is horizontal. Symbol *i* represents a fold with a vertical axial plane that strikes north; the axis is vertical. Three symbols of the type just described have been inserted beneath each of the six folds in Fig. 17. In each case the symbol farthest to the right shows the attitude of the axial plane. The symbol farthest to the left shows the attitude of the axis. The middle symbol is a combination of these two.

In order to visualize the three dimensional attitude of folds, take a sheet of paper and bend it back on itself to make an isoclinal fold. The crease is the axis of the fold and the plane of the paper not only represents the two limbs of the fold but the axial plane as well. The fold may then be held in any position desired to show the distinction between the attitude of the axial plane and the attitude of the axis.

In a larger fold which cannot be observed in a single outcrop or in a series of closely adjacent outcrops, the attitude of the axial plane and the axis cannot be measured directly. Nevertheless the same principles apply, and the geologist should always think of folds in three dimensions.

#### Plotting attitude of beds

The most common way to recognize folds that are larger than an outcrop is to plot the strike and dip of beds on a map. In Fig. 49A, the dips indicate an asymmetric anticline, the axial plane of which strikes north and dips to the west. In Fig. 49B, the symbols indicate a symmetrical syncline that plunges south at an angle of 14 degrees.

The serviceability of this method depends upon the complexity of the structure and the number of exposures. If the structure is simple, a few exposures may suffice. On the other hand, if the structure is complex, many exposures are necessary. In regions of extremely complex structure, this method may fail—even though exposures are reasonably good—unless other significant data are available. The use of sedi-

mentary features in connection with this method are discussed on pp. 67-76.

### Map pattern

The pattern shown by the different mappable units may be very useful in deducing the structure. Fig. 50A represents the geological map of a region where the actual outcrops might constitute 25 per cent of the area. In practically all of the exposures, the strata strike northeast and dip steeply to the northwest. A traverse across the region from *M* to *N* suggests that there are five stratigraphic units: two sandstones, two conglomerates, and one slate. The map shows, however, that the two sandstones at opposite ends of *MN* belong to the same formation. Moreover, the map reveals that there is only one conglomerate. The pattern is that of a plunging fold—either an anticline that plunges southwest, or a syncline that plunges to the northeast. Without some additional data, a solution would not be possible. At some such place as *I*, the nose of the fold might be exposed. By following the base of the conglomerate, one might be able to ascertain that it plunges to the northeast. If this were so, the sandstone would be the oldest formation, and the slate would be the youngest formation. Primary features (pp. 67-76) might solve the problem. If cross-bedding in the conglomerate at locality *2* shows the top to be to the southeast, the fold is a syncline plunging northeast. Fossils might give the answer to the problem; if fossils in the slate are younger than those in the sandstone, the fold is a syncline plunging northeast.

A cross section along the line *MN* of Fig. 50A is given in Fig. 50B. The section must satisfy the condition that the beds dip steeply to the northwest. Moreover, although no direct evidence for subsidiary folds may be obtained along the line *MN*, it is obvious from the map that such folds must exist, and, assuming harmonic folding, the number and location of these folds can be predicted from the map. Every anticline shown by the map must also appear in the structure section. The depth of each anticlinal crest and synclinal trough depends upon the value of the plunge. In this case the plunge is about 60 degrees to the northeast.

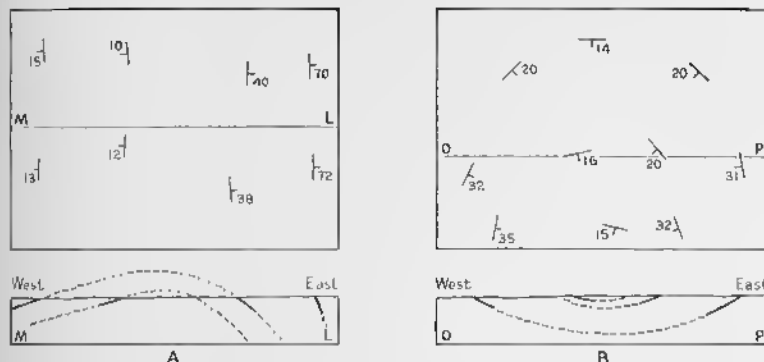


FIG. 49—Fold Shown by Dip-Strike Symbols. Map is above, structure section is below. A. Asymmetric, non-plunging anticline. B. Symmetrical syncline plunging south.

### Topography

Topography is often useful in the study of folds. In heavily forested or deeply weathered regions, it may be possible to trace key units for long distances by means of the topography. A resistant formation will stand up in ridges, an easily eroded bed will be followed by valleys, and a limestone may be traced by karst topography. In reconnaissance studies, particularly by airplane, the topography may give important clues to the geological structure.

Fig. 51 is a topographic map of an area in which ridges rise more than 1500 feet above sea level. The ridges are heavily wooded, and exposures are scanty. But a good section

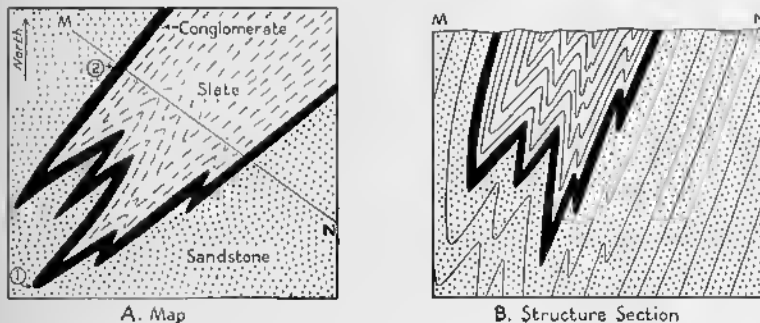


FIG. 50—Fold Shown by Pattern of Formations on a Map. A. Geological map. B. Inferred structure section.

is exposed at the water gap where the Red River cuts through the ridge. At this locality, hard quartzites dipping 45 degrees to the north are right-side-up. Apparently this same quartzite holds up Pine Mountain throughout its extent. The zig-zag pattern of the ridge indicates that the strata are folded.

The observations at the water gap reveal that this portion of the ridge is on the south limb of a syncline. The axis of the syncline must lie at Lookout Point, where the ridge makes a sharp bend. In plan, the ridge is concave toward the north-

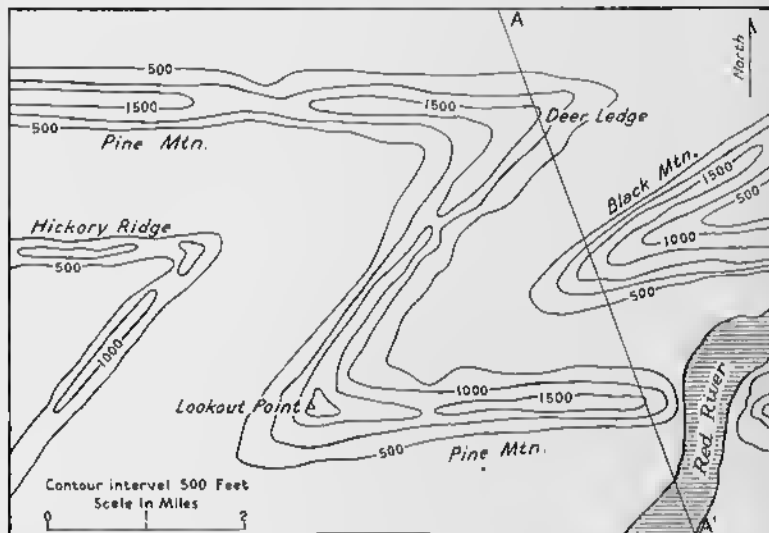


FIG. 51—Zig-zag Ridges That Indicate Plunging Folds.

east; the syncline, therefore, plunges to the northeast, because the pattern of a plunging syncline is concave in the direction of plunge (Fig. 33, p. 47).

Another fold axis must be located at Deer Ledge. This is an anticlinal axis and it must plunge to the northeast, because the pattern of the plunging anticline is convex in the direction of plunge.

It follows that Black Mountain is held up by some resistant formation stratigraphically higher than the quartzite on Pine Mountain. Hickory Ridge is held up by a formation stratigraphically lower than the quartzite on Pine Mountain. The inferred structure is shown in Fig. 52. The value of the dips at

Deer Ledge and Black Mountain are necessarily schematic, unless actually observed in the field.

The careful field geologist would consider such an interpretation suggestive, and he would feel compelled to visit as many outcrops as his time permitted.

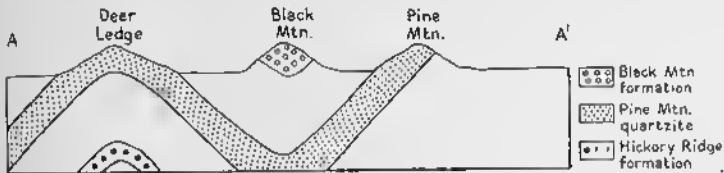


FIG. 52—Cross Section Along Line AA' of Fig. 51.

The illustration given above manifests how topography may be utilized to extrapolate from observations made at a single locality—in this case the water gap through Pine Mountain.

The attitude of beds may be determined quantitatively from the relation of bedding to contours. If the contact between two formations is rigorously parallel to the contours, the strata are horizontal (Fig. 53A). If, regardless of the topography, a contact maintains a uniform strike, the strata are

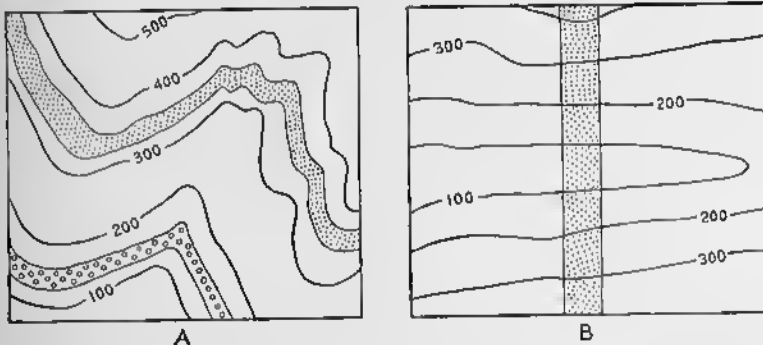


FIG. 53—Relation of Outcrop Pattern to Topography. Every hundred foot topographic contour is shown; special beds are shown by dots and circles. A. Horizontal beds. B. Vertical beds.

vertical (Fig. 53B). Dipping strata have an outcrop pattern that is partially controlled by the contours. The strike and dip of the beds may be calculated, as is shown by Fig. 54. The southern boundary of the stippled bed crosses the 300-foot contour at *a* and *b* on opposite sides of the valley. Inasmuch

as those two points are at the same altitude, the line *ab* is horizontal; moreover, *ab* lies in the plane of the bedding. It is apparent, therefore, that *ab* gives the strike of the bedding; in this instance it is east-west. Similarly, the lines *cd* and *ef* are parallel to the strike. The dip may be readily determined. The line *xy* is perpendicular to *ab* and *cd*, and it is 160 feet

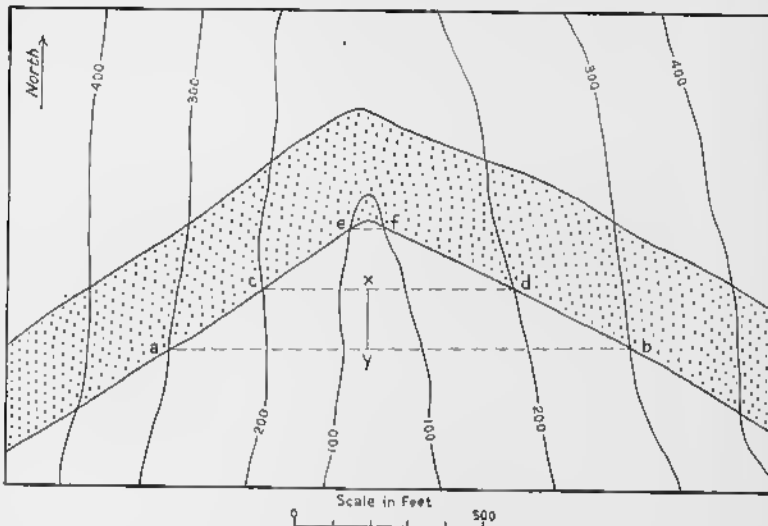


FIG. 54—Relation of Outcrop Pattern of a Dipping Bed to Topography.

long; that is, the bed drops 100 feet vertically in 160 feet horizontally. The dip is found by the equation

$$\tan \delta = \frac{100}{160}$$

and

$$\delta = 32^\circ.$$

The reliability of this method depends upon the accuracy of the topographic map and upon the precision of the geological mapping.

The interpretation of topography in areas for which no geological information is available, may be hazardous. Cuestas indicate gently dipping formations, whereas hogbacks indicate steeply dipping formations. The strata dip in the same direction as the gentler slopes of such ridges. A concentric series of ridges, with steep inner slopes, but with gentle outer slopes, indicate a domical structure.

**Drilling.** Where exposures are rare or absent, the structure may be deduced from drilling. If some bed is sufficiently distinctive, either because of lithology or because of fossil content, its altitude in various drill holes can be recorded and the structure can be determined. If drill cores are obtained, the angle of dip of the bedding can be determined.<sup>1</sup> The more complex the structure, the greater should be the number of drill holes per unit area. This method is expensive, however, and has been used only where the possibility of financial return has justified the cost.

**Mining.** Mining operations give the most complete information concerning geological structure. Coal mining, especially, furnishes valuable data, because individual beds are followed for long distances. The Northern Anthracite Basin of Pennsylvania is unusually well known, and Darton has recently published an invaluable series of structure sections of this region.<sup>2</sup> Two of these sections are reproduced in Fig. 40. It is obvious that this method can be used only where there is economic incentive, and ordinarily the structural geologist must rely on other, less precise methods.

**Geophysical methods.** During the last two decades, under the impetus of the exploration for petroleum and metals, various geophysical methods have been utilized in order to determine geological structure. The principal methods may be classified as *gravimetric*, *magnetic*, *seismic*, and *electric*. These methods will be discussed in Chapter 19.

### Determination of Top of Beds by Primary Features

#### Nature of the problem

In overturned folds and in recumbent folds the strata on one limb are overturned. Obviously, it would greatly facilitate the solution of structural problems if methods were available to determine whether the beds are right-side-up or overturned. Where the folds are exposed on the face of a great cliff, the whole

<sup>1</sup> Lahee, F. H., *Field Geology*, 4th edition. Cf. especially pp. 565-568. New York: McGraw-Hill Book Company, 1941.

<sup>2</sup> Darton, N. H., Some structural features of the Northern Anthracite Coal Basin, Pennsylvania: U. S. Geological Survey Professional Paper 193, pp. 69-81, 1940.

structure may be clearly observed, and special methods are unnecessary. In some instances, even in regions of low relief, the exposures may be sufficiently continuous to show a progressive change from beds that are right-side-up to those that are overturned. Fig. 55A illustrates such a case. At *a* the beds are in normal position, but toward the east they become progressively steeper, and are vertical at *b*; still farther east, as at *c*, they dip to the west and must be overturned. In many areas,

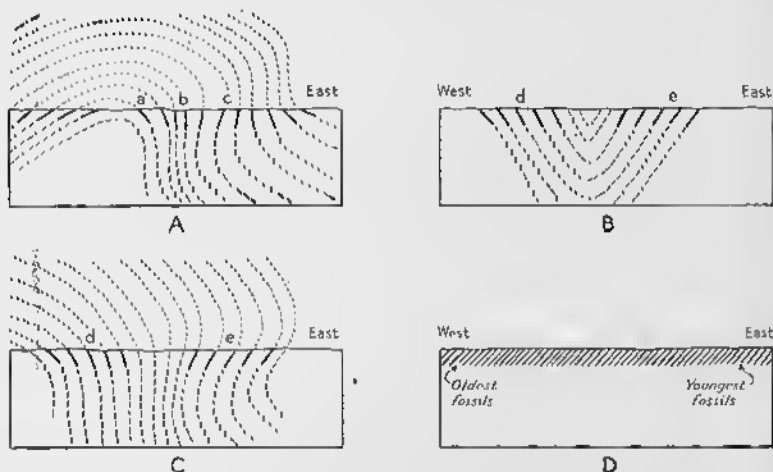


FIG. 55—Importance of Determining Top and Bottom of Beds. A. The gradual change from beds that are right-side-up at *a* through vertical beds at *b* to overturned beds at *c* may be observed. B. Beds at *d* and *e* dip toward each other, suggesting a syncline. C. If beds at *e* are overturned, the structure cannot be a simple syncline such as shown in diagram B. D. Beds dip west; fossils indicate that the strata are overturned.

however, exposures are not sufficiently numerous to show the gradual change. In Fig. 55B, for example, the beds at *d* and *e* dip toward each other, and at first it might be supposed that the structure is a simple syncline. If, however, the strata at *e* are overturned, such an interpretation is impossible, and the structure would be that shown in Fig. 55C.

#### Paleontological methods

Paleontological methods, of course, may be of great aid in indicating whether beds are right-side-up or not. In Fig. 55D the beds dip 48 degrees to the west. If the youngest fossils

are at the east end of the section, it is apparent that the strata are overturned.

### Use of primary features

In many localities, however, fossils are either absent, or, if present, they are not sufficiently diagnostic to be used in distinguishing top from bottom. Other means must be employed. The most reliable information is furnished by features developed during the deposition of sediments<sup>3</sup> or during the eruption of lavas; they are commonly called *primary structures*, or, more suitably, *primary features*. Those features most commonly employed are ripple-marks, cross-bedding, and graded bedding. Other features are mud-cracks, local unconformities, channeling, rain-imprints, and related characteristics. In lavas, the original top may be shown by pillow structure, vesicular zones, or oxidized zones.

### Ripple-marks

Ripple-marks may be aqueous or eolian in origin; that is, ripple-marks may form on the bottom of a body of water or, by wind action, at the surface of the earth. The origin and formation of ripple-marks is a subject that cannot be fully discussed here, and only those phases of the subject that are significant to the structural geologist will be considered.

*Oscillation ripples*, as shown in Fig. 56A, are symmetrical, and they consist of broad troughs that are convex downward, and of sharp crests that point upward. Ideally, oscillation ripples form in bodies of standing water. Whenever waves disturb the upper surface of the body of water, the individual water particles move in vertical orbits that are nearly circular. Although the wave form moves across the water, the individual particles do not. The motion of the particles is transmitted downward with decreasing intensity. The sand or mud on the bottom is affected by the same motion and is thrown into ripples.

*Current ripples*, as shown in Fig. 56C, are asymmetrical, and both the crest and trough are rounded. Such ripples

<sup>3</sup> Twenhofel, W. H., *Principles of Sedimentation*. Cf. especially pp. 494-568. New York: McGraw-Hill Book Company, 1939.

develop when a current, either of water or of air, moves across sand or mud. In Fig. 56C, the current moved from left to right.

Forms transitional between oscillation ripples and current ripples are not uncommon; although these forms are asymmetrical, they have sharp crests which point upward. There are other forms of ripple-marks, but they do not concern the structural geologist.

Either the original ripple-mark itself or its cast may be preserved. In Fig. 56A, original oscillation ripple-marks are represented on the lower block; the upper block is the cast. Fig. 56B shows the cast after it has been removed from the original and has been turned over. In Fig. 56C, original current ripple-marks are represented on the lower block; the upper block is the cast. Fig. 56D shows the cast after it has been removed from the original and has been turned over.

Oscillation ripple-marks can readily be used to tell whether a bed is right-side-up or overturned. The sharp crest points toward the younger beds, whereas the rounded trough is convex toward the older beds. This is true whether the specimen is an original or a cast. In Fig. 57 the beds at outcrop *I* dip to the west at an angle of 30 degrees. At *a* the originals of ripple-marks are preserved; the crests point upward to the left, indicating that the beds are right-side-up. At *b* there is an overhanging cliff on which the casts of ripple-marks are preserved; here, also, the crests point upward to the left, confirming the conclusion that the beds are right-side-up. At outcrop *II*, the beds dip 50 degrees to the west. On the sloping surface of the outcrop at *c*, the casts of ripple-marks are preserved; the crests point downward to the right, indicating that the beds are overturned. On the face of the overhanging cliff at *d*, the originals are preserved, and again the crests point downward to the right. The inferred structure is indicated by a broken line.

A brief consideration of Fig. 56 shows that current ripples cannot be used to determine top from bottom. An overturned current ripple has the same form as one that is right-side-up.

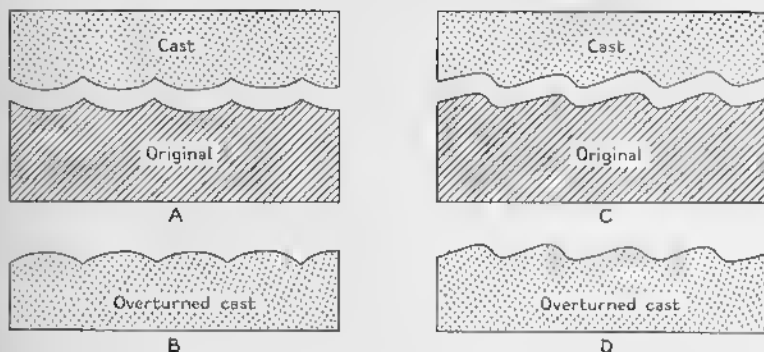


FIG. 56—Ripple-marks. A. Original oscillation ripple-marks and the cast. B. Overturned cast of oscillation ripple-marks. C. Original current ripple-marks and the cast. D. Overturned cast of current ripple-marks.

### Cross-bedding

Cross-bedding, which is also known as *cross-lamination* or *false-bedding*, is illustrated by Fig. 58A. Whereas the true bedding in this figure is horizontal, the cross-bedding is inclined at varying angles. Cross-bedding develops wherever sand has dropped over the edge of a growing sand bar, over the front of a sand dune, or over the edge of a small delta. The upper extremity of each cross-bed is commonly inclined at a considerable angle to the true bedding, whereas the lower extremity is essentially parallel to the true bedding. The cross-beds thus are sharply truncated above, and are tangential to the true bedding below. The cross-beds in *torrential cross-bedding* are inclined to the true bedding at a considerable angle at both their upper and lower extremities (Fig. 58B).

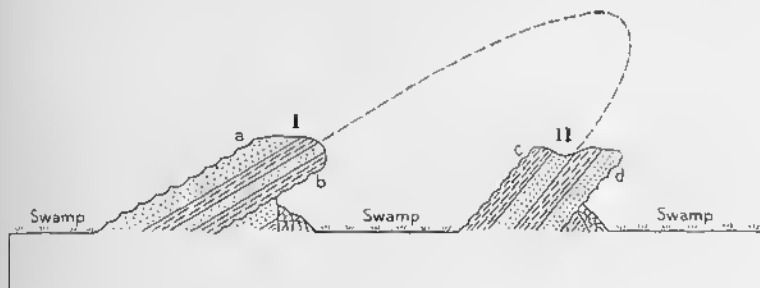


FIG. 57—Use of Ripple-marks to Determine Top of Beds.

The use of cross-bedding to distinguish the top from the bottom of beds is apparent from Fig. 58A. The cross-beds are tangential downward, but are truncated upward. Thus, in Fig. 59A, the beds, which dip 45 degrees to the left, are right-side-up. The top of the vertical beds in Fig. 59B is to the right. The beds in Fig. 59C, which dip 45 degrees to the left, are overturned. In order to use cross-bedding properly, the tangential portion must be observed; it is insufficient to observe that the cross-beds are sharply truncated. It would be incorrect to assume in Fig. 60A that the top is to the right, because the cross-bedding may be of the torrential type, as is shown in Fig. 60B; in such a case the evidence is inconclusive.

### Graded bedding

In many instances the grains in a thin bed are progressively finer from bottom to top (Fig. 61A). This feature is known as *graded bedding*. The materials comprising a sediment are transported when the currents are swifter than usual. As the velocity subsides, the largest particles are dropped first, and then progressively finer particles are deposited. Although this generalization may seem correct, field experience proves that there are many exceptions, especially among such coarse sedimentary rocks as conglomerate. On the other hand, in the finer sedimentary rocks—notably shales and siltstones, where the individual beds are a fraction of an inch thick—the method is more reliable, but by no means infallible.

If this method is applied to the examples shown in Fig. 61, the beds in Fig. 61B are right-side-up; the tops of the beds in Fig. 61C are to the right; and the beds in Fig. 61D are overturned.

### Local unconformities, channeling, and related features

During the accumulation of sediments, particularly those laid down by rivers, erosion may alternate with deposition. In Fig. 62A, for example, conglomerate occupies a channel in shale. After the original mud had been deposited, swiftly flowing streams in flood carved a channel. When the flood was subsiding, or at some later time, gravel was deposited in the channel. The base of the conglomerate truncates the bedding of the shale.

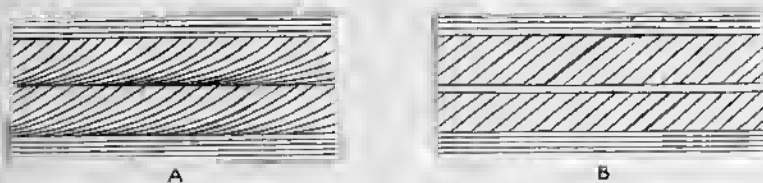


FIG. 58—Cross-bedding. A. Normal cross-bedding. B. Torrential cross-bedding.

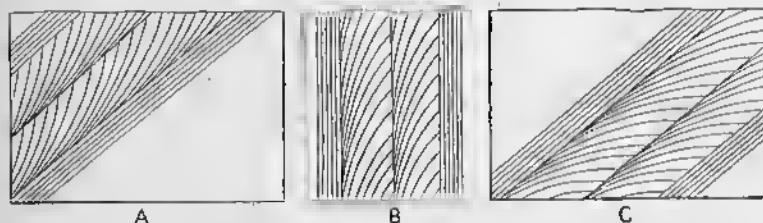


FIG. 59—Use of Cross-bedding to Determine Attitude of Beds. A. Beds are right-side-up. B. Top is to the right. C. Beds are overturned.

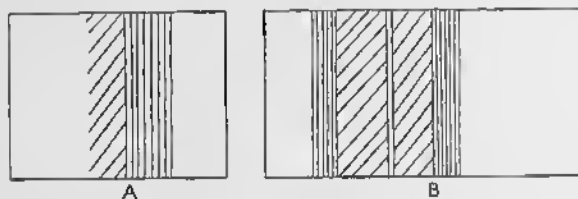


FIG. 60—Torrential Cross-bedding in Vertical Strata.  
A. Truncation of cross-beds observed on one side only.  
B. Truncation of cross-beds observed on both sides.

A related feature is illustrated by Fig. 62B, where sandstone lies on top of shale. The currents that transported the sand, ripped up pieces of mud, fragments of which are preserved as shale in the sandstone. Similarly, fragments of lava may be found in the sedimentary rocks directly above a lava flow.

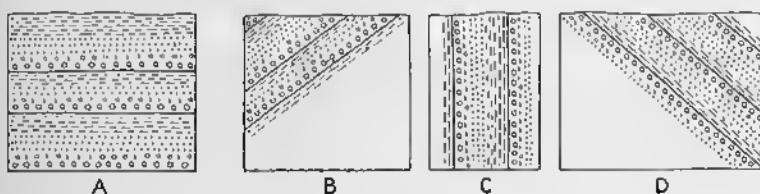


FIG. 61—Graded Bedding. A. As deposited in horizontal beds; each bed gets finer toward the top. B. Dipping beds, right-side-up. C. Vertical beds, top toward the right. D. Dipping beds, overturned.

Features that are the results of short intervals of erosion during a period of sedimentation are known as local unconformities.

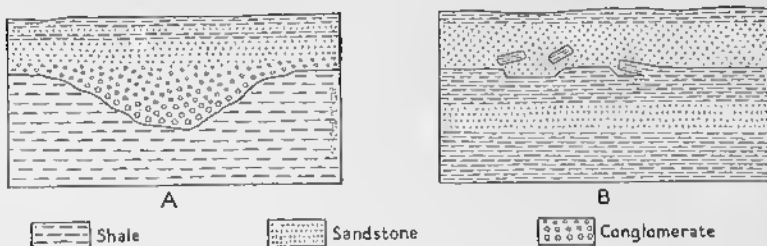


FIG. 62—Channeling and Local Unconformity. A. Channel cut into shale has been filled by conglomerate. B. Fragments of shale deposited in overlying sandstone.

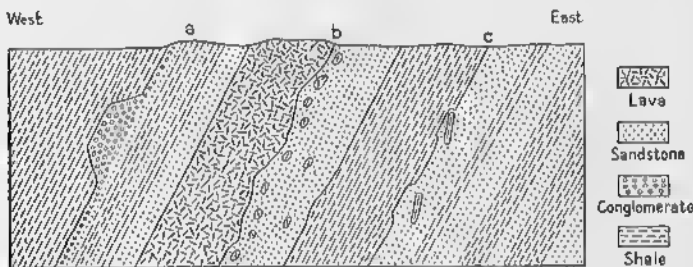


FIG. 63—Overturned Beds. Shown by channeling, pebbles of lava in sandstone, and fragments of shale in sandstone.

In Fig. 63 the beds dip to the west. By following the contact of the conglomerate and shale at *a*, it becomes obvious that the conglomerate truncates the shale and fills a channel in it. Also, at *b*, the sandstone contains pebbles of the lava to the west, and the sandstone at *c* contains fragments of the shale directly west of it. All the evidence thus indicates that the beds are overturned.

### Mud-cracks

Mud-cracks, which are sometimes called *sun-cracks* or *shrinkage-cracks*, are polygonal in plan and taper downward (Fig. 64A). They characteristically form in mud and ooze that are exposed to the atmosphere and have dried out; under special conditions mud-cracks may form under water. Because of the loss in volume that accompanies desiccation, tensional

stresses are set up, and ruptures develop. The sediments deposited on top of the mud-cracked layers fill in the cracks. The east, therefore, shows a polygonal system of ridges, whereas the original shows a polygonal series of cracks. The strata in the western outcrop in Fig. 64B are right-side-up. At *b* the mud-cracks form a polygonal series of cracks that taper

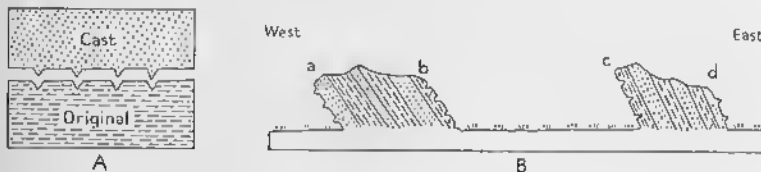


FIG. 64—Mud-cracks. A. Cross section. B. Use of mud-cracks to tell top and bottom.

downward to the left; they are originals. On the overhanging cliff at *a*, a series of polygonal ridges are casts, and again show that the beds are right-side-up. In the eastern outcrop, the originals at *c* and the casts at *d* reveal that these beds are overturned.

Rain-imprints, animal tracks, root-holes, and worm burrows may be used in a similar way.

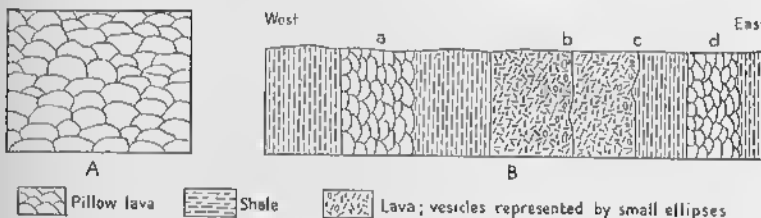


FIG. 65—Top of Lava Flows. A. Pillow structure, right-side-up. B. Pillow structure and vesicular structure shows the top is to right.

### Pillow structure

Some lavas, particularly those of basaltic composition, are characterized by pillow structure (Fig. 65A). The individual pillows are roughly ellipsoidal, and they range from a foot to several feet in diameter. In flat lavas, the tops and bottoms of the pillows are generally convex upward. This method of

distinguishing top from bottom has been used with particular success in the pre-Cambrian rocks of the Canadian shield.<sup>4</sup>

### Vesicular or oxidized tops of lavas

Whereas the base of a lava flow is generally massive, the top tends to be vesicular—that is, full of gas bubbles. If the lava on one side of a contact is vesicular, whereas the lava on the other side is massive, the latter is likely to be younger than the former. The reddened, oxidized tops of lava flows may be used in a similar way.

Fig. 65B illustrates the use of these methods in a series of beds that are vertical. The pillows in lava flows at *a* and *d* are convex toward the east. At *b*, vesicular lava lies to the west of the contact, whereas massive lava is to the east. The eastern contact of the lava at *c* is vesicular and oxidized, but the western contact of this same flow is not. All observations show that the top is toward the east.

### Field methods

In those areas where primary features such as those described above are preserved, and where these primary features must be utilized in order to solve the structure, some systematic method of recording the data should be employed. Special symbols that are used for the different primary features indicate the direction of the top of beds.

## Determination of Top of Beds by Drag Folds

### Relation of drag folds to axes of major folds

On p. 43 it has been shown that drag folds develop when beds slide past each other—especially if an incompetent stratum lies between two competent strata (Fig. 27).

Ordinarily, the upper beds slide away from the synclinal axes relative to the lower beds, as is shown by the arrows in Figs. 66 and 67. This fact is of the utmost importance in using drag folds to deduce the larger structures (Pl. VIII).

<sup>4</sup> Wilson, M. E., Structural features of the Kewatin volcanic rocks of western Quebec: *Bulletin Geological Society of America*, Vol. 53, pp. 53-70 (especially pp. 62-64), 1942.



PLATE VIII.—Plastic Deformation in Ice.—Aerial view of folded moraines between Steller glacier (left) and Bering glacier (right), Alaska. Note thinning on limbs of folds, thickening in troughs. Analyzing the folds as drag folds, the glacier to the right was moving down-hill (toward the bottom of the picture) more rapidly than the glacier to the left. (Photo by Bradford Washburn.)



PLATE IX. Joints and Sheeting. The rock is quartz diorite. Two joints, on the left-hand side of the picture, strike diagonally to the road and dip steeply to the left. The sheeting dips toward the road. San Diego County, California. (Photo by D. L. Everhart.)

The drag folds in an incompetent bed between two competent beds assume the attitudes shown in Figs. 66 and 67. The acute angles between the axial planes of the drag folds and the

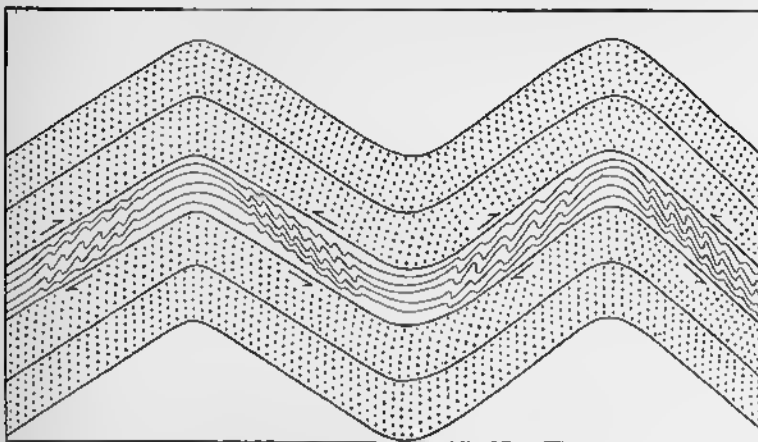


FIG. 66—Structure Section of Symmetrical Folds Showing Relation of Drag Folds and Direction of Shearing.

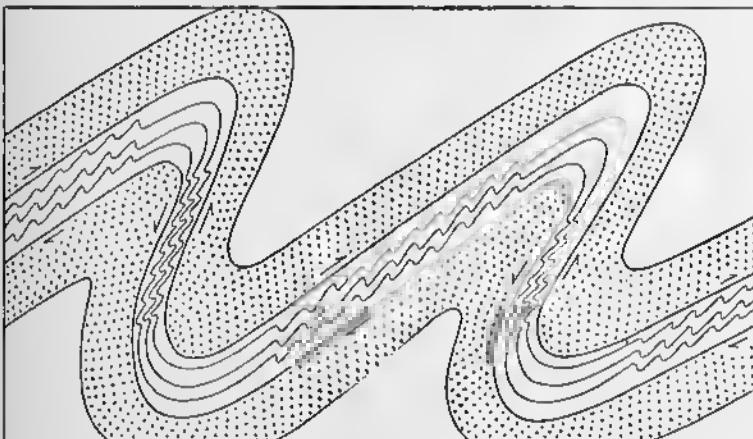


FIG. 67—Structure Section of Overturned Folds Showing Relation of Drag Folds and Direction of Shearing.

main bedding planes point in the direction of differential movement.

#### Drag folds in cross section

The use of drag folds in deducing the larger structures is illustrated by Figs. 68, 69, 70, and 71. At *a* in Fig. 68, the

strata are vertical and the drag folds show that the beds slipped past each other in the manner indicated by the arrows. The synclinal axis must lie to the east. The beds at *b* dip to the west, and the drag folds show that the bed to the left moved upward relative to the bed to the right; the synclinal axis must lie to the

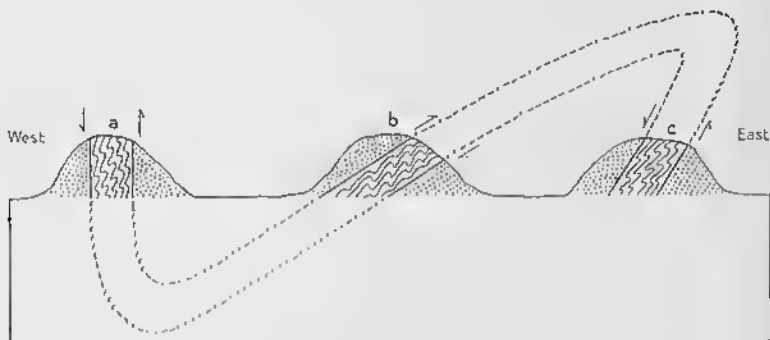


FIG. 68—Use of Drag Folds in Determining Major Structure. Letters are referred to in text.

west, and the strata are right-side-up. At *c* the beds also dip to the west, but the drag folds reveal that the beds to the right moved upward relative to the beds to the left. The synclinal axis must lie to the right. Assuming that the beds at *a*, *b*, and *c* are the same, the probable structure is indicated by the broken lines.

### Drag folds in three dimensions

So far we have considered drag folds only in vertical sections, and have tacitly assumed that the axes of the major folds are horizontal. Under such circumstances, the beds would slide parallel to the direction of dip, as is shown by the arrow in Fig. 69A, and the axes of the drag folds would be horizontal. If, however, the major folds are plunging, there will be a component of the movement parallel to the strike of the beds. Fig. 69C shows an anticline plunging 45 degrees away from the observer. The younger beds move upward relative to the older beds in the direction of the arrow—that is, at right angles to the axis of the fold. In such a case the axes of the drag folds will also plunge 45 degrees away from the observer. If the plunge of the

major fold is vertical, the beds slide past one another horizontally (Fig. 69B). The axes of the drag folds will have a vertical plunge.

A major principle is suggested by these facts: drag folds plunge in harmony with the major folds, and the axes of the drag folds are parallel to those of the major folds.

Each of the three diagrams in Fig. 69 illustrates the appearance of the bedding on a horizontal surface and on a vertical section at right angles to the strike of the axial plane of the fold. In Fig. 69A the drag folds appear on the vertical plane *cdef*.

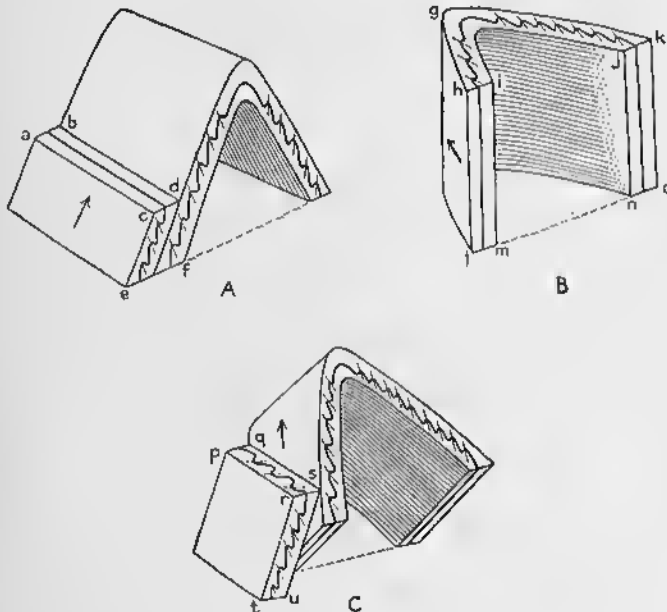


FIG. 69—Drag Folds in Three Dimensions. The small blocks on the left side of diagrams A and C show the appearance of the drag folds on a map and on a vertical section that strikes perpendicular to the axial plane of the fold.

These drag folds are not apparent on the horizontal plane *abcd*, where the trace of the bedding forms a straight line, because the fold does not plunge. In Fig. 69B the drag folds appear on the horizontal plane *ghijk*. In the vertical sections *hilm* and *jkno*, however, the trace of the bedding forms a straight line. In the most general case, illustrated by Fig. 69C, the drag folds

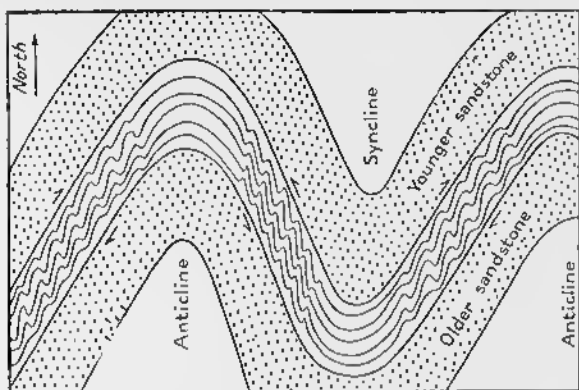


FIG. 70—Geological Map of Drift Folds. The large folds, as well as the drag folds, plunge north. Horizontal component of shear is shown by arrows.

appear on both the horizontal plane *pqrs* and on the vertical plane *rstu*.

Fig. 70 is a map of folds that plunge to the north, a major syncline lying between two anticlines. The wavy lines show the pattern of the drag folds, and the arrows indicate the horizontal component of differential movement.

In utilizing drag folds to determine the top of beds, a vertical section that strikes at right angles to the bedding is analyzed to ascertain in which direction the synclinal and anticlinal axes are located. The horizontal section is then studied in order to determine the direction of plunge.

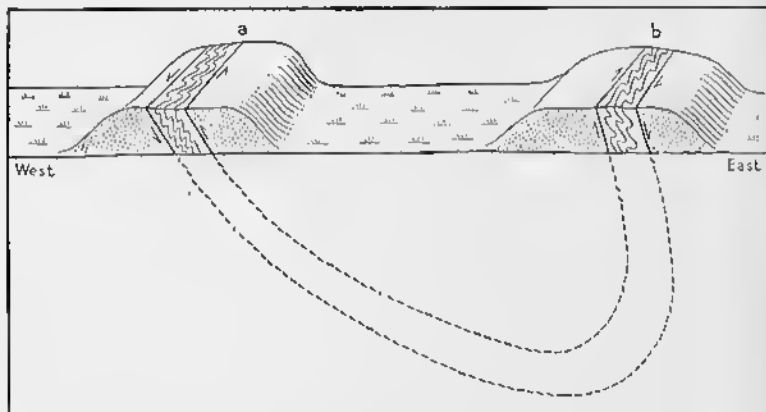


FIG. 71—Use of Drag Folds in Determining Major Structure.

### Example of use of drag folds

Fig. 71 shows the drag folds in two different outcrops. In both instances the vertical face shows that the beds dip steeply to the east. In outcrop *a*, the drag folds reveal that the more easterly beds moved upward relative to the more westerly beds. In outcrop *b*, the more westerly beds moved upward relative to the more easterly beds. A synclinal axis must lie between the two outcrops. The top of outcrop *a* shows that the eastern bed moved north relative to the western bed; the major fold, therefore, must plunge north. Outcrop *b* corroborates this conclusion.

Even in those cases where only a flat exposure is available, the plunge of the drag folds may be observed directly if the surface of the outcrop is somewhat rough.

### Minor folds

In many regions all the strata have essentially the same competency. Drag folds, in the narrowest sense of the word, do not form. Nevertheless, large masses of rock move past one another, and the strata are thrown into *minor folds*. The minor folds usually bear the same relation to the major folds as do drag folds, and they are even called drag folds by many geologists.

### Limitations of method

Drag folds are not infallible indicators of the location of major folds axes. The interpretation is based on the assumption that the upper beds slide away from the synclinal axes relative to the lower beds. If for any reason the beds slide in some different direction, the drag folds will not necessarily bear any systematic relation to the major folds.

Under some conditions, very plastic rocks may flow toward the center of a syncline, just as, in hot weather, tar on a highway flows away from the crown on the road. The resulting folds, which have an orientation opposite to that of drag folds, have been called *flowage folds*.<sup>4</sup>

<sup>4</sup> Bain, G. W., Flowage folding: *American Journal of Science*, 5th series, Vol. 22, pp. 503-530, 1931.

### Representation of folds

#### Photographs and sketches

Folds may be represented in a variety of ways. Where direct observation is possible, as in cliffs or artificial cuts, photographs may be taken or sketches may be made. Articles describing the structure of the Alps are replete with significant sketches (Figs. 41 and 45), but even here the largest folds are too large to be included in a single view. Moreover, although great cliffs give the vertical aspect of the structure, they give only one horizontal dimension. In such ranges as the Appalachians, the Jura, and even the North American Cordillera, the larger structures can not be photographed or sketched in the field.

#### Maps

A good geological map may adequately represent the folds. Such maps vary greatly in elaboration. Some are simple black and white maps on which each formation is shown by a special pattern; in order to be useful, such maps must include dip and strike symbols, or, as described below, they must be accompanied by structure sections. Fig. 72A is a simple geological map. If no other data are given, however, numerous interpretations of the structure are possible; four possible interpretations are given in the accompanying structure sections (Fig. 72B). If there is no topographic relief, the structure could be either a doubly plunging syncline (diagram 1) or a doubly plunging anticline (diagram 2). On the other hand, the pattern would also be consistent with a hill (diagram 3), or with an enclosed depression in horizontal strata (diagram 4). If such maps are accompanied by dip and strike symbols to show the attitude of the bedding, as in Fig. 49, there is no ambiguity.

The most satisfactory geological maps, however, are those which show not only topography, drainage, and culture, but which also indicate the geology by numerous colors and patterns. These maps may be accompanied by elaborate symbols to reveal the attitude of bedding and other structural features. Such maps are expensive to print, however, and usually only government organizations can afford to issue them. The

geological folios of the U. S. Geological Survey are excellent examples of this type of map. The ease with which such maps may be interpreted depends upon the complexity of the geology and the skill of the reader.

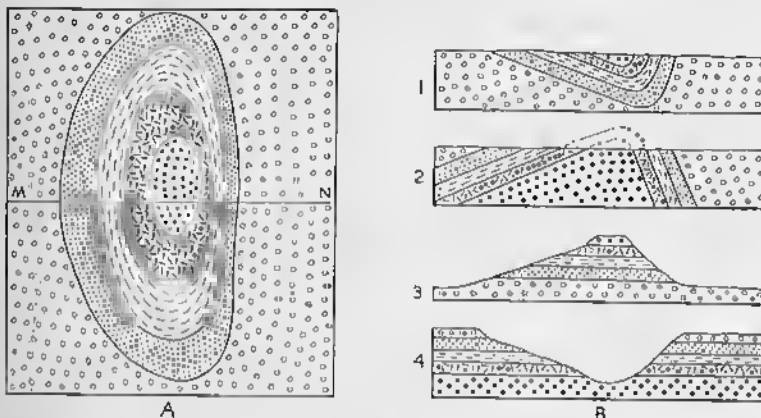


FIG. 72—Geological Map with Alternate Interpretations of Structure.  
A. Geological map. B. Alternate interpretations.

### Structure sections

Structure sections, such as Fig. 73, are highly satisfactory means by which to represent geological structure. These structure sections purport to show the structure of folds as they would appear in imaginary vertical slices down into the earth.

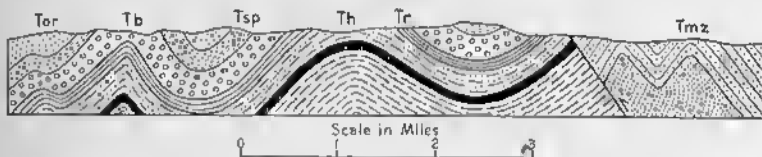


FIG. 73—Folds in the Coast Range of California. Formations are of Tertiary age. *Tmz* = Martinez formation; *Th* = Hombre sandstone; *Tr* = Rodeo shale; *Tb* = Briones sandstone; *Tsp* = San Pablo formation; *Tor* = Orinda formation. (Part of section *CC'*, Concord quadrangle, San Francisco Folio, U. S. Geol. Survey; after A. C. Lawson.)

In themselves, however, such representations are inadequate, because, although they show the vertical dimension, they can show only one horizontal dimension. The accuracy of such sections depends upon many factors. If the sections are based solely upon data obtained at the surface of the earth, they are

at best only approximations, and their precision depends upon the complexity of the geology, the number of exposures, the care and skill of the field geologist, and the time available for the field work.

In many publications the folds are represented by a combination of the methods described above; a geological map is accompanied by a series of structure sections and pertinent photographs and sketches.

### Structure contours

Structure contours, an example of which is given in Fig. 74, provide the most precise way by which to represent folds in three

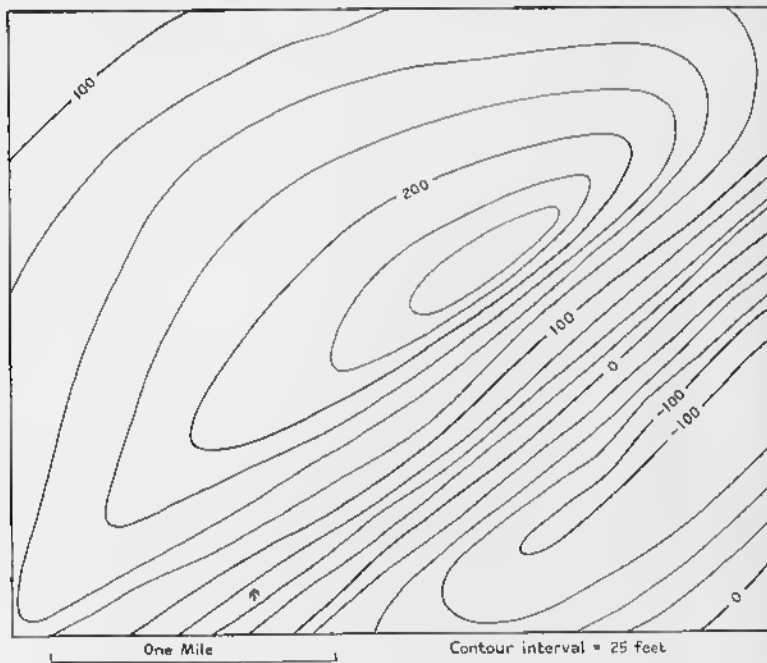


FIG. 74.—Structure Contour Map.

dimensions. Such a map is read in the same way as is a topographic contour map. The contours are based on a single horizon, such as the bottom or top of some particular bed. The position of the bed is given in reference to some datum plane, usually mean sea level. Inasmuch as the key horizon may go below sea level, negative contours are not uncommon. For a

given contour interval, the dip is steepest where the contours are closest together. In Fig. 74 the contour interval is 25 feet, and every 100-foot contour is labeled. The structure shown is an asymmetric doubly plunging anticline, bounded on the southeast by a syncline that plunges to the northeast. The southeast limb of the anticline, where the contours are close together, is much steeper than the northwest limb, where the contours are far apart. The southwestward plunge of the southwestern end of the anticline is gentler than the northeastward plunge of the northeastern end. If one knows the scale of the map, one can determine the dip at any place in feet per mile, and, if that is desirable, one can then readily convert it into degrees. On the northwestern limb of the anticline, the key bed drops from 200 feet to 100 feet in one mile. The dip on this limb is thus 100 feet per mile, or approximately one degree.

Structure contour maps are particularly useful in regions where the dips are low. Obviously, where strata are overturned, such maps are difficult to use, although broken lines or some other device could be used for overturned beds.

### Block diagrams

Folds may be shown by block diagrams, such as Figs. 28 and 31. Block diagrams are particularly useful to illustrate the

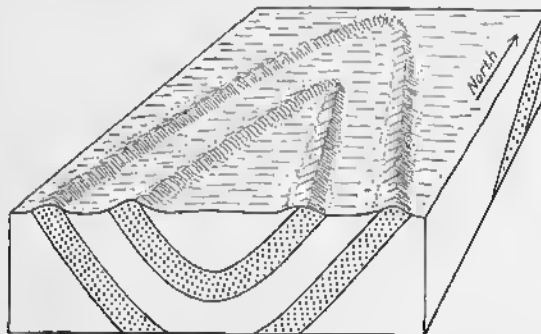


FIG. 75—Block Diagram Showing Relation Between Geological Structure and Topography. The topography indicates that the syncline plunges south.

general features of the structure, and, especially, to indicate the relation between folds and topography (Fig. 75). Block diagrams cannot be used, however, to show the structure of an

area precisely, because, first, the scale is variable in different directions; again, only two sides of the block are available for structure sections; and, finally, the upper surface of the block is generally used to show topography.

### Models

Both the surface geology and topography may be shown on models made of wood, plaster, or some similar substance. The correlation between geology and topography is clearly portrayed, and these models are of great aid to a person not trained in reading geologic maps. The folds, however, can be shown only on the four sides of the model. Obviously this method is not very useful in distributing information to thousands of geologists all over the world.

For very special purposes, cross sections of the folds may be drawn on vertical sheets of glass that are mounted in their appropriate positions. A view of the folds in three dimensions is thus available. As in the case of the models, however, structural information cannot be readily published in this way.

## 5

## Mechanics and Causes of Folding

### Mechanics of Folding

In general, four principal types of folding may be recognized, but transitions are common. The four principal types are: (1) flexure folding; (2) flow folding; (3) shear folding; and (4) folding due to vertical movements.

#### Flexure folding

*Flexure folding*, also known as *true folding*, may result from either compression or a couple. For purpose of analysis, the behavior of flat beds under a compressive force acting parallel to the bedding may be discussed (Fig. 76A). A single bed,

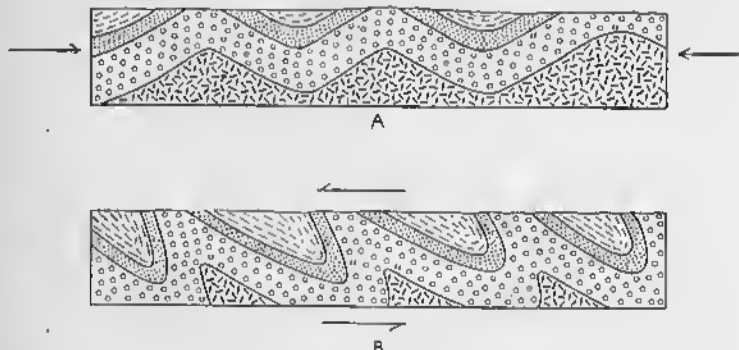


FIG. 76—Flexure Folding. A. Folds resulting from simple compression. B. Folds developed by (1) a couple or (2) compression and a couple combined.

which has small thickness compared to its horizontal extent, should be considered first. Engineering is not much concerned with the failure of bodies of this shape under compression, but engineering does deal with struts. Struts, however, are placed in an engineering structure to give it strength, and they themselves are not supposed to fail. If they do fail, it is usually by

rupture, although under certain conditions they may bend. The simplest analogy to the folding of a single stratum is the behavior of a sheet of paper under compression; the paper arches upward or downward to form a fold.

In nature, of course, many strata are involved in folding. Each bed changes shape by plastic deformation; minute adjustments between and within the grains permit this permanent change in form (pp. 25-29). Folding is analogous to the bending of a thick package of paper, and a very important factor is the sliding of beds past one another, as illustrated in Fig. 77. Each bed slips past the beds on either side of it. Of two adjacent beds, the upper one moves away from the synclinal axis relative to the lower bed (Fig. 77B). This principle is of great importance in interpreting certain types of drag fold (pp. 76-81) and cleavage (pp. 223-228).

In the folding of sedimentary rocks, some formations are competent, whereas others are incompetent. *Competency* is a relative property. A *competent formation* is strong and can transmit the compressive force much farther than a weak, *incompetent* formation. Many factors determine whether or not a formation is competent. The crushing strength is one of these factors. If specimens from two different formations are tested in the laboratory, the one with the greater crushing strength will

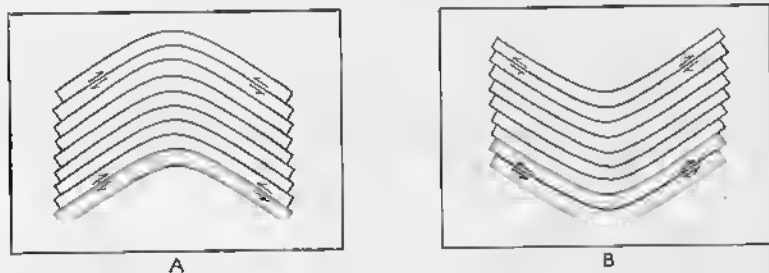


FIG. 77—CROSS SECTIONS ILLUSTRATING FLEXURE FOLDING. A. Anticline. B. Syncline.

be the more competent in folding, provided, of course, that all other factors are equal.

Table 1, p. 19, gives the compressive strength of common rocks. Quartzite and marble are stronger than sandstone and limestone, and shale is the weakest of all.

The massiveness of the formation is an important factor. If, in two formations composed of the same kind of limestone, the beds of one formation are a foot thick, whereas in the other the beds are 100 feet thick, the thick-bedded formation will be the more competent.

The ability of fractures to heal may be an important factor. If a stratum fails by rupture, it is no longer competent to transmit a compressive force. A sandstone may be inherently stronger than an adjacent limestone. But once the sandstone has broken, the fracture may heal with difficulty, whereas the rupture in the limestone may heal relatively rapidly.

If the column of sedimentary rocks is composed of materials of greatly differing competency, the competent beds transmit the force, whereas the incompetent beds behave more or less passively, and are either lifted by the rising arch of competent rock, or flow into potential cavities beneath the arch.

In summary, flexure folding involves the bending or buckling of the more competent layers under compressive force, the more passive behavior of the incompetent beds, and the sliding of beds past one another.

### **Flow folding**

All transitions exist between flexure folding and flow folding. *Flow folding* is typical of regions where thick, competent beds are absent and where all the rocks are plastic, either because of inherent characteristics or because of high temperature or high confining pressure. Under such conditions, individual strata cannot transmit the compressive force any great distance. The whole mass is forced to move under compression, but its behavior is analogous to that of a viscous liquid rather than that of a solid. The problem is one in hydromechanics. This type of deformation is characteristic of the central part of some orogenic belts, where thin-bedded shales and sandstones were rendered even more incompetent by high temperatures and moving solutions. If sufficiently small volumes of sedimentary rocks are considered, however, the folding is similar to flexure folding. The more competent beds may transmit forces for short distances, and the strata slide past one another as in flexure folding.

In many respects flow folds do not differ in appearance from flexure folds, but minor folds are more abundant.

### Shear folding

*Shear folding*, also known as *slip folding*, results from minute displacements along closely-spaced fractures. In Fig. 78A, original horizontal strata are broken into blocks by fractures

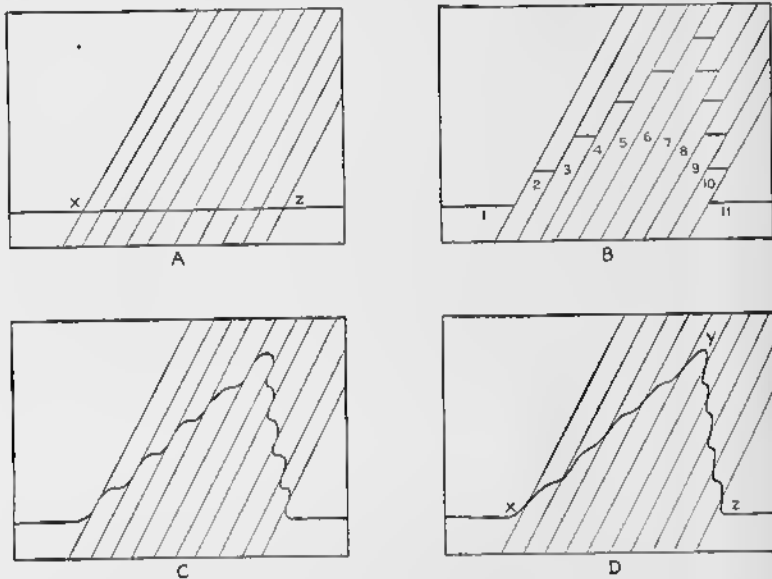


FIG. 78—Cross Sections Illustrating Shear Folding. Heavy black line,  $xx'$ , is a bedding plane. Inclined light lines are fractures. A. Before displacement on fractures. B. After displacement. C. Due to friction, beds tend to parallel the fractures. D. Fold results if bed maintains continuity.

that dip 60 degrees to the left. In Fig. 78B, blocks 1 and 11 remain undisturbed. Block 6 has moved upward the greatest amount; the blocks on either side of it have moved upward in amounts that decrease progressively. Each fracture is actually a fault. If, however, the fractures are only a fraction of an inch apart, and the beds, because of friction, tend to parallel the fractures, as is shown in Fig. 78C, the resulting structure is a major fold with many associated minor folds (Fig. 78D). In the simplest case, such shear folds should always be accompanied by visible fractures, usually cleavage. It is conceivable, how-

ever, that such fractures could be eliminated by later recrystallization of the rocks.

It is evident from Fig. 78 that in pure shear folding the beds are thinned, but are never thickened. Inasmuch as blocks 1 and 11 have not moved toward each other during the folding, the beds that originally had a length  $xz$  have been stretched so that they now have a length of  $xyz$ .

In the example cited, the beds were assumed to have been horizontal at the beginning of the deformation, and all of the folding is of the shear type. After earlier folds develop by some other mechanism, however, their form may be modified by shear folding. The presence of visible fractures with conspicuous, even though minute, offsets, is no proof that the folding was entirely of the shear type. Under conditions of extreme deformation, after an initial phase of flexure folding or flow folding, closely spaced fractures may develop and slippage may take place. In the experience of the author, most shear folds evolve in this way.

#### Folds due to vertical movements

*Differential vertical movements*, unassociated with any fractures, may cause folds in the outer shell of the earth. A bed

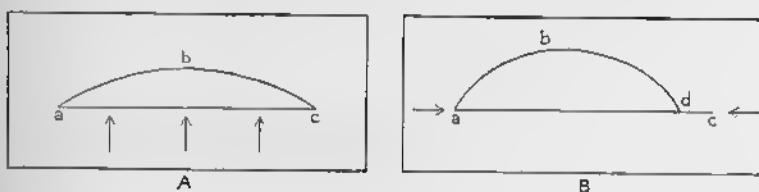


FIG. 79—Folds Due to Vertical Movements. A. Mechanics of doming.  
B. Mechanics of flexure folding.

with an original length  $ac$  (Fig. 79A) is uplifted into a dome by vertical forces. Points  $a$  and  $c$  remain the same horizontal distance apart during the deformation and, consequently, the beds are stretched to form the arc  $abc$ . This mechanism is different, of course, from flexure folding. In flexure folding, as is illustrated by Fig. 79B, the two ends move toward each other, and ideally there is no lengthening of the sedimentary bed; actually there may be some lengthening, but it is incidental to the process and is not essential.

Some geologists do not classify as folds the domes and basins resulting from vertical movements. Willis calls them flexures,<sup>1</sup> and Cloos calls them "swellings" (German, *die Beule*)<sup>2</sup> if they are convex upward. Such a distinction, although commendable in some ways, seems undesirable, because in many cases it is difficult to determine the true nature of the forces involved. It seems far better to use "fold" for all such structural features.

### Causes of Folding

Folds may originate in many ways. The folds in the major orogenic belts have been variously explained as due to (1) horizontal compression, (2) horizontal couple, or (3) convection currents. Some folds, usually domical in form, are due to (4) the intrusion of igneous rocks, (5) the intrusion of rock salt, or (6) vertical forces of unknown origin. Other folds, related to volume changes in the rocks, are due to (7) differential compaction of sediments, or (8) changes in chemical composition. Of minor importance are folds caused by (9) glacial ice, or (10) contemporaneous deformation.

#### Horizontal compression

In horizontal compression, the compressive force acts essentially parallel to the surface of the earth, as is illustrated in Fig. 76A. In most cases the active force, analogous to a moving piston, operates on one side of the orogen, whereas a resisting force is induced by a stationary block on the other side.

Over a period of many years, laboratory experiments have been performed to produce folds by compression. The most exhaustive study was made approximately 50 years ago by Bailey Willis,<sup>3</sup> who sought to understand more thoroughly the folds of the Appalachian Province. The experiments were performed in a pressure box (Fig. 80), the interior of which was 39 $\frac{3}{8}$  inches long, 5 inches wide, and 20 inches deep. A movable piston was at one end. Alternating layers, representing sedi-

<sup>1</sup> Willis, B., and Willis, R., *Geologic Structures*, 3d edition, p. 19. New York: McGraw-Hill Book Company, 1934.

<sup>2</sup> Cloos, H., *Einführung in die Geologie*, pp. 196-200. Berlin: Gebrüder Borntraeger, 1936.

<sup>3</sup> Willis, Bailey, The mechanics of Appalachian structure: *U. S. Geol. Survey 13th Annual Report*, pt. 2, pp. 211-281, 1893.

mentary rocks, were laid in the box. The various layers differed in thickness from one-sixteenth of an inch to  $2\frac{1}{2}$  inches. Each layer consisted of wax, plaster, and turpentine, the pro-

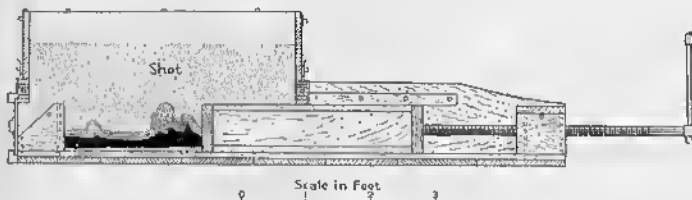


FIG. 80—Pressure Box for Producing Folds. (After B. Willis.)

portions having been varied in order to produce strata of different strength. A layer of B-B shot, more than a foot thick, was placed over the artificial sedimentary rocks. The piston was then slowly moved from right to left to produce folds such as those shown in Fig. 81. A represents the first stage, D repre-

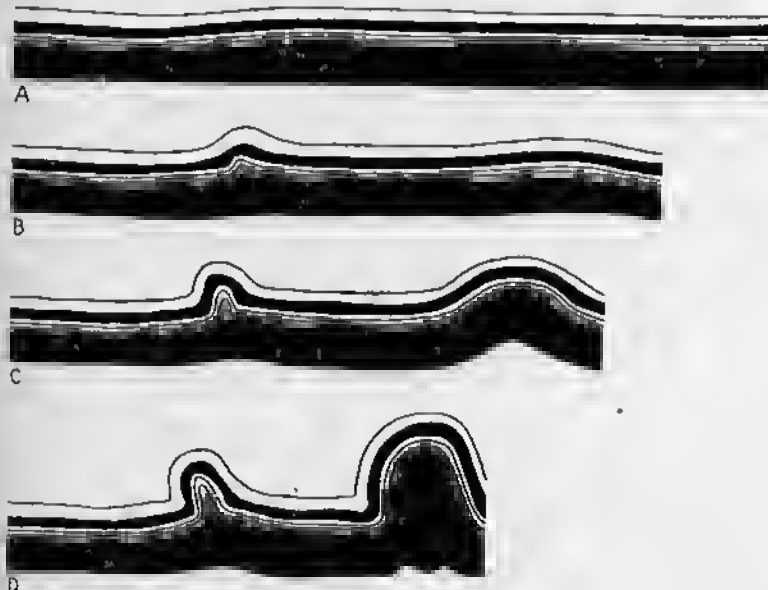


FIG. 81—Folds Produced in Pressure Box. Piston active on right hand end. (After B. Willis.)

sents the last stage. The resulting folds, very similar to those in the Appalachian and Jura Mountains, indicate the effectiveness of horizontal compression to produce folds.

It is supposed, in applying this principle to orogenic belts, that the primary force acted at right angles to the trend of the folds.

If the intensity of the compressive force diminishes downward, the uppermost layers moving more than the lower layers, a couple is superimposed upon the simple compression (Fig. 76B). This causes asymmetry and overturning of the folds.

The cause of these primary forces need not be treated here. Under such an interpretation, the primary forces in the Appalachian Province, where the folds trend northeast, were acting along northwest-southeast lines. In the North American Cordillera, where the folds trend northwest, the compressive forces acted along northeast-southwest lines.

#### Horizontal couple

Horizontal compression, however, may merely be the resultant of a primary horizontal couple. This has been shown

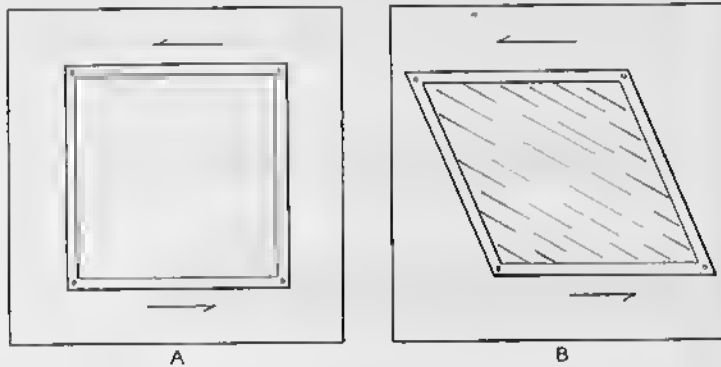


FIG. 82—Folds Produced by a Horizontal Couple. A. Iron frame before deformation. B. After deformation. (After W. J. Mead.)

experimentally by Mead.<sup>4</sup> A sheet of rubber is placed across a rectangular iron frame, with hinges at each of the four corners (Fig. 82A). A thin veneer of wax is placed on the rubber sheet, and the frame is then subjected to a couple (Fig. 82B). The axes of the folds trend diagonally across the frame, making an angle of approximately 45 degrees to the direction in which

<sup>4</sup> Mead, W. J., Notes on the mechanics of geologic structures: *Journal of Geology*, Vol. 28, pp. 505-523, 1920.

the couple is acting. A circle under a similar force is deformed into an ellipse; the axes of the folds are parallel to the long axis of the ellipse.

Such folds may be minor features in a large orogenic belt. It has been suggested that some folds in California are due to a couple resulting from horizontal movement along vertical faults.

Some geologists, however, believe that entire orogenic belts are due to gigantic terrestrial couples. It has recently been suggested that the northwestward trending folds of the Sierra Nevada are due to a southward movement of the central part of North America relative to the Pacific Coast, and that the northeastward trending ranges of China<sup>5</sup> are due to a southward movement of the interior of Asia relative to the Pacific Ocean.

### Convection currents

The principle of a couple may be applied in another way. It is supposed that currents are flowing horizontally beneath the outermost shell of the earth. These currents, caused by convection, exert a drag on the overlying rocks, and they set up a couple such as that represented in Fig. 76B. The axial planes of the resulting folds dip in the direction in which these currents flow.<sup>6</sup>

At the present stage of our knowledge, it is impossible to evaluate the relative importance of horizontal compression, horizontal couples, and convection currents upon the formation of orogenic belts.

### Intrusion of magma, intrusion of salt, and vertical forces of unknown origin

Forces acting upward at right angles to the surface of the earth may be due to a number of causes. The intrusion of magma may dome the overlying rocks as described on p. 271. Uplifts associated with salt domes will be described in Chapter 14. Even laccoliths and salt domes, however, are relatively small structural features, seldom more than a few miles in

<sup>5</sup> Lee, J. S., *The Geology of China*, pp. 282-366. London: Thomas Murby and Co., 1939.

<sup>6</sup> Griggs, David, A theory of mountain building: *American Journal of Science*, Vol. 237, pp. 611-650, 1939.

diameter. Broad domes covering thousands of square miles or even large parts of a continent, must be due to large-scale vertical movements in the outer shell of the earth. The fundamental cause of such movements is a problem which has not yet been satisfactorily solved.

### Differential compaction of sediments

Some folds, anticlinal and synclinal, are due to downward movements of rock masses directly under the influence of

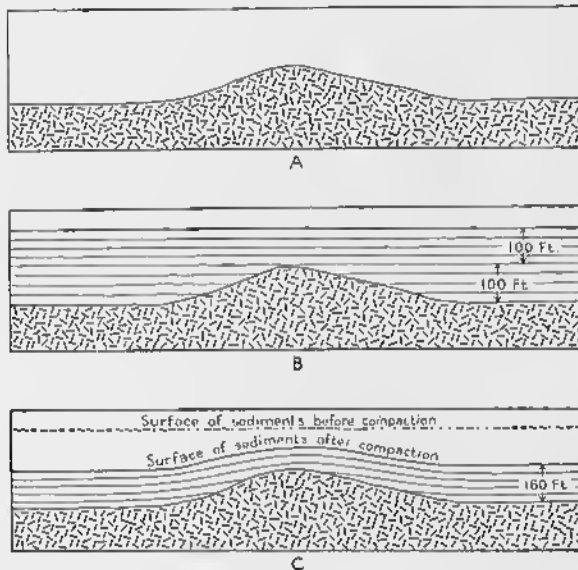


FIG. 83—Folds Resulting from Differential Compaction of Sediments. A. Ridge left by erosion. B. Same ridge covered by mud, but before compaction of mud. C. Same, but after compaction of mud.

gravity. Although anticlines that result from the differential compaction of sediments over buried ridges have comparatively low dips, they form important traps for the accumulation of petroleum. The general principles are illustrated by Fig. 83. Diagram A represents a land surface carved on solid rocks; the hill is 100 feet high. Later, as shown in diagram B, sediments are deposited on this surface; these sediments are only 100 feet thick on the top of the hill, but are 200 feet thick over the surrounding lowlands. For purposes of illustration, these sedi-

ments have been shown as absolutely horizontal. Actually, of course, there would be some minor irregularities, and particularly on the flanks of the hill there would be some outward initial dips. If at some subsequent time the mud compacts 20 per cent over the top of the hill, the highest sedimentary bed will sink 20 feet—that is, 20 per cent of 100 feet. Beyond the limits of the hill, the highest sedimentary bed sinks 20 per cent of 200 feet—that is 40 feet. Consequently, the highest beds will dip away from the center of the buried hill.

### Chemical changes

Calcium sulphate is precipitated from evaporating water as anhydrite. Water is subsequently added to convert the anhydrite into gypsum, and the increase in volume is approximately 40 per cent. If the beds are flat lying, and if all the expansion takes place upward, the beds thicken, but no folds develop. If, however, much of the expansion is horizontal, compressive forces are set up and folding ensues. The resulting folds are small, with a height of only a fraction of an inch, or, at the most, of a few feet. Moreover, gypsum is not an abundant rock.

### Ice push

Glacial ice, pushing against the steep slope of a cuesta, may throw the strata, if they are poorly consolidated, into folds. Moreover, ice may override weak sediments and cause drag folds. Folds due to glacial action are well developed near the southern limits of the Pleistocene ice caps on Martha's Vineyard, an island off the southeastern coast of Massachusetts.

### Contemporaneous deformation

Some folds may form in sediments during their deposition (Fig. 84); even small faults may form, as beneath *a* and *b* of Fig. 84. In the strictest sense, of course, the deformation is subsequent to the deposition of the bed that is deformed, but is contemporaneous with the sedimentation as a whole. Beds of soft mud, sand, and ooze may slide because of a number of reasons. The slope on which deposition takes place may be inclined and, although the rocks are relatively stable for long

periods of time, any disturbing factor may set them in motion. Slight tilting, excessive local deposition, or an earthquake may set masses of mud and ooze into motion. Local subaqueous erosion may leave the beds with inadequate support. The upper beds may slide over the lower, developing small folds. If the lower portion of a bed is held back by a buttress, the upper part may slide under the influence of gravity, and the beds may buckle. Movements of this type may occur on slopes as low as  $2\frac{1}{2}$  degrees.

The drag of floating objects, such as icebergs and trees, causes contemporaneous deformation. The resulting folds and

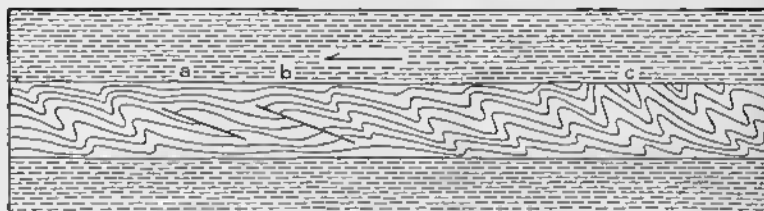


FIG. 84—Folds Formed by Contemporaneous Deformation. The upper layer slid from right to left over the middle layer.

faults, however, would presumably be rather irregular and unsystematic. Faults are shown at *a* and *b* in Fig. 84.

It may be difficult to distinguish between features resulting from contemporaneous deformation and those due to later forces. If, as is sometimes observed, the folds are truncated by younger beds of the same sedimentary series, as at *c* in Fig. 84, it is evident that the deformation was contemporaneous. The folds resulting from contemporaneous deformation are similar to drag folds. If the major structure is known, the orientation of the minor folds may be useful in deciding whether they are contemporaneous or secondary. If they are true drag folds, they should be related to the major structure in the manner indicated on p. 76; otherwise they are probably the result of contemporaneous deformation. Obviously, however, this criterion is unreliable, and it may lead to erroneous interpretations.

# 6

## Failure by Rupture

### Introduction

In Chapter 2 it has been shown that rocks first undergo elastic deformation, then plastic deformation. If deformation proceeds far enough, the rock eventually may fail by rupture—that is, by breaking. The orientation of the planes of rupture depends upon the nature of the external forces, the kind of rock, the temperature, and the confining pressure.

The most precise information about the relation between external forces and rupture comes, of course, from engineering practice, especially from controlled laboratory experiments. Geologists have also performed numerous experiments in their laboratories. In other cases where experiments are impossible, certain deductions from field geology seem justified. It is essential, however, to distinguish between observation and deduction.

All ruptures may be classified as *tension fractures* and *shear fractures*. *Tension fractures* result from local forces that tend to pull the specimen apart. When the specimen finally breaks, the two walls move away from each other. *Shear fractures* result from local forces that tend to slide one part of the specimen past the adjacent part.

It is of the utmost importance to distinguish between the character of the external force and the type of fracture. Tension fractures may result not only from tension, but also from couples and even from compression; as will be shown later, however, a special name is given to tension fractures formed by compression. Shear fractures may develop not only under compression, but also from couples and from tension.

### Tension

In the simplest type of tension, the opposite ends of a rod are pulled apart. After elastic and plastic deformation, the

specimen fails by rupture. The nature of the rupture depends upon the brittleness of the material. In brittle substances, such as wrought iron or a piece of blackboard chalk, a single tension fracture forms at right angles to the axis of the rod (Fig. 85A).

In more ductile substances, rupture may be preceded by "necking"; that is, the central part of the rod thins more rapidly than the ends (Fig. 85B). A conical fracture develops and, when failure ultimately occurs, a conical protuberance withdraws from a conical depression. In this case, the specimen has failed

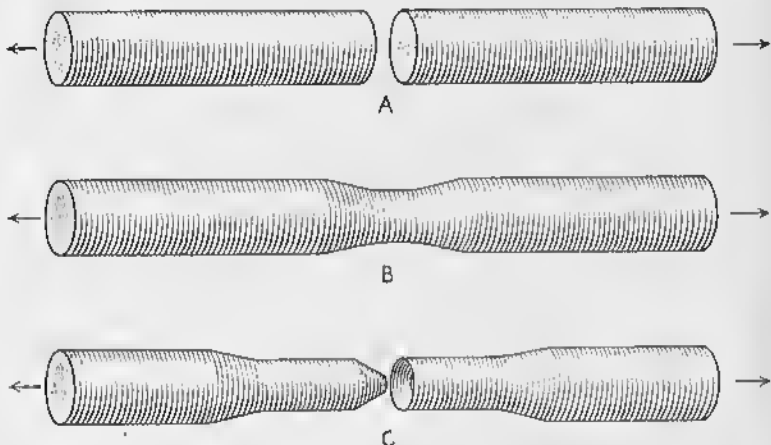


FIG. 85—Rod Subjected to Tension. A, Brittle material, with a tension fracture at right angles to the axis of the rod. B, Ductile material that has "necked," but not ruptured. C, Ductile material that has ruptured; the conical surface is due to failure along shear fractures; the blunt end of the cone is due to failure along a tension fracture.

along shear fractures. In some material the rupture is a combination of a shear fracture and a tension fracture (Fig. 85C).

Consolidated rocks near the surface of the earth are brittle substances and, when they are subjected to tension, we should generally expect them to fail by the formation of tension cracks. In other words, fractures should form at right angles to the tensional forces.

Rocks have a much lower tensile strength than compressive strength, as is shown by Table 1. Sandstone, for example, has a compressive strength of 500 to 1500 kilograms per square centimeter, but the same rock possesses a tensile strength of only 10 to 30 kilograms per square centimeter.

### Compression

In the simplest type of compression, the test specimen, usually a cylinder or a square prism, is subjected to a compressive force at two opposite ends, and the sides are free to expand outward. Under such a force, an imaginary sphere in the

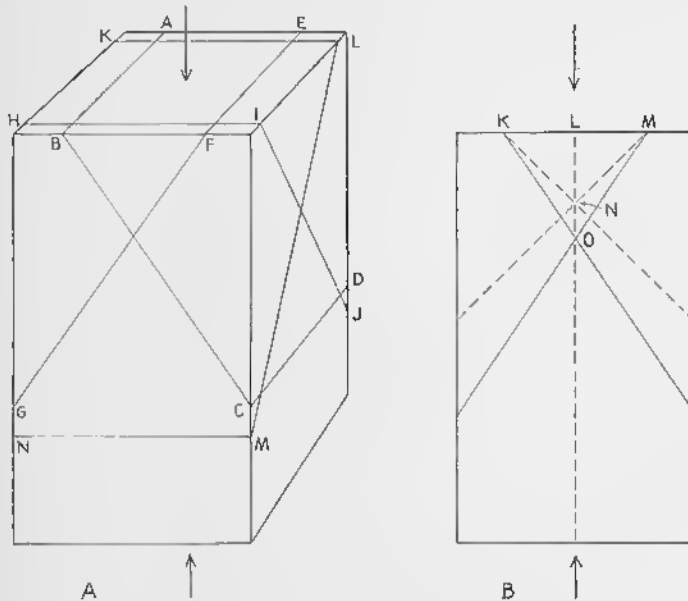


FIG. 86—Shear Fractures Due to Compression. Arrows indicate compressive force. A. In a square prism subjected to simple compression four sets of shear fractures develop; they are parallel to the planes  $ABCD$ ,  $EFG$ ,  $HIJ$ , and  $KLMN$ . B.  $KN$  and  $MN$  represent planes of maximum shearing stress deduced mathematically;  $KO$  and  $MO$  represent approximate position of shear fractures that form in experiments.

specimen would be deformed into an oblate spheroid. In other experiments, a square prism is again compressed at the two ends, but it is confined on two opposite sides; the other two sides are free to move. Under such conditions, an imaginary sphere in the specimen would be deformed into an ellipsoid.

If the block is a square prism, unconfined on the sides, four sets of shear fractures develop. The four planes parallel to which the fractures form are illustrated in Fig. 86A by the planes  $ABCD$ ,  $EFG$ ,  $HIJ$ , and  $KLMN$ . Ordinarily, many fractures

develop parallel to each of these four planes. As the compressive force is increased, the fractures increase in number and size, until, eventually, one fracture cuts all the way across the specimen and the block collapses. Some sets may be much more extensively developed than others, especially if the specimen lacks homogeneity.

It may be shown mathematically that the maximum shearing stress is along planes inclined at an angle of 45 degrees to the

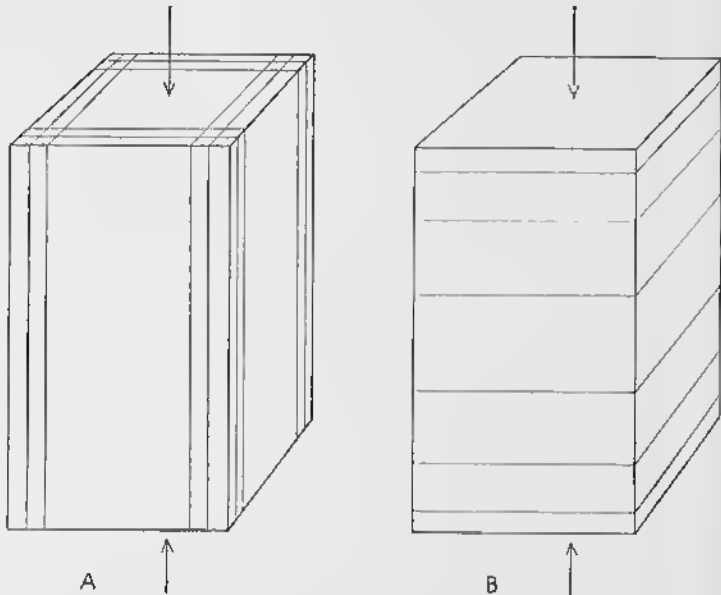


Fig. 87—Extension Fractures and Release Fractures Due to Compression. Arrows indicate compressive force. A. Extension fractures; form parallel to sides of the prism. B. Release fractures; form parallel to top of prism. (After D. T. Griggs.)

compressive force, and we might expect the planes of rupture to intersect at right angles. In Fig. 86B, these planes make angles  $KNL$  and  $MNL$  with the compressive force  $LN$ . In all experimental work, however, the angle is less than 45 degrees, and the planes of rupture form angles such as  $KOL$  and  $MOL$  with the compressive force. The angle depends upon the material. Available information indicates that even if the test specimen is under high confining pressure, the angle is less than 45 degrees. The statement commonly made in geological literature that the angle is greater than 45 degrees in ductile material, is unjustified.

If the square prism is confined on two opposite sides, two sets of fractures dip toward the unconfined sides of the specimen. If the front and back of the block shown in Fig. 86A were confined, only two sets of fractures, represented by *ABCD* and *EFG*, would form.

If the test specimen is cylindrical, the surfaces of rupture tend to assume a conical form; this is similar to the shear fractures that form in ductile materials under tension.

In many cases, however, specimens under compression fail along fractures parallel to the sides of the prism, especially if a lubricant is placed along the contact of the specimen and the piston exerting the compressive force (Fig. 87A). From one point of view these are tension fractures, on the principle that active compression in one direction sets up tensional forces at right angles. There are, however, theoretical objections to such an analysis, and ruptures of this type are preferably called *extension fractures*.<sup>1</sup>

Yet another type of fracture results indirectly from compression.<sup>2</sup> The specimen, while immersed in a fluid and under high confining pressure, is subjected to compression. After the load is released and the specimen removed, there are numerous fractures at right angles to the axis of compression (Fig. 87B). Such fractures are, in a sense, tension fractures caused by expansion of the specimen upon the release of load, but because there is no active tension they may be called *release fractures*.

### Couples

The relation of ruptures to couples may be rather simply shown by means of the frame mentioned previously (p. 94). While the frame is still square, a sheet of rubber is mounted on it and coated with a thin layer of paraffin. If the frame is then sufficiently deformed by a couple, the paraffin is broken by numerous cracks (Fig. 88). The first ruptures are vertical tension fractures (*t* of Fig. 88B) which strike parallel to the short diagonal of the parallelogram. This is not unexpected, for obviously the paraffin is being stretched parallel to the long

<sup>1</sup> Bridgman, P. W., Reflections on rupture: *Journal of Applied Physics*, Vol. 9, pp. 517-528, 1938.

<sup>2</sup> Griggs, D. T., Deformation of rocks under high confining pressures: *Journal of Geology*, Vol. 44, pp. 541-577, 1936.

diagonal of the parallelogram. After further deformation, vertical shear fractures (*s* of Fig. 88B) develop parallel to the sides of the wooden frame. These fractures are also not unexpected, for they are analogous to the shear fractures that develop under compression. Their orientation, however, is controlled by the sides of the frame. Small thrust faults (*th* of Fig. 88B), which develop in the last step of the deformation, strike parallel to the long diagonal of the parallelogram.<sup>3</sup>

### Torsion

If the two ends of a piece of blackboard chalk are pulled apart, a tension fracture forms at right angles to the long axis of the specimen, as in Fig. 85A. If the same material is twisted, a helical fracture develops, as is shown in Fig. 89A. Although chalk illustrates the difference between the ruptures produced by tension and torsion, the rock masses with which the structural geologist deals can scarcely be compared to rods. The twisting of sheet-like bodies, involving either a single bed, a formation, or the whole outer shell of the earth, is far more significant than the twisting of a rod.

The stresses developed in a twisted sheet can be resolved into the simpler stresses, tension or compression, and the ruptures obey the generalizations already set forth. Many years ago rather simple experiments were performed by twisting a sheet of glass. As shown in Fig. 89B, the upper right and lower left-hand corners were moved down, whereas the upper left and lower right-hand corners were moved up. Two sets of fractures developed.<sup>4</sup> On the upper surface the fractures were diagonal, and they extended from the upper left to the lower right-hand corner. On the under side the fractures were also diagonal, but they extended from the upper right to the lower left-hand corner.<sup>5</sup> A brief consideration explains why the glass fractures in this manner. If a sheet is bent, as in Fig. 90, the upper part is subjected to tension, the lower part to compression.

<sup>3</sup> Mead, W. J., Notes on the mechanics of geologic structures: *Journal of Geology*, Vol. 28, pp. 505-523, 1920.

<sup>4</sup> Daubrée, A., *Études synthétiques de géologie expérimentale*, pp. 306-314. Paris, 1879.

<sup>5</sup> Mead, W. J., *op. cit.*

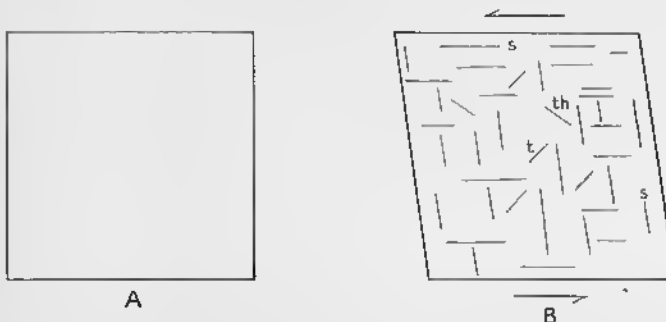


FIG. 88—Ruptures Due to a Couple. A. Square frame that is covered by a sheet of rubber, on which is a layer of paraffin. B. Fractures that develop due to couple; *t* = tension fractures (perpendicular to plane of paper); *s* = shear fractures (perpendicular to plane of paper); *th* = thrust faults (inclined to plane of paper). (After W. J. Mead.)

Between the two parts is a surface of no strain. In the sheet of glass that was twisted, the upper side was subjected to tensional forces acting from the upper right to the lower left-hand corner. Conversely, the tensional forces on the lower side acted from the upper left to the lower right-hand corner. The tension fractures

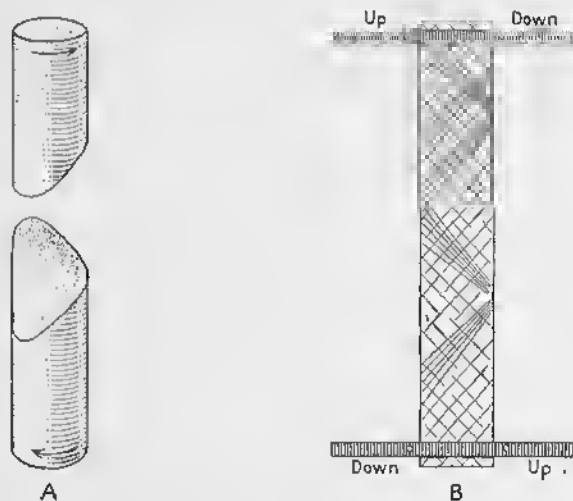


FIG. 89—Rupture Due to Torsion. A. Helical fracture due to twisting of a piece of blackboard chalk. B. Tension fractures on a piece of glass. Fractures that extend from upper left to lower right hand corner are on upper side of sheet of glass; those that extend from upper right to lower left hand corner are on under side of the sheet of glass.

formed because the tensile strength is less than the compressive strength.

It is difficult to evaluate the importance of torsion as a cause of rupture in the rocks of the earth. It seems probable that torsion is an important type of deformation, but in any particular case it may be hard to decide whether local tension or local compression was due to regional torsion.

### Rupture and the Strain Ellipsoid

As has been stated on p. 29, the understanding of deformation may be aided by visualizing the behavior of a sphere under stress. The sphere is changed into an ellipsoid, two special cases of which are the oblate spheroid and the prolate spheroid. A sphere can be deformed into an ellipsoid by tension, by compression, or by a couple.

If tension fractures form, they are parallel to the plane that contains the least axis and the intermediate axis of the strain ellipsoid (Fig. 92A); that is, tension fractures form at right angles to the greatest axis of the strain ellipsoid (Fig. 92B). If the attitude of the strain ellipsoid is known, the position of the tension fractures may be predicted. Conversely, if fractures can be identified as of tensional origin, the greatest axis of the strain ellipsoid is readily determined; the plane containing the least and intermediate axes is also defined, but the position of these axes within this plane can be determined only if additional data are available.

The relation between the strain ellipsoid and the shear fractures cannot be stated so simply. If a circle is deformed into an ellipse, as in Fig. 91, all lines parallel to  $AA'$  are lengthened and all lines parallel to  $CC'$  are shortened. Somewhere between  $AA'$  and  $CC'$ , therefore, there must be two lines that are neither lengthened nor shortened. These lines,  $SS'$  and  $S''S'''$ , are called *lines of no distortion*.

Every ellipsoid has three mutually perpendicular axes, the greatest ( $AA'$ ), intermediate ( $BB'$ ), and least ( $CC'$ ) strain axes (Fig. 92A). Moreover, every ellipsoid has two circular cross sections, which intersect in  $BB'$ . These circular sections are illustrated by Figs. 92C and 92D.

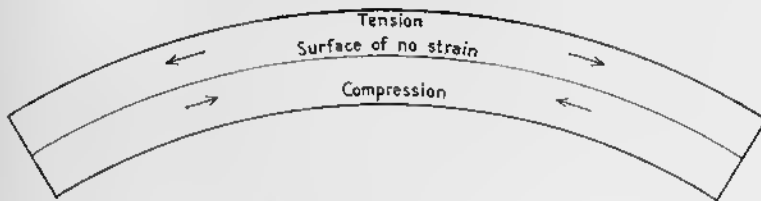


FIG. 90—Stresses in a Bent Sheet.

It may be shown that the two circular sections of the strain ellipsoid are *surfaces of no distortion* if the intermediate axis,  $BB'$ , is neither lengthened nor shortened. These two surfaces of no distortion are considered to be the surfaces of maximum shearing strain and, consequently, the surfaces parallel to which rupture takes place. It is often stated that shear fractures form parallel to the circular sections of the strain ellipsoid. That is, if a body of rock is compressed in such a way that an imaginary sphere within the rock changes to an ellipsoid (Fig. 92C), whatever shear fractures develop are parallel to the circular sections of this imaginary ellipsoid.

There are, however, several objections to this generalization. The circular sections are surfaces of no distortion only if the intermediate axis,  $BB'$ , is neither lengthened nor shortened. If  $BB'$  does not remain constant during deformation, the surface of no distortion is a double cone. If  $BB'$  shortens, the axis of the cone is  $AA'$ . If  $BB'$  lengthens, the axis of the cone is  $CC'$ .

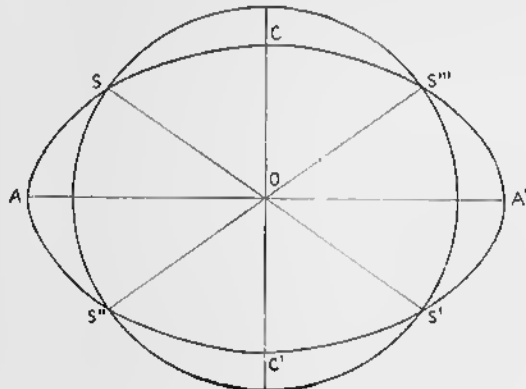


FIG. 91—Strain Ellipse.  $AA'$  is the greatest strain axis.  $CC'$  is the least strain axis.  $SS'$  and  $S''S'''$  are the lines of no distortion.

There is no proof that the surfaces of no distortion are planes of maximum shearing strain.

Experimental data show that shear fractures are not directly related to surfaces of no distortion. In Fig. 91 the ellipse may be considered the result of a compressive force acting along the line  $CC'$ . The lines of no distortion,  $SS'$  and  $S''S'''$ , make angles of  $SOC$  and  $S'''OC$ , respectively, with the compressive force. These angles are greater than 45 degrees. This is true no matter how slight the deformation is. But experimental work indicates that these angles are always less than 45 degrees.

We may generalize and say that experimentally-produced shear fractures make an angle of less than 45 degrees with the least strain axis, whereas the surfaces of no distortion of the strain ellipsoid make angles of greater than 45 degrees with the least strain axis. It is apparent that shear fractures are approximately parallel to the surfaces of no distortion, but the angular difference may be as great as 30 degrees.

A simple example may serve to illustrate the use of the concept of the strain ellipsoid in relation to ruptures. Fig. 93A is a cross section through a fault—that is, a fracture along which the blocks on opposite sides have been displaced relative to each other. Scratches on the surface of the fault indicate that the movement was parallel to the dip of the fault. The problem is to decide whether the eastern block moved up or down relative to the western block—that is, which arrows, those at  $a$  or those at  $b$ , represent the movement?

On the east side of the fault are short, open tension fractures, arranged *en échelon* as shown in Fig. 93A. The long axis of the strain ellipse,  $AA'$ , is therefore vertical, as is shown in Fig. 93B, and the ellipse is oriented as shown. If the couple along the fault acted as shown by the arrows at  $b$ , the long axis of the ellipse would be horizontal. If the couple acted as shown by the arrows at  $a$ , the long axis of the ellipse would be vertical. Inasmuch as the latter corresponds to the orientation deduced from the tension cracks, it is concluded that the east wall moved up relative to the west wall. This problem has been analyzed by omitting the third dimension, but in this case the intermediate axis of the strain ellipsoid is perpendicular to the plane of the paper and may be neglected.

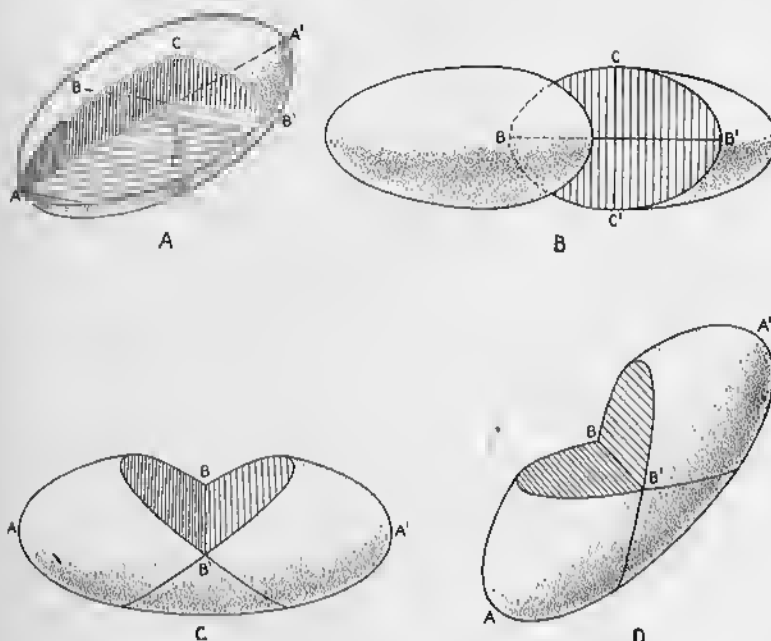


FIG. 92—Strain Ellipsoid. A.  $AA'$  is the greatest strain axis,  $BB'$  is the intermediate strain axis, and  $CC'$  is the least strain axis. B. Tension fractures form perpendicular to the greatest strain axis. C. and D. Every ellipsoid has two circular sections that intersect at the intermediate axis  $BB'$ . Shear fractures are approximately parallel to these circular sections.

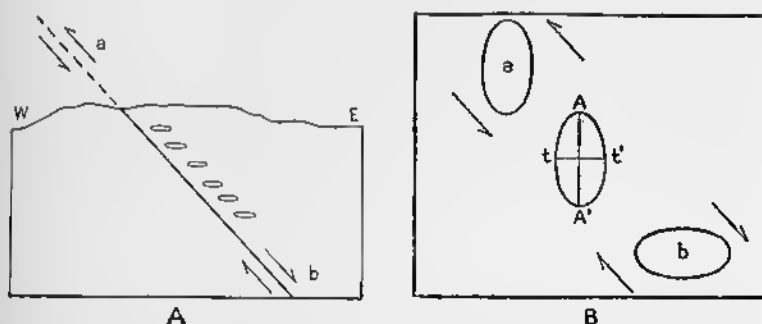


FIG. 93—Use of Strain Ellipse in a Structural Problem. A. Cross section; heavy diagonal line is a fault; problem is to decide whether movement has been of type represented by arrows at  $a$  or by arrows at  $b$ . Small ovals are open tension cracks. B. The tension cracks of Fig. 93A are represented by  $tt'$ ; therefore the greatest strain axis lies in direction  $AA'$ , which is the long axis of the strain ellipse. The movement represented by the arrows at  $a$  would give such an orientation of the strain ellipse; the movement represented by the arrows at  $b$  would not.

Other examples of the use of the strain ellipsoid can be cited more intelligently in later sections of the book.

The concept of the strain ellipsoid is used extensively in the literature on structural geology. It has been used particularly in attempts to relate ruptures to strain and to external forces; the student should be familiar with the methods employed. On the other hand, many geologists feel that little is to be gained by analyzing field problems in this way. In general, however, the concept of the strain ellipsoid is exceedingly useful if it is employed with discrimination. It is helpful in visualizing in three dimensions the change in shape that masses of rock may undergo. Moreover, it is clear that tension fractures form at right angles to the greatest strain axis. Shear fractures are approximately parallel to the surfaces of no distortion, but the angular difference may be as great as 30 degrees.

#### Rupture in Rocks

Failure by rupture is expressed in the rocks of the outer shell of the earth by joints, faults, and some kinds of cleavage. The next few chapters are devoted, therefore, to these subjects. Many ruptures are now occupied by veins or dikes. Although the origin of the ruptures is the concern of the structural geologist, the nature of the material that fills them is the concern of the economic geologist or the petrologist.



PLATE X. Joints. These joints cutting pre-Cambrian granite in the Ozark Mountains, Missouri, have been widened by weathering. (Photo by K. Fowler-Billings.)



PLATE XI. Joining. View looking northeast up Tenaya Canyon from Glacier Point, Yosemite National Park, California. Half Dome is on the right. The sheer side of Half Dome is about 2000 feet high, but the top of Half Dome is 4770 feet above the bottom of the canyon at 11,100 feet. The attitude of the sheer cliff has been determined by a series of traverses extending vertically.

## Joints

### General Features

The visible rocks of the earth are characteristically broken by smooth fractures known as joints. *Joints* may be defined as divisional planes or surfaces that divide rocks, and along which there has been no visible movement parallel to the plane or surface. Although joints are characteristically planes, some are curved surfaces. There has been no visible movement parallel to the surface of the joint; otherwise it would be classified as a fault. Movement at right angles to the surface of the joint may take place, however, and produce an open fracture (Pl. IX, X, XI).

Joints may have any attitude; some joints are vertical, others are horizontal, and many are inclined at various angles. The strike and dip of joints are measured in the same way as in bedding. The strike is the direction of a horizontal line on the surface of the joint; the dip, measured in a vertical plane at right angles to the strike of the joint, is the angle between a horizontal plane and the joint. In Fig. 94 the geographic directions are shown. The front of the block (plane *ABCD*) is a joint that strikes east and has a vertical dip. The right-hand side of the block (plane *BEDF*) is a joint that strikes north and has a vertical dip. The plane *GHIJ* is a joint that strikes north and dips 50 degrees east.

Joints differ greatly in size. Some joints are only a few feet long, but observations in quarries show that others may be followed for hundreds of feet along the strike and for similar distances down the dip. Joints which are hundreds and even thousands of feet in length and in height may be observed in mountainous regions.

Joints never occur alone. The interval between them may be hundreds of feet or only a few inches. As will be shown on

p. 217, if the interval is a fraction of an inch, the term fracture cleavage is applied.

The term joint is said to have originated in the British coal fields because the miners thought that the rocks were "joined" along the fractures, just as bricks are put together in a wall.

Joints may be classified either geometrically or genetically. A geometrical classification is strictly descriptive and comparatively easy to apply, but does not indicate the origin of the joints. A genetic classification is more significant, but, as will be seen, is not readily applied in many cases.

### Geometrical Classification

In a geometrical classification, the joints may be classified on the basis of their attitude relative to the bedding or some similar structure in the beds that they cut. *Strike joints* are those which strike parallel or essentially parallel to the strike of the bedding of a sedimentary rock, the schistosity of a schist, or the gneissic structure of a gneiss. In Fig. 95, in which the bedding is shown in solid black, *BDEF* and *MNO* are strike joints. *Dip joints* are those that strike parallel or essentially parallel to the direction in which the bedding, schistosity, or gneissic structure dips. In Fig. 95, *ABCD* and *GHI* are dip joints. *Oblique* or *diagonal* joints are those striking in a direction that lies between the strike and direction of dip of the associated rocks. In Fig. 95, *PQR* and *STU* are oblique joints. Bedding joints are parallel to the bedding of the associated sedimentary rocks. In Fig. 95, *JKL* is a bedding joint.

Characteristically a large number of joints are parallel. A *joint set* consists of a group of more or less parallel joints. A *joint system* consists of two or more joint sets or of any group of joints with a characteristic pattern. Two perpendicular sets of joints are frequently referred to as a *conjugate joint system*.

Joints may be classified according to their strike. It is thus possible to speak of the north-south set, the northeast set, or the east-west set. In some regions there may be several north-south sets; one set may be vertical, a second set may dip 40 degrees east, and a third set may dip 60 degrees west.

In order to ascertain the number of sets present, the joints can be plotted on a map. Fig. 96 shows at a glance that in the

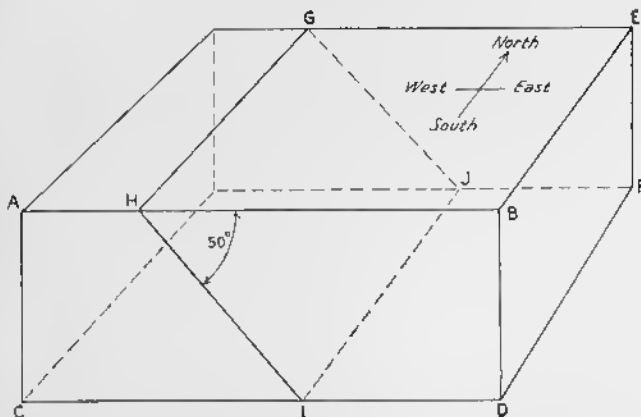


FIG. 94—Attitude of Joints. Plane  $ABCD$  represents a vertical joint that strikes east-west; plane  $BDEF$  represents a vertical joint that strikes north-south; plane  $GHIJ$  represents a joint that strikes north-south and dips 50 degrees east.

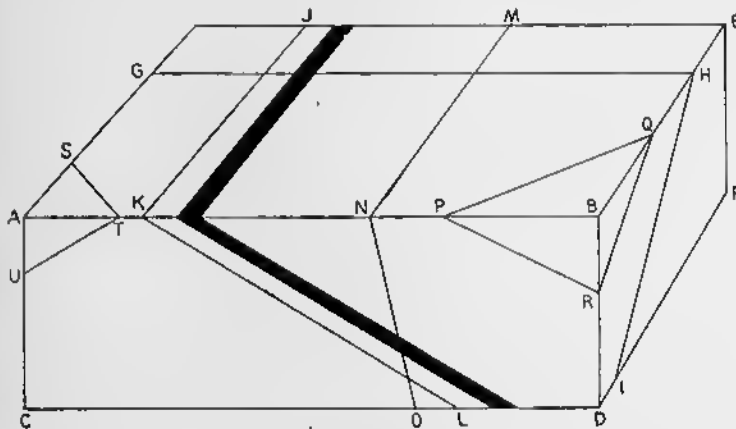


FIG. 95—Geometrical Classification of Joints. Heavy black band is bedding.  $ABCD$  and  $GHI$  are dip joints;  $BDEF$  and  $MNO$  are strike joints.  $JKL$  is a bedding joint.  $PQR$  and  $STU$  are diagonal joints.

Adirondack Mountains of New York there are two prominent sets of joints that are essentially vertical, and that one set strikes northeast, the other northwest. In the imaginary region portrayed by Fig. 97, the most prominent set of joints strikes northwest and dips between 40 and 60 degrees to the northeast; a less conspicuous set strikes northeast and dips steeply northwest. Some of the joints are diversely oriented.

Various types of diagrams may be used to portray the attitude of the joints in an area. In one kind of diagram the strikes are plotted on one semicircle, the dips on a second; Fig. 98 is such a diagram, and represents the joints shown in Fig. 97. Both semicircles are divided into sectors—in this case by radii at

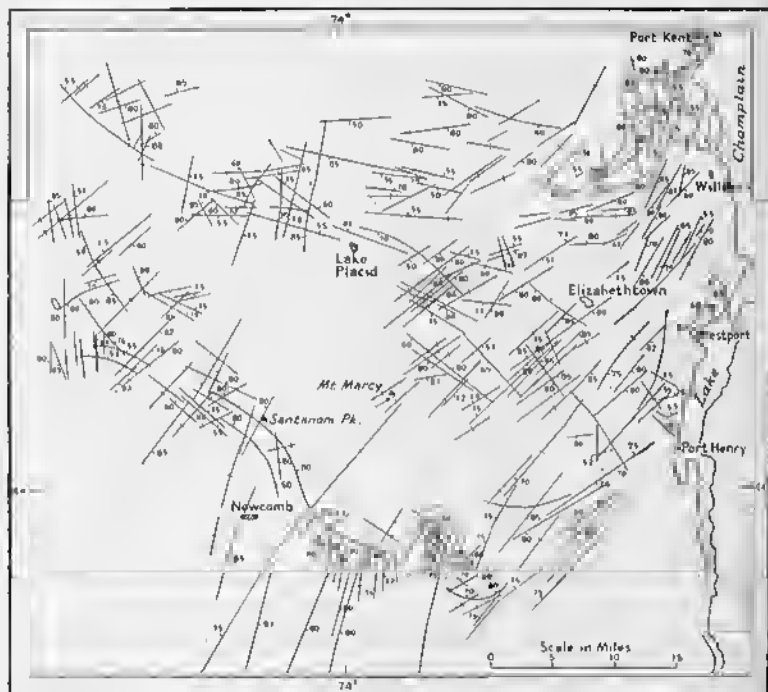


FIG. 96—Joint Map of Part of the Adirondack Mountains of New York. Generalized from detailed maps; data for many joints are combined into one dip-strike symbol. Length of lines is intended to show relative importance of different groups of joints, but does not mean that one can be followed for that distance. (After R. Balk.)

every 10 degrees. The number of joints in each sector is indicated by some scale—in this instance approximately  $\frac{1}{16}$  inch for each joint. The upper diagram shows that most of the joints strike either northwest or northeast. The lower diagram reveals that about half the joints are nearly vertical, and that the other half dip about 45 degrees in an easterly direction. This method of representing the attitude of joints is obviously deficient, because it does not indicate which joints have the vertical dips

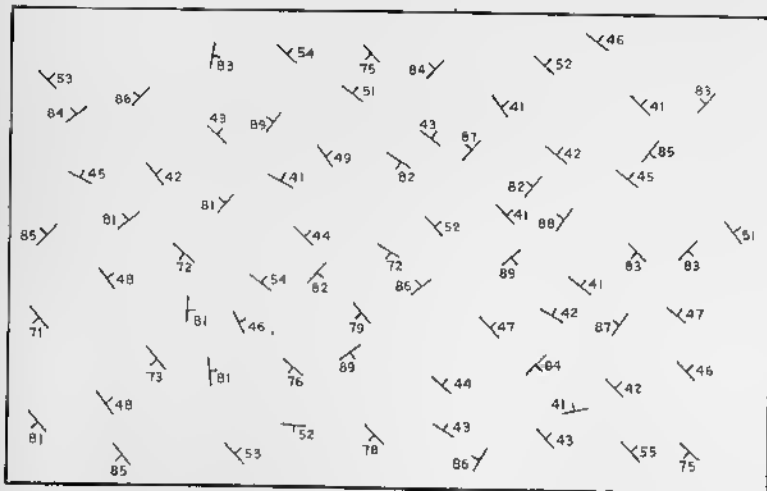


FIG. 97—Joint Map of a Hypothetical Area. Attitude of individual joints shown by dip-strike symbols.

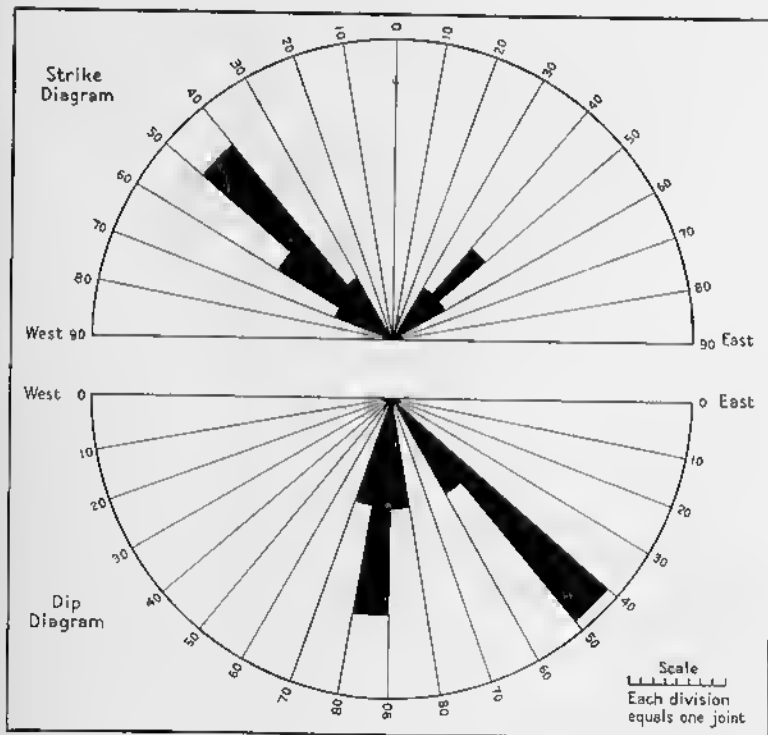


FIG. 98—Joint Diagrams of Area Shown in Fig. 97.

and which have the 45-degree dip. Moreover, it can indicate only the general direction of dip, and not the exact direction.

A precise, and therefore a more useful way of representing joints, is to plot the poles of perpendiculars to the joints. All the joints are imagined to be at the center of a sphere. A line drawn perpendicular to each joint will pierce the sphere at two points, called the poles. In Fig. 99 the poles of a horizontal

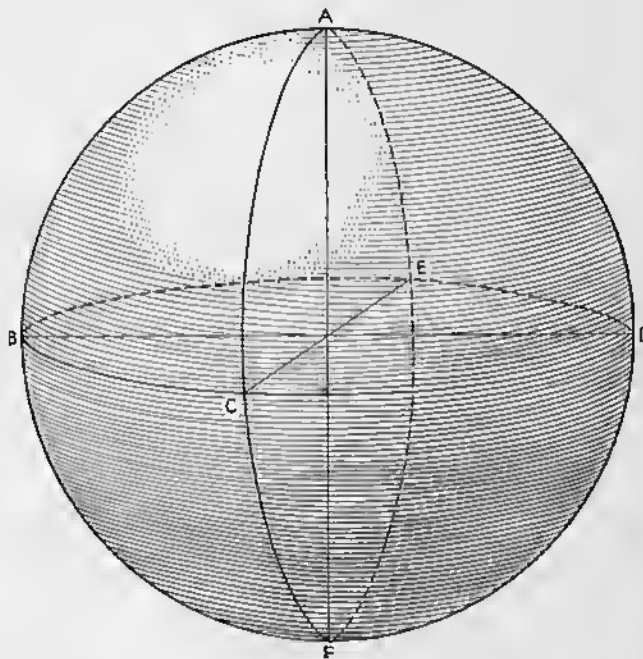


FIG. 99—Sphere with All Joints Passing through Center.  
ABFD, ACFE, and BCDE are joints.

joint,  $BCDE$ , are at  $A$  and  $F$ . The poles of a vertical joint,  $ABFD$ , parallel to the page, lie at  $C$  and  $E$ . The poles of a vertical joint,  $ACFE$ , perpendicular to the page, are at  $D$  and  $B$ . It is obvious that, for plotting data, one need use only the top or bottom half of the sphere, because the poles on one hemisphere are the mirror image of those on the other. Moreover, it is far more convenient to project the surface of the hemisphere on to the plane of the paper. Fig. 100 is an example of a projection in which the upper hemisphere was used. Point 1 represents a horizontal joint; point 2 represents a vertical joint that strikes

north; point 3 represents a vertical joint that strikes east; and point 4 represents a vertical joint that strikes northwest. Point 5 represents a joint striking east and dipping 45 degrees south. Point 6 represents a joint striking northwest and dipping 45 degrees southwest. All vertical joints, of course, can be represented by two points, and points 2', 3', and 4', respectively, represent the same joints as 2, 3, and 4. But only one point

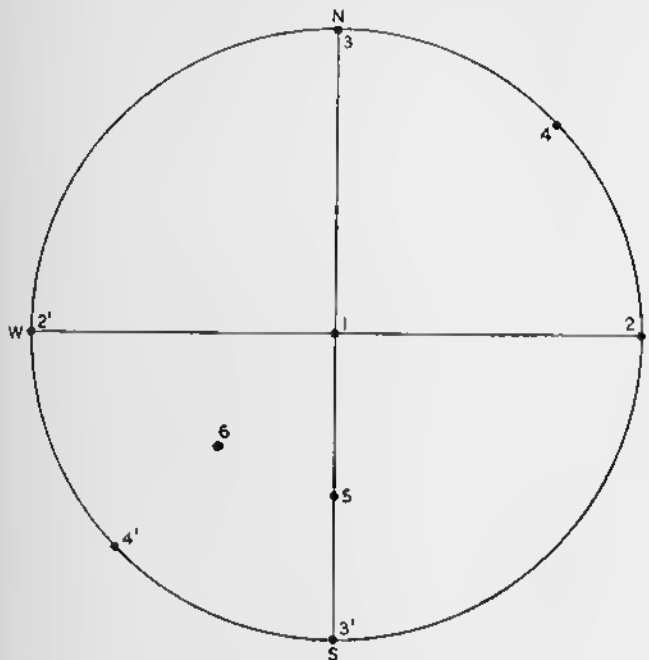


FIG. 100—Poles of Joints Plotted in a Circle. Numbers represent different joints. (See text.)

should be plotted for each vertical joint, or the reader may derive a wrong impression of their abundance. Which of the two possible points is to be plotted is an arbitrary matter.

The exact distance that a point lies from the center of the circle depends upon the size of the projection circle, the dip of the joint, and the type of projection used. The stereographic projection, as used in mineralogy, could be employed. More useful, however, is the *equal area projection*, which is also used in structural petrology (Chapter 18). The scale for a projection circle with a radius of 10 centimeters is shown in Fig. 101.

To plot the projection of the pole of a particular joint, one draws a line from the center of the circle at right angles to the strike of the joint and in the direction of dip. Using the scale

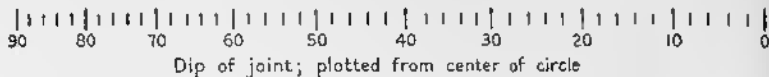


FIG. 101—Scale Used for Plotting Poles of Joints. To be used on a circle with a radius of 10 centimeters; based on equal area projection.

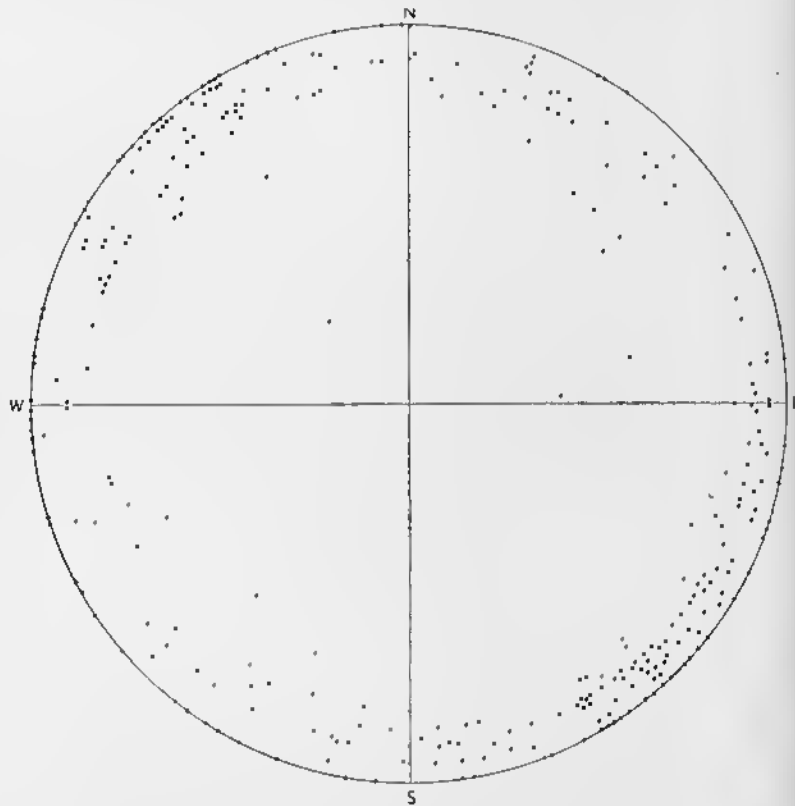


FIG. 102—Point Diagram of 311 Joints in Adirondack Mountains Shown in Fig. 96. Plotted on upper hemisphere.

in Fig. 101, one plots the dip outward from the center of the circle, which has a radius of 10 centimeters.

Fig. 102, which is a plot of the poles of the joints in the Adirondack Mountains shown in Fig. 96, is known as a *point diagram*. Points on the circumference of the circle indicate

vertical dips; such points could be placed at either end of a diameter and have been distributed arbitrarily in order to equalize the number of points on the circumference in opposite quadrants. This plot shows that practically all of the joints dip steeply, for the points are at or near the circumference of the circle. More-

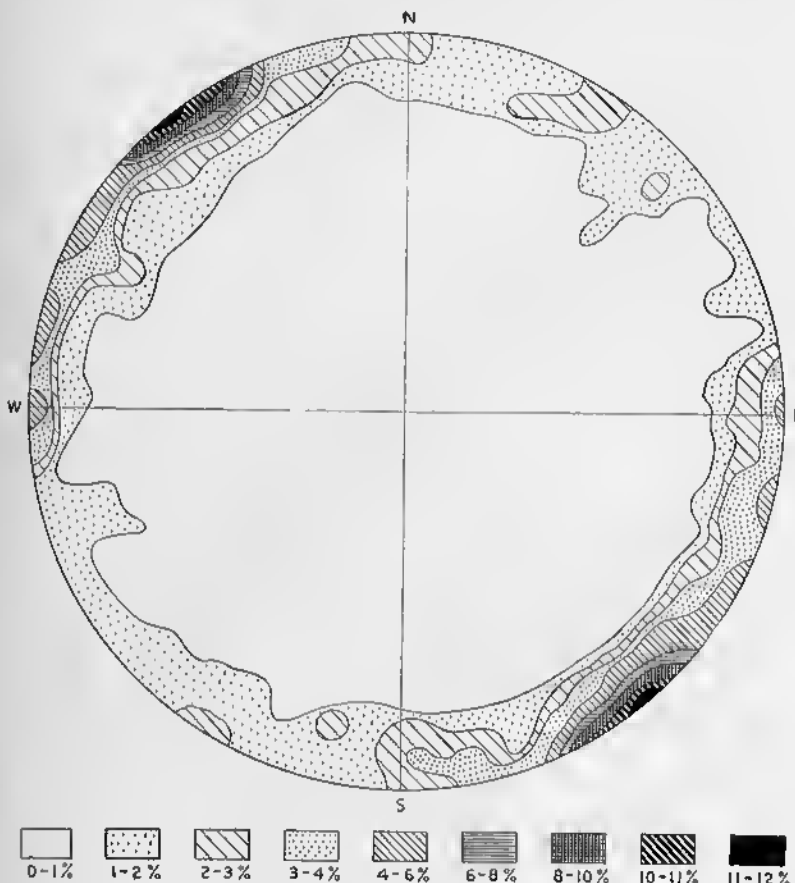


Fig. 103—Contour Diagram of 311 Joints in Adirondack Mountains Shown in Fig. 96. Plotted on upper hemisphere.

over, the greater concentration of points in the northwest and southeast quadrants indicates that the majority of the joints strike in a general northeasterly direction. This fact is also apparent from the map; Fig. 96.

From the point diagram a *contour diagram* may be prepared, such as that shown in Fig. 103. The solid black area, labeled

"11-12%," means that 11 to 12 per cent of all the points shown in the point diagram (Fig. 102) lie within an area equal to one per cent of the total area of the diagram. That is, if a small circle, covering an area equal to one per cent of the area of the large circle, were placed over this solid black area, it would contain 11 to 12 per cent of the points. The high percentages on

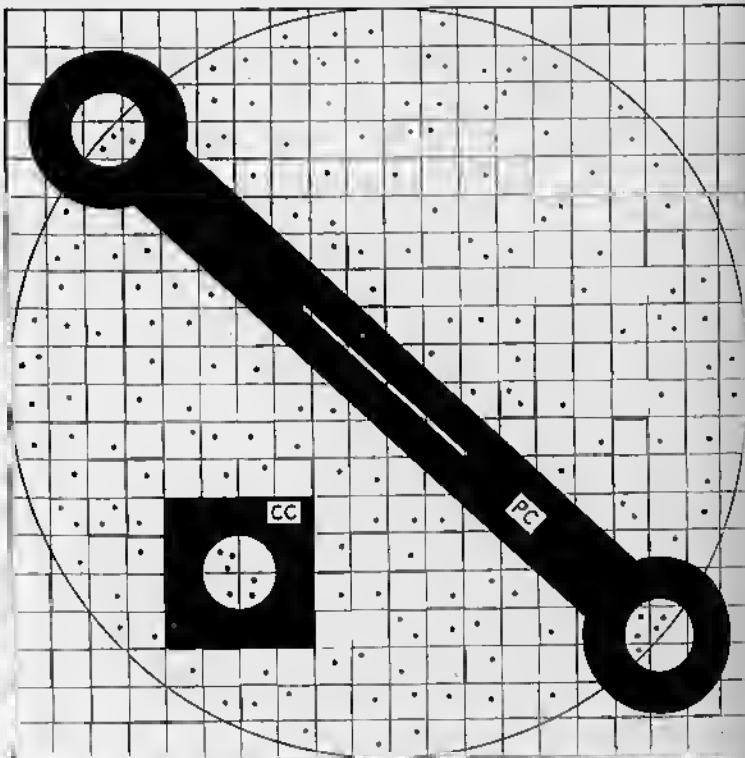


FIG. 104.—Method of Counting Points in Making Contour Diagram.  
CC = Center counter; PC = peripheral counter.

the circumference in the northwest and southeast quadrants indicate that the majority of the joints strike northeast and that they are essentially vertical.

The preparation of such a contour diagram from a point diagram is illustrated by Fig. 104. A piece of tracing paper is placed over the point diagram. The center counter, CC of Fig. 104, consists of a circular hole in the center of a piece of paper, celluloid, or any satisfactory material. The area

of this circle is equal to one per cent of the area of the large circle; if the large circle has a radius of 10 centimeters, the small circle has a radius of 1 centimeter. Two hundred points are plotted on Fig. 104. (Some of the 200 points are covered by the counters.) Six of these points lie within the center counter; six points are 3 per cent of the total number of points in the large circle, and the figure 3 is written in the center of the center counter. The center counter is moved over the whole diagram, and the percentage of points at each place is recorded. In order that the sampling may be systematic, a grid system is placed on the point diagram—or beneath it if the point diagram is on tracing paper—and the center counter is moved from left to right one centimeter at a time. After a traverse from left to right has been completed, the counter is moved down one centimeter, and a second traverse is run. It should be noted that a single point in the point diagram may lie within the center counter several times in its successive positions. The point is counted each time.

For points closer to the circumference than a distance equal to the diameter of the center counter—one centimeter if the large circle is 10 centimeters—a special technique is required. The peripheral counter (*PC* of Fig. 104) is used for such points; it is made of paper, cardboard, celluloid, or any satisfactory material. Half of each of the two circles at either end extends beyond the circumference of the large circle. The points in each circle are added together. In Fig. 104 they total 8, which is 4 per cent of the total 200. The figure 4 is then entered on the diagram in the center of *both* circles at the ends of the peripheral counter.

After the diagram has been covered with percentage figures, contours are drawn in the same manner by which topographic contours are prepared from points of known altitude.

There are various modifications of the technique outlined above, and for more complete discussion the reader is referred to Knopf and Ingerson.<sup>1</sup>

Representing the attitude of joints by point diagrams and contour diagrams is by far the most satisfactory method yet devised. Once a geologist has learned to read such diagrams,

<sup>1</sup> Knopf, E. B., and Ingerson, E., Structural Petrology, *Memoir 6, Geological Society of America*, pp. 245-251, 1938.

the diagrams are very serviceable. The same type of diagram may be used for faults, veins, and dikes. These diagrams are superior to maps because, although any systematic strike can be readily discerned on the map, one must read each dip figure in order to determine the attitude. These diagrams are useful only if the joint pattern is relatively homogeneous over the whole area being studied. They do not distinguish between joints in different parts of the area. The diagram for a group of vertical joints radiating from a common center would consist of points distributed more or less evenly around the circumference of the diagram. Vertical joints that strike in various directions, but are haphazardly distributed throughout the area, would give a diagram that is similar to or identical with that given by radiating joints.

Any method of recording joints on maps or diagrams introduces a quantitative problem. The strike and dip of the joint can be expressed quantitatively, but curving joints present a problem. Ordinarily, the average attitude is recorded. The joints may differ greatly in size, and it may be necessary to adopt some arbitrary system (such as using a heavy line for a "big" joint, a medium weight line for an "intermediate" joint, and a light line for a "little" joint) in order to indicate the magnitude of a joint. What is "big," "intermediate," or "little" is strictly relative, depending upon the local geology. Unless a very large scale map is employed, it may be impossible to plot all the joints on a map, and one symbol may have to represent 5 to 10 joints in those parts of the area where joints are abundant. If so, the weight of the line might indicate the number of joints represented by the symbol.

### Genetic Classification

In many instances it is difficult to ascertain the origin of joints. It is not always possible to distinguish *tension joints*, which form perpendicularly to forces tending to pull the rock apart, from *shear joints*, which are due to forces tending to slide one part of the rock past an adjacent part. Even if this can be done, and the attitude of the axes of strain can be established, it may be impossible to deduce with satisfaction the character of the external forces.

PLATE XII. Columnar Jointing in Lava at Great Face, Staffa, off the West Coast of Scotland. (Photo by K. Fowler-Billings.)





PLATE XIII. Columnar Jointing in Lava, at Fingal's Cave, Staffa, off the West Coast of Scotland. (Photo by K. Fowler-Billings.)

Tension joints due to a decrease in volume are one of the easiest types of joints to recognize. The columnar jointing in basalt is of this origin; this is the origin too of mud-cracks and joints in loess. An ideal example is a cooling horizontal sheet of basalt, either a flow or a sill. The basalt solidifies at about 1000° C., and during subsequent cooling it contracts. The resulting tensional forces act primarily in the horizontal plane, and are equal in all directions within this plane. When rupture eventually takes place, three vertical fractures, making angles of 120 degrees with each other, radiate out from numerous centers (Fig. 105). If the centers are evenly distributed, the

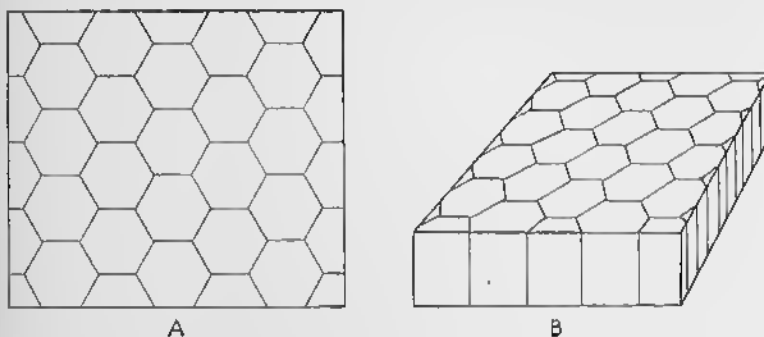


FIG. 105—Hexagonal Fractures in a Sheet. The tension results from loss of volume, due either to cooling of lava or desiccation of mud. A. Upper surface of sheet. B. Block diagram of sheet.

fractures bound vertical hexagonal columns. Actually, of course, the perfection of the hexagonal columns differs greatly, depending on many factors. In many instances the fractures are so irregularly distributed that the hexagonal form is unrecognizable (See also Pl. XII and XIII).

Theoretically, of course, the cooling of a horizontal sheet of solid basalt is a three-dimensional problem. Because of gravity, however, tension does not necessarily develop in the vertical direction, because the top of the basalt gradually lowers to take care of shrinking in this direction. In the horizontal plane, however, the sheet cannot shrink in size, and the tensional forces develop. Even in the vertical direction, however, tension is set up, and the hexagonal columns may be broken by horizontal cross fractures. In places, the cross fractures assume a "cup

and socket" form similar to the conical fractures found experimentally in ductile materials.

For simplicity of discussion it has been assumed that the sheet of basalt is horizontal. An analogous situation is found, however, if the sheet of basalt is vertical, as in a dike (p. 279). In this case the axes of the hexagonal columns are horizontal. The basalt is frozen to its walls, and, despite gravity, the shrinking sheet can not move as a unit. The tensional forces which develop are equal in all directions in the vertical plane.

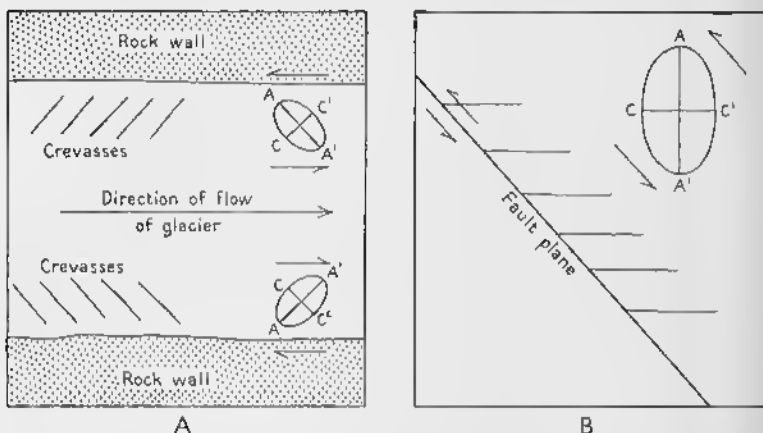


FIG. 106—Tension Fractures. A. Crevasses along side of glacier. Couples caused by friction are shown by smaller arrows. Ellipses represent orientation of strain ellipsoid. B. Cross section to show feather joints, which are represented by horizontal lines to right of fault plane. Arrows near fault show relative movement along it. Orientation of ellipse resulting from this movement shown in upper right hand corner. (After E. Cloos.)

Mud-cracks form because of forces similar to those in the cooling sheet of solid basalt. In this case, however, the shrinkage is due to the loss of water consequent to the desiccation of the wet mud.

Tension fractures due to a couple are represented by some of the crevasses in glaciers and by feather joints. Fig. 106A is a diagrammatic map of vertical crevasses that are diagonal to the contact between a glacier and the rock walls; the direction in which the ice flows is shown by the large arrow. The friction with the walls sets up couples, the nature of which is indicated by the smaller arrows. The intermediate axis of the strain ellipsoid is perpendicular to the surface of the ice, and the

greatest and least axes are respectively  $AA'$  and  $CC'$ . The tension cracks develop at right angles to the greatest strain axis,  $AA'$ .

Feather joints are tension fractures related to faulting. Fig. 106B is a vertical section of a fault on which the right-hand block has moved up relative to the left-hand block, as shown by the arrows along the fault. The intermediate axis of the strain ellipsoid is perpendicular to the plane of the paper, and  $AA'$  and  $CC'$  are oriented as shown in the figure. Tension joints which form perpendicularly to  $AA'$  may be confined to one side of the fault if the rocks on that side have a lower tensile strength than the rocks on the other side.

Tension joints in rising granite massifs will be described in Chapter 16.

Joints perpendicular to the axes of folds are common in orogenic belts (Fig. 107, plane  $ABCD$ ). Such joints may be *extension joints*, resulting from slight elongation parallel to the axes of the folds. They would be analogous to the ruptures that form parallel to the sides of specimens under compression (Fig. 87A).

Joints parallel to the axial planes of folds (Fig. 107, plane  $EFGH$ ) may be *release joints*, similar to those that form at right angles to the axis of compression when the load is released (Fig. 87B). Other joints with this attitude may be due to tension on the convex side of a bent stratum (Fig. 90).

Shear joints are difficult to recognize. If a joint is slicken-sided (p. 157), the opposite walls have obviously slipped past one another. But this is not proof that the fracture originated under shearing stress. The stress may have been tensional, and the sliding of walls past each other could be a later phenomenon. It is often supposed that tension fractures break around the pebbles of conglomerates, and that only shear fractures cut indiscriminately across pebbles and matrix. Although this may be true for loosely-consolidated conglomerates, apparently it is not a reliable criterion in well-cemented conglomerates.

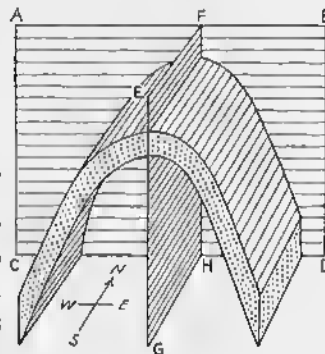


FIG. 107—Fold with Vertical Dip and Vertical Strike Joint.  $ABCD$  = Vertical dip joint.  $EFGH$  = Vertical strike joint. Modified from B. and R. Willis, *Geologic Structures*, 3d ed., McGraw-Hill Book Co., 1934.

Two sets of joints that intersect at a high angle to form a conjugate system are often considered shear fractures, especially if they are symmetrically disposed about the strain axes. Such a disposition simulates the two circular sections of the strain ellipsoid. Fig. 108A is a block diagram of an area in which horizontal fold axes trend north-south. There are two sets of vertical joints, one of which strikes northwest, and the other of which strikes northeast. The attitude of the folds indicates that the compressive force was acting along east-west lines. In the light of experimental observations, the joints could be interpreted as shear fractures that developed due to a compressive

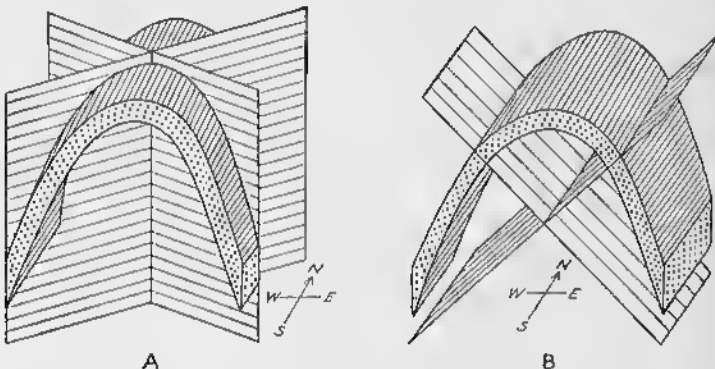


FIG. 108—Folds with Conjugate Joint Systems. A. Fold with vertical diagonal joints. B. Fold with strike joints dipping about 45 degrees. Modified from B. and R. Willis, *Geologic Structures*, 3d ed., McGraw-Hill Book Co., 1934.

force acting in an east-west direction, with the easiest relief in a north-south direction.

Interpreting such joints in terms of the strain ellipsoid, the intermediate axis is parallel to the intersection of the two sets of joints, and it is therefore perpendicular to the surface of the earth. The least and the greatest strain axes are horizontal, and they bisect the angles between the shear fractures; one axis strikes east-west, the other strikes north-south. The attitude of the joints gives no direct clue whether the least or the greatest strain axis strikes north-south. The least strain axis, because it is presumably at right angles to the axis of the fold (Fig. 108A), must strike east-west.

Fig. 108B is a block diagram of an area in which the horizontal fold axes trend north-south and in which the axial planes

are vertical. Two sets of joints strike north-south, but one set dips about 45 degrees east, whereas the other set dips about 45 degrees west. Such a conjugate system can also be interpreted as shear fractures due to an east-west compressive force, but under such conditions that the easiest relief was upwards. In terms of the strain ellipsoid, the intermediate axis of the strain ellipsoid is horizontal and trends north-south; the least strain axis is horizontal and trends east-west, and the greatest strain axis is perpendicular to the surface of the earth.

Shear joints can result from a couple. Fig. 109, for example, is a map of an area in which there are two sets of vertical joints,



FIG. 109—Map Showing Vertical Shear Joints Caused by a Couple. Solid black is key bed. Faults are vertical; movement parallel to strike of fault.

one set striking northeast, the other striking northwest. These joints are in a block bounded by two northwesterly-striking vertical faults, along both of which the northeasterly wall has moved northwest relative to the southwest wall. The central block was subjected to a couple; utilizing the concept of the strain ellipsoid, as illustrated in the lower right-hand corner, the intermediate axis would be perpendicular to the surface of the earth, and the strain axes  $AA'$  and  $CC'$  would trend respectively north-south and east-west. The shear fractures would be essentially parallel to the two circular sections,  $SS'$  and  $S''S'''$ , corresponding to the joints shown on the map.

Although such explanations of conjugate joint systems as those given on the preceding pages are plausible and account

for all the facts, other interpretations cannot always be eliminated. A conjugate system might conceivably form if the rocks are subjected to tension which acts in one direction at one time and in a different direction at another time. In such a case, the younger set would generally abut against the older set. Dikes or veins might fill some joints in one set, but none in the second. If, however, the two sets of joints are shear fractures, no essential difference in age should be apparent. Although individual joints of one set may be younger or older than joints of the other set, there should be no systematic age difference.

In general, the structural geology of a large area must be well-understood in order that the joints may be interpreted correctly. Even under such circumstances, several interpretations may explain the facts equally well, and a unique solution cannot be obtained.

A discussion of joints related to magmatic intrusion has been reserved for Chapter 16, in which granite tectonics will be discussed.

### Sheeting

Sheeting, a form of rupture similar to jointing, is best exposed in artificial openings, such as quarries. The sheeting surfaces are somewhat curved and are essentially parallel to the topographic surface, except in regions where there has recently been rapid erosion. The fractures are close together at the surface of the earth, and in many places the interval between them is measured in inches. The interval increases with depth, and a few tens of feet beneath the surface the visible sheeting disappears. At greater depths, however, invisible planes of weakness parallel to the sheeting are utilized by quarrymen in their work. Although sheeting is best developed in granitoid rocks, it is also observed in sandstone.

Various hypotheses have been developed to explain sheeting. According to one of these, the sheeting in granite is parallel to the upper contact of the intrusive body and formed as tension cracks during the cooling of the rock after it had crystallized. In such an interpretation the topography is controlled by the sheeting, rather than the sheeting by the topography. Numerous field examples, however, show that this hypothesis is

untenable, because the sheeting is unrelated to the igneous contacts.

According to a second hypothesis, the sheeting is a tensional phenomenon due to the release of load during erosion. Although it is evident that a mass of rock approaching the surface is under a constantly decreasing load and will expand, it is difficult to understand why the expansion should lead to rupture. Nevertheless, as has been stated on p. 103, the release of the compressional force on specimens that have been under high confining pressure sometimes causes ruptures perpendicular to the axis of compression.

A third hypothesis is similar in some respects to the second hypothesis. Because of progressive lowering of the surface of the earth due to erosion and consequent decrease in the confining pressure, the rock expands in all directions. The vertical expansion is unimpeded and only air has to be pushed away. The horizontal expansion is hindered by rock. Compressional forces parallel to the surface of the earth develop and cause rupture. Shear fractures would be inclined at angles of about 45 degrees to the surface of the earth. Extension fractures, as described on p. 103, would be parallel to the surface. This is the most acceptable interpretation of sheeting.

## Description and Classification of Faults

### General Characteristics

Faults are ruptures along which the opposite walls have moved past each other. The essential feature is differential movement parallel to the surface of the fracture. Some faults are only a few inches long, and the total displacement is measured in fractions of an inch. At the other extreme, there are faults that are hundreds of miles long with a displacement measured in miles and even tens of miles.

The strike and dip of a fault are measured in the same way as they are for bedding or jointing. The strike is the trend of a horizontal line in the plane of the fault. The dip is the angle between a horizontal surface and the plane of the fault, and is measured in a vertical plane that strikes at right angles to the fault. The *hade* is the complement of the dip; that is, the hade equals ninety degrees less the angle of dip. The hade may also be defined as the angle between the fault plane and a vertical plane that strikes parallel to the fault. Hade is a relatively obsolete term, but is common in the older literature. In Fig. 110 the front of the block is a plane that strikes east-west and dips vertically. The right-hand side of the block strikes north-south and has a vertical dip. The fault is an inclined plane that strikes north-south, dips 35 degrees east, and has a hade of 55 degrees east.

The block above the fault is called the *hanging wall* (Fig. 110); the block below the fault is the *footwall*. A person standing upright in a tunnel along a fault would have his feet on the footwall, and the hanging wall would hang over him. It is obvious that vertical faults have neither a footwall nor a hanging wall.

Although many faults are clean-cut, in many instances the displacement is not confined to a single fracture, but is dis-

tributed through a *fault zone*, which may be hundreds, even thousands, of feet wide. The fault zone may consist of numerous interweaving small faults, or it may be a confused zone of breccia or mylonite (p. 158). *Distributive faulting* occurs if the differential movement takes place by systematic small displacements along a large number of closely spaced fractures.

The intersection of the fault with the surface of the earth is known as the *fault line*, *fault trace*, or *fault outcrop* (Fig. 110). In most instances, the fault line, as it appears on a map, is

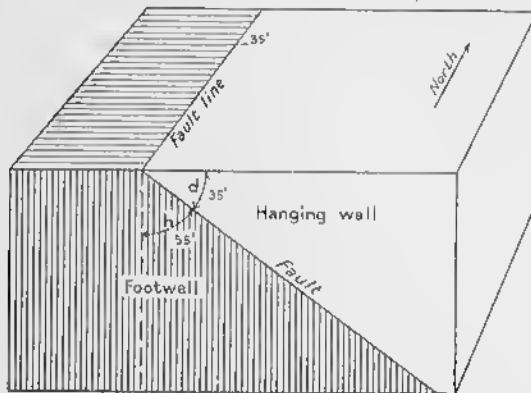


FIG. 110—Terminology for a Fault Plane.  $d$  = dip,  
 $h$  = hade.

reasonably straight or somewhat sinuous. If, however, the dip of the fault is low and the topographic relief high, the fault line may be exceedingly irregular.

### Nature of Movement along Faults

#### Translatory and rotational movements

The movement along faults may be translatory or rotational. In Fig. 111, diagrams *A* and *B* illustrate translatory movement, whereas diagrams *C* and *D* illustrate rotational movement.

In *translatory movement* there has been no rotation of the blocks relative to each other; all straight lines on opposite sides of the fault and outside the dislocated zone that were parallel before the displacement, are parallel afterwards.

In Fig. 111A, two points, *a* and *a'*, contiguous before faulting, have been separated by the faulting. The right-hand block has

moved directly down the dip of the fault relative to the left-hand block. The lines  $bc$  and  $c'd$ , which were parallel before faulting, are also parallel after faulting. In Fig. 111B, the right-hand block has moved diagonally down the fault; the lines  $bc$  and  $c'd$ , parallel to each other before faulting, are also parallel after faulting.

*Rotational movements* are those in which some straight lines on opposite sides of the fault and outside the dislocated zone, parallel before the displacement, are no longer parallel afterwards. In Fig. 111C, the right-hand block has gone down relative to the left-hand block, but the displacement increases toward the front; at point  $a$  there has been no displacement, but  $b$  and  $b'$  were contiguous before faulting. Lines  $ca$  and  $ad$ , parallel before faulting, are not parallel after faulting. In Fig. 111D, the back part of the right-hand block has gone up relative to the left-hand block, but the forward part of the right-hand block has gone down. The lines  $dc$  and  $c'e$ , parallel before faulting, are no longer parallel after faulting. A line within the fault plane, and separating that part of the right-hand block that has gone up from that part that has gone down, is known as the *hinge* or *hinge line*.

In a sense, all faults have a certain amount of rotational movement. The displacement increases or decreases along the strike of all faults, and the blocks must rotate somewhat relative to one another. But if the rotation is not too great, the movements at any one locality may be treated as if the fault were a translatory one.

#### *Relative movements*

A rather elaborate terminology has, of necessity, been devised to describe the movement along faults and the effects on disrupted strata. The terminology has been devised primarily for translatory movements, but it may be used with modifications for rotational movements.<sup>1</sup>

<sup>1</sup> Throughout this book the terminology advocated by a committee of the Geological Society of America has been followed. See Reid, H. F., and others, Report of the committee on the nomenclature of faults: *Bulletin Geological Society of America*, Vol. 24, pp. 163-186, 1913.

Faults in themselves never offer any direct evidence as to which block actually moved. Thus, in Fig. 111A, the right-hand block may have gone down and the left-hand block may have remained stationary, or, the left-hand block may have gone

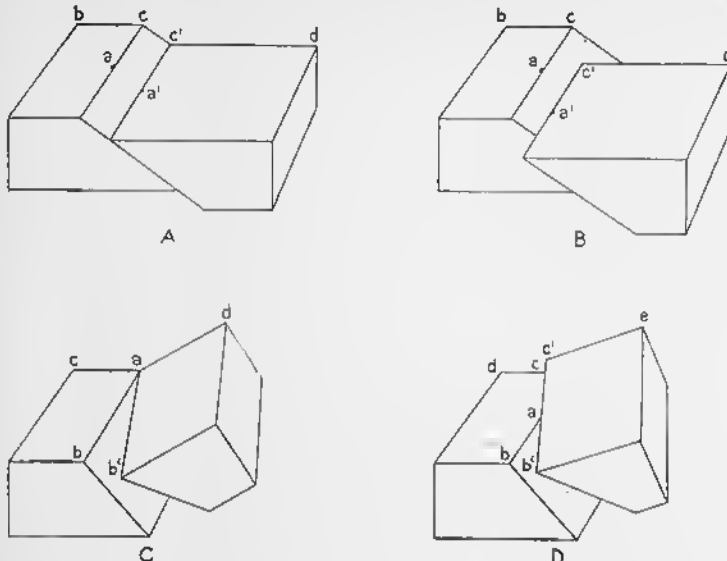


FIG. 111.—Translatory and Rotational Movements. A. and B. Translatory movements. C. and D. Rotational movements. Small letters are referred to in text.

up and the right-hand block may have moved down; both blocks may have gone down, but the right-hand block may have gone down more than the left-hand block, or, both blocks may have gone up, but the left-hand block may have gone up more than the right-hand block. Because in most cases no direct evidence is available concerning the absolute movements, the terminology is based chiefly on relative movements.

Fig. 112 illustrates some of the various kinds of relative movements that may take place along a translatory fault. In diagram *A* the hanging wall has moved directly down the dip relative to the footwall; in diagram *B* the hanging wall has moved parallel to the strike; and in diagram *C* the hanging wall has moved diagonally down the fault plane. In diagram *D* the hanging wall has moved directly up the dip of the fault, and in diagram *E* the hanging wall has moved diagonally up the fault plane.

The term *slip* is used to indicate the relative displacement of formerly-adjacent points on opposite sides of the fault, and it is measured in the fault surface. The *net slip* ( $ab$  of Fig. 112) is the total displacement, and is the distance measured on the

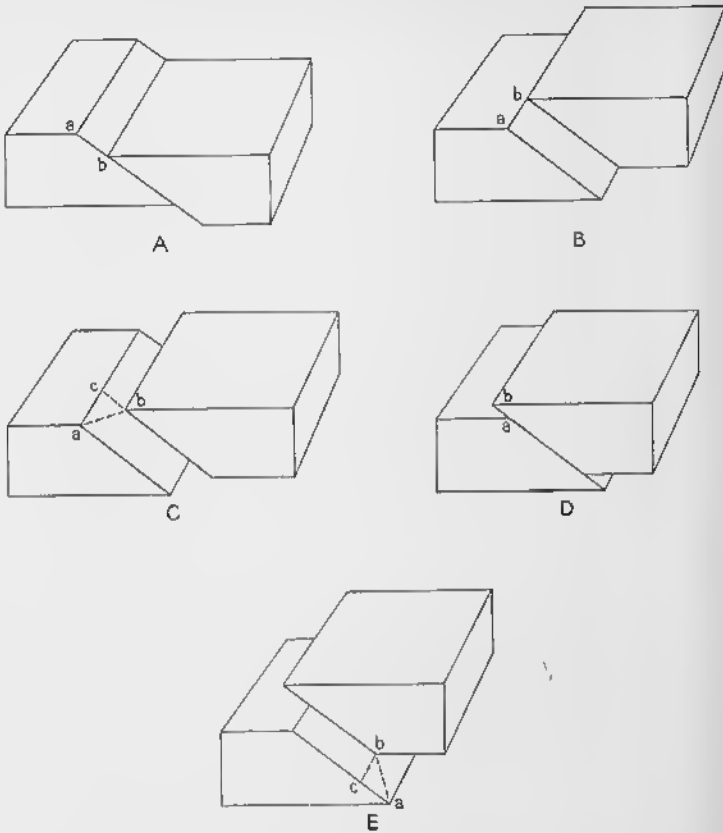


FIG. 112—Net Slip, Dip Slip, and Strike Slip. A.  $ab$  = net slip = dip slip; strike slip is zero. B.  $ab$  = net slip = strike slip; dip slip is zero. C.  $ab$  = net slip;  $cb$  = dip slip;  $ac$  = strike slip. D.  $ab$  = net slip = dip slip; strike slip is zero. E.  $ab$  = net slip,  $bc$  = strike slip,  $ac$  = dip slip.

fault surface between two formerly-adjacent points situated on opposite walls of the fault. It is defined in terms of the distance and the angle it makes with some line in the fault plane, such as a horizontal line or a line directly down the dip. In Fig. 112C, the net slip,  $ab$ , makes an angle of  $35^\circ$  with a horizontal line in the fault plane; the distance depends, of course, on the scale. It is

also necessary to state the relative movement; in this case the hanging wall went down relative to the footwall. It is equally correct to say that the footwall went up relative to the hanging wall. The *strike slip* is the component of net slip parallel to the strike of the fault; it is indicated by  $ac$  in Fig. 112C. The *dip slip* is the component of the net slip measured parallel to the dip of the fault plane; it is  $bc$  of Fig. 112C. In Figs. 112A and 112D,

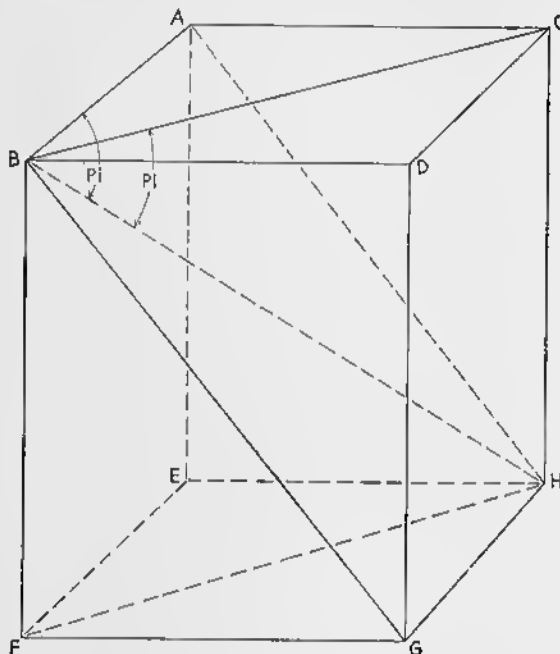


FIG. 113—Pitch and Plunge. The line  $BH$  lies in the plane  $ABGH$ . Angle  $ABH$  = pitch; angle  $CHH$  = plunge.

the dip slip equals the net slip, and the strike slip is zero. In Fig. 112B, the strike slip equals the net slip,  $ab$ , and the dip slip is zero. In Fig. 112E, inasmuch as the movement is diagonal, there is both a dip slip,  $ac$ , and a strike slip,  $bc$ , component to the net slip,  $ab$ .

The *pitch* is the angle that a line in a plane makes with a horizontal line in that plane. Thus, in Fig. 113, the plane  $ABGH$  dips to the right and contains the line  $BH$ . The angle  $ABH$  is the pitch of  $BH$ . Plunge was defined on pp. 43–44; the only vertical plane in Fig. 113 that contains  $BH$  is the plane

*BCFH.* The angle  $CBH$  is the plunge. The pitch, the angle  $ABH$ , as measured in the plane  $ABGH$ , is about  $57^\circ$ ; the plunge, the angle  $CBH$ , as measured in the plane  $BCFH$ , is about  $45^\circ$ .

In Fig. 112C, the pitch of the net slip is the angle  $bac$ ; in Fig. 112E, the pitch is the angle  $cba$ .

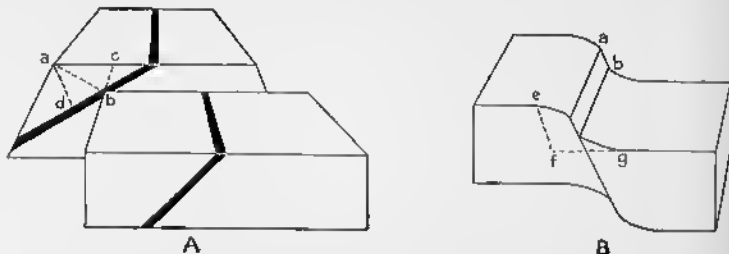


FIG. 114—Slip and Shift. A, Fault dips toward reader; black is a stratum of rock.  $ab$  = net slip,  $ac$  = strike slip,  $cb$  = dip slip,  $db$  = trace slip,  $ad$  = perpendicular slip. B,  $ab$  = net slip = dip slip; strike slip is zero.  $ef$  = net shift = dip shift; strike shift is zero.

In Fig. 114A, the fault intersects a bed or vein, which is shown in solid black; the fault dips toward the reader. The *trace slip* is that component of the net slip parallel to the trace of the bed on the fault. In Fig. 114A, the net slip is  $ab$ , the strike slip is  $ac$ , and the dip slip is  $bc$ . The trace slip is  $db$ .

The *perpendicular slip* is that component of the net slip measured perpendicularly to the trace of the bed on the fault; it is  $ad$  of Fig. 114A.

A vertical plane perpendicular to the strike of the fault contains the dip slip. The front of the block shown in Fig. 115 represents such a plane, and  $ad$  is the dip slip. The horizontal component of  $ad$  is  $ed$ , and the vertical component is  $ae$ . By some geologists  $ed$  is called the heave and  $ae$  is called the throw.

FIG. 115—Components of Dip Slip.  $ab$  = net slip,  $ac$  = strike slip,  $cb$  =  $ad$  = dip slip.  $ae$  = vertical component of dip slip, called *throw* by many geologists.  $ed$  = horizontal component of dip slip, called *heave* by many geologists.

As will be shown later, however, this usage is undesirable.

The slip refers to the displacements along the fault plane itself. If there is drag along the fault, however, the total

displacement may be of more significance than the slip. The term *shift* is used to refer to the displacement on opposite sides of the fault and outside the dislocated zone. Fig. 114B illustrates a fault along which there has been drag; the movement has been directly down the dip. The dip slip,  $ab$ , equals the net slip in this case. The net shift is  $ef$ ; the dip shift is the same. The strike shift in this case is zero.

#### Effects on disrupted strata

The above discussion has been confined to the relative movements along faults, and it has not considered the effects on the

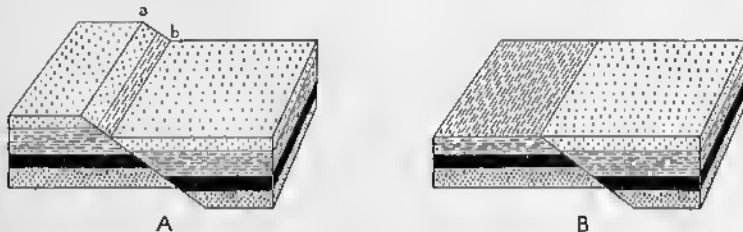


FIG. 116—Apparent Displacement in a Vertical Section Equals the Net Slip. A. Before erosion;  $ab$  = net slip = dip slip. B. After erosion of top of footwall block.

disrupted strata or veins. The apparent movement of the disrupted stratum may be very different from the net slip. This point is very important and cannot be overemphasized. The apparent movement is a function of many variables, and depends not only on the net slip, but also on the strike and dip of the fault, the strike and dip of the disrupted stratum, and the attitude of the surface on which the observations are made. It is possible for the apparent movement to be zero, although the net slip may be great.

Figs. 116 to 125 show the relationship between the net slip and the apparent movement under different conditions. In Fig. 116, the beds are horizontal, and the net slip  $ab$  is directly down the dip. Fig. 116A illustrates relations before erosion, and Fig. 116B illustrates the relations after the left-hand block has been eroded down to the level of the right-hand block. On the map—the upper surface of Fig. 116B—different beds outcrop on opposite sides of the fault. On the front of the blocks, the apparent movement equals the net slip. A deep valley or an

## 138 DESCRIPTION AND CLASSIFICATION OF FAULTS

artificial opening, such as a quarry or mine, might produce an exposure of this sort.

In Fig. 117, the net slip,  $ab$ , is parallel to the strike of the fault. In Fig. 117B, the front of the left-hand block has been eroded back to coincide with the front of the right-hand block.

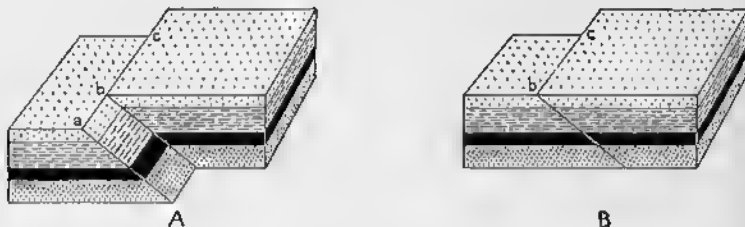


FIG. 117—Apparent Displacement in a Vertical Section Is Zero. A.  $ab$  = net slip = strike slip. B. After removal of front of footwall block.

Such an exposure might be found on the side of a valley or in an artificial opening. The apparent movement in such a section is zero, although the net slip may be considerable. If the net slip were diagonally down the fault plane, a vertical section at right angles to the strike of the fault would show an apparent movement, but the value would be less than the net slip.

Figs. 118 to 121 illustrate faults that strike at right angles to the strike of the bedding. In Fig. 118, the net slip,  $ab$ , is

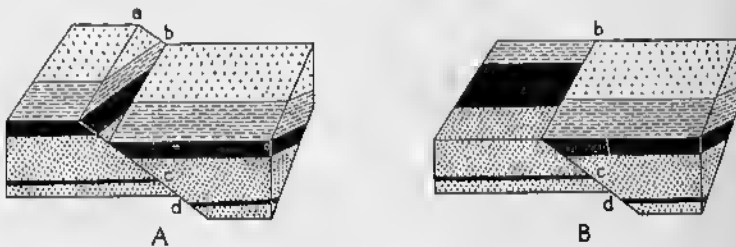


FIG. 118—Apparent Displacement in Vertical Section Equals Net Slip. A.  $ab = cd$  = net slip = dip slip. B. After erosion of top of footwall block.

directly down the dip. Fig. 118A shows the relations before erosion; Fig. 118B shows the relations after the left-hand block has been eroded down to the level of the right-hand block. On the map—the upper surface of Fig. 118B—the apparent movement is such as to suggest that the left-hand block moved back a

considerable distance parallel to the strike of the fault. If the beds have a low dip, a comparatively small net slip down the dip can give a large apparent displacement on the map. The apparent movement on the front of the blocks, Fig. 118, equals the net slip.

In Fig. 119, the net slip is parallel to the strike of the fault; Fig. 119A depicts the relations before erosion; Fig. 119B indicates the relations after the removal of the front of the left-hand block.

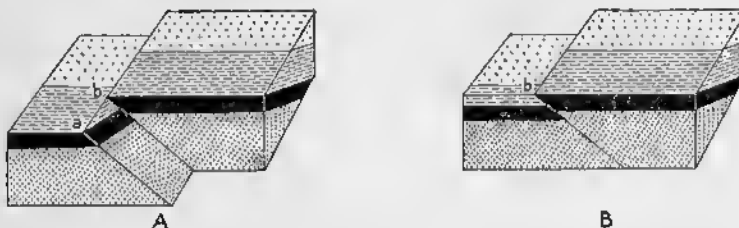


FIG. 119—Apparent Displacement in a Vertical Section Gives Erroneous Impression That Hanging Wall Has Gone Up. A.  $ab$  = net slip = strike slip. B. After removal of front of footwall block.

cates the relations after the front of the left-hand block has been eroded back to coincide with the front of the right-hand block. On the map the apparent movement equals the net slip. But the apparent movement on the front of the block, Fig. 119B, gives the false impression that the hanging wall has moved up.

In Fig. 120, the net slip,  $n$ , has been diagonally down the dip. After the surface and front of the left-hand block have

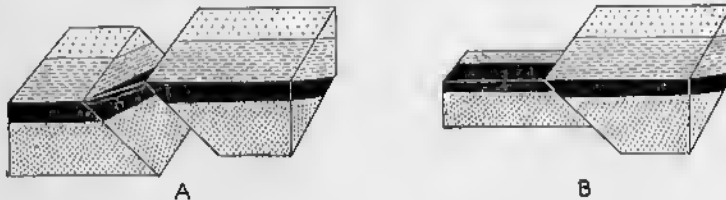


FIG. 120—Apparent Displacement in Vertical Section Is Less than Net Slip. A.  $n$  = net slip. B. After removal of top of footwall block.

been eroded to the surface and front of the right-hand block, respectively, the relations are those illustrated in Fig. 120B. On the map, the left-hand block has apparently moved back; in the structure section the right-hand block has apparently moved down.

Fig. 121 illustrates the special case in which the net slip is parallel to the trace of the bedding on the fault plane. Fig.

Fig. 121B shows the relations after erosion of the top and front of the left-hand block. There is no apparent movement either on the map or on the front of the block. In fact, the generalization may be made that wherever the net slip is parallel to the trace of the disrupted stratum on the fault plane, there is no

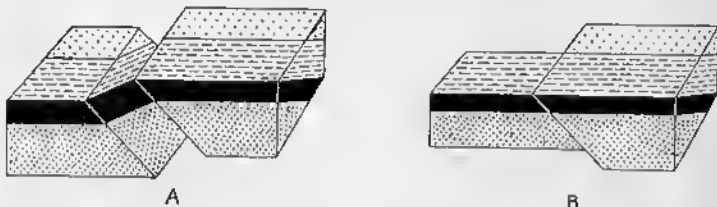


FIG. 121.—Net Slip Parallel to Trace of Bedding on Fault. Apparent movement in a vertical section and in map is zero. A. Immediately after faulting. B. After removal of top and front of footwall block.

apparent movement on the map or cross sections.<sup>2</sup> Fig. 117 also illustrates this principle.

Fig. 122 is an example of a fault that strikes parallel to the strike of the disrupted strata. The hanging wall has gone down relative to the footwall. The apparent movement in the front of the block in Fig. 122A equals the net slip. On the map of Fig. 122B, some of the beds are repeated because of the faulting. If the net slip were parallel to the strike of such a fault, there would be no apparent movement, because the net slip would be

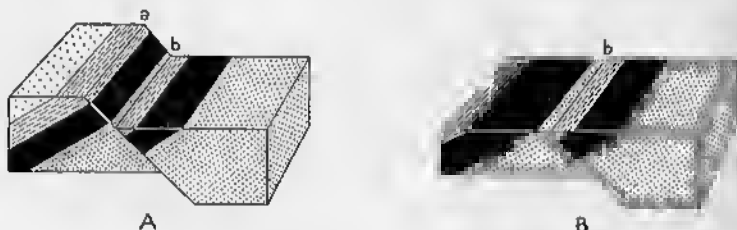


FIG. 122.—Apparent Displacement in Vertical Section Equals Net Slip. A.  $ab = \text{net slip} = \text{dip slip}$ . B. After removal of top of footwall block.

parallel to the trace of the beds on the fault. If the hanging wall were to move diagonally down the dip, some of the beds would be repeated, but the apparent movement on a cross section at

<sup>2</sup> Beckwith, R. H., Trace-slip faults: *Bulletin American Association Petroleum Geologists*, Vol. 25, pp. 2181-2193, 1941.

right angles to the strike of the fault would be less than the net slip.

Fig. 123 illustrates a fault that strikes parallel to the strike of the strata, but the hanging wall has moved up relative to the footwall. The net slip is the same as the apparent movement

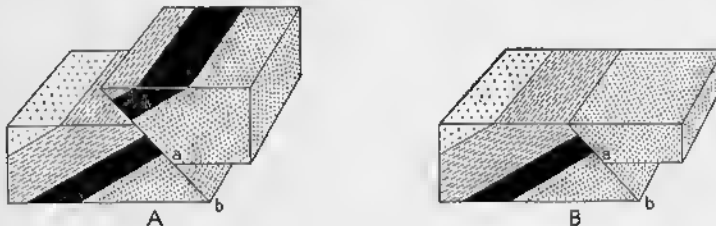


FIG. 123—Apparent Displacement in Vertical Section Equals Net Slip. A.  $ab =$  net slip = dip slip. B. After removal of top of hanging wall block.

on the front of the block in Fig. 123A. If the right-hand block is eroded to the level of the left-hand block, the bed shown in solid black does not crop out at the surface.

Fig. 124 is the special case in which the fault and the strata have not only the same strike, but have also the same dip. It is obvious that, in such a case, the apparent movement on the map and in the cross section is zero, regardless of the value of the net slip.

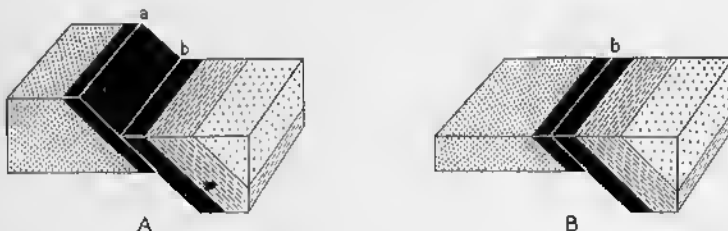


FIG. 124—Fault Is Parallel to Bedding, and Hence There Is No Apparent Displacement. A.  $ab =$  net slip = dip slip. B. After removal of top of footwall block.

Fig. 125 represents the case where the fault strikes diagonally to the strata, and where the hanging wall has moved directly down the dip of the fault. After erosion, as shown in Fig. 125B, the apparent movement on the map suggests that the hanging wall has moved back relative to the footwall.

These numerous examples have been cited to emphasize that the apparent movement may be very deceiving. Moreover, it is disconcerting to realize that even if we know the dip and strike of the fault, the dip and strike of the disrupted strata, and the apparent movement, it is nevertheless impossible to determine the net slip. Suppose, for example, that the geologist mapped an area such as that shown on the top of the block diagram in Fig. 118B. The attitude of the bedding and of the fault are known; moreover, the apparent movement along the fault is given by the map. Actually, the net slip was directly down the dip. But the observed, apparent movement on the map could have resulted equally well from a horizontal movement parallel to the strike of the fault—that is, if the left-hand block moved backward relative to the right-hand block. Moreover, diagonal movement down the dip of the fault would have produced the same effect on the map.

### Calculation of net slip

The amount and nature of the movement can be determined, however, if the strike and dip of the fault and the strike and dip of two or more planes with different attitudes are broken by the fault. Fig. 126A is an example of two dikes,  $aa'a''a'''$  and  $bb'b''b'''$ , that have different attitudes and are displaced along a fault. This problem can be solved by graphical methods; the pitch of the net slip is 85 degrees toward the northeast, and the hanging wall (north block) has moved up relative to the footwall; the value of the net slip is 175 feet. The disrupted bands may be dikes, veins, bedding planes, or older faults.

Even if data are available for only one disrupted band, the problem can be solved if the direction of movement is known. The striations on a slickensided surface (p. 157) may show the direction of movement, but this method is dangerous, for as is stated on p. 157, slickensides may record only the last movements along the fault plane. Fig. 126B shows how this method may be used. In addition to the data indicated on the map, it is known that the striations pitch 45 degrees toward the northeast. The net slip may be calculated by graphical methods to be 260 feet. See also pp. 444-453.

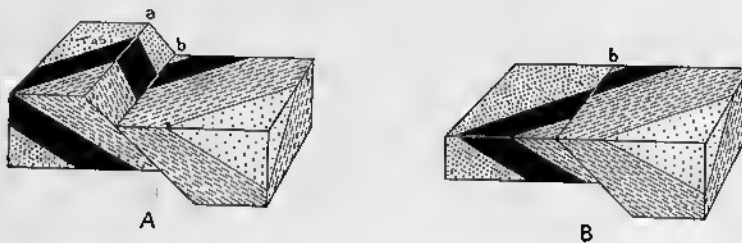


FIG. 125—Apparent Displacement on Map Does Not Equal the Net Slip. A.  $ab = \text{net slip} = \text{dip slip}$ . B. After removal of top of footwall block.

### Throw and heave

The *throw* and *heave* are measured in a vertical section that is perpendicular to the strike of the fault. The throw is the vertical component of the apparent movement in such a section; heave is the horizontal component.

Figs. 127 and 128 illustrate these terms. Fig. 128 is an example in which the fault strikes parallel to the strata, and in which the movement has been directly down the dip. Fig. 128A is a block diagram, and Fig. 128B, a cross section at right angles to the fault, is the same as the front of the block diagram. The throw is  $ad$ , and the heave is  $db$ . In this particular case, they are respectively the vertical and horizontal components of the net slip, which also equals the dip slip. However, this is not always true. Fig. 127 shows a fault that is diagonal to the strike of the disrupted stratum. Fig. 127A is a block diagram, and Fig. 127B is a vertical section perpendicular to the strike of the

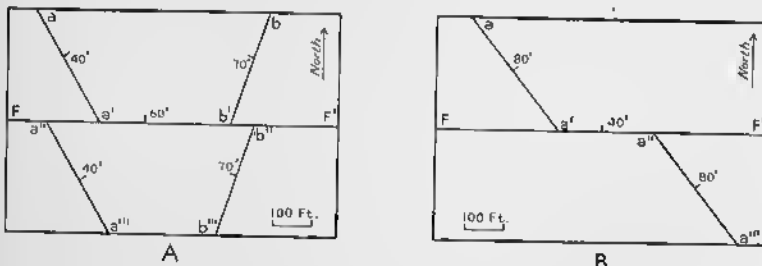


FIG. 126—Calculation of Net Slip. A.  $aa'a''a'''$  and  $bb'b''b'''$  are two veins displaced along the fault  $FF'$ . With these data the net slip can be calculated. B.  $aa'a''a'''$  is a vein displaced along the fault  $FF'$ . The net slip cannot be calculated unless some additional data are available.

fault; the throw is  $df$ , and the heave is  $fe$ . The vertical component of the dip slip ( $cb$ ) is  $ib$ , and the horizontal component of the dip slip is  $ci$ . They are obviously different from the throw and heave.

It is clear that throw and heave refer to the effects on the disrupted band. If two bands with different attitudes, such as two dikes, are broken by a fault, each of them has a different value for the throw and heave. Many geologists feel that the terms should refer only to the movement along the fault, and that they should be independent of the effect on the disrupted bands. These geologists use throw for the vertical component

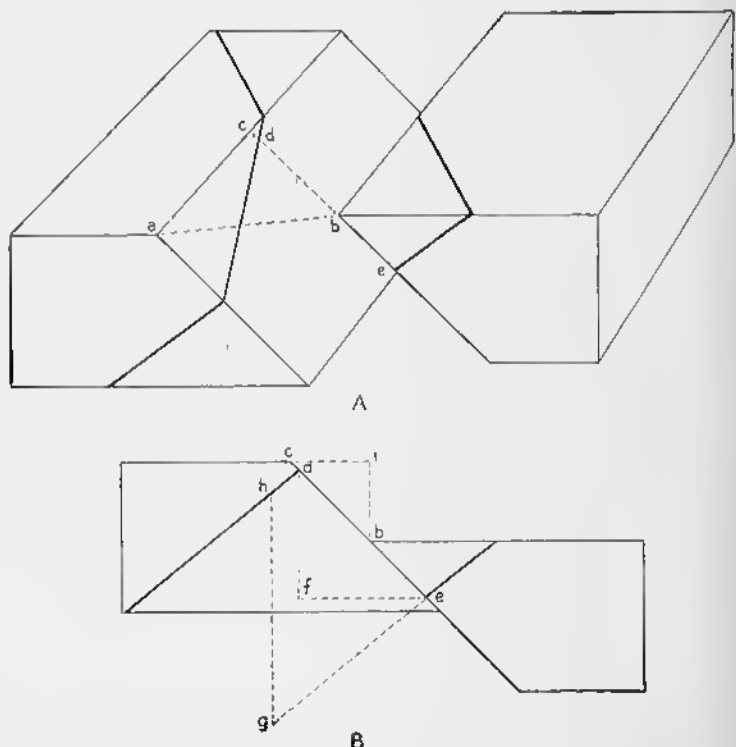


FIG. 127—Throw and Heave. Heavy black band is disrupted stratum. A. Block diagram;  $ab$  = net slip,  $ac$  = strike slip,  $cb$  = dip slip. B. Vertical cross section perpendicular to the strike of the fault; along same plane as front of hanging wall block of block diagram.  $cb$  = dip slip;  $ib$  = vertical component of dip slip, *throw* to some geologists;  $ci$  = horizontal component of dip slip, *heave* to some geologists;  $de$  = apparent displacement;  $df$  = *throw*;  $fe$  = *heave*;  $hg$  = vertical separation.

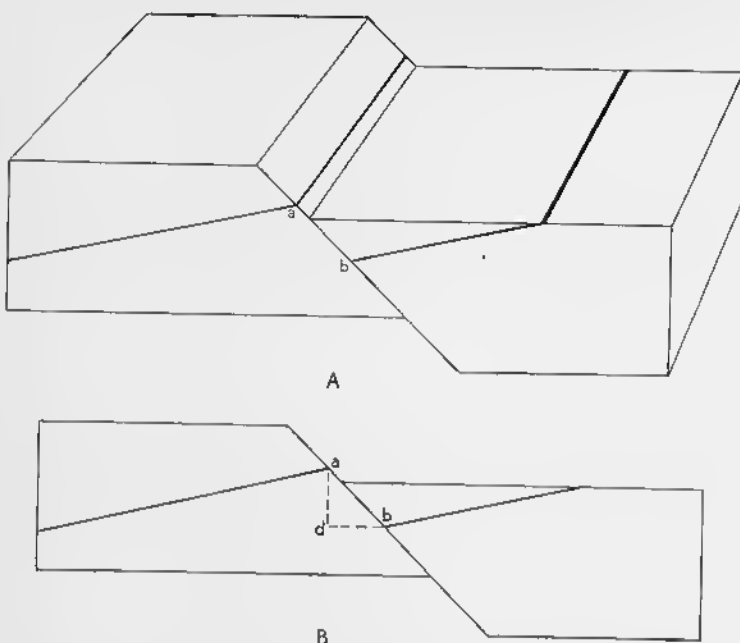


FIG. 128—Throw and Heave. Heavy black band is disrupted stratum. A. Block diagram;  $ab$  = net slip = dip slip. B. Vertical cross section perpendicular to strike of fault. Same as front of block diagram above.  $ab$  = net slip = dip slip,  $ad$  = throw,  $db$  = heave.

of the dip slip ( $ib$  of Fig. 127B), and they use heave for the horizontal component of the dip slip ( $ci$  of Fig. 127B).

### Separation

*Separation* indicates the distance between the two parts of the disrupted horizon measured in any indicated direction. The *vertical separation* is the separation measured along a vertical line. In Fig. 130B, a vertical section perpendicular to the fault,  $eg$  is the vertical separation. A measurement along any other vertical line, such as  $hi$ , would give the same value. The *horizontal separation* is the separation measured in any indicated horizontal direction. Fig. 131A is a map of a fault and a disrupted horizon;  $we$  is the horizontal separation in an east-west direction;  $ns$  is the horizontal separation in a north-south direction;  $hi$  is the horizontal separation parallel to the strike of the fault. A special term, *offset* or *normal horizontal separation*, is

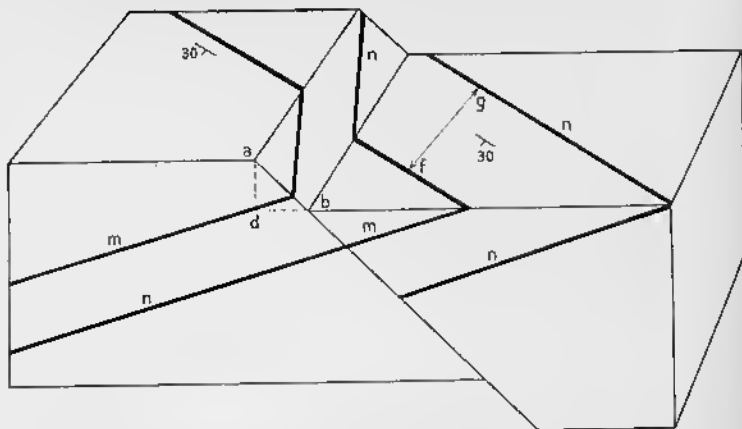


FIG. 129—Stratigraphic Throw. Heavy black lines are two disrupted beds,  $m$  and  $n$ .  $ab$  = net slip = dip slip;  $ad$  and  $db$  are vertical and horizontal components, respectively, of dip slip.  $gf$  = breadth of outcrop between beds  $m$  and  $n$ . Stratigraphic throw can be calculated as shown in text.

used if the horizontal separation is measured perpendicularly to the strike of the disrupted horizon;  $ji$  in Fig. 131A is the offset. The *overlap* is  $hj$ . In Fig. 131B,  $mn$  is the offset and  $ln$  is the *gap*.

In sedimentary rocks, faults bring into contact beds that are normally separated by intervening strata with a definite thickness. The thickness of these intervening beds is the *stratigraphic separation* or *stratigraphic throw* along the fault. Fig. 129 shows how the stratigraphic separation may be determined. Along the fault, bed  $m$  in the right-hand block is brought into contact with bed  $n$  in the left-hand block. From the top of the right-hand block it is possible to calculate the thickness of the beds between  $m$  and  $n$ , according to the equation

$$t = gf \times \sin \delta.$$

In this equation  $t$  = thickness of beds between  $m$  and  $n$ ;  $gf$  = breadth of outcrop between  $m$  and  $n$ , measured perpendicular to the strike of the strata; and  $\delta$  = angle of dip of beds. The stratigraphic separation is one of the most important measurements of all, because in sedimentary rocks it can be determined with precision if the stratigraphy is known.

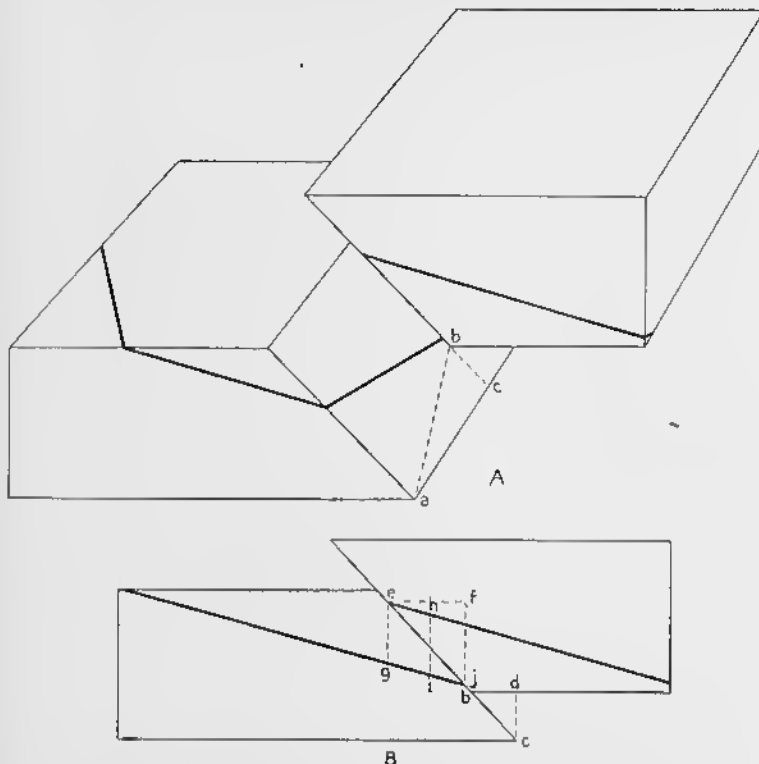


FIG. 130—Separation. Heavy black band is disrupted bed. A. Block diagram;  $ab$  = net slip;  $bc$  = dip slip;  $ac$  = strike slip. B. Vertical cross section perpendicular to strike of fault.  $eg = hi$  = vertical separation;  $eb$  = apparent displacement;  $fj$  = throw;  $ef$  = heave.

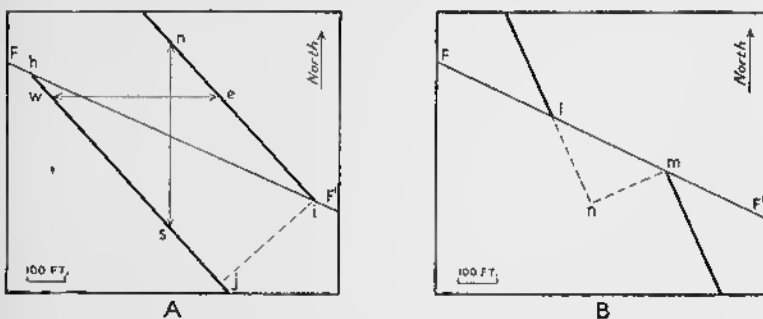


FIG. 131—Separation as Shown on Geological Map. Heavy black band is disrupted bed.  $FF'$  = fault trace. A.  $ns$  = north-south horizontal separation;  $we$  = east-west horizontal separation;  $hi$  = horizontal separation parallel to trace of fault;  $ji$  = offset;  $hj$  = overlap. B. Geological map.  $lm$  = horizontal separation parallel to trace of fault;  $mn$  = offset;  $ln$  = gap.

### Classifications

#### Geometrical classifications

**Bases of classification.** Faults, like joints, may be classified on the basis of their geometry or their genesis. Because no interpretation is involved, geometrical classifications are obviously less hazardous than genetic classifications. It is partly for this reason that the geometrical classifications will be considered first.

The bases of five different geometrical classifications are: (1) the pitch of the net slip; (2) the attitude of the fault relative to the attitude of the adjacent rocks; (3) the pattern of the faults; (4) the angle at which the faults dip; and (5) the apparent movement on the fault.

**Classification based on pitch of net slip.** A *strike slip fault* is one in which the net slip is parallel to the strike of the fault (Fig. 119A); that is, the strike slip equals the net slip and there is no dip slip component. The pitch of the net slip is therefore zero.

A *dip slip fault* is one in which the net slip is down the dip of the fault (Fig. 118A); that is, the dip slip equals the net slip and there is no strike slip component. The pitch of the net slip is therefore 90 degrees.

A *diagonal slip fault* is one in which the net slip is diagonally down the fault plane (Fig. 120A). There is both a strike slip and dip slip component; the pitch of the net slip is greater than zero, but less than 90 degrees.

**Classification based on attitude of fault relative to attitude of adjacent beds.** The second of these geometrical classifications, which is based on the attitude of the faults relative to the attitude of the adjacent rocks, would be highly involved if all the variables were considered. In general, therefore, the terms refer merely to the relations as observed in plan—that is, on a geological map. A *strike fault* is one that strikes essentially parallel to the strike of the adjacent rocks. Figs. 122 and 123 are examples of strike faults. The strike of the adjacent rocks is ordinarily measured on the bedding, but if the bedding is absent, the strike may be measured on the schistosity of metamorphic rocks or on the flow structure of igneous rocks.

A *bedding fault* is a variety of strike fault that is parallel to the bedding; Fig. 124 is an example of a bedding fault. A *dip fault* strikes essentially parallel to the direction of dip of the adjacent beds; that is, its strike is perpendicular to the strike of the adjacent beds. Figs. 119, 120, and 121 are examples of dip faults. An *oblique* or *diagonal fault* is one that strikes obliquely or diagonally to the strike of the adjacent rocks; Fig. 125 is an example of a diagonal fault.

A *longitudinal fault* is one striking parallel to the strike of the regional structure; *abcd* of Fig. 132 is an example of a longi-

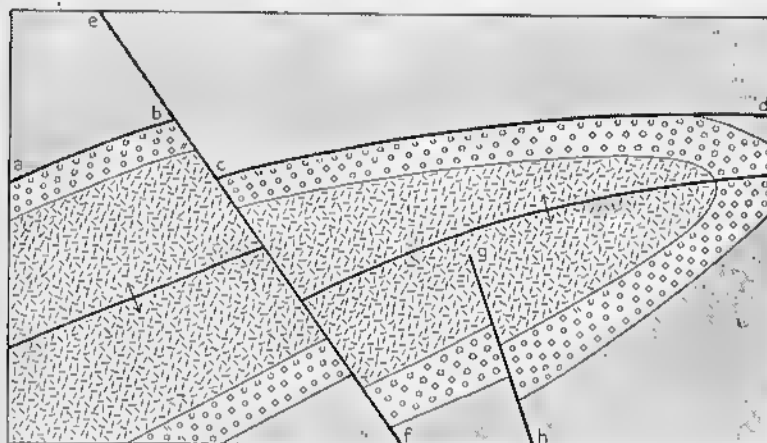


FIG. 132.—Longitudinal and Transverse Faults. Anticline plunging toward the east (right) is broken by faults. *abcd* = longitudinal fault; *ecef* and *gh* are transverse faults.

tudinal fault. Along most of its course it is a strike fault, but locally the adjacent rocks may strike at a high angle to the fault. A *transverse fault* is one striking perpendicularly or diagonally to the strike of the regional structure; *ef* and *gh* of Fig. 132 are examples of transverse faults. Along most of its course a transverse fault is a dip or diagonal fault, but locally the adjacent rocks may strike parallel to the fault.

**Classification based on fault pattern.** A third geometrical classification is based on the pattern shown by the faults; ordinarily the classification is based on the pattern on a map, but it may be based on the pattern in a cross section. The attitude of the adjacent rocks is unimportant. In some localities, the

faults have essentially the same dip and strike, and thus belong to a set of *parallel faults* (Fig. 133A). If the strikes are the same, but the dips differ, the faults are assigned to two or more sets of parallel faults. *En échelon faults* are relatively short faults that overlap each other (Fig. 133B). *Peripheral faults* are circular or arcuate faults that bound a circular area or part of a circular area (Fig. 133C). *Radial faults* belong to a system of faults that radiate out from a point (Fig. 133D).

In some areas, the strike and dip of the faults may differ so markedly that the arrangement appears to be quite haphazard.

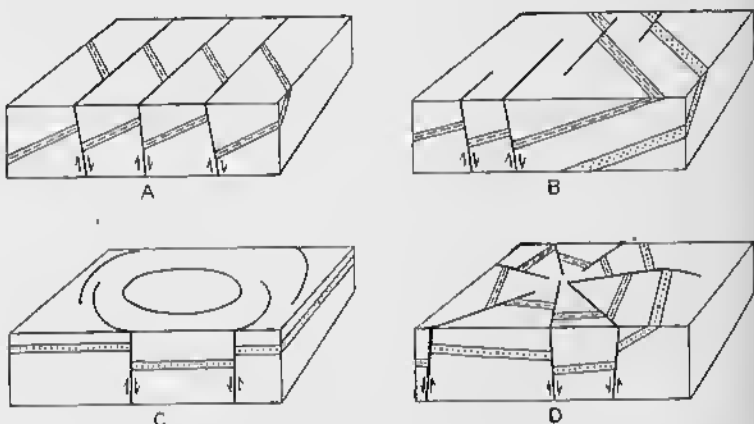


FIG. 133—Geometrical Classification of Faults by Pattern. A. Parallel faults. B. *En échelon* faults. C. Peripheral faults. D. Radial faults.

In many such cases, however, the faults may be grouped into several sets.

**Classification based on value of dip of fault.** The fourth geometrical classification is based on the angle of dip of the fault. *High angle faults* are those that dip greater than 45 degrees; *low angle faults* are those that dip less than 45 degrees.

**Classification based upon apparent movement.** A fifth geometrical classification is based upon the apparent movement in vertical sections at right angles to the fault. A *normal fault* is one in which the hanging wall has apparently gone down relative to the footwall. A *reverse fault* is one in which the hanging wall has apparently gone up relative to the footwall. Normal faults are illustrated by Figs. 116, 118, 120, and 122. Reverse

faults are illustrated by Figs. 119 and 123. It should be noted that the apparent movement is not necessarily the same as the true movement. In Fig. 119 the movement along the fault was parallel to the strike of the fault. In Fig. 134 the hanging wall actually moved down, but in the vertical section at right angles

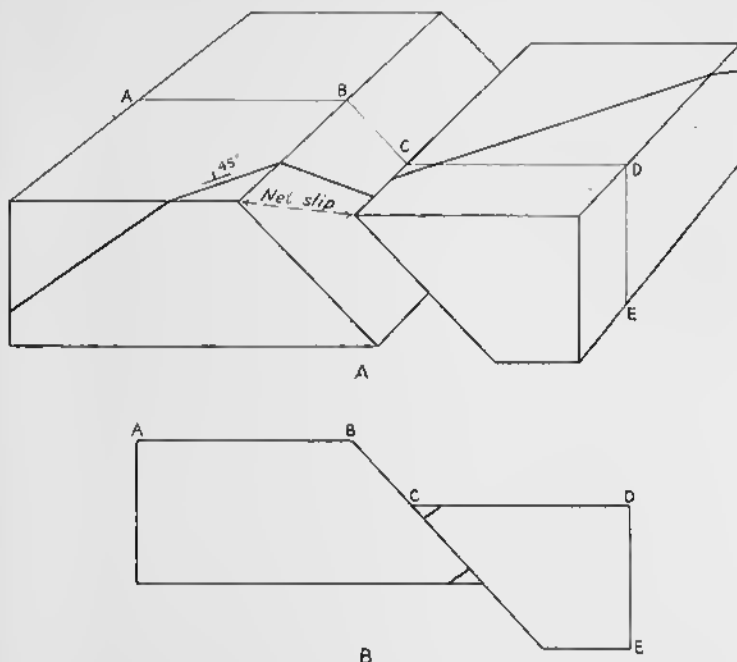


FIG. 134—Contrasting True and Apparent Movement on a Fault.  
A. Block diagram. Heavy black band is disrupted bed. B. Vertical cross section along ABCDE of the block diagram. Although the hanging wall has gone down relative to footwall, the disrupted horizon suggests the opposite.

to the strike of the fault (Fig. 134B), the hanging wall appears to have moved up.

It is obviously hopeless to attempt to establish a single set of terms that will take into consideration all the factors enumerated above. A far better system is to describe faults by using several terms from the various classifications given above. Thus the faults in one locality may be described as high angle, *en échelon*, dip faults. In another locality the faults may be low angle, parallel, longitudinal faults.

### Genetic classifications

**Ideal classification.** The most satisfactory classifications in natural science are those based on genesis. An ideal genetic classification of faults would be based primarily on the nature of the forces involved. Such a classification should consider not only whether the forces were compressional, tensional, shearing, or torsional, but it should consider also the direction in which these forces were acting. In the present state of our knowledge, however, such a classification is impossible.

**Classification based on relative movements.** The most satisfactory genetic classification that can be established at present is based on the nature of the relative movement along the fault. A *thrust fault* or *thrust* is a fault along which the hanging wall has moved up relative to the footwall. A *gravity fault* is a fault along which the hanging wall has moved down relative to the footwall. *Rifts* are longitudinal faults along which the displacement has been parallel to the strike of the fault; *tear faults* and *flaws* are transverse faults along which the displacement has been parallel to the strike of the fault. Thrust faults indicate shortening of the outer shell of the earth, and generally result from horizontal compression. Gravity faults indicate lengthening of the outer shell of the earth, and generally result from tension. Rifts, tear faults, and flaws indicate horizontal displacement of bodies of rock past one another. They are evidence of a couple acting in a plane parallel to the surface of the earth.

Because the relative movement along the fault plane is not necessarily parallel to either the strike or the dip, but may be diagonal, the terminology should make allowance for these possibilities. The most satisfactory solution is to divide the fault plane into four quadrants by two lines making an angle of 45 degrees with a horizontal line on the fault plane. This has been done in Fig. 135, which represents the footwall of the fault. If the relative movement of the hanging wall is such that the net slip lies in the upper quadrant, the fault is a thrust fault; if the net slip lies in the lower quadrant, the fault is a gravity fault; if the net slip lies in the right or left quadrants, the fault is a rift, tear fault, or flaw. If the net slip is not directly down the dip or

parallel to the strike, a modifying clause should be added to the appropriate term. Thus if the net slip is in the upper quadrant, but makes an angle of 60 degrees with a horizontal line in the fault plane, the fault can be called a thrust fault with a large component parallel to the strike of the fault.

**Classification based on absolute movements.** The classification outlined above is based on relative movements. A more elaborate classification would be based on absolute movements relative to some datum plane, such as sea level. Thus four

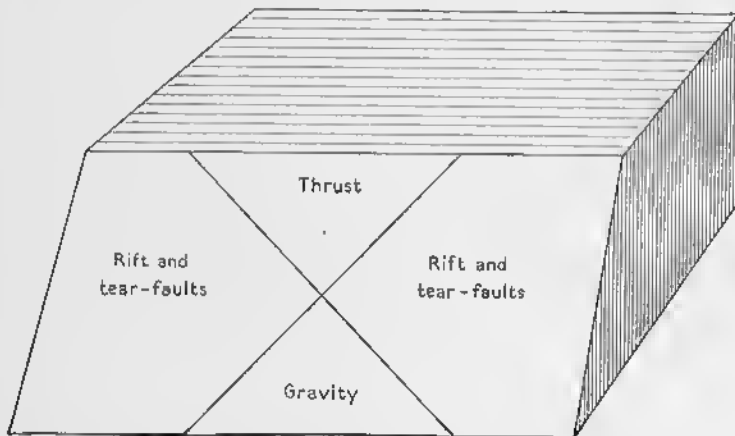


FIG. 135—Genetic Classification of Faults. Fault dips toward reader, and hence the block represents the footwall. If hanging wall moves into top sector, the fault is a thrust; if hanging wall moves into lower sector, the fault is a gravity fault; if hanging wall moves into either the right or left sectors, the fault is a rift or tear fault.

kinds of gravity faults might be recognized: (1) those in which the footwall stayed in place, but in which the hanging wall moved down; (2) those in which the footwall moved up, while the hanging wall stayed still; (3) those in which both blocks moved down, but in which the hanging wall moved a greater amount; and (4) those in which both blocks moved up, but in which the hanging wall moved less than the footwall.

Similarly, four kinds of thrust faults might be established.

In most instances, however, data are not available to indicate the absolute movement on faults. Many attempts have been made to establish criteria, based on the pattern of the faults, the dip of the fault plane, or the comparative intensity of the

## 154 DESCRIPTION AND CLASSIFICATION OF FAULTS

deformation in the two blocks. Knowledge of that phase of mechanics known as *statics* indicates that such criteria are unreliable.

In a few instances, where movements along faults near the ocean have occurred within historic times, it is possible to ascertain which block moved. Moreover, from a consideration of crustal forces, it is sometimes possible to theorize about the absolute movements along faults. Under certain conditions, therefore, terms based on absolute movements may be of value. *Upthrusts* are high angle faults along which the relatively uplifted block has been the active element. If the hanging wall of a high angle thrust fault has moved up while the footwall stayed in place, or if the footwall of a high angle gravity fault has moved up while the hanging wall stayed in place, the fault is an *upthrust*.

Sometimes the term *underthrust* is used for those thrust faults in which the footwall has been the active element, whereas *overthrust* is used for those thrust faults in which the hanging wall has been the active element.

## Criteria for Recognition of Faults

### Introduction

Faults may be recognized in various ways. If a fault is exposed in a cliff, a road cut, or a mine working, it may be readily observed, and precise data may be obtained concerning its attitude and the displacement of the disrupted strata. In other instances the observations may not be so direct, but careful field work may bring to light data which permit a complete analysis of the fault. In still other cases some information about the fault may be obtained, but a complete analysis may be impossible. Finally, there may be instances where the data are so incomplete that it is impossible to decide whether a fault is present or not. On some maps separate symbols are used to differentiate observed faults, inferred faults, and possible faults from each other.

The criteria for the recognition of faults may be considered under the following headings: (1) discontinuity of structures; (2) repetition or omission of strata; (3) features characteristic of fault planes; (4) silicification and mineralization; (5) sudden changes in sedimentary facies; and (6) physiographic data.

Some of the features characteristic of faults are also typical of unconformities, and in some places it is difficult to determine whether a fault or an unconformity is present. Methods of distinguishing between the two cannot be considered intelligently, however, until unconformities have been discussed. Criteria for distinguishing between faults and unconformities will be discussed in Chapter 13.

### Discontinuity of Structures

If strata suddenly end and abut against different beds, a fault may be present. On a map, cliff, or artificial exposure, the discontinuity occurs along a line, but this is merely the trace of a

surface of discontinuity. In some instances the disrupted strata may be found in the same outcrops or in nearby exposures, but often this is not so. The discontinuity of strata along faults is illustrated in Figs. 116 and 118-120. Dikes, veins, or older faults also may end suddenly along some line, and the displaced parts may appear elsewhere. In such cases, however, the observer must realize that dikes, veins, or faults may form with a discontinuous pattern. Moreover, discontinuity of structures is, in itself, not proof of faulting; the truncation of structures is also typical of unconformities (p. 242), intrusive contacts (p. 264), and, on a small scale, cross-bedding.

In summary, discontinuity of structures is characteristic of faults, but it is a proof of faulting only if other possible interpretations have been eliminated.

#### Repetition and Omission of Strata

Fig. 136 is a geological map of a region of folded and faulted sedimentary rocks. A syncline lies near the center of the map,

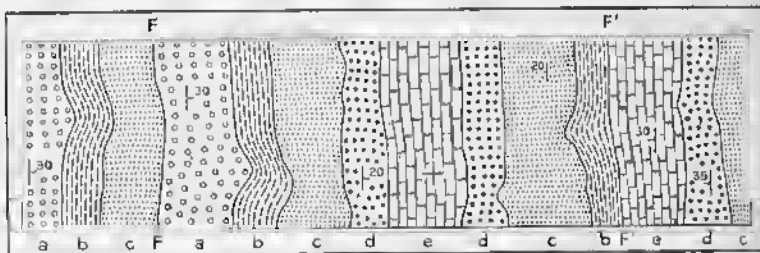


FIG. 136—Faults Indicated by Repetition and Omission of Strata. Strata, from oldest to youngest, are *a*, *b*, *c*, *d*, and *e*. *FF* and *F'F'* are faults. Dip-strike symbols indicate attitude of bedding.

as is shown by the dips, and the formations are progressively younger from *a* to *e*. In certain places, however, one or more formations are missing, as, for example, along the line *FF*, where formation *b* is absent, and along the line *F'F'*, where *c* and *d* are missing. The lines *FF* and *F'F'* must be the trace of faults, but no data are given to indicate the direction and value of the dip of the faults.

The omission of strata, however, may be due to an unconformity (Chap. 13).

### Features Characteristic of Fault Planes

Many faults are accompanied by such distinctive features as slickensides, mullion structure, gouge, breccia, and mylonite; these features are conclusive proof of faulting, although if care is not exercised, some of them may be confused with phenomena of a different origin.

*Slickensides* are polished and striated surfaces that result from friction along the fault plane. The scratches or striations are parallel to the direction of movement, but caution is necessary in employing such information, because some faults show

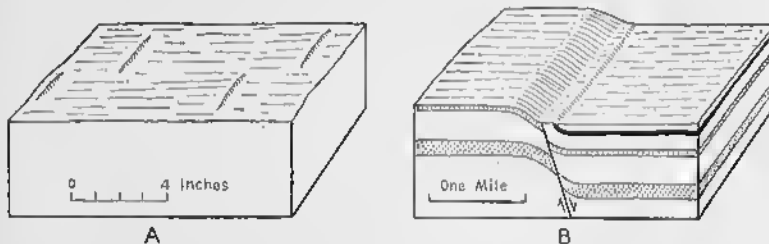


FIG. 137—*Features Associated with Faults.* A. Slickensides with small associated steps; lines parallel to front of block are scratches; at right angles to them are small "steps." B. Drag along a fault. Slipping and solid black represent special beds.

many slickensided layers, in each of which the striations have different trends. Moreover, a slickensided layer may record only the last movements along the fault, and the earlier displacements may have been in some other direction.

Many slickensided surfaces are accompanied by sharp, low steps that trend at right angles to the striations (Fig. 137A). These sharp little rises are commonly only a fraction of an inch high, and may be so small that they are difficult or even impossible to see. These rough surfaces can be used to determine the relative movement along the fault plane, in much the same way that *roches moutonnées* indicate the direction in which glacial ice was moving. In Fig. 137A, the upper block, which is not shown, moved from left to right relative to the lower block, on which the slickensides are shown. Even if the small irregularities are not visible, however, a person with sensitive fingers may be able to tell the direction of movement. The surface feels smooth if the fingers slide in the direction that the missing block

was displaced, whereas in the reverse direction the fault feels rough.

*Mullion structure* consists of large grooves or furrows that may be several feet from crest to crest and several inches deep; it is parallel to the direction of displacement.

*Drag* is in some cases an aid in divulging the relative motion along the fault, as is shown in Fig. 137B. Because of friction the beds in the hanging wall are dragged up in this particular case, whereas the beds in the footwall are dragged down. This method is subject to the same limitation as are slickensides, because the observed drag may be due to the last movements along the fault, and may even be the opposite of the major movement.

Some of the rock along a fault may be pulverized to a fine-grained *gouge*, which looks and feels like clay. In fact, gouge differs in no important way from clays of glacial origin, because both are pulverized rock.

*Breccia* consists of angular to subangular fragments of various sizes, characteristically associated with a more finely-crushed matrix. The fragments typically range from an inch to several feet in diameter, but much larger blocks may occur. Fault breccias may be many tens of feet thick.

Large blocks may be caught along faults, as shown in Fig. 138. Such blocks are separated from the foot and hanging walls by faults which may or may not be accompanied by breccia. Such large blocks are called *horses* or *slices*. The term *horse* (Fig. 138A) usually refers to such a block caught along a gravity fault (p. 152), and *slice* (Fig. 138B) refers to a block caught along a thrust fault (p. 152). This distinction is of no great import-

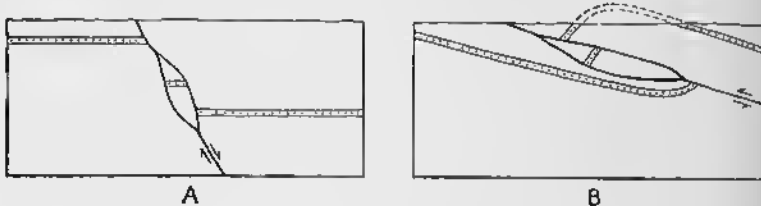


FIG. 138—Horse and Slice. A. Horse along a gravity fault. B. Slice along a thrust fault.

tance, and merely reflects the fact that the terms were first used in two different countries.

A *mylonite* is a microbreccia that maintained its coherence during the deformation.<sup>1</sup> It is characteristically dark and fine-grained, and may be difficult to distinguish from sedimentary or volcanic rocks. The brecciated character is generally apparent only from microscopic study. Although usage varies, the term *mylonite* should be restricted to those microbreccias with a streaked or platy structure; they may look like slate. Uncrushed fragments of the parent rock can be recognized under the microscope. An *ultramylonite* forms if the crushing is so complete that no such fragments remain. An ultramylonite may be difficult to recognize unless transitions to mylonite and the parent rock are preserved. *Flinty crush-rock* and *pseudo-tachylite* are massive microbreccias that lack the platy structure. Flinty crush-rock looks like chert. Pseudo-tachylite looks like tachylite, which is a variety of basaltic glass. Flinty crush-rock and pseudo-tachylite that are exceedingly fine-grained—the individual grains are 0.001 millimeter in diameter—may fill irregular fractures near the fault, and may simulate dikes of igneous rocks. Although some geologists believe that these rocks were actually molten at one time, there is no unanimity of opinion on this matter.

Although slickensides, gouge, breccia, mylonite, and related phenomena are found along many faults, they are not necessarily present. It is often assumed that the larger the fault, the greater the amount of breccia, gouge, and mylonite. This is by no means true. In general, gouge and breccia form near the surface of the earth, where the confining pressures are comparatively small, and mylonite forms at greater depth, where the confining pressure forces the rocks to retain their coherence. Parts of some of the great overthrusts in the Alps are so devoid of slickensides, gouge, breccia, and mylonite that they passed unnoticed and were for a time mapped as sedimentary contacts. It was only after paleontological evidence was obtained and after areal mapping was extended that the existence of the great faults was recognized.

<sup>1</sup> Waters, A. C., and Campbell, C. D., Mylonites from the San Andreas fault zone: *American Journal of Science*, Vol. 29, pp. 473-503, 1935.

### Silicification and Mineralization

Faults, because they are extensive fractures or branches of large fractures, are often the avenues for moving solutions. The solutions may replace the country rock with fine-grained quartz, causing *silicification*. This phenomenon in itself is not proof of faulting, but in some localities it may be highly suggestive. In New Hampshire, for example, several large faults have been extensively silicified. Some of the silicified zones are in granitoid rocks in which it is impossible to utilize stratigraphic means to demonstrate faulting. It seems likely, however, that all the silicified zones in this area are along faults.

Mineralization along faults is typical of many mining districts.

### Sudden Changes in Sedimentary Facies

A fault with a large horizontal displacement, such as an over-thrust (p. 176), is suggested if contiguous strata of exactly the

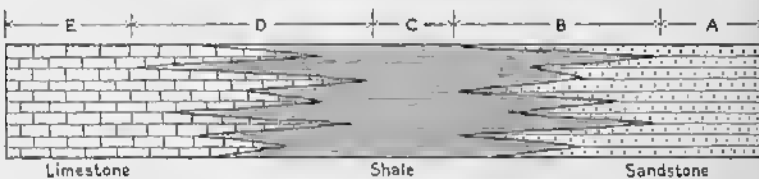


FIG. 139—Changes in Sedimentary Facies Across a Basin of Deposition.  
A = Sandstone facies, B = sandstone-shale facies, C = shale facies,  
D = shale-limestone facies, E = limestone facies.

same age show very different *sedimentary facies*. Fig. 139 illustrates a basin of deposition in which sandstones are deposited near shore, shales farther out, and limestones farthest from shore. The transition from sandstone to shale, and from shale to limestone, will be gradual and there will be considerable inter-fingering of beds. The rocks of this particular age are said to be represented by a sandstone facies in region *A*, a sandstone-shale facies in region *B*, a shale facies in region *C*, a shale-limestone facies in region *D*, and a limestone facies in region *E*. Even if the strata are strongly folded and exposed by erosion, the various facies will grade into each other. On the other hand, a large overthrust (Fig. 151) might bring the sandstone facies of region *A* into contact with the limestone facies of region *E*.

Conversely, if contemporaneous strata are represented in the same area by radically different sedimentary facies, a fault of large displacement is suggested. It is not possible to deduce the amount of the displacement, because at present we do not know precisely the distances involved in the change from one facies to another. The Alps are a classic area for the juxtaposition of different facies due to overthrusting.

### Physiographic Criteria

In some instances, the more direct geological evidences of faulting may be unobtainable, particularly if the downthrown block is completely buried by alluvium. But some of the topographic features may indicate the presence of a fault. The physiographic criteria include offset ridges, scarps, scarplets, triangular facets, truncation of structure by a mountain front, modified drainage patterns, and springs.

Resistant sedimentary formations are generally expressed topographically by ridges (Fig. 75). A dip fault or diagonal fault will displace the strata, as in Fig. 118B, and, consequently, the ridge held up by some resistant bed will be discontinuous, and an *offset ridge* will result.

A *scarp* is a relatively steep, straight slope of any height (Fig. 140). A scarp may be ten feet high or thousands of feet high. Although the inclination of a scarp is steep compared to that of the surrounding region, it may be only ten or twenty degrees; slopes steeper than 45 degrees are not common. As erosion wears a scarp back, the scarp may lose its straightness and become irregular, but there is no precise way of defining when it ceases to be called a scarp.

A scarp is not, of course, proof of the presence of a fault, because scarps may develop quite independently of faulting. The steeper slope of a *cuesta*, formed by subaerial erosion, may be relatively straight and be a typical scarp. Marine erosion may form a wave-cut cliff, which may also have all the attributes of a scarp. Erosion may be locally controlled by a joint or by a series of joints, and a low scarp may develop. All too frequently a fault is assumed because of the presence of a scarp, but additional evidence is necessary to establish a fault. The essen-

tial point is that scarps, although compatible with faulting, are not proof of faulting.

Scarps associated with faults are of three types—fault scarps, fault-line scarps and composite fault scarps.

A *fault scarp* owes its relief directly to the movement along the fault, even though erosion may have greatly scarred the initial topography. Fig. 140A illustrates a very fresh fault scarp. A surface of low relief has been broken by a gravity fault, and the height of the scarp ( $h$ ) is equal to the vertical component ( $v$ ) of the dip slip. Because of erosion on the upthrown block and deposition of alluvium on the downthrown block (Fig. 140B), the height of the scarp will gradually decrease. As long as the slope retains any resemblance to straightness, it is classed as a scarp.

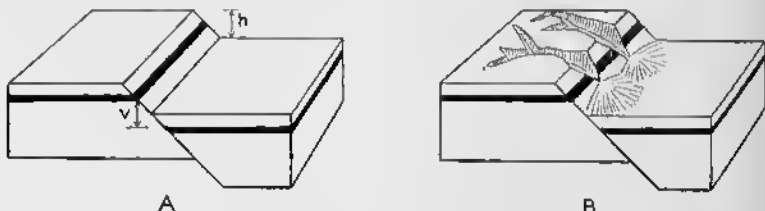


FIG. 140—Fault Scarp. A. Before erosion;  $h$ , height of scarp, equals  $v$ , the vertical component of the dip slip. B. After some erosion the material removed from deep valleys on the footwall block has been deposited as alluvial fans on hanging wall block.

A *fault-line scarp* is a scarp which owes its relief to differential erosion along a fault-line. Fig. 141 illustrates some of the ways in which fault-line scarps may form. In Fig. 141A, the initial relief due to faulting has been destroyed by erosion. The region is then bodily uplifted and a new baselevel of erosion established at  $abc$ . The soft rocks, shown by parallel lines, are rapidly reduced to the new baselevel, but the resistant sandstone, shown by dots, protects the left-hand block. The resulting scarp (Fig. 141B) is a *resequent fault-line scarp*.

Under certain conditions the downthrown block may be topographically higher than the upthrown block. After the stage illustrated in Fig. 141B, the whole area may be reduced to the baselevel  $abc$ , and the resistant bed is worn off the upthrown block. Because of still later uplift of the whole region, a new baselevel is established at  $def$ . In the ensuing erosion the

resistant bed protects the downthrown block, and an *obsequent fault-line scarp* forms (Fig. 141C). In the example cited, more than one cycle of erosion has been assumed, but it is possible to develop an obsequent fault-line scarp from a fault scarp in a single cycle.

A *composite fault scarp* is one that owes its height partly to differential erosion and partly to actual movement on the fault. Fig. 141B is an example of a fault-line scarp. If there were

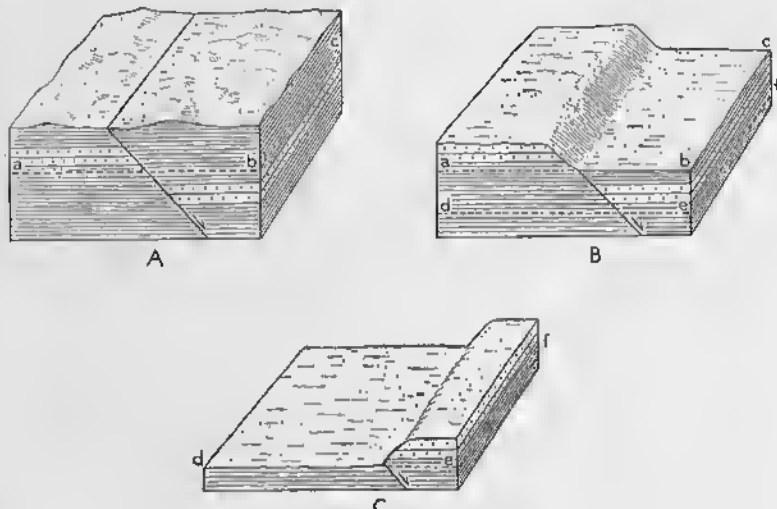


FIG. 141—Fault-line and Fault-line Scarp. A. Fault-line without scarp. Dotted formation is resistant to erosion; formations shown by parallel lines are not resistant to erosion; abc = new baselevel of erosion. B. Resequent fault-line scarp. Easily eroded rocks on hanging wall block have been reduced to new baselevel; rocks resistant to erosion on footwall have been only partially eroded; the plane def represents a new baselevel of erosion. C. Obsequent faultline scarp developed on the downdropped (relatively) block.

renewed movement on the fault—the right-hand block dropping still lower—the height of the scarp would be increased. Part of the height of such a scarp would be due to erosion along a fault-line, whereas the remaining part of the height would be due to movement on the fault. The scarp is therefore composite in character.

It is frequently difficult to distinguish fault scarps, fault-line scarps, and composite fault scarps from each other. Criteria for doing so are discussed on pp. 168–171.

*Scarpets*, also known as *piedmont scarps*, are indicative of active faults. Scarplets lie at or near the foot of mountains, and they trend essentially parallel to the base of the range. The height is commonly measured in tens of feet, and scarplets over 100 feet high are rare. They are usually confined to unconsolidated deposits such as alluvial fans, glacial moraines, and lake terraces, but bedrock is exposed on some of them. It is evident that such scarps must be very young geologically, because they would not have lasted long in unconsolidated materials.

Some scarplets that cut unconsolidated deposits represent the emergence, at the surface of the earth, of a fault that cuts bedrock (Fig. 142A). This is necessarily true wherever bedrock

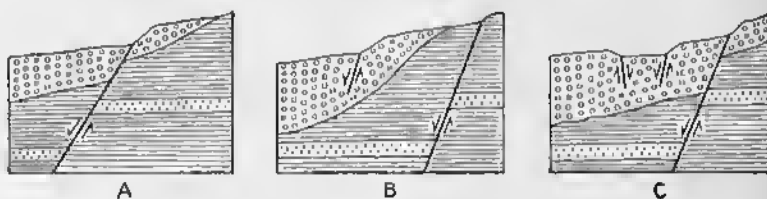


FIG. 142—Scarplets or Piedmont Scarps. Dotted and lined patterns represent bedrock. Open circles represent unconsolidated material. A. Scarplet that is direct continuation of a fault in the bedrock. B. Right hand scarp is direct continuation of fault in bedrock, but left hand scarp is not. C. Graben bounded by faults that do not extend into bedrock.

is exposed on the face of the scarp. In the Owens Valley, California, some of the scarplets produced in the earthquake of 1872 may be traced along their strike from alluvium into bedrock without any change in the height of the scarp.<sup>2</sup> If the scarp cannot be observed to cross bedrock in any part of its course, the term *fan scarp* may be used.

In other instances the piedmont scarp may be only indirectly related to the master fault (Fig. 142B). Tension may develop in the alluvium because it tends to slide down hill when movements take place on the master fault. The passage of earthquake waves may develop brief, but significant, tensional forces. Some piedmont scarps face toward the mountain front (Fig. 142C); in most cases, an outward-facing scarp lies nearer the

<sup>2</sup> Hobbs, W. H., The earthquake of 1872 in the Owens Valley, California: *Beiträge zur Geophysik*, Vol. 10, pp. 352-385, 1910; p. 375 and Pl. XI.

mountains, and the down-dropped block of alluvium constitutes a graben (see p. 201).

Piedmont scarps formed in historic time are known from several localities. During the Pleasant Valley, Nevada, earthquake in 1915, one of the piedmont scarps that formed was 18 miles long and had a maximum height of 15 feet.<sup>3</sup> In the Owens Valley earthquake of 1872, the maximum height of the scarps was 23 feet.<sup>4</sup>

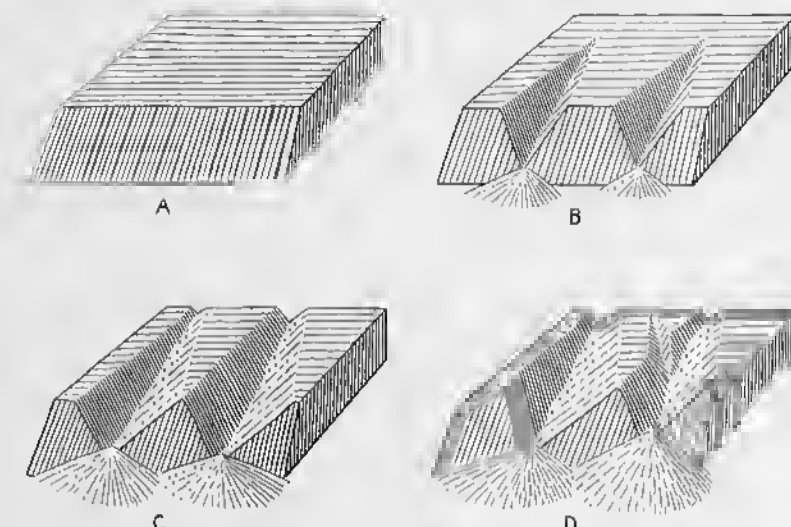


FIG. 143—Evolution of Triangular Facets. A. Fault scarp prior to erosion. B. Partially eroded fault scarp. C. Triangular facets representing remnants of original fault scarp. D. Triangular facets that represent the original fault scarp driven back somewhat by erosion.

*Triangular facets* are developed on some scarps associated with faulting. Fig. 143 illustrates how triangular facets may form. Fig. 143A is the uneroded fault scarp, but such a perfect scarp is quite hypothetical—at least for scarps more than 100 feet high. The total movement on most faults is the result of many relatively small displacements, and erosion goes on during the whole period of movement. In Fig. 143B, deep V-shaped valleys have cut into the scarp and, in Fig. 143C, the valleys have been widened, so that only half of the face of the original

<sup>3</sup> Jones, J. C., The Pleasant Valley, Nevada, Earthquake of October 2, 1915: *Bulletin Seismological Society of America*, Vol. 5, pp. 190–205, 1915.

<sup>4</sup> Hobbs, W. H., *loc. cit.*

scarp remains. The spurs between the valleys are thus truncated by triangular facets, which have a broad base and an apex pointing upward. In Fig. 143C, the dip of the facets is the same as the dip of the fault, but this would be true only if erosion does not attack the face of the fault. In most cases, however, the upper part of the scarp is subjected to erosion, as is shown in Fig. 143D, and the slope of the scarp is less than the slope of the fault. In Nevada and Utah the scarps slope 20 to 35 degrees, but the associated faults dip 50 to 70 degrees.

Triangular facets may also develop along fault-line scarps. Moreover, they are not confined to scarps associated with faults. Wherever interstream spurs are truncated by erosion, such triangular facets may form. If a maturely dissected region is attacked by marine or lacustrine erosion, the triangular facets that develop on the ends of the interstream spurs are aligned, and the resulting scarp simulates a fault scarp. Glaciers also truncate interstream spurs to develop triangular facets.

It is apparent that triangular facets, although a characteristic feature of scarps associated with faults, may evolve in other ways. Triangular facets normally are associated with gravity faults; they are associated with thrust faults only under exceptional circumstances.

A *break in a stream profile* or an *offset stream* may occur at a fault-line. If the stream cannot erode with sufficient rapidity to maintain grade while faulting is in progress, the profile of the stream may be unusually steep in the vicinity of the fault. After the 1915 earthquake at Pleasant Valley, Nevada, a stream flowed over a waterfall 10 feet high.<sup>6</sup> Such breaks are not common, however, because faulting is relatively slow compared to the speed with which streams may be incised. Moreover, the deposition of alluvium on the downthrown block tends to smooth out the profile. Broken stream profiles, however, may be due to causes other than faulting.

Wherever the movement is dominantly horizontal and essentially parallel to the strike of high-angle faults, a map of the streams may show distinct offsets. Such relations have been observed in California, where the northwesterly-trending Hayward fault zone near San Francisco is crossed by streams

<sup>6</sup> Jones, J. C., *loc. cit.*

that flow southwestward.<sup>6</sup> The stream courses southwest of the fault are displaced toward the northwest 25 to 1000 feet. In some instances the lower end of a valley has been abandoned, and the valley abuts directly against a scarp. But offsets in stream courses can also develop wherever a valley crosses a zone of weakness, such as a soft bed, a set of joints, or a fault.

The truncation of the internal structure of the range at the mountain front is highly suggestive of a fault. Fig. 144 illustrates such a case. The western part of the region is an alluvial

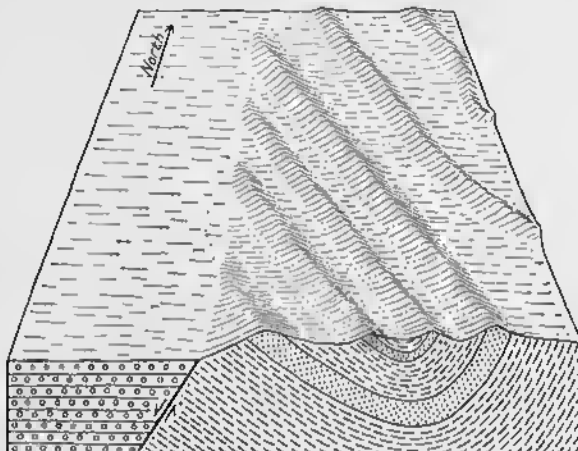


FIG. 144—Mountain Front Truncating Internal Structure of a Range. Resistant sandstones, shown by dots, hold up ridges; main valley is underlain by unconsolidated alluvium, shown by open circles.

flat, but to the east a series of ridges trends northwest. The ridges are held up by resistant sandstones in a syncline trending northwest. All the ridges end suddenly at the north-south line that separates the alluvial flat from the mountains. Under normal conditions of erosion, the ridges would not end this way, and a fault separating the alluvial flat from the mountains is implied. Additional data would be necessary to determine both the direction and value of the dip of the fault, and the nature and amount of the displacement.

*Springs in alignment along the foot of a mountain range are highly suggestive of faulting, especially if the water is hot.* The

<sup>6</sup> Russell, R. J., *Journal of Geology*, Vol. 34, pp. 507-511, 1926; J. P. Buwalda, *Bulletin Seismological Society of America*, Vol. 19, pp. 187-200, 1929.

alignment suggests the presence of a major plane of weakness, and the hot water indicates a fracture that permits deep penetration of circulating waters.

The physiographic criteria for faulting are important, but they must be employed with discretion. Some of the physiographic features mentioned, such as scarps, triangular facets, broken stream profiles, offset streams, and springs, may be unrelated to faulting and may be due to other causes. They are most significant when used in conjunction with other kinds of evidence, such as those described on pp. 155-161. Scarplets and the truncation of the internal structure of the range, on the other hand, are in themselves usually acceptable evidence for the presence of a fault.

#### Distinction between Fault Scarps, Fault-line Scarps, and Composite Fault Scarps

It is difficult—and in many instances practically impossible—to distinguish fault scarps, fault-line scarps, and composite fault scarps from each other. Nevertheless, this is an important problem for both structural geologists and physiographers, and both should strive for a solution of the problem.<sup>7</sup>

Features suggesting that the scarp is a true fault scarp are: (1) piedmont scarps; (2) lakes; (3) frequent severe earthquakes; and (4) a poor correlation between rock resistance and surface form.

Piedmont scarps have been discussed above, and it has been shown that they are associated with active faulting. It is likely that the entire scarp, at the foot of which the piedmont scarp lies, is a fault scarp. Under certain conditions, however, if faulting is renewed along a fault-line scarp, a piedmont scarp would form, and the false impression would be given that the entire scarp is a fault scarp.

Lakes associated with a fault-line suggest a fault scarp. A lake may form if a fault cuts across a stream and the block on the downstream side is uplifted (Fig. 145A). Depressions also develop if the down-dropped block settles different amounts along the strike of the fault, and lakes or swamps may occupy

<sup>7</sup> Blackwelder, E., The recognition of fault scarps: *Journal of Geology*, Vol. 36, pp. 289-311, 1928.

those depressions (Fig. 145B). *Sagponds* occupy depressions along active faults in California. But lakes associated with faults are not likely to last very long, because the outlet may be lowered very rapidly or sediments from the nearby hills and mountains may fill up the lake.

Lakes are not a normal accompaniment of fluviaatile erosion, and they are not to be expected along fault-line scarps. On the other hand, lakes at the foot of fault-line scarps may result from local overdeeping by glaciers, damming by landslides and lava flows, and from other causes.

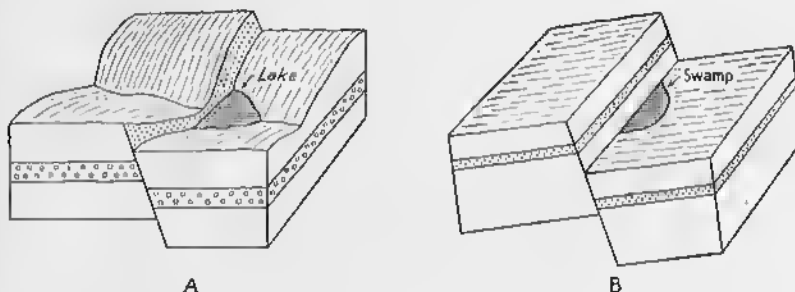


FIG. 145—Lakes and Swamps along a Fault Scarp. A. A stream that flowed toward the left has been dammed by the fault scarp. B. Swamp occupies depression at foot of fault scarp caused by tilted fault blocks.

Frequent severe earthquakes in the vicinity of a scarp associated with a fault indicate a fault scarp, because the earthquakes are presumably due to movement along the fault. In Shensi and Kansu provinces, China, recurrent destructive earthquakes at the base of high scarps are evidence that the mountains are young, active fault blocks.

A poor correlation between rock resistance and surface form suggests a fault scarp. If the scarp were due entirely to erosion, the hard formations would form hills and mountains, and the soft formations would be occupied by valleys. On the other hand, if the soft rocks rise above the hard rocks, a fault scarp is indicated. But it is obvious that such a situation could not long withstand the ravages of erosion.

There are several lines of evidence that may be used to show that a scarp is a fault-line scarp: (1) scarp on the downthrown side of the fault, (2) close correlation between rock resistance,

structure, and topography; and (3) evidence of baseleveling subsequent to faulting.

It is self-evident that if the downthrown block is topographically higher than the upthrown block (Fig. 141C), the scarp is an obsequent fault-line scarp. The relief along the fault must be caused by differential erosion.

Locally the evidence may be noncommittal, as in the front part of the block diagram shown in Fig. 146. The scarp could

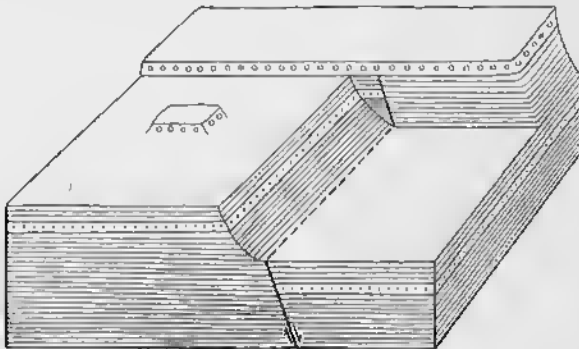


FIG. 146—Fault-line Scarp. Dots = sandstone; parallel lines = shale; circles = conglomerate. (See text.)

be either a fault scarp or a fault-line scarp. At the back of the block, however, a younger conglomerate, shown by circles, overlies the older rocks and is unaffected by the fault. It is evident that the original topographic expression of the fault

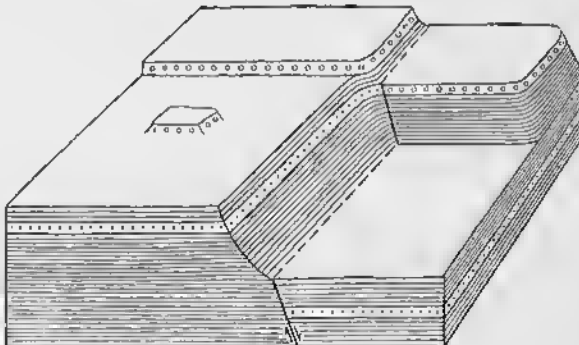


FIG. 147—Composite Fault Scarp. Dots = sandstone; parallel lines = shale; circles = conglomerate. (See text.)

had been destroyed by erosion of the whole region to the surface directly beneath the conglomerate. The conglomerate was then deposited. Finally, in a renewed cycle of erosion, the conglomerate in the foreground and many older beds in the right foreground were eroded, and a fault-line scarp developed.

A close correlation between topography and rock resistance is indicative of a fault-line scarp. The scarp is high and abrupt where the contrast in lithology is greatest, is more subdued where the contrast is slight, and may disappear if rocks on opposite sides of the fault are equally resistant.

The recognition of composite fault scarps must be based upon combinations of the criteria given above, and the local conditions are so variable that a general discussion here is inadvisable. One type of evidence is illustrated by Fig. 147, which may be considered a later stage than that illustrated by Fig. 146. Part of the height of the scarp in the foreground of Fig. 147 is directly due to movement along the fault, because the conglomerate has been displaced by the fault.

## Thrust Faults

### Introduction

*Thrust faults*, often simply called *thrusts*, are those faults in which the hanging wall moves up relative to the footwall. Such a process involves crustal shortening and implies compression, but the compression may be the indirect result of a couple. Ordinarily, it is impossible to ascertain which wall has been the active element; but, as has already been stated, if it is possible to determine which block moved, an underthrust is one on which the footwall is thrust under the hanging wall, whereas an overthrust is one in which the hanging wall is thrust over the footwall. Overthrust is also used in another sense (p. 176). The term *upthrust* may be used for high-angle thrust faults in which the hanging wall is the active element.

The most useful classification of thrust faults is based upon their origin. Some thrusts develop from folds and represent ruptures that formed when additional plastic deformation was impeded. Other thrusts are quite independent of folds, and in many instances they form without any previous folding. Some thrusts emerge at the surface of the earth, and the hanging wall moves over an erosion surface. Many thrusts have been folded, usually after motion along the fault has ceased.

### Terminology

A *break thrust* develops when a fracture forms across one limb of a fold, at a high angle to the bedding; the relative movement is such that the strata nearer the center of an anticline move over the strata nearer the center of an adjacent syncline. In Fig. 149A, which illustrates a break thrust, *ab* is the net slip.

A *stretch thrust* develops when the inverted limb of an overturned or recumbent fold becomes so stretched that it finally ruptures. The relative motion is such that the strata nearer

the center of the anticline move over those nearer the center of an adjacent syncline. In Fig. 149B, which illustrates a stretch thrust, *ab* is the net slip.

A *shear thrust* is independent of folding. In many cases the fracture cuts across horizontal strata (Fig. 149C), and the resulting fault may be called an *initial shear thrust*. In other instances, the fracture may cut across strata that have already been folded (Fig. 149D), producing what may be called a *subsequent shear thrust*. In this case, although the strata have been previously folded, the fracture itself is quite independent of the folds.

A thrust that follows a bedding plane is known as a *bedding thrust*. On p. 88 it has been shown that all folding involves some slipping of the beds past each other, but ordinarily the amount is so slight that it is measured in fractions of an inch. If, however, the movement is great enough to cause slickensiding, brecciation, or a displacement of at least several inches, the surface may be properly called a bedding thrust wherever the hanging wall moves up relative to the footwall.

In areas of flat or gently-dipping strata, a fracture may follow a bedding plane for a long distance, and the upper formations may slide thousands of feet or even miles over the lower beds (Fig. 149E). Although such fractures are bedding thrusts, they are a special kind, and may be called *strip thrusts* or *décollements* (see also p. 55). In many instances, especially if the upper block is rigid and cannot fold, the frontal part of the fracture (*bc* of Fig. 149F) must cut across the strata as a shear thrust. Thrusts of this type in Nevada have been described.<sup>1</sup>

Thrust faults may emerge at the surface of the earth (Fig. 149F); in this case the hanging wall moves over an erosion surface. Such faults are called *erosion thrusts* (*cd* of Fig. 149F). If the advancing thrust sheet undergoes erosion, a veneer of gravel or alluvium may be deposited in front of it; the thrust sheet ultimately overrides these gravels. Such an example in Norway has been described.

It is apparent that different parts of the same thrust fault may fall into various categories. Thus, in Fig. 149F, that part

<sup>1</sup> Longwell, C. R., Thrust faults of peculiar type: *Bulletin Geological Society of America*, Vol. 44, p. 93 (abstract), 1933.

of the fault designated *ab* is a bedding thrust or strip thrust; *bc* is an initial shear thrust; and *cd* is an erosion thrust. Most thrusts can be observed in only a small part of their total extent and that designation is used which applies to the exposed section. Erosion thrusts are particularly susceptible to destruction because of their proximity to the surface of the earth.

Older rocks are thrust over younger formations along break thrusts, stretch thrusts, and initial shear thrusts (Fig. 149A, B, and C). In fact, thrusts are commonly recognized by the fact that the rocks in the hanging wall are older than those in the footwall. It is apparent, however, that under certain conditions, younger rocks may be thrust over older rocks. In subsequent shear thrusts such as that illustrated in Fig. 149D, in some places, as at *c*, younger rocks rest on older rocks; elsewhere, as at *a*, older rocks are on younger rocks; and locally, as at *d*, the rocks above the thrust are the same age as those beneath it. Along erosion thrusts, younger rocks may lie on older ones. In Fig. 149F, older rocks are on younger rocks at *c* and *d*; if, however, the hanging wall were to move over the

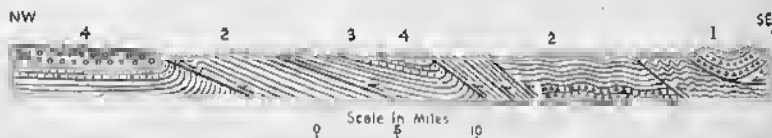


FIG. 148—Imbricate Structure in the Appalachian Province. Vicinity of Bristol, Tennessee. Formations in order of decreasing age: arc 1, 2, 3, and 4. 1 = Cambrian, 2 = Cambrian and Ordovician, 3 = Silurian and Devonian; 4 = Carboniferous. (After M. R. Campbell.)

erosion surface as far as *e*, formation 2 would lie on formation 1. Thrusts in which younger rocks rest on older rocks may be difficult to recognize, and it may be particularly hard to distinguish such thrusts from unconformities.<sup>2</sup>

*Folded thrusts* are not uncommon. One example is shown at the southeast end of Fig. 43. The data here are particularly good, because a tunnel gives a continuous section some distance beneath the surface of the earth, and it crosses the thrust in three places. Other examples are discussed on p. 183 and are

<sup>2</sup> Billings, M. P., Thrusting younger rocks over older: *American Journal of Science*, 5th ser., Vol. 25, pp. 140-165, 1933.

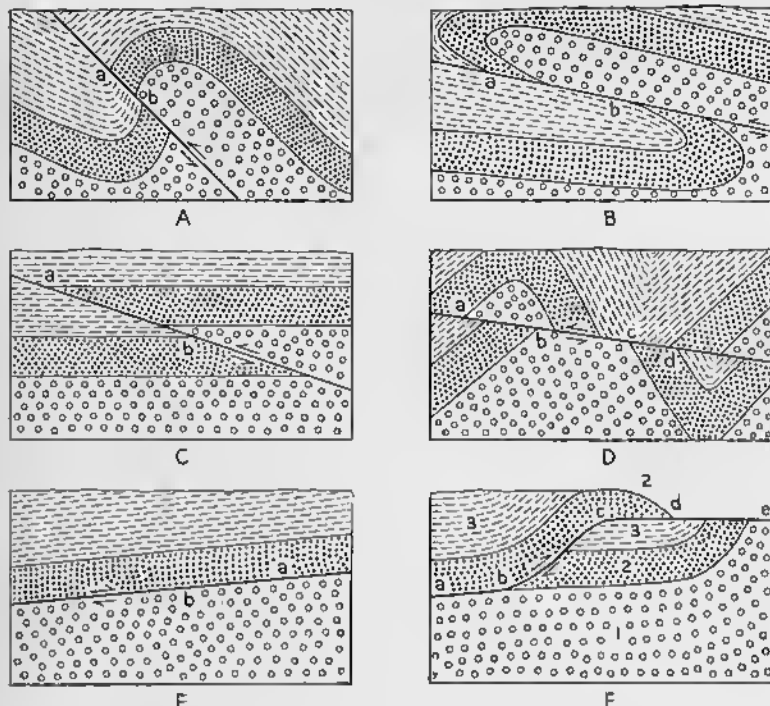


FIG. 149—Terminology of Thrust Faults. A. Break thrust;  $ab$  = net slip. B. Stretch thrust;  $ab$  = net slip. C. Initial shear thrust;  $ab$  = net slip. D. Subsequent shear thrust;  $ab$  = net slip; at  $c$  younger rocks are thrust over older; at  $d$  the rocks above and below the thrust plane are the same age. E. Bedding thrust. F. Erosion thrust; 1 = oldest beds, 2 = beds of intermediate age, 3 = youngest beds.  $ab$  = strip thrust,  $bc$  = initial shear thrust,  $cd$  = erosion thrust. If thrust block moves to  $e$ , younger rocks would be thrust over older.



FIG. 150—Imbricate Structure in the Canadian Rockies. Formations in order of decreasing age are 1, 2, 3, 4, and 5. 1 = Cambrian, Ordovician, Devonian; 2 = Carboniferous, 3 = Triassic, 4 = Jurassic, 5 = Cretaceous. (After Raymond and Willard.)

illustrated by Figs. 151, 153, 154, and 156–158. Such folded thrusts are relatively smooth planes at one stage in their development, and are later folded.

*Imbricate structure*, sometimes called *shingle-block structure*, consists of several thrust faults dipping in the same direction.

Ordinarily, the strata dip in the same direction as the thrusts and at similar, but not necessarily identical, angles. Excellent examples of imbricate structure are found in the Valley and Ridge Province of the Southern Appalachian Mountains (Fig. 148)<sup>3</sup> and in the Canadian Rockies (Fig. 150).<sup>4</sup>

### Overthrusts

*Overthrusts* are spectacular geological features along which large masses of rock are displaced great distances. An *overthrust* may be defined as a thrust fault with an initial dip of 10 degrees or less and a net slip that is measured in miles. For another usage of the term, see p. 172. The *overthrust sheet* or *overthrust block* is the block above the fault plane. Although the initial dip is low, the overthrust may be folded to assume a steep dip, and it may even become overturned.

Our knowledge of overthrusts is largely due to the fact that they are folded and eroded. Fig. 151 is a map and structure section of a folded overthrust in a region of low relief. The attitude of the thrust plane is given by dip-and-strike symbols. The rocks above are shown by a dotted pattern, whereas those beneath the thrust plane are shown by diversely-oriented short dashes. The overthrust sheet originally extended as far west as the line *xy*, but has been subsequently eroded from the central part of the area. The broken line in the upper part of the structure section shows the original top of the overthrust sheet. *K* is a remnant of the overthrust sheet, now isolated by erosion from the main thrust sheet. It is called a *Klippe*, a German word for *cliff*, because many such erosional remnants of overthrust sheets in northern Switzerland are high mountains bounded by steep cliffs. Erosion has broken through the upper sheet at *F*, exposing the rocks beneath the fault. This area is a *Fenster* or *window*, because it is possible to look through the upper sheet to the lower. In Fig. 151, in which the surface of the earth is flat, the Klippe is preserved in a doubly plunging syncline, and the Fenster is due to a doubly plunging anticline.

<sup>3</sup> Campbell, M. R., Bristol folio, No. 59; *Geologic Atlas of the United States*, U. S. Geological Survey, 8 pages, 1899.

<sup>4</sup> Raymond, P. E. and Willard, B., A structure section across the Canadian Rockies: *Journal of Geology*, Vol. 39, pp. 97-116, 1931.

Erosion alone may be chiefly responsible for Klippe and Fensters in regions of high relief. The term *window* is frequently misused in American geological literature to refer to inliers, which occur in a normal stratigraphic sequence wherever erosion has broken through the younger strata to expose a circular, elliptical, or irregular area of older rocks.

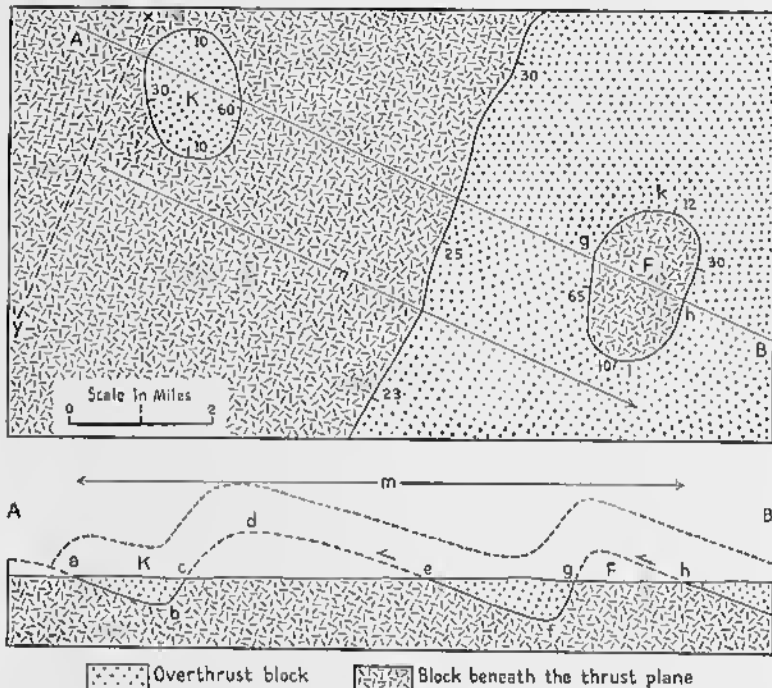


FIG. 151—Folded Overthrust. Map above, structure section below. Dip of thrust plane shown by figures. *K* = Klippe, *F* = Fenster (window). *A-B* = line of structure section. *m* = minimum breadth of overthrust block. *xy* = original western limit of overthrust block. Other letters are referred to in text.

The *root zone* of an overthrust is the exposure of the overthrust nearest its source. Thus in Fig. 151 the root zone is at *h*.

The stratigraphic throw along overthrusts may be many thousands of feet, and in many instances it may be determined with considerable precision.

The calculation of the net slip on an overthrust may be difficult. It is apparent, however, that if the strata were essentially flat when thrusting began, and that if the dip of the fault

plane was low, the net slip would be many times the stratigraphic throw. In fact, a simple trigonometric relation exists, and, as shown in Fig. 152,

$$ab = \frac{ac}{\sin \delta}.$$

In this equation  $ab$  = net slip,  $ac$  = stratigraphic throw, and  $\delta$  = dip of the fault plane. This assumes that the movement is directly up the dip of the fault; that is, there is no strike slip component.

Even if the fault and the beds have been subsequently folded,  $\delta$  may be taken as the angle between the bedding and the fault. In practice this method can seldom be applied, because measure-

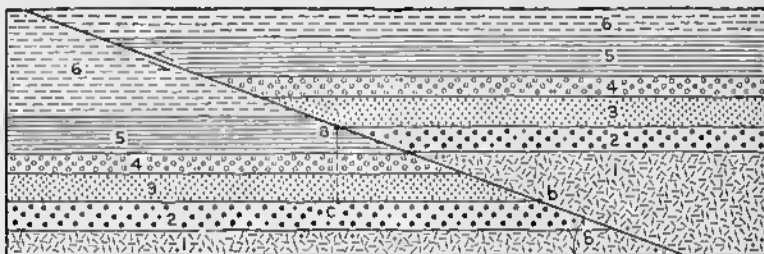


FIG. 152—Calculation of Net Slip from a Cross Section of an Initial Shear Thrust. Formations in order of decreasing age are 1, 2, 3, 4, 5, and 6.  $ab$  = net slip;  $ac$  = stratigraphic throw;  $\delta$  = dip of thrust plane.

ment of this critical angle may be impossible because of drag and brecciation along the fault.

If sufficient data are available to prepare an adequate structure section, the net slip may be measured by noting the position of some key horizon both above and below the plane of the over-thrust. In the structure section of Fig. 153, the net slip  $ab$  is five miles. The bottom of formation 3 below the thrust plane is truncated by the fault at point  $b$ . The same horizon above the thrust is truncated by the fault at  $a$ .

The erroneous assumption is often made that a minimum value for the net slip may be obtained by measuring  $m$  (Figs. 151 and 153); this is the distance between the most advanced exposure of the fault in a Klippe and the most recessive exposure in a window, and it is measured at right angles to the strike of the main outcrop of the overthrust. Actually,  $m$ , as measured

on the map, is the horizontal component of a somewhat greater distance measured along the fault plane. In Fig. 151, for example,  $m$ , of the map, is the horizontal component of  $abcdefg$  of the structure section; in the structure section of Fig. 153,  $m$  is the horizontal component of  $cabde$ . The distance  $m$  may be called the *minimum breadth* of the overthrust. The true

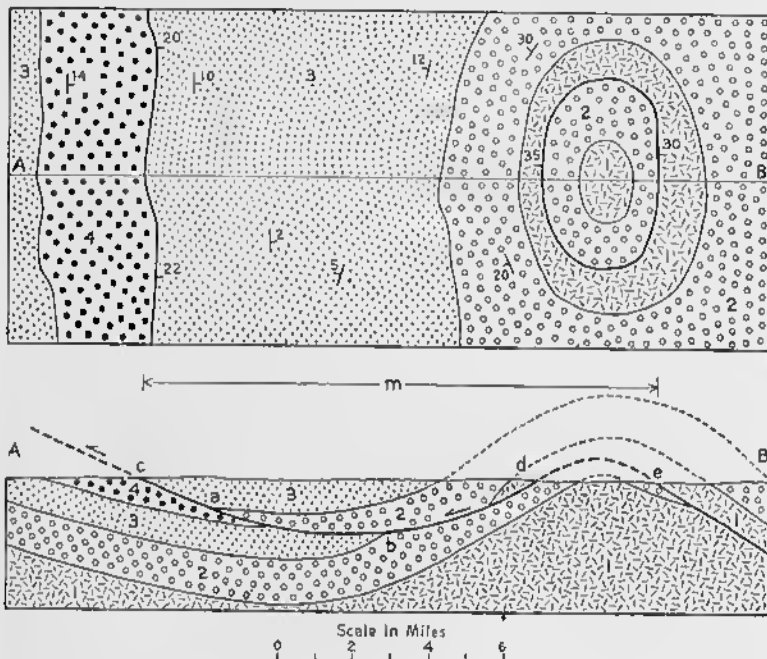


FIG. 153—Measuring Net Slip on an Overthrust. Map above, structure section beneath. Formations in order of decreasing age are 1, 2, 3, and 4. Thrust is shown in heavier black line, with figures to indicate dip.  $ab$  = net slip.  $m$  = minimum breadth of overthrust block, is really horizontal component of  $cabde$ .

breadth of the overthrust is a much larger value, and would be measured along the plane of the fault from the original most advanced position of the thrust block to that unknown place within the crust where the fault originated. Obviously, it is impossible to measure the true breadth of overthrusts. In Fig. 153, the distance  $m$  is 13.7 miles, but the net slip,  $ab$ , is only 5 miles.

In many regions there may be more than one overthrust. In Fig. 155, three overthrusts,  $ab$ ,  $cd$ , and  $ef$ , dip east, and along

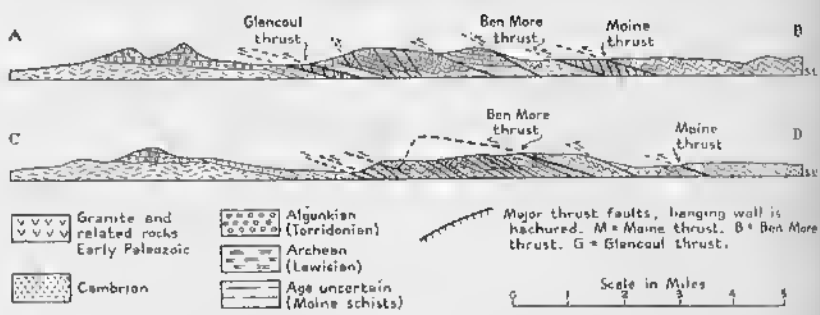
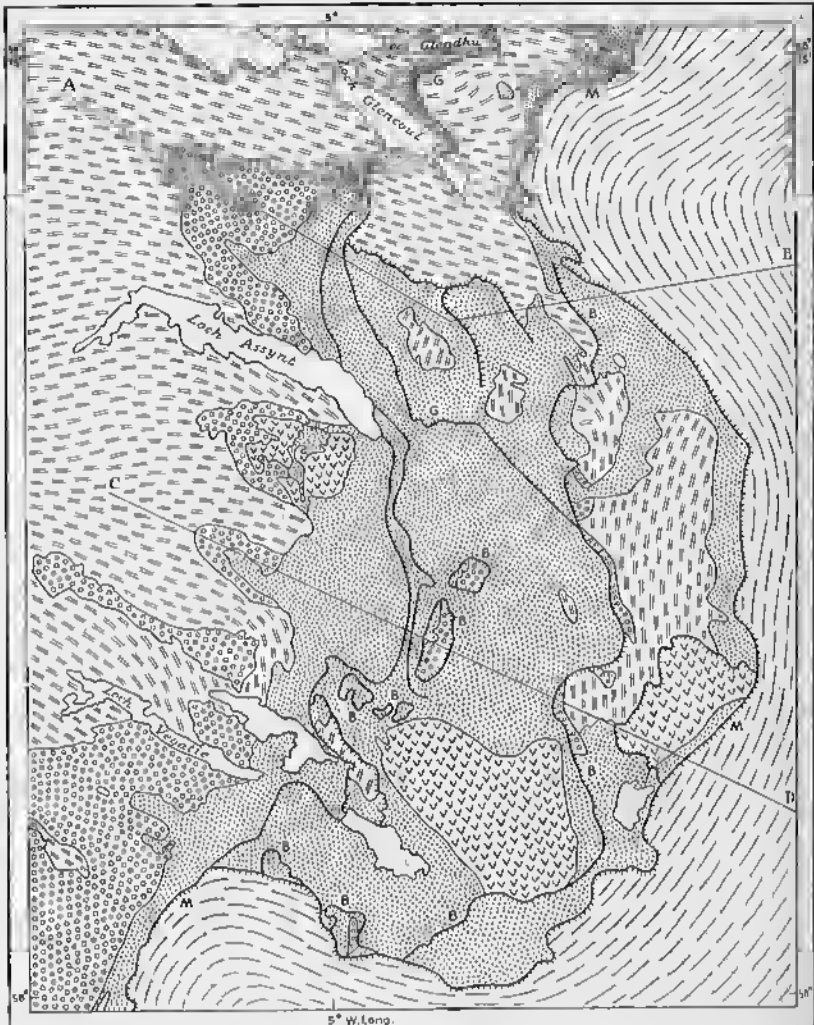


FIG. 154—Overthrusts of the Assynt District in the Northwest Highlands of Scotland. (Simplified from the Geological Survey of Scotland, Assynt district, 1923.)

each of them the net slip is measured in miles. Each block between two overthrusts is an overthrust sheet; there are three overthrust sheets in Fig. 155.

The region in front of the overthrusts is often called the *foreland* (Fig. 155). Small thrusts, with a net slip of hundreds or even thousands of feet, may occur in the foreland, but there are no overthrusts.

The rocks of the foreland are essentially where they were deposited and are said to be *autochthonous*—that is, developed where found; these rocks are sometimes called the *autochthon*. Although *foreland* and *autochthon* are somewhat similar terms, the former refers to the place, the latter to the rocks in that place.

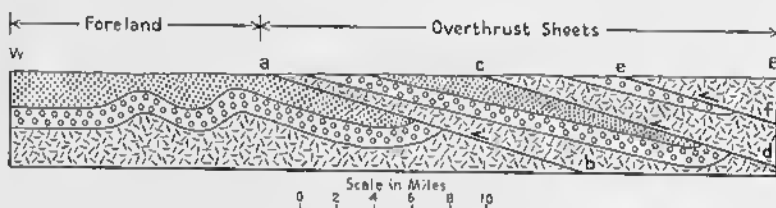


FIG. 155.—Foreland of an Overthrust Belt. *ab*, *cd* and *ef* = thrust planes.

The rocks in the overthrust sheets have traveled many miles from their original place of deposition and are said to be *allochthonous*—that is, formed somewhere else; these rocks are sometimes called the *allochthon*.

A *nappe* is a large body of rock that has moved forward more than one mile from its original position, either by overthrusting or by recumbent folding. The term is thus not synonymous with either *overthrust sheet* or *recumbent fold*. A large recumbent fold is a nappe, but a small one is not.

Some overthrusts are shown in Figs. 154, and 156–158. The Northwest Highlands of Scotland, a classic region of overthrusting,<sup>5</sup> are illustrated by a map and structure sections of the Assynt district in Fig. 154. To the west is the foreland, composed of Archean, Algonkian, and Cambrian rocks. The western edge of the overthrust belt trends somewhat east of

<sup>5</sup> Peach, B. N., Horne, J., Gunn, W., Clough, C. T., Hinxman, L. W., and Teall, J. J. H., The geological structure of the North-west Highlands of Scotland: *Memoir Geological Survey of Great Britain*, pp. 463–594. Glasgow: 1907.

## THRUST FAULTS

north across the center of the map. The Moine overthrust, designated by the letter *M*; is the major overthrust, and along it the Moine schists have been thrust westward. It is apparent

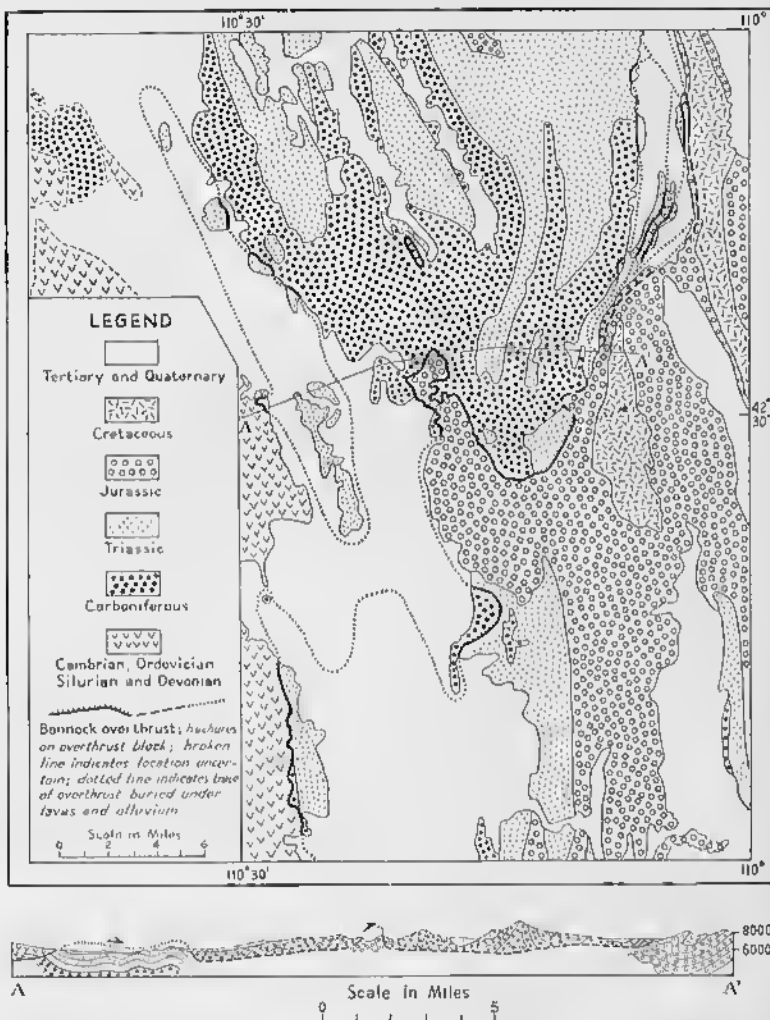


FIG. 156—Bannock Overthrust of Southeastern Idaho. (Simplified from G. R. Mansfield.)

that the Moine schists at one time extended at least as far west as Loch Assynt, but that they have been removed from the central part of the area by erosion. Evidence to the north of

the Assynt district indicates that the net slip along the Moine overthrust is at least 15 miles.

The Ben More thrust, designated by the letter *B*, outcrops west of the Moine thrust. Several Klippe of the Ben More thrust lie in the vicinity of section line *CD*.

The lowest thrust, separating the rocks that are essentially in place from those that have been moved, is known as a *sole*. Many minor thrusts, all dipping steeply to the east, produce a well-developed imbricate structure.

The Bannock overthrust<sup>6</sup> of southeastern Idaho is illustrated by Fig. 156. The main trace of the overthrust is very sinuous, extending southwestward from the northeast corner of the map.

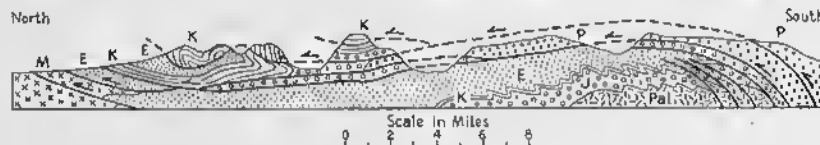


FIG. 157—Overthrusts of the Glarus District, Switzerland. Thrusts shown in heavy black. *Pal* = Paleozoic, *P* = Permian, *J* = Triassic and Jurassic, *K* = Cretaceous, *E* = Eocene, *M* = Miocene. (After J. Oberholzer.)

The irregularities are due to erosion of a folded overthrust. A large window appears in the northwest part of the map, and a smaller window appears in the north-central part.

Some of the great overthrusts of the Glarus district of Switzerland<sup>7</sup> are shown in Fig. 157. The autochthonous rocks in the lower part of the section are separated from the allochthonous rocks in the upper part by a great overthrust, along which the net slip is at least 20 miles. The great drag folds in the autochthon show that the relative movement of the overthrust sheets was toward the north.

Fig. 158 shows two large overthrust sheets in the Swiss Alps 15 miles southeast of Lake Geneva.<sup>8</sup> Cretaceous rocks have been pushed over Eocene along the lower thrust; Cretaceous

<sup>6</sup> Mansfield, G. R., Geology, geography, and mineral resources of southeastern Idaho: *U. S. Geological Survey Professional Paper* 152, pp. 150-159, 1929.

<sup>7</sup> Bailey, E. B., *Tectonic Essays, Mainly Alpine*, pp. 36-56. Oxford: Clarendon Press, 1935.

Heim, A., *Geologie der Schweiz*, Vol. 1 and Vol. 2. Leipzig: C. H. Tauchnitz, 1919, 1921, and 1922.

<sup>8</sup> Lugeon, M., "Les Hautes Alpes Calcaires entre la Lizerne et la Kander," *Materiaux pour la carte géologique de la Suisse, Nouvelle Série*, Vol. 30, 94 pp. Berne: 1914.

rocks have been thrust over Cretaceous and Eocene formations along the upper thrust. The thrusts dip north, and the overthrust sheets have traveled northward relative to the underlying formations. The drag folds are consistent with this interpretation.

It is not always easy to determine the direction of movement along overthrusts. The early geologists assumed that the net slip was directly up the dip of the fault. This would probably be correct for an unfolded overthrust. Fig. 151 is a hypothetical case in which the overthrust sheet moved from

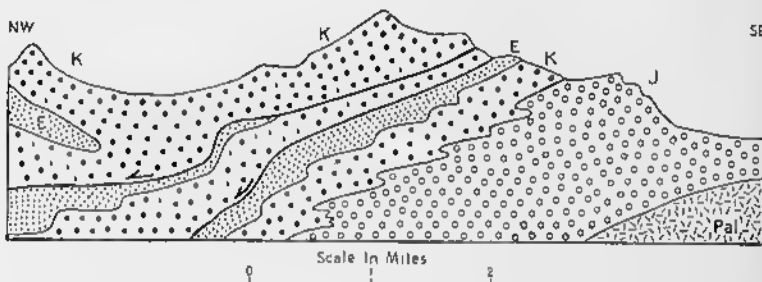


FIG. 158—Overthrusts in High Calcareous Alps of Switzerland. Thrusts shown in heavy black. *Pal* = Paleozoic, *J* = Triassic and Jurassic, *K* = Cretaceous, *E* = Eocene. (Simplified from M. Lugeon.)

southeast to northwest parallel to the line *AB*. The present dip of the overthrust has little significance with reference to the direction of movement. Around both the Klippe and the window, the strike of the overthrust boxes the compass.

At *h* on the map of Fig. 151, the net slip is up the dip; at *g*, it is down the dip; and at *k* and *l*, it is parallel to the strike of the overthrust.

It is believed that in most instances the movement was essentially at right angles to the average strike of the overthrust. Thus, in Fig. 154, the movement was essentially parallel to *CD*. More precise evidence is offered, however, by drag folds and minor thrusts beneath the overthrust. Drag folds are overturned in the direction of movement (Figs. 157 and 158). Minor thrusts dip in the direction from which the overthrust was moving (Fig. 154).

Some of the large overthrusts may be followed for long distances along the strike. The Bannock overthrust of Idaho

is at least 270 miles long,<sup>9</sup> and the Lewis overthrust along the Rocky Mountain front in Montana is at least 135 miles long and is probably more than 300 miles long.<sup>10</sup>

The stratigraphic throw may amount to several miles. Along the Bannock overthrust, the maximum stratigraphic throw is 15,000 feet;<sup>11</sup> along the Lewis overthrust, the stratigraphic throw is approximately 40,000 feet.<sup>12</sup> On the Muddy Mountain overthrust of Nevada, the stratigraphic throw is at least 11,000 feet.<sup>13</sup> Near Buffalo Mountain, Tennessee, where lower Cambrian quartzites are thrust over Ordovician limestone and shales, the stratigraphic throw is approximately 14,000 feet.<sup>14</sup>

The net slip along some of the large overthrusts is to be measured in miles and even tens of miles. Unfortunately, however, many of the data in the geological publications are unreliable, because the observers have actually measured the minimum breadth (p. 179), but have erroneously stated it to be the net slip. A minimum displacement of 12 miles along the Bannock overthrust is well authenticated; a larger figure of 35 miles that is also cited in the geological literature is actually the value for the minimum breadth. A minimum figure for the net slip along the Lewis overthrust is 15 miles. Although the net slip along the overthrust in the vicinity of Buffalo Mountain, Tennessee, is approximately 6 miles, the minimum breadth is 12 miles, and this has been erroneously stated to be the net slip. A structure section of the Glarus district in the Alps (Fig. 157) indicates that the net slip along the Glarus overthrust is not less than 20 miles.

### Mechanics of Thrusting

It is not possible to analyze with any precision the mechanics of thrusting, because too many of the physical data are unknown.

<sup>9</sup> Mansfield, G. R., *op. cit.*

<sup>10</sup> Billings, M. P., Physiographic relations of the Lewis overthrust in northern Montana: *American Journal of Science*, 5th series, Vol. 35, pp. 260-272, 1938.

<sup>11</sup> Mansfield, G. R., *op. cit.*, p. 158.

<sup>12</sup> Clapp, C. H., Geology of a portion of the Rocky Mountains of northern Montana: *Montana Bureau of Mines and Geology*, Memoir 4, p. 25, 1932.

<sup>13</sup> Longwell, C. R., Geology of the Muddy Mountains, Nevada: *U. S. Geological Survey Bull.* 798, p. 110, 1928.

<sup>14</sup> Keith, A., Roan Mountain Folio, No. 151: *Geologic Atlas of the United States*, U. S. Geological Survey, 1907.

Nevertheless, certain principles may be established and applied qualitatively to the problems involved. The chief factors to consider are the angle of dip of the fault plane, the coefficient of friction along the thrust plane, the strength of the rocks, and inertia. The problem also involves the formation of the original fracture and the movement along that fracture. It is axiomatic that at every point along the thrust, the fracture must form before any movement can take place. This, however, does not preclude the possibility that the fault begins as a small fracture at some place, accompanied by displacement, and then gradually extends itself in all directions. In fact, this seems to be the most reasonable sequence of events.

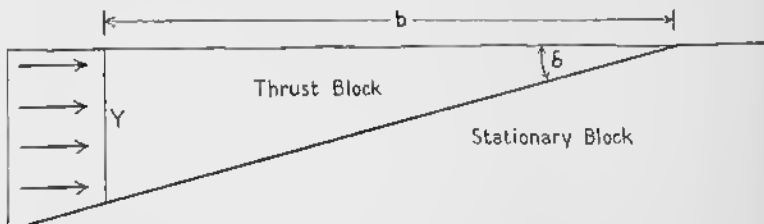


FIG. 159.—Theoretical Thrust Block.  $b$  = breadth of thrust block;  $\delta$  = angle of dip of thrust plane;  $Y$  = surface where force is applied.

The formation of the initial fracture depends upon the strength of the rocks. When the stress exceeds a critical value, the rocks will rupture. The value of this stress depends not only upon the crushing strength of the rock as determined in the laboratory (under atmospheric pressure and room temperatures), but depends also upon the confining pressure, temperature, abundance and character of solutions in the pore spaces, massiveness of the rock, and speed of application of force. Although weak rocks will fail under compression more readily than will strong rocks, overthrust sheets of considerable size should be composed of strong rocks, or they could not long maintain their coherence.

The importance of friction along a thrust plane is obvious. With an increase in the coefficient of friction, the force necessary to cause movement along the fault must also be raised. Large-scale overthrusting is obviously aided by a low coefficient of friction, and European geologists tend to emphasize that in some cases weak rocks along the thrust plane served as lubri-

cants. In North America, however, there is little evidence of such lubricants along thrust planes, where the rocks seem to have the normal coefficient of friction of 0.3 to 0.5.

A. C. Lawson has derived an equation that considers several factors, including the angle of dip of the fault and the coefficient of friction.<sup>15</sup>

The assumed conditions are illustrated by Fig. 159, in which the thrust block is assumed to move directly up the fault; the dip of the fault is  $\delta$ . A horizontally-directed force is applied at  $Y$  to cause the movement.

The equation is

$$S = \frac{bw(f + \tan \delta)}{2}$$

In this equation  $S$  = force per unit area necessary to move the overthrust block along the plane,

$b$  = breadth of thrust sheet,

$w$  = weight of rock per unit volume,

$f$  = coefficient of friction,

$\delta$  = angle of dip of thrust plane.

We may assume, as an example, that the dip of the fault is 10 degrees, the breadth of the thrust sheet 10 miles (52,800 feet), and the coefficient of friction 0.3. The weight of rock per unit volume is relatively uniform. For an average rock with a specific gravity of 2.7, the weight per cubic foot is 168 pounds or 0.084 tons. In such an example the force,  $S$ , that must be applied at  $Y$  in order to move the block, is 1056 tons per square foot.

Fig. 160 is a graph showing the relation between the angle of dip of the fault and the force necessary to move the prism; the breadth of the thrust sheet is assumed to be 10 miles, the coefficient of friction 0.3, and the weight of the rock 168 pounds per cubic foot. If the dip of the fault increases, the force necessary to move the thrust block also increases; as the dip approaches 90 degrees, the force approaches infinity.

Fig. 161 is a graph showing the relation between the coefficient of friction and the force necessary to move the prism. The

<sup>15</sup> Lawson, A. C., Isostatic compensation considered as a cause of thrusting: *Bulletin Geological Society of America*, Vol. 33, pp. 337-351, 1922.

breadth of the thrust block is assumed to be 10 miles, the dip of the fault 10 degrees; and the weight of the rock 168 pounds per cubic foot.

Fig. 160 shows that if the fault dips 60 degrees—the other conditions being what we have previously assumed—the force,  $S$ , necessary to move the block is 4500 tons per square foot. But the crushing strength of the strongest rocks is only slightly

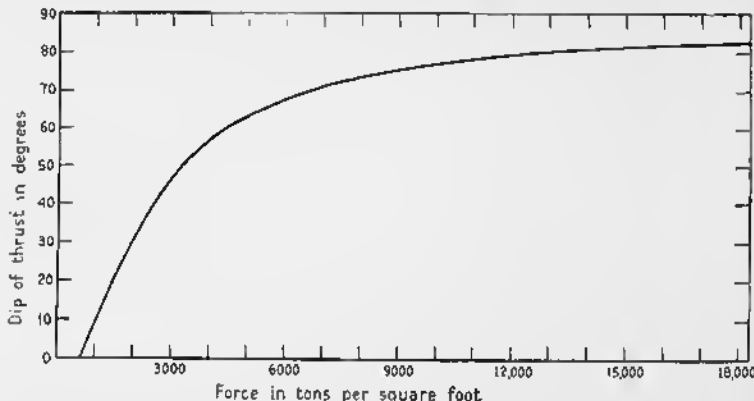


FIG. 160—Relation between Angle of Dip of Thrust Plane and Force Necessary to Move Thrust Block. Breadth of thrust block is assumed to be 10 miles, coefficient of friction 0.3, and weight of rock 168 lb./ft.<sup>3</sup>

more than 2000 tons per square foot. Such a thrust block would be impossible. Before the force necessary to move the block could be attained, the block would fail by one or more minor ruptures. The critical point on the curve is about 35 degrees; for the postulated conditions, thrusts with a dip of over 35 degrees are impossible.

The equation may be expressed in a somewhat different form:

$$B = \frac{2S}{w(f + \tan \delta)},$$

where  $B$  = maximum possible breadth of thrust block,

$S$  = crushing strength of strongest rocks,

$w$ ,  $f$ , and  $\delta$  as before.

The results are given in the form of graphs in Fig. 162. In this case  $w$  is considered 0.084 ton per cubic foot, and  $S$  is considered 2160 tons per square foot. The equation has been solved for four different values of the coefficient of friction—

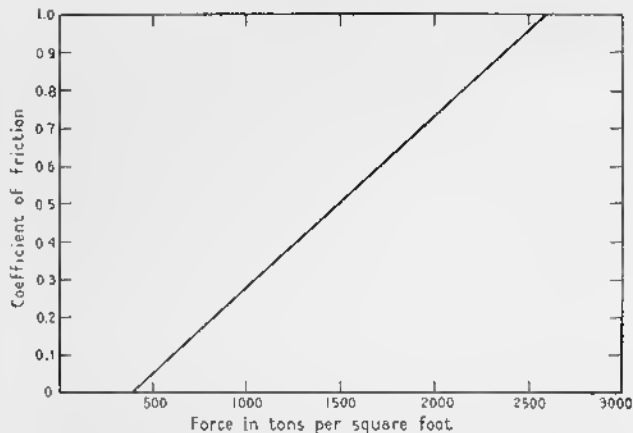


FIG. 161—Relation between Coefficient of Friction and Force Necessary to Move Thrust Block. Breadth of thrust block assumed to be 10 miles, dip 10 degrees, and weight 168 lb./ft.<sup>3</sup>

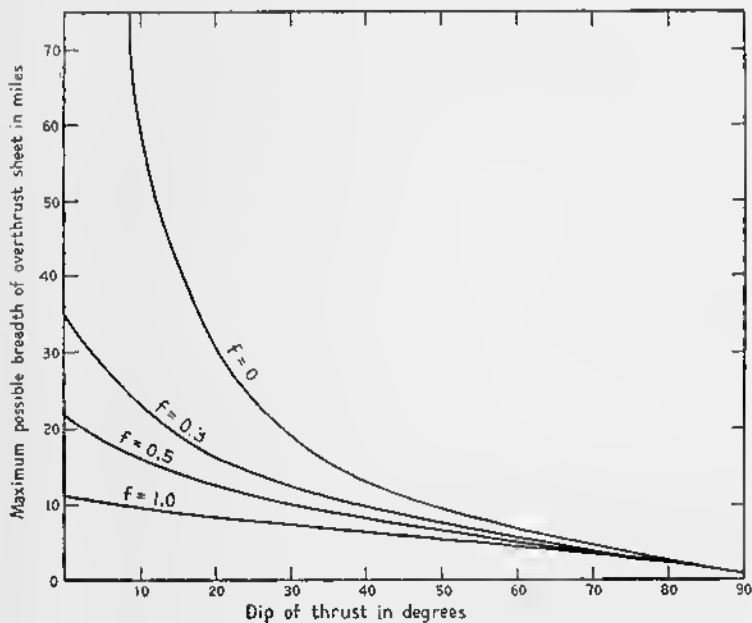


FIG. 162—Theoretical Maximum Breadth of Overthrust Block, with Varying Angles of Dip and with Four Different Values for Coefficient of Friction.

0, 0.3, 0.5, and 1.0; different values of dip for the thrust plane are plotted on the abscissa.

For example, if the dip of the fault is 10 degrees and the coefficient of friction is 0.3, the maximum possible breadth of the thrust sheet is 26 miles; if the dip is 10 degrees and the coefficient of friction is 0.5, the maximum possible breadth is 18 miles.

The graph (Fig. 162) shows that the breadth of the thrust sheet decreases with an increase in the angle of dip of the fault and an increase in the coefficient of friction.

Although the above discussion is on a quantitative basis, the results should be used only in a qualitative way. The equations and graphs bring out the importance of the angle of dip and the coefficient of friction. Too many unknowns enter into the equations, however, to permit quantitative applications.

Perhaps the greatest objection to a rigorous application of the method is the tacit assumption that the compressive force acts parallel to the surface of the earth. The really critical value is not the angle of dip of the thrust plane, but the angle between the compressive force and the thrust plane. If the force that causes displacement is acting parallel to the thrust plane, then the critical angle is zero, and relatively large thrust blocks are possible.

*Inertia* is a factor that must be considered.<sup>16</sup> Motion along faults is not a continuous process, but is very spasmodic. The actual movement takes place within a few seconds or fractions of a second. Even a greater force is necessary than that indicated by the equations in order to overcome inertia and to start the block moving.

Another assumption that has entered into the above analysis is that the force is non-rotational. A piston pressing on the back of the block would give the type of force visualized. Some European geologists believe, however, that many of the lower overthrust sheets of the Alps were dragged along by higher, over-riding thrust sheets. Although such an explanation may be correct for the lower overthrust sheets, it is obvious that there must be some other explanation for the highest sheet. Many

<sup>16</sup> Stevens, E. H., Inertia as a possible factor in the mechanics of low-angle thrust faulting; *Journal of Geology*, pp. 729-736, 1935.

geologists believe, moreover, that in most overthrusts the foot-wall is the active element, and that it is dragged along by convection currents beneath the solid crust.

In the preceding discussion of the mechanics of thrusting, emphasis has been placed upon horizontally-directed compressional forces. We must recognize, however, that some thrusts—particularly high-angle thrusts—are probably due to vertically-directed forces that push up large masses of rock.

## 11

# Gravity or Normal Faults

### Introduction

*Gravity faults* are those in which the hanging wall has gone down relative to the footwall; they involve lengthening of the crust of the earth. There are many possibilities concerning the actual movement as measured from some datum, such as sea level or the center of the earth. The footwall may remain stationary and the hanging wall go down; or the hanging wall may remain stationary and the footwall go up; or both blocks may move down, but the hanging wall more than the footwall; or both blocks may move up, but the footwall more than the hanging wall. In the present state of our knowledge it is impossible in most cases to determine the absolute movement, and hence an elaborate terminology is unnecessary and undesirable. In some instances, where there is evidence that the footwall has moved up along a high-angle gravity fault or that the hanging wall block has moved up along a high-angle thrust fault, the term *upthrust* may be used.

Many geologists use the term *normal fault* in preference to gravity fault, but as indicated on p. 150, normal fault has a different meaning. But most normal faults, as the term is defined in this book, are also gravity faults.

### Attitude, Size, and Pattern

The dip of gravity faults may range from almost horizontal to vertical, but dips greater than 45 degrees are more common than dips less than 45 degrees. Gravity faults may range from microscopic size to those that are tens of miles long and have a net slip that is measured in thousands of feet. Some of the great northeasterly-trending faults of Scotland are 150

miles long.<sup>1</sup> The fault that bounds the Triassic rocks of Pennsylvania, Maryland, and Virginia on the northwest is 250 miles long according to the 1933 geological map of the United States. Gravity faults in the Colorado Plateaus of Arizona and Utah are shown on the same map to be 100 to 300 miles long. In most instances, such long faults are not single fractures throughout their length, but locally are fault zones. The gravity fault bounding the west side of the Wasatch Range of Utah is mapped by Gilbert as a single, somewhat sinuous fault at least 80 miles long.<sup>2</sup> More detailed mapping by Eardley shows that at the south end of the range there are several *en échelon*, overlapping faults.<sup>3</sup>

The minimum throw along the Great Glen fault of Scotland is said to be 6000 feet.<sup>4</sup> The minimum net slip along a gravity fault bounding the Triassic rocks of Connecticut on the east side is 13,000<sup>5</sup> feet and perhaps as much as 35,000 feet.<sup>6</sup> The probable net slip along the gravity fault on the west side of the Wasatch Range of Utah is 17,900 feet.<sup>7</sup>

The pattern shown in plan by gravity faults is varied. The individual faults are generally rather straight, but they may be sinuous or irregular, with sudden changes in strike. In many instances two or more gravity faults are parallel to one another (Fig. 133A). *Step faulting* occurs wherever the downthrow is systematically on the same side of several parallel faults. In many localities the gravity faults show an *en échelon* pattern (Fig. 133B). Elsewhere they may be peripheral (Fig. 133C), radial (Fig. 133D), or irregular.

The most conspicuous structural features that result from gravity faults are belts of *en échelon* faulting, tilted fault blocks, horsts, and graben.

<sup>1</sup> Peach, B. N., and Horne, J., *Chapters on the Geology of Scotland*, Pl. I. London: Oxford University Press, 1930.

<sup>2</sup> Gilbert, G. K., Studies of Basin Range structure: *U. S. Geological Survey Prof. Paper 158*, Fig. 12, 1928.

<sup>3</sup> Eardley, A. J., Structure and physiography of the southern Wasatch Mountains: *Papers Michigan Academy Science, Arts, and Letters*, Vol. 19, pp. 377-400, 1933.

<sup>4</sup> Peach, B. N., and Horne, J., *op. cit.*, p. 198.

<sup>5</sup> Longwell, C. R., Sedimentation in relation to faulting: *Bulletin Geological Society of America*, Vol. 48, pp. 433-442; cf. especially p. 436, 1937.

<sup>6</sup> Krynine, P. D., Triassic sediments of Connecticut: *Bulletin Geological Society of America*, Vol. 52, p. 1919 (abstract), 1941.

<sup>7</sup> Gilbert, G. K., *op. cit.*, p. 52.

### En Échelon Gravity Faults

In some areas gravity faults show an *en échelon* pattern, such as that illustrated by Fig. 163A. The individual faults strike at an angle of approximately 45 degrees to the trend of the faulted belt as a whole. The active tension is in the direction  $TT'$  (Fig. 163B), but a regional tension acting in this direction would not account for the *en échelon* pattern. The long axis of a strain ellipse is oriented northeast ( $aa'$  of Fig. 163C). A couple caused by a northerly block moving toward

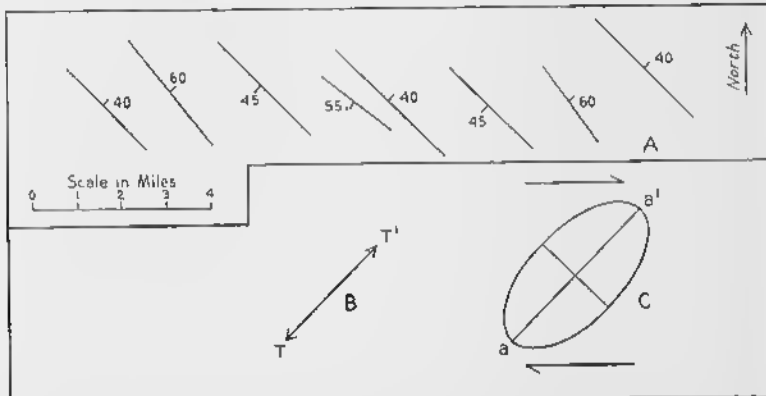


FIG. 163.—*En Échelon* Gravity Faults. A. Diagrammatic map of an area of *en échelon* gravity faults; each line represents a fault several miles long; angle of dip shown in degrees. B. Direction of active tension. C. Strain ellipse, caused by a couple; tension fracture will trend at right angles to long axis,  $aa'$ , of the ellipse.

the east relative to a southerly block, would produce the type of fracture observed.

Faults of this type are common in northeastern Oklahoma.<sup>8</sup> The belts of faulting, of which there are several, trend north-south, whereas most of the individual faults trend north-northwest to northwest. The largest fault is  $3\frac{1}{4}$  miles long, and the maximum stratigraphic throw is 130 feet.

A similar belt of *en échelon* faulting in central Montana trends east-southeast for some 56 miles.<sup>9</sup> More than 90 northeasterly-

<sup>8</sup> Fath, A. E., The origin of the faults, anticlines, and buried "granite ridge" of the northern part of the Mid-Continent oil and gas field: U. S. Geological Survey Prof. Paper 128C, pp. 75-84, 1920.

<sup>9</sup> Hancock, E. T., Geology and oil and gas prospects of the Lake Basin field,

trending faults have been mapped, many of them over 5 miles long and one, at least, is 10 miles long. The dips of the faults range from 10 to 80 degrees, but average about 45 degrees; the maximum recorded stratigraphic throw is between 500 and 600 feet. Most of the faults are of the gravity type, but some are reverse faults, and in some there has been a strike slip component to the displacement. This belt of faulting is due to a couple, the northerly block moving west relative to the southerly block, as in Fig. 163.

### Tilted Fault Blocks

Gravity faulting is accompanied in many instances by rotation of the blocks on one or both sides of the fault, and *tilted fault blocks* result. Examples are shown in Fig. 165. In many cases there is no topographic expression of the fault blocks (Figs. 165A and 165B). In other instances, the topography expresses the underlying structure more or less faithfully (Figs. 165C and 165D). The situation is seldom as simple, however, as in these very diagrammatic figures, because erosion attacks the highest areas, and the resulting debris is deposited in the valleys (Fig. 166A). The mountains that rise above the valleys in such cases are one variety of *fault block mountains*. Some fault block mountains are horsts (p. 201).

Tilted fault blocks are most readily recognized by the tilting of one or more datum planes, such as the bedding (Figs. 165A, 165B, and 165C). In some cases a late-mature or old-age erosion surface may be broken and tilted (Fig. 165D). Such erosion surfaces are particularly useful in those regions that are underlain by granitic rocks, or in those areas where the strata were highly deformed prior to the gravity faulting. In some mountains a thin lava flow may serve as the key bed that shows rupture and tilting (Fig. 166B).

The Triassic rocks of eastern North America display tilted fault blocks that have little topographic expression. In Connecticut (Fig. 167), the easterly-dipping Triassic rocks rest

Montana: U. S. Geological Survey Bull. 691, pp. 101-147, 1918.

Chamberlin, R. T., A peculiar belt of oblique faulting: *Journal of Geology*, Vol. 27, pp. 602-613, 1919.

Chamberlin, R. T., Diastrophic behavior around the Bighorn Basin: *Journal of Geology*, Vol. 48, pp. 673-716, 1940.

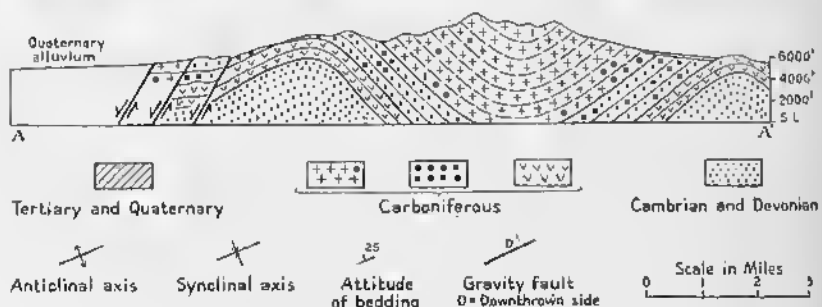


FIG. 164—Tilted Fault Block of the Oquirrh Range, Utah. (After Giluly.)

unconformably on the older crystalline rocks to the west. On the east a large, westerly-dipping gravity fault, with a net slip of at least 13,000 feet, separates the Triassic rocks from the crystalline rocks to the east. The Triassic strata dip toward the east at an angle of 20 degrees, except near the fault, where the easterly dip reaches a maximum of 40 degrees. Longwell<sup>10</sup> has shown that the fault was active during deposition. A num-

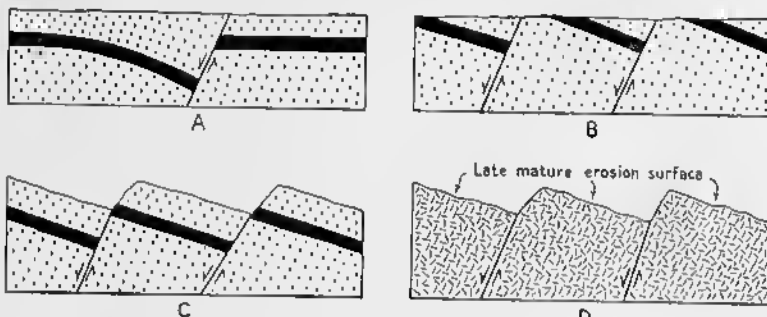


FIG. 165—Tilted Fault Blocks. Solid black = shale; dots = sandstone; diversely oriented dashes = granite. A. and B. Tilted fault blocks that are not expressed topographically. C. Topographically expressed tilted fault blocks. D. Topographically expressed tilted fault blocks developed on granite; a late mature erosion surface has been broken and tilted by the faulting.



FIG. 166—Tilted Fault Blocks. Diversely oriented dashes are granite; circles are alluvium; solid black is lava. A. Alluvium derived from erosion of higher parts of the fault blocks accumulates in depressions. B. A broken and tilted lava bed that serves as a key bed.

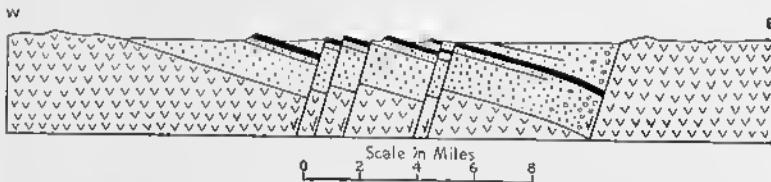


FIG. 167—Tilted Fault Block of the Connecticut Valley, Connecticut. Checks = pre-Triassic crystalline rocks; dots = arkose, sandstone, shale; circles = conglomerate; solid black = volcanic rocks. (Modified from Barrell.)

<sup>10</sup> Longwell, C. R., *op. cit.*

ber of northeasterly-trending gravity faults lie within the Triassic rocks.

Tilted fault blocks that are expressed topographically are well developed in the Great Basin of the western United States. Fig. 164 shows the Oquirrh Range of central Utah.<sup>11</sup> These mountains rise 5000 feet above the alluvial valley to the west, south, and east. The Paleozoic rocks are thrown into broad, open folds, the axes of which trend northwest. The western side of the range is broken by a series of gravity faults, the most significant of which trend north-northwest. Where the faults have actually been observed, the dip ranges from 40 to 64 degrees to the west-southwest, and it averages 57 degrees. In all instances the hanging wall has gone down relative to the footwall. The maximum measured stratigraphic throw, which is along the fault with the greatest length in Fig. 164, is 3500 feet. The greatest displacement may be along the most southwest-erly of the faults, but the downthrown block is buried under alluvium.

The manner in which the internal structure of the range is truncated by the western front of the mountains is clearly brought out by the map. A piedmont scarp, 40 feet high, which cuts alluvium, testifies to the recency of some of the movements. In general, however, the faults are not well expressed in the topography (see cross section in Fig. 164), and triangular facets are poorly defined. These facts indicate that considerable erosion has modified whatever scarps may have existed.

It is obvious that the mountain block has been uplifted along the faults many thousands of feet relative to the valleys to the west. A mature erosion surface, which developed on the site of the range prior to the normal faulting, has been tilted eastward at an angle of approximately 4 degrees.

The Wasatch Range of Utah is a tilted fault block<sup>12</sup> illustrated by Figs. 168-170. The Wasatch Mountains extend north from Salt Creek in the southern part of Fig. 168. The Juab Valley, which lies to the west of Mt. Nebo, the highest

<sup>11</sup> Gilluly, James, Geology and ore deposits of the Stockton and Fairfield quadrangles, Utah: U. S. Geological Survey Prof. Paper 173, 1932.

<sup>12</sup> Eardley, A. J., *op. cit.*

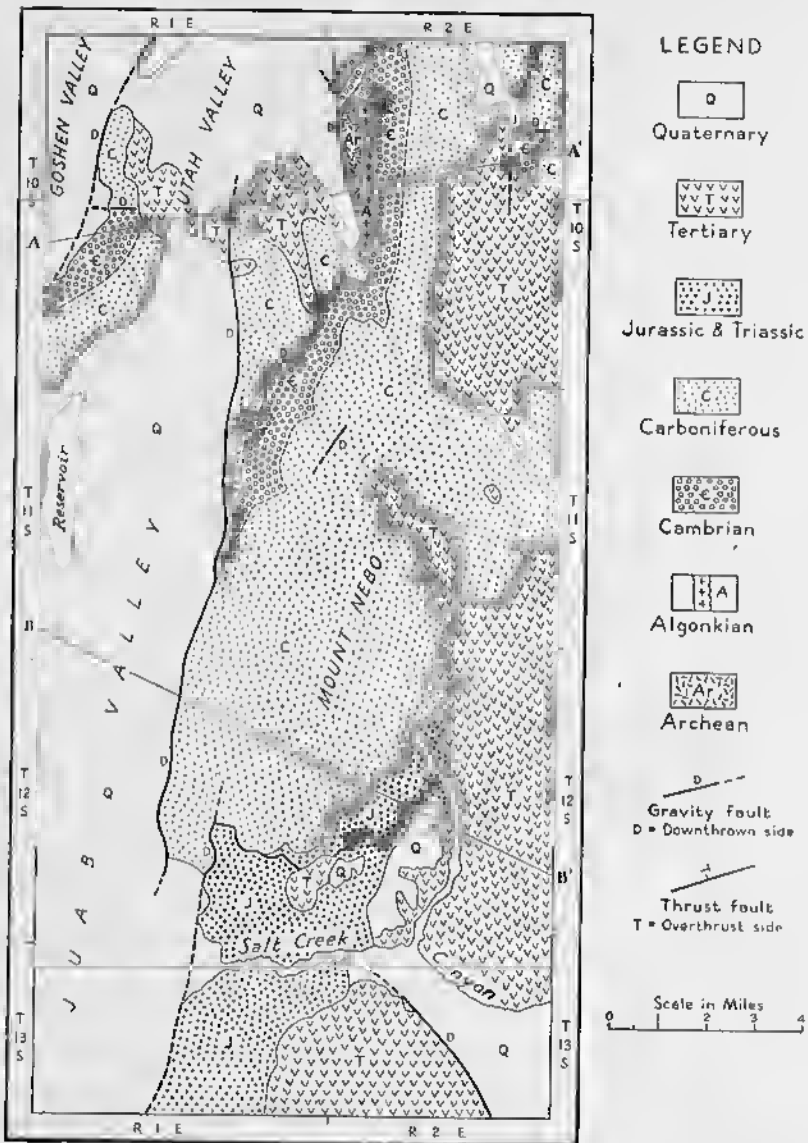


FIG. 168—Geological Map of the Tilted Fault Block of the Southern Part of the Wasatch Range, Utah. Cross sections along lines AA' and BB' are in Fig. 169. (After Eardley.)

peak in this part of the Wasatch Range, is underlain by Quaternary alluvium many hundreds of feet thick.

The Jurassic and older rocks in the mountains were greatly deformed by the Laramide folding at the end of the Cretaceous; consequently, the Tertiary and Quaternary rocks rest unconformably (see Chapter 13) on the older rocks. Mt. Nebo has been eroded from the eastern limb of an overturned anticline; this is shown on section *BB'*, Fig. 169, where the younger, Jurassic rocks dip under the older, Carboniferous rocks. A break thrust of considerable breadth, but slight net slip, cuts

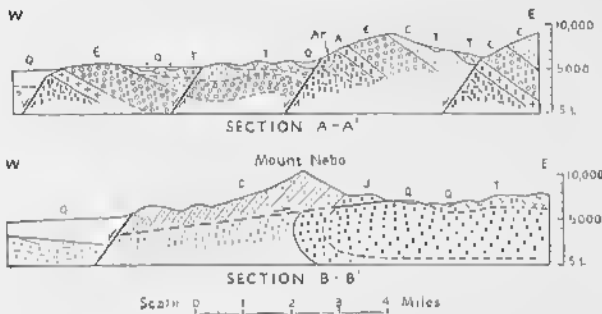


FIG. 169—Cross Sections of the Southern Part of the Wasatch Range, Utah, along Lines *AA'* and *BB'* of Fig. 168. *Ar* = Archean; *A* = Algoukian; *E* = Cambrian; *C* = Carboniferous; *J* = Triassic and Jurassic; *T* = Tertiary; *Q* = Quaternary. (After Bardley.)

the overturned limb. Toward the north, the strata are less intensely overturned and the dips progressively change from overturned toward the west into vertical and, finally, into easterly, dips. Along the line of section *AA'*, the Wasatch Range is carved out of the eastern limb of an anticline that is not overturned.

The gravity faults, the pattern of which is shown by the map, are much younger than the anticline and the thrust fault. Along the line of section *BB'*, a single large fault bounds the range on the west. Farther north, however, another fault appears *en échelon* to the east, and north of section *AA'* this is the fault that bounds the range on the west. Two of the fault planes that may be observed dip 50° W. The net slip on the major faults ranges from 6500 to 7800 feet. Fig. 170 is a block diagram to illustrate the character of the gravity faults as seen

from west of the area. The front of the block corresponds to the west side of the geological map, Fig. 168. The block diagram illustrates very strikingly the *en échelon* character of the faults. The surface of this block is an arbitrary horizontal datum plane, and in the area no such surface exists.

Many lines of evidence demonstrate the presence of the faults. Not only may the fault planes be observed, but triangular facets are well developed, and piedmont scarps cut alluvial fans, a fact that testifies to the recency of the movements.

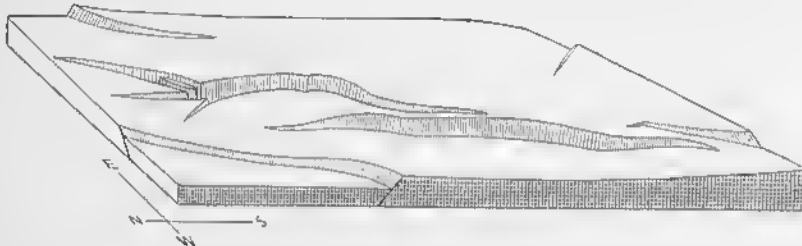


FIG. 170—Highly Diagrammatic Block Diagram of the Gravity Faults of the Southern Part of the Wasatch Range, Viewed from West. The surface of the block is an arbitrary surface, essentially horizontal. (After Eardley.)

Prior to gravity faulting, the region had been dissected to a mature topography with a relief of at least 3000 feet.<sup>13</sup> Eardley has calculated that the fault block has been tilted to the east at an angle of 3 to 4 degrees.

### Graben and Horsts

Many fault blocks are bounded on both sides by faults along which the displacement is more or less equal, and, consequently, there is little or no tilting. A *graben* is a block, generally long compared to its width, that has been lowered relative to the blocks on either side. A *horst* is a block, generally long compared to its width, that has been raised relative to the blocks on either side. The border faults are generally steep, and in most cases, if not all, they are either gravity faults or are essentially vertical. In some cases the border faults have been described as steep reverse faults, but the validity of these observations is questionable.

<sup>13</sup> Eardley, A. J., Strong relief before block faulting in the vicinity of the Wasatch Mountains, Utah: *Journal of Geology*, Vol. 41, pp. 243-267, 1933.

Graben and horsts, like most geological structures, may differ greatly in size. Fig. 171, which is a map of small faults formed during the earthquake of December 20, 1932, near Cedar Mountain, Nevada, shows some small graben.<sup>14</sup> The black lines are open fissures that are essentially vertical; the weight of the line shows the relative strength of the fissures, but the width

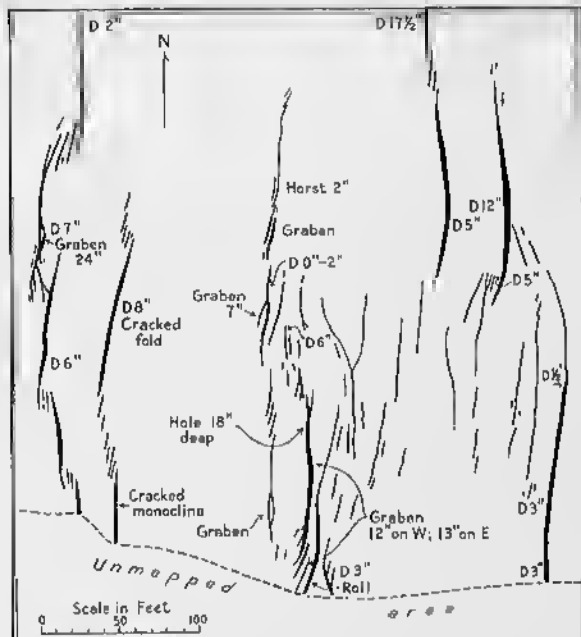


FIG. 171.—Fissures, Horsts, and Graben Formed during Cedar Mountain, Nevada, Earthquake. Solid black lines are open fissures; width of lines indicates relative magnitude of the fissures, but is not to scale.  $D$  = Downthrown side of fissure, the amount being given in inches. (After Gianella and Callaghan.)

has been exaggerated. The surface of the ground was the datum plane displaced by the fissures. In the northeast corner of the map, a small graben, 35 feet wide and 140 feet long, is shown. The throw on the east wall is 12 inches, and on the west wall it is 5 inches. Some of the graben are even smaller; in the south-central part of the map, a graben is 120 feet long, 5 to 20 feet

<sup>14</sup> Gianella, B. P., and Callaghan, E., The Cedar Mountain, Nevada, earthquake of Dec. 20, 1932: *Bulletin Seismological Society of America*, Vol. 24, pp. 345-377, 1934.

wide, and the displacement along the faults is approximately one foot.

In the Wasatch Plateau of Utah numerous graben that trend north-south cut the gently-dipping Mesozoic and Cenozoic strata. One of these, the Joe's Valley graben, is more than

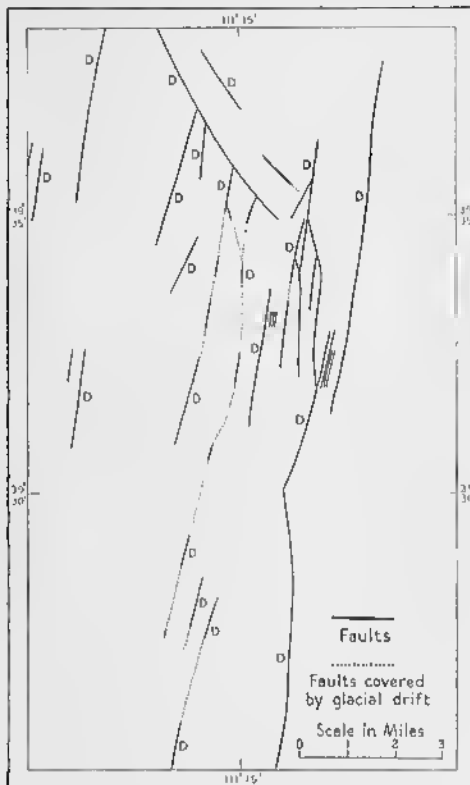


FIG. 172—Pattern of Gravity Faults at North End of Joe's Valley Graben, Utah. D = Downthrown side. (After Spieker and Billings.)

60 miles long, and is 2 to  $2\frac{1}{2}$  miles wide.<sup>15</sup> The *en échelon* pattern of the faults at the north end of this graben (Fig. 172) is similar to the pattern formed during the Cedar Mountain earthquake (Fig. 171). The maximum displacement on the faults through-

<sup>15</sup> Spieker, E. M., and Billings, M. P., Glaciation in the Wasatch Plateau, Utah: *Bulletin Geological Society of America*, Vol. 51, pp. 1173-1198; especially Pl. 5, 1940.

ont the entire graben ranges from 1500 to 3000 feet, but in the area covered by Fig. 172, it is from 1400 to 1600 feet. None of

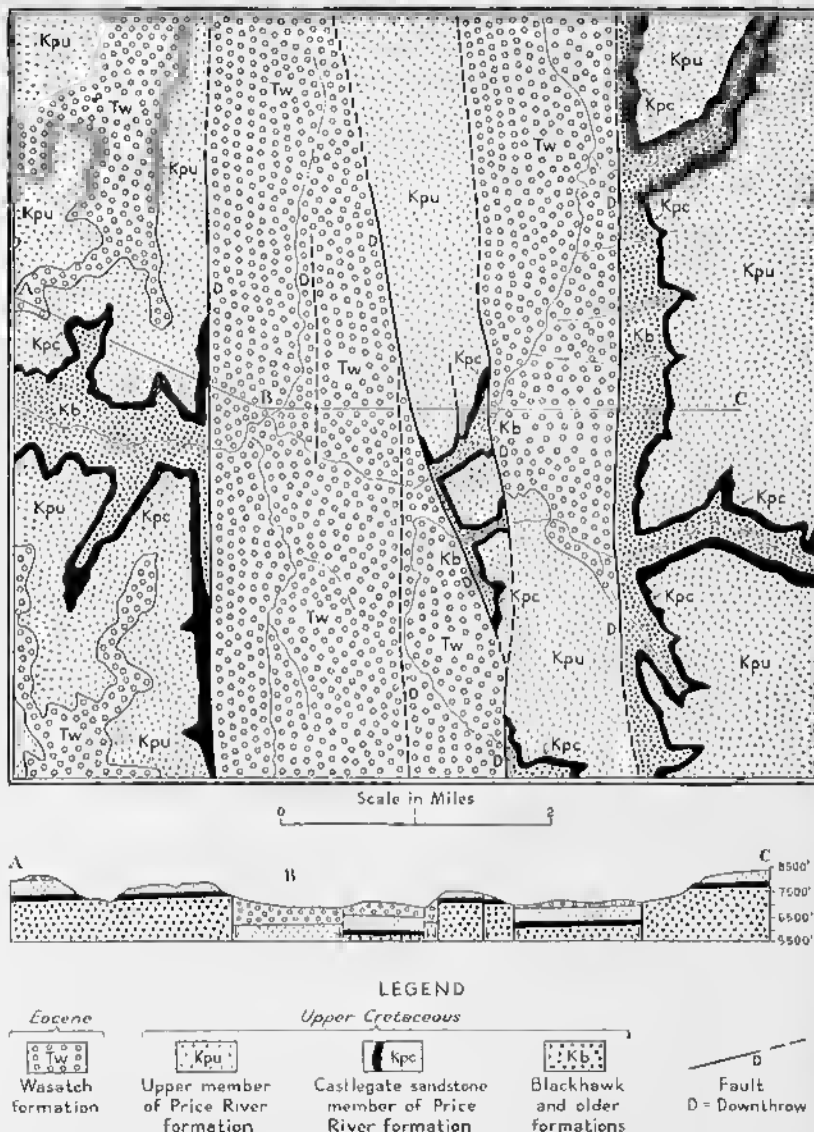


FIG. 173—Musinia Graben, Utah. (After Spieker and Baker.)

the faults has been observed, but the evidence indicates that the dips are steep.

A geologic map and structure section of part of a similar structural feature in another part of the Wasatch Plateau, the Musinia graben,<sup>16</sup> are shown in Fig. 173. None of the faults has been observed, but the dips are essentially vertical. The displacement along the most easterly fault increases from south to north; at the south end of the map it is only 500 feet, but at cross section *ABC* it is 1300 feet; at the north end of the map, the displacement increases to 2500 feet. The displacement along the western fault at structure section *ABC* is 2000 feet. A notable feature of this graben is a central horst, which increases in width toward the north and which wedges out to the south.

The size of some of the largest graben of Europe and Africa is indicated by Fig. 177, in which the pattern of the faults has been considerably simplified.<sup>17</sup>

The main Rhine graben is 180 miles long and 20 to 25 miles wide. The eastern border fault, where it is crossed by a tunnel, dips about 55 degrees toward the west, and occupies a crushed zone about 50 feet wide. The main part of the Great Graben, to the east of Lake Victoria in Africa, is approximately 300 miles long and is as much as 35 miles wide. The displacement along the faults bordering the Nyassa graben is as much as 8000 feet.

In experimental graben, formed by subjecting clay to tension, *antithetic faults*<sup>18</sup> are extensively developed under certain conditions. These faults dip toward the master fault (Fig. 174), but the displacement along them is dominantly of the gravity type. Such antithetic faults are common in a tunnel section that cuts the eastern border fault of the Rhine graben.

Horsts range in size from those that are only a few inches wide to those that are many miles wide. A small horst is illustrated in the north-central part of Fig. 171. The horst that occupies the center of the Musinia graben (Fig. 173) is at least 5 miles long, one mile wide at maximum; the displacement along the border faults is 1000 to 1500 feet.

<sup>16</sup> Spicker, E. M., and Baker, A. A., Jr., Geology and coal resources of the Sulina Canyon district, Sevier County, Utah: *U. S. Geological Survey Bull.* 796, pp. 125-170, 1928.

<sup>17</sup> Cloos, H., "Hebung, Spaltung, Vulkanismus," *Geologische Rundschau*, Band 30, Zwischenheft 4A, pp. 406-527; cf. especially p. 434, 1939.

<sup>18</sup> Cloos, H., *op. cit.*, p. 416.

The Ruby-East Humboldt Mountains of Nevada (Fig. 175) are essentially a large, complex horst that trends north-northeast for at least 53 miles and averages 7 miles in width.<sup>19</sup> The faults bounding the range are gravity faults that dip away from the mountains at angles of 60 to 70 degrees. The displacement on the eastern faults is 5500 to 6000 feet, whereas that on the western faults is only 2000 feet. The range is thus a westward tilted horst. Many of the criteria given in Chapter 9 may be employed to prove the presence of the faults: the internal structure of the range is truncated by the mountain front; piedmont

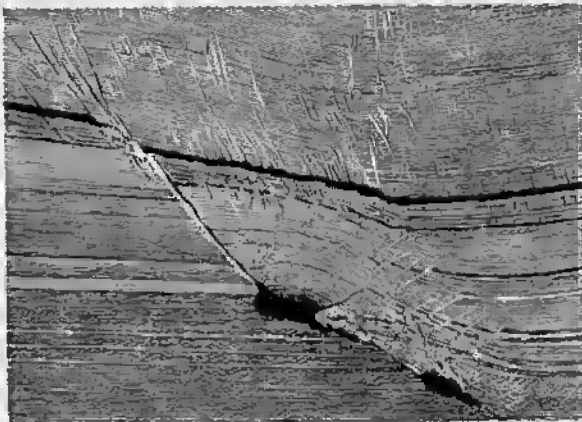


FIG. 174—Edge of an Artificial Graben. Produced by subjecting clay to tension. The master fault and many subsidiary faults dip to the right. Antithetic faults dip to the left. All the faults are of the gravity type. (After H. Cloos.)

scarps as much as 200 feet high cut bedrock, alluvium, and glacial moraines; triangular facets are exposed on the west side of the range; and in two localities the fault plane is exposed.

#### Intermittent Faulting

Movement along gravity faults is intermittent, and a period of relatively rapid movements may be followed by a long interval of quiescence, during which erosion partially or completely destroys the topographic expression of the fault. In a renewed cycle of rapid movements a new scarp can develop.

<sup>19</sup> Sharp, R. P., Basin-range structure of the Ruby-East Humboldt Range, northeastern Nevada: *Bulletin Geological Society of America*, Vol. 50, pp. 881-920, 1939.

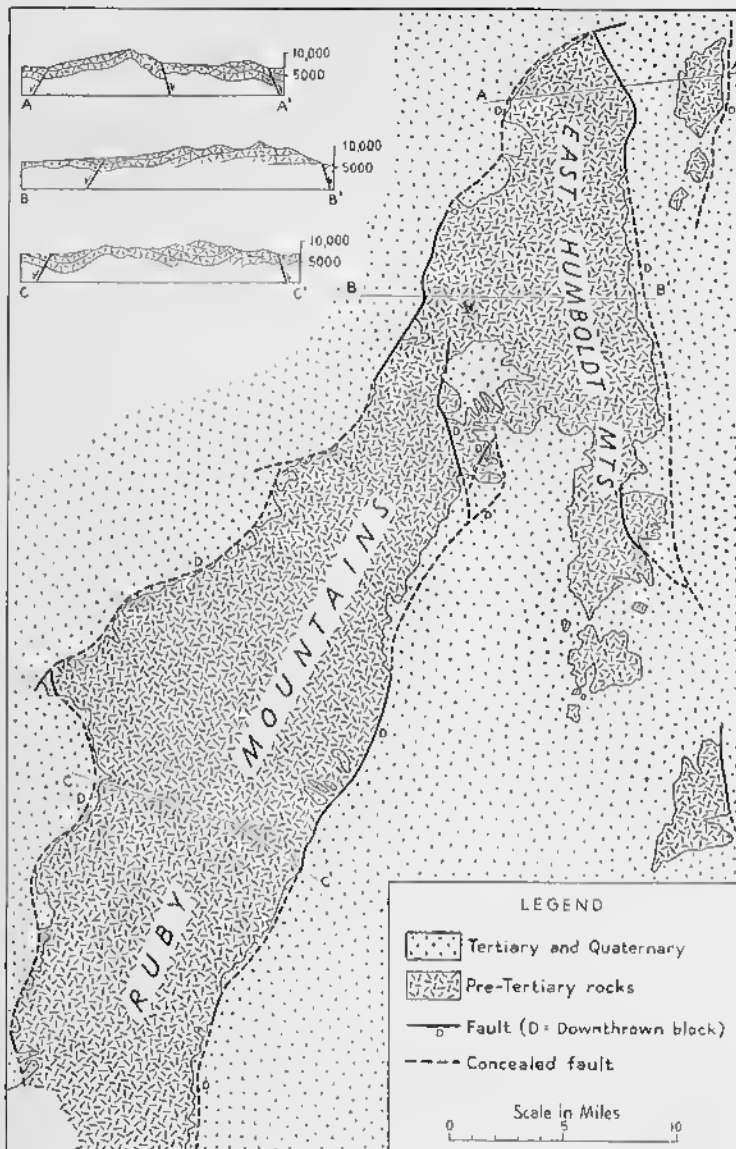


FIG. 175—Horst of the Ruby-East Humboldt Range, Nevada. (After R. P. Sharp.)

Fig. 176 illustrates the intermittent character of movement along the Hurricane fault of Utah and Arizona.<sup>20</sup> This fault extends at least 170 miles in a direction somewhat east of north, and the displacement ranges from 1500 to 10,000 feet. After eruption of Miocene (?) volcanics (Fig. 176A), the Hurricane fault formed in late Miocene or Pliocene time and the western block dropped 8000 feet relative to the eastern block (Fig. 176B). In a subsequent interval of quiescence, all topographic expression of the fault was destroyed, and a surface of low relief developed. During Quaternary time basalts were erupted on this surface

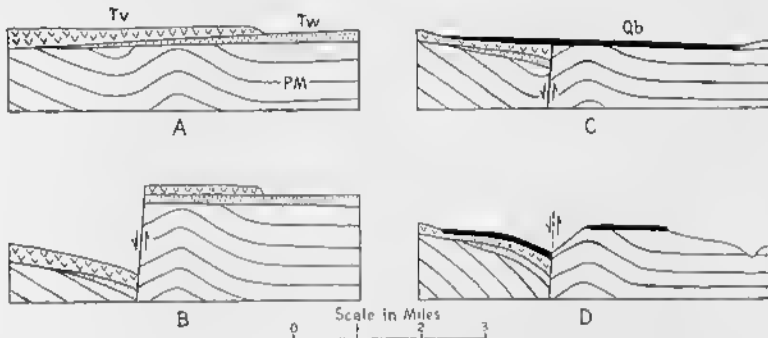


FIG. 176—Evolution of the Hurricane Fault, Utah and Arizona. PM = Paleozoic and Mesozoic rocks; Tw = Wasatch formation (Eocene); Tv = Miocene (?) volcanoes; Qb = basalt (Quaternary). A, B, C, and D represent successive stages. (After L. Gardner.)

(Fig. 176C). During the last disturbance, which occurred during the Quaternary, the western block dropped 700 to 1000 feet (Fig. 176D).

### Origin of Gravity Faults

The nature of the forces that cause gravity faulting is a subject upon which complete agreement has not been reached. It is obvious, however, that gravity faulting is associated with a stretching of the rocks involved; wherever the hanging wall goes down relative to the footwall, the total area occupied by the blocks is increased. On the assumption that the stretching causes the fracturing, most geologists have concluded that gravity faults are the result of tension. This does not preclude

<sup>20</sup> Gardner, L. S., The Hurricane fault in southwestern Utah and northwestern Arizona: *American Journal of Science*, Vol. 239, pp. 241-260, 1941.

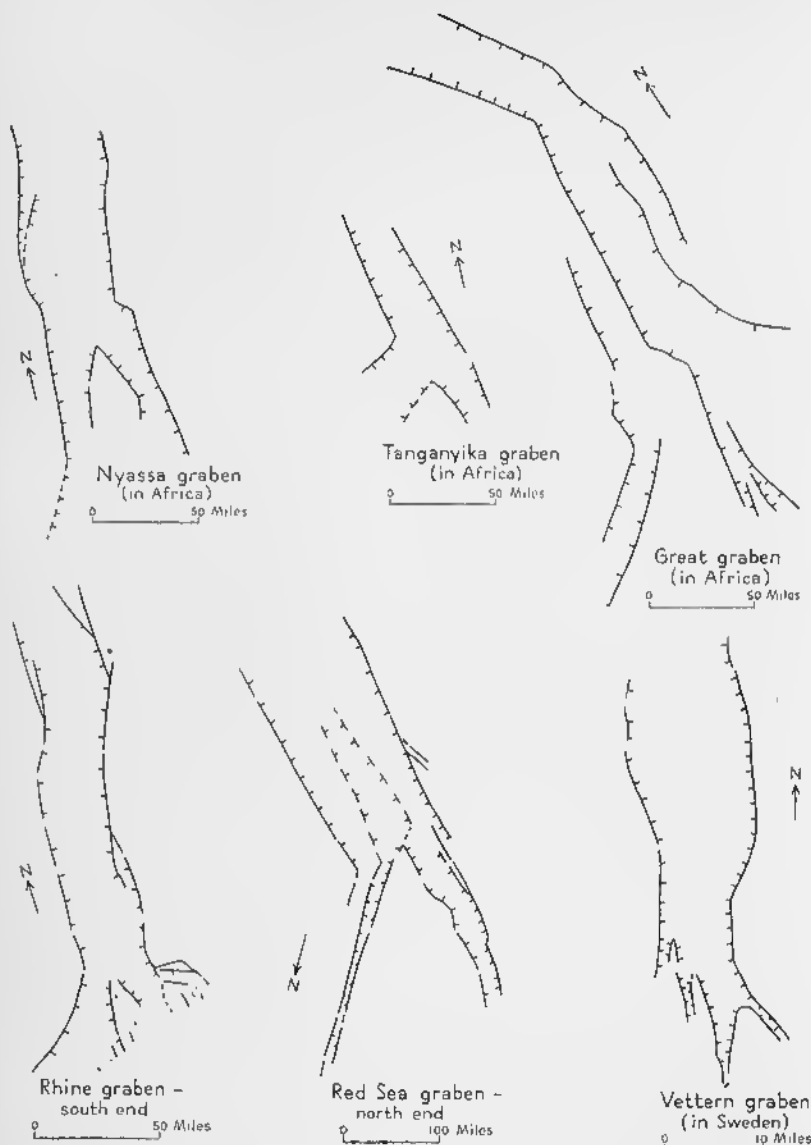


FIG. 177—Generalized Pattern of Some Large Graben. Arrow marked N indicates North, which is generally not toward top of page. (After H. Cloos.)

the possibility that the tension is the indirect result of compressional, rotational, or torsional forces.

Among the various suggestions that have been advanced to explain the origin of the tension, the following are the most worthy of consideration: (1) If the interior of the earth were to expand, an outer shell would be subjected to tension.<sup>21</sup> Most gravity faults are too closely related to local structures, however, to be explained in this way. (2) Differential vertical movements cause stretching (Fig. 79), as a result of which the rocks are subjected to tension; if the rocks are brittle enough, they will fail by rupture. Many gravity faults, even the largest, are most satisfactorily explained in this way; the subject is treated more fully below. (3) If rocks are left unsupported by the removal of material beneath, they tend to sag, and tensional stresses are set up. (4) Field observations show that gravity faulting often follows folding, which suggests that tensional stresses follow the relaxation of the compressional forces. (5) The horizontal movement of masses of rock past each other (Fig. 163) may induce couples that cause tension in preferred directions. (6) The passage of earthquake waves subjects the rocks alternately to compression and tension, and this mechanism has been cited to explain some gravity faults. It is evident, however, that such faults would be of minor importance.

A discussion of the origin of graben<sup>22</sup> is particularly pertinent to the question of the genesis of gravity faults. The small graben shown in Fig. 171 are clearly the result of tension. The gaping fissures offer undeniable evidence that the rocks have been stretched. The tensional forces operated in a direction somewhat north of west. The tension was caused, however, by a couple, in which the rocks to the northeast were moving southeasterly relative to the rocks to the southwest.

The origin of small graben at the foot of large fault scarps has been discussed on p. 164.

Some graben in volcanic regions are presumably due to the withdrawal of lava. At the east end of the Island of Hawaii, a small graben was deepened in 1924. The graben is about one

<sup>21</sup> Bucher, W. H., *The Deformation of the Earth's Crust*, pp. 119-123. Princeton: Princeton University Press, 1933.

<sup>22</sup> Taber, Stephen, Fault troughs: *Journal of Geology*, Vol. 35, pp. 577-606, 1927.

mile wide, and the movement, which lasted several days, affected a section four or five miles long. The displacement on the northeast wall was 10 to 12 feet, and was 1 to 2 feet on the southwest side. Similar features, known as collapse depressions, are described on p. 315.

Many graben, both large and small, are associated with plateaus and domes, some of which are of continental proportions.<sup>23</sup> Because of the stretching of the rocks (Fig. 79), tensional forces develop, the rocks fail by rupture, and movement along the resulting fractures ensues (Fig. 178). The formation

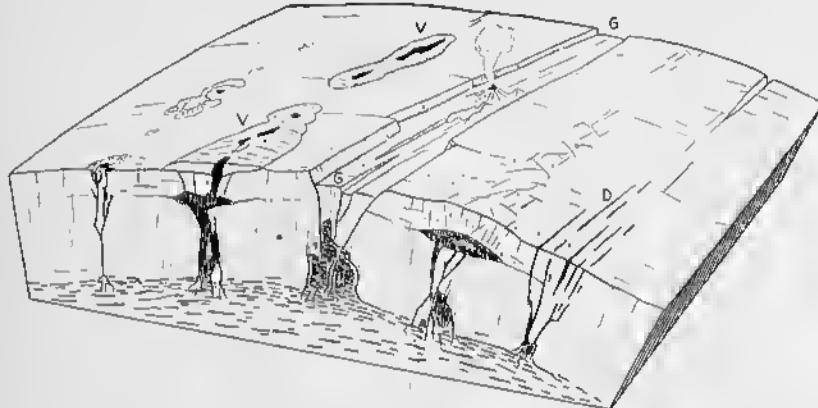


FIG. 178—Origin of Graben. *G* = graben; *D* = dikes; *V* = volcanics, with associated intrusives in solid black. (After H. Cloos.)

of the larger graben has often been associated with extensive volcanism, which is notably true of the graben of Africa, the Oslo graben, and the Rhine graben. The relation is generally not simple; that is, the master faults bounding the graben are not necessarily the fractures up through which the magma moves. In some instances, the most extensive volcanism is in the vicinity of, but beyond the limits of, the graben (Fig. 178).

The horst and graben structure of southeastern Idaho has been ascribed to tension which served "as a method of relief for overstrained or overcompressed structural features."<sup>24</sup>

Fault block mountains—both the tilted fault blocks and horsts—are similar in origin to graben. Although some may be

<sup>23</sup> Cloos, Hans, *op. cit.*

<sup>24</sup> Mansfield, G. R., Geology, geography, and mineral resources of southeastern Idaho: *U. S. Geological Survey Professional Paper* 152, 1929, p. 390.

due to tension that followed excessive compression during folding, most of them seem to be due to stretching induced by vertical movements. The domed area is broken by fractures, along which differential movement takes place. It was supposed in some of the older hypotheses that doming took place first and was later followed by collapse. It is apparent, however, that doming and faulting can go on simultaneously. If doming continues after a number of fractures have formed, the individual blocks will be uplifted differentially, and some blocks may subside.

The cause of the vertical movements is a moot question. Gilbert and Gilluly favor the hypothesis that a brittle surface layer adjusts itself to folds induced by regional compression in a deep-seated layer.<sup>25</sup>

---

<sup>25</sup> Gilluly, James, *op. cit.*, p. 88.

## Secondary Foliation and Lineation

### Introduction

The ability of rocks to break along approximately parallel surfaces is called *foliation* or *foliate structure*.<sup>1</sup> In some rocks this is a primary feature, inherited from the time of their formation. Many sedimentary rocks, particularly those that are fine-grained, tend to part parallel to the stratification, and thus they possess what is often called *bedding fissility*. Bedding fissility is due to differences in the grain size or composition of the particles in the various layers, or to platy and elongate grains more or less parallel to the stratification. Many igneous rocks, both intrusive and extrusive, possess a primary foliation, but discussion of this subject has been reserved for Chapter 16. The present chapter is concerned exclusively with those foliate structures which are of secondary origin, and which develop some time—often millions of years—after the original formation of the rock. Such structures may develop in rocks of either sedimentary or igneous origin, and the product is a metamorphic rock.

*Cleavage*, sometimes called *rock cleavage*<sup>2</sup> in order to distinguish it from *mineral cleavage*, is the ability of rocks to break along parallel surfaces of secondary origin (Pl. XV). Much rock cleavage is inclined to the bedding, but in some instances it may be parallel to the bedding. *Schistosity* is a term applied to the variety of rock cleavage found in rocks that are sufficiently recrystallized to be called *schist* or *gneiss*. Thus the secondary foliation of a slate would be called *cleavage*, but a similar structure in a mica schist would be termed *schistosity*. Obviously,

<sup>1</sup> Mead, W. J., Folding, rock flowage, and foliate structures: *Journal of Geology*, Vol. 48, pp. 1007-1021, 1940.

<sup>2</sup> Leith, C. K., Rock cleavage: *U. S. Geological Survey Bull.* 239, 1905.

there are transitional rocks in which either term might be appropriately used.

The attitude of cleavage and schistosity is measured in the same way as is the attitude of bedding. The strike is the direction of a horizontal line in the plane of cleavage; the dip, which is the angle between the cleavage and a horizontal plane, is measured at right angles to the strike (Fig. 16).

Special symbols are employed to represent cleavage and schistosity on geological maps. Because the symbols are not

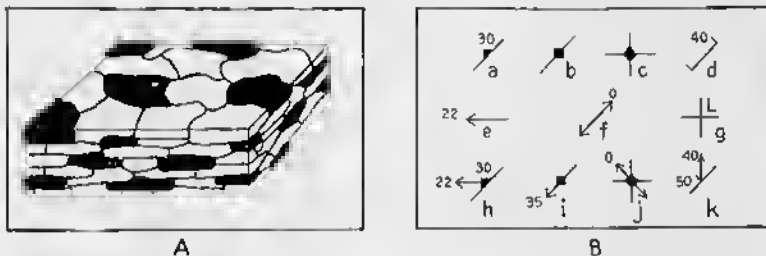


FIG. 179—Flow Cleavage and Map Symbols. A. Flow cleavage due to parallel orientation of platy minerals. Black = biotite mica or chlorite; white = feldspar and quartz. B. Map symbols: *a* = cleavage dipping  $30^{\circ}$  NW.; *b* = vertical cleavage striking N.  $45^{\circ}$  E.; *c* = horizontal cleavage; *d* = another type of symbol to represent cleavage that dips  $40^{\circ}$  NW.; *e* = lineation plunging  $22^{\circ}$  W.; *f* = horizontal lineation striking N.  $45^{\circ}$  E.; *g* = vertical lineation; *h* = cleavage dipping  $30^{\circ}$  NW., lineation plunging  $22^{\circ}$  due west; *i* = vertical cleavage, lineation plunging  $35^{\circ}$  SW.; *j* = horizontal foliation, horizontal lineation striking N.  $45^{\circ}$  W.; *k* = bedding dipping  $50^{\circ}$  NW., lineation plunging  $40^{\circ}$  due north.

standardized, it is necessary to look at the legend accompanying the map in order to understand the meaning of the symbols. In one type of symbol, represented by *a*, *b*, and *c* in Fig. 179B, a long line gives the strike, and a triangle, either open or solid black, shows the direction of dip; the value of the dip is given by a numeral. Symbol *a* indicates that the cleavage (or schistosity) strikes N.  $45^{\circ}$  E. and dips  $30^{\circ}$  NW. Symbol *b* indicates that the cleavage strikes N.  $45^{\circ}$  E. and is vertical. Symbol *c* indicates horizontal cleavage. On many older maps a different type of symbol is used; symbol *d* of Fig. 179B indicates a cleavage that strikes N.  $45^{\circ}$  E. and dips  $40^{\circ}$  NW.

A *schist* is a metamorphic rock that possesses schistosity, but which is not characterized by layers of differing mineral composition. A *gneiss* is a metamorphic rock characterized by



PLATE XIV. Fault Cutting Santa Fe Formation, Rio Puerco,  
New Mexico. (Photo by H. E. Wright.)



PLATE XV. Cleavage. Bedding dips 60 degrees to the left. Flow cleavage in argillaceous beds dips 85 degrees to the right. Fracture cleavage in arenaceous beds dips 60 degrees to the right. Analysis of relation of cleavage to bedding indicates that beds are right-side-up, and that synclinal axis lies to the left. (From a photo by G. K. Gilbert, U S. Geological Survey.)

alternating bands, usually a few millimeters or centimeters thick, of differing mineral composition. In many cases, some bands are rich in light minerals, others are rich in dark minerals. The layers may or may not possess foliation. *Paraschists* and *paragneisses* are, respectively, schists and gneisses of sedimentary origin. *Orthoschists* and *orthogneisses* are, respectively, schists and gneisses of igneous origin. *Metasediments*, *metavolcanics*, and *meta-igneous rocks* are metamorphic rocks derived, respectively, from sedimentary, volcanic, and igneous rocks. A slate derived from a shale is a metasediment, but none of the other terms would apply to it. A mica schist derived from a shale could be called either a metasediment or a paraschist. A marble that is devoid of schistosity is a metasediment, but none of the other terms would apply to it. Rocks that result from the injection of thin layers of magma into older metamorphic rocks, or from the partial replacement of older metamorphic rocks by solutions of igneous origin, are sometimes called *migmatites*.<sup>3</sup>

Structural geology is not concerned with the question whether the rocks are of sedimentary, igneous, or mixed origin, because such problems belong to the stratigrapher, petrographer, and metamorphic geologist. The cleavage and schistosity of such rocks, however, lies in the domain of structural geology. In actual field work, of course, it is usually impossible to divorce the subjects of genesis and tectonics, and the geologist working in cleaved and schistose rocks must be well-versed in tectonics, metamorphism, and petrography.

The principal secondary foliate structures may be classified as flow cleavage, fracture cleavage, shear cleavage, and bedding cleavage. For some of these the term *schistosity* would be as appropriate as cleavage, but certain desirable distinctions become apparent below.

### Types of Cleavage

#### Flow cleavage

Flow cleavage, sometimes called *slaty cleavage* and *axial plane cleavage*, is due to the parallel orientation of platy minerals,

<sup>3</sup> Sederholm, J. J., On migmatites and associated Precambrian rocks of southern Finland: *Commission Géologique de Finlande Bulletins* 58, 77, and 107, 1923, 1926, and 1934.

such as the micas and chlorites (Fig. 179), or of elongate minerals, such as hornblende. The cleavage planes are present throughout the rock, and are a fraction of a millimeter apart. They form at right angles to the least strain axis of the strain ellipsoid; in other words, they lie in the plane that includes the intermediate and greatest strain axes. In Fig. 180A, the flow cleavage is parallel to the plane represented by  $AA'$ . If it is caused by simple compression, flow cleavage is perpendicular to the compressive force, but if it is caused by a couple, flow

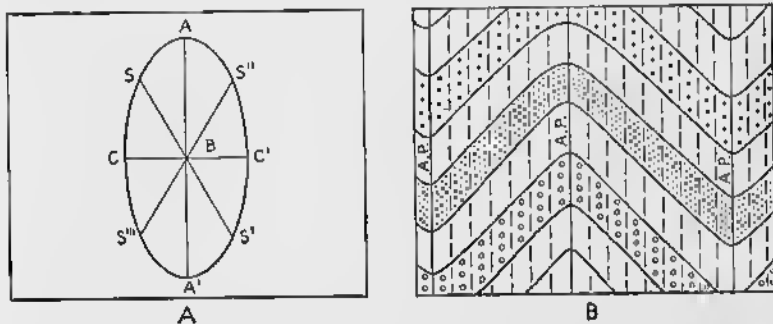


FIG. 180—Flow Cleavage. A. Flow cleavage forms at right angles to the least strain axis ( $CC'$ ) of the strain ellipsoid; it includes the greatest strain axis ( $AA'$ ) and the intermediate strain axis ( $BB'$ ), which is perpendicular to the plane of the paper. Fracture cleavage and shear cleavage develop essentially parallel to the planes represented by  $SS'$  and  $S''S'''$ . B. Structure section of folds. Flow cleavage, represented by vertical broken lines, is parallel to the axial planes ( $AP$ ) of the folds.

cleavage is inclined to the deforming forces. In all cases, however, it bears the same relation to the strain ellipsoid. Inasmuch as the axial planes of folds are essentially perpendicular to the least strain axis, it follows that flow cleavage is parallel to the axial planes of the folds, as is illustrated in Fig. 180B. The significance and use of this principle is discussed on p. 228.

Flow cleavage is the result of plastic deformation. The rock mass changes shape by becoming shorter perpendicular to the cleavage and longer parallel to it. The internal readjustments in the rock are similar to those in any plastic deformation (pp. 25-29), involving the granulation and rotation of grains, gliding, and recrystallization. Platy and elongate minerals are rotated to assume an attitude more nearly at right angles to the

least strain axis. Individual minerals, by gliding, change in shape (Fig. 13) so that the shortest axis of the deformed mineral is parallel to the least strain axis. If they are platy, the new minerals that form by recrystallization have the shortest dimension parallel to the least strain axis. The net result is to develop a rock made up of platy and elongate minerals, lying with their greatest dimensions in the plane that contains the intermediate and greatest strain axes. The rock will obviously cleave most readily parallel to this direction.

### Fracture cleavage

Fracture cleavage is essentially closely-spaced jointing. The distance between individual planes of cleavage can be measured, and it is commonly a matter of millimeters or centimeters. The minerals in the rock are not parallel to the cleavage. Fracture cleavage is a shear phenomenon that obeys the laws of shear fractures; consequently, fracture cleavage is inclined to the least strain axis at an angle of approximately 45 degrees. In Fig. 180A, the fracture cleavage is parallel to the planes represented by  $SS'$  and  $S''S'''$ . Under simple compression, the fracture cleavage forms at approximately 45 degrees to the compressive force, but, under a couple, one set of cleavage planes is roughly parallel to the deforming forces, and the other set is inclined at a high angle. Ordinarily, for reasons that are discussed on p. 230, only one set of these cleavage planes forms.

### Shear cleavage

Although fracture cleavage is a shear phenomenon, no visible displacement takes place along the planes of rupture. If, however, there is differential movement along the fractures, they become small faults. The cleavage is then more appropriately called *shear cleavage* or *slip cleavage*. The platy minerals may be dragged into parallelism with the cleavage, and new minerals may crystallize in the cleavage plane. Under such conditions shear cleavage may simulate flow cleavage, but it may be distinguished from flow cleavage if the various evolutionary stages are preserved.

Inasmuch as shear cleavage is essentially fracture cleavage along which there has been displacement, it bears the same

relation to the strain ellipsoid and to the deforming force as does fracture cleavage.

Shear cleavage is often considered a variety of fracture cleavage, rather than a category separate from fracture cleavage.

### Bedding cleavage

In some metamorphic rocks the cleavage is parallel to the bedding, and hence it may be called *bedding cleavage* or *bedding schistosity*. Cleavage parallel to bedding may be due to (1) isoclinal folding; (2) mimetic recrystallization; (3) flow parallel to bedding; and (4) load metamorphism.

(1) The bedding on the limbs of an isoclinal fold is parallel to the axial plane. Because the flow cleavage is parallel to the axial plane, it will also be parallel to the bedding on the limbs. But on the nose of such folds the flow cleavage cuts across the bedding at a considerable angle.

(2) In many localities, however, the schistosity follows the bedding, and wraps around the noses of the folds. Such schistosity is probably *mimetic*; during the recrystallization of the rock, the new platy minerals grew with their long dimensions parallel to the bedding. Little or no plastic deformation need accompany such reerystallization.

(3) In some localities characterized by bedding cleavage, originally spherical pebbles have been flattened so that the shortest axis is perpendicular to the bedding; conversely, the rocks must be elongated parallel to the bedding. In places, this type of deformation may be due to the upward pressure of magma more or less perpendicular to the bedding. Another mechanism is discussed on p. 235.

(4) Bedding cleavage has sometimes been ascribed to *load metamorphism*.<sup>4</sup> According to this hypothesis, the weight of an overlying thick column of rocks exerts vertically-directed pressure on flat strata. Such a load, however, would produce a confining pressure that is essentially hydrostatic, and the proposed mechanism does not seem competent to explain bedding cleavage.

---

<sup>4</sup> Daly, R. A., Metamorphism and its phases: *Bulletin of Geological Society of America*, Vol. 28, pp. 375-418, 1917.

The field geologist must be exceedingly cautious in concluding that bedding and schistosity are parallel. Under some conditions of metamorphism, where shales and sandstones are interbedded, the more plastic shale may be squeezed into inclined planes of cleavage that cut the sandstones. The resulting structure is *cleavage banding* (Fig. 181A). The individual bands of shale are characteristically a fraction of an inch thick. In other rocks, notably those that have been thoroughly recrystallized under conditions of high metamorphic intensity, the light and dark minerals may segregate into alternate bands

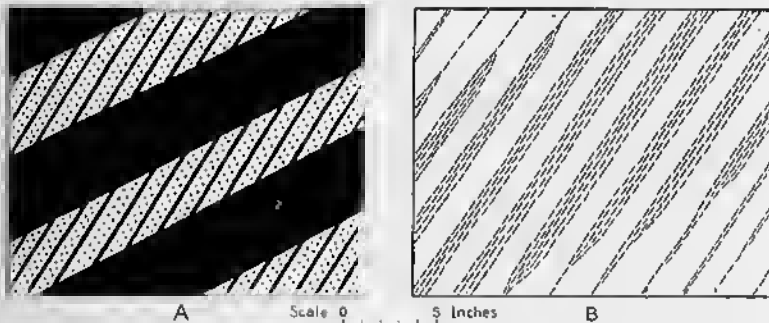


FIG. 181—Cleavage Banding and Segregation Banding. A. Cleavage banding. Solid black represents shale, dots represent sandstone. Bedding dips 25 degrees to left; cleavage dips 60 degrees to left. The more plastic shale has been injected along cleavage in the sandstone to produce a rhythmic alternation of shale and sandstone that simulates bedding. B. Segregation banding. Short dashes represent bands rich in dark minerals. White areas are rich in light mineral. Bedding dips 25 degrees to the left.

parallel to the schistosity (Fig. 181B); the individual bands are a fraction of an inch to an inch thick. This may be called *segregation banding*. The original rock may have been homogeneous, but during recrystallization the various elements moving in solution tended to accumulate in different bands. Segregation banding thus differs from the plastic injection characteristic of cleavage banding.

In such cases the ordinary criteria for recognizing bedding—compositional and textural differences—cannot be applied. If, however, the layers that differ in composition are many inches or feet thick, they presumably represent bedding. In the final analysis, however, each case must be decided on its own merits.

### Classification

The above discussion of foliation may be conveniently summarized in Table 2. For the sake of completeness, the foliate structures of igneous rocks are included, although detailed description is reserved for Chapter 16.

TABLE 2  
CLASSIFICATION OF FOLIATION

- A. Primary:
  - 1. Sedimentary rocks—*bedding fissility*
  - 2. Plutonic rocks—*primary foliation*
  - 3. Extrusive rocks—*flow structure*
- B. Secondary: in rocks of both sedimentary and igneous origin.
  - 1. *Flow cleavage* (also called slaty cleavage or axial plane cleavage)
  - 2. *Fracture cleavage*
  - 3. *Shear cleavage (skip cleavage)*
  - 4. *Bedding cleavage*

### Alternate interpretation of cleavage

The distinction made in the preceding sections between flow cleavage and fracture cleavage is not accepted by many structural geologists. They believe that both of these supposed types of cleavage are one and the same, forming parallel to the shear planes of the strain ellipsoid.

### Secondary Lineation

*Lineation*, also called *linear parallelism* and *linear structure*, is due to the parallelism of some directional property in the rock. For example, a rock in which the long axes of hornblende crystals are essentially parallel, would possess a lineation. All transitions exist between rocks that possess no lineation and rocks with excellent lineation. In one rock the long axes of 90 per cent of the hornblende crystals might lie within a few degrees of each other; such a striking linear parallelism would be recognized immediately. In another rock, however, the long axes of the hornblende crystals might be rather evenly oriented in all possible directions within the rock; in such a case no lineation would exist.

Igneous rocks may possess a *primary lineation*—that is, a lineation due to the flow of the magma. Although the lineation of metamorphic rocks may be inherited from the original rock, more commonly it is a secondary feature developed during

deformation. At present we are concerned only with *secondary lineation*, and for the sake of brevity throughout the rest of this chapter, it will be referred to simply as lineation.

Lineation can occur with or without foliation; that is, a rock without cleavage or schistosity may, nevertheless, possess lineation. More commonly, however, lineation is associated with foliation, and the linear feature is parallel to the plane of cleavage or schistosity.

Lineation may be expressed in various ways. Elongated or "stretched" pebbles or boulders are one of the most impressive types of lineation (Fig. 182A). Each pebble is an irregular ellipsoid, the longest axis of which may be several times as long as the shortest axis. The long axes of the pebbles are more or less parallel to one another. The short and intermediate axes of the different pebbles are likewise parallel, and the short axis is perpendicular to whatever schistosity is present. The amount of the elongation permits an estimate of the extent of the plastic deformation. If the original shape of the pebbles is unknown, however, a precise quantitative measurement is difficult. Locally, however, a conglomerate may have escaped intense deformation, so that the original shape of the pebbles may be known.

Lineation is more commonly expressed by the minerals constituting the rock. As noted above, hornblende crystals, which have one long dimension, with the result that individual crystals are more or less needle shaped, may display an excellent lineation (Fig. 182B). In some instances, biotite occurs as elliptical plates, the long axes of which are parallel. In other cases, although the individual plates are circular, they are strung out in groups, the long dimensions of which are parallel (Fig. 182C). In still other instances, an original, more or less spherical mineral, may be granulated into numerous fragments which become strung out into an ellipsoidal group.

The schistosity or cleavage may be thrown into small corrugations or crinkles, with a wave length and an amplitude that are measured in millimeters (Fig. 268). In such a case the lineation results from the parallel arrangement of the crests of minute drag folds formed by the sliding of different layers over one another.

The intersection of bedding and cleavage produces a lineation, because the intersection of two planes is a line. If the rock breaks parallel to the cleavage, the trace of the bedding appears as parallel streaks on the cleavage. In Fig. 182D, the top of the block is parallel to the cleavage; the trace of the bedding on the cleavage is parallel to  $b$ . On the other hand, if the rock breaks parallel to the bedding, the trace of the cleavage appears as minute fractures on the bedding.

The attitude of the lineation is defined by the strike of its horizontal projection and its plunge. Fig. 29, although designed primarily to illustrate the method of measuring the attitude of the axis of a fold, may be used equally well to illustrate the measurement of lineation. The lineation is  $FD$ ; the horizontal projection ( $AD$ ) of the lineation trends northwest, and this is said to be the strike of the lineation. The angle  $P$  is the plunge of the lineation.

On geological maps the attitude of the lineation is represented by an arrow (symbol  $e$  of Fig. 179B). The trend of the arrow is parallel to the strike of the lineation. The arrow points in the direction of plunge, and an arabic numeral gives the value of the plunge. Thus symbol  $e$  of Fig. 179B indicates a lineation which plunges 22 degrees in a direction N.  $90^{\circ}$  W. A special symbol such as  $f$ , with arrowheads at both ends, is employed for horizontal lineation. Symbol  $f$  means that the strike of a horizontal lineation is N.  $45^{\circ}$  E. Symbol  $g$  is used for vertical lineation; to distinguish this symbol from a similar symbol used for the axes of vertical folds, an  $L$  may be placed at the side of the lineation symbol, an  $F$  may be placed at the side of the fold symbol.

Because lineation usually lies in the plane of the foliation, the two symbols are generally combined. Symbol  $h$  of Fig. 179B indicates a schistosity that strikes N.  $45^{\circ}$  E. and dips  $30^{\circ}$  NW.; lying in the plane of the schistosity is a lineation, the horizontal projection of which strikes N.  $90^{\circ}$  W. and plunges  $22^{\circ}$  W. Symbol  $i$  indicates a vertical schistosity that strikes N.  $45^{\circ}$  E., and on which is a lineation plunging  $35^{\circ}$  SW. Symbol  $j$  indicates a horizontal foliation with a horizontal lineation that strikes N.  $45^{\circ}$  W. Symbol  $k$  indicates bedding that strikes

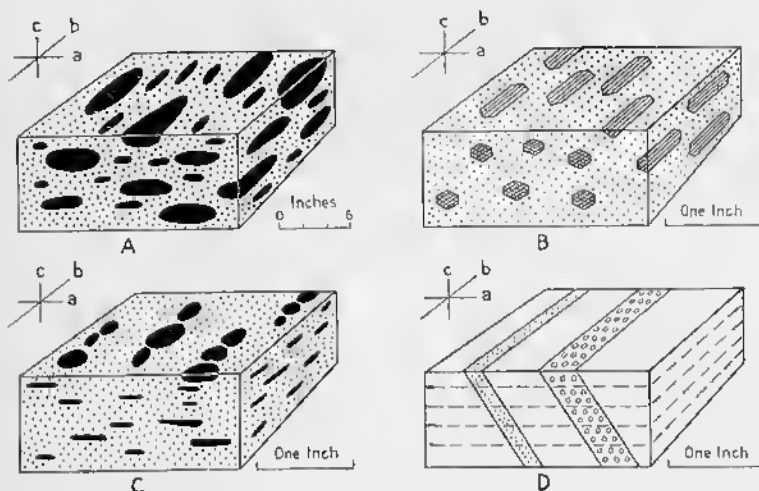


FIG. 182—Lineation. A. Elongated pebbles are shown in solid black. Each pebble is an irregular ellipsoid, the long axis of which is parallel to  $b$ , the short axis parallel to  $c$ , and the intermediate axis parallel to  $a$ . B. Elongate crystals of hornblende, the long axes of which are parallel to  $b$  in the diagram. C. Lineation caused by circular plates of mica, shown in solid black, strung out like beads on a string. D. Cleavage is represented by top of block and by planes shown by broken lines. Bedding is shown by dots and open circles. Trace of bedding on cleavage gives a lineation.

N. 45° E., and dips 50° NW. On this is a lineation that strikes N. and plunges 40° N.

In the field, a careful record should be made concerning the kind of lineation, as all types of lineation are not formed in the same way.

A discussion of the origin of secondary linear features is given on p. 233.

### Relation of Cleavage to Major Structure

#### Introduction

Empirical observation in the field has shown that in many localities the cleavage and lineation bear a standard relationship to the major structure. The systematic pattern shown by folds, cleavage, and lineation is of the utmost importance to the structural geologist attempting to solve complicated field problems. The constancy of this relationship is, after all, not unexpected. Inasmuch as folds, cleavage, and lineation generally develop contemporaneously under the same forces, a

definite correlation is to be expected. Even in those areas where the folds, cleavage, and lineation are not contemporaneous, if they developed under similar forces they would be related to one another. In some regions, of course, the tectonic history was more complicated; if the various structural features under consideration developed successively under forces acting in different directions, no relationship would occur.

The simpler case, in which folds, cleavage, and lineation developed under the same force, or under successive applications of forces acting along the same lines, will be treated first; the more complicated situation will be discussed later.

### Flow cleavage

Flow cleavage may be confined to relatively thin, incompetent beds between more competent strata (Fig. 183). On

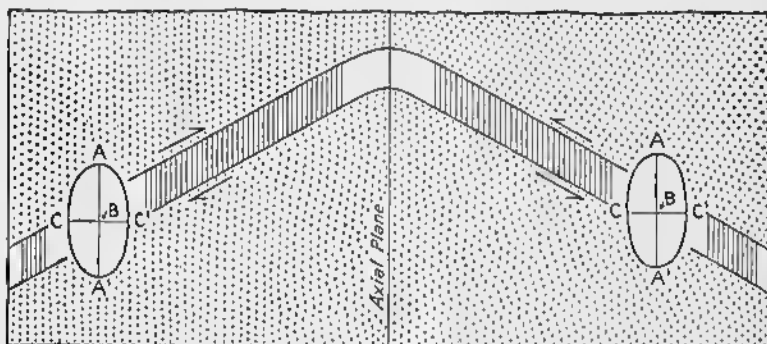


FIG. 183—Flow Cleavage in a Thin Incompetent Bed in a Symmetrical Fold. Cleavage represented by closely spaced lines. Arrows show manner in which beds shear past one another. The ellipse indicates orientation of the strain ellipsoid under these conditions. The flow cleavage forms perpendicularly to the least strain axis,  $CC'$ , of the strain ellipsoid.

p. 88 it has been shown that the younger beds in folding strata shear upward relative to the older beds. Most of the differential movement takes place either at the contact of the competent and incompetent beds, or within the incompetent strata. As a consequence of these couples, the strain ellipse is oriented with the long axis inclined to the bedding as shown in Fig. 183. The intermediate axis is perpendicular to the page. Inasmuch as flow cleavage forms perpendicularly to the short axis of the ellipsoid, it has the attitude shown in Fig. 183. This principle

may be stated in another way by saying that the acute angle between the bedding and the flow cleavage points in the direction of shear.

Even in overturned folds a similar situation exists (Fig. 184); the younger beds shear upward relative to the older beds, and the acute angle between the flow cleavage and the bedding points in the direction of shear.

The mechanism described above emphasizes the shearing of the beds past each other. Theoretically, the beds do not slip

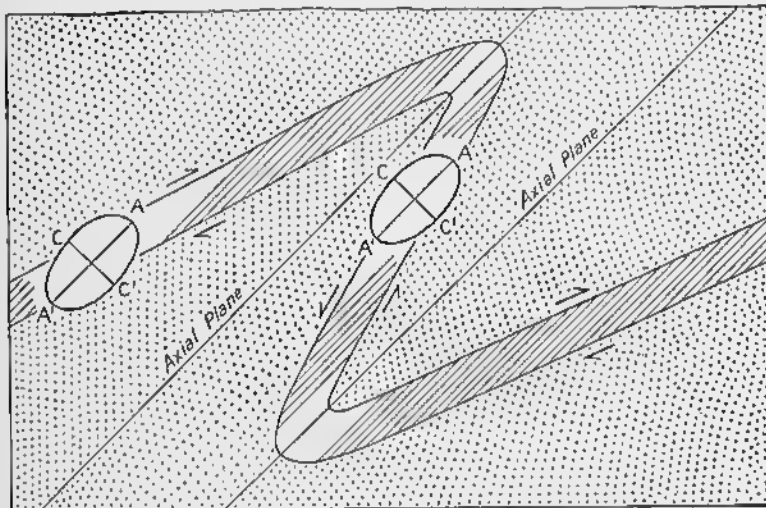


FIG. 184—Flow Cleavage in a Thin Incompetent Bed in an Overturned Fold. Cleavage represented by closely spaced lines. The cleavage is perpendicular to the least strain axis,  $CC'$ , of the strain ellipsoid.

past one another near the axes of the folds, and at these places no cleavage has been shown in Figs. 183 and 184. Another way in which flow cleavage, confined to incompetent beds, may form is discussed on p. 230.

The use of flow cleavage in incompetent beds to solve larger structural problems is illustrated in Fig. 185, which represents a series of vertical exposures as they are seen on small cliffs. In Fig. 185A, the cleavage and bedding dip in the same direction, but the cleavage is the steeper. The arrows indicate the direction of shear as deduced from the relation of bedding and cleavage. The synclinal axis must lie to the west and the anti-

clinal axis to the east; but the actual distance to these axes is unknown.

In Fig. 185B, the beds are vertical, and the flow cleavage dips to the west. The deduced directions of shear are shown by the arrows. The synclinal axis must lie to the east and the anticlinal axis to the west, but the distance to these axes is unknown.

In Fig. 185C, the bedding and cleavage dip to the west, but the bedding is steeper than the cleavage. The deduced direction of shear is shown by the arrows. The synclinal axis lies to the east, the anticlinal axis lies to the west, and the beds at the outcrop must be overturned.

In the preceding discussion, the relation of cleavage to bedding has been discussed as a two-dimensional problem, whereas it should be treated in three dimensions. The relations were considered only in the vertical plane. In a non-plunging fold (Fig. 186A), the beds shear past one another directly up the dip. There is no component of motion parallel to the strike of the strata. Consequently, the intermediate axis of the strain ellipsoid ( $BB'$ ) is horizontal and parallel to the strike of the beds. From this it follows that the flow cleavage, because it includes the intermediate axis, strikes parallel to the bedding.

In plunging folds, the beds do not shear directly up the dip; there is a horizontal component, the relative importance of which increases as the plunge becomes steeper. This point is illustrated by the limiting case, Fig. 186B, in which the plunge is vertical. The beds shear past each other as shown by the arrows, and in this case there is no vertical component of motion. The long and short axes of the strain ellipsoid,  $AA'$  and  $CC'$ , respectively, have the horizontal attitude shown in the figure, but the intermediate axis ( $BB'$ ) is vertical. The trace of the flow cleavage, which includes the long and intermediate axes, will be inclined to the trace of the bedding on a horizontal surface, but on a vertical surface, such as the front of the block, it will be parallel to the trace of the bedding. The most general case, in which the fold plunges at some angle greater than zero degrees, but less than ninety degrees, is shown in Fig. 186C. The cleavage is diagonal to the bedding on horizontal and vertical sections.

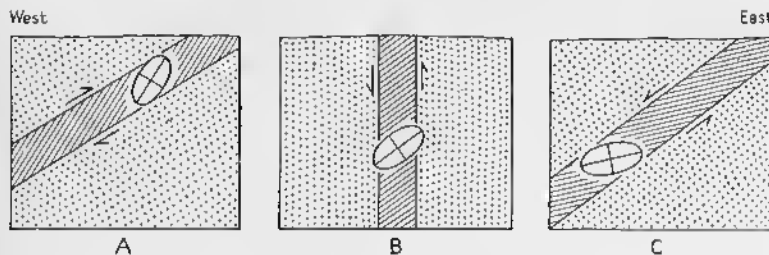


FIG. 185—Two-dimensional Representation of Flow Cleavage in Thin Incompetent Bed. The strain ellipsoid is oriented so that the short axis is perpendicular to the cleavage. The direction of shear deduced from the orientation of the ellipsoid is shown by arrows.

It is apparent, therefore, that a three-dimensional analysis shows not only the direction in which the fold axes lie, but also gives evidence on the direction of plunge. The customary procedure is to consider first a vertical section essentially at right angles to the strike of the bedding; from this section one

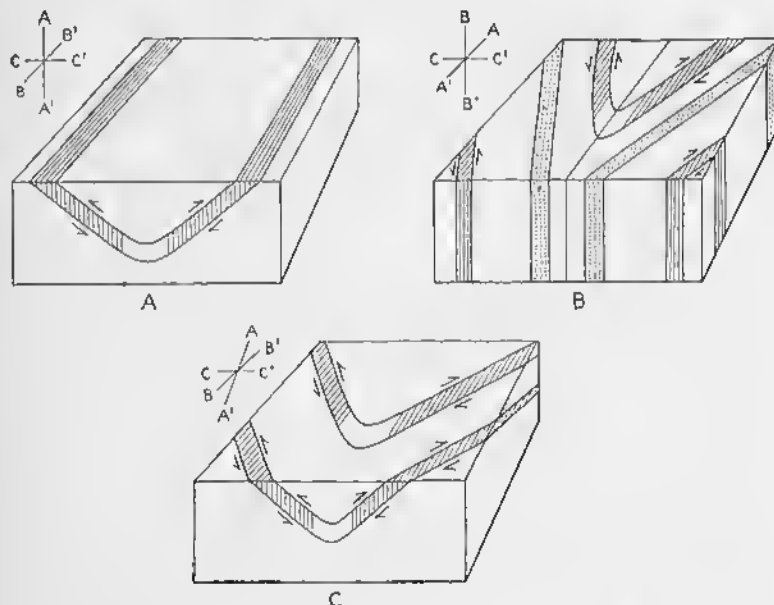


FIG. 186—Flow Cleavage in Three Dimensions. Cleavage represented by closely spaced lines, shear direction shown by arrows. Axes of strain ellipsoid shown in upper left hand corner of each diagram. A. Symmetrical, non-plunging fold. B. Symmetrical fold that plunges vertically. C. Symmetrical fold that plunges north.

determines the direction in which synclinal and anticlinal axes are located. The horizontal section is then studied in order to determine the direction of plunge. In Fig. 187 three vertical beds are illustrated. In bed *a*, the relation of cleavage and bedding in the vertical section on the front of the block indicates a syncline to the east. On the horizontal surface, the trace of the cleavage is parallel to the trace of the bedding, indicating that the fold does not plunge. In bed *b*, the vertical section shows that the syncline lies to the east; the horizontal section indicates that the fold plunges north. In bed *c*, the vertical section shows that the syncline lies to the east; the horizontal section indicates that the plunge is south.

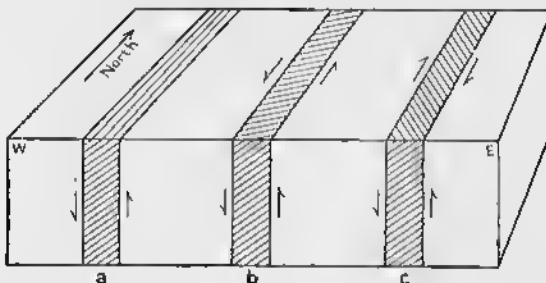


FIG. 187—Three-dimensional Analysis of Flow Cleavage in Thin Incompetent Beds. Closely spaced lines represent flow cleavage. Arrows show inferred directions of shear.

The relation of flow cleavage to bedding in incompetent beds may thus be an extremely significant guide to the structural geologist working in the field.

In regions of thick argillaceous sediments, a widespread flow cleavage may form parallel to the axial planes of the folds. The reasons are apparent. If strata are subjected to horizontal compression (Fig. 188), they are thrown into folds with vertical axial planes. The intermediate and long axes of the strain ellipsoid, parallel to which the flow cleavage forms, will likewise be perpendicular to the compressive force. Hence the cleavage and axial planes are parallel. If the deforming force is a couple, the same is true (Fig. 189).

Such widespread flow cleavage in thick argillaceous sediments has essentially the same attitude as the flow cleavage

that is confined to thin incompetent beds. Consequently, in both cases the same methods may be employed to deduce the location of fold axes and the direction in which they plunge. In fact, the value of the plunge may be measured. In Fig. 190,

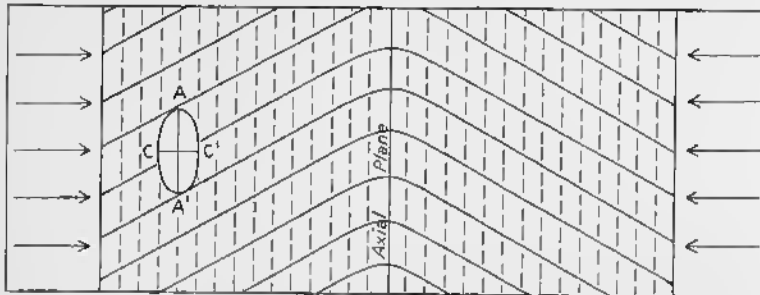


FIG. 188—Flow Cleavage in a Thick Series of Argillaceous Strata in a Symmetrical Fold. Solid lines represent bedding. Broken lines represent flow cleavage. Arrows at either end show nature of force that caused the fold and the cleavage. Ellipse represents strain ellipsoid.

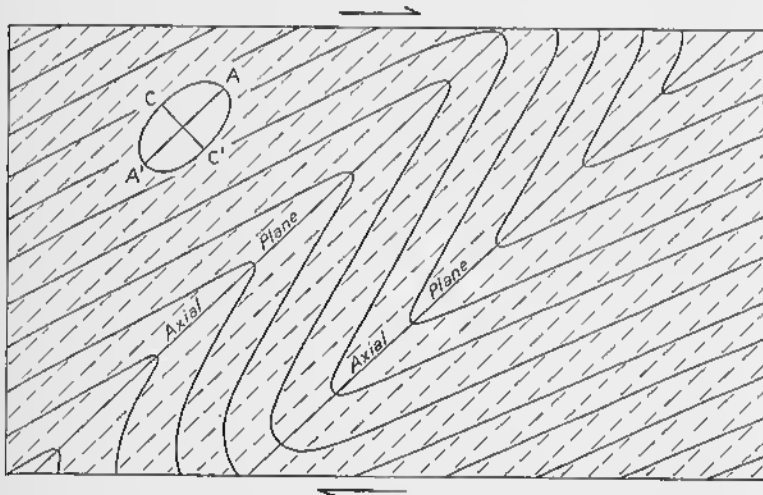


FIG. 189—Flow Cleavage in a Thick Series of Argillaceous Strata in an Overturned Fold. Solid lines represent bedding, broken lines represent flow cleavage. Ellipse represents strain ellipsoid. Arrows above and below indicate nature of the couple that caused folds and cleavage.

the axial plane, and hence the cleavage, of a southerly plunging syncline is vertical. The angle  $P$  which the trace of the bedding on the cleavage makes with the horizontal, is equal to the plunge of the fold.

Even in regions where the strata consist of alternating competent and incompetent beds, a flow cleavage may develop in the incompetent beds because of regional forces. That is, the flow cleavage in such a case is not primarily due to the slipping of the beds past one another, but is directly caused by the regional compressive force. Flow cleavage formed in this way would be as well-developed on the anticlinal axes and in the synclinal axes as it would be on the limbs of the folds.

### Fracture cleavage

Inasmuch as fracture cleavage is a shear phenomenon, its relation to the deforming forces will be different from that of flow cleavage. Fracture cleavage is characteristically developed in incompetent beds that lie between competent beds. Empirical observation shows that fracture cleavage in a fold has the relations shown in Fig. 191A. The cleavage is inclined to the bedding, and the acute angle between the bedding and cleavage points in the direction of differential movement. The same is true of fracture cleavage in a fault zone (Fig. 191B); fault *a* is a thrust, fault *b* is a gravity fault.

It is apparent, therefore, that fracture cleavage may be used in the same way to determine larger structures as is flow cleavage. Observations made in vertical sections at right angles to the strike of the bedding may be used to deduce the direction in which anticlinal and synclinal axes are located. Observations made on horizontal surfaces may be used to deduce the direction in which the folds plunge. Thus Figs. 185-187, although intended to illustrate the use of flow cleavage in determining the structure, are equally valid for fracture cleavage. For practical purposes it is not essential to distinguish fracture cleavage from flow cleavage.

The origin of fracture cleavage in these incompetent beds is a subject upon which there is not complete agreement. The most common interpretation supposes that fracture cleavage is essentially parallel to one of the two shear planes of the strain ellipsoid. The long axis ( $AA'$ ) of the ellipsoid is inclined to the bedding (Fig. 192). One of the shear directions,  $SS'$ , is so nearly parallel to the bedding that the formation of new rupture planes is unnecessary, and any differential movements will utilize

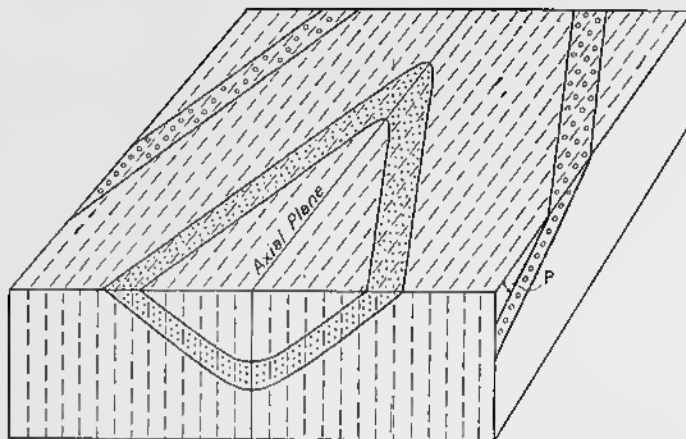


FIG. 190—Three-dimensional Representation of Flow Cleavage. Cleavage represented by broken lines. Value of plunge of fold is equal to  $P$ , which is measured on the cleavage; it is the angle between the trace of the bedding and a horizontal line.

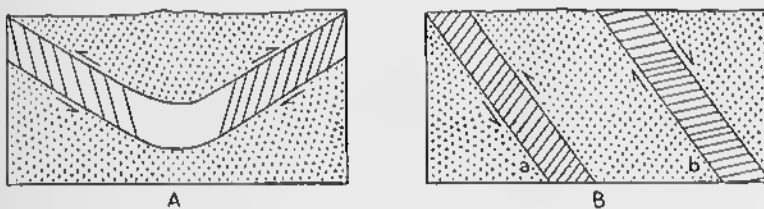


FIG. 191—Fracture Cleavage. A. On the limbs of a fold. B. In fault zones.

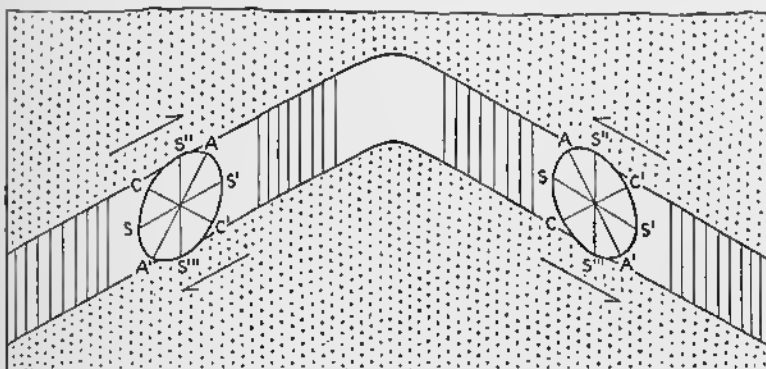


FIG. 192—Origin of Fracture Cleavage, Which Is Represented by Vertical Lines. It is essentially parallel to the shear plane  $S''S'''$  of the strain ellipsoid.

the already existing planes of weakness parallel to the bedding. But the other set of shear planes,  $S''S'''$ , are inclined at such a high angle to the bedding that new ruptures must form to satisfy the conditions of strain.

Fracture cleavage is not necessarily confined to thin, incompetent beds. It may be extensively developed in thick argillaceous formations.

### Shear cleavage

Shear cleavage is fracture cleavage along which there has been measurable differential movement. It may be used in the same way to determine major structure as is fracture cleavage.

### Bedding cleavage

Bedding cleavage has the same significance as bedding in determining the major structure.

### Repeated deformation

In the preceding discussion it has been assumed that the cleavage was contemporaneous with the folding, or, if later,

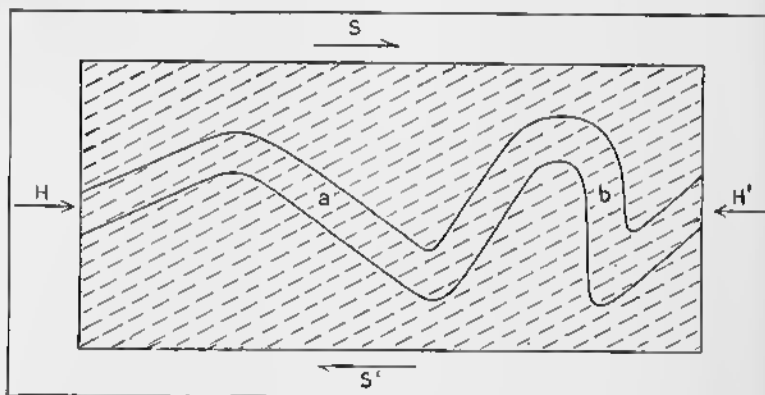


FIG. 193—Flow Cleavage That Is Not Parallel to Axial Planes of Folds. The folds resulted from simple compression, represented by  $H$  and  $H'$ , and the axial planes are essentially vertical. The flow cleavage, represented by the broken lines, was formed by a couple represented by  $S$  and  $S'$ .

that it was caused by similar forces. On the other hand, it is conceivable that the forces producing the cleavage may be later and different from those causing the folding. In Fig. 193, the

folds formed by simple horizontal compression,  $H$  and  $H'$ , are essentially symmetrical. The flow cleavage, which dips to the north, was formed by a later couple,  $S$  and  $S'$ ; consequently, the flow cleavage is not parallel to the axial planes of the folds. In such a case, use of the methods outlined above to determine the major structure, would not necessarily give the correct solution. At  $b$ , one would correctly deduce that a synclinal axis lay to the right. But at  $a$ , one would deduce that a synclinal axis lay to the left; that is, of course, incorrect.

### Summary

Inasmuch as there are several kinds of cleavage, and their usefulness in interpreting major structure has limitations, it is obvious that discretion is necessary in field investigations. In some areas the nature of the cleavage may be readily apparent; in others, a long study may be necessary. As Mead<sup>5</sup> has said: "No hard and fast specifications can be written for the identification of foliate structures. The problem perhaps falls more into the category of an art than a science. Experience and familiarity with a wide variety of occurrences is of value."

### Use and Origin of Lineation

The secondary lineation so characteristic of metamorphic rocks is an aid in solving the major structure. In many localities the lineation is parallel to the axes of the folds. This is almost universally true of elongated pebbles and elongate minerals, and, to a lesser extent, of crinkles and streaks of minerals. The reasons why certain types are more reliable than others can be made apparent only after the origin of lineation is discussed.

The use of lineation in the field is comparatively simple. If the lineation is horizontal, the axes of the folds are horizontal; if the lineation plunges 35 degrees northwest, the folds must plunge 35 degrees northwest. If one utilizes flow cleavage and lineation combined, the complete attitude of the folds is defined. If a vertical flow cleavage that strikes north carries a lineation that plunges 40 degrees north, the folds are symmetrical and plunge 40 degrees north.

---

<sup>5</sup> Mead, W. J., *op. cit.*, p. 1018.

The origin of secondary lineation is a problem that has engaged the attention of structural and metamorphic geologists for only a few years. Although its existence has been known for a long time, no systematic consideration was given to the subject. Obviously, the various kinds of lineation may have different origins, and each type should therefore be considered independently.

Small crinkles and corrugations such as those shown in Fig. 268C are the result of the sliding of layers of rock over one another. The axes of the crinkles are oriented at right angles to the direction of movement, and they do not differ in any major essential from drag folds. The cleavage that is crinkled may have formed in any one of the various ways discussed in previous pages; it may be flow cleavage, fracture cleavage, shear cleavage, or bedding cleavage. In all cases, however, the crinkles must be subsequent to the formation of the cleavage itself.

This type of lineation, under the simplest conditions, should be parallel to the axes of the major folds. The direction of shear on bedding cleavage is directly away from the axes of the folds (Fig. 69); the same would be true for shear cleavage. In a non-plunging fold, for example, the shear direction is directly up the dip. The axes of any minor crinkles will be at right angles to the direction of shear; that is, the axes would be horizontal. Thus the axes of crinkles are parallel to the axes of the major folds.

Younger than the cleavage itself, however, the crinkles are a late tectonic phenomenon, and it is possible that at this stage the direction of shear is different from that normally expected. Under such conditions the crinkles would not be parallel to the axes of the major folds.

Those types of lineation represented by elongated pebbles, elongate minerals, and streaks of minerals, are a somewhat different problem. This subject is one of those treated by students of structural petrology, which is more fully discussed in Chapter 18. These investigators assume that elongated pebbles<sup>6</sup> and elongate minerals are due to forces similar to those causing the

<sup>6</sup> Fairbairn, H. W., Elongation in deformed rocks: *Journal of Geology*, Vol. 44, pp. 670-680, 1936.

crinkles. As the layers of rock slide over one another, each grain is elongated at right angles to the direction of motion. A crude analogy may be drawn to the rolling of dough between the hands. An original spherical mass of dough becomes deformed into a prolate spheroid, the long axis of which is at right angles to the motion of the hands. If all the hundreds of grains that comprise one pebble are similarly deformed, the whole pebble is elongated in the same sense as are the individual grains.

This explanation, however, is by no means entirely satisfactory. The necessary amount of differential movement would be tremendous. Each grain would have to be rolled over many times, and there is evidence that this has not occurred.

A more satisfactory explanation of elongated pebbles assumes that they have been squeezed out of their original shape. If a cube of unstratified clay or of any plastic material were subjected to horizontal compression (Fig. 194A), but was unrestrained vertically and in the horizontal direction at right angles to the deforming force, it would deform into a square prism (Fig. 194B).

Even if the mass of sediments is well bedded, it will attempt to assume the form of the square prism. The upward lengthening of the mass is accomplished by folding. But the horizontal lengthening at right angles to the compression can be accomplished only if the individual beds lengthen in that direction. Conversely, each bed must become thinner. As a consequence of this type of deformation, each bed becomes thinner, but is lengthened parallel to the axes of the folds. Each imaginary sphere in the original sediments is thus lengthened parallel to the axes of the folds. Any actual spheres, such as round pebbles, would be similarly deformed (Fig. 194C).

The objection may be raised that in nature, because the folds are restrained in a direction parallel to the axes of the folds, the strata are not free to elongate in that direction. But salients and plunging folds show that elongation parallel to the axes of the folds is an important factor. Salients, in so far as they represent a differential forward movement of a folded belt, necessitate stretching parallel to the axes of the folds. As is shown by Fig. 195A, the difference between the length of the

folds,  $S$ , as measured around the salient, and the length of the chord,  $C$ , measured directly across from one recess to the other, gives the amount of the elongation.

A far more important factor, however, is the plunge of folds. In Fig. 195B, which is a vertical longitudinal section,  $P$  represents the axis of a fold that changes its direction of plunge at several places. Before folding, however, the line had the length  $O$ . In this case the elongation is equal to the difference between  $P$  and  $O$ .

If sufficient data are available, therefore, the amount of elongation shown by the pebbles may be checked quantitatively against the amount of stretching indicated by the salients and plunging folds. The actual stretching may be confined to relatively small areas where the pebbles will be greatly elongated, whereas in the intervening areas the pebbles may be only slightly deformed.

The type of lineation that is due to the parallelism of the long axis of some elongate mineral, such as hornblende (Fig. 182B), may be explained in several ways. If deformation is later than crystallization, the mineral may be mechanically oriented by shearing. As the thin sheets of which the rock is composed slide over one another, any elongate particles are gradually swung around until the long axes are at right angles to the direction of motion. The amount of differential movement along each plane of cleavage would be considerable. Moreover, the minerals would be rather battered by the process, and they would inevitably be granulated and fractured. In most instances this has obviously not taken place. It is conceivable, however, that the granulated material might recrystallize to clear and unfractured minerals that would preserve the preferred orientation.

In most instances, elongate minerals seem to have crystallized simultaneously with the "stretching" of the rock mass as a whole. While the rock was being compressed, each bed was yielding parallel to the axes of the folds, and all new inequidimensional minerals grew with the long dimension parallel to the fold axes.

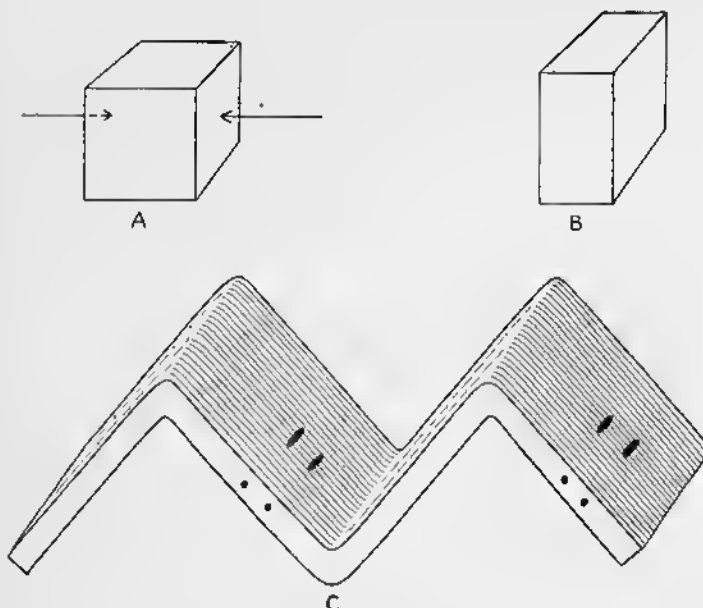


FIG. 194—Origin of "Stretched" Pebbles. A. Cube subjected to simple compression. B. Square prism that results. C. Symmetrical folds; as a result of elongation parallel to the fold axes, the original spherical pebbles have been "stretched" into ellipsoids (solid black), the long axes of which are parallel to the fold axes.

In some cases the lineation may be mimetic; the elongate mineral crystallizes after the deformation, but its growth is controlled by a predetermined direction.

Lineation that is caused by streaks of several equidimensional grains of the same mineral strung out in a line, is susceptible of more than one interpretation. In some rocks streaking is

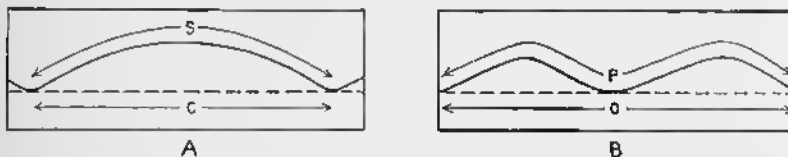


FIG. 195—Mechanics of Elongation Parallel to a Folded Belt. A. Map of a salient convex toward the north. Broken line is position of axis of an embryonic fold prior to the development of the salient; solid line is position of same fold axis after formation of the salient. Amount of elongation is equal to the difference between *S* and *C*. B. Vertical longitudinal section along a folded belt. Broken line is position of axis of an embryonic fold prior to development of plunge, solid line is position of same fold axis after folds have assumed a plunging attitude. Amount of elongation is equal to difference between *P* and *O*.

similar in origin to crinkles and corrugations, and is due to differential movements at right angles to the lineation. In other rocks, particularly if the streaking is accompanied by striations similar to those in slickensides, the differential movement is parallel to the lineation. The author has observed folds in which both types of lineation are present (Fig. 196A). One, which is parallel to the axis of the fold, is the "crinkling" type; the other, at right angles to the axis of the fold, is the "slickensiding" type.

Lineation due to fracture cleavage and shear cleavage is normally parallel to the axes of the major folds. Fig. 196B is

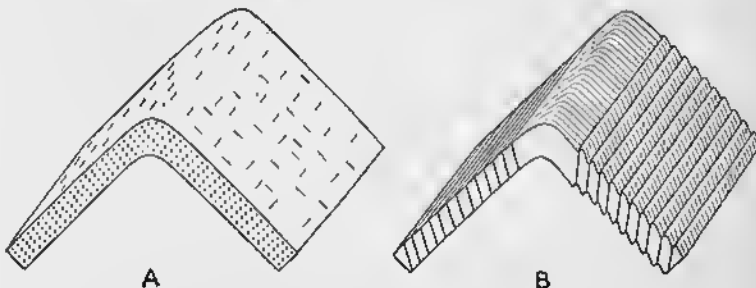


FIG. 196—Different Kinds of Lineation on Folds. A. Two lineations, one parallel to axis of fold and other at right angles. B. Left-hand limb shows lineation due to intersection of fracture cleavage with bedding. Right-hand limb shows lineation due to intersection of shear cleavage with bedding; displacement on the cleavage causes either tiny faults or small crinkles.

a symmetrical fold formed by simple compression. The trace of fracture cleavage on the bedding is parallel to the axis of the fold, as is illustrated by the left hand limb of the fold in Fig. 196B. The intersection of shear cleavage with the bedding may cause tiny fault scarps; small, asymmetric crinkles develop if there is drag along these faults. In either case, the fault scarps or crinkles are parallel to the axis of the fold, as is illustrated by the right hand limb of the fold in Fig. 196B.

If the forces causing the cleavage are oriented differently than are those that produced the fold, no simple relationship will exist between the trace of the fracture cleavage or the shear cleavage with the bedding.

Experience indicates that of the various kinds of lineation discussed above, elongated pebbles and elongate minerals are

most likely to be parallel to the axes of the fold. Crinkles and the intersection of fracture cleavage or shear cleavage with bedding are less likely to be reliable, because they tend to form in the later stages of deformation when stress conditions—or at least the direction of relief—may differ from those in the earlier stages. Streaking of minerals, especially if associated with slickensides, may actually be at right angles to the fold axes.

# 13

## Unconformities

### Introduction

The structural geologist is concerned with unconformities for several reasons. Unconformities are definitely structural features, although their origin involves erosional as well as tectonic processes. Moreover, unconformities may be confused with some kinds of faults. Most important of all, however, is the use of unconformities in dating orogenic and epeirogenic movements. Unconformities are also important to students of stratigraphy, sedimentation, and historical geology.

An *unconformity* (Pl. XVI) is a surface of erosion or non-deposition—usually the former—that separates younger strata from older rocks. The development of an unconformity involves several stages. The first stage is the formation of the older rock. Most commonly this is followed by uplift and subaerial erosion. Finally, the younger strata are deposited.

Rocks of various origins may participate in unconformities; sedimentary rocks, volcanic rocks, plutonic rocks, or metamorphic rocks may be involved.

In Fig. 197 the unconformities are labeled *ab*. In some instances, as in Fig. 197A, the rocks both above and below the unconformity are sedimentary. After the lower limestone was deposited, the region was uplifted and eroded; then the upper sandstones and shales were deposited. In Fig. 197B, the rocks beneath the unconformity are limestone, those above the unconformity are volcanic. After the deposition of the limestone, there was uplift, erosion, and, finally, eruption of the volcanics. In Fig. 197C, after the eruption of the lower volcanics there was erosion—with or without a preceding uplift—and then eruption of the upper volcanics. Figs. 197D and 197E involve plutonic rocks. The plutonic rocks were intruded and then eroded, with or without a preceding uplift. Upon the erosion surface,

younger sediments were deposited (Fig. 197D) or volcanics were erupted (Fig. 197E).

The relief on unconformities differs greatly. In some localities the older rocks were reduced to an extensive peneplane. In other localities, only a mature stage in the erosion cycle was reached before the younger rocks began to accumulate. The relief on the unconformity may amount to hundreds or even

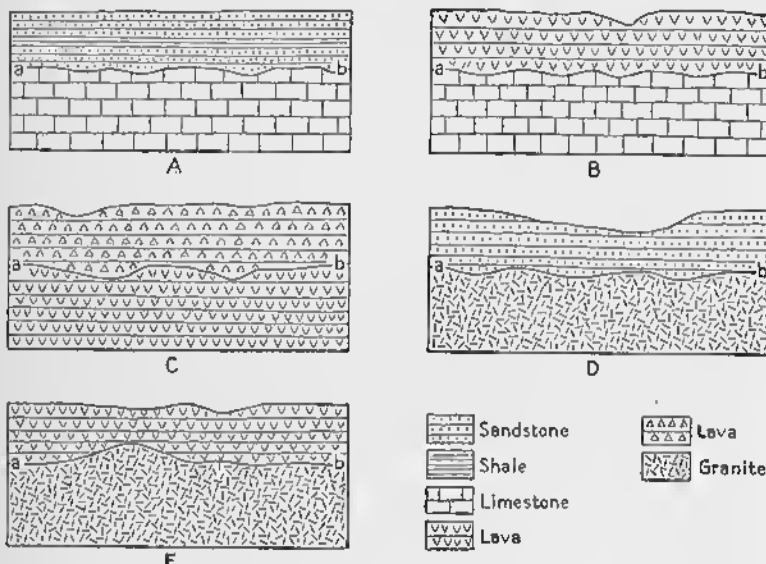


FIG. 197—Rocks Participating in Unconformities. Unconformities are labelled *ab*. A. Sedimentary rocks both above and below the unconformity. B. Volcanic rocks above, sedimentary rocks below. C. Volcanic rocks above and below. D. Sedimentary rocks above, plutonic rocks below. E. Volcanic rocks above, plutonic rocks below.

thousands of feet. The Cambrian sedimentary rocks of the Grand Canyon were deposited on a surface with a known maximum relief of 800 feet.<sup>1</sup> The Algonkian rocks of the Northwest Highlands of Scotland were deposited over hills at least 2,000 feet high.<sup>2</sup> The Carboniferous sedimentary rocks around

<sup>1</sup> Sharp, R. P., Ep-Archean and Ep-Algonkian erosion surfaces, Grand Canyon, Arizona: *Bulletin Geological Society of America*, Vol. 51, pp. 1235-1270; cf, especially p. 1244, 1940.

<sup>2</sup> Peach, B. N., Horne, J., Clough, C. T., Hincksman, L. W., Teall, J. J. H., *The Geological Structure of the North-west Highlands of Scotland: Memoirs Geological Survey Great Britain*, Glasgow, p. 4, 1907.

Boston, Massachusetts, rest upon an unconformity with a relief of at least 2,100 feet.<sup>3</sup>

### Kinds of Unconformities

There are various kinds of unconformities, the distinction depending upon the rocks involved and the tectonic history that is implied. The most important varieties are: angular unconformity, disconformity, local unconformity, and nonconformity.

As is illustrated by Fig. 198, the rocks on opposite sides of an *angular unconformity* are not parallel. Fig. 198A is a cross section, such as an exposure in a cliff; Fig. 198B is a map of a different region. The first event recorded in Fig. 198A is

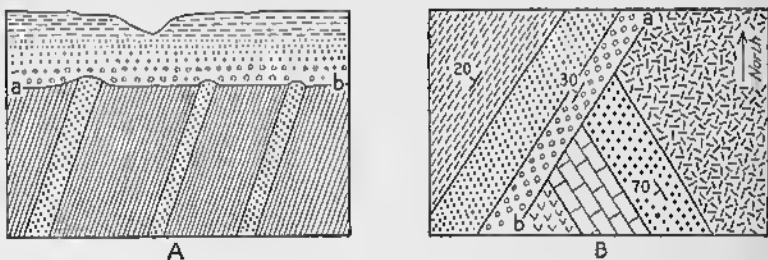


FIG. 198—Angular Unconformity. A. Cross section. B. Map, not same region as shown in A.

deposition of sandstone and shale. These rocks were then deformed to assume dips of 70 degrees, either by folding or tilting of fault blocks. The ensuing erosion, probably accomplished by streams, but possibly marine, reduced the region to the surface *ab*. Eventually, erosion ceased and the younger conglomerate, sandstone, and shale were deposited. Although the rocks both above and below the unconformity represented in Fig. 198A are sedimentary, either one or both may be volcanic.

The precision with which the period of deformation can be dated depends upon the age of the rocks on either side of the unconformity. If the rocks beneath *ab* are upper Permian and the rocks above *ab* are lower Triassic, the deformation was late Permian or early Triassic. If, however, the rocks beneath the unconformity are upper Silurian and those above are lower

<sup>3</sup> Billings, M. P., Loomis, F. B., Jr., and Stewart, G. W., Carboniferous topography in the vicinity of Boston, Massachusetts: *Bulletin Geological Society of America*, Vol. 50, pp. 1867-1884, 1939.



PLATE XVI. Angular Unconformity, Salina Canyon, Utah. Vertical Mesozoic strata are overlain by horizontal Tertiary strata. (Photo by K. Fowler-Billings.)



PLATE XVII. Volcanic Plug and Dike. Aerial photograph of Shiprock, New Mexico. Shiprock is a plug which rises 300 feet above its surroundings. A conspicuous black dike extends outward from the plug. (Photo and copyright by Barnum Brown, American Museum of Natural History.)

Jurassic, the deformation could have occurred at any time between late Silurian and early Jurassic. (See also Pl. XVI).

In a *disconformity*, the formations on opposite sides of the unconformity are parallel. A disconformity covers a large area and represents a considerable interval of time; the meaning of this somewhat vague statement will be more apparent after local unconformities have been discussed. Figs. 197A, 197B, and 197C represent disconformities, and the history implied has been given above (page 240).

A *local unconformity* (Fig. 62) is similar to a disconformity, but, as the name implies, it is distinctly local in extent; the time involved is short. In the deposition of continental sediments, such as gravels, sands, and clays, the streams may wander back and forth across the basin of deposition. At times of flood these streams may scour out channels scores of feet wide and many feet deep. As the flood subsides, or some days or even years later, the channel may be filled up again. Such an unconformity is local in extent and, in most instances, can not be identified beyond the limits of the outcrop in which it is found. The time involved is short.

In a sense, a local unconformity is a disconformity of small extent representing a short interval of time. Under certain conditions it may be difficult to decide which term is the more appropriate.

Although the term *nonconformity* is used in various ways in the geological literature, it may be utilized most satisfactorily for unconformities in which the older rock is of plutonic origin (Figs. 197D and 197E).

### Recognition of Unconformities

#### Exposed in one outcrop

Unconformities may be recognized in various ways, of which direct observation in a single outcrop is the most satisfactory. The outcrop may be small and only a few feet across; it may be an artificial opening, such as a quarry; or it may be the wall of a canyon, such as the Grand Canyon of the Colorado River.

If the unconformity is an angular one, the lack of parallelism of the beds on opposite sides of the contact will be readily apparent (Pl. XVI). This may be observed in a vertical section, such as

a cliff (Fig. 198A), or on the surface of the outcrop (Fig. 198B). The lowest beds above the unconformity may consist of conglomerate with pebbles derived from the underlying formations. If the conglomerate is thin, it may be concentrated in small depressions eroded out of soft beds in the strata beneath the unconformity. But basal conglomerates are not necessarily present along angular unconformities. Faults and dikes may be truncated at the contact. The Grand Canyon of the Colorado, of course, displays two major unconformities in a striking way.<sup>4</sup>

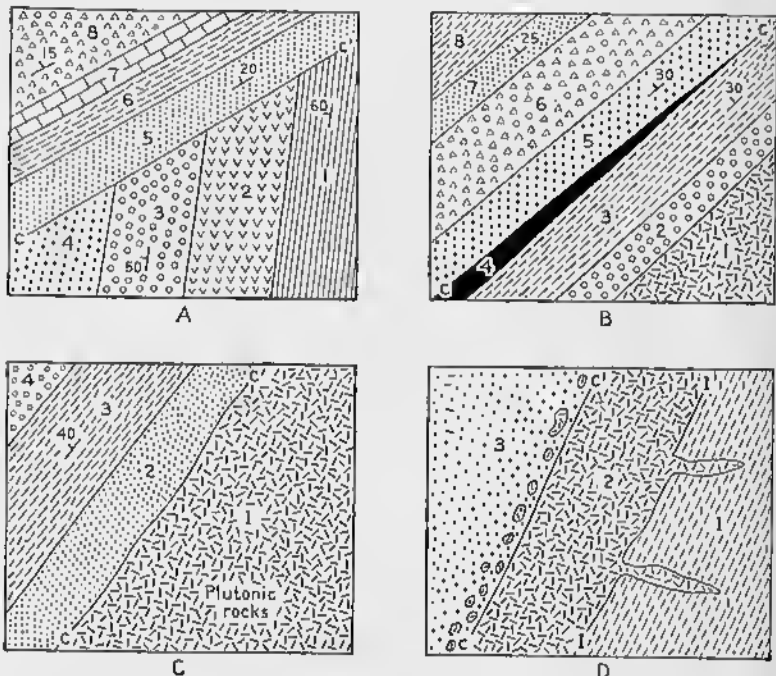


FIG. 199—Unconformities Shown by Areal Maps. Formations in order of decreasing age: 1, 2, 3, 4, 5, 6, 7, and 8. CC' = Unconformity. A. Angular unconformity. B. Disconformity. C. Nonconformity. D. Nonconformity (CC') and intrusive contact (II').

Under favorable conditions, disconformities may be readily recognized in outcrops, road cuts, and quarries. If there is a sharp contrast in color between the rocks above and below the disconformity, if the disconformity is somewhat wavy, and

<sup>4</sup> Sharp, R. P., *op. cit.*

especially if there is a thin conglomerate just above the disconformity, the nature of the contact is apparent. Regional relations must be considered (p. 243), in order to distinguish between a disconformity and a local unconformity. But disconformities may be difficult to recognize, and in many cases paleontological evidence indicates considerable gaps in the geological record without any accompanying physical evidence.

Nonconformities must be distinguished from intrusive igneous contacts. The rocks above a nonconformity may contain fragments of the older igneous rock, either as readily recognized pebbles and boulders or as small fragments recognized only under the microscope. Some nonconformities are characterized by an arkose many feet thick, so that the plutonic rock seems to grade into the overlying strata. Along an intrusive contact, of course, dikes might be expected to penetrate the adjacent rocks; in some cases the intrusive is chilled against the older strata.

Many unconformities are not exposed in an outcrop. This may be due to poor exposures, igneous intrusions, or faulting. In such cases other methods must be employed to detect the unconformity.

### Areal mapping

A geological map showing an angular unconformity is illustrated by Fig. 199A. A group of older rocks, 1, 2, 3, and 4, strikes into the base of a group of younger rocks, 5, 6, 7, and 8. Formation 5 is in contact with all the older formations along the line  $CC'$ , and the relations can be interpreted to mean an angular unconformity. But a fault between 5 and the older formations is equally plausible. The presence of pebbles of 1, 2, 3, and 4 in formation 5 would indicate an unconformity, but even in this case the mapped contact,  $CC'$ , could be a fault. In the last analysis, therefore, it is necessary to see the contact of formation 5 with the older rocks. The areal mapping is suggestive, but not conclusive.

Areal mapping may bring out a disconformity in a similar way (Fig. 199B). Although, in any one exposure, the strata on opposite sides of a contact ( $CC'$ ) may appear to be parallel to each other, the mapping may show that the younger beds truncate the older. But, just as in the case described above,

the truncation may be due to faulting; consequently, a solution is obtained only if the contact is visible.

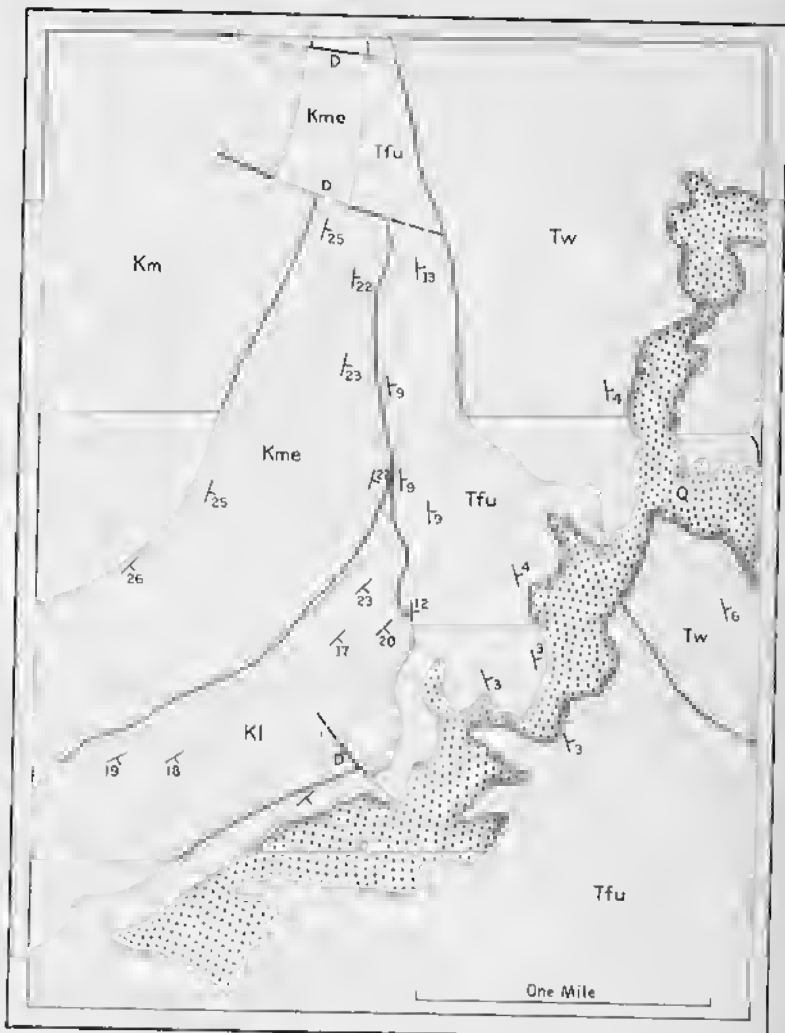


FIG. 200—Angular Unconformities of Meeteetse Area, Wyoming.  
*Km* = Mesaverde formation, *Kme* = Meeteetse formation, *Kl* = Lance formation, *Tfu* = Fort Union formation, *Tw* = Wasatch formation, *Q* = Quaternary gravels. *D* = Downthrown side of gravity faults. (After D. F. Hewett.)

A nonconformity may be suggested by areal studies. If the sedimentary rocks, such as formation 2 of Fig. 199C, contain

pebbles of the plutonic rock, a nonconformity must exist. But the contact  $CC'$ , exposed at the surface, could be a fault, and the nonconformity itself is not necessarily exposed. If dikes of the igneous rock do not cut the sediments, or if inclusions of the sedimentary rocks are not found in the plutonic rock, a nonconformity rather than an intrusive contact is implied, but not proved. As in the case of the angular unconformity and disconformity, for a satisfactory solution of the problem it is highly desirable to see the contact.

Three angular unconformities are shown in Fig. 200.<sup>5</sup> The oldest unconformity is at the base of the Fort Union formation ( $Tfu$ ), which clearly truncates the older rocks; the Fort Union formation rests on the Meeteetse formation ( $Kme$ ) in the northern part of the area, and on the Lance formation ( $KL$ ) in the southern part. A second unconformity is at the base of the Wasatch formation ( $Tw$ ); the faults that cut the Mesaverde ( $Km$ ), Meeteetse ( $Kme$ ), and Fort Union ( $Tfu$ ) formations in the northern part of the map, are truncated by the base of the Wasatch formation ( $Tw$ ). The third and youngest unconformity is at the base of the Quaternary gravels ( $Q$ ), which are in contact with the Fort Union and Wasatch formations.

#### Sharp contrasts in degree of induration

A sharp contrast in the degree of induration indicates an unconformity. If unconsolidated sands and clays are associated with well-cemented sandstones and compact shales, it may be presumed that the unconsolidated material is unconformable on the consolidated rocks. Some caution must be exercised, however, because an unconsolidated rock may be locally indurated. Conversely, consolidated rocks may locally weather to loose sands and clays.

#### Sharp contrasts in the grade of metamorphism

If rocks of sharply contrasting metamorphism are found in the same region, it is probable that the less metamorphosed rocks were deposited unconformably upon the more metamorphosed rocks.

<sup>5</sup> Hewett, D. F., Geology and oil and coal resources of the Oregon, Meeteetse, and Grass Creek Basin quadrangles, Wyoming: *U. S. Geological Survey Prof. Paper 145*, Fig. 5, 1926.

The grade of metamorphism<sup>6</sup> is commonly defined by the nature of the minerals resulting from recrystallization; a complete discussion of this subject is beyond the scope of this book. Under conditions of regional metamorphism, a shale becomes a slate or phyllite, with such minerals as sericite and chlorite.

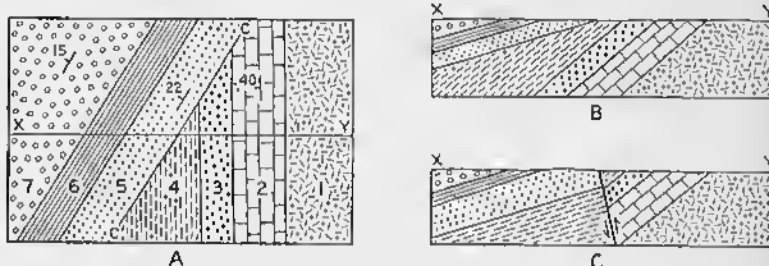


FIG. 201—Faults and Unconformities. Formations in order of decreasing age are 1, 2, 3, 4, 5, 6, and 7. A. Map; contact  $CC'$  may be either an unconformity or fault. B. Cross section along line  $XY$ ;  $CC'$  of Fig. 201A interpreted as an unconformity. C. Cross section along line  $XY$ ;  $CC'$  of Fig. 201A interpreted as a fault.

Biotite, garnet, staurolite, and sillimanite appear successively as zones of greater metamorphic intensity are approached. All of these minerals persist into the higher zones; for example, a sillimanite schist may contain biotite, garnet, and staurolite. Thus, if a sufficiently large area is studied, a single formation that was originally shale may be represented by the following different *metamorphic facies*: slate, biotite schist, biotite-garnet schist, biotite-garnet-staurolite schist, and biotite-garnet-staurolite-sillimanite schist. Normally, a geological map will show that the change from one facies to another is gradual.

If slate and sillimanite schist are found in adjacent outcrops, an unconformity probably exists, and the more metamorphosed rock is the older. This criterion, however, must be used with some caution. A large overthrust, in particular, may bring together different metamorphic facies of the same formation.

#### Sharp contrasts in the intensity of folding

If some formations in an area are highly folded, whereas others are gently inclined or horizontal, the less deformed rocks

<sup>6</sup> Harker, Alfred, *Metamorphism*, 2d edition. London: Methuen and Co., 1939.

are probably unconformable above the more deformed rocks. Due regard, however, must be given to the relative competency of the formations involved. Whereas thick, massive sandstone may be thrown into a few broad, open folds, thin-bedded shales deformed at the same time may be crumpled into many small folds. Moreover, even the same formation may be much more folded in some tectonic zones than in others. It is apparent that variations in the degree of folding are not a very reliable criterion of an unconformity.

#### Relation to intrusives

Two formations, such as *1* and *3* in Fig. 199D, may be separated from each other by granite (*2*), and may nowhere come into contact with each other. Formation *1* is intruded by the granite, but *3* is resting on the granite unconformably, and it contains pebbles of the granite. It is apparent, therefore, that *3* is above an unconformity and that *1* is beneath the unconformity.

#### Criteria for Distinguishing Faults from Unconformities

Reference has been made in several places to the danger of confusing faults with unconformities. Dip, diagonal, and transverse faults offer no difficulties. But if the bedding on one or both sides of the contact has the same strike as the contact, as in Fig. 201A, either an unconformity or a fault may exist. Formation *5* may lie unconformably above formations *1*, *2*, *3*, and *4*, or the contact may be a fault, with either group of formations the older. Even if formations *1*, *2*, *3*, and *4* are known to be older, the contact can be either an unconformity or a fault. In Fig. 201B, a cross section along *XY* of Fig. 201A, the contact is interpreted as an unconformity, but in Fig. 201C it is interpreted as a fault.

Several methods of attack may prove fruitful if the contact cannot be observed. The contact is a fault if formations *5*, *6*, and *7* are older than *1*, *2*, *3*, and *4* (Fig. 201C). Moreover, in a region of sufficient relief, it may be possible to ascertain the attitude of the contact, *CC'*, from its relation to topography. Under the simplest conditions, the dip of the unconformity would be essentially parallel to the dip of the beds in formation *5*. The greater the divergence of the dip of the contact from the

dip of formation 5, the more likely it is that the contact is a fault.

The presence of pebbles of formations 1, 2, 3, or 4 in formation 5 would indicate an unconformity between the two formations, but even under such circumstances the contact  $CC'$  could be a fault.

If the younger beds strike or dip into the contact, a fault is indicated. This point is illustrated by Fig. 202A, where younger formations, 5 and 6, strike into an older formation, 3.

In the final analysis, every effort should be made in the field to observe the actual contact. If it is an unconformity,

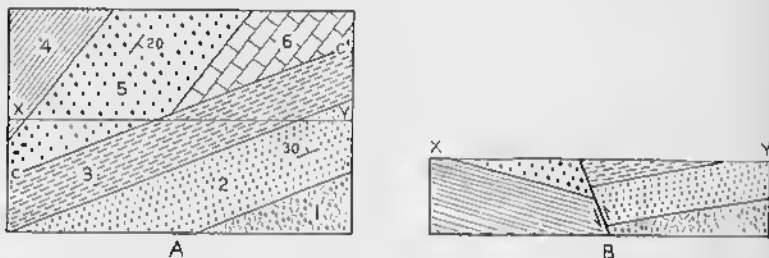


FIG. 202—Contact That Is Very Probably a Fault. Formations in order of decreasing age are 1, 2, 3, 4, 5, and 6. A. Geological map. B. Cross section along line XY of Fig. 202A.

small ridges of the older rock may project into the younger rocks, and a conglomerate or sandstone, with fragments of the older rock, may lie above the contact. Slickensides, gouge, and breccia would be absent from an unconformity, but would likely be present along a fault. Some faults, however, are sharp, knife-like contacts devoid of such features.

Additional complexity is introduced by the fact that faults may follow unconformities, particularly angular unconformities. In the Wasatch Plateau of Utah, for example, a hard, brittle, Eocene limestone was deposited with a strong angular unconformity on underlying weak shales. Subsequently the region was subjected to horizontal compression; the weak shales folded, but the brittle limestone slid along the unconformity.<sup>7</sup>

<sup>7</sup> Billings, M. P., Thrusting younger rocks over older: *American Journal of Science*, Vol. 25, pp. 140-165; especially pp. 153-155, 1933.

## Salt Domes

### Introduction

Salt domes are of particular interest to the structural geologist. They constitute a superb example of the plastic movement of large bodies of rock, and their structural evolution is unusually fascinating. Moreover, very little information has been obtained from surface exposures. The data have been supplied by drill holes, geophysical methods, and a few mines. The growth of our knowledge of salt domes is an unparalleled example of co-operative enterprise, in which thousands of geologists—chiefly petroleum geologists—have participated.<sup>1</sup> Moreover, salt domes are of great economic importance, principally as a source of petroleum, sulphur, and salt.

A *salt dome* consists of a central core of rock salt and a surrounding dome of sedimentary strata. The core of many salt domes has pierced the adjacent sedimentary rocks, but this cannot be proved in all cases.

Salt domes have been found in a number of regions, notably Texas, Louisiana, Germany, Russia, and Iran. In Texas and Louisiana one hundred and forty-one salt domes were known in 1936. Approximately one hundred salt domes were known in 1938 in the Emba district of Russia on the northeast coast of the Caspian Sea.<sup>2</sup>

<sup>1</sup> DeGolyer, E. L., and others, *Geology of Salt Dome Oil Fields*. Chicago: American Association Petroleum Geologists, 1926.

Powers, S., and others, *Structure of Typical American Oil Fields*, Vol. 1 and Vol. 2. Tulsa: American Association Petroleum Geologists, 1929.

Barton, D. C., and Sawtelle, G., *Gulf Coast Oil Fields*. Tulsa: American Association Petroleum Geologists, 1936.

<sup>2</sup> Sanders, C. W., Emba salt dome region, U.S.S.R., and some comparisons with some other salt dome regions: *Bulletin American Association Petroleum Geologists*, Vol. 23, pp. 492–516, 1939.

### Shape, Size, and Composition

In considering the shape, size, and composition of salt domes, one should make a clear distinction between the anticlinal dome of sediments and the core, which is composed of rock salt overlain by a relatively thin cap rock. Although the core is thought to be a great pillar, with a much greater vertical than horizontal extent, our direct knowledge of the core is confined to its uppermost part.

Some American salt domes are expressed topographically, but many are not. The hills, which rise from a few feet to 40 feet above the surrounding lowlands, and, in exceptional instances, as much as 80 feet, cover an area a mile or so in diameter. Lakes occupy depressions above some of the domes. Oil seeps and salt springs were the means of discovering some salt domes.

The cores of American salt domes are essentially circular in plan, and they characteristically range in diameter from  $\frac{1}{2}$  to 2 miles; some cores, however, are as much as 5 miles in diameter. The German salt domes are comparable in size.<sup>3</sup> In some of the largest Russian domes, on the northeast shore of the Caspian Sea, the cores are 3.1 to 7.5 miles in diameter. The cores of the Rumanian salt domes are elliptical in plan, and the longer axis is parallel to the trend of the associated folds.<sup>4</sup>

In many salt domes the walls dip steeply outward; the top may be flat (Fig. 203A) or domical (Figs. 203B and 203D). Some cores are symmetrical, the wall dipping at essentially the same angle on all sides; other cores are asymmetrical, the wall dipping steeper on some sides than on others. In at least a dozen salt domes in the United States, the core overhangs or "mushrooms"; that is, although in the uppermost levels of the earth the diameter of the core increases downward, at greater depth it narrows again (Fig. 203C).

<sup>3</sup> Stille, Hans, *The Upturist of the Salt Masses of Germany: Geology of Salt Dome Oil Fields*, pp. 142-166. Chicago: American Association Petroleum Geologists, 1926.

<sup>4</sup> Voitesti, I. P., *Geology of the Salt Domes in the Carpathian Region of Rumania: Geology of Salt Dome Oil Fields*, pp. 87-128. Chicago: American Association Petroleum Geologists, 1926.

Mason, S. L., *Rumanian Oil Fields: Geology of Salt Dome Oil Fields*, pp. 129-141. Chicago: American Association Petroleum Geologists, 1926.

The core consists principally of rock salt overlain by cap rock. Rock salt is the common name for the mineral halite (Fig. 1), which is sodium chloride. In the United States the salt is remarkably homogeneous, with no trace of shale or other material. Argillaceous beds and potash-rich beds are interbedded with the salt in the German salt domes. The salt in

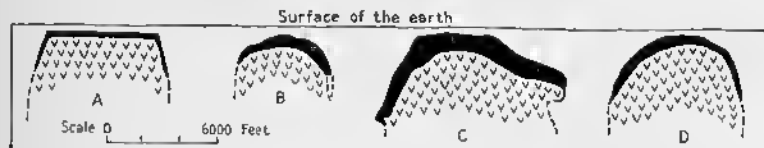


FIG. 203—Shape of the Core of Salt Domes. Checks = rock salt; solid black = cap rock. A. Palanguna, Texas. (After D. C. Barton.) B. Hoskins Mound, Texas. (After A. H. Marx.) C. High Island, Texas. (After M. T. Halbouty.) D. Brenham, Texas. (After S. O. Burford.) Data from Bulletin American Association Petroleum Geologists.

the core of a salt dome is thousands of feet thick. In the United States wells have been drilled 3000 feet into the salt, and in Germany wells have been driven nearly 4000 feet through salt; the depth to the bottom is a matter of conjecture. In the search for petroleum there is ordinarily little incentive to drill any great distance into the salt. The probable shape of some salt domes is illustrated in Fig. 204. Fig. 204A is a domical body rising from a bed of salt. Fig. 204B is a domical body with

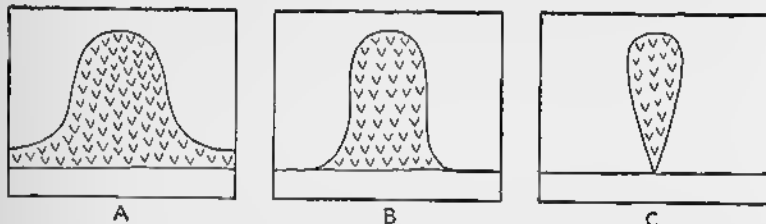


FIG. 204—Hypothetical Shape of Salt Domes. (After Barton, Bulletin American Association Petroleum Geologists.)

vertical walls. Fig. 204C is a stream-lined body that tapers downward.

Because the salt is so massive and homogeneous, little can be said about the internal structure of the American salt domes. The rocks constituting the core of the German salt domes are highly folded.

The cap rock (Fig. 203) overlies the salt and may be over 100 feet thick, but in some domes it is missing. The cap rock characteristically consists of limestone, gypsum, and anhydrite; the limestone is on top, the anhydrite on the bottom. Commercial deposits of sulphur occur in the cap rock of a few domes.

The sediments surrounding the core are uplifted into an anticlinal dome (Fig. 205). The sediments in many instances are sharply truncated by the rock salt in the core (Fig. 205A); borrowing a term from igneous geology, we might describe the structure as *discordant* (p. 264). Elsewhere the bedding of sediments is parallel to the contact with the core (Fig. 205B);

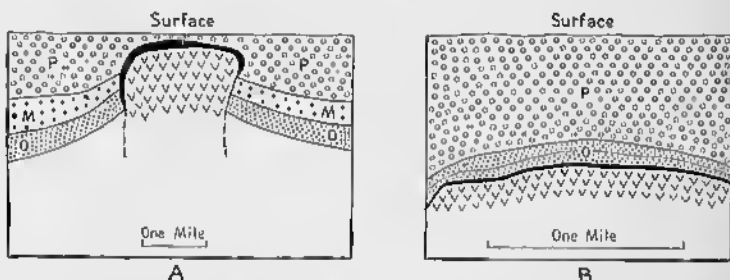


FIG. 205—Pierceinent and Non-pierceinent Salt Domes. Checks = rock salt; solid black = cap rock. Sedimentary rocks: *O* = Oligocene, *M* = Miocene, and *P* = Pliocene and Pleistocene. A. Barbers Hill dome, Texas. (After S. A. Judson and R. A. Stamey.) B. Sugarland salt dome, Texas. (After W. A. McCarler and P. H. O'Bannon.) Data from Bulletin American Association Petroleum Geologists.

In igneous geology we would describe the relations as *concordant*. On this basis salt domes are classified by some geologists into *pierceinent domes* and *non-pierceinent domes*, the former being discordant, the latter concordant. Some domes, however, may show both relationships; the core may truncate the older formations on its flanks, but not the younger strata near the roof.

The sedimentary rocks adjacent to the core have been dragged upward many thousands of feet. The exact amount may be calculated rather readily by comparing the depth of a bed near the core with its depth where it is undisturbed beyond the influence of the salt (Fig. 205A).

A zone of gouge has been recorded from some of the American domes at the contact of the core and the surrounding sediments. Thick breccias locally surround the salt core of some of the

Rumanian salt domes. The fragments, derived from the surrounding sediments, are embedded in a matrix of salt or, less commonly, gypsum.

The domed sediments overlying the cores of some salt domes are broken by gravity faults. These faults may be radial (Fig. 206A), but more commonly they belong to a more or less parallel system in which one or more graben are conspicuous (Fig. 206B).

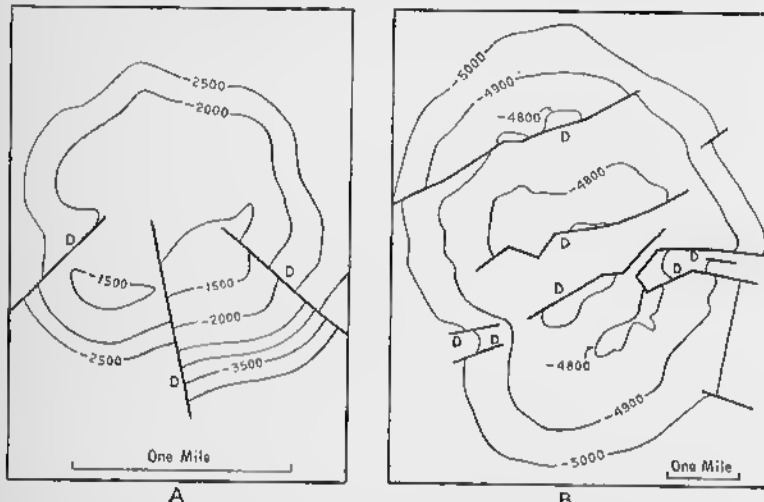


FIG. 206—Faulting on Salt Domes. Heavy black lines are faults, *D* = downthrown side. A. Clay creek salt dome, Texas; structure contours on top of cap rock; contour interval 500 feet. (After W. B. Ferguson and J. W. Minton.) B. Conroe oil field, Texas; structure contours on top of main Conroe sand; contour interval 100 feet. (After F. W. Michaux, Jr. and E. O. Buck.) Data from Bulletin American Association Petroleum Geologists.

These gravity faults show clearly that the sediments in the dome have been under tension.

The depth of the core beneath the surface differs greatly, and salt domes are sometimes classified on this basis.<sup>5</sup> *Deep domes* are those in which the top of the core is 5000 feet or more beneath the surface; in many so-called deep domes, the core has not been reached. *Intermediate-depth domes* are those in which the top of the core is 3500 to 5000 feet beneath the surface. *Shallow domes* are those in which the top of the core is less than 3500 feet beneath the surface.

<sup>5</sup> Sanders, C. W., *op. cit.*, p. 503.

In some of the Rumanian domes the rock salt is exposed at the surface of the earth, and in some of the Iranian domes the salt literally flows out on the surface to form spectacular "glaciers" composed of rock salt.

### Origin of Salt Domes

Salt domes result from the plastic intrusion of halite (rock salt) into the surrounding sediments. The salt is derived from some underlying source bed, although in Texas and Louisiana this source bed has not been reached by wells that penetrate the sediments beyond the limits of the domes. In Germany, however, Permian salt beds form part of the normal stratigraphic sequence in the undisturbed sediments. All structural transitions are known from gently-dipping beds through simple anticlinal domes to true salt domes.

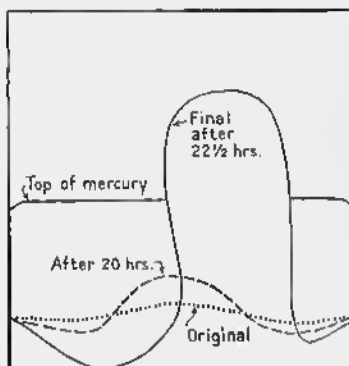


FIG. 207—Fluid Mechanics of Salt Domes. At start a layer of paraffin lies beneath the dotted line, and mercury is above. (After L. L. Nettleton. Data from Bulletin American Association Petroleum Geologists.)

The American salt domes have risen independently of tectonic forces. The motive force is the difference in density between the salt and the surrounding sediments. The salt, which is of lower specific gravity than the sediments, has moved upward somewhat in the same way that a fluid rises through an overlying heavier fluid. Nettleton<sup>6</sup> has investigated this subject experimentally, and he has obtained structures remarkably simulating salt domes (Fig. 207). According to his investigations, if a small anticlinal flexure exists on top of the original salt bed, upward movement starts here, and salt is drained away from the surrounding region. Eventually, the salt bed in the adjacent area may become so thin and constricted that further addition of salt is impossible. In fact, many salt domes may have been pinched from the source beds, and they may have a

<sup>6</sup> Nettleton, L. L., Fluid mechanics of salt domes: *Bulletin American Association Petroleum Geologists*, Vol. 18, pp. 1175-1204, 1934; also *Gulf Coast Oil Fields*, pp. 79-108, Tulsa: American Association Petroleum Geologists, 1936.

stream-lined shape with a rounded top and a sharp downward termination (Fig. 204C).

Barton has emphasized that, although the rock salt has moved upward relative to the surrounding sediments, it may have stayed at essentially the same position relative to sea level.<sup>7</sup> In other words, the surrounding sediments went down while the salt was remaining stationary; salt domes are the result of *downbuilding* rather than of *upthrusting*. Although this is probably essentially correct, such a distinction is mechanically unimportant.

In Rumania, horizontal compression has been an important factor in the development of salt domes. The salt, forced upward by orogenic pressure, has penetrated the sediments at the crests of the anticlines to form diapir folds (see also p. 54). Sanders has suggested that the American and Rumanian salt domes are two extreme types of a more or less transitional series.<sup>8</sup> Orogenic forces, which have played an important rôle in the formation of Rumanian salt domes, have also affected the German salt domes. The Russian domes around the Caspian sea and the Iranian domes have been only slightly influenced by compressive forces.

The origin of the cap rock is a problem upon which there is no unanimity of agreement. According to one theory the cap rock is residual material left when salt is dissolved at the top of the rising dome. Another theory supposes that the cap is sedimentary material deposited on top of the original salt bed; this material has been pushed ahead of the rising body of salt.

### Structural Evolution of Salt Domes

A vast amount of precise information has accumulated on the structural evolution of salt domes, both in America and abroad. Some, and perhaps many, of the American salt domes have been rising throughout Tertiary time. The evidence is primarily stratigraphic. An angular unconformity, such as that illustrated in Fig. 208A, shows that considerable uplift

<sup>7</sup> Barton, D. C., Mechanics of formation of salt domes with special reference to Gulf Coast salt domes of Texas and Louisiana: *Bulletin American Association Petroleum Geologists*, Vol. 17, pp. 1025-1083, 1933; also *Gulf Coast Oil Fields*, Tulsa: American Association Petroleum Geologists, pp. 20-78, 1936.

<sup>8</sup> Sanders, C. W., *op. cit.*, pp. 511-512.

occurred after the deposition of formation *a*, but before the deposition of formation *b*. The salt rose up through formation *a*, truncating the bedding and doming up the sediments. Erosion followed, removing many of the younger beds in formation *a*. Formation *b* was subsequently deposited, and this was followed by renewed upward movement that slightly domed formation *b*.

In other instances a formation may become thinner over the top of the dome. This indicates, as illustrated in Fig. 208B, that the dome was actively rising throughout the deposition of formation *d*, but unconformities within formation *d* may be

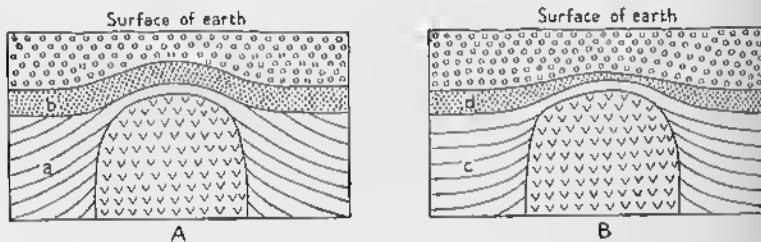


FIG. 208—Criteria for Dating Movements in Salt Domes. Checks = core of rock salt and cap rock. Rest are sedimentary rocks. A. Unconformity between formation *a* and *b*. B. Formation *d* thins over core of rock salt.

difficult to detect. It must be remembered that all the data are obtained from drill holes.

Topographically-expressed salt domes have probably been active in relatively recent times. Moreover, if Pleistocene or recent gravels on the dome are uplifted relative to their position in the surrounding region, it is obvious that the salt has been active during the Quaternary.

### Economic Resources

A detailed discussion of the resources of salt domes is not appropriate in this book, but salt domes are of such great economic importance that a brief discussion is desirable. Petroleum is trapped in the sediments that flank the core of rock salt, and in some instances it has been found in the cap rock. Large quantities of sulphur have been obtained from the cap rock of some salt domes. This sulphur has probably been derived from the anhydrite and gypsum normally present in the cap

rock, but there is no agreement concerning the details of the process of formation. The rock salt in the core has also been exploited economically. Potash salts have been extensively mined in the German salt domes, where the potash salts occur in strata that were deposited during the accumulation of the sediments.

## Plutons

### Introduction

Some magma pours out on the surface of the earth as lava, or is blown into the air; *extrusive igneous rocks* result from these processes. Much magma, however, consolidates beneath the surface of the earth to form bodies of *intrusive igneous rock*, and it is with these latter bodies that the present chapter is concerned.

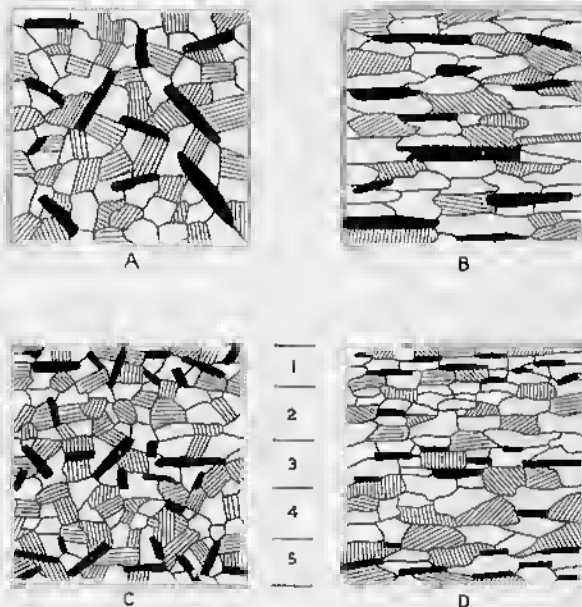


FIG. 209—Internal Structure of Intrusive Igneous Rocks. Natural scale. Solid black represents platy dark minerals, such as biotite; lined pattern represents feldspar; white represents quartz. A. Massive rock. B. Foliated rock. C. Banded or layered rock. D. Banded and foliated rock. In C and D layers 1, 3, and 5 are richer in dark minerals than layers 2 and 4.

It is by no means easy to define the limits of petrology and structural geology in this particular subject. The petrologist is primarily concerned with the mineralogy, chemistry, and origin of these intrusive rocks. The structural geologist is interested in the shape of these rock bodies, because they play an important rôle in the architecture of the earth. He is concerned with the mechanics of intrusion, involving the movement of large masses of potential rock under the influence of gravity or tectonic forces. The internal structure of the intrusive rocks—such as foliation and layering—is of importance in so far as it bears upon the mechanics of intrusion or upon the influence of later forces acting on a consolidated rock.

Ideally, the student of intrusive igneous rocks should be both a petrologist and a structural geologist; a good field geologist and a good petrographer, he should possess a thorough knowledge of the physical chemistry of igneous rocks. This book, however, is concerned only with the structural phases of the problem.

A *pluton* is a body of intrusive igneous rock of any shape or size. At first, such a general term may seem of little value, but when the data are insufficient it is far better to call a body a *pluton* than to use a term with a definite meaning. All too often in the past when the field data were quite inadequate, a body of intrusive igneous rock has been called a *laccolith* or a *batholith*. A geologist can call a body a *pluton*, and then tell exactly what he knows about it.

A structural study of plutons involves a consideration of their internal structure, shape, and size, as well as the structural and chronological relations to the adjacent rocks.

#### Internal Structure

Many igneous rocks are *massive*, showing no preferred orientation of the constituent minerals (Fig. 209A). Others, however, are characterized by *foliation*, due to the parallel arrangement of platy minerals (Fig. 209B). The perfection of the foliation differs greatly, being well-marked in some instances and barely perceptible in others. *Primary foliation* forms during the crystallization of the magma, whereas *secondary foliation* develops after the rock has consolidated. Secondary foliation

is similar in this respect to the schistosity of metamorphic rocks. Means of distinguishing primary from secondary foliation are discussed on p. 307. *Banded or layered intrusive rocks* are those that consist of alternate layers of different mineral composition. In Fig. 209C, the dark minerals, shown in solid black, are abundant in layers 1, 3, and 5, but are rare in layers 2 and 4. The layers typically range in thickness from an inch to several inches, but in exceptional cases the thickness may be greater or less than that. If the minerals in such a layered rock are platy and lie parallel to one another, the rock is foliated as well as banded (Fig. 209D).

*Primary lineation* is discussed on p. 300.

*Inclusions* are fragments of older rock surrounded by igneous rock. They may be angular, subangular, or round. A *xenolith* is an inclusion that has obviously been derived from some older formation genetically unrelated to the igneous rock itself, as, for example, a fragment of sandstone in granite. An *autolith*, sometimes called a *cognate xenolith*, is an inclusion of an older igneous rock that is genetically related to the rock in which it occurs. Thus an inclusion of diorite in granodiorite is called an *autolith*, if it can be shown that both were derived from a common parent magma. Whether or not the two rocks have a common parentage is, however, primarily a problem of petrology.

A *segregation* is a round or irregular body, a few inches to many feet in diameter, and in some cases hundreds of feet across, that has been enriched in one or more of the minerals composing the igneous rock. Thus a hornblende granite may contain clots that have much more hornblende than the surrounding granite. These clots are segregations if they formed while the granite was consolidating, and if their formation was due to concentration of the atoms of which hornblende is composed. Petrographic methods may be necessary to distinguish a segregation from an inclusion, particularly if the latter has been modified by reaction with the magma.

*Schlieren* are somewhat wavy, streaky, irregular sheets, usually lacking sharp contacts with the surrounding igneous rocks. Schlieren may be either darker or lighter than the rock in which they occur. Some are disintegrating, altered inclu-

sions, some may be segregations, and some may represent concentrations of residual fluids into layers in a rock that had otherwise crystallized.

### Age Relative to the Adjacent Rocks

An intrusive igneous rock can be either older or younger than the adjacent formations. If the intrusive rock is older, the adjacent rocks must rest on it unconformably (Fig. 210A). The bedding in the sedimentary rocks above the unconformity is essentially parallel to the contact. Debris from the igneous

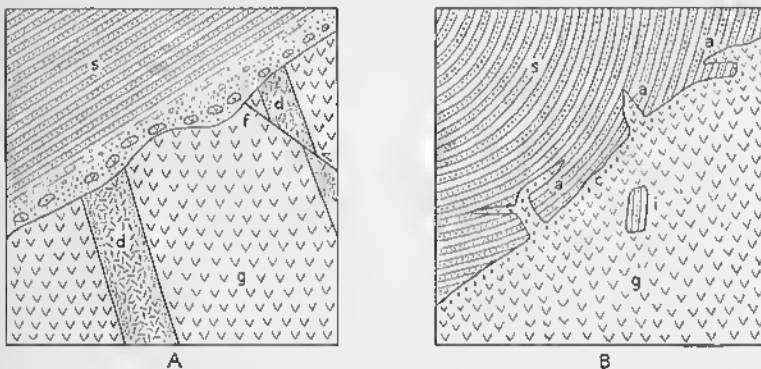


FIG. 210.—Relative Age of Pluton and Adjacent Rocks. *s* = sandstone and shale; *g* = granite; *d* = dike of diorite; *f* = fault; *i* = inclusion; *a* = apophyses; *c* = chilled contact of granite. A. Unconformity. B. Intrusive contact.

rock, either in the form of pebbles or mineral fragments, may generally be found in the overlying formations. The igneous rock is coarse up to the contact, and faults and dikes (see p. 279) in the igneous rock may be truncated at the contact.

If the igneous rock is younger than the adjacent formations, an *intrusive contact* must exist (Fig. 210B). Small dikes or sills (pp. 267-270) of the igneous rock may cut the adjacent formations, and inclusions of the latter may be found in the intrusive. The igneous rock may become finer-grained adjacent to the older rocks, giving a *chilled contact*. The bedding in the adjacent formations may or may not be truncated by the contact. Conclusive data may be difficult to obtain along many contacts, but assiduous search will usually reveal critical information.

### Structural Relations to the Surrounding Rocks

In many instances, the older rocks into which a pluton is intruded are characterized by bedding or schistosity. A body is said to be *concordant* if the contacts are parallel to the bedding or schistosity of the older rocks (Fig. 211A). A body is said to be *discordant* if the contacts cut across the bedding or schistosity of the older rocks (Fig. 211B). In many cases, of course, a contact may be concordant in some places, discordant in others. When one refers to the larger plutons, the terms *concordant* and *discordant* may be used to a certain extent in a relative sense.

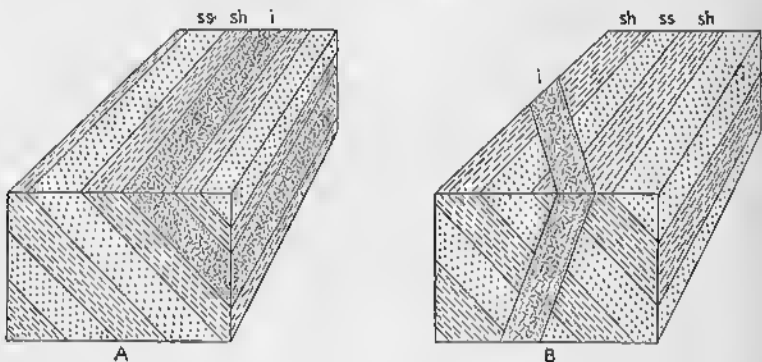


FIG. 211—Concordant and Discordant Intrusions: ss = sandstone, sh = shale, i = igneous rock of pluton. A. Concordant pluton. B. Discordant pluton.

For example, an intrusive that is regionally concordant may locally transgress the structure of the older rocks.

The most satisfactory classification of plutons is based upon whether the contact is concordant or discordant, but shape and size are also factors. The concordant bodies include sills, laccoliths, lopoliths, and phacoliths. The discordant bodies include dikes, volcanic vents, batholiths, and stocks.

The structural relations to the surrounding rocks may be determined in various ways. The smaller bodies, a few feet or tens of feet across, may be observed directly in a single outcrop, and the concordant or discordant nature may be established directly (Fig. 211). For larger plutons, more indirect methods are necessary. Fig. 212A, for example, is a map of a pluton, 100 feet wide, trending northeast. At localities *a* and *c*, the

bedding dips 40 degrees to the southeast. At locality *b*, the southeast contact of the pluton is exposed, and it dips 40 degrees to the southeast. At locality *d*, the northwest contact of the pluton is observed to dip 40 degrees to the southeast. It is

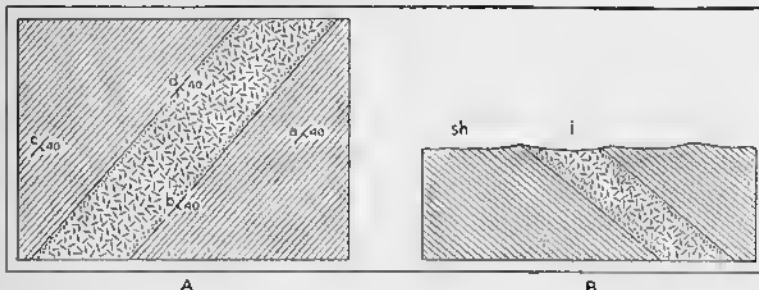


FIG. 212—Concordant Pluton, the Contacts of Which Are Exposed; *sh* = shale, *i* = igneous rock of pluton. A. Geological map; letters are mentioned in text. B. Inferred cross section.

apparent, therefore, that the body is concordant, as shown in Fig. 212B, at least within the zone of observation.

Fig. 213A is a map of another region. As in the previous case, the bedding dips 40 degrees to the southeast. But the southeast contact at *b* and the northwest contact at *d* dip 80 degrees to the northwest; the pluton must be discordant (Fig. 213B).

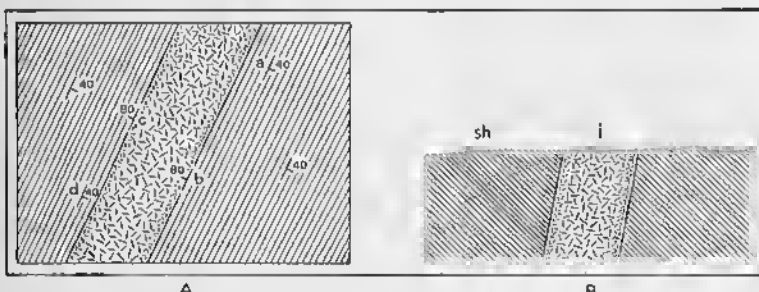


FIG. 213—Discordant Pluton, the Contacts of Which Are Exposed; *sh* = shale, *i* = igneous rock of pluton. A. Geological map; letters are mentioned in text. B. Inferred cross section.

Several indirect methods are available to ascertain the attitude of contacts that are not exposed. One of these methods is based upon topography. In Fig. 214A, the strata dip 40 degrees to the southeast. The contacts of the pluton are not

exposed, but the outcrops are good enough to permit location of the contact within a few feet. The contact bends downstream where it crosses a valley. If the altitudes of the southeastern contact at *c*, *d*, and *e* are known, the dip of the contact may be calculated by the three-point method (pp. 65, 417). Similarly,

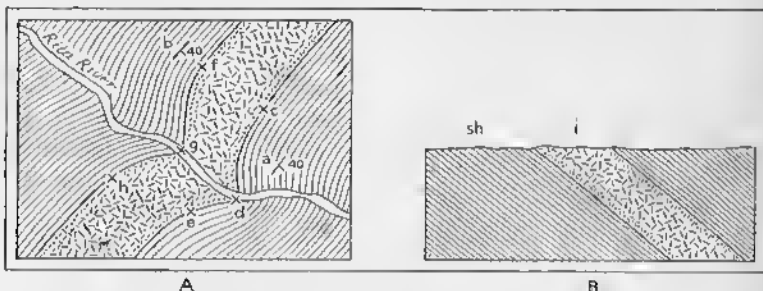


FIG. 214—Concordant Pluton—Attitude of Contacts Deduced from Relations to Topography: *sh* = shale; *i* = igneous rock of pluton. A. Geological map; letters referred to in text. B. Inferred cross section.

the attitude of the northwestern contact may be determined if the altitude of points *f*, *g*, and *h* are known. If both contacts dip 40 degrees to the southeast, the pluton is concordant.

Another method utilizes whatever primary foliation may be present in the igneous rock. In Fig. 215A, the bedding dips

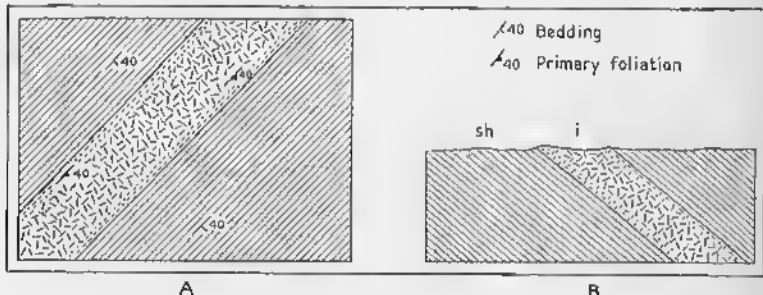


FIG. 215—Concordant Pluton—Attitude of Contacts Deduced from Attitude of Foliation: *sh* = shale; *i* = igneous rock of pluton. A. Geological map. B. Inferred cross section.

40 degrees to the southeast, but the actual contact of the pluton is nowhere exposed. The primary foliation near both contacts also dips 40 degrees to the southeast. Observations in many parts of the world show that the primary foliation is commonly parallel to the adjacent contacts. This subject is discussed

more fully on p. 299. It is inferred, therefore, that the contact in this case dips 40 degrees to the southeast, and that the pluton is concordant.

The attitude of a contact may be determined by artificial means such as tunnels, mines, or drill holes. Geophysical methods (chapter 19) may also be used.

### Determining the Shape and Size of Plutons

The shape and size of plutons are almost always a matter of conjecture. This is true of even the smaller bodies. An intrusion such as that illustrated in Fig. 212 is presumably tabular, but only the thickness is known with any precision. The northeast-southwest dimensions can be ascertained if exposures are available. But the dimension down the dip is unknown—unless by some artificial means, such as drilling or mining—and the former extent up the dip is forever lost by erosion.

For the larger plutons, the ground plan is determined by areal mapping, which may show that the body is linear, circular, arcuate, or irregular. The attitude of the contact is determined by the methods discussed above—direct observation, relation to topography, or attitude of primary foliation. The application of these principles is discussed more fully in those sections treating of the various kinds of pluton. The downward extent of the body is beyond the realm of observation, however, and is of necessity a matter of extrapolation. In regions of high relief, the contacts may be exposed throughout a vertical range of thousands of feet, or data throughout a considerable depth may be obtained wherever there has been mining or drilling.

### Concordant Plutons

#### Sills

*Sills*, sometimes called *sheets*, are tabular plutons that are parallel to the bedding or schistosity of the adjacent rocks (Fig. 216). The rock in the sill is younger than the rock on either side of it. Sills are horizontal, vertical, and inclined; the concept that a sill must be horizontal is quite erroneous. Sills are relatively thin compared to their extent parallel to the

structure of the adjacent rocks. Sills and lava flows (p. 313) have some features in common. Both are sheet-like bodies lying parallel to the structure of the adjacent rocks. They differ, however, in origin. A flow pours out on the surface of the earth, and it is older than the overlying rocks. A sill, on the other hand, is younger than the strata both above and below; moreover, it consolidated beneath the surface of the

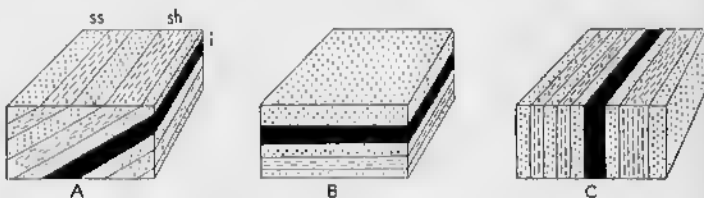


FIG. 216—Sills: *ss* = sandstone; *sh* = shale; *i* = igneous rock of sill.  
A. Dipping sill. B. Horizontal sill. C. Vertical sill.

earth. Criteria for distinguishing sills from lava flows are given on p. 316.

Sills range in size from tiny sheets less than an inch thick to large bodies many hundreds of feet thick. The smaller sills can usually be traced for only a few feet or scores of feet, but the larger sills cover thousands of square miles.

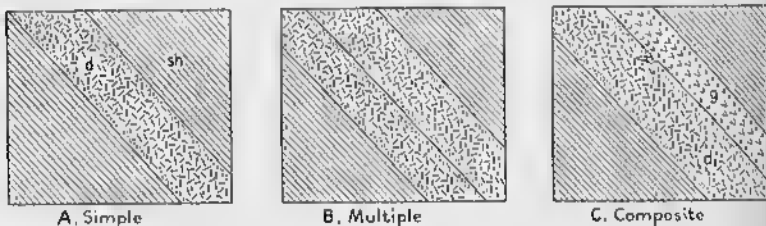


FIG. 217—Cross Sections of Sills: *sh* = shale; *d* = diorite; *g* = granite.  
A. Simple sill. B. Multiple sill. C. Composite sill.

A *simple sill* results from a single injection of magma (Fig. 217A). A *multiple sill* results from two or more injections of the same kind of magma (Fig. 217B). Ideally, a simple sill is chilled only at the margins. A multiple sill, although possessing chilled margins, also possesses a medial zone, the position of which depends upon the relative thickness of the individual sills. The greater the number of separate

injections comprising the multiple sill, the greater will be the number of chilled zones. If the injections followed one another in relatively rapid succession, the chilled zones may be obscure. A *composite sill* results from two or more injections of magma of differing composition. Fig. 217C illustrates a sill formed by separate injections of diorite and granite. A small offshoot of the granite cuts the diorite, indicating that the granite is younger than the diorite.

*Differentiated sills* (Fig. 218) are of particular interest to petrographers, because of their bearing on the problem of magmatic differentiation.<sup>1</sup> Such sills are generally hundreds of feet thick, and they are initiated by the injection of a hori-

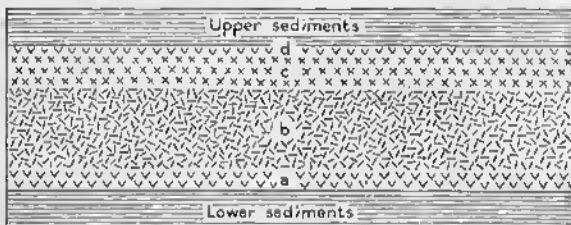


FIG. 218—Differentiated Sill; *a* and *d* = rock with chemical composition of original magma; *b* = part of rock richer in dark minerals than *a* and *d*; *c* = part richer in light minerals than *a* and *d*.

zontal sheet of magma. The magma cools slowly and, under the influence of gravity, separates into layers of different composition. As crystallization proceeds, any minerals that are heavier than the magma tend to sink, whereas crystals lighter than the magma tend to rise. Rising gases play a rôle the importance of which is as yet undetermined. In the ideal case, such as is illustrated in Fig. 218, a differentiated sill will have at both the top and the bottom relatively thin layers, *a* and *d*, of fine-grained rock, representing the rapidly cooled original magma. Above the bottom layer are heavier rocks, *b*, which contain minerals of relatively high specific gravity. Still higher is a layer of lighter rocks, *c*, containing minerals with relatively low specific gravity. The combined chemical composition of *b*

<sup>1</sup> Daly, R. A., *Igneous rocks and the depths of the earth*, pp. 333-344. New York and London: McGraw-Hill Book Company, 1933.

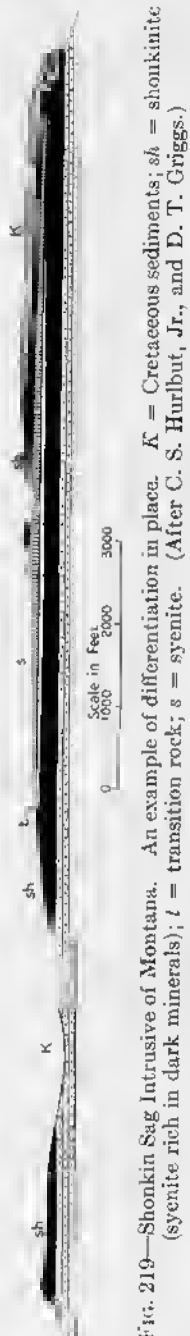


FIG. 219—Shonkin Sag Intrusive of Montana. An example of differentiation in place.  $K$  = Cretaceous sediments;  $sh$  = shonkinite ( $s$  = syenite);  $t$  = transition rock;  $s$  = syenite. (After C. S. Hurlbut, Jr., and D. T. Griggs.)

and  $c$  will equal the combined composition of  $a$  and  $d$ . In the simplest case, the contacts between the four layers are gradational.

Many complications may exist in detail in differentiated sills. For example, one would suppose that if any density stratification occurred within layer  $b$ , the layers would be progressively heavier downward. A detailed study of a similar body at Shonkin Sag, Montana (Fig. 219),<sup>2</sup> shows that the heaviest rocks are many feet above the bottom of layer  $b$ . Moreover, the contacts of layer  $c$  are relatively sharp, rather than gradational; this is due to movement of the partially-liquid magma after differentiation took place.

To distinguish a differentiated sill from a composite sill may be difficult. (1) Obviously, a sill in which the lighter rocks are at the bottom cannot be due to differentiation in place under the influence of gravity. (2) Differentiation in place is implied if the various layers are gradational into one another. But this is by no means an infallible criterion, because under some conditions two intrusives of different ages show gradational, rather than sharp, contacts. A younger intrusive may react with an older rock to produce a transition zone that is many feet wide. (3) Although sharp contacts seem to imply successive injections, the liquid resulting from differentiation in place may move several scores of feet and produce sharp contacts.

It is quite possible, of course, for a differentiated sill to be deformed in a later orogenic episode, and even to assume a vertical or overturned attitude.

<sup>2</sup> Hurlbut, C. S., Jr., and Griggs, D. T., Igneous rocks of the Highwood Mountains, Montana, pt. 1, 'The laccoliths; *Bulletin Geological Society of America*, Vol. 50, pp. 1043-1111, 1939.

### Laccoliths

A *laccolith*<sup>3</sup> is an intrusive body that has domed up the strata among which it has been inserted (Fig. 220). If the floor is relatively horizontal (Figs. 220 and 221A), the laccolith may be described as *plano-convex*, but if the floor is bowed



FIG. 220.—Asymmetric Laccolith at Mount Hillers, Henry Mountains, Utah. Solid black is igneous rock (trachyte); other symbols represent Mesozoic sedimentary rocks. (After G. K. Gilbert.)

down (uppermost laccolith of Fig. 221B), the laccolith may be described as *doubly convex*. Such a distinction, however, is rarely possible, because, as will be shown later, critical data concerning the nature of the floor are usually impossible to obtain. Laccoliths are usually two to four miles in diameter, and the thickness is measured in thousands of feet.

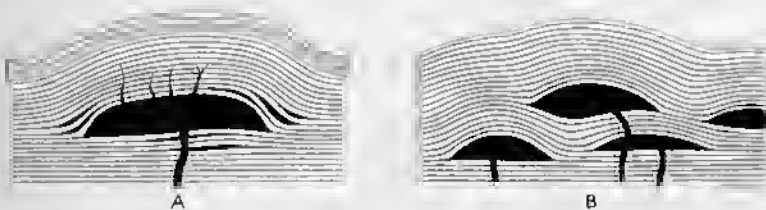


FIG. 221.—Laccoliths. Solid black represents igneous rock; lined pattern represents sedimentary rocks. A. Ideal cross section of laccolith with accompanying dikes and sills. B. Ideal cross section of grouped laccoliths. (After G. K. Gilbert.)

It is apparent that all transitions may exist between laccoliths and sills. In a typical laccolith, the diameter is only a few

<sup>3</sup>Gilbert, G. K., Report on the geology of the Henry Mountains: *U. S. Geographic and Geologic Survey of the Rocky Mountain Region*, 1880.

Jaggar, T. A., Jr., The laccoliths of the Black Hills: *U. S. Geological Survey 21st Annual Report*, pt. 3, pp. 163-303, 1901.

times greater than the thickness. In a typical sill, the diameter is many times the thickness. The body may be termed a *laccolith* if the ratio of the diameter to the thickness is less than ten; if the ratio is greater than ten, the body should be called a *sill*. This is an arbitrary figure, but in all geological classifications continuous series must be artificially assigned to compartments.

The typical laccolith has a floor; a small central pipe or conduit, through which the magma was intruded, is shown in most diagrams (Fig. 221). Inasmuch as the floor and feeder

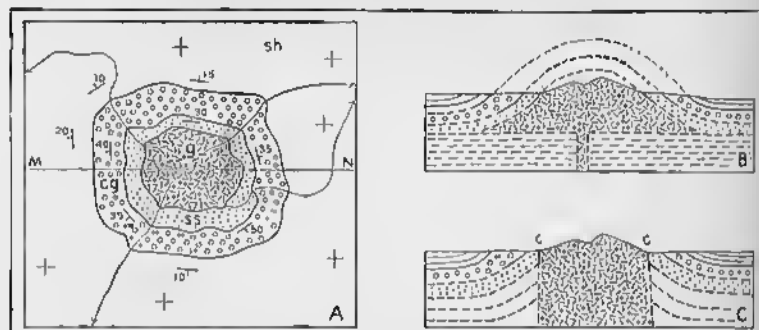


FIG. 222—Intrusive Rock in the Center of Domed-up Sediments: *g* = granite porphyry; *ss* = sandstone; *cg* = conglomerate; *sh* = shale; *c* = contact of intrusive. The granite intrudes the sandstone. A. Geological map. B. Interpreted as a laccolith. C. Interpreted as a "bottomless" stock.

are seldom, if ever, observed, they are largely based on inference. If a valley were eroded directly across a laccolith, a floor, and perhaps even the central conduit, might be exposed. But most laccoliths, particularly in the western United States, are resistant rock bodies from which the drainage is radial. Ordinarily, all that one observes is a central body of igneous rock, surrounded by outwardly-dipping sedimentary rocks (Fig. 222A). Sills and dikes (p. 279) derived from the igneous core may intrude the sedimentary rocks. In the accompanying cross section (Fig. 222B), the observed data are indicated in heavy, solid lines. The supposed structure is in broken lines, and it is obvious that the floor and feeder are merely inferred.

An alternate interpretation, shown in Fig. 222C, is that the intrusive is "bottomless." In such a case, however, the con-

tacts are crosscutting. It is obvious that the contacts, *c*, are the critical places at which to obtain data. If the intrusive is a laccolith, the contacts must be concordant. Even such data are not conclusive, because, as is shown in Fig. 223A, the body could be concordant at the surface, yet discordant at depth and "bottomless." Of course, the exact shape of an intrusive could be determined by drilling or mining, but ordinarily the expense is prohibitive.

It is obvious from the preceding discussion that the location and nature of the feeding conduit is also a problem. Its very existence is questioned by some geologists. It is possible that some laccoliths have been fed from the side (Fig. 223B); some laccoliths may be great protuberances on a sill.

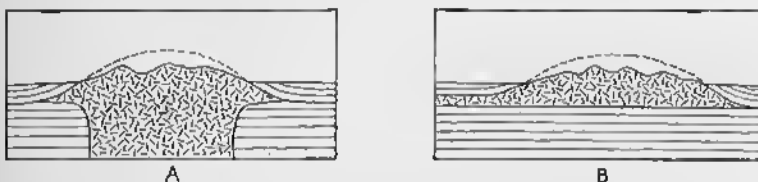


FIG. 223.—Dome-like, Concordant Intrusion. Diversely oriented dashes represent intrusive rock; lined pattern represents sedimentary rocks. A. Interpreted as the concordant top of a body that is mostly discordant and "bottomless." B. Interpreted as a large bulge at the end of a sill.

An *asymmetric laccolith* is one in which the dip of the roof rocks differs considerably in different sectors (Fig. 220). An *interformational laccolith* is one injected along an unconformity. A *bysmalith* is a variety of laccolith the roof of which has been uplifted along cylindrical faults. It is obvious, however, that in the field it would ordinarily be impossible to distinguish such a body from a "bottomless" intrusion.

Whether a laccolith or a sill develops when magma spreads along horizontal bedding planes, depends upon several factors, of which the most important is the viscosity of the magma. Low viscosity will cause thin, wide-spread intrusions such as sills; high viscosity, because it prevents lateral spreading of the magma, causes laccoliths.<sup>4</sup>

The roof of the laccolith is lifted by the hydrostatic pressure of the magma. The overlying sedimentary rocks, compressed

<sup>4</sup> Paige, S., The bearing of progressive increase of viscosity during intrusion on the form of laccoliths: *Journal of Geology*, Vol. 21, pp. 541-549, 1913.

by the force of the magma, are elongated parallel to the bedding. The amount of the elongation depends, of course, upon the shape of the laccolith, but in some cases it is as great as 10 per cent and even more. Similarly, the thickness of the overlying sedimentary rocks is reduced. Tension cracks may form because of this "stretching" of the roof, and the roofs of some experimental laccoliths<sup>5</sup> are broken by radiating and concentric cracks. There is little field evidence for fractures of this type. This is partly because the roof rocks have generally been destroyed by erosion; but even where the roof is preserved, such fractures are rare—apparently because the rocks were sufficiently plastic to yield without rupture.

The conditions that determine the horizon at which the magma will be intruded are not well understood. When laccoliths were first described, it was supposed that the magma rose in a relatively narrow pipe until it was in hydrostatic equilibrium with the sedimentary rocks through which it was moving. Supposedly, the specific gravity of the sedimentary rocks increased downward more or less systematically. The magma, having a lower specific gravity than the lower part of the sedimentary column, would rise until it reached that horizon where the specific gravities of magma and sedimentary rocks were approximately equal. Unable to rise any higher, the magma would spread laterally. A more important factor may be the physical character of the intruded sedimentary rocks. The magma may rise until it reaches a series of beds that it cannot penetrate, perhaps because of their strength or plasticity; at this horizon the magma spreads laterally.

### Lopoliths

A *lopolith*<sup>6</sup> is a concordant intrusion associated with a structural basin (Fig. 224). In the simplest and ideal case, the sediments above and below the lopolith dip inward toward a common center. The diameter of a lopolith is commonly measured

<sup>5</sup> Howe, E., Experiments illustrating intrusion and erosion: *U. S. Geological Survey 21st Annual Report*, pt. 3, pp. 291–303, 1901.

MacCarthy, G. R., Some facts and theories concerning laccoliths: *Journal of Geology*, Vol. 33, pp. 1–18, 1925.

<sup>6</sup> Grout, F. F., The lopolith; an igneous form exemplified by the Duluth gabbro: *American Journal of Science*, 4th series, Vol. 46, pp. 516–522, 1918.

in tens or even hundreds of miles, and the thickness in thousands of feet. Superb examples are furnished by the Bushveld igneous complex of South Africa, where there are two lopoliths (Fig. 225), an upper one composed of granite, and a lower one composed of norite and related rocks.<sup>7</sup> If a lopolith is injected along an angular unconformity, the rocks above the intrusion will display

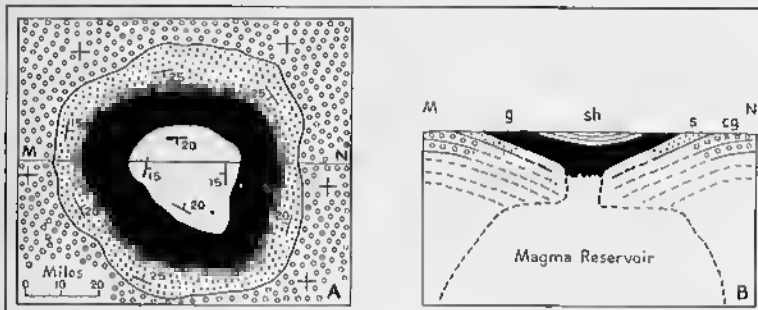


FIG. 224—Lopolith: *cg* = conglomerate; *s* = sandstone; *sh* = shale; *g* = gabbro of lopolith. Usual dip-strike symbols; + = flat strata. A. Geological map. B. Structure section.

the inward dip, but the underlying rocks will not, because they have been previously folded. The Duluth lopolith of Minnesota is such a body, but is incomplete, because it is chiefly confined to the northwestern quadrant of the structural basin. At Sudbury, Ontario, a large intrusion, with which nickel ores are associated, is considered by many to be a lopolith.



FIG. 225—Lopoliths of the Bushveld Igneous Complex of South Africa: *OG* = older granite; *T* = Transvaal system; *K* = Karroo system; *N* = norite of the lower lopolith; *G* = newer granite of the upper lopolith; *S* = younger syenites, unrelated to lopolith. (After A. L. Hall.)

The nature of the feeder of a lopolith is problematical. It may be a relatively narrow, centrally-located conduit, as is shown in Fig. 224B, or it may be much larger. No data pertinent to this subject are available. The basining is probably

<sup>7</sup> Hall, A. L., The Bushveld igneous complex of the central Transvaal: *Geological Survey of South Africa, Memoir 28*, 1922.

contemporaneous with the intrusion. The overlying rocks sag downward while large masses of magma are being withdrawn from the underlying magma reservoir (Fig. 224B). In fact, some geologists consider this contemporaneous basining an essential part of the definition of a lopolith. If a large, concordant sheet injected into flat sedimentary rocks were deformed into a basin, during some later orogenic period, these geologists would use the term *sill*, rather than *lopolith*.

Lopoliths, like sills, can be simple, multiple, composite, or differentiated. Differentiation is characteristic of lopoliths. The Duluth lopolith is primarily gabbro, but a granite that is the product of gravitational differentiation has accumulated near the top. The differentiation of the norite lopolith of the Bushveld complex is simple in its larger features, but very complicated in detail.

### Phacoliths

*Phacoliths*<sup>8</sup> are concordant intrusives confined to the crests of anticlines (Fig. 226B) or to the troughs of synclines. Phaco-

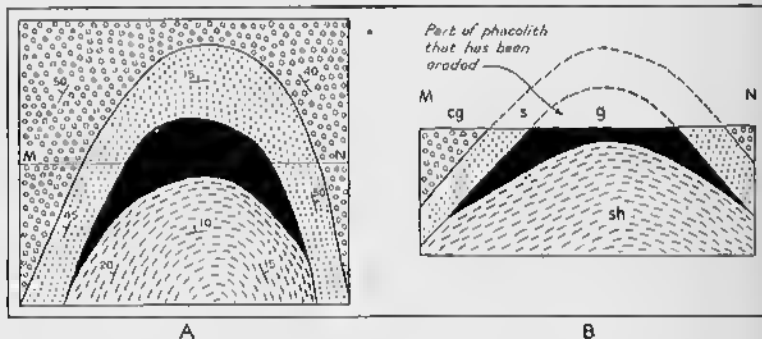


FIG. 226—Phacolith; *sh* = shale; *s* = sandstone; *cg* = conglomerate; *g* = granite. A. Map of granite phacolith in a northerly-plunging anticline. B. Cross section of the same phacolith.

liths are not only crescentic in cross section, but also in plan, because they are commonly associated with plunging folds. Fig. 226A is a geological map of a northerly-plunging anticline intruded by a phacolith, shown in solid black. The thickness of phacoliths is measured in hundreds, or, at the most, several

<sup>8</sup> Harker, A., *The Natural History of Igneous Rocks*, pp. 77-78. New York: The Macmillan Company, 1909.

thousands, of feet. In plan, phacoliths are seldom more than a few thousand feet long, as measured around the crescent. Whereas sills, laccoliths, and lopoliths characteristically force their way into place, some geologists believe that phacoliths are passively intruded, the magma filling potential cavities that form during the folding. In an anticline, for example, the upper beds may pull away from the lower beds. It seems probable, however, that the magma must be under some pressure, and that it actually makes space for itself.

### Other concordant plutons

It is becoming increasingly apparent that large, more or less concordant intrusions are an integral part of orogenic belts.

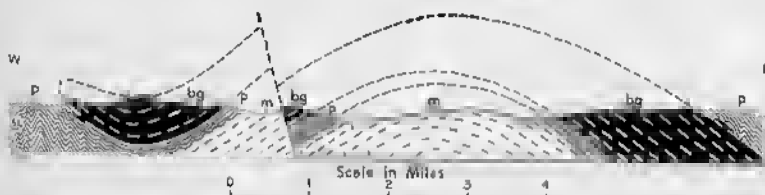


FIG. 227.—Large Concordant Pluton, Masecoma Quadrangle, New Hampshire. *P* = Paleozoic schists; *m* = granitic rocks of Masecoma group; *bg* = Bethlehem gneiss, which forms a large concordant pluton. (After C. A. Chapman.)

Although special names might be given to such bodies, depending upon their shape and size, it seems better to use the general term, *pluton*, rather than to coin new words.

In western New Hampshire a large sill-like body of orthogneiss, the Mt. Clough pluton, is 100 miles long. In cross section it is a great sheet, several thousand feet thick (*bg* of Fig. 227).<sup>9</sup> It is possible that this pluton was intruded as a horizontal sheet and was subsequently folded. On the other hand, it may have been intruded with its present curved form. The intruding magma moved from the east toward the west.

Other plutons are great lenses forced into the older sedimentary rocks. Balk<sup>10</sup> states that the anorthosite complex of the Adirondack Mountains is such a body, the magma having

<sup>9</sup> Chapman, C. A., Geology of the Masecoma quadrangle, New Hampshire: *Bulletin Geological Society of America*, Vol. 50, pp. 127-180, 1939.

<sup>10</sup> Balk, R., Structural geology of the Adirondack anorthosite: *Mineralogische Petrographische Mittheilungen*, Vol. 41, pp. 308-432, 1931.

moved upward toward the southwest. Similar bodies, such as the Kinsman quartz monzonite in the vicinity of Mt. Cardigan,<sup>11</sup> are common in western New Hampshire.

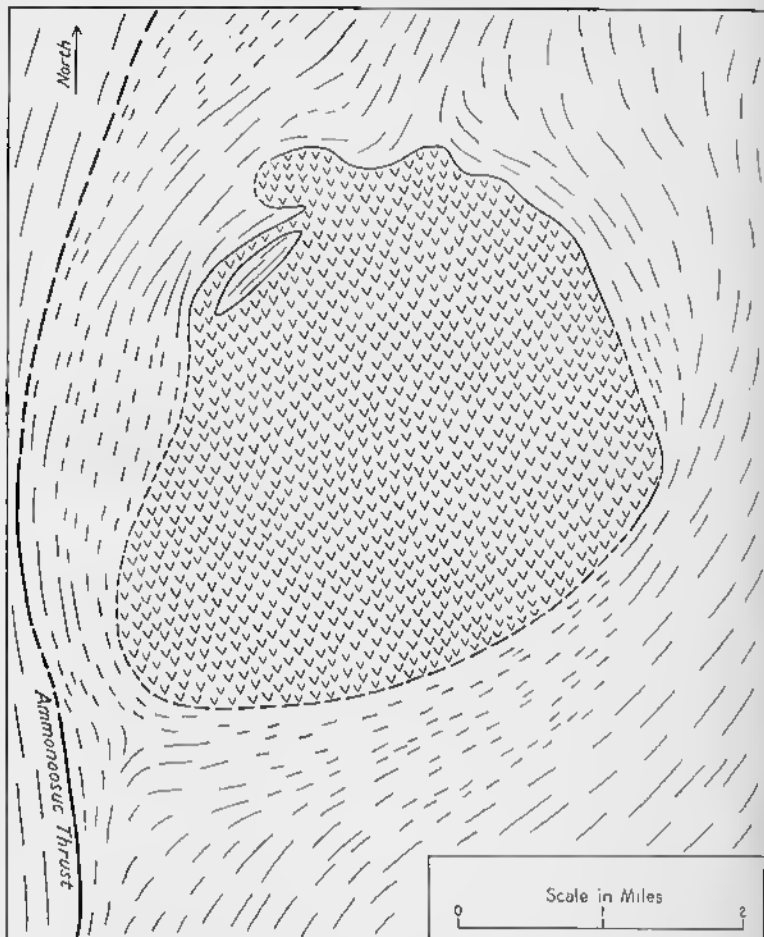


FIG. 228—Cylindrical Concordant Pluton, French Pond Pluton, near North Haverhill, New Hampshire. Checks = granite of pluton; longer lines = strike of steeply dipping schists; shorter lines = probable strike of schists that are covered by glacial deposits.

Some concordant bodies are essentially circular in plan, and have steep to vertical contacts. The bedding and schistosity

<sup>11</sup> Billings, Katharine F., Geological map of the Cardigan quadrangle, New Hampshire: *Bulletin Geological Society of America*, Vol. 53, pp. 177-178, 1942.

of the surrounding sediments wrap around the intrusive (Fig. 228). How deep the "bottom" of such an intrusive may be is a matter of conjecture, but the upper part, at least, is presumably cylindrical.

### Discordant Plutons

#### Dikes

*Dikes* are tabular bodies of igneous rock that cut across the structure of the intruded formations (Fig. 211B). Tabular intrusive bodies cutting massive, structureless rocks are also called dikes. Most dikes are formed by the injection of magma into a fracture; the walls may be pushed apart by the pressure exerted by the intruding magma, or the magma may quietly well up into fractures opened by tensional forces. Some bodies that appear to be dikes have been formed by replacement; that is, solutions moving through a fracture have altered the adjacent rock into igneous-looking material.<sup>12</sup>

The terms *simple*, *multiple*, *composite*, and *differentiated* may be applied to dikes in the same sense that they are used for sills. A *simple dike* is the result of a single intrusion of magma. A *multiple dike* is the result of two or more intrusions of the same kind of magma. A *composite dike* is the product of the intrusion of two or more kinds of magma. A *differentiated dike* is one that was intruded as a homogeneous magma, but from which two or more varieties of rock have formed *in situ*.

Dikes may be very small, and dikes a fraction of an inch wide and a few inches long may be associated with larger igneous bodies. Most dikes are one to twenty feet wide, but wider and narrower dikes are not uncommon. The distance for which a dike may be followed depends in part upon the nature of the exposures (Pl. XVII). In Iceland, dikes 10 miles long are common, and some are 30 miles long; at least one is 65 miles long. In England, the Cleveland dike is 110, and perhaps 190, miles long.

The Medford dike near Boston, Massachusetts, is 500 feet wide in places. A differentiated dike at Brefven, Sweden, is 20 miles long and one mile wide. The Great Dike of Rhodesia is

<sup>12</sup> Goodspeed, G. E., Dilation and replacement dikes: *Journal of Geology*, Vol. 48, pp. 175-195, 1940.

300 miles long and 2 to 7 miles wide, but it may not be a true dike in the sense of being tabular.

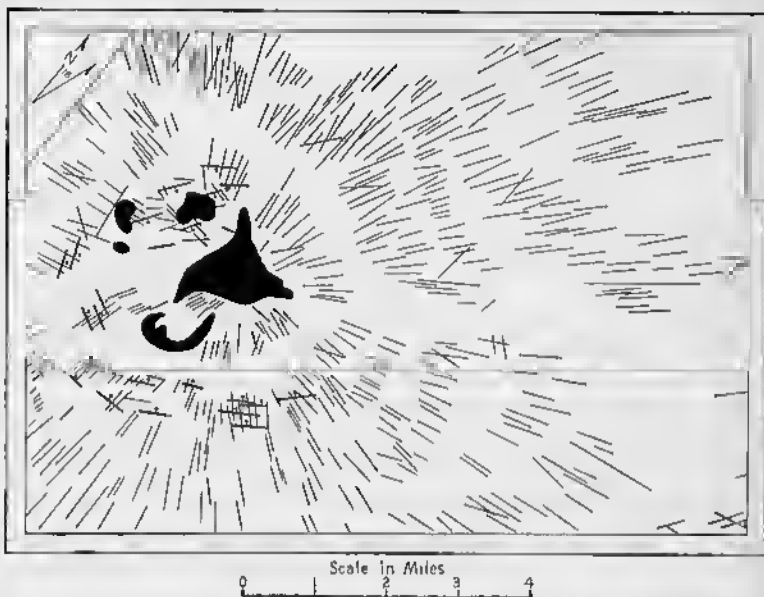


FIG. 229—Radiating Dikes and Cone Sheets of the Sunlight Area, Wyoming. Straight lines are dikes; heavier lines, with dip symbol, are cone sheets. (After W. H. Pursons.)

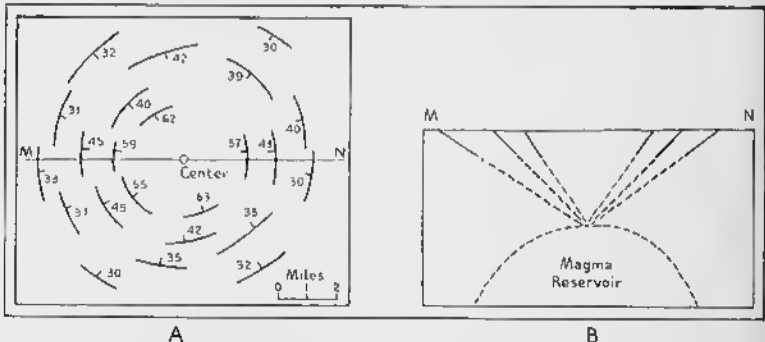


FIG. 230—Cone Sheets. A. Map; direction and value of dip is indicated.  
B. Cross section along line *MN*.

A *dike set* consists of parallel dikes; where the dikes are very abundant, the term *dike swarm* may be applied. In some areas several sets may be present, and each set may be characterized by its own peculiar petrography, indicating that the various sets

are of different ages. The fractures occupied by isolated dikes, dike sets, and dike swarms are commonly initiated by tension. The forces are in many instances regional in character, and they may even be the indirect result of compression or a couple. Any magma that is available injects the rupture. Elsewhere the pressure exerted by a large body of magma may initiate extension fractures (p. 103) more or less perpendicular to the walls of the reservoir. The pressure exerted by the magma may play an important rôle in pushing apart the walls of the fracture. Moreover, the wedging action of the magma will be important in extending the fracture farther.

*Radiating dikes* are found around volcanic centers. Most of the dikes—some of which can be followed for miles—radiate from the central volcanic region. In the Sunlight area of Wyoming (Fig. 229), the radiating dikes extend 5 to 7 miles from the central area.<sup>13</sup> There are thousands of dikes averaging 4 feet in width, although some are 20 feet wide.

The original fractures, now filled by the dikes, are tensional in origin. In some cases, the magma in the conduit within the cone of the volcano exerts a horizontally-directed compressive force on the surrounding rocks. The resulting extension fractures constitute a vertical, radiating system. In other instances, the fractures may be related to forces initiated by the magma reservoir underlying the volcano. The upward pressure exerted by the magma would cause vertical, radiating extension fractures.

*Cone sheets* are dikes that belong to a concentric, inward-dipping system (Fig. 230). None of the cone sheets extends all the way around the central area; in fact, a cone sheet can be followed for only a few miles at the most. The average dip is 45 degrees, but the outer cone sheets tend to dip more gently than the inner. If the Scottish cone sheets,<sup>14</sup> which are Tertiary in age, are projected downward, they meet at a focus approximately 3 miles beneath the present surface (Fig. 230B). Cone sheets, typically a few feet thick, may attain a thickness of

<sup>13</sup> Parsons, W. H., Volcanic centers of the Sunlight area, Park County, Wyoming: *Journal of Geology*, Vol. 47, pp. 1-26, 1939.

<sup>14</sup> Richey, J. E., The Tertiary volcanic districts: *British Regional Geology, Scotland*, Edinburgh, 1935.

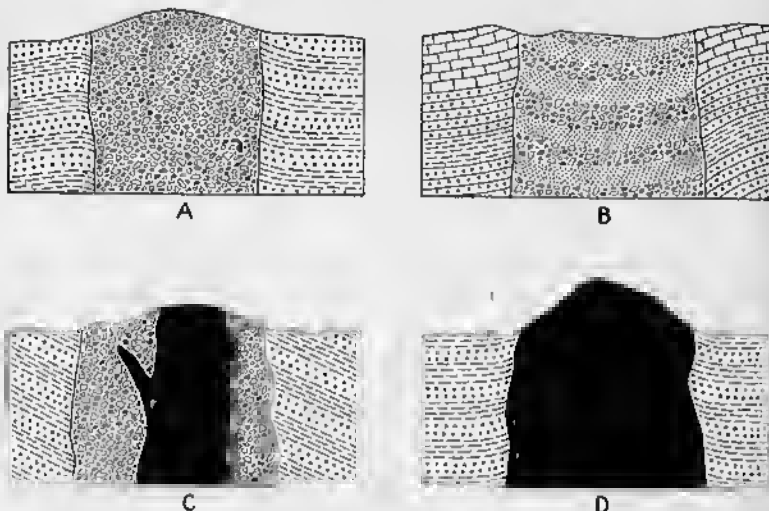


FIG. 231—Volcanic Vents. A. Vent filled with agglomerate. B. Vent filled with crudely stratified tuff and breccia. C. Vent filled with agglomerate and intrusive rock. D. Vent filled entirely by intrusive rock.

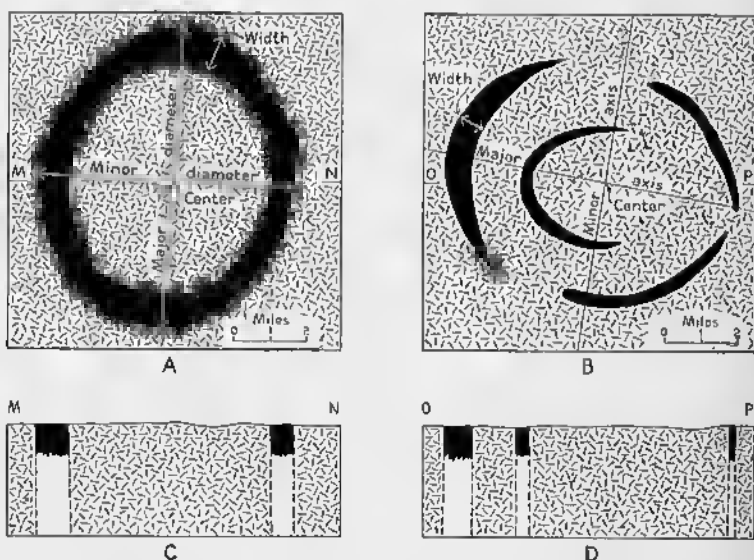


FIG. 232—Ring-dikes. Solid black represents igneous rock of ring-dikes. A. Circular (complete) ring-dike. B. Arcuate (incomplete) ring-dikes. C. Structure section along line *MN* of diagram A. D. Structure section along line *OP* of diagram B.

40 feet. In Mull, an island off the west coast of Scotland, they are concentric about two distinct centers. The cone sheets of the older center are cut by those associated with the younger center. Cone sheets are apparently not extensively developed in North America. Some have been mapped, however, from the Sunlight area of Wyoming (Fig. 229).

Fig. 230B illustrates the formation of cone sheets. The focal point is believed to lie approximately at the top of the original magma reservoir. Because of upwardly-directed magmatic pressure, the rocks in the roof were broken by conical, inwardly-dipping shear fractures similar to those formed under compression in the laboratory (p. 103). Magma injected into these fractures formed cone sheets.

Few direct data are available concerning the direction of movement of magma in dikes. It is commonly assumed that the magma moved upward, and for many dikes this is undoubtedly correct. There is reason to believe, however, that the magma in the radiating dikes of the Sunlight area moved horizontally.

*Apophyses* (singular, *apophysis*) and *tongues* are dikes, in some instances rather irregular, that obviously have been derived from a nearby igneous body.

#### Volcanic vents

*Volcanic vents*, also called *necks* and *plugs*, are the filled channels through which the magma that fed volcanoes moved. They are circular, subcircular, or even irregular in plan, and are a few score feet to a mile in diameter.<sup>15</sup> In a few cases they are even larger, but such necks are compound and have resulted from several successive eruptions. The contacts of volcanic necks with the surrounding country rock are typically steep; they are either vertical or inward-dipping, rarely outward-dipping.

The material filling a volcanic neck is variable and heterogeneous. In some instances it is coarse, unstratified pyroclastic material known as agglomerate (see p. 317), as illustrated by Fig. 231A. Some vents are filled by crudely-stratified tuff and breccia (Fig. 231B). Other vents are filled by a heterogeneous

<sup>15</sup> Geikie, A., *The Ancient Volcanoes of Great Britain*: Vol. 1 and Vol. 2. New York: The Macmillan Company, 1897.

mixture of agglomerate and fine-grained intrusive rocks (Fig. 231C). Still others are occupied exclusively by fine-grained intrusive rocks (Fig. 231D). (See also Pl. XVII).

### Ring-dikes

*Ring-dikes* are oval (Fig. 232A) or arcuate (Fig. 232B) in plan; the contacts are steep, either vertical or dipping steeply inward or outward (Figs. 232C and 232D). The diameter (Fig. 232A) ranges, in different examples, from one to sixteen miles; the width (Fig. 232A) may reach a maximum of one mile, and probably more; arcuate ring-dikes, of course, pinch out at both ends.

Fig. 233, a geological map of the Belknap Mountains of New Hampshire,<sup>16</sup> is typical of an area in which ring-dikes are present. The older rocks, chiefly schist and quartz diorite, are labeled *or*. An outer ring-dike, consisting of the units labeled *m*, *sqs*, and *am*, has a maximum diameter of 7 miles and a maximum width of one mile. An inner ring-dike, consisting of the units labeled *aqs*, *pqs*, the dike-like bodies of *cg*, and the more southerly of the two bodies labeled *s*, also has a maximum diameter of 7 miles and a maximum width of one mile. A central stock (see p. 289) consists chiefly of *cg*, *eb*, and the northern body of *s*.

The intrusion of ring-dikes is preceded by the formation of a circular or oval fracture that dips steeply outward in many cases (Fig. 234A). While the central block subsides (Fig. 234B), magma rises from a reservoir and fills the potential void left between the stationary walls and the sinking block. If erosion subsequently cuts deeply enough, to a level such as *OP* in Fig. 234B, the circular or oval intrusion, with steeply dipping contacts, is exposed. If the central block subsides several times (Fig. 234C and 234D), a number of concentric ring-dikes will form. A remnant of the older country rock left between two ring-dikes is called a *screen* (Fig. 234D).

Many ring-fractures extend to the surface of the earth (Fig. 235B); volcanies, erupted during the same magmatic cycle, may be preserved within the ring-dike (Fig. 235D).

<sup>16</sup> Modell, D., Ring-dike complex of the Belknap Mountains, New Hampshire: *Bulletin Geological Society of America*, Vol. 47, pp. 1885-1932, 1936.

The mechanism by which ring-dikes are formed is called *cauldron subsidence*. If the fracture extends to the surface (Fig. 235), we may use the term *surface cauldron subsidence*. If,

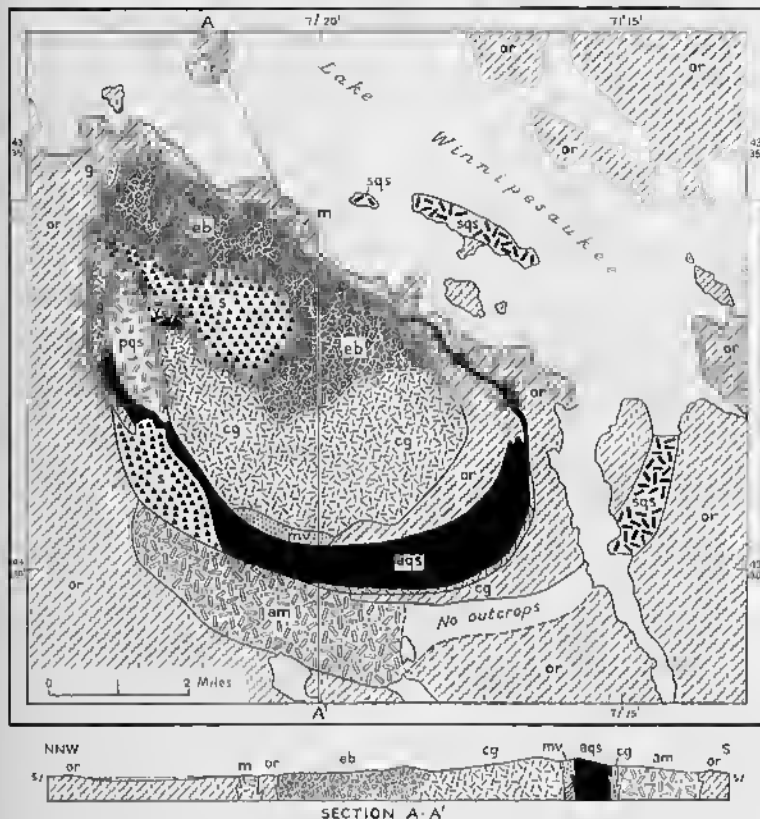


FIG. 233.—Ring-dikes of the Belknap Mountains, New Hampshire.  
*or* = older rocks, chiefly schist and quartz diorite; *mv* = Moat volcanics;  
*g* = gabbro; *m* = monzodiorite; *am* = augite monzodiorite; *s* = syenite;  
*pqs* = pink quartz syenite; *sgs* = subporphyritic quartz syenite; *ags* =  
Albany quartz syenite; *cg* = Conway granite; *eb* = Conway granite with  
many inclusions of diorite; *va* = vent agglomerate filling a volcanic vent.  
(After Modell.)

however, the fracture is entirely beneath the surface (Fig. 234), we may use the term *underground cauldron subsidence*.

The mechanism described above is adequate if the fractures dip outward. In some areas, where the contacts of the ring-dikes are vertical, an additional process must have been in operation. Magma entering such a vertical fracture may push

aside the walls of the fracture, the amount being controlled by the elasticity and plasticity of the country rock. Field evidence suggests, however, that very little of the space occupied by the ring-dikes was made in this way. In some cases the subsiding block was not bounded by a single fracture, but by a brecciated zone many hundreds of feet wide. The intruding magma was able to clean out this breccia, partly by piecemeal

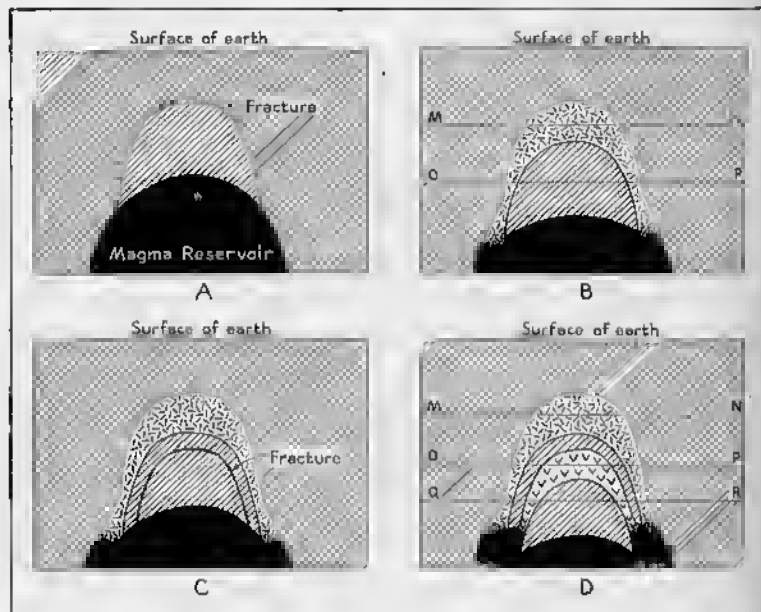


FIG. 234—Underground Cauldron Subsidence. Diagonal lining represents older country rock; diversely oriented short dashes represent one intrusion; checks represent a second intrusion. A, B, C, and D represent successive stages of intrusion. MN, OP, and QR are a few of the many levels to which erosion may cut.

stoping (p. 293), partly by carrying the fragments up to the surface, where they were poured out in surface eruptions.

In the simplest case of cauldron subsidence, the width of the ring-dike should be essentially uniform. Many ring-dikes are arcuate, however, and some have blunt ends. If the subsiding block crowds toward one wall (Fig. 236A), an incomplete ring-dike may form. The width of the ring-dike will differ if the dip of the initial fracture is not uniform (Fig. 236B); the width of the ring-dike is proportional, among other things, to

the angle of dip of the fracture; no ring-dike will form where the dip is vertical. A younger intrusion may eliminate part of what was originally a complete ring-dike. In Fig. 236C<sub>1</sub> a younger

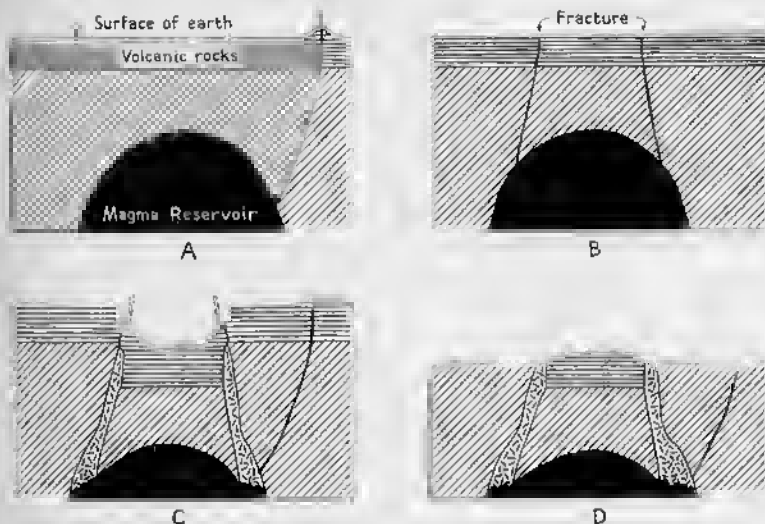


FIG. 235—Surface Cauldron Subsidence. Diagonal lining represents older country rock. Diversely oriented short dashes represent intrusive rock of a ring-dike. A. After eruption of volcanoes. B. Fracture forms. C. Subsidence accompanied by some volcanism; drag that commonly occurs near ring-dikes has been omitted. D. Erosion to present topography.

intrusion, shown by checks, has cut out the western part of an older ring-dike which is shown in solid black where it still remains; broken lines indicate the location of the western part

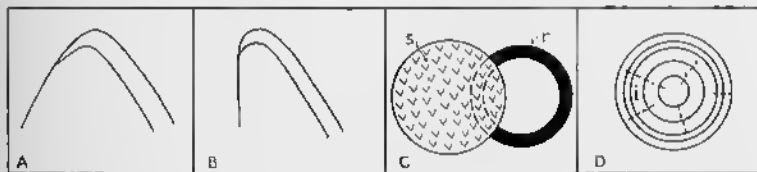


FIG. 236—Origin of Arcuate Ring-dikes. A. Cross section; subsiding block moves to one side. B. Cross section; dip of fracture is vertical in places. C. Map; younger intrusion cuts out part of ring-dike; *r* = ring dike; *s* = younger stock. D. Map; block *i*, bounded by concentric and radiating fractures, subsides.

of the ring-dike before it was cut out. In some cases, an arcuate block may be isolated by two circular and two radial fractures (block *i* of Fig. 236D). Subsidence of such a block, accom-

panied by the intrusion of magma, would form an arcuate ring-dike with blunt ends.

The ring-fracture itself is undoubtedly tensional in origin. According to one hypothesis, the magmatic pressure in the reservoir may at times become less than the pressure exerted by the roof. Under such conditions, the tension is relieved by the formation of outward-dipping fractures.<sup>17</sup> Any block that becomes completely isolated by fractures, will sink into the lighter magma below. According to this same hypothesis, cone sheets form when the magmatic pressure increases to such an extent that it exceeds the strength of the roof and causes shear fractures. In the Tertiary igneous complexes of western Scotland, ring-dikes and cone sheets are characteristically associated.

According to a second hypothesis, the ring-fractures may be in the nature of cylindrical extension fractures, resulting from the upward pressure of the magma.

### Batholiths and stocks

The term *batholith*, because it was originally defined rather vaguely, has been used in subsequent years in different ways by various geologists. In 1885, Suess described batholiths as large igneous bodies which were intrusive into the surrounding rocks, and which had the form of large, irregular loaves of bread.<sup>18</sup> Almost any large intrusive would fit such a definition, and for many years geologists used the term in this broad sense. In 1895 Suess said: "We should clearly distinguish the expression *batholith*, used for a stock-shaped or shield-shaped mass resulting from complete melting, which with further erosion maintains its cross section or becomes wider into the 'everlasting depths'; and the expression *laccolith*, used for a laterally injected cake, which, with erosion, may at first, of course, become wider, but then disappears."<sup>19</sup> In a still later definition, published in 1909, subsequent to the appearance of Daly's classic studies at Mt.

<sup>17</sup> Anderson, E. M., Tertiary and post-Tertiary geology of Mull, Loch Aline, and Oban; *Memoirs Geological Survey of Scotland*, pp. 11-12, 1924.

<sup>18</sup> Suess, E., *Das Antlitz der Erde*, Band 1. Cf. p. 217. Leipzig: G. Freytag, 1885.

<sup>19</sup> Suess, E., "Einige Bemerkungen über den Mond," *Sitzungsberichte der Mathematisch-Naturwissenschaftlichen Klasse der Kaiserlichen Akademie der Wissenschaften*, Band CIV, Abtheilung I, pp. 21-54; cf. especially pp. 52-54, 1895.

Ascutney, Vermont,<sup>20</sup> he said: "But a renewed examination of the Erzgebirge made in 1893 . . . convinced me of the fact that the contours of these intrusive masses cut through both the strike and the folds in the most uncompromising fashion, much as a white-hot iron thrust through a plank cuts across the grain."<sup>21</sup>

According to Daly,<sup>22</sup> batholiths have the following objective characteristics: (1) they are located in orogenic belts; (2) they

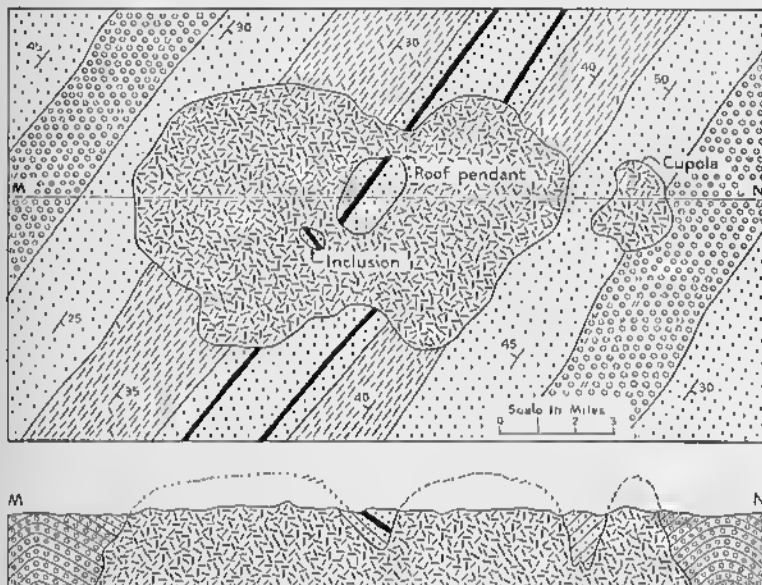


FIG. 237—Batholith. Circles, dots, parallel dashes, and solid black are sedimentary rocks. Diversely oriented dashes are granite. Map is above, structure section is below.

are large, the area exceeding 40 square miles; a body covering less than 40 square miles, but otherwise having the essential features of a batholith, is called a *stock*; (3) they are discordant bodies, crossecutting the structure of the country rock; this is true in both plan and section (Fig. 237); (4) they possess an

<sup>20</sup> Daly, R. A., The geology of Ascutney Mountain, Vermont: *U. S. Geological Survey Bull.* 209, 1903.

<sup>21</sup> Suess, E., *Das Antlitz der Erde, Band 3, Hälftie 2*, p. 633. Leipzig: G. Freytag, 1909.

<sup>22</sup> Daly, R. A., *Igneous Rocks and the Depths of the Earth*, pp. 113-134. New York: McGraw-Hill Book Company, 1933.

irregular, domical roof; *roof pendants* are downward projections of the roof; *cupolas* are upward protrusions from the batholith; (5) the walls are steep, smooth, and dip outward, so that the body enlarges downward; there is no visible or inferable floor; (6) most batholiths are composite, consisting of a number of separate intrusions.

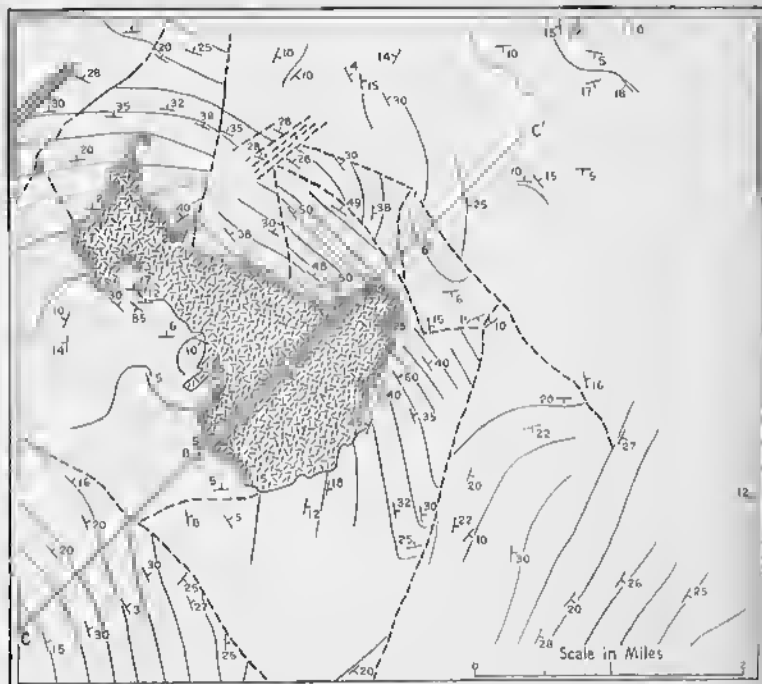


FIG. 238—Map of Marysville Stock, Montana. Diversely oriented dashes are quartz diorite. Rest of area consists of sedimentary rocks. Dip-strike symbols refer to bedding. Light lines are structure contours, contour interval about 500 feet. Heavy broken lines are inferred faults. Heavy solid lines are observed faults. For cross section along line CC', see Fig. 239. (After J. Barrell.)

Most of these principles are illustrated by the pluton at Marysville, Montana,<sup>23</sup> which, because of its relatively small size, should be classified as a stock rather than a batholith (Figs. 238 and 239).

<sup>23</sup> Barrell, J., Geology of the Marysville mining district, Montana: a study of igneous intrusion and contact metamorphism: U. S. Geological Survey Prof. Paper 57, 1907.

Fig. 240, a map of the Castle Peak pluton in the vicinity of the international boundary between British Columbia and Washington, also illustrates the crosscutting nature of stocks.<sup>24</sup>

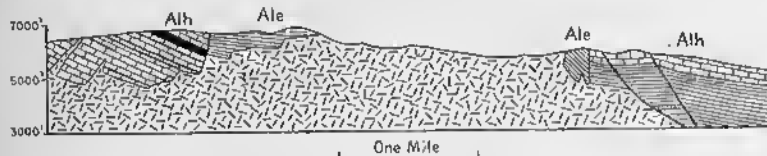


FIG. 239.—Structure Section of Marysville Stock, Montana. Along line CC' of Fig. 238. Diversely oriented dashes are quartz diorite. Ale = Empire shale; Alh = Helena limestone. (After J. Barrell.)

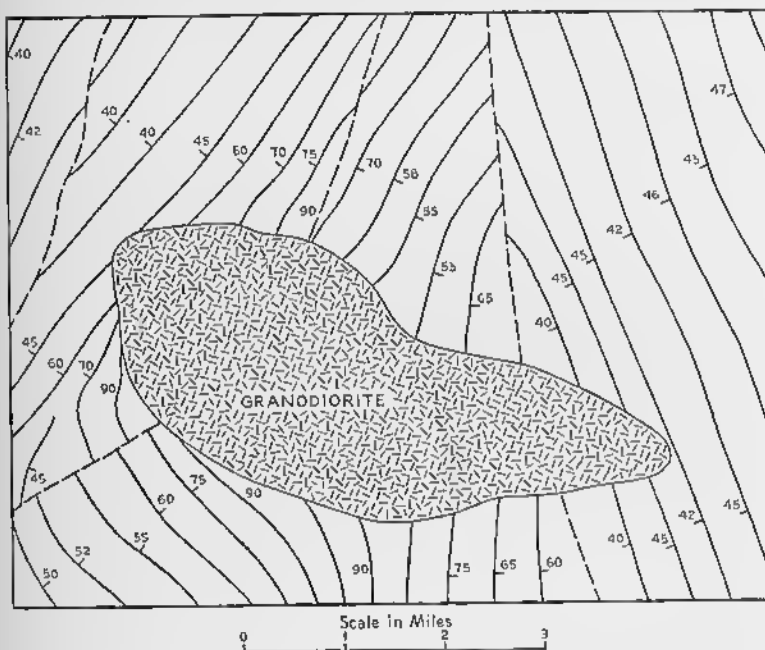


FIG. 240.—Castle Peak Stock, British Columbia. Solid lines indicate attitude of the Pasayten formation; broken lines are faults. (After R. A. Daly.)

Fig. 241 demonstrates clearly the crosscutting nature of the stock at Mt. Ascutney, Vermont, which consists of gabbro-diorite, syenite, and granite.<sup>25</sup> The intrusive not only cuts

<sup>24</sup> Daly, R. A., Geology of the North American Cordillera at the forty-ninth parallel: *Geological Survey of Canada, Memoir 38*, pp. 492-499, 1912.

<sup>25</sup> Chapman, R. W. and C. A., Cauldron subsidence at Ascutney Mountain, Vermont: *Bulletin Geological Society of America*, Vol. 51, pp. 191-212, 1940.

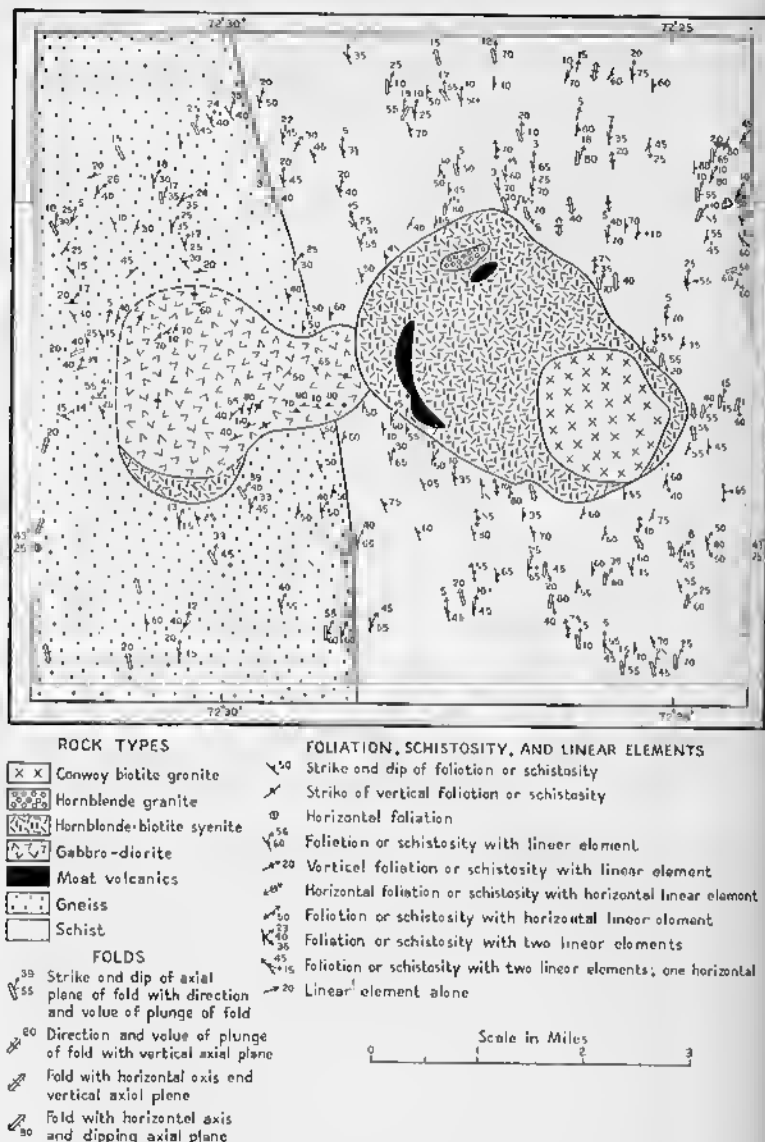


FIG. 241—Composite Stock at Mt. Ascutney, Vermont. (After R. W. and C. A. Chapman.)

across the foliation, but across the axes of the folds also. Moreover, the lineation, which on the average strikes north and dips gently north, is undisturbed by the intrusion.

For many years the tendency was to assume that any large intrusive body was a batholith, unless it was obviously a laccolith or some related form. In recent years, however, it has become apparent that many of the bodies called batholiths actually are great sheets or lenses, and have floors. For such masses the more general term "pluton" should now be used (p. 277).

How do batholiths and stocks form? It is obvious that the magma has not forced its way in, because the older country rock

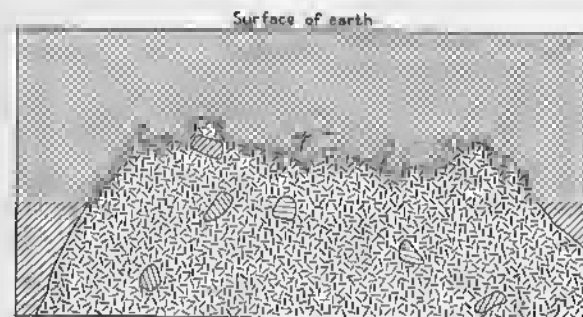


FIG. 242—*Magmatic Stoping*. Diagonal lines are older rocks. Diversely oriented dashes are plutonic rock.

has not been pushed aside; indeed, the older rocks have disappeared (Figs. 237, 238, and 239). The structure of the roof indicates that the older rocks have not been pushed upward and out of the way (Fig. 239). The existing relations are most satisfactorily explained by *magmatic stoping*, a process whereby pieces of the older rocks are ripped off by the magma, and are removed. *Piecemeal stoping*, one variety of the process, is illustrated in Fig. 242. The roof of the magma chamber is shattered, and blocks are surrounded by apophyses. Any block that is isolated by the magma will sink—provided, of course, that the specific gravity of the block is greater than that of the magma. The blocks may sink to great depth, where they may be reacted upon by the magma and assimilated. By this stoping process, the magma can gradually eat its way upward into the country rock. The size of the individual blocks is measured in

feet, tens of feet, or even hundreds of feet. The shattering of the country rock may be due to thermal or mechanical causes. Inasmuch as the country rock is heated by the magma, it expands and cracks, especially if the heating is rapid. Mechanical shattering is probably even more important, because the roof rocks will be subjected to numerous forces, particularly tensional and torsional forces.

In favor of the hypothesis of piecemeal stoping, it is possible to cite examples of the process "caught in the act." Xenoliths and antoliths attest to the actuality of stoping, and at some contacts it is possible to observe apophyses of igneous rock enveloping the country rock (Fig. 242).

On the other hand, xenoliths are surprisingly rare in many batholiths and stocks. Moreover, the specific gravity of the rocks involved must be favorable. In general, the specific gravity of magma is 7 to 10 per cent less than that of the corresponding solid rock. Thus a magma could stop its way into a rock of the same chemical composition. But the specific gravity of gabbro or diorite magma is as high as that of crystalline granite; in such a case piecemeal stoping could not be very effective. Furthermore, many sedimentary rocks have a lower specific gravity than has magma.

Cauldron subsidence differs from piecemeal stoping only in the size of the blocks involved. Whereas in piecemeal stoping the sinking blocks are measured in feet, the blocks involved in cauldron subsidence are measured in miles. The term *ring-fracture stoping* may be used synonymously with *cauldron subsidence*. Underground cauldron subsidence (p. 285) may produce either a ring-dike or a stock, depending upon the amount the central block subsides and upon the depth of erosion. In Fig. 234D, for example, if erosion penetrates to the level *QR*, two ring-dikes will be exposed. If, however, erosion penetrates only to *MN*, a circular intrusive with all the characteristics of a stock will be exposed. The mechanism of cauldron subsidence explains the rarity of small inclusions in many batholiths and stocks. Moreover, this hypothesis is in accord with the smooth walls so typical of batholiths and stocks; piecemeal stoping should produce jagged, irregular walls. Specific gravities, however, would play the same rôle as in piecemeal stoping, and

a subsiding block must be heavier than the magma in the reservoir.

The alkalic batholiths and stocks of New Hampshire are composite complexes made up of ring-dikes and stocks, and they have therefore attained their position in the outer shell of the earth by ring-fracture stoping. Available data indicate that such ring-dike complexes are rather exceptional in orogenic belts. Underground cauldron subsidences may have been important in other batholiths, but the individual subsidences may have been of such magnitude that only stocks, rather than ring-dikes, are exposed.

If the term *batholith* is used in the broader sense of any large igneous body that enlarges downward, other intrusive mechanisms must be considered.

Such bodies may be emplaced by forceful injection. The great mass of magma pushes its way into the older rocks, driving them aside or ahead, in much the same way that salt domes rise (Chapter 14). The intrusion may be entirely due to gravity, the lighter magma rising through older, heavier rocks. In other cases, however, the magma may be pushed around by orogenic forces.

It has recently been proposed that some large igneous bodies, such as the Sierra Nevada pluton of California, are emplaced neither by stoping nor by forceful injection. Rather, the intrusion was "permissive." Potential cavities, resulting from horizontally-directed tectonic forces, are believed to have been filled by magma as rapidly as they formed. It is doubtful, however, whether a body as large as the Sierra Nevada pluton could have formed in such a way.

Some bodies of coarse-grained igneous rock may attain their position by *replacement*. Hot solutions, coming from below, add some elements to the pre-existing rocks, but they subtract others; in this way older sedimentary rocks may be "made over" into granitic rocks.

It may be recalled that, in 1895, Suess assumed that batholiths "resulted from complete melting" (p. 288). In recent years this idea has been advocated for some igneous bodies, and the process of forming a plutonic rock by melting in place has been called *palingenesis*. A rise in the temperature of the outer

shell of the earth might cause melting. Moreover, large bodies of solid rock might be depressed to such great depths by orogenic processes that melting ensued. These rocks, however, would form at such great depths that they could not be exposed by erosion. The products of such melting might rise, and they would then behave as magma. Palingenesis might be aided near the surface of the earth by hot solutions. Replacement granites have never been molten, because the older rocks were replaced atom by atom; the change in chemical composition is considerable. Palingenetic granites were actually molten and, in the simplest case, they have the same chemical composition as the rocks from which they were derived.

In the present state of our knowledge it is impossible to evaluate the relative importance of the various mechanisms outlined above. Although many geologists have strong opinions on the subject, they often fail to realize that their personal experience may be limited, and that if they were to conduct research in other areas, they might reach different conclusions. In many cases, furthermore, the opinions are based on scanty and inadequate field work. The problem of the mechanics of emplacement of large plutons is a challenge to geology, and only by careful and assiduous field studies can correct solutions be obtained.

#### Time of Intrusion

For many years geologists have known that the intrusion of large plutons may be associated with orogenic movements. *Atectonic plutons* are those which are unrelated to orogenic movements and which are found in horizontal strata. *Pre-tectonic plutons* are those that are older than a period of folding; they may be genetically related to the orogeny, or they may be much older and may bear no genetic relation to the orogeny. *Syn-tectonic* or *synchronous plutons* are emplaced during the orogeny. *Post-tectonic* or *subsequent plutons* are later than the orogeny; they may be genetically related to the folding, or they may be much later and may bear no genetic relation to the folding. The situation is complicated, of course, if there has been more than one period of folding in the region. In such a case, an igneous body could be post-tectonic relative to the first orogeny,

but pre-tectonic relative to the second. The ensuing discussion applies, therefore, to a region in which there has been only one period of folding.

Post-tectonic intrusions are undeformed, the associated dikes and sills are not folded, the rocks are not granulated, and they do not have a secondary foliation (p. 213). All ring-dike complexes and true batholiths are post-tectonic, because stoping is not likely to occur in regions which are subjected to compressive forces.

Syntectonic and pre-tectonic intrusions are more difficult to distinguish from each other. The rocks in each are likely to be *granulated*; that is, the individual crystals are broken, strained, and rounded, with the result that the rock has a sugary texture. This is particularly true along the contacts, where most of the strain is concentrated. Apophyses of such intrusions will be folded. Syntectonic intrusives are always forcefully injected bodies, because the magma was moving under the influence of orogenic pressures; some replacement may have occurred in association with these processes. Syntectonic intrusions generally have the form of great sheets or lenses, or perhaps even of "domes." Primary foliation is characteristic. Such bodies may cut across some of the older thrust faults, but may themselves be broken by later thrust faults.

Igneous rocks that lie unconformably beneath highly folded sedimentary rocks, are obviously older than the deposition of the overlying sedimentary rocks; hence they are older than the orogeny. Such igneous rocks are pre-tectonic—at least relative to the orogeny that has been impressed upon the sedimentary rocks.

## Granite Tectonics

### Introduction

Geologists have discovered during the last two decades that many of the structural features in a pluton may be genetically related to one another. In many instances the foliation, lineation, joints, dikes, and faults are expressions of the movement of the magma, and, if systematically studied, they contribute valuable data concerning the history of the intrusion. This field of geology, called *granite tectonics*, was initially developed by a German geologist, Hans Cloos. The most complete treatments in English are by two of his former students, Robert Balk<sup>1</sup> and Ernst Cloos.<sup>2</sup>

If the magma attains its destination before crystallization begins, it will be massive and will possess neither foliation nor lineation. Some of the schlieren and inclusions, however, may be oriented in the manner discussed below.

If the magma is crystallizing as it moves, and especially if the movement continues until after the rock is completely consolidated, a series of structural features develops. Even after the magma in the outer and upper parts of the intrusion has frozen, the liquid or semi-liquid material below may continue to rise, subjecting the consolidated parts of the intrusion to systematic stresses. For convenience, the structures may be considered under the following headings: (1) structures of the flow stage; (2) structures of the transition stage; and (3) structures of the solid stage.

---

<sup>1</sup> Balk, R., *Structural Behavior of Igneous Rocks*. Geological Society of America, Memoir 5, 1937.

<sup>2</sup> Cloos, E., The application of recent structural methods in the interpretation of the crystalline rocks of Maryland: *Maryland Geological Survey*, Vol. 13, pp. 27-105; cf. especially pp. 27-49, 1937.

### Structures of the Flow Stage

#### Movement of magma

Moving liquids are characterized by either turbulent flow or lamellar flow. In *turbulent flow*, the movement of the individual particles is irregular and unsystematic, and the particles are not confined to any one layer in the liquid. In *lamellar flow*, on the other hand, the individual particles move in parallel sheets which slide over one another like the cards in a sheared playing pack. In such a viscous substance as magma beneath the surface of the earth, the flow is lamellar. The sheets tend to be parallel to nearby contacts, and at such localities the differential speed of the various layers will be much greater than in the interior of the body of the magma.

#### Platy flow structure

*Platy flow structure*, also referred to as *planar flow structure* or *planar structure*, forms during the flow stage. Any platy

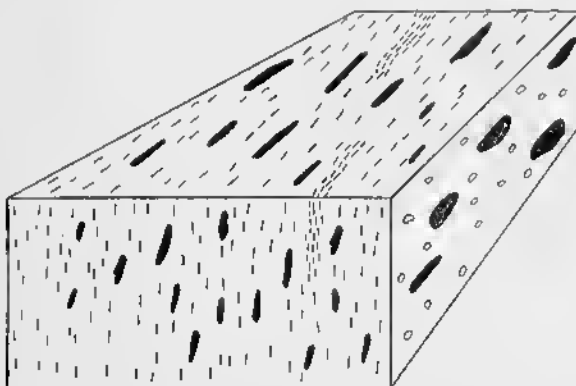


FIG. 243—Platy Flow Structure in an Intrusive Rock.  
Shown by parallel arrangement of platy inclusions (solid black), platy minerals (short dashes, except on side of block, where they appear circular), and schlieren (closely spaced dashes).

material immersed in a magma characterized by lamellar flow, tends to become oriented with the largest face parallel to the liquid layers. Consequently, platy inclusions, such as slabs of shale, sandstone, or schist, become oriented parallel to one

another. Schlieren and platy minerals, such as biotite, align themselves in the same way. Feldspar crystals, if well-formed, will tend to lie with the largest faces parallel to the layers. Prismatic minerals—those shaped like a short pencil—also become oriented so that the long axis lies in the flow layers. If inclusions, schlieren, and platy minerals are all present, they will ordinarily be parallel to one another, as shown by Fig. 243. *Primary foliation* is that variety of platy flow structure that is due to the parallelism of platy minerals. Platly flow structure is thus a more inclusive term, because it refers to the parallelism of slab-like inclusions and schlieren as well as to the parallelism of platy minerals.

#### Linear flow structure

*Linear flow structure*, also called *linear structure* and *lineation*, is also formed during the flow stage. The long axes of prismatic

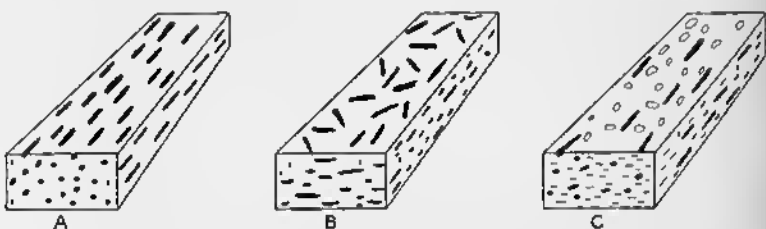


FIG. 244—Linear Flow Structure. Solid black is a prismatic mineral, such as hornblende; dashes and circles represent a platy mineral, such as mica. A. Linear flow structure due to parallelism of crystals of a prismatic mineral; no platy flow structure. B. Platly flow structure due to orientation of crystals of a prismatic mineral parallel to the top of the block; no linear flow structure. C. Linear flow structure, due to parallelism of crystals of a prismatic mineral, associated with a platy flow structure, due to parallelism of a platy mineral.

minerals may be oriented parallel to one another (Fig. 244A). This is particularly true of a mineral such as hornblende, the longest dimension of which is ordinarily parallel to the *c*-crystallographic axis. Feldspar is also longer parallel to the *c*-crystallographic axis than it is in any other direction.

Fig. 244A is an example of a rock with lineation, but with no platy flow structure; such a rock would break into rods parallel to the lineation. Fig. 244B is an example of a rock composed, at least in part, of prismatic minerals; it also possesses

platy flow structure, but has no lineation. It would break into sheets parallel to the top of the block. Fig. 244C is a rock that possesses both lineation and platy flow structure; it would break into sheets parallel to the top of the block.

On surfaces that are parallel to the lineation, such as the top or side of the block (Fig. 244), the long dimension of the mineral is quite apparent. On a surface at right angles to the lineation, however, prismatic minerals appear to be equidimensional (Fig. 244A and 244C). A more tabular mineral, such as feldspar, lies with the long and intermediate axes parallel to the platy flow structure; even in sections perpendicular to the lineation, the tabular habit is apparent.

The manner of measuring the attitude of lineation and of recording it on a map has been described on p. 222.

The long axes of spindle-shaped inclusions may also be parallel to one another, thus showing the lineation. In some cases, although the individual inclusions are more or less spherical, they may be strung out in lines, like the beads on a string.

It is often assumed that the lineation indicates the direction in which the magma was flowing. Vertical lineation would, under such circumstances, indicate a vertically-rising magma, whereas a horizontal lineation would indicate horizontally-flowing magma. In applying these ideas, however, two points should be emphasized. It is obviously essential to distinguish primary lineation from secondary lineation—that is, to distinguish linear features formed during the liquid or semiliquid stage from those formed when the rock was solid. Many attempts to apply granite tectonics to specific areas have led to erroneous conclusions, because secondary lineation was assumed to be primary. This problem is discussed on p. 311. Secondly, even if the lineation is primary, it is not necessarily parallel to the direction in which the magma flows. Although some attempts have been made to study this subject under laboratory conditions, our information on the subject is not complete. In general, however, it is probably safe to assume that primary lineation is parallel to the magmatic flow. If a viscous substance is squeezed through a tube, the long axes of any needle-like particles become oriented parallel to the tube. Moreover, as is shown below, inferences concerning the direction

of movement may also be made from the fracture pattern; in many instances these inferences confirm the results obtained by assuming that the movement of the magma is parallel to the lineation.

### Structures of the Transition Stage

#### Condition of magma

When the magma is nearly consolidated, and when only a small percentage of it is still liquid, special structures, unlike those formed in the flow and solid stages, may develop. These structures include flexures and shears, the latter occupied by pegmatite or coarse granite.

#### Flexures

Planar flow structures may be thrown into flexures by additional flowage. These flexures (*fo* of Fig. 247) are analogous to drag folds, because they are due to sheets of rocks slipping past each other. Moreover, these flexures may be used to determine

the relative motion in the same way that drag folds may be employed. Apparently, such flexures are not extensively developed, because they have been recorded in comparatively few localities. Such flexures are believed to have formed during the transition stage, because the rocks must have been still plastic.

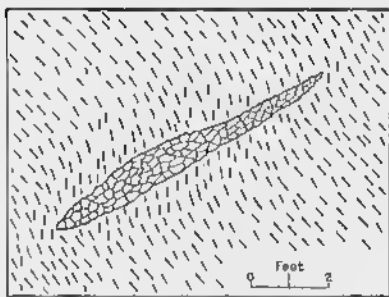


FIG. 245—Shear Filled with Pegmatite. Short dashes represent primary platy flour structure—that is, a primary foliation. Granular pattern is pegmatite or coarse granite.

Flowage becomes increasingly difficult as the magma consolidates, and eventually failure by rupture occurs. The planar flow structures may be broken by small shears (Fig. 245), into which some of the liquid still remaining in the rock may concentrate. This material is rich in the late-crystallizing constituents of the magma, and hence will form light colored minerals. The abundant gases tend to make the minerals coarser than they are

#### Granite-filled shears

Flowage becomes increasingly difficult as the magma con-

in the main body of the rock; moreover, the boundaries of this material are vague. Such granite-filled shears are important in demonstrating that the foliation is primary and not secondary.

### Structures of the Solid Stage

#### Condition of magma

After the outer shell of the intrusion has completely consolidated, the interior may still be liquid or partially liquid. Continued movement of this interior will subject the consolidated shell to stresses that are systematically related to the structures formed in the flow stage. But the solid rock fails by rupture. In the early stages of the intrusion, the contact of the magma with the wall rock was not only a lithologic boundary, but also a dynamic boundary. Liquid magma was moving past solid rock. As the wall rock became heated and the outer shell of the intrusion consolidated, the contact became less important as a dynamic boundary. The wall rock began to participate in the movements; consequently, many of the fractures of the solid stage extend out into the country rock.

#### Cross joints

*Cross joints*, also known as *Q-joints*, are essentially perpendicular to the linear structure (Figs. 246 and 247). Regardless of its precise origin, the lineation is parallel to the direction of maximum elongation in the rock. Any tension cracks would obviously form at right angles to the elongation. The cross joints are thus tensional in origin. Where the lineation is vertical, the cross joints are horizontal; cross joints associated with a horizontal lineation that strikes north, would strike east and would have a vertical dip. Cross joints may be barren; some are coated with hydrothermal minerals such as chlorite, muscovite, quartz, pyrite, and fluorite; some are occupied by quartz veins, pegmatites, or other kinds of dikes.

#### Longitudinal joints

*Longitudinal joints*, also called *S-joints*, are steep and strike parallel to the lineation (Fig. 246). They are best developed

where the linear structures have low plunges. If a horizontal lineation strikes north, the longitudinal joints would strike north and would have a steep dip. According to Balk, they are rougher than the cross joints, and the coatings of hydrothermal minerals are thinner. In many instances the longitudinal joints are clearly related to the intrusion of the magma, because they are occupied by aplite, pegmatite, and other kinds of dikes.

The origin is not clearly understood. The lineation is a direction of weakness, parallel to which later fractures might tend to develop.

#### Diagonal joints

*Diagonal joints* are steep; they strike approximately 45 degrees to the strike of the lineation (Fig. 246). If a horizontal linear structure strikes east, the diagonal joints are essentially vertical, striking northwest and northeast. They may be barren, have a thin coating of hydrothermal minerals, or be intruded by dikes.

Diagonal joints are interpreted as shear fractures. The lineation is parallel to the maximum elongation of the rock mass. According to the principles discussed on p. 106, shear fractures form at approximately 45 degrees to the elongation.

#### Marginal fissures

After the margin of the intrusive has consolidated, the liquid interior may continue to push upward. The marginal rocks are subjected to a couple; in accordance with the principles set forth on p. 103, tension cracks dipping 45 degrees into the intrusive develop. These are known as *marginal fissures* (Figs. 246 and 247).

#### Primary flat-lying joints

*Primary flat-lying joints* have low dips and, like other primary fractures, may be barren, coated with hydrothermal minerals, or occupied by aplite, pegmatite, or other dikes. Where barren, they may be difficult to distinguish from sheeting.

These fractures probably form when the magmatic pressure decreases. As has been shown on p. 103, laboratory specimens

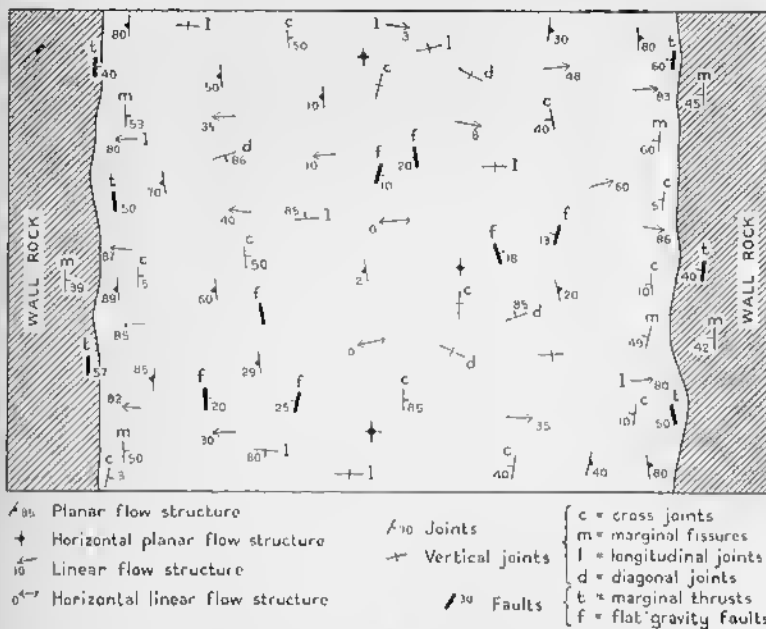


FIG. 246—Map of a Hypothetical Pluton.

subjected to compression under high confining pressure may develop fractures perpendicular to the axis of compression after the compressive force has been released. Similar fractures might develop when the magmatic pressure is lowered.

### Flat-lying gravity faults

*Flat-lying gravity faults*, also called *planes of stretching*, have low dips, and the displacements are of the gravity type (Fig. 247). They strike more or less at right angles to the trend of the lineation (Fig. 246). Such faults indicate lengthening of the rock mass, due to horizontal stretching of the consolidated rocks caused by the upward pressure of the still-liquid magma below.

### Marginal thrusts

*Marginal thrusts*, also called *marginal upthrusts*, are found along the borders of large intrusives, into which they dip at angles of 20 to 45 degrees (Fig. 247). Although barren in

places, they are elsewhere occupied by quartz veins, or by aplite, pegmatite, and other kinds of dikes. Flow layers, inclusions, and even the contact of the intrusive with the country rock are displaced along these fractures, the hanging wall having moved upward relative to the footwall. Initially, the fracture is apparently a marginal fissure. Subsequently, as the upper part of the intrusive is expanding laterally, these marginal fissures are utilized for thrusting.

### Relation of Structures to Each Other

The structures described above are developed with various degrees of perfection in different intrusive bodies. In some plutons, particularly those composed of massive rocks, these structures are rare; in others, many of them are well developed, but all are seldom found in a single body. Moreover, if present, their perfection differs greatly throughout the pluton.

Fig. 247 illustrates the relation of the structures to one another in a hypothetical pluton that has steep walls and a broadly-arched roof. The planar flow structures, controlled by platy minerals (short parallel lines), inclusions (*i*), and schlieren (not shown), form a great arch, the axis of which is perpendicular to the plane of the paper. The lineation, also represented by the short dashes, lies in the plane of the paper. Where the contact of the intrusion is vertical, the planar and linear flow structures are steep, but near the roof they are horizontal.

Some of the planar flow structures have been thrown into flexures (*fo*) by the upward movement of the magma. Moreover, before the rock had completely crystallized, small shears (*sh*) developed, and residual liquid drained into them.

After the outer shell of the intrusive had consolidated, it began to fail by rupture. Cross joints (*c*) developed because of the elongation of the rock parallel to the lineation; marginal fissures (*m*) formed because of couples near the contacts. In a dome, such as that illustrated in Fig. 247, the cross joints and marginal fissures together make a great "fan." Flat-lying gravity faults (*f*) developed because of stretching of the roof. The longitudinal joints are not shown in the illustration, because they are parallel to the plane of the paper.

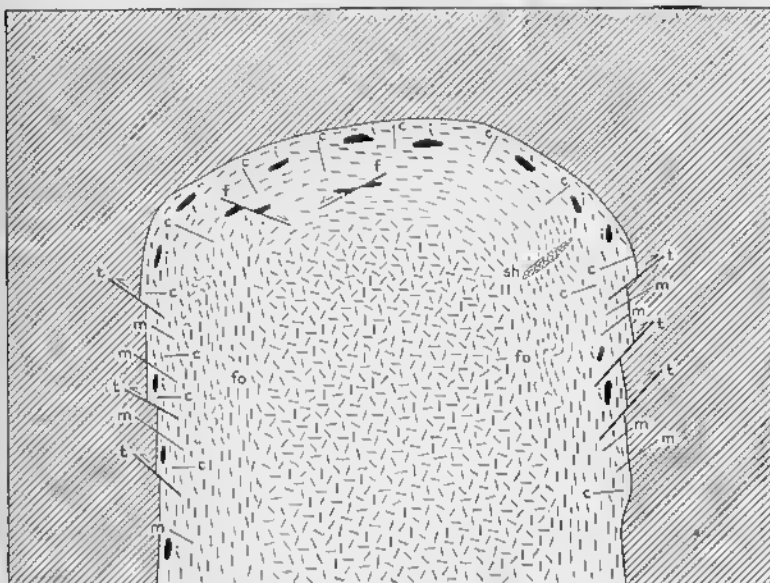


FIG. 247—Cross Section of a Hypothetical Pluton. Section is parallel to strike of the linear flow structures. Short dashes are platy minerals; *i* = inclusion; *fo* = flexure; *sh* = shear filled with pegmatite or coarse granite; *c* = cross joint; *m* = marginal fissure; *t* = marginal thrust; *f* = flat-lying gravity fault.

### Distinction between Primary and Secondary Structures

#### Problem

A clear distinction between primary and secondary planar and linear structures is essential for a correct interpretation of the tectonics of plutons. The distinction becomes particularly difficult if primary structures are utilized for later secondary movements.

#### Planar structures

Several criteria may be particularly useful in demonstrating that a planar structure—particularly a foliation—is primary. In regions unaffected by orogenic movements, any foliation in an igneous rock must be primary, because the forces essential for the development of secondary structures never existed. A second line of evidence is based on the attitude of inclusions.

A foliation to which the inclusions are parallel (Fig. 248A), is probably primary. If a secondary foliation were imposed upon a rock with diversely oriented inclusions (Fig. 248B), the long axes of the inclusions would be unrelated to the foliation. In the example illustrated by Fig. 248A, the flat inclusions must have been oriented while the host rock was still molten; obviously, they would lie parallel to the foliation of the igneous rocks, because the platy minerals and the slab-like inclusions are oriented by the same forces.

Two exceptions to the use of these criteria may be mentioned. In one case, platy inclusions might be oriented during

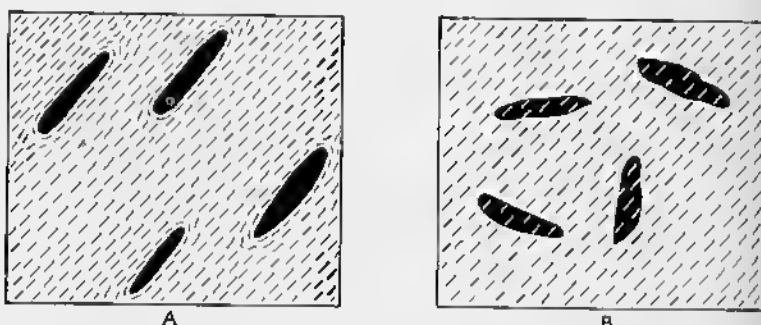


FIG. 248—Relation of Inclusions to Foliation. Solid black = platy inclusions; black and white short dashes = foliation due to platy minerals. A. Platy inclusions parallel to primary foliation. B. Platy inclusions, diversely oriented, cut by a secondary foliation.

the flow stage, but a foliation might fail to develop in the intrusive rock. During a later orogenic movement, a secondary foliation superimposed on the igneous rock might coincide with the oriented inclusions. In this example, the orientation of the inclusions would be primary, but the foliation would be secondary. In a second case, the "stretching" during the formation of a secondary foliation could be so great that inclusions, regardless of their original orientation, might be elongated to such an extent that they become parallel to one another and to the secondary foliation.

A third line of evidence that the foliation is primary has been mentioned (p. 302), and is illustrated in Fig. 245. The foliation is flexed, but along the axis of the flexure a dike-like body, rich in the lighter colored minerals, grades into the main body of

the rock; the material in the dike was derived from the liquid that was still uncrystallized in the rock.

### Lineation

In regions unaffected by orogeny, lineation in igneous rocks must be primary. The orientation of hornblende needles in a

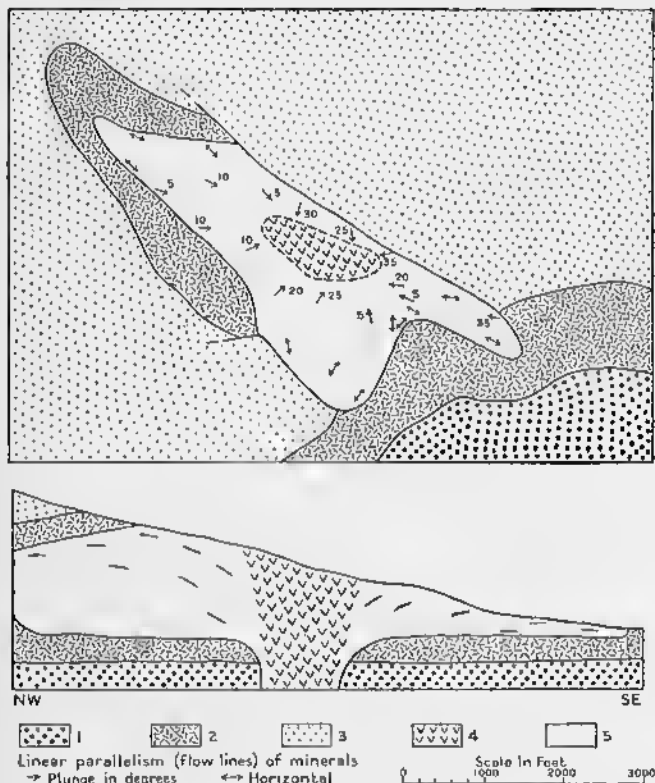


FIG. 219—Deer Creek Laccolith. Map is above, northwest-southeast cross section is below. 1 = early basic breccia, 2 = early basalt sheets, 3 = late basic breccia, 4 = decayed quartz diorite porphyry, 5 = quartz diorite porphyry. (After J. T. Rouse.)

dike, sill, or laccolith injected into flat sediments is primary (Fig. 249).<sup>3</sup> In orogenic belts, on the other hand, a clear distinction between primary and secondary lineation may be very

<sup>3</sup> Rouse, J. T., The structure, inclusions, and alteration of the Deer Creek intrusive, Wyoming: *American Journal of Science*, Vol. 26, pp. 139-146, 1933.

difficult. If the lineation is obviously due to the granulation and dragging out of older minerals, it is presumably secondary. On the other hand, if the minerals in the igneous rock appear to be unstrained and ungranulated, the lineation may be primary; but the recrystallization of a highly-granulated rock is a possibility that would have to be considered. Structural petrology may in some instances offer a solution to the problem (Chapter 18). In general, no hard and fast rules can be established, and each case must be considered by itself.

### Criticism

Granite tectonics has contributed greatly to the understanding of plutons. The mapping of igneous bodies has been revolutionized by the introduction of this technique. Many data that were formerly neglected or were only casually noted are now carefully recorded on field maps. Moreover, granite tectonics attempts to co-ordinate many facts, and to interpret them in terms of a single dynamic process.

The interpretation given to joints by the students of granite tectonics has been criticized. It has been pointed out that the possible sets of joints are so numerous and varied that any chance fracture would fit the system. This is particularly true if it is realized that every pluton has some joints that are classified as "anomalous." Any chance joint could be assigned to a place in this "unbeatable system." For example, let us assume that magma consolidates to form an unjointed rock. Many geologic periods later, it may be subjected to regional forces, with the result that a large number of joints develop. Many of these joints would by chance be parallel to some one of the various joint systems of granite tectonics. The unsuspecting geologist, studying such a pluton, would relate many of the joints to the period of intrusion.

This criticism is, in part, justified. But a close connection between rupture and igneous activity is implied wherever hydrothermal minerals, aplite, pegmatite, or other dikes occupy the fractures. Even in such cases, however, the possibility of later magmatic cycles must be considered.

Students of granite tectonics should always make a clear distinction between primary and secondary structures. A

secondary foliation, due to later compressive forces acting on solid rocks, has often been used as if it were primary. A secondary lineation may, in like manner, be confused with a primary lineation. In some areas, a secondary lineation has been interpreted as if it were primary. Buddington believes that most of the lineation in the Adirondack Mountains is secondary rather than primary.<sup>4</sup>

Regardless of the difficulties involved, the methods of granite tectonics should be applied to as many plutons as possible, particularly in regions where no subsequent deformation has complicated the problem. Each pluton should be considered as an independent problem, because no two plutons will be exactly alike. All data must be faithfully recorded, and the subjective element must be eliminated.

### Bearing on Mechanics of Intrusion

As a result of their observations, many students of granite tectonics have argued that all plutons are forcefully injected, and that magmatic stoping is unimportant. They state that an analysis of many intrusions, such as that shown diagrammatically in Fig. 247, indicates upward-moving magma. The great arch shown by the planar structures, as well as fan structure of the cross joints and marginal fissures, indicates upward movement. The attitude of the inclusions shows that they too have participated in this upward movement; there is no opportunity for downward stoping. Moreover, lateral expansion of the upper part of the intrusive, as indicated by the marginal thrusts and flat gravity faults, is a process not in harmony with the concept of a magma rising quietly by magmatic stoping. According to the students of granite tectonics, the magma rises as a viscous mass, pushing ahead or aside whatever older rocks may be in the way. The rise of the magma may be solely under the influence of gravity, the lighter magma rising through heavier, older rocks; in other instances orogenic forces may play an important rôle in pushing the magma around.

These deductions are undoubtedly correct for many plutons. It is fallacious to assume, however, that there is only one way

<sup>4</sup> Buddington, A. F., Adirondack Igneous Rocks and Their Metamorphism: *Geological Society of America, Memoir 7*, pp. 305-333, 1939.

in which igneous rocks can be emplaced. Cauldron subsidence and piecemeal stoping are of unquestioned importance in some localities. What factors control the mechanics of intrusion is a problem for the future. Undoubtedly, the time of intrusion relative to mountain building is significant; the physical condition of the country rock, and the depth beneath the surface of the earth are important.

## 17

# Extrusive Igneous Rocks

### Introduction

In considering extrusive igneous rocks, the exact limits of structural geology are particularly difficult to define. The petrography and chemistry of these rocks is primarily the concern of the petrologist. The geomorphic forms assumed at the time of eruption are of interest to the physiographer. All phases of the subject fall within the domain of the volcanologist.<sup>1</sup> The structural geologist is interested, however, because volcanic masses contribute to the architecture of the earth. In some instances, moreover, folds, joints, and faults are intimately related to volcanic processes. In this book, therefore, the emphasis will be placed upon the structures resulting from extrusive igneous activity, but nothing will be said about the mineralogy, texture, or chemistry. Some nonstructural material must be introduced, however, in order to present the proper background.

The fundamental units resulting from extrusive igneous activity are lava flows and pyroclastic beds. A large number of these units are usually associated to constitute volcanoes, which result from central eruptions, and volcanic plateaus and plains, which generally result from fissure eruptions.

### Lava Flows

#### Characteristics of lava flows

Lava flows develop when magma wells out at the surface of the earth in a relatively quiet fashion, with little or no explosive activity. Lava flows are tabular igneous bodies, thin compared to their horizontal extent. The attitude corresponds in a

---

<sup>1</sup> Tyrrell, G. W., *Volcanoes*. London: Thornton Butterworth, 1931.

general way to that of the surface upon which they are erupted; on flat plains, the lava flows are more or less horizontal, but, on the slopes of volcanoes, they may consolidate with a considerable inclination.

The surface of a lava flow is never smooth, but is covered by irregularities of different magnitudes. *Pahoehoe lava* has a ropy top. *Aa lava* consists of irregular blocks that are covered with small spines. *Block lava* is composed of irregular blocks that lack spines. In general, pahoehoe and aa lavas are typical of basalts, whereas block lava is typical of siliceous igneous rocks.

*Tumuli* (singular, *tumulus*), also called *Schollendome* and *lava blisters*, are low domical hills 20 to 60 feet long and 5 to 10 feet high. An open fracture, parallel to the long axis of the uplift, is not uncommon, and ropy masses of lava may issue from this crack. Some geologists believe that tumuli are due to the hydrostatic pressure of fluid lava beneath the crust of a gently-dipping flow. Others believe that tumuli are caused by gigantic gas bubbles trapped beneath the crust of the lava.

*Pressure ridges* are long sharp ridges, many of which are broken by a central crack. In a flow in New Mexico, the shortest pressure ridge is said to be 130 feet long, but some pressure ridges are more than 1200 feet long; they are 10 to 25 feet high and as much as 100 feet wide.<sup>2</sup> Some pressure ridges are due to a compressive force imparted to the crust of a lava flow by the viscous drag of slowly-moving subcrustal lava. Those cited from New Mexico are considered to be due to the collapse of the crust of a lava flow that was initially domical in cross section.

*Squeeze-ups*, small excrescences a few feet or tens of feet long on the surface of a flow, are due to the extrusion of viscous lava through an opening in the solidified crust. They may be bulbous or linear in form. *Dribble cones*, also called *spatter cones*, form if sufficient gas is present to cause rapid effervescence of the magma; they may be as much as 25 feet high and have steep walls. The successive layers of lava overlap one another in much the same way as does the accumulated wax on the sides

<sup>2</sup> Nichols, R. L., Pressure ridges and collapse depressions on the McCarty's basalt flow, New Mexico: *Transactions American Geophysical Union*, pt. 3, pp. 432-433, 1939.



PLATE XVIII. Cinder Cone, Composed of Cinders of Basalt, near Flagstaff, Arizona. (Photo by R. L. Nichols.)



PLATE XIX. Obsidian Lava Flow, Paulina Mountains, Oregon. This view faces northeast toward East Lake, beyond which are the walls of the caldera. The obsidian flow, characterized by wave-like block ridges, came from a vent to the right. Height of front of flow is 115 feet. (Photo by R. L. Nichols.)

of a partly-burned candle. Lava flows that were very viscous at the time of eruption, may possess concentric wave-like block ridges (Plate XIX).<sup>3</sup>

*Lava tunnels*, as the name implies, are long caverns beneath the surface of a lava flow; in exceptional cases they may be 12 miles long.<sup>4</sup> They are due to the withdrawal of magma from an otherwise solidified flow. Tunnels may be partially or completely filled with pyroelastic material or sediments that wash in through small fissures.

Depressions, circular or elliptical, are found on the surface of lava flows. Many depressions are due to the collapse of the roofs of lava tunnels. In a lava flow in New Mexico, the largest *collapse depression* is nearly a mile long and 300 feet wide, whereas the smallest is only a few feet across; one is 28 feet deep.<sup>5</sup>

A single flow may consist of several *flow units*.<sup>6</sup> Lava may flow in a series of spurts rather than at a constant velocity. A few hours or days after the advance guard of the lava has ceased to move and has consolidated, more liquid from the same flow may bury the part that has already stopped. This process may be repeated several times, and what is to all intents and purposes a single eruption, is actually composed of several flow units.

Individual flows differ greatly in size. Some are only a few feet thick; flows more than 300 feet thick are rare. The average thickness in the Columbia Plateaus of the northwestern United States is probably less than 50 feet; in India the average thickness of basaltic flows is less than 60 feet; in Iceland the average flow is 15 to 30 feet thick. The area may be a few acres or many square miles. In Iceland, single flows covering over 100 square miles are known, and one flow is said to cover 400 square miles.

#### Criteria for distinguishing lava flows from sills

Lava flows and sills are tabular bodies of igneous rock that are parallel to the bedding of the overlying and underlying forma-

<sup>3</sup> Williams, H., Newberry volcano of central Oregon: *Bulletin Geological Society of America*, Vol. 48, pp. 253-304, 1935.

<sup>4</sup> Stearns, H. T., Volcanism in the Mud Lake area, Idaho: *American Journal Science*, 5th series, Vol. 11, pp. 353-363, 1926.

<sup>5</sup> Nichols, R. L., *op. cit.*

<sup>6</sup> Nichols, R. L., Flow-units in basalt: *Journal of Geology*, Vol. 44, pp. 617-630, 1936.

tions. It is essential, therefore, to establish criteria by means of which the two may be distinguished. These criteria are based primarily on the fact that sills are younger than the rocks above and below, whereas lava flows, although younger than the underlying rocks, are older than those above.

The essential differences between flows and sills are illustrated by Fig. 250. A sill (Fig. 250B) is characterized by a relatively smooth, fine-grained top, in which vesicles (gas bubbles) are rare. In particular, the overlying rocks may be penetrated by apophyses of the sill, and they may occur as inclusions in the sill.

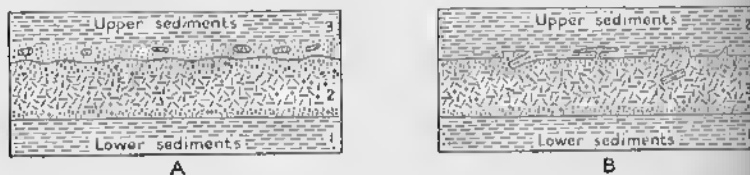


FIG. 250—Criteria for Distinguishing Sill from a Flow. Diversely oriented dashes represent igneous rock; black dots are gas bubbles. A. Lava flow. B. Sill.

A lava flow (Fig. 250A), on the other hand, has a rolling, vesicular top. In particular, fragments of the lava may occur in the overlying rocks. Lava flows are likely to be cut by irregular dikes of sedimentary or pyroclastic material, representing debris washed into cracks in the lava. Moreover, if they are present, all the characteristics of lava flows described above are diagnostic. In many instances the evidence may not be clear, and assiduous search may be necessary in order to find critical data.

### Pyroclastic Beds

Pyroclastic rocks, volcanic in origin, are composed of fragments that range in size from a fraction of an inch to many feet.<sup>7</sup> Some fragments are composed entirely or partially of volcanic glass, thrown into the air as liquid, that hardened before it hit the ground or shortly thereafter. Some fragments are individual crystals which were floating in the magma when the eruption began, or which were phenocrysts in the wall rock of the

<sup>7</sup> Wentworth, C. K., and Williams, H., The classification and terminology of the pyroclastic rocks: *Bulletin National Research Council*, No. 89, pp. 19-53, 1932.

volcanic pipe. Some fragments are composed of older volcanic rocks, either glassy or fine-grained, that were ripped from the sides of the volcanic vent. Still other fragments have been derived from the country rock through which the magma erupted.

Uncemented pyroclastic detritus is classified, on the basis of size and origin, into dust, ash, lapilli, cinders, blocks, and bombs. *Volcanic dust* consists of uncemented pyroclastic fragments that are mostly less than 0.25 mm. in diameter. *Volcanic ash* consists of uncemented pyroclastic fragments that are mostly 0.25 to 4.0 mm. in diameter. *Lapilli* are uncemented pyroclastic fragments that are mostly 4 to 32 mm. in diameter; if the fragments are vesicular and glassy, they are called *cinders*. *Blocks* are fragments, usually angular and larger than 32 mm. in diameter, that were ejected in a solid state. *Bombs* are ejected as plastic magmatic material and have forms (in many instances that of a spindle) acquired during flight through the air. They are larger than 4 mm. in diameter. Material of similar shape and origin, but less than 4 mm. in diameter, is classified as *ash* or *dust*.

Indurated (cemented) pyroclastic material is classified into tuff, tuff-breccia, breccia, volcanic conglomerate, and agglomerate. *Tuff* is composed primarily of material less than 4 mm. in diameter. *Breccia*, more precisely called *volcanic breccia*, is composed chiefly of angular fragments larger than 4 mm. in diameter. If much of the matrix of such material is less than 4 mm. in diameter, the term *tuff-breccia* may be applied. *Agglomerate* is composed of rounded or subangular fragments, larger than 4 mm. in diameter, set in a finer matrix. The round or semi-round shape of the fragments is not due to the action of running water; it may be original or it may result from constant churning in the volcanic pipe, and from the consequent attrition of the fragments. A *vent agglomerate* is the variety that is confined to a volcanic vent. *Volcanic conglomerate* is similar to breccia, but the fragments are rounded by the action of running water.

The material thrown high into the air during an eruption may stay where it settles, thus forming rocks which, because of variations in the size of the fragments ejected at different times,

are stratified. Sometimes *nueés ardentes*, which are masses of fragmental rock charged with interstitial gas, speed down the mountain slope as great avalanches. In 1902, such hot clouds killed 28,000 persons at the foot of Mt. Pelée, Martinique.<sup>8</sup> The rock deposited by such a cloud is an unstratified tuff or breccia. Sometimes, because of torrential rains, the pyroclastic material resting on the mountain slopes becomes saturated with water, and moves as a *mud flow*. The consolidated rock is a typical breccia or tuff which may be difficult to distinguish from one deposited by *nueés ardentes*. Some of the material erupted from a volcano either falls in standing water or, more commonly, is carried for considerable distances by running water. Under either of these circumstances it becomes stratified like sedimentary rocks. The finer-grained rocks are tuff, the coarser are volcanic conglomerate.

A body of pyroclastic material deposited during a single eruption or phase of an eruption, tends to be tabular in shape; it is relatively thin compared to its lateral extent. A deposit of tuff blown directly from a volcano in one eruption may be only a few inches or a few feet thick, but it may cover hundreds or thousands of square miles. Such a bed may be a great aid in correlation. A bed of breccia that was deposited as a mud flow may have been confined to a valley; consequently, it would be very long compared to its width.

### Fissure Eruptions

In fissure eruptions the lava is extruded through a relatively narrow crack, and flows out on the surface of the earth. The eruption of a whole succession of such flows produces a lava plateau or plain. Although pyroclastic rocks are rare, they may result from violent local explosions. Under favorable conditions, the dikes that served as feeders for the fissure eruptions are exposed by erosion.

Several of the great lava plateaus of the world have been constructed primarily by fissure eruptions. This is true of the Columbia Plateau of the northwestern United States, and of western India, South Africa, South America, and the North

---

<sup>8</sup> La Croix, A., *La Montagne Pelée et ses Éruptions*. Paris: Masson et Cie, 1904.

Atlantic volcanic field, remnants of which are found in Great Britain, Iceland, and Greenland. In each of the plateaus, which cover tens of thousands of square miles, the total thickness of the volcanics ranges from 3000 to nearly 10,000 feet. Basalts constitute 90 or 95 per cent of the lavas participating in fissure eruptions.

### General Character of Central Eruptions

The major forms that develop at the surface of the earth as a result of central eruptions, although really no more important than fissure eruptions, are more spectacular, partly because of their form and height, partly because of the violence that may attend their activity. These major forms may be classified as volcanoes, craters, and calderas.

## Volcanoes

### General features

*Volcanoes* are bodies of rock built up by the eruption of magma; they rise above their surroundings. Volcanoes may be classified in several different ways, depending upon the emphasis that the investigator wishes to make. A petrographic classification is based upon the lithology. A physiographic classification is based in part upon the stage of erosion. A structural classification is based primarily upon the internal structure of the volcano and, secondarily, upon the map pattern displayed by a number of volcanoes.

### Classification based on internal structure

On the basis of internal structure, volcanoes may be conveniently classified into pyroclastic cones, lava cones, composite cones, volcanic domes, large spines, and compound volcanoes.

The various kinds of cones may be considered first. Such volcanoes are conical in shape, the apex of the cone pointing upward (Fig. 251). A depression, either a crater or caldera (see p. 325), is commonly present at the top of the cone, unless erosion has been so extensive as to destroy it. The slopes of the cone are concave upward, and the steepest slopes, found at the top, are controlled by the angle of repose of the material when it was erupted. Internally, the cones consist of successive

layers, either lava, pyroclastic material, or both; these layers dip outwardly more or less parallel to the slope of the cone.

*Lava cones*, more commonly called *shield volcanoes*, are built chiefly of lava that was very mobile at the time of eruption; they are broad cones with low angles of slope (Fig. 251A).

*Hornitos* are relatively small, steep-sided lava cones constructed by the eruption of great plastic blobs of lava that were too cool to flow (Fig. 251D).

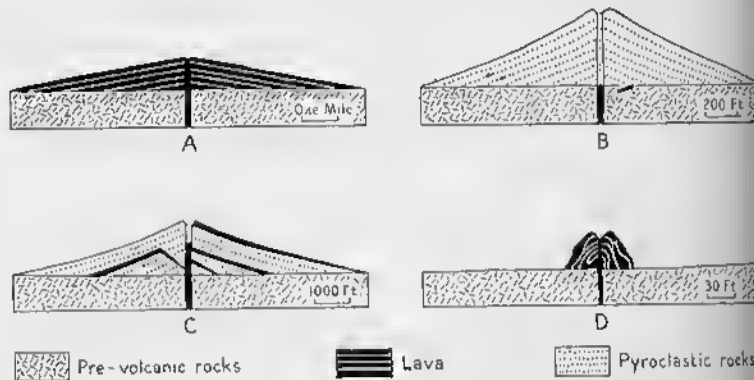


FIG. 251—Volcanic Cones. A. Lava cone. B. Pyroclastic cone. C. Composite cone. D. Hornito.

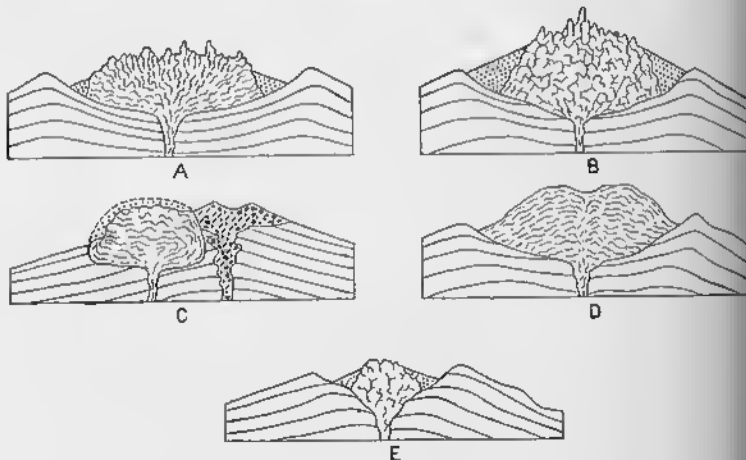


FIG. 252—Internal Structure of Volcanic Domes. A. Fan-structure of flow planes; dots represent talus. B. Dome with crude concentric banding and irregular fissures. C. Endogenous dome on side of a cone. D. Exogenous dome. E. Plug dome, irregularly fissured. (After H. Williams.)

*Pyroclastic cones*, built chiefly of pyroclastic material, may possess very steep upper slopes (Fig. 251B); the variety that is composed chiefly of cinders is called a *cinder cone*.

*Composite cones*, also called *strato-volcanoes*, are built of alternating layers of lava and pyroclastic material (Fig. 251C).

In the simplest type of volcanic cone, the pyroclastic rocks were blown out of the summit crater, from which much of the lava may have issued as overflows. Some of the lava—and in many instances most of it—pours out from fractures on the sides of the mountain. *Adventive* or *parasitic* cones are subsidiary cones on the flanks of a larger volcano.

Volcanic cones differ greatly in size. Small cinder cones and hornitos may be only a few tens of feet high. On the other hand, some great giants tower five or ten thousand feet above the adjacent lowlands, and the base may be many miles in diameter. Some of the largest volcanoes in the San Francisco Mountains of Arizona rise 6000 feet above the Colorado Plateau and contain 33 cubic miles of rock.<sup>9</sup> Mt. Etna, in Sicily, rises 11,000 feet above sea level, and the base is 30 miles in diameter. The great volcanoes of the Hawaiian Islands rise 30,000 feet above the floor of the Pacific Ocean, attaining altitudes of 14,000 feet above the level of the sea.

*Volcanic domes* are steep-sided, bulbous bodies of lava usually so viscous at the time of extrusion that normal flows could not develop (Fig. 252). Many volcanic domes form inside a crater, but this is not always true. The height of domes ranges from a few tens of feet to 2500 feet. Many domes are difficult to study because the surface is covered by a jumble of irregular blocks caused by the rupture of the original dome; this rupture is partly due to thermal contraction of the lava, partly to stresses resulting from extrusion. Moreover, the steep sides of most domes are buried under talus.

*Exogenous domes* are those built by a series of surface eruptions, much in the way that lava cones are constructed. Successive layers of viscous lava are plastered on top of each other. Volcanic domes of this type differ from lava cones by having steeper slopes.

<sup>9</sup> Robinson, H. R., The San Francisco volcanic field, Arizona: U. S. Geological Survey Prof. Paper 76, 1913.

*Endogenous domes* are those that grow primarily by expansion from within (Fig. 253). Some endogenous domes are characterized by concentric shells,<sup>10</sup> but such a structure apparently forms most readily if a slight cover of older rocks overlies the rising magma (Fig. 252C). Most endogenous domes are intensely fissured and brecciated (Fig. 252B).

During the rise of a dome, irregular dikes that are continuously injected into the outer shell may serve as feeders to small surface flows.

FIG. 253—Dome Formed by Squeezing Viscous Material Through a Narrow Opening. (After E. Reyer.)

During the rise of a dome, irregular dikes that are continuously injected into the outer shell may serve as feeders to small surface flows.

gests that such a structure is due to the fact that the earliest lavas spread out from the vent at a low angle, forming a constricting ring that acted as a levee. The later flows, because they were restricted, rose at increasingly high angles.

Any pointed projecting eminence is a *spine*; spines associated with volcanic rocks may range in length from a fraction of an inch to many hundreds of feet. The classic example of a large spine is that of Mt. Pelée, in the West Indies (Fig. 254).<sup>12</sup> Two months after the disastrous eruption of May 8, 1902, a spine was first noted. Successive spines formed during the summer, but each was destroyed by explosions. The most permanent of the spines, which began to rise in October, 1902, reached its greatest height on May 31, 1903, when it was over 1000 feet high; the diameter was approximately 450 feet. Thereafter the spine gradually lost height.

*Compound volcanoes* are those that consist of two or more of the types described above. Thus, a composite volcano that has an associated volcanic dome, either in its crater or on its flanks, would be a compound volcano.

<sup>10</sup> Reyer, E., *Theoretische Geologie*, Fig. 84. Stuttgart: E. Schweizerbart'sche Verlagsbuchhandlung, 1888.

<sup>11</sup> Williams, H., The history and character of volcanic domes: *University of California, Department Geological Sciences Bulletin*, Vol. 21, pp. 51-146, 1932.

<sup>12</sup> La Croix, A., *op. cit.*

### Classification based on grouping of volcanoes

A *volcanic cluster* consists of a group of volcanoes without any apparent systematic arrangement. A *volcanic chain* consists of a group of aligned volcanoes, the arrangement apparently controlled by a single fracture.



FIG. 254—Spine of Mt. Pelée, March 15, 1903. Height 1145 feet.  
(After A. LaCroix.)

### Craters, Caldera, and Related Forms

Many volcanoes are characterized by depressions to which the term *crater* is often loosely applied. The depressions differ, however, in origin, and because a more elaborate terminology is necessary, *crater* should be reserved for one kind of depression.

#### Craters

A *crater* is the normal depression at the top of a volcanic cone, and it is directly above the pipe that feeds the volcano.

A crater, in its simplest form, is a flat-bottomed or pointed, inverted cone more or less circular in horizontal section. Immediately after an eruption, the diameter of the bottom of the crater (probably the same as the diameter of the feeding pipe) is seldom over 1000 feet. Subsequent landslides from the walls, however, may partially fill the bottom of the crater. The walls

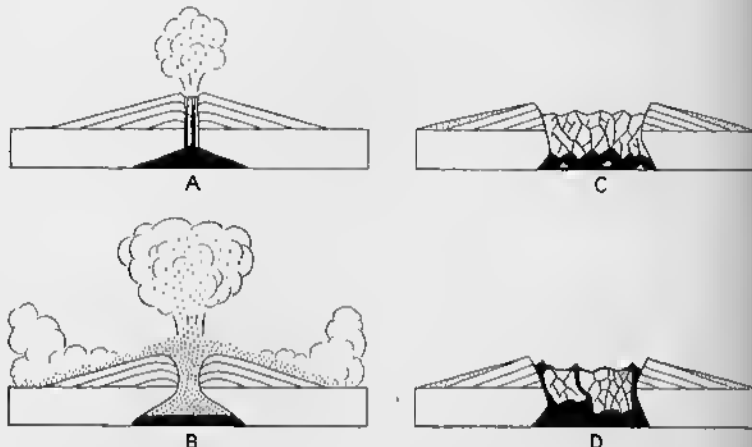


FIG. 255—Collapse Caldera of the Krakatoa Type. A. Mild explosion of pumice. B. Violent explosions: part of pyroclastic material is thrown into air, part rushes down slopes as *nées ardentes*. C. Collapse of the top of the cone. D. Renewed volcanic activity. (After H. Williams.)

of a crater are composed of interbedded lava and pyroclastic rocks, but the ratio of the two depends upon the type of volcano; some crater walls are composed exclusively of lava, others are composed exclusively of pyroclastic material. An unusually strong explosion may blow away part of the crater wall, thus exposing the layers of which the top of the cone is composed.

Craters are primarily due to explosions at the top of the pipe feeding the volcano. Fragmental rocks are blown into the air, and the largest material, landing within some hundreds of feet, builds a circular wall. Whenever magma rises in the pipe, it melts and dissolves whatever may be directly above it; it thus helps to maintain the depression.

*Pit craters*, typically exposed in the Hawaiian Islands, are circular depressions with steep walls. In the Kau district,<sup>13</sup>

<sup>13</sup> Stearns, H. T., and Clark, W. O., Geology and water resources of the Kau district, Hawaii: U. S. Geological Survey Water-Supply Paper 616, pp. 29-194, 1930.

where pit craters range in diameter from 50 feet to nearly a mile, the depth of some is many hundreds of feet. Some are floored by solid lava; those that are occupied by a lake of lava are sometimes called *lava pits*.

Stearns believes that at some place along a crack, the magma works upward by stoping and fluxing to form a more or less cylindrical chamber occupied by magma. After the magma subsides, the roof of the chamber collapses, forming a circular pit. The pit may be widened later by landsliding and circular faulting.

*Maars*, also called *embryonic volcanoes* and *explosion pits*, are flat-floored explosion craters that are either devoid of cones or have very small cones. There is little or no associated magmatic material, because the cones consist largely or entirely of fragments of the country rocks. They have been described from Swabia in Germany, and from Abyssinia.

### Calderas

Following Williams, we may classify all large volcanic depressions as *calderas*.<sup>14</sup> More or less circular in form and miles in diameter, calderas are much larger than the pipe feeding the volcano. Calderas may be classified into three major types: *explosive calderas*, *collapse calderas*, and *erosion calderas*.

*Explosive calderas* are due to a violent explosion that blows out a huge mass of rock. A classic example is Bandai-San in Japan, which blew up within a minute. The volcano had not erupted for more than a thousand years, but on the morning of July 15, 1888, 15 or 20 explosions occurred within little more than a minute. Although much rock was blown into the air, the last explosion, which was horizontal, initiated a great avalanche containing  $1\frac{1}{4}$  cubic kilometers of rock. The summit and much of the northern side of the volcano were blown away, leaving a great amphitheatre  $1\frac{1}{2}$  square miles in area, with walls more than 1200 feet high. No lava appeared, and the cataclysm was caused by a *phreatic explosion*; that is, ground water was converted to steam by volcanic heat until such a great pressure was generated that an explosion ensued.

<sup>14</sup> Williams, H., Calderas and their origin: *University of California, Department Geological Sciences, Bulletin*, Vol. 25, pp. 239-346, 1941.

*Collapse calderas* are most common. The essence of this mechanism is collapse of the superstructure of the volcano because of withdrawal of the underlying support. The details may differ; a single large cylindrical block may sink as a unit, or the collapse may be piecemeal, either during the eruption or immediately thereafter. The collapse may be due to one of several factors, or it may be due to a combination of factors.



FIG. 256—Caldera Due to Withdrawal of Magma by Rissures Far Down on Slope of Mountain. A. Original condition. B. Withdrawal of lava to give flow, *l*, causes collapse and formation of caldera, *c*. (After H. Williams.)

The rapid eruption of great volumes of ash or *pumice*, which is frothy volcanic glass so charged with gas that it floats, may lower the level of the magma in the main reservoir to such an extent that the whole superstructure of the volcano is left unsupported (Fig. 255). Collapse is apparently piecemeal



FIG. 257—Caldera Due to Change in Shape of Reservoir. A. Steep-sided reservoir. B. Reservoir changes shape, followed by collapse. (After H. Williams.)

(Fig. 255C); good examples of this type are Krakatau in the Dutch East Indies, which violently erupted in 1888, and Crater Lake, Oregon. Collapse apparently followed the eruption of the pumice—probably within the hour. In the past, many such calderas have been considered explosive in origin, similar to Bandai-San. If this were the case, however, the erupted material would consist of fragments of older volcanics. But pumice is the chief visible product of such eruptions, indicating the inadequateness of the explosion hypothesis.

Katmai, in Alaska, is a similar type; but collapse and eruption were simultaneous, and vast quantities of the original cone

collapsed into the reservoir, only to be hurled out after being assimilated by the magma.

The rapid outflow of lava from fissures far down on the slopes of the mountain may cause collapse. A volcano may be underlain by a reservoir several miles in diameter. If magma withdrawn from this reservoir by lateral fissures (Fig. 256) is not replenished, the roof is left unsupported. The *volcanic sinks* of Hawaii, exemplified by Kilauea, are of this type.

A change in the shape of the magma reservoir may cause collapse. For example, a steep-sided reservoir may arch the overlying rocks, as in Fig. 257A. If the magma then spreads laterally without being replenished, the roof of the reservoir will collapse (Fig. 257B). This mechanism has been advocated to explain the Morro Caldera of San Luis, Argentina, but, by the very nature of the case, the proof is difficult to establish.

Surface cauldron subsidence, as described on p. 285, must produce calderas. If the collapse is due to the withdrawal of magma, the mechanism is not fundamentally different from the Kilauea type or the Morro type. The mechanism is dissimilar, however, if the initial ring fracture is due to upward pressure of the magma, and if collapse is due to the greater specific gravity of the subsiding block compared to that of the magma.

The origin of the *cryptovolcanic type* of caldera is not entirely clear. Depressions that are considered to be cryptovolcanic in origin are more or less circular, range from 1 to 15 miles in diameter, and are from 200 to 1700 feet deep. Such calderas are located in non-volcanic rocks, and in most instances little or no volcanic material is found in the neighborhood. Perhaps the best known of these is the Ries Basin in southern Germany (Fig. 259).<sup>15</sup> The basin itself is approximately 14 miles in diameter, and is floored by upper Miocene fresh water deposits, beneath which is a tumultuous assemblage of granite, Triassic sedimentary rocks, and Jurassic sedimentary rocks. Surrounding the basin is a zone, several miles wide, of outwardly-driven thrust slices. In still another zone, which is as much as 15 miles wide, rootless slices and isolated blocks of various sizes are common. In the outermost zone, small blocks of limestone are

<sup>15</sup> Bentz, A., "Drehwaagmessungen im Ries bei Nördlingen, Geologische Einführung," Zeitschrift für Geophysik, Band 7, pp. 1-6, 1931.

scattered about. The most commonly accepted interpretation is that a broad laccolith was injected and, aided by a series of explosions, lifted its cover, perhaps more than 1200 feet. The larger thrust blocks are probably due to outward sliding of the cover of the laccolith. Some geologists believe that the caldera itself was caused by a great explosion. It is probably due to a later collapse of the summit of the dome along ring fractures, resulting from loss of gases and from contraction of a cooling rock that had consolidated from magma.

*Erosion calderas* are the result of the enlargement of craters or calderas by erosional processes.

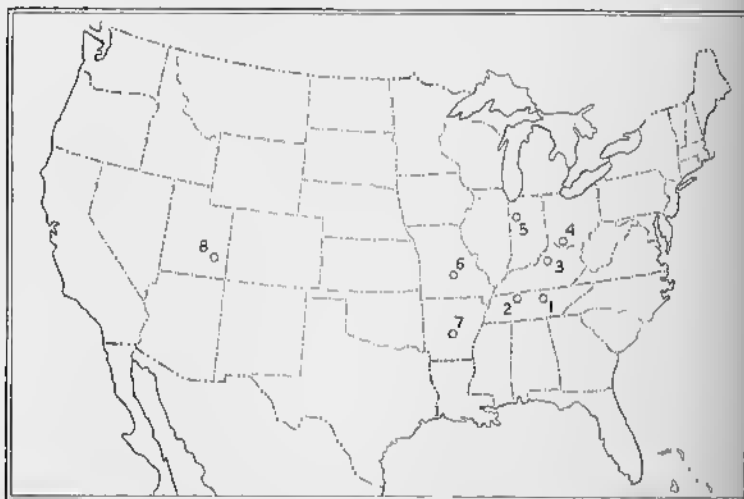


FIG. 258—Location of Cryptovolcanic Structures in the United States.  
1, Flynn Creek disturbance, Tenn.; 2, Wells Creek Basin, Tenn.; 3, deptha Knob, Kentucky; 4, Serpent Mound structure, Ohio; 5, Kentland structure, Indiana; 6, Decaturville structure, Missouri; 7, Magnet Cove, Arkansas; 8, Upheaval dome, Utah. (After Bucher and Wilson.)

### Cryptovolcanic Structures of the United States

A somewhat different type of cryptovolcanic structure is found in the United States (Fig. 258). Some examples of such structures are topographically expressed by hills, others by basins. Ranging from 2 to  $8\frac{1}{2}$  miles in diameter, a central area has been uplifted 350 to 1200 feet. There is characteristically

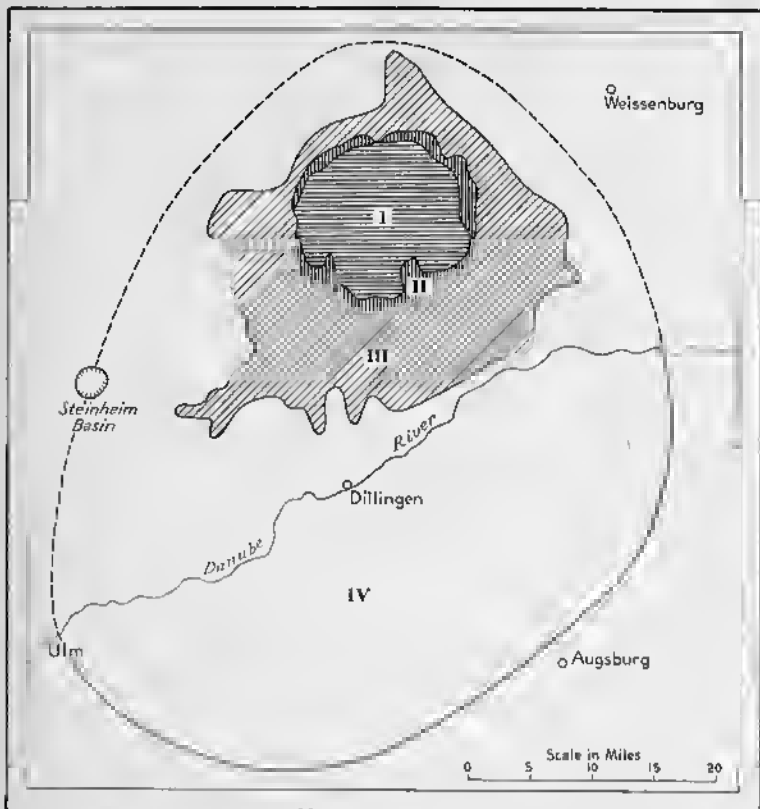


FIG. 259—Cryptovolcanic Type of Caldera. The Ries Basin in Germany. I. Basin, floored by upper Miocene fresh-water deposits. II. Zone of thrust slices. III. Zone of rootless slices. IV. Zone of isolated blocks. (After A. Bentz.)

a circular structural depression surrounding the central uplift. Faults, both radial and peripheral, are common.

Fig. 261, a geologic map of the Wells Creek Basin in Tennessee,<sup>16</sup> is an example of American cryptovolcanic structure. The central domical uplift has carried the lower Ordovician limestones 1000 feet above their normal position. In the surrounding syncline ( $s_1$ ), the Mississippian formations are 300 feet below their normal position. An incomplete circular anticline

<sup>16</sup> Bucher, W. H., Cryptovolcanic structures in the United States: *18th International Geological Congress*, pp. 1055-1084, 1936.

( $a_1$ ) and an outer ring syncline ( $s_2$ ) are still farther from the center. Peripheral, radial, and irregular faults are common.

Bucher believes that cryptovolcanic structures of the United States are due to an explosion caused by the sudden liberation of volcanic gases. Inasmuch as there are no visible volcanic rocks, the term *cryptovolcanic* (*hidden-volcanic*) is used. It is possible, however, that these structures are caused by long continued vertical forces unrelated to volcanism. If this is true, the use of the term *cryptovolcanic* is inadvisable.

### Volcanic Pipe

The central conduit that supplies the magma (Fig. 251) can never be observed, of course, in active volcanoes; but after erosion has removed the superstructure of lava and pyroclastic rocks, the shape and filling of the *pipe* may be observed. Such

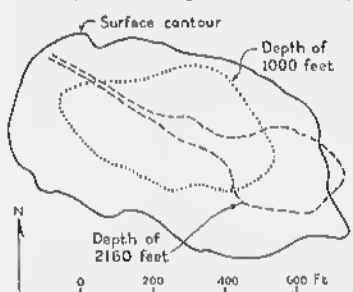
filled pipes are called *vents*, *necks*, and *plugs* (see p. 283). They indicate that the pipe is relatively small and circular, seldom over a few hundred or thousand feet in diameter.

The mechanics of formation of such circular pipes is by no means clear. Some may be localized by the intersection of two fractures. Others, particularly where a number of central eruptions are aligned, may develop along a master fissure that

FIG. 260—Changing Form of Volcanic Vent with Depth, Kimberly Mine, South Africa. Plan of neck at different levels is shown. (After Wagner.)

is locally widened by melting, gas fluxing, stoping, or explosion. Some volcanoes may form directly over cupolas in magma reservoirs. Mining operations in South Africa have demonstrated that volcanic necks pass downward into dikes (Fig. 260).<sup>17</sup> Apparently the magma rose through a fissure, but, when it approached the surface, the gas began to come out of solution with such rapidity that a violent explosion occurred. This was localized at a point of weakness, and a circular hole (*diatreme*) was blown through the crust.

<sup>17</sup> Wagner, P. A., *The Diamond Fields of Southern Africa*. Johannesburg: The Transvaal Leader, 1914.



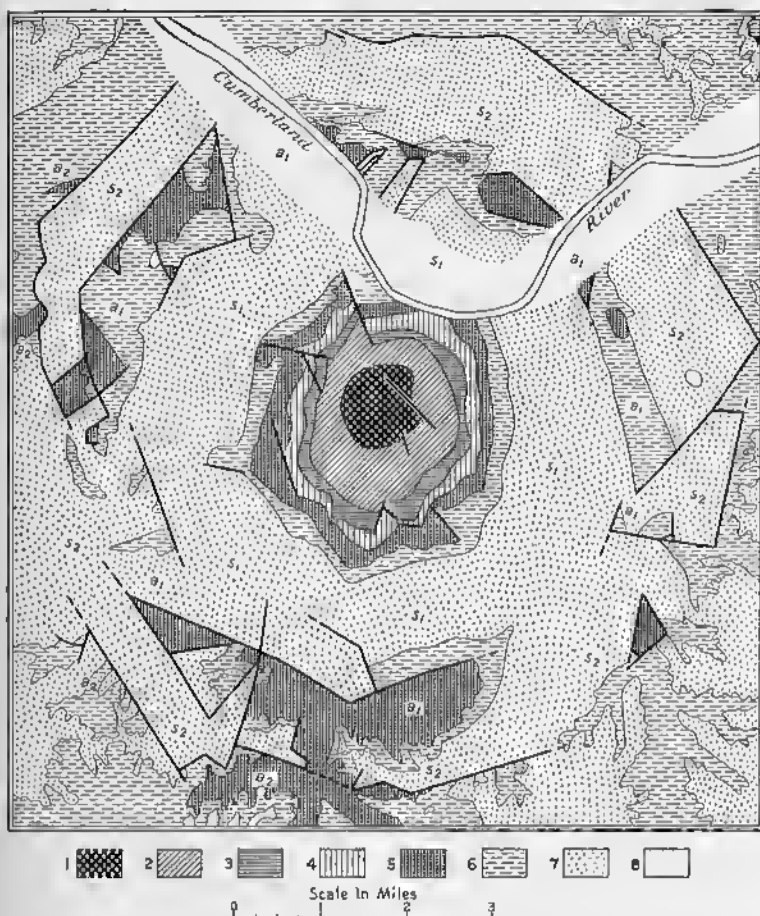


FIG. 261—Geological Map of Wells Creek Basin, Tennessee. 1, lower Ordovician; 2, and 3, middle Ordovician; 4, Silurian and Devonian; 5, lower Mississippian; 6 and 7, middle Mississippian; 8, Quaternary; *s<sub>1</sub>*, inner syncline; *a<sub>1</sub>*, inner anticline; *s<sub>2</sub>*, outer syncline; *a<sub>2</sub>*, outer anticline. Heavy lines are faults. (After W. H. Bucher.)

## Structural Petrology

### Introduction

*Structural petrology* or *petrofabric analysis* is the study of the internal structure of rocks and its relation to the movements involved in their formation or deformation. It may be used to investigate rock deformation as well as the genesis of sedimentary and igneous rocks. *Petrotectonics* is that phase of the subject which deals with the relation existing between the internal structure of deformed rocks and their tectonic history.

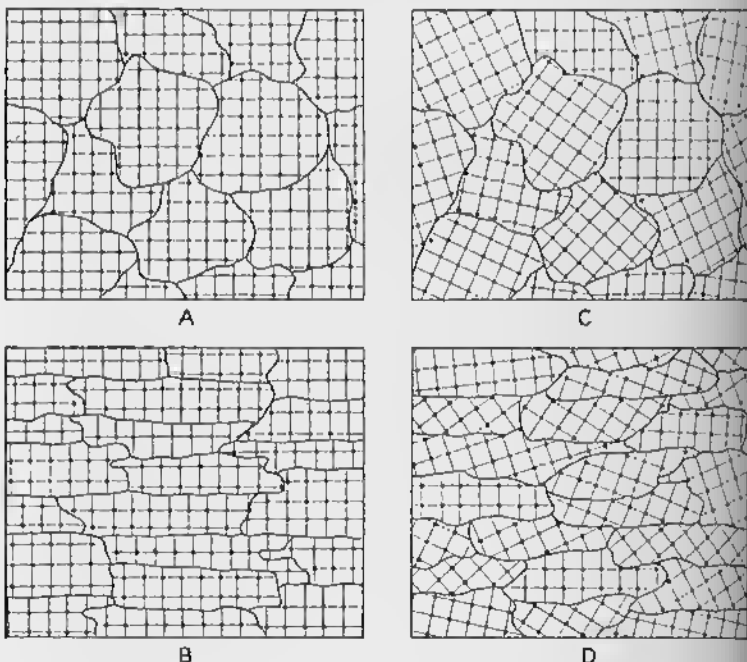


FIG. 262—Diagrammatic Two-dimensional Representation of Preferred Orientation. Dots represent centers of atoms. A. Space lattice orientation, grains equidimensional. B. Space lattice and shape orientation. C. No orientation. D. Shape orientation, but no space lattice orientation.

The fundamental principles of structural petrology were developed by Bruno Sander, an Austrian, and by Walter Schmidt, a German. The most complete treatments in English are by Knopf and Ingerson,<sup>1</sup> and by Fairbairn.<sup>2</sup>

*Structural fabric*, or *fabric*, refers to the arrangement of the units that comprise any kind of external form. The term *fabric* as used in structural petrology has a different meaning than it has in petrography. If many of the grains in a rock composed of mica, quartz, and feldspar are platy or ellipsoidal in habit and lie parallel to one another, the fabric may be described as *foliated* (p. 213). If many of these platy grains are oval in shape, and if the long axes of the ovals tend to lie parallel to one another, the fabric is *linear* as well as *foliated*. On the other hand, although many of the grains may be tabular or ellipsoidal, they may lie in a random orientation, so that the rock, lacking both foliation and lineation, may be described as *isotropic* (Fig. 209A); that is, the properties of the rock are equal in all directions.

The type of fabric just described is controlled by the shape of the individual mineral grains. We may also think of the atoms that comprise the individual minerals. Each mineral species is characterized by its own peculiar arrangement of atoms, usually referred to as the *atomic lattice* or *space lattice* (Fig. 1). In some rocks, the space lattices of all the grains of a single mineral species may have approximately the same orientation. In the diagrams of Fig. 262, which are simple, very diagrammatic, two-dimensional representations of rocks composed of grains of a single mineral species, each dot indicates the center of an atom. In Fig. 262A, the space lattices are parallel. On the other hand, the space lattices may be oriented at random, as represented in Fig. 262C.

In many cases a lattice orientation is associated with a shape orientation (Fig. 262B). But a shape orientation without a space lattice orientation is quite possible. Lenticular grains of quartz may be parallel to one another, but the space lattices may be diversely oriented (Fig. 262D).

<sup>1</sup> Knopf, E. B., and Ingerson, E., *Structural Petrology*, Geological Society of America, Memoir 6, 1938.

<sup>2</sup> Fairbairn, H. W., *Structural Petrology of Deformed Rocks*. Cambridge: Addison-Wesley Press, Inc., 1942.

The structural fabric may be displayed by units of larger size than atoms or minerals. The "stretched pebbles" in a deformed conglomerate may lie with the long axes parallel to one another, thus giving a distinctive fabric (Fig. 182A).

If, regardless whether they are pebbles, minerals, or atoms, the units tend to be oriented in a particular direction, the fabric shows a *preferred orientation*. In Figs. 262A and 262B, the space lattice shows a preferred orientation; in Figs. 262B and 262D, the grains show a preferred orientation according to shape. In contrast to a preferred orientation, we may speak of a *random orientation*.

In many instances, the preferred orientation may be so well marked that there is no doubt of its existence. Obviously,

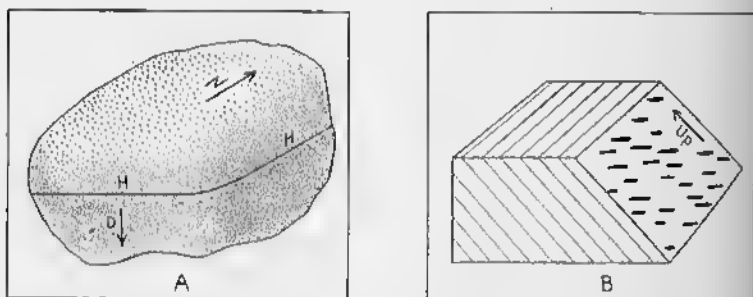


FIG. 263—Methods of Labeling Specimens in Field. A. Completely labeled. B. Partially labeled; attitude of foliation (parallel lines) and lineation (dark streaks) have been measured in the field.

there are all transitions from random orientation to a well-marked preferred orientation. By means of the statistical analysis applied in petrofabric analysis, it is possible to express quantitatively the degree of preferred orientation.

The essence of structural petrology is that the fabric is the result of the conditions existing at the time the rock formed, and particularly that the fabric of deformed rocks has been controlled by differential movements. The fabric of an igneous rock that crystallizes quietly from stationary molten magma will be different from that of an igneous rock that crystallizes from flowing magma. The fabric of a sediment quietly deposited at the bottom of a body of water will be different from that of a rock that has been involved in strong differential movements. The aim of that phase of structural petrology known as *petro-*

*tectonics* is to determine the number of periods of deformation and the nature of the differential movements during the deformation.

### Field Technique

Inasmuch as one of the aims of structural petrology is to relate the internal structure of the rocks to the larger structural features, a careful field study, conducted by customary field methods, is essential. In particular, such features as foliation, lineation, faults, joints, and all other directional elements in the rock must be measured and recorded on maps.

These field methods are supplemented by structural studies involving the use of the microscope. It is essential, therefore, to collect *oriented specimens* from which thin sections may be cut. An oriented specimen is one whose exact arrangement in space is known; the fabric of the rock may show either a preferred orientation or a random orientation. The dual use of the word *orient*, in one instance referring to the arrangement of the specimen in space and in the other instance referring to the fabric of the rock, is perhaps somewhat confusing. The specimen may be oriented by reference to the geographic co-ordinates. In Fig. 263A, for example, a horizontal plane (*H*), north (*N*), and the down direction (*D*) are all marked. At any subsequent time it is possible to orient the specimen as it was in its natural relations.

A specimen that possesses foliation and lineation, the attitude of which was recorded in the field, can be properly oriented at any subsequent time, provided that the top or bottom of the specimen is indicated (Fig. 263B).

### Laboratory Technique

Thin sections for microscopic study are prepared from the specimens. The sections can be cut in any desired direction, but if only one section is to be prepared, it is usually cut perpendicularly to the schistosity and lineation. It may be necessary to give rather careful instructions to the man making the thin sections.

A conventional system of labeling the thin sections has developed (Fig. 264A); *c* is perpendicular to the plane of schis-

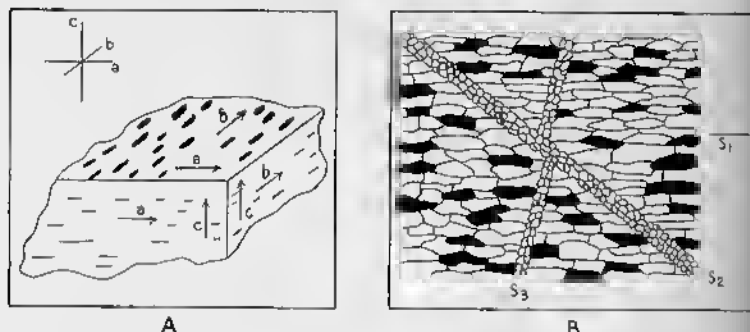


FIG. 264—Labeling Material. A. Conventional system of labeling a specimen that has foliation and lineation;  $c$  is perpendicular to foliation;  $b$  is lineation;  $a$  lies in plane of foliation and is perpendicular to  $b$ . B. Thin section showing three  $S$ -planes. Black = platy dark mineral; white = platy light-colored minerals.

tosity;  $b$ , the direction of lineation as observed in the hand specimen, lies in the plane of schistosity;  $a$  lies in the plane of schistosity and is perpendicular to the lineation. These three axes are thus at right angles to one another. In some cases, which can not be discussed here,  $B$  or  $R$  may be used instead of  $b$ . If two lineations are visible on the schistosity, the more prominent is called  $b$ , whereas the less conspicuous is labeled  $b'$ . If more than one plane of schistosity is present,  $c$  is oriented perpendicularly to the most prominent one. If the rock is

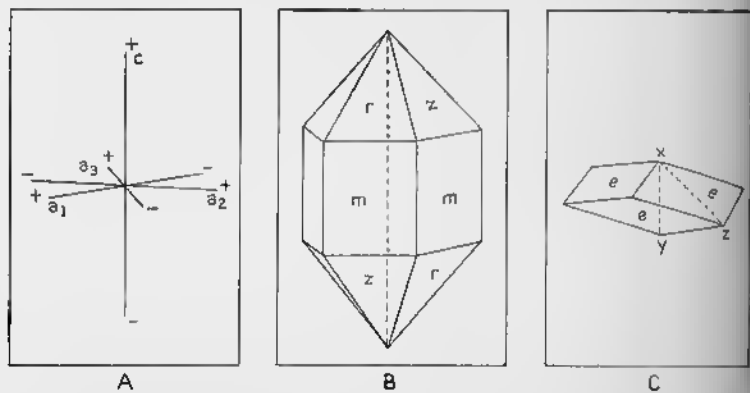


FIG. 265—Hexagonal Minerals. A. Conventional system of designating axes of hexagonal minerals. B. Quartz crystal;  $m$  = unit prism;  $r$  = positive unit rhombohedron;  $z$  = negative unit rhombohedron. Broken line =  $c$ -crystallographic axis = optic axis. C. Calcite crystal;  $e$  = negative rhombohedron;  $xy$  =  $c$ -crystallographic axis = optic axis;  $zz$  = short diagonal of rhombohedron.

massive, lacking both schistosity and lineation, the thin section may be labelled by geographic directions or by some other system.

For convenience, a plane parallel to the schistosity may be referred to as the *ab* plane, because it contains the *a* and *b* axes. The plane perpendicular to the schistosity and lineation is the *ac* plane. The plane perpendicular to the schistosity and parallel to the lineation is the *bc* plane. Each thin section may be similarly labelled according to the two axes that it contains. Ingerson<sup>3</sup> prefers to designate a thin section by the axis that is perpendicular to it; thus the thin section parallel to the schistosity would be the *c-section* in his terminology.

The thin section is first studied by ordinary microscopic methods, and the minerals are determined. Special attention is given to the orientation and abundance of *S-surfaces*, which may be planes of stratification, schistosity, or shear planes. Fig. 264B is an example of a thin section with three *S-surfaces*. The most prominent surface is customarily labelled *S*<sub>1</sub>; the others are designated by arabic numerals in order of their importance.

A *petrofabric diagram* is then prepared from the thin section. Separate diagrams must be prepared, of course, for each mineral species. Quartz, biotite, muscovite, and calcite are most commonly studied. The diagram may be based on any of the following four properties of the mineral: the space lattice, the cleavage, twin lamellae, or the shape of the mineral. Such diagrams are prepared by means of the *Universal Stage*, which is so designed that the thin section, by rotation about three mutually perpendicular axes, may be brought into any desired position. The technique is petrographic in character, and its description is beyond the function of this book. Two excellent discussions are available in English, one by Knopf and Ingerson,<sup>4</sup> the other by Fairbairn.<sup>5</sup> It is possible, however, to understand such diagrams without being familiar with the technique involved in their preparation.

The diagrams that consider the space lattice of the minerals are really based on optical properties. The *optic axis* of a

<sup>3</sup> Knopf, E. B., and Ingerson, E., *op. cit.*, p. 218.

<sup>4</sup> Knopf, E. B., and Ingerson, E., *op. cit.*

<sup>5</sup> Fairbairn, H. W., *op. cit.*

hexagonal mineral such as quartz, for example, is parallel to the *c*-crystallographic axis. Fig. 265B is a drawing of a perfect quartz crystal, the *c*-crystallographic axis of which is shown by the broken line; this is also the optic axis. Although most quartz grains in rocks are spherical, elliptical or irregular, each

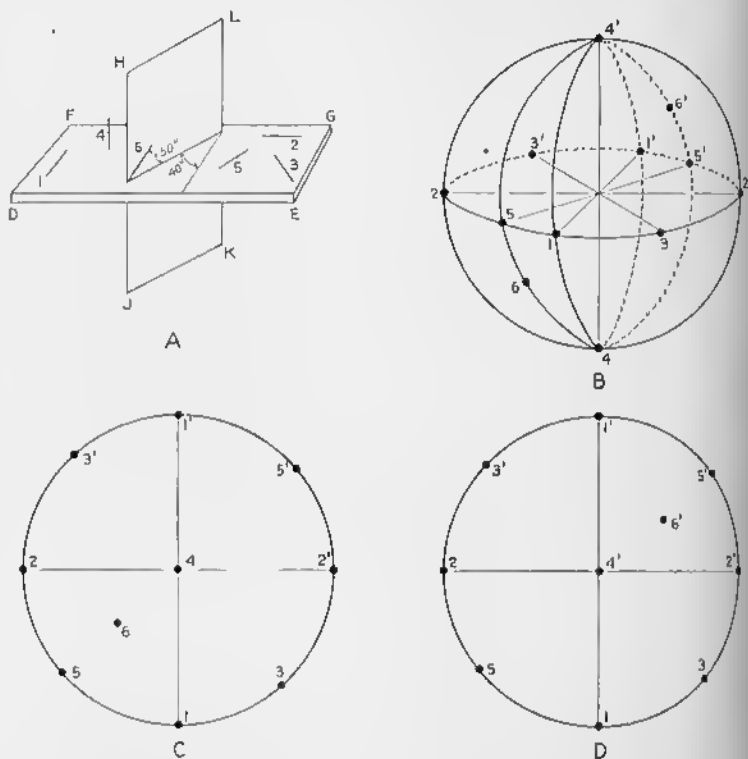


FIG. 266—Meaning of a Point Diagram. A, Thin section is plane *DEFG*; 1, 2, 3, 4, 5, and 6 represent optic axes of six different quartz crystals. B, Sphere showing poles of axes shown in Fig. 266A. C, Projection on to lower hemisphere. D, Projection on to upper hemisphere.

possesses an optic axis. By means of the Universal Stage, the exact orientation of this optic axis relative to the thin section may be determined.

In a thin section, such as that represented by the plane *DEFG* in Fig. 266, one optic axis of quartz might occupy the position 1, lying parallel to the plane of the thin section and parallel to *DF*. Another optic axis might be in the position 2, parallel to the plane of the thin section and parallel to *DE*.

A third is in position 3, lying parallel to the plane of the thin section, but diagonally to the sides. A fourth optic axis, 4, is perpendicular to the plane of the thin section. A fifth optic axis, 5, lying in the plane of the thin section, is diagonal to the sides. A sixth optic axis, 6, is inclined to the plane of the thin section; this is the most general case. This optic axis lies in the vertical plane *HJKL*, which makes an angle of 40 degrees with *DF*; optic axis 6 is inclined 50 degrees to the plane of the thin section.

If each of these grains is imagined to be at the center of a sphere, the optic axis 1 would pierce the sphere at 1 and 1'; (Fig. 266B); optic axis 2 would cut it at 2 and 2'; 3 at 3 and 3'; 4 at 4 and 4'; and 5 at 5 and 5'. The optic axis 6 would pierce the lower, left-hand, front part of the sphere at 6 and the upper, right-hand, back part of the sphere at 6'.

Inasmuch as each optic axis pierces the sphere in two places, all the data may be represented on one hemisphere, the upper or the lower one. For practical reasons, these data are more satisfactorily plotted on a plane surface that is a projection of the sphere. In Fig. 266C, the data of Figs. 266A and 266B have been plotted on the lower hemisphere. Any optic axis that lies parallel to the plane of the thin section intersects the circumference of the circle at two points, and it can be plotted in either of these two positions; ordinarily only one point is plotted, the choice being arbitrary. Optic axis 2 intersects the circle at 2 and 2', and the plot may be made at either of these two points. An optic axis such as 4, which is perpendicular to the plane of the thin section, lies in the center of the circle. An inclined optic axis, such as 6, appears between the center and the circumference. The steeper the angle of inclination, the nearer it will be to the center of the circle.

Fig. 266D shows the same data plotted on the upper hemisphere. For optic axes parallel or perpendicular to the plane of the thin section, this diagram is identical with Fig. 266C. For inclined optic axes, such as 6, however, the position is diagonally across from that in Fig. 266C. Inasmuch as inclined optic axes are the most common, a plot made on one hemisphere will be a mirror image of that made on the other hemisphere—except, perhaps, for optic axes lying on the circumference of the circle, where an arbitrary choice is permissible.

The exact distance that a point, such as 6, appears from the center of the circle, depends not only upon its angle of

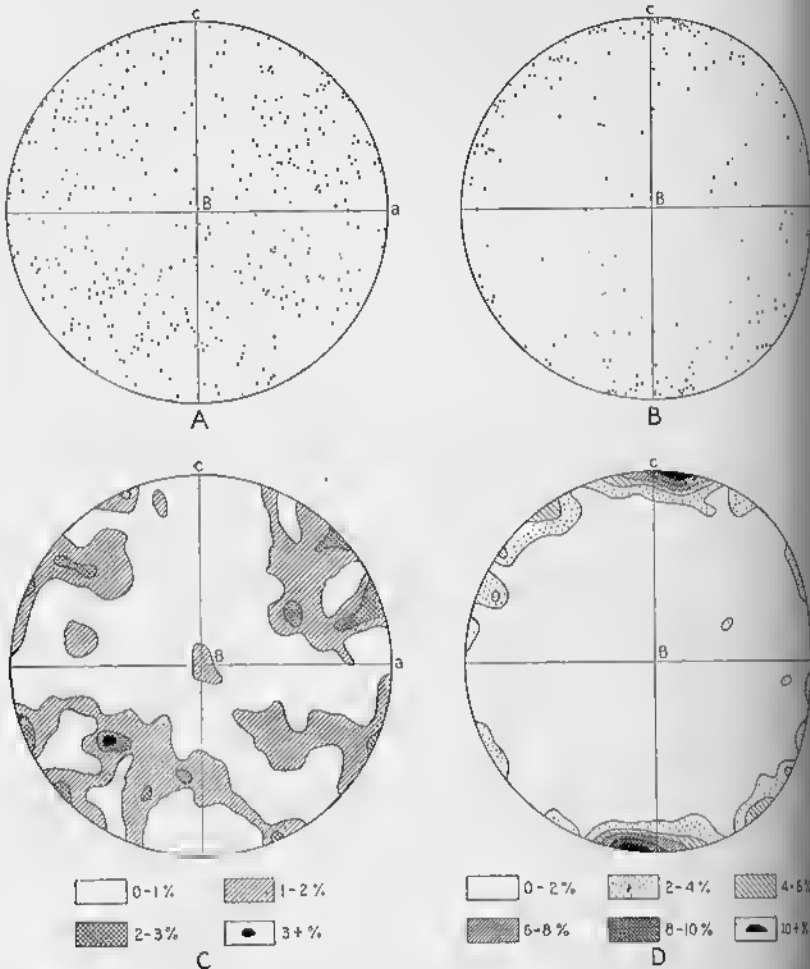


FIG. 267.—Point Diagrams and Contour Diagrams. A. Point diagram, 400 optic axes of quartz from mica schist, Mt. Clough, New Hampshire. B. Point diagram, 200 poles of cleavage of biotite from mica schist, Mt. Clough, New Hampshire. C. Contour diagram of Fig. 267A. D. Contour diagram of Fig. 267B.

inclination relative to the plane of the thin section, but also upon the type of projection used. In structural petrology, the Schmidt equal-area net<sup>6</sup> is used.

<sup>6</sup> Knopf, E. B., and Ingerson, E., *op. cit.*, p. 227.

When all the optic axes have been plotted, the resulting diagram is known as a *point diagram* (see also p. 118). Fig. 267A is an example of a point diagram of the optic axes of quartz.

The optic axis of calcite may be measured and plotted in the same way that the optic axis of quartz is plotted.

The biaxial minerals—those with two optic axes—are more difficult to study. Biotite, however, is so nearly uniaxial, like quartz and calcite, that point diagrams may be readily prepared. Moreover, the optic axes of biotite are essentially perpendicular to its cleavage, a fact that is a great help in orienting the mineral on the universal stage.

Many petrofabric diagrams show the attitude of the cleavage rather than the orientation of the optic axes. Minerals like biotite and muscovite, which have one good cleavage, are easy to study. Calcite, with three cleavages, is more difficult to study. The attitude of a line perpendicular to the cleavage is determined and plotted. The point where the perpendicular to a plane intersects the projection sphere is called the *pole* of that plane. The preparation of point diagrams for the poles of cleavage planes is similar to the method used in making point diagrams for the poles of joints, as described on p. 118. Fig. 267B is a point diagram of the poles of 200 biotite flakes.

In some diagrams, notably those of calcite, the plot may be based on perpendiculars to twin lamellae (see also p. 353).

The number of grains that must be measured and plotted depends upon the degree of the preferred orientation. In some instances 100 grains are adequate, and usually 200 grains will suffice; if 400 grains reveal no evidence of preferred orientation, it is very probable that none exists.

After the point diagrams have been prepared, they may be converted into *contour diagrams* by the method described in pp. 119-121. Fig. 267C shows a contour diagram of the optic axes of quartz; Fig. 267D is a contour diagram of the perpendiculars to the cleavage of biotite.

Each high point on a contour diagram is a *maximum*. Actually, there may be several such high points, so that several *maxima* may exist.

Most petrofabric diagrams are based on only a small percentage of all the grains of a mineral species in a thin section.

A thin section may thus contain several thousand quartz grains, but usually a few hundred are sufficient to indicate whether there is a preferred orientation. Ordinarily, the person preparing the diagram must select the grains at random, and must not make any selection, either conscious or unconscious, of grains of a particular color, size, or shape. A *non-selective diagram* is one prepared by an indiscriminate measurement of grains. A *selective or partial diagram* is one prepared by deliberately choosing grains of a certain size, shape, or position within or outside of shear zones. A *collective diagram* is prepared by making a single diagram from several selective diagrams.

Published diagrams should always contain certain fundamental information, preferably on the diagram itself or in the description directly beneath it. The mineral represented by the diagram and the number of grains measured should always be stated. The *a*, *b* and *c* directions and the contour interval should be indicated. A clear statement should be made, either under the figures or at the start of the paper, whether the projection is on the lower or the upper hemisphere. If no statement

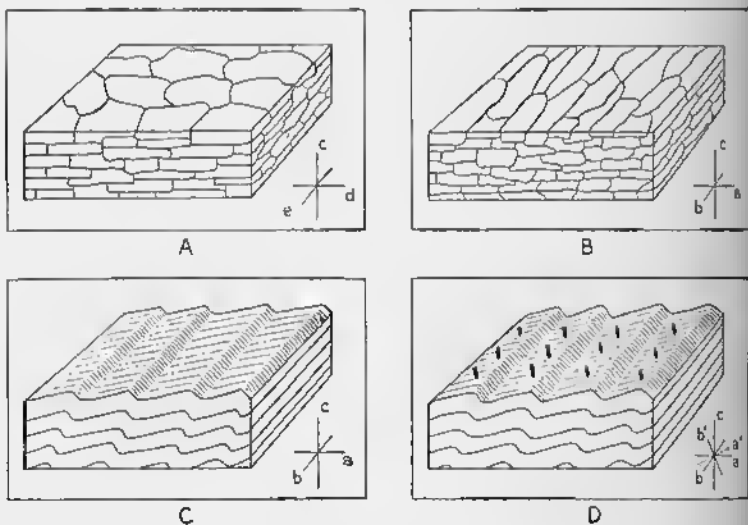


FIG. 268—Symmetry of Hand Specimens. A. Axial Symmetry. B. Orthorhombic Symmetry. C. Monoclinic Symmetry; wavy lines are schistosity. D. Triclinic Symmetry; wavy lines are schistosity; black streaks represent an oval mineral lying in the plane of schistosity.

is made, it may be assumed that the projection is on the lower hemisphere.

### Symmetry of Fabric

The rock fabric may be classified according to its symmetry, in somewhat the same way that minerals may be grouped into systems. In fact, the terminology used to describe the symmetry of rocks has been partially borrowed from mineralogy. It was formerly thought that the symmetry of the rock fabric bore a rather simple and direct relation to the movements in the rock during their formation and deformation. It is now realized, however, that the relation is more complicated than that, and broad generalizations are difficult to make. Each case must be considered individually. Moreover, the symmetry shown by the hand specimen may differ from that revealed by the petrofabric diagram prepared from the thin section. A clear distinction must be made, therefore, between the *megascopic fabric symmetry* and *microscopic fabric symmetry*.

The four kinds of fabric symmetry are: (1) spheroidal, or axial; (2) rhombic, or orthorhombic; (3) monoclinic; and (4) triclinie.

*Spheroidal symmetry (axial symmetry)* is the symmetry of a spheroid, either oblate or prolate. There is an axis of symmetry; that is, the fabric is the same in all directions perpendicular to the axis.

A megaseopic example is a schist that lacks lineation. The fabric is uniform in all directions within the plane of schistosity. In Fig. 268A the grains appear to be equidimensional in a plane parallel to the schistosity. At right angles to the schistosity, parallel to  $c$ , the grains are much shorter. Not only is the plane of schistosity a plane of symmetry, but any plane passing through  $c$  is a plane of symmetry.

Spheroidal symmetry is displayed in a petrofabric diagram by concentration at a point (Fig. 269A). Any diameter of the diagram is a line of symmetry.

*Orthorhombic symmetry (rhombic symmetry)* is the symmetry of an ellipsoid; the three axes are of unequal length. Fig. 268B is a schistose rock with a distinct lineation. If we suppose that each grain is 1 mm. long, 0.5 mm. wide, and 0.1 mm. thick, the

rock will have three planes of symmetry, corresponding to the front, side, and top of the block. But the fabric differs parallel to the three principal axes. In the direction *b*, the grains are 1 mm. long; in the direction *a*, they are 0.5 mm. long; and in the direction *c*, they are 0.1 mm. long.

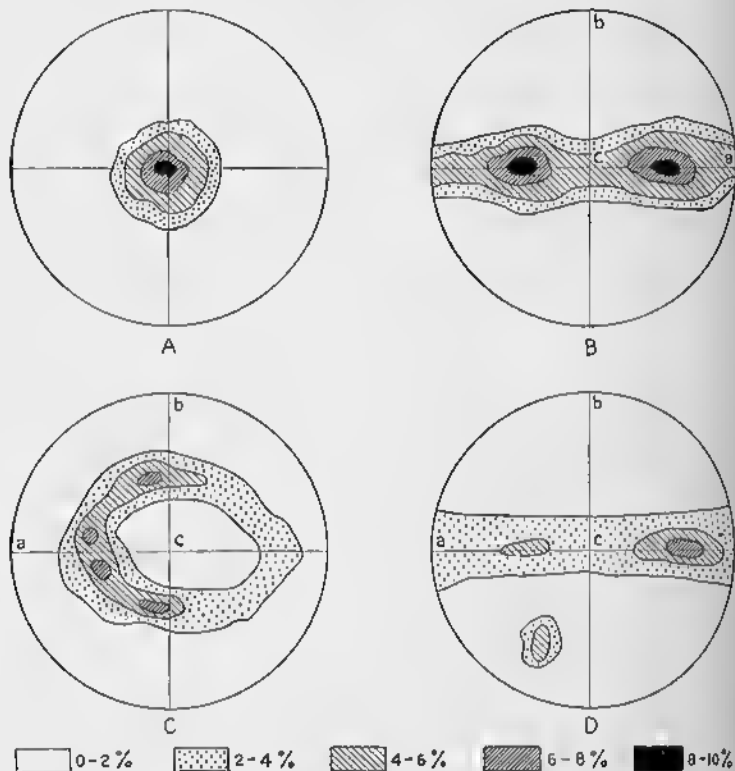


FIG. 269—Symmetry of Petrofabric Diagrams. A. Axial symmetry. B. Orthorhombic symmetry. C. Monoclinic symmetry. D. Triclinic symmetry.

Fig. 269B is a petrofabric diagram showing orthorhombic symmetry. The two principal diameters, *a* and *b*, are lines of symmetry.

*Monoclinic symmetry* is characterized by a single plane of symmetry which is perpendicular to the lineation. Fig. 268C is a metamorphic rock, the schistosity of which has been thrown into tiny asymmetric crinkles. Only the front of the block is a plane of symmetry.

In petrofabric diagrams, monoclinic symmetry is characterized by a single line of symmetry, as in Fig. 269C. This line is usually perpendicular to the *b* fabric axis.

*Triclinic symmetry*, which has no planes of symmetry, is illustrated by Fig. 268D. The schistosity has been thrown into crinkles trending parallel to the side of the block, but in addition there is a lineation that trends diagonally across the top of the block. Fig. 269D is a petrofabric diagram showing triclinic symmetry. There is no line of symmetry in the diagram.

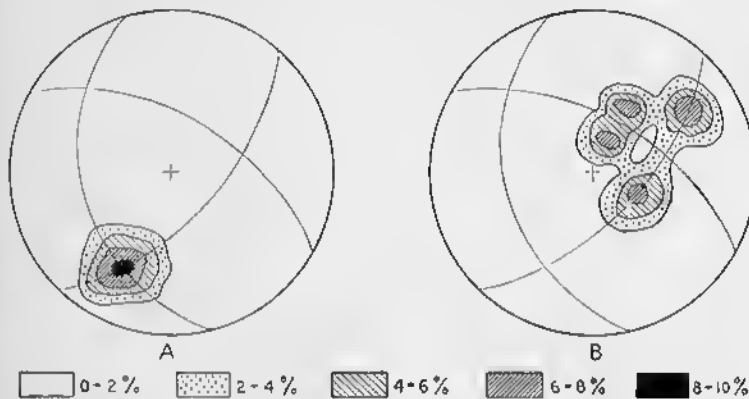


FIG. 270—Eccentric Symmetry Diagrams. A. Axial symmetry. B. Monoclinic symmetry.

The lines of symmetry in the petrofabric diagrams are not necessarily diameters that pass through the center of the circle. Fig. 270A, for example, possesses axial symmetry, whereas the symmetry of Fig. 270B is monoclinic. If the thin section is cut diagonally to the fabric axes *a*, *b*, and *c*, the whole diagram will be eccentric. Ordinarily, thin sections are cut perpendicularly to one of the megascopic fabric axes, because the symmetry is much more readily recognized if the petrofabric diagram is centered.

### Symmetry of Movement

During the formation or deformation of rocks, the individual grains move under the influence of an external force. Detrital sediments settle from stagnant bodies of water under the influence of gravity, or from running water under the combined influence of gravity and the current. In deformed rocks

the individual grains move under the influence of tectonic forces. Each type of movement is characterized by a particular symmetry.

*Axial symmetry of movement* is typified by the settling of sediments from stagnant water. The individual particles move perpendicularly to the surface of the earth under the influence of gravity. Parallel to the surface of the earth, all directions are equal and interchangeable in relation to the movement. The symmetry is that of a spheroid, and it is referable to one axis. The motion involved in the deformation of a sphere into an oblate spheroid under simple compression, is also an example of axial symmetry of motion.

*Orthorhombic symmetry of movement* is exemplified by the motion that occurs when a sphere, subjected to simple compression acting along a vertical line, is constrained on two opposite sides. The sphere would be deformed into an ellipsoid.

*Monoclinic symmetry of movement* occurs when the cards in a playing pack slide past one another because of shear. Each card moves in the same direction relative to the card directly beneath it. The surfaces along which the movement takes place are *slip planes*.

*Triclinic symmetry of movement* may be illustrated by a simple example. Water flowing in a stream between two banks, the frictional effect of which is neglected, might represent monoclinic symmetry of movement. Because of friction the bottom layers move more slowly than the upper layers. Any individual particle of water would move directly downstream, but those near the surface move faster. Irregularities and frictional resistance of the banks, however, may cause eddies about vertical axes; these eddies are superimposed on the downstream movement. Such movement is triclinic in character.

#### Correlation of Fabric Symmetry and Movement Symmetry

One object of structural petrology is to determine the nature of the movement involved in the formation and deformation of rocks. In many instances, the movement symmetry and fabric symmetry may be directly correlated; that is, an axial fabric symmetry may indicate an axial movement symmetry, and a monoclinic fabric symmetry may indicate a monoclinic

movement symmetry. Some simple examples will illustrate this point.

Small mica flakes settling in stagnant water are an example of axial symmetry of movement. These flakes would lie flat on the bottom of the body of water. If a thin section were cut parallel to the bedding, and if a petrofabric diagram were prepared for the normals to the cleavage of the mica, a maximum would appear in the center (Fig. 269A); that is, the diagram would show axial symmetry. Thus, an axial movement results in an axial fabric.

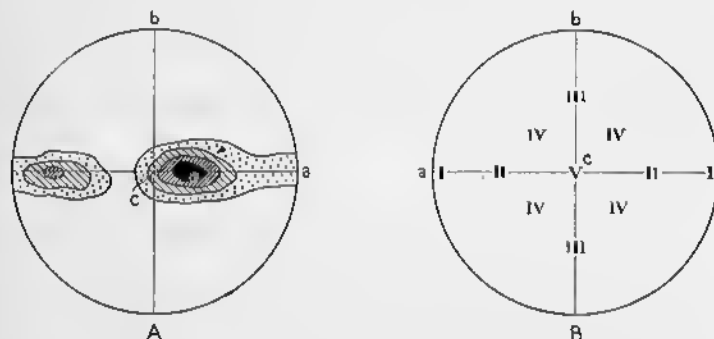


FIG. 271—Mica and Quartz. A, Petrofabric diagram of mica. Type of diagram expected from a crinkled schist of kind shown in Fig. 268C. B, Maxima in quartz diagrams. The maxima found in many diagrams tend to occupy the positions shown by the Roman numerals.

The normals to the cleavage of the mica in the crinkled schist illustrated in Fig. 268C would, in a section cut parallel to the top of the block, give a diagram such as that shown in Fig. 271A. This is a monoclinic fabric symmetry, the *a*-axis being the line of symmetry. In such a crinkled schist each successively higher layer slid to the right relative to the layer directly beneath it. This is a monoclinic symmetry of movement. Thus a monoclinic movement results in a monoclinic fabric.

In the Austrian Alps it was early demonstrated that *a* is parallel to the direction of movement, whereas *b* is perpendicular to it. Thus the fabric axes are rather directly and simply related to the movements in the rock.

That the lineation is perpendicular to the direction of movement is one of the fundamental tenets of structural petrology.

Although the symmetry of fabric may sometimes be directly correlated with the symmetry of movement, there are numerous exceptions. In fact, future studies may show that the exceptions are so numerous that the application of the concept of symmetry to structural petrology is not particularly useful. But the problem needs further investigation. In any case, clear distinctions must be made among megascopic fabric symmetry, microscopic fabric symmetry, and symmetry of movement.

The significance of triclinic symmetry is not clear. It is possible that in some instances triclinic fabric symmetry results from triclinic movement symmetry. In most cases, however, triclinic fabric symmetry is probably the result of two superimposed stages of deformation. Traces of the older deformation were not completely destroyed by the later deformation. Thus, in the schist illustrated by Fig. 268D, the diagonal lineation shown by one of the minerals is presumably younger or older than the crinkles. Such an interpretation does not mean that there were two distinct periods of orogeny; the two stages may well have been part of one orogenic period. The deforming forces were acting along somewhat different directions during the two stages.

### Mechanics of Mineral Orientation

The reality of the preferred orientation of minerals is a fact that can not be questioned, but the causes of this orientation are only partially understood. Most students of structural petrology believe that the orientation is a mechanical phenomenon, and that recrystallization is not essential to the process of orientation. According to the most widely accepted hypothesis, the deformation is controlled by slip planes in the rock and by glide planes in the minerals.

The rock undergoing deformation is characterized by one or more sets of *slip planes*—that is, surfaces along which differential movements may occur. The slip planes are analogous to the surfaces separating the individual cards in a sliding pack of playing cards. There may be more than one set of slip planes in a rock; the sets may be utilized simultaneously or successively.

As stated on p. 26, some minerals have no glide planes, others have one or more sets; the number depends upon the mineral species. Each grain rotates until a glide plane coincides with or is close to a slip plane; then translation along the glide planes begins (p. 26). In studying the subject of gliding it is essential to consider the glide direction, because a mineral can not glide in any direction in the glide plane. The glide direction must lie essentially parallel to the direction of translation (movement) in the slip plane of the rock. When the glide plane and the glide direction of the mineral are essentially parallel, respectively, to the slip plane and to the direction of movement in the rock, gliding may take place.

Studies in metallurgy suggest that perhaps too much emphasis has been placed on slip planes in structural petrology. Metallurgical investigations indicate that gliding will begin when the grain has rotated to such a position that the shearing stress parallel to the glide plane exceeds a critical value.

The minerals that have been utilized most extensively in structural petrology are quartz, calcite, biotite, and muscovite; hornblende and feldspar have been used to a lesser extent, and a few studies have been made on epidote, gypsum, fluorite, kyanite, tourmaline, and scapolite. Knowledge concerning glide planes and glide directions is based partly on experimental data, but much has been inferred from a consideration of petro-fabric diagrams.

Quartz, although it is one of the most common minerals in metamorphic rocks and one of those most extensively used in structural petrology, is least understood. It is believed by some that quartz possesses several glide planes, but none of these glide planes has been revealed by experiments.

According to the prisin rule, glide planes in quartz are parallel to the prism face  $m$  ( $10\bar{1}0$ ), and the glide direction is parallel to the *c*-crystallographic axis, which is also the optic axis (Fig. 265B). These planes and directions would exist, of course, in all quartz grains, even though the external form may be spherical or irregular. Each quartz grain rotates until the glide plane and glide direction coincide, respectively, to the slip plane and to the translation direction of the rock. Gliding then begins. Fig. 272A shows a quartz crystal oriented in the direction most

favorable for gliding in accordance with this rule; a prism face is parallel to the slip plane of the rock, and the *c*-crystallographic axis is parallel to the movement direction, *a*, of the rock. The use of a well-formed crystal in such an example is merely for

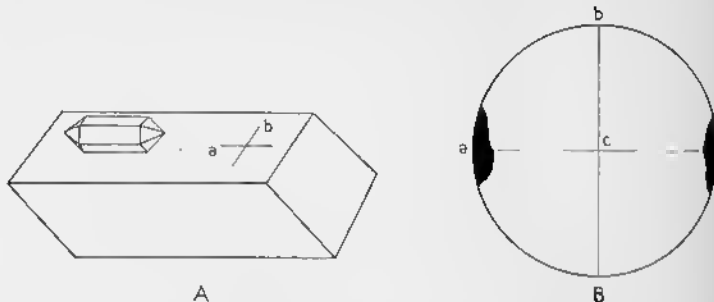


FIG. 272—Prism Rule for Orientation of Quartz. A. Top of block is slip plane of rock; *a* = translation direction in this slip plane; *b* = perpendicular to *a* in the slip plane. B. Resulting petrofabric diagram; black = maximum.

purposes of illustration; the grains in rocks are spherical, ellipsoidal, or irregular. A petrofabric diagram of quartz grains that have been oriented in accordance with this rule would show a strong maximum at *a* (Fig. 272B).

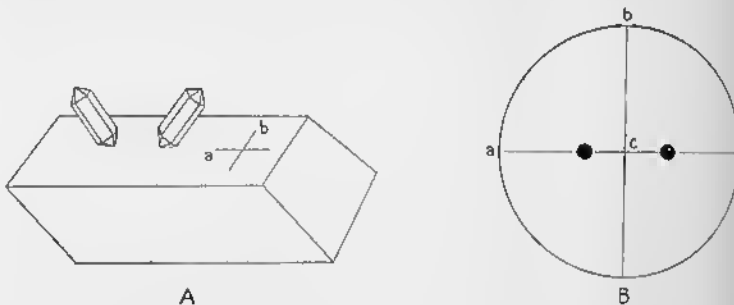


FIG. 273—Orientation of Quartz According to a Rhombohedron Rule. A. Flat rhombohedron, near  $\omega$  (0113) is parallel to slip plane of rock; trace of *c*-crystallographic axis on this rhombohedron is parallel to *a*. B. Resulting petrofabric diagram. Black = maxima.

A second possible glide plane in quartz is parallel to a flat rhombohedron, near  $\omega$  (0113). The glide direction is parallel to the trace of the *c*-crystallographic axis on this rhombohedron. Well-formed quartz crystals oriented in accordance with this

rule would occupy either of the two positions shown in Fig. 273A. A petrofabric diagram of quartz grains oriented in this way would show two maxima lying in the *ac* plane, approximately 20 to 23 degrees on either side of *c* (Fig. 273B).

Other glide planes in quartz have been suggested, but they need not be considered here.

In Fig. 272B, the maximum is at *a*. But this is not always true, and Fig. 271B shows, by Roman numerals, where maxima occur in different diagrams. In many petrofabric diagrams, for example, the concentration is at *II*—that is, in the *ac* plane, halfway between *a* and *c*. In other diagrams, maxima are found at *III*, in the *bc* plane, halfway between *b* and *c*.

Students of structural petrology explain these maxima in different ways. Some believe that quartz, following the prism rule, glides principally on the prism in a direction parallel to the *c*-crystallographic axis, but that the slip planes in the rock may occupy many different positions. Thus maxima *II* can be explained by two slip planes which intersect at *b* and which are inclined about 45 degrees to the *ab* plane; the translation direction is supposedly parallel to the *ac* plane (Fig. 271B). Gliding along the prism face parallel to the *c*-crystallographic axis will explain the maxima at *II*. Maxima *III* can be explained by slip planes intersecting in *a* and making an angle of approximately 45 degrees to the *ab* plane. All other maxima can be explained by slip planes that dip in the appropriate direction.

Other students of structural petrology believe that there is commonly only one set of slip planes in the rock, but that quartz possesses several glide planes. Thus maxima *II* may be explained by gliding on the pyramid (2 $\bar{1}$ 12) in a direction perpendicular to (2113). Maxima *III* are explained as due to gliding on rhombohedron (1011) in a direction perpendicular to (2110). Maximum *V* is explained as due to gliding on the base *c* (0001).

Because there is no experimental evidence of glide planes in quartz, Griggs and Bell<sup>7</sup> have suggested that, under stress, quartz breaks into needle-like slivers, the long axes of which

<sup>7</sup> Griggs, D. T., and Bell, J. F., Experiments bearing on the orientation of quartz in deformed rocks: *Bulletin Geological Society of America*, Vol. 49, pp. 1723-1746, 1938.

are parallel to a limited number of directions in the quartz lattice. It is believed that the long axes of many of the slivers are parallel to the *c*-crystallographic direction in the quartz; other slivers are either parallel to the trace of the *c*-crystallographic axis on any rhombohedron, to the intersection of two rhombohedrons, or to the intersection of a rhombohedron and

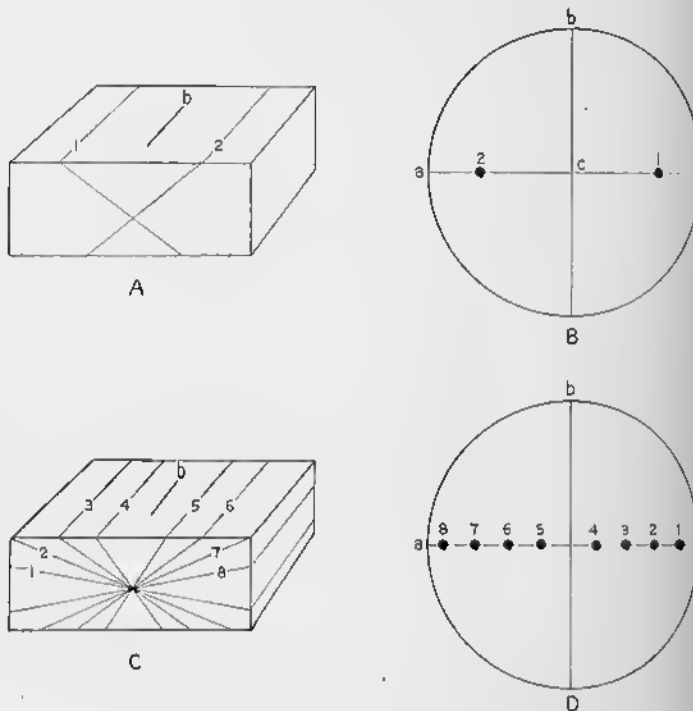


FIG. 274—Origin of Girdles. A. Rock with two slip planes, 1 and 2; *b* = lineation. B. Petrofabric diagram of quartz oriented according to prism rule on these two slip planes. C. Rock with numerous slip planes, 1, 2, 3, 4, 5, 6, 7, and 8. D. Petrofabric diagram of quartz oriented according to prism rule in these slip planes.

the base. If the long axes of the needles become oriented parallel to the direction of movement in the slip planes of the rock, the orientation of the *c*-crystallographic axis would bear a definite mathematical relation to the direction of translation. If the hypothesis were correct, however, we should expect to find many rocks containing such slivers of quartz. Actually, they are very rare.

Experimental data show that calcite glides on the rhombohedron  $c$  ( $01\bar{1}2$ ), as is illustrated in Fig. 265C; the short diagonal ( $zx$  of Fig. 265C) of the rhombohedron is parallel to the translation direction  $a$  of the rock. Moreover, the acute angle between this short diagonal and the  $c$ -crystallographic axis ( $yxz$  of Fig. 265C) generally opens in the  $a$  direction.

Many thin sections of calcite show that a single grain is composed of alternating sheets or layers with different optical behavior. When the nicols of the microscope are crossed, one set may be dark when the other set is light. These are twin lamellae, commonly parallel to the rhombohedron  $c$  ( $01\bar{1}2$ ). Many petrofabric diagrams of calcite represent the attitude of the perpendiculars to these twin lamellae.

The glide plane of mica is the basal pinacoid  $c$  ( $001$ ). In muscovite, the glide direction is parallel to the  $a$ -crystallographic direction.

### Kinds of Tectonites

A *tectonite* is a deformed rock, the fabric of which is due to the systematic movement of the individual units under a common external force. A *non-tectonite* is a rock that results from the accumulation of many separate components, each of which moved into place independently of its neighbors; all undeformed sedimentary and igneous rocks belong in this category.

The two principal kinds of tectonites are *S*-tectonites and *B*-tectonites. In an *S*-tectonite, the prominent structure is an *S*-plane, such as a plane of schistosity, a slip plane, or a bedding plane. The petrofabric diagram of an *S*-tectonite is generally characterized by one or two, occasionally more, clearly-separated maxima (Fig. 272).

In a *B*-tectonite a lineation is prominent, and in some instances *S*-planes may be absent. The petrofabric diagram of a *B*-tectonite is usually characterized by a girdle, a more or less complete belt in which the points are concentrated; there may be one or more maxima within this girdle (Fig. 269B).

The girdle characteristic of *B*-tectonites develops for several reasons. Such girdles are usually perpendicular to  $b$ . Fig. 274A illustrates a rock in which two sets of slip planes, labelled 1 and 2, intersect in  $b$ . It is assumed that both planes are

utilized equally, and that the direction of translation is parallel to the dip of these planes. If quartz were oriented according to the prism rule, the optic axes of some grains would lie in the plane 1 and would be parallel to its direction of dip; the optic axes of the other grains would lie in the plane 2 and would be parallel to its direction of dip. In a petrofabrie diagram of quartz plotted on the lower hemisphere (Fig. 274B), two maxima would appear, 1 corresponding to those grains whose axes lie parallel to plane 1 of Fig. 274A, 2 corresponding to those grains whose axes lie parallel to plane 2 of Fig. 274A. Two maxima would thus appear in the *ac*-plane.

A rock might be characterized by a large number of slip planes that intersect in *b* (Fig. 274C). Under conditions similar to those outlined above, a maximum would correspond to each plane (Fig. 274D). The result would be an *ac*-girdle with a number of maxima.

Actually, it is unlikely that so many slip planes would ever develop in a rock. The same result is obtained, however, if the rock is being rotated during deformation. Only one slip plane, which maintains a constant attitude relative to the surface of the earth, may exist. Relative to the rotating rock, however, the slip plane is constantly changing its position; this results in a situation similar to that shown in Fig. 274C.

Girdles also result from the rotation of individual grains. The amount of gliding is limited, and, after a grain has deformed as much as possible by gliding, it will be forced to rotate again about the *b* fabric axis. The *c*-crystallographic axis will rotate, of course, with the grain, but it will remain within the *ac* plane.

### Field Applications

Structural petrology has been applied to regional geological problems in many parts of the world—especially in Austria, Switzerland, Finland,<sup>8</sup> Scotland,<sup>9</sup> New Zealand,<sup>10</sup> Quebec,<sup>11</sup>

<sup>8</sup> Hietanen, A., On the petrology of Finnish quartzites; *Bulletin de la Commission Géologique de Finlande*, No. 122, 1938.

<sup>9</sup> Phillips, F. C., A fabric study of some Moine schists and associated rocks; *Quarterly Journal Geological Society of London*, Vol. 93, pp. 581–620, 1937.

<sup>10</sup> Turner, F. J., Structural petrology of the schists of eastern Otago, New Zealand; *American Journal of Science*, Vol. 238, pp. 73–106, 153–191, 1940.

<sup>11</sup> Osborne, F. F., and Lowther, G. K., PetroTECTONICS at Shawinigan Falls, Quebec; *Bulletin Geological Society of America*, Vol. 47, pp. 1343–1370, 1936.

Maryland, and Pennsylvania.<sup>12</sup> The purpose of most of these investigations has been to obtain more precise data concerning the tectonic history of the region, and concerning the nature of the deforming forces.

---

<sup>12</sup> Cloos, E., and Hietanen, A., Geology of the "Martic overthrust" and the Glenarm series in Pennsylvania and Maryland: *Geological Society of America Special Papers 35*, 1941.

## Geophysical Methods in Structural Geology

### Introduction

For many years structural geologists relied exclusively upon data obtained by direct observation. Most of the information came from natural exposures, although some facts were revealed by artificial openings such as mines, tunnels, railroad cuts, and highway cuts. Data obtained from drill holes may also be considered in this category, because the cores or cuttings are studied megascopically and microscopically in much the same manner as are surface outcrops. In the last two decades, however, geophysical methods have been greatly amplified, chiefly under the impetus of the petroleum and mining industries. By these methods, much information about the invisible rocks beneath the surface has been obtained.

At the outset it should be emphasized that the geophysical instruments do not make geological maps and structure sections. Rather they produce numerical data concerning the physical properties of the subsurface rocks. These data, if properly interpreted, shed much light on the lithology of the rocks, and, if sufficient data are available, on the shape of rock bodies too.

During the early stages of extensive application of geophysical methods to geology, especially in the 1920's and early 1930's, there was a rather sharp division between what were classified as geophysical methods and geological methods. The geophysicist produced numerical data, but in some instances he lacked the geological experience to interpret them properly; or the geologist, if called upon to translate the numerical data into geological structure, did not understand the principles by which the geophysical data were obtained, and hence could not make full use of them. This situation is fortunately being remedied at the present time; geophysicists and geologists now understand each other's problems more fully. In the future, many of the

investigations that utilize geophysical methods will be carried on by men trained in structural geology and in geophysics.

It is beyond the scope of this book to discuss the techniques involved in geophysical studies, and only a rather general discussion of the subject can be presented. For a complete treatment, the student is referred to textbooks on geophysics.<sup>1</sup> But the student of structural geology should be thoroughly familiar with the methods that can be employed, the extent of their usefulness, and their limitations. The broad physical principles underlying the various methods are discussed briefly here, and some examples of geophysical studies of structural problems are presented.

The precision of the information given by geophysical investigations depends upon several factors, such as the method employed, the time spent on the problem, the skill and knowledge of the investigator, and the nature of the problem. Although one geophysical method may be most suited for a particular problem, in another case some other method may be more useful.

In many instances, the geophysical methods merely indicate the presence of a rock body that differs in composition from its surroundings; that is, the results are qualitative. In other cases, the numerical data may suggest, with varying degrees of precision, the lithology and areal extent of this body. By some of the methods, the subsurface structure of sedimentary rocks and the shape of rock bodies may be determined with considerable accuracy.

In some instances geophysical methods are used to extend information obtained from a study of surface outcrops. Suppose, for example, that two areas of good exposures are separated by several miles of alluvium. Contacts between formations may be traced beneath the alluvium by some geophysical method; thus, the structural relations between the isolated areas may be determined. In other cases, where the exposures are good, it may be desirable to determine the depth to which some

---

<sup>1</sup> Heiland, C. A., *Geophysical Exploration*. New York: Prentice-Hall, Inc., 1940.  
Jakosky, J. J., *Exploration Geophysics*. Los Angeles: Times-Mirror Press, 1940.  
Nettleton, L. L., *Geophysical Prospecting for Oil*. New York: McGraw-Hill Book Company, 1940.

of the structural units extend. Some of the geophysical methods may be very useful in achieving this purpose.

In many cases the geophysical methods are employed in areas where surface exposures are rare or absent. In countries that have not been adequately studied geologically, the interpretation of the data may be difficult. In geological provinces that are reasonably well known, however, the correct solution might be readily obtained. If, for example, in the Gulf Coast of the United States a circular area a mile or so in diameter is occupied by a rock that transmits elastic waves with much greater speed than do its surroundings, a salt dome is probably present. In the Lake Superior region, strong positive magnetic anomalies indicate a deposit of iron ore.

### Geophysical Methods

The principal geophysical methods may be classified into four groups: gravitational, magnetic, seismic, and electrical. The first two methods involve the measurement of forces that are inherent in the earth, in contrast to the seismic method in which the forces are artificially introduced by the investigator. Most of the electrical methods also involve the introduction of energy by man, but in some instances natural electrical currents are measured. The investigator cannot control those forces that are naturally present in the earth, and, consequently, the vertical extent of the structural features involved cannot be determined very readily. Whenever the forces are artificially introduced, however, the depth of penetration can be controlled by the investigator; the vertical dimension of the structure can therefore be determined more satisfactorily.

### Gravitational Methods

#### Principles Involved

*Gravitation* is the force by which, due to mass, all bodies attract each other. This force is directly proportional to the mass of the two bodies concerned, and is inversely proportional to the square of the distance separating them. This principle may be expressed as

$$F \propto \frac{m_1 m_2}{r^2} \quad (1)$$

Here  $F$  is the force,  $m_1$  and  $m_2$  are the masses of the two bodies, and  $r$  is the distance between them. In the form of an equation,

$$F = \frac{k \cdot m_1 \cdot m_2}{r^2}. \quad (2)$$

In this equation  $m_1$  and  $m_2$  are measured in grams,  $r$  is in centimeters, and  $F$  is in dynes. A *dyne* is the force necessary to give a mass of one gram an acceleration of one centimeter per second per second. If two masses, each weighing a gram apiece, are one centimeter apart, equation (2) becomes  $F = k$ . That is,  $k$ , known as the *gravitational constant*, is the force of attraction of two equal masses of one gram each at a distance of one centimeter;  $k = 6.673 \times 10^{-8}$  C.G.S. units. This is about 1/15,000,000,000 part of gravity.

*Gravity* is the force by which the earth attracts bodies toward it. If a stationary body suspended in air a short distance above sea level is released, it will move toward the earth with a constantly increasing speed; that is, it accelerates. The acceleration is independent of the mass of the released body. It is thus more satisfactory to express the force of gravity in terms of the acceleration it causes. A *gal* is an acceleration of one centimeter per second per second; a *milligal* is one thousandth of a gal. At sea level the acceleration of gravity is approximately 980 gals (approximately 32 feet per second per second).

Because the earth is an oblate spheroid, flattened at the poles, the normal acceleration of gravity differs with latitude; at the equator it is 978.049 gals, at the poles it is 983.221 gals. The general equation is

$$g = 978.049(1 + 0.0052884 \sin^2 \phi - 0.0000059 \sin^2 2\phi). \quad (3)$$

In this equation  $g$  is normal gravity at sea level, and  $\phi$  is the latitude.

Equation (3) is based on data for the whole earth. In an ideal, homogeneous earth, the value of gravity could be calculated if the latitude were known. Actually, however, gravity usually differs from the theoretical value. This is due in part to the fact that the earth is heterogeneous; even at the surface, the rocks are by no means uniform. If an unusually heavy

rock is near the surface, gravity will exceed the theoretical value; if an unusually light rock is near the surface, gravity will be less than the theoretical value. The actual value of gravity also differs from the theoretical value because of a lack of isostatic adjustment. But within small areas—a few miles or a few tens of miles across—the differences due to isostatic factors are uniform, and hence they can be neglected in the study of local structural features.

Some of the gravitational methods, such as those utilizing pendulums and gravimeters, measure the value of gravity directly. Other methods, such as those using torsion balances, measure the rate of change of gravity and the deviation of equipotential surfaces from a spherical shape.

### Methods

**Pendulum method.** By swinging a simple pendulum, we may determine the value of gravity according to the equation

$$g = 4\pi^2 n^2 L. \quad (4)$$

In this equation  $g$  is the value of gravity,  $L$  is the length of the pendulum, and  $n$  is the number of vibrations the pendulum makes in unit time; in the C.G.S. system  $L$  is measured in centimeters and  $n$  in seconds;  $g$  is in gals.

This method has been used for many years by the U. S. Coast and Geodetic Survey and similar organizations to obtain precise values of gravity. A single observation, however, consumes considerable time—several hours—and for this reason the method is not practical for ordinary field mapping.

**Gravimeter method.** Within the last few years, instruments have been designed whereby the force of gravity can be measured directly within a few minutes. These instruments are known as gravimeters. The mechanical gravimeters use the elastic force of springs and the torsion of wires; the deformation is magnified by optical, mechanical, or electrical means to give an accuracy of 1 in 10,000,000.

**Corrections applied in pendulum and gravimeter methods.** In order to compare gravity measurements at adjacent stations, it is necessary to make a number of corrections. After the value of gravity is determined by the instruments, the following cor-

rections are made: (1) free air correction; (2) Bouguer reduction, (3) terrain (topographic) correction; (4) isostatic correction.

*Free air correction.* Most stations are above sea level, and the force of gravity becomes progressively less as the altitude becomes greater. For example, if gravity at some station at sea level were 980.000 gals, gravity measured from a captive balloon 300 meters above the station would be only 979.907 gals. For all stations above sea level, therefore, a correction must be added proportional to the altitude. A few examples of the correction at latitude 45 degrees are given in Table 3, which comes from Heiland.<sup>2</sup>

TABLE 3

Altitude in Meters	Correction in Milligals
100	+ 30.9
200	+ 61.7
300	+ 92.6
500	+154.3
1000	+308.6

*Bouguer reduction.* The rock between the station and sea level increases the value of gravity; the amount is proportional to: (1) the altitude of the station and (2) the density of the rocks between the station and sea level. For example, if the gravity station is at an altitude of 300 meters on a flat tableland underlain by granite, the rock between the station and sea level exerts a gravitational attraction of 33 milligals. This correction, therefore, must be subtracted when one calculates the value of gravity at sea level.

Thus, whereas the free air correction is positive, the Bouguer correction is negative; but the free air correction is the greater—approximately three times as large as the Bouguer correction. Moreover, it is obvious that the free air and Bouguer corrections can be combined into one correction according to the equation

$$g_0'' = g + H(0.0003086 - 0.0000421\delta) \text{ gals.} \quad (5)$$

In this equation  $g_0''$  = gravity at sea level with free air and Bouguer corrections;  $g$  = measured value of gravity;  $H$  = altitude in meters;  $\delta$  = density of rocks between station and sea level.

<sup>2</sup> Heiland, C. A., *op. cit.*, p. 136.

*Topographic (terrain) correction.* Hills that rise above the instrument, or depressions that descend below it, exert an influence on the measured value of gravity. If good contour maps are not available, it may be necessary for the field party to obtain sufficient data for calculating the topographic data. This is particularly true if considerable relief exists near the station.

One procedure is to divide the country into compartments by radii extending out from the station and by circles concentric about it, as illustrated in Fig. 275, where  $S$  is the station. The gravitational effect of each compartment, such as  $abcd$ , is

$$\Delta g = k \cdot \delta \cdot \phi(r_1 + \sqrt{r_2^2 + h^2} - \sqrt{r_1^2 + h^2} - r_2). \quad (6)$$

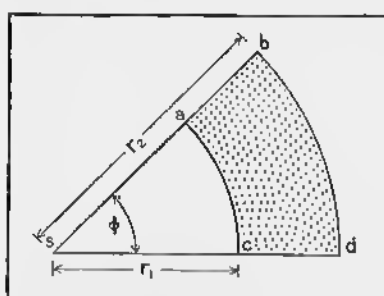


FIG. 275—Calculation of Terrain Correction in Gravity Measurements. See text. (After C. A. Heiland.)

$r_1$  = radius in centimeters of inner circle bounding compartment;  $r_2$  = radius in centimeters of outer circle bounding compartment; and  $h$  = average elevation in centimeters of the compartment above the instrument.

Charts and tables for making these corrections have been recently published by Hammer.<sup>3</sup>

If the average altitude of the compartment is greater than that of the instrument, the observed gravity is too low. In other words, the correction,  $\Delta g$ , should be added to the observed gravity. If the average altitude of the compartment is less than that of the instrument, the correction is subtracted from the observed gravity.

*Isostatic correction.* A correction for isostatic compensation is unnecessary in the study of local structure. On the other hand, such corrections are of great importance in geodetic work and structure of continental proportions.<sup>4</sup>

<sup>3</sup> Hammer, S., Terrain corrections for gravimeter stations: *Geophysics*, Vol. 4, pp. 184-194, 1939.

<sup>4</sup> Daly, R. A., *Strength and Structure of the Earth*, pp. 120-128. New York: Prentice-Hall, Inc., 1940.

**Calculation of gravity anomaly.** The theoretical or normal value of gravity for a station is calculated by equation (3). The corrected value of gravity is obtained from the observed value by making the free air, Bouguer, and terrain corrections. The difference between the corrected value and the normal value is the *gravity anomaly*. That is,

$$\Delta g_0'' = g_0 - g_0'', \quad (7)$$

where  $\Delta g_0''$  = gravity anomaly,  $g_0''$  = normal gravity, and  $g_0$  = observed gravity, with free air, Bouguer, and terrain corrections. The gravity anomaly is usually expressed in milligals. The gravity anomalies calculated by geodesists include an isostatic correction.

The gravity anomalies for each station are plotted on a map, and then isogams are drawn. *Isogams* are lines of equal gravity anomaly, and they are drawn in the same way as contour lines, interpolating wherever necessary. Fig. 277A is an isogam map of the Wellington field in Colorado;<sup>5</sup> the isogam interval is 0.2 milligals.

In some areas, the effects of the local structure may be concealed by a strong regional change in the gravity anomalies, and some method of adjustment must be used. In Fig. 277A, the value of gravity increases toward the south at the rate of 2.2 milligals per mile; the average east-west change is zero. Fig. 277B is the adjusted map, after the regional effect has been eliminated. Fig. 277C is the structure contour map of the region; it is referred to on p. 368.

**Torsion balance method.** For approximately 20 years, before gravimeters were developed, torsion balances were used for gravitational studies. These instruments do not measure the value of gravity, but give the gradient of gravity and the curvature of equipotential surfaces.

In essence, a torsion balance consists of a small beam, about 20 to 40 centimeters long, suspended from a vertical wire. This beam may be a simple horizontal beam, as in Fig. 276A, with weights at either end. In another type of beam, Fig. 276B,

---

<sup>5</sup> Wilson, J. H., Gravity meter survey of the Wellington field, Larimer County, Colorado: *Geophysics*, Vol. 6, pp. 264-269, 1941.

the weight at one end is suspended from a vertical wire. In more recent years, a tilted beam (Fig. 276C) has been used. Each observation takes from 20 to 30 minutes.

One of the values measured by the torsion balance is the *horizontal gradient of gravity*, also referred to simply as *gradient*. The unit of measurement is the *Eötvös* or *Eötvös unit*, which is  $1 \times 10^{-9}$  dyne per horizontal centimeter.

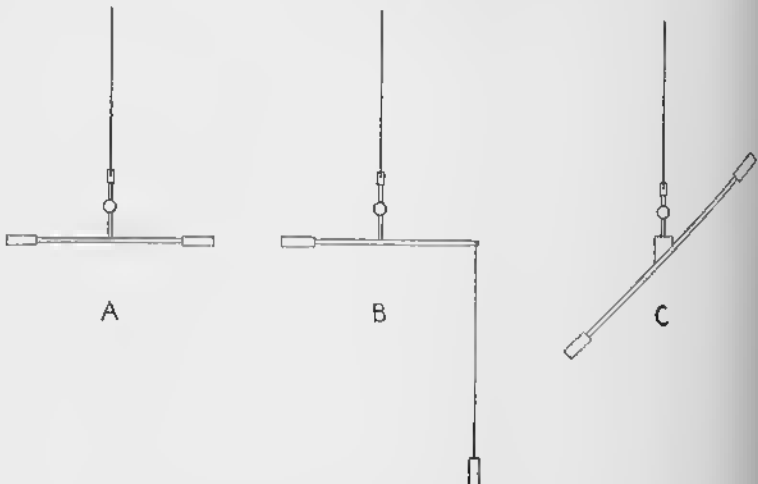


FIG. 276—Three Types of Eötvös Torsion Balance. See text. (After C. A. Heiland.)

After the field measurements have been made, corrections similar to those described for the pendulum and gravimeter methods must be made; these are the free air, Bouguer, terrain, and latitude corrections.

The gradient can be shown on maps or on profiles. On maps the gradient is indicated by an arrow pointing in the direction of increasing gravity; the length of the arrow is proportional to the magnitude of the gradient. The tail of the arrow is placed on the map at the point at which the observation is made.

Fig. 278 is a gradient map of the Fannett salt dome in Jefferson County, Texas.<sup>6</sup> The arrows point toward the center of the map, indicating that at this point the value of gravity is

<sup>6</sup> Eby, J. B., and Clark, R. P., Relation of geophysics to salt dome structures: *Bulletin American Association Petroleum Geologists*, Vol. 19, pp. 356-377, 1935.

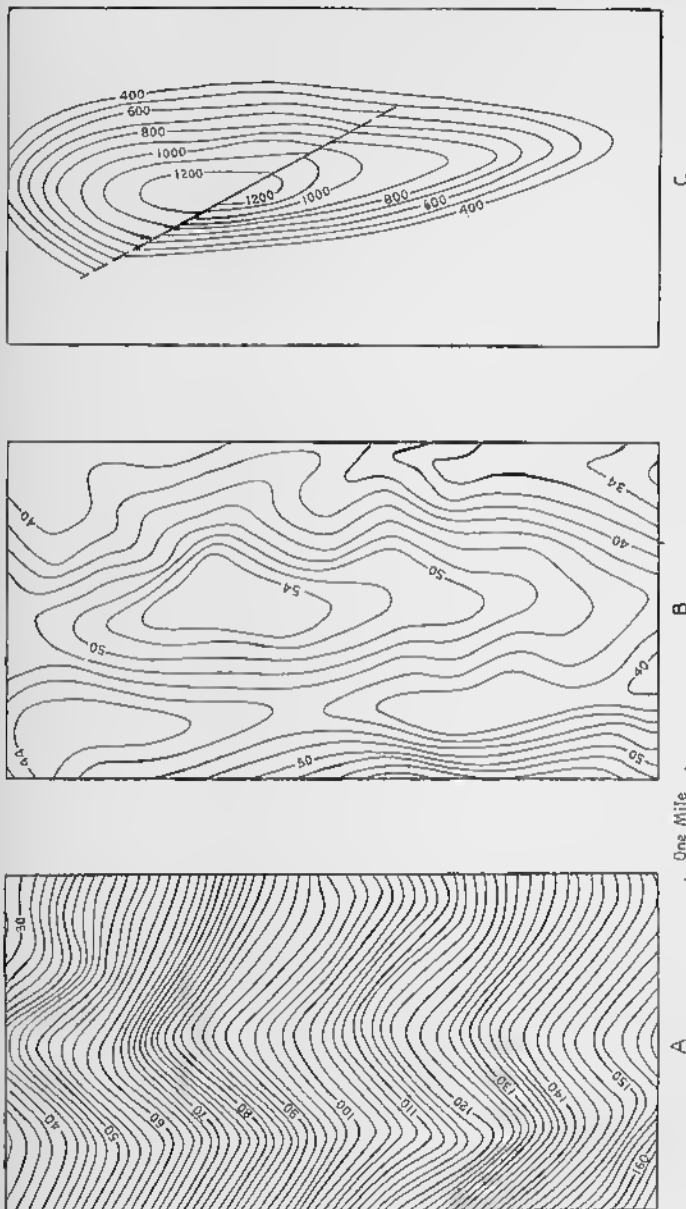


FIG. 277—Wellington Field, Colorado. A. Isogam map; contour interval is 0.2 milligals. B. Isogam map, adjusted for regional gradient of 2.2 milligals per mile south; contour interval is 0.2 milligals. C. Structure contour map on the Muddy Sand; contour interval is 100 feet. (After J. H. Wilson, *Geophysics*.)

at a maximum. The highest gradient is near the circular line marked "2000 ft. cap rock." At a point, such as *a*, the arrow shows that gravity is increasing toward the southeast, at a rate of about 33 Eötvös units (see scale in lower right-hand corner of the map).

If the observations are confined to a single line on the map, the gradient may be plotted on a graph, in which the horizontal distance is given on the abscissa, and in which the gradient in Eötvös units is given on the ordinate (Fig. 279).

A second value measured by the torsion balance is the *differential curvature*, also known as the *Eötvös curvature value*,

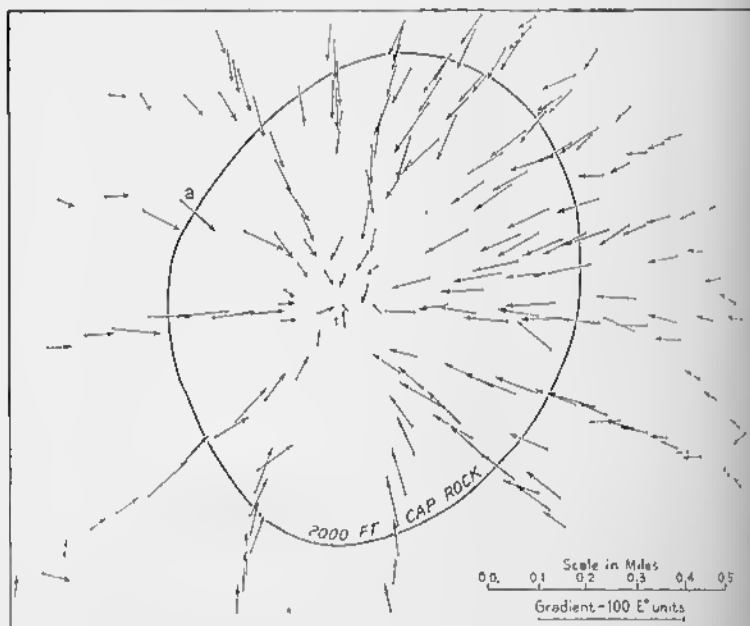


FIG. 278—Horizontal Gradient of Gravity, Fannett Salt Dome, Jefferson County, Texas. (After J. B. Eby and R. P. Clark, American Association Petroleum Geologists.)

*horizontal directing force*, or *R* value. For the significance of these terms, the reader is referred to textbooks on geophysics.

The torsion balance gives only the relative values of gravity. But if the absolute value of gravity at one station is known, from the pendulum or gravimetric methods, the gradient map may be converted into an isogam map. Even if the absolute

value of gravity is not known, an isogam map can be prepared on an assumed base.

### Relation between Gravity and Structure

Systematic local differences in gravity are directly related to differences in the density of the underlying rock. In some instances these may have no structural significance; for example, a local lava flow or basic sill in flat-lying sediments would cause differences in gravity. In many instances, however, the indicated lithologic changes are related to the geological structure. Anticlines, buried ridges, salt domes, faults, and igneous intrusions are commonly indicated by changes in gravity.

Many anticlines are expressed by an increase in gravity. This is due, of course, to the fact that older stratigraphic units tend to be heavier than younger formations. This is notably true where a crystalline basement is overlain by sedimentary rocks. An example of a map showing a correlation between the gravity anomalies and the structure is given in Fig. 277. Fig.

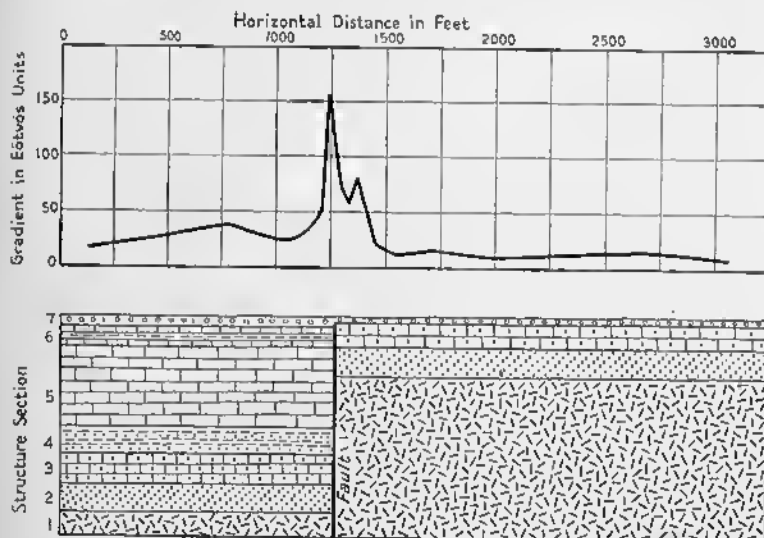


FIG. 279—Hull-Gloucester Fault at Leitrim, Ontario. Lower diagram is structure section: 1 = pre-Cambrian, sp. gr. 2.8; 2 = Potsdam sandstone, sp. gr. 2.5; 3 = dolomite, sp. gr. 2.8; 4 = Chazy, shale and sandstone, sp. gr. 2.5; 5 = limestone, sp. gr. 2.7; 6 = shale and limestone, sp. gr. = 2.6; 7 = glacial drift, sp. gr. = 1.8. Upper diagram is a graph showing horizontal gradient of gravity. (After A. H. Miller, C. A. French, and M. E. Wilson.)

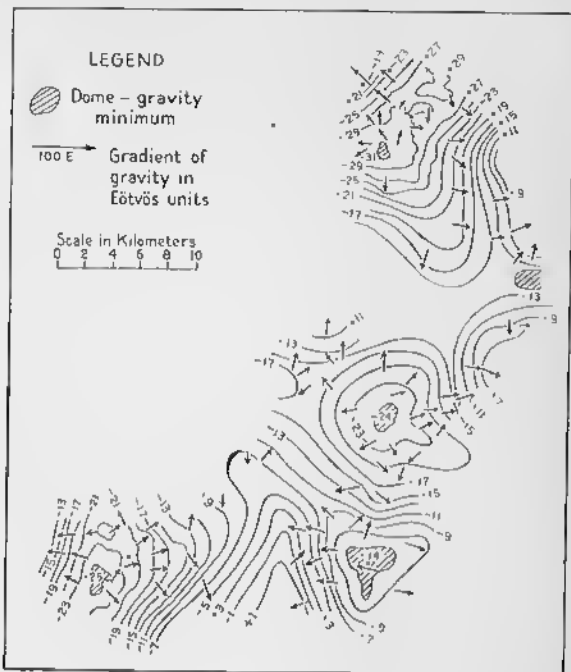


FIG. 280—Horizontal Gradient of Gravity and Isogam Map of Emba Region, Near Dossor, Russia. (After Numerov.)

277B is the adjusted isogam map of the Wellington field of Colorado. Fig. 277C, which covers exactly the same area as does Fig. 277B, is a structure contour map on the Muddy Sand. It shows a doubly plunging anticline with a closure of at least 800 feet. The correlation between the anticline and the adjusted isogam map is apparent.

Salt domes are commonly well-displayed by gravity data. Fig. 278 shows the horizontal gradient of gravity for the Fannett salt dome in Texas. The outline of the cap rock at a depth of 2000 feet below sea level is shown. Gravity increases radially inward toward the center of the dome. Fig. 280 is a map of a district in Russia, showing the gravity gradient and the isogam map.<sup>7</sup> In this case gravity increases radially outward from the

<sup>7</sup> Numerov, B., Results of the general gravity survey in the Emba district; *Zeitschrift für Geophysik*, Vol. 5, pp. 268-270, 1929.

salt domes. Whether a salt dome is a gravity minimum or maximum depends upon the nature of the surrounding sediments, as well as upon the nature and size of the cap rock on the dome.

Faults, if they bring rocks of different density into juxtaposition, will be indicated by gravity data. Fig. 279 shows the geological structure section, as well as the gravity gradient, of the Hull-Gloucester fault at Leitrim, Ontario.<sup>8</sup> As would be expected, the gradient reaches a maximum directly over the fault. The maximum is not directly over the outcrop of dipping faults, but its exact position depends upon numerous variables.

Gravity anomalies are not always related to local structure. In a recent gravity survey in the Appalachian area, Nettleton found that the anomalies could not be entirely explained by the known structure, and he suggests that masses rather deep within the outer shell of the earth must play an important rôle.<sup>9</sup>

### Magnetic Methods

#### Principles

Magnets are characterized by two *poles*, one of which is known as the *north-seeking* or *north pole*, the other as the *south-seeking* or *south pole*. Like poles repel each other, unlike poles attract. The force between two magnetic poles is proportional to the strength of each pole and inversely proportional to the square of the distance between the poles. That is,

$$F = \frac{SS'}{d^2} K. \quad (8)$$

In this equation  $F$  is the force;  $S$  and  $S'$  are the strengths of the two poles;  $d$  is the distance between the two poles; and  $K$  is a constant of proportionality that depends upon the units chosen. A magnetic pole placed in a field that has a strength of one *gauss* is acted upon by a force of one dyne. In magnetic studies

<sup>8</sup> Miller, A. H., French, C. A., and Wilson, M. E., Geophysical survey of the Hull-Gloucester and Hazeldean faults: *Geological Survey of Canada, Memoir 165*, pp. 190-209, 1931.

<sup>9</sup> Nettleton, L. L., Relation of gravity to structure in the Northern Appalachian Area: *Geophysics*, Vol. 6, pp. 270-286, 1941.

related to geological problems, it is more convenient to use the *gamma*, which is 1/100,000 part of a gauss. That is,

$$1 \text{ gamma} = 1 \text{ gauss} \times 10^{-5}.$$

The *magnetic field* of a magnet is that region in space into which the influence of the magnet extends. The *lines of force* of a magnetic field are the imaginary lines drawn through the field in such a way that they extend in the direction in which small magnetic poles would tend to move. Fig. 281A illustrates the field surrounding a bar magnet. The orientation of

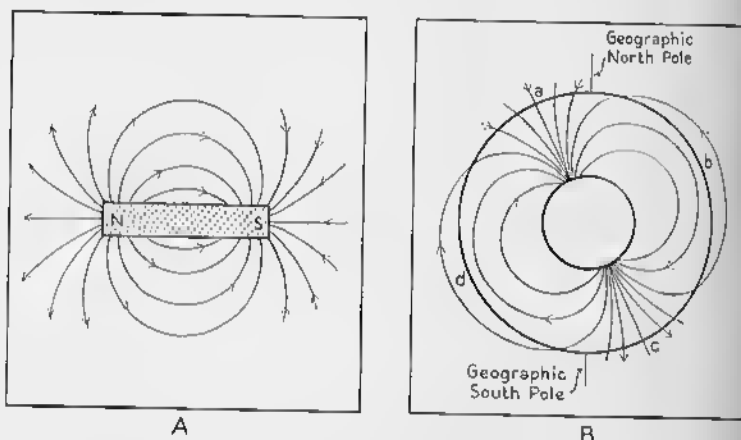


FIG. 281—Magnetic Fields. A. Magnetic field around a bar magnet.  
B. Magnetic field of the earth.

lines of force about a magnet is shown very clearly by scattering iron filings in the field, because the filings align themselves parallel to the lines of force.

The earth is a gigantic magnet; in a cross section through the earth, the magnetic lines of force are distributed as shown in Fig. 281B. The magnetic poles, far below the surface of the earth, are displaced relative to the geographical poles. Point *a* is on the west side of Hudson Bay at about 70° N. latitude.

A magnetic needle suspended in such a way that it is free to turn in all directions, tends to align itself parallel to the lines of force. At points *b* and *d* of Fig. 281B, the needle would be horizontal; at points *a* and *c*, it would be perpendicular to the surface of the earth. At any intermediate point it would be

inclined, and the *magnetic dip* is the angle between the lines of force and the horizontal. The *magnetic declination* at a point is the angular difference between geographic north and the vertical plane that contains the inclined needle.

In Fig. 282, which applies to the northern hemisphere, *X* points north and *Y* points east. If *T* is the total intensity of the magnetic force, *H* is the horizontal component, *Z* is the vertical component, *X* is the north horizontal component, and *Y* is the east horizontal component. The magnetic dip *I* is measured in the plane containing *H* and *T*; the magnetic declination, *D*, is measured in the horizontal plane that contains *H*, *X*, and *Y*.

In the United States, the magnetic dip ranges from 57 to 80 degrees, and the horizontal intensity ranges from 0.15 to 0.26 gauss.

The lithosphere lacks homogeneity in its magnetic properties. Some rocks are relatively magnetic, others are weakly magnetic. Consequently, the intensity of the magnetism and the attitude of the lines of force differ from place to place.

Magnetic prospecting methods date back to 1640, and since that time various types of instruments have been devised. Of modern design are the Schmidt vertical intensity magnetometer, the Schmidt horizontal magnetometer, and the Hotchkiss superdip. Simpler instruments are the Swedish mining compass and the dip-needle. In the Schmidt vertical intensity magnetometer, the magnetic system is suspended on a knife edge that is oriented at right angles to the magnetic meridian (magnetic north). It measures the relative value of the vertical component of magnetic intensity. The Schmidt horizontal magnetometer, in which the magnetic system is oriented parallel to the magnetic meridian, measures the value of the horizontal component of the magnetic intensity.

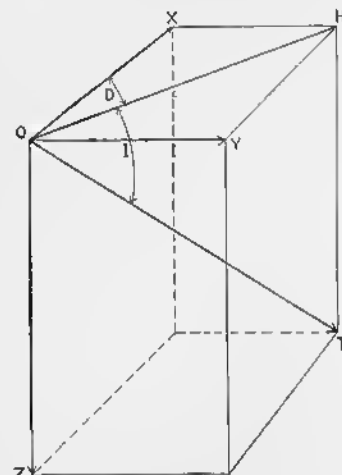


FIG. 282—Vector Diagram of the Earth Magnetic Field in the Northern Hemisphere. (After C. A. Heiland.)

If the Schmidt vertical magnetometer is used, several readings are made with the magnetic system oriented at right angles to the magnetic north. After the system has been turned 180 degrees, several additional readings are made. All the readings, which give the vertical intensity in gammas, are averaged in order to determine the reading for the station. The number of stations occupied depends on the detail with which the work is being done.

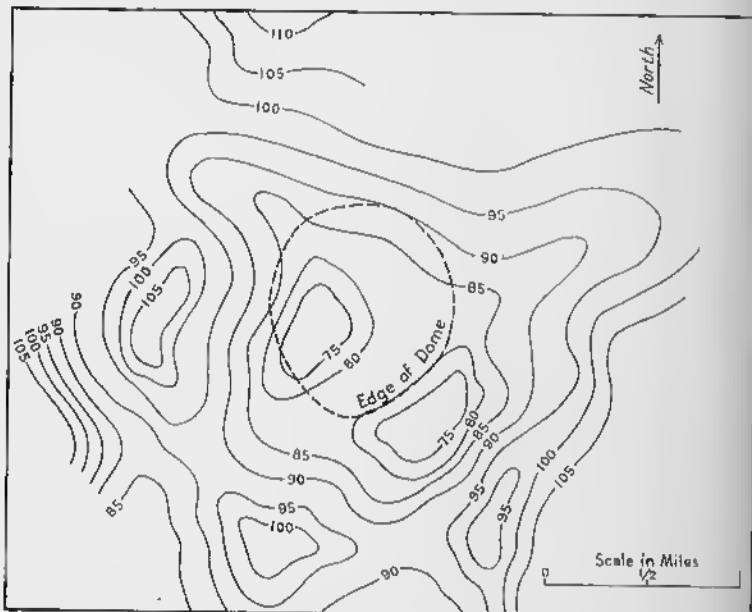


FIG. 283—Isonomy Map of Magnetic Vertical Intensity of the Fannett Salt Dome, Jefferson County, Texas. Contour interval 5 gamma. (After J. B. Eby and R. P. Clark, *Bulletin of the American Association of Petroleum Geologists*.)

Several corrections have to be applied before a map is prepared. A correction for *diurnal variation* is necessitated by more or less systematic daily variations in the magnetic intensity. Another correction must be made because of *magnetic storms*. Both these corrections are made together in one of two ways. A permanent instrument is left at a base station, and observations are made throughout the day on the value of the vertical intensity. Variations from the assumed or true value of the intensity at this station are plotted for the day, a curve is

prepared, and the corrections are applied to the field stations. This method necessitates, of course, two instruments and an additional observer. If only one instrument is available, the party must return several times a day to the base station in order to determine the correction. In some instruments, a correction must also be made for variations in temperature, measured by means of a thermometer inside the instrument. If the survey extends over many months, or if surveys made in different years are to be tied together, a correction must be made for long-period changes in the magnetic field of the earth. Charts published by the U. S. Coast and Geodetic Survey give the essential information. In order to show local structure adequately, a correction must be made for the terrestrial variations in the vertical magnetic intensity that is shown in Fig. 281B. This correction is obtained from the most recent "Equal Magnetic Vertical Intensity Chart" published by the U. S. Coast and Geodetic Survey.

For each station, the *magnetic anomaly* is determined algebraically by subtracting the theoretical values of the intensity from the observed value as corrected. The anomalies are then plotted on a map, and lines of equal anomaly are drawn. These lines, called *isonomalies* or *isanomalies*, show magnetic highs and lows. Near the center of the map illustrated by Fig. 283, there are two magnetic lows.<sup>10</sup> Profiles at right angles to the strike of the geologic structure may also be used, as in Fig. 284.<sup>11</sup> The abscissa represents the distance, and the ordinate represents the magnetic intensity, in this instance given in gauss. Curve

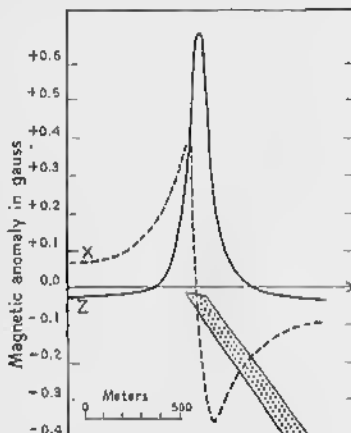


FIG. 284—Profile Showing Magnetic Anomaly Associated with Magnetite Body at Kiruna, Sweden. Z = curve for vertical intensity, X = curve for horizontal intensity. (After Haalek.)

<sup>10</sup> Eby, J. B., and Clark, R. P., *op. cit.*

<sup>11</sup> Haalek, H., "Zur Frage der Erklärung der Kursker magnetischen und gravimetrischen Anomalie, pt. 2," *Gerlands Beiträge zur Geophysik*, Band 22, pp. 385-399, 1929.

*Z* refers to the vertical intensity, whereas curve *X* refers to the horizontal intensity.

### Relation of magnetic intensity to geological structure

A magnetic ore body will obviously be betrayed by an increase in the vertical magnetic intensity. An anticline or buried ridge may bring a relatively magnetic formation near the surface; this is especially true if crystalline basement rocks are overlain by weakly magnetic sediments. A fault may bring together rocks of differing magnetic properties. Igneous intrusions and salt domes may also be shown by an isonomaly map.

A magnetite ore body at Kiruna, Sweden, profoundly affects the vertical and horizontal intensity of gravity, as shown by Fig. 284. Rather weak magnetic lows are associated with the Fannett salt dome (Fig. 283). In the Witwatersrand district of South Africa, the gold-bearing conglomerates are overlain by shales, some beds of which are highly magnetic. Toward the southwest, all these formations are overlain unconformably by younger formations, usually dolomite, which in places are as much as 3000 feet thick. By magnetic methods, it proved possible to trace the magnetic shales, then to predict the subsurface location of the gold-bearing conglomerates.

## Seismic Methods

### Principles

The essence of the seismic method is the accurate observation of artificially generated elastic waves that are transmitted through the rocks. These waves are generally induced by explosions, occasionally by the dropping of weights. The speed of transmission varies with the rock, and, in general, it is a function of the degree of consolidation. Heiland<sup>12</sup> says that in alluvium and glacial drift, the velocities range from 1900 to 6400 feet per second; in shales and sandstones the velocities are from 3000 feet to 14,000 feet per second; in granite and gneiss the velocities are from 13,000 feet to 25,000 feet per second; and in salt the velocity is 15,000 to 25,000 feet per second.

<sup>12</sup> Heiland, C. A., *op. cit.*, pp. 468-472.

All seismic methods are similar in that there is a *shot point* and one or more *receiving points* (Fig. 285). At the shot point, a hole is drilled a few feet to 100 feet deep, occasionally more, depending upon the type of prospecting and upon local conditions. After the charge, which varies from a fraction of a pound to several pounds of dynamite, has been placed, the hole is tamped with water or dirt. The instant of the explosion may be transmitted to the recording apparatus in various ways. Where the distance between the shot point and the recording apparatus is not great, the instant of shot is transmitted by wire. A contact in an electrical circuit is broken or made at the instant of explosion. If the distance is large, the instant of shot is trans-

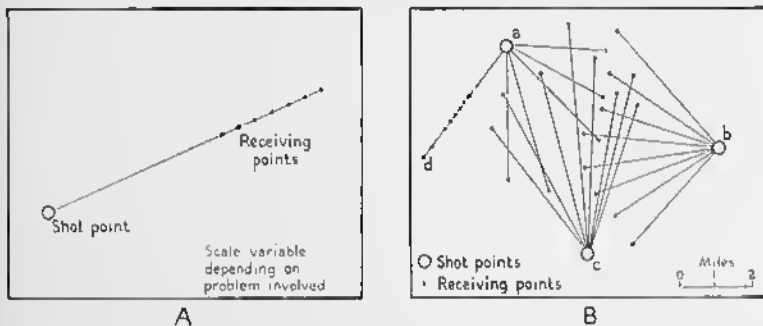


FIG. 285—Seismic Surveying. A. Profile shooting. B. Fan shooting.

mitted by radio. A third method, used in the earliest work, and not as accurate as the others, is to compute the instant of explosion from the time of arrival of the sound wave, which reaches the receiving points after the first waves transmitted through the rocks. The velocity of sound in air is 1086 feet per second at 0° C.; corrections must be made for temperature, barometric pressure, wind direction, and wind velocity.

At each receiving point is a *detector*, known also as a *geophone*, *phone*, or *pickup*. In some kinds of work, as many as 36 detectors, set up along a profile line a few hundred feet long, record the energy sent out by one explosion. The detectors are connected by wire to amplifiers and a recording camera, often placed in a specially-designed truck. The vibrations received by the detectors are recorded on rapidly-moving photographic paper; a timing device, usually a tuning fork, marks every

hundredth of a second. The instant of explosion is also recorded on this same paper. Fig. 286 is an example of such a record, which shows that the first impulse arrived 0.06 second after the

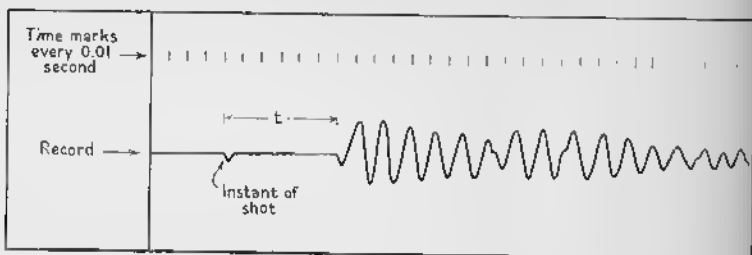


FIG. 286—Seismogram to Show Interval of Time Between Instant of Shot and Arrival of First Waves at Receiving Instruments.

instant of shot. Knowing the distance, it is possible to calculate the velocity of the elastic waves through the rocks.

$$v = \frac{x}{t} \quad (9)$$

Here  $v$  = velocity,  $x$  = distance, and  $t$  = time.

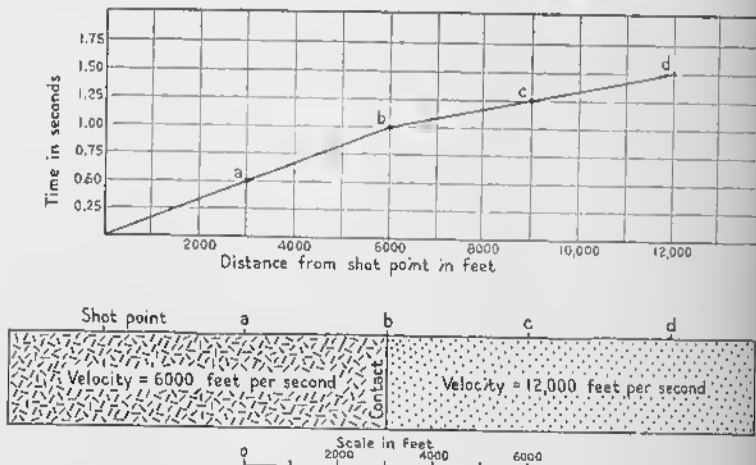


FIG. 287—Travel-time Curve (Upper Diagram) Obtained If Relations Are Those Shown in Cross-Section Below. (In part after C. A. Heiland.)

The data are plotted on a travel-time curve, an example of which is shown in the upper part of Fig. 287. The horizontal scale is the distance from the shot point to the detector; the vertical scale is the time that elapses between the instant of

shot and the arrival of the first elastic wave. The less the slope of the curve, the higher the velocity. The velocity can be determined directly from the curve by the equation

$$v = \frac{x_2 - x_1}{t_2 - t_1}. \quad (10)$$

In this equation  $v$  = velocity,  $x_2$  and  $x_1$  are distances represented by two points on the curve, and  $t_2$  and  $t_1$  are the times represented by the same two points.

In the upper part of Fig. 287, it is apparent that the part of the curve to the left of  $b$  indicates a velocity of 6000 feet per second, whereas the part of the curve to the right of  $b$  represents a velocity of 12,000 feet per second.

### Refraction methods

In *fan shooting*, which has been particularly successful in locating salt domes, the receiving points are placed at similar distances near the circumference of a circle, at the center of which the shot point is located (Fig. 285B). For each shot point there are ordinarily 5 to 20 receiving points, which are 4 to 8 miles from the shot point. Several overlapping fans are usually employed.

In a region that has not been previously studied, the normal travel-time curve is determined by "shooting a profile"; that is, the travel-time from a single shot point to 5 or 10 receiving points on the same straight line is determined. In Fig. 285B, the line *ad* is such a profile. If the intervening rocks are relatively homogeneous, the curve should be a straight line.

If a body of unusual composition is present in the area, the travel-times for some of the receiving points on the fan will lie off the normal curve. If a salt dome is present, the travel times are less, and the points lie below the normal curve; this is because the waves travel faster in salt than in the surrounding sediments. By noting on the map which receiving points are characterized by a lowered travel-time, it is possible to locate the salt dome approximately. Other methods are usually utilized to outline the dome more accurately.

In *refraction profile shooting*, the shot point and the detectors are placed on a straight line. The same shot point may be used for successive locations of the detectors.

By way of introduction, the case of a vertical geological boundary may be considered, although the principles of refraction are not involved. This contact may be a fault, a sedimentary contact, or an intrusive contact. If the velocity of the seismic waves on opposite sides of the contact are different, a distinct break in the travel-time curve will be observed. In the lower diagram of Fig. 287, for example, the velocity in the formation on the left side of the vertical contact is 6000 feet per second, whereas on the right side the velocity is 12,000 feet per second. The shot point is near the left side of the diagram; at the end of half a second, the seismic waves will have reached *a*. At the end of one second, they will have reached *b*. But, after

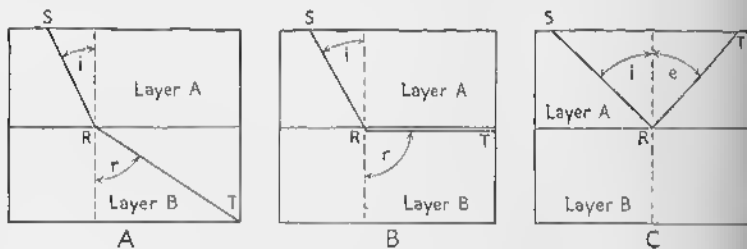


FIG. 288—Principles of Refraction. (See text.)

crossing the vertical contact, they will travel at the rate of 12,000 feet per second. One and one-quarter seconds after the instant of shot, the waves will be at *c*, and at the end of 1.5 seconds, they will be at *d*. The travel-time curve is given in the graph above the structure section. No matter where the shot point or the receiving points, the break in the travel-time curve will always be at locality *b*.

Refracted seismic rays obey the same general laws as do refracted light waves. In Fig. 288, the velocity in layer *A* is 10,000 feet per second; in layer *B* the velocity is 20,000 feet per second. If an explosion occurs at *S*, the energy moves outward in all directions. Some of it, which follows the path *SR* (Fig. 288A), is, upon meeting layer *B*, refracted to follow *RT*; as in

$$q = \frac{\sin i}{\sin r} = \frac{v_1}{v_2}. \quad (11)$$

In this equation  $q$  = index of refraction;  $i$  = angle of incidence;  $r$  = angle of refraction;  $v_1$  = velocity in upper layer;  $v_2$  = velocity of lower layer.

The greater the angle of incidence, the greater the angle of refraction. There is a critical angle of incidence for which  $r$  is  $90^\circ$ ; that is,  $RT$  is parallel to the contact; in the case illustrated (Fig. 288B), the critical angle is 30 degrees. In the general case

$$\sin c = \frac{v_1}{v_2} = q. \quad (12)$$

Here  $c$  = critical angle, and the other letters have the same meaning as in equation (11). If the angle of incidence exceeds

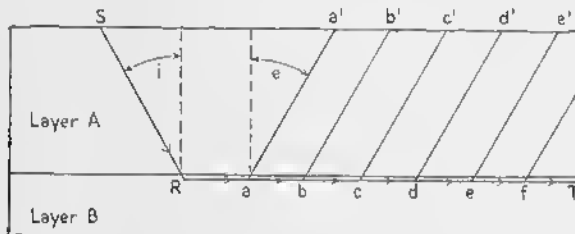


FIG. 289—Paths Followed by Refracted Ray. (See text.)

the critical value, as in Fig. 288C, the energy is reflected; the angle of reflection,  $e$ , equals the angle of incidence,  $i$ .

The wave that follows the path  $RT$  (Fig. 289) travels with the velocity of the lower layer, but it sends energy into the overlying layer. This energy is transmitted upward with the velocity of the upper layer. The angle of emergence is the same as is the angle of incidence. There are an infinite number of such rays; in Fig. 289, rays  $aa'$ ,  $bb'$ ,  $cc'$ ,  $dd'$ , and  $ee'$  are only examples. Of the total energy expended at  $S$ , only a small percentage behaves in this way.

The lower part of Fig. 290<sup>13</sup> illustrates the character of the wave fronts where the upper layer, 3000 feet thick, has a velocity of 10,000 feet per second; in the lower layer the velocity is 20,000 feet per second.  $S$  is the shot point; the position of

<sup>13</sup> Modified from Thornburgh, H. R., Wave-front diagrams in seismic interpretation; *Bulletin American Association Petroleum Geologists*, Vol. 14, pp. 185-200, 1930.

the wave front at every tenth of a second is shown in arabic numerals. At the end of 0.5 second, the waves have reached locality *a*; the energy has traveled directly along the surface of the earth at the rate of 10,000 feet per second. At the end of 1.0 second the energy has reached locality *b*, also having traveled along the surface of the earth at a speed of 10,000 feet per second. At the end of 1.1 seconds, energy that has followed the more circuitous route, *Smnc*, reaches *c* before energy that has traveled directly from *S* to *c*. At all points to the right of *b*, the energy that travels in the lower layer arrives first. The travel-time curve for this case is given in the upper part of Fig. 290. The break in this curve occurs directly above *b*.

A *reversed profile* should be shot in order to ascertain that the contact between the two layers is horizontal; that is, the shot point should be at the right end of the section (Fig. 290), and the receiving points should be at the left end of the section. If the contact is horizontal, the travel-time curve will be identical with that obtained previously.

In actual field practice the travel-time curve is used for determining the velocities in the different layers. The slope of the curve is inversely proportional to the velocity (see p. 377). In Fig. 290, it is apparent from the left end of the travel-time curve that in one second the energy has traveled 10,000 feet; this is the velocity in the upper layer. The right hand part of the curve, between 1.0 and 1.45 seconds, indicates a velocity of 20,000 feet per second. This is the velocity in the lower layer.

One would suppose that the travel-time curve for the uppermost layer would always intersect the abscissa and ordinate at zero, as in Fig. 290. Often, however, the curve strikes the time scale above zero. This is due to a "weathered zone" in which the rocks, because of fracturing and weathering, are characterized by abnormally low velocities.

The thickness of the upper layer may be calculated in various ways. One equation is

$$d = \frac{x}{2 \sqrt{\frac{1+q}{1-q}}}. \quad (13)$$

In this equation  $d$  = depth of the contact;  $x$  = "critical" distance on travel-time curve—that is, the distance from the origin to the break in the curve; and  $q$  is the index of refraction (see equation 12).

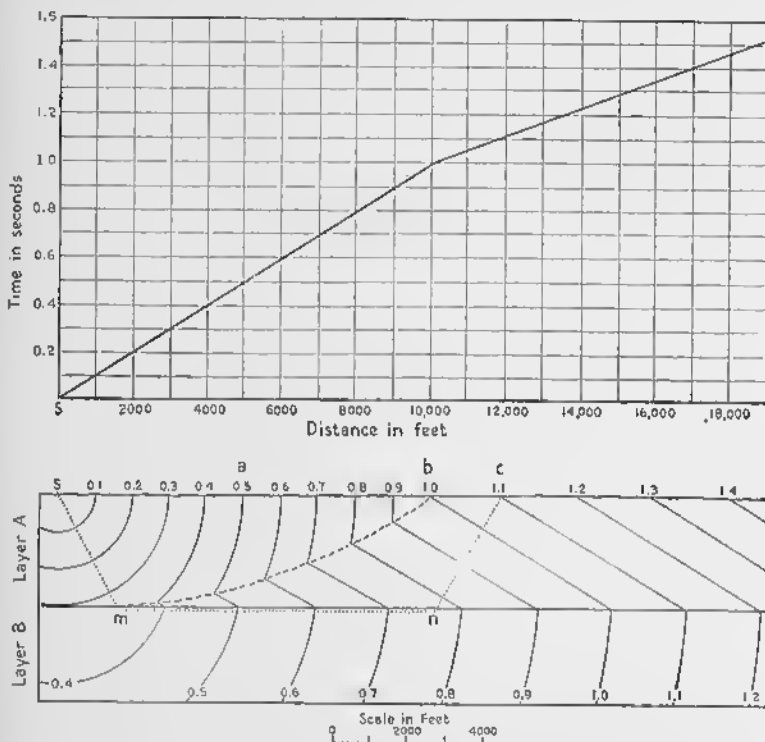


FIG. 290—Lower diagram shows wave front each tenth of a second if  $S$  is shot point, if velocity in layer  $A$  is 10,000 feet per second, and if velocity in layer  $B$  is 20,000 feet per second. Upper diagram is travel-time curve for this case. (After H. R. Thornburgh, Bulletin American Association Petroleum Geologists.)

Travel-time curves may be used to obtain velocities and depths of more than two layers.

The problem is more complicated if the contact between two layers is inclined. The reversed profile does not give the same travel-time curve as does the first profile. Depths and angles of dip may be calculated, but space does not permit consideration of the methods employed in such cases.

### Reflection methods

The reflection method can detect reflecting horizons at depths of 300 to 30,000 feet, although it is commonly used for depths of 2,000 to 10,000 feet. If two layers of different velocities are in contact, some of the energy released by the explosion is reflected back toward the surface of the earth. In Fig. 291,  $S$  is the shot point,  $R$  is a receiving point. Of all the possible rays radiating from  $S$ , one is  $SE$ ; the energy following this path is reflected at  $E$ , and follows the path  $ER$ . The angle of reflection,  $e$ , equals the angle of incidence,  $i$ .

If the beds are essentially horizontal, *correlation shooting* is employed. The shot point and the receiving points are on

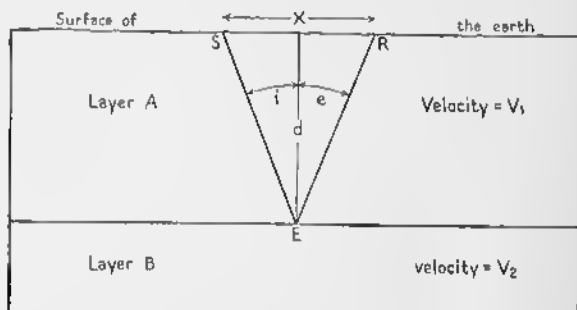


FIG. 291—Path Followed by a Reflected Wave. (After C. A. Heiland.)

the same straight line (Fig. 285A). Six or more geophones operate simultaneously at receiving points that are 20 to 100 feet apart. The distance from the shot point to the middle geophone is 100 to 2,000 feet.

The waves from a reflecting horizon produce in the seismogram a striking change in amplitude, which is followed by one to four oscillations. Fig. 292 shows the seismograms for six geophones that are placed 100, 200, 300, 400, 500, and 600 feet from the shot point. Such a record could be obtained from one shot, with the six geophones recording simultaneously. The time is given at the bottom of the figure, each mark representing  $\frac{1}{100}$  of a second. The instant of shot is marked zero. The greater the distance between the shot point and the receiver, the greater is the time interval between the instant of shot and

the arrival of the direct waves. The record of the direct waves is often blurred or lost because of the magnification by the instrument. In the uppermost record, in which the shot point and

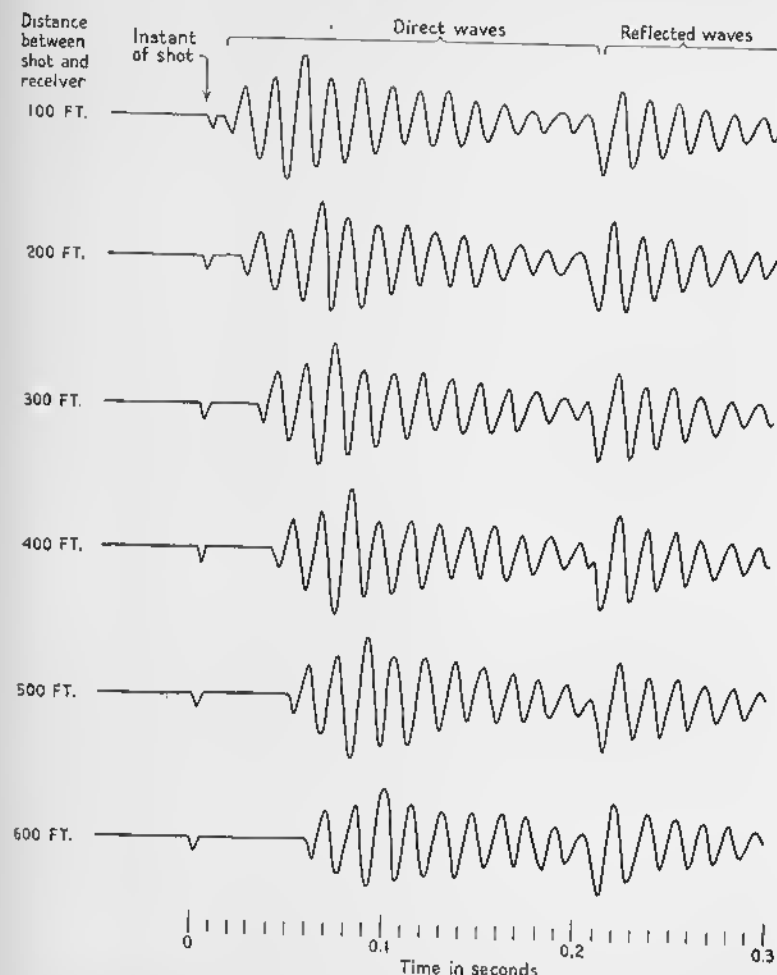


FIG. 292—Direct and Reflected Waves Obtained When the Distance Between the Shot Point and the Receiving Point Ranges from 100 to 600 feet. Velocity in layer above reflecting horizon is 10,000 feet per second.

geophone are 100 feet apart, the reflected waves begin to arrive at 0.2 second. In all the seismograms the reflected waves arrive at approximately the same time, although, as is to be expected,

they are a little later where the distance between the shot point and geophone is large.

The depth of a horizontal reflecting horizon is readily calculated:

$$d = \frac{1}{2} \sqrt{v_1^2 t^2 - x^2}. \quad (14)$$

In this equation  $d$  = depth;  $v_1$  = velocity in upper layer;  $t$  = time interval between instant of shot and arrival of reflected wave; and  $x$  is the distance between shot point and receiving point. The value of  $v_1$  is determined for the surface waves by dividing the distance  $x$  by the time interval  $t$ .

Applying these equations to Fig. 292, it is first necessary to calculate the velocity in the surface layer. The lowest seismogram shows that the waves travel 600 feet in 0.06 seconds, indicating a velocity of 10,000 feet per second. This same seismogram shows that the reflected waves begin to arrive at approximately 0.21 second. Calculating the depth by equation (14), we get a depth of 1006 feet. Using equation (15), we get a depth of 1050 feet.

If  $x$  is small compared to  $d$ , as is the case in *vertical shooting*,

$$d = \frac{1}{2} v_1 t. \quad (15)$$

These equations assume that the average velocity in the upper layer is the same as the velocity at the very surface of the earth. It is possible, however, to calculate the *effective average velocity* by the equation

$$V_a = \sqrt{\frac{x_2^2 - x_1^2}{t_2^2 - t_1^2}}. \quad (16)$$

Here  $V_a$  is the average effective velocity,  $x_2$  and  $x_1$  are the distances from the shot point to two separate receiving stations, and  $t_2$  and  $t_1$  are the travel-times for the same receiving stations. More commonly, the squares of the distances are plotted against the squares of the travel-times; the cotangent of the angle that the average curve makes with the abscissa is the square of the average velocity.

Fig. 293 illustrates how data obtained from a series of localities may be correlated. All the localities are on the same straight line on the map. Each vertical line gives the data for

one locality. Good reflections are shown by solid circles, fair reflections by open circles. At locality *a*, for example, strong reflections were obtained at 3500 feet and 1650 feet, fair reflections at 4100 feet and 1000 feet. The broken lines show how the reflections may be correlated and the structure deduced.

For inclined strata, *dip shooting* must be employed by reversing the profile. It is possible to calculate both the depth of the reflecting horizon and its dip. After the dip for every reflection

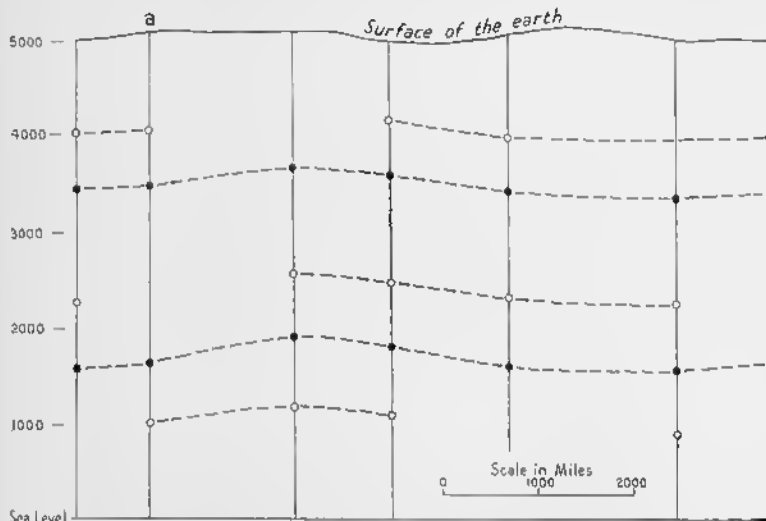


FIG. 293—Reflection Correlation Logs. Solid circles = good reflection; open circles = fair reflections. (Modified after C. A. Heiland.)

is plotted on a structure section, an imaginary, or *phantom horizon*, is sketched on the section to show the structure.

### Geological applications of seismic methods

Seismic methods are not only useful in recognizing the presence of rock bodies of unusual composition, such as salt domes, but they may also provide some data concerning the characteristics of these rocks. Moreover, the depth and dip of beds and contacts may be determined. At the present time, the reflection method is the best of all the geophysical methods for obtaining a precise structural picture. Folds, faults, salt domes, and igneous bodies may be delineated.

Fig. 294 is a structure contour map of the South Cotton Lake area in Texas, based upon a reflection seismograph survey.<sup>14</sup> The broken lines show the location of the profiles. The major features of this map, prepared in 1936, were subsequently verified by drilling. Fig. 295, the Sheppards Mott dome, Texas,<sup>15</sup> is another example of a structure contour map prepared

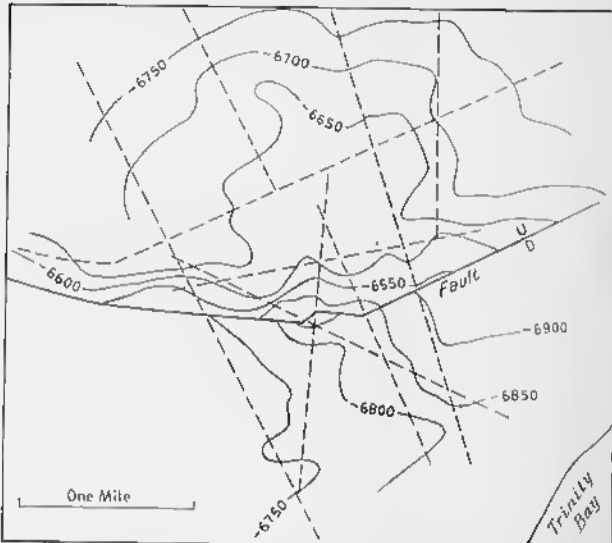


FIG. 294.—Structure Contour Map of the South Cotton Lake Area, Chambers County, Texas. Made by reflection method, contoured on a phantom horizon near the top of the Frio sand. Contour interval 50 feet. Broken lines show location of the seismic profiles. Petroleum is trapped in the anticline north of the fault. (After J. M. Wilson, *Bulletin of the American Association of Petroleum Geologists*.)

by reflection methods; the contour interval is 100 feet, but the absolute values of the contours are not given in the original paper.

### Electrical Methods

#### Introduction

The electrical methods for deducing geological structure are many and varied, both in technique and in the properties

<sup>14</sup> Wilson, J. M., South Cotton Lake field, Chambers County, Texas: *Bulletin American Association Petroleum Geologists*, Vol. 25, pp. 1898-1920, 1941.

<sup>15</sup> Elby, E. B., and Clark, R. P., *op. cit.*

measured. Some methods utilize natural electrical currents that flow through the lithosphere. Other methods use artificial currents that are introduced into the rocks by direct contact or by induction. Only some of the more common methods can be considered.

The flow of electricity may be compared to the movement of water in a pipe. The rate of flow of electricity is measured in

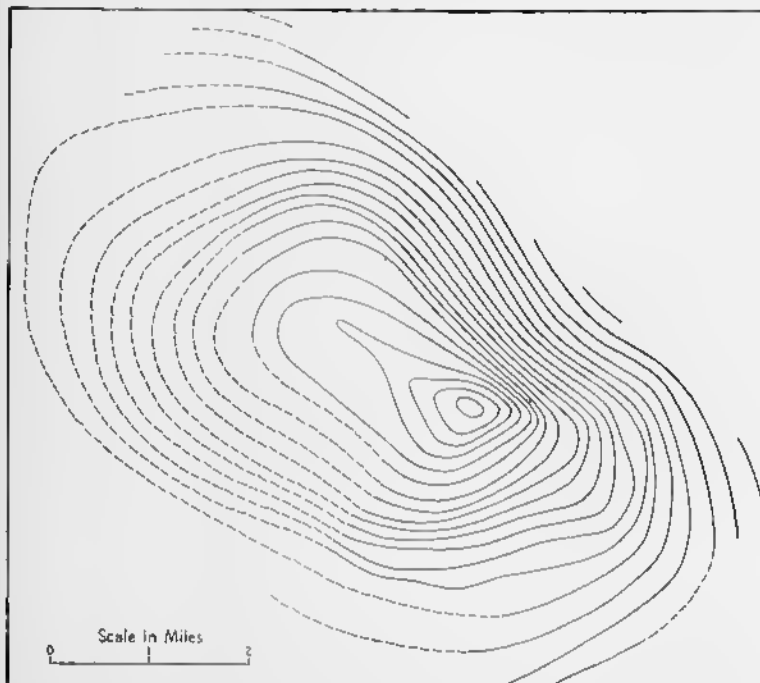


FIG. 295—Structure Contour Map of Sheppards Mott Dome, Matagorda County, Texas. Made by reflection method. Contour interval 100 feet, but absolute values of contours and name of horizon contoured are not given in the original paper. (After E. B. Eby and R. P. Clark, *Bulletin of the American Association of Petroleum Geologists*.)

amperes. Although the ampere might be defined in terms of the magnetic effect of the current, in practice it is defined in terms of its chemical effect. If two silver plates are placed in a jar of silver nitrate solution, and if the positive terminal of a battery is connected to one plate and the negative terminal is connected to the other plate, silver is dissolved from one plate and added to the other. The quantity of electricity that deposits 0.001118

gram of silver is one *coulomb*, and the current that deposits silver at a rate of 0.001118 gram per second is one *ampere*. In geophysical work, measurements are often made in *milliamperes*—that is, in thousandths of an ampere.

All substances offer resistance to the passage of electrical current, just as the friction in a pipe impedes the flow of water.

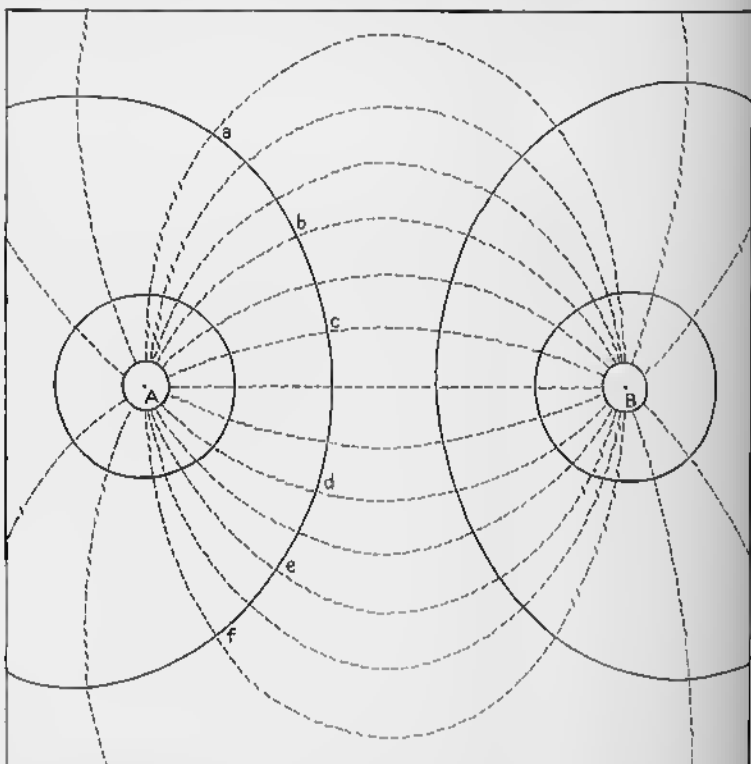


FIG. 296—Current Flow-lines (broken lines) and Equipotential Lines (solid lines) about Two Electrodes *A* and *B*.

An *ohm* is the resistance offered by a column of mercury 106.3 centimeters long, weighing 14.4521 grams, at 0° centigrade.

The *electromotive force* causes electricity to flow or tend to flow, and it may be compared to the hydrostatic head causing water to flow. The unit of measurement is the *volt*, which is the electromotive force needed to drive a current of one ampere through a resistance of one ohm. In geophysical work, the *millivolt*, one thousandth of a volt, is the unit normally used.

*Difference of potential* is the difference in electric pressure between two points in an electric circuit, and it is measured in volts.

*Resistivity* ( $\rho$ ), or *specific resistance* of a substance, is the resistance between opposite faces of a centimeter cube. *Conductivity* ( $\gamma$ ) is the reciprocal of resistivity.

$$\rho = \frac{I}{\gamma} \quad (17)$$

If electricity flows from one end of a thin homogeneous rectangular plate to the other, as from  $A$  to  $B$  in Fig. 296, we may think of the electricity as moving along an infinite number of current flow lines, some of which are illustrated by broken lines. Along each of these lines there is a drop in potential. If the difference in potential between  $A$  and  $a$ ,  $A$  and  $b$ ,  $A$  and  $c$ ,  $A$  and  $d$ ,  $A$  and  $e$ , and  $A$  and  $f$  is the same, it follows that there is no difference in potential along the line  $abcdef$ , which is therefore an *equipotential line*. There are an infinite number of such equipotential lines, at right angles to the current flow lines, and in Fig. 296 some of them are shown in solid lines. Within the lithosphere, which is three-dimensional, we must think of equipotential surfaces. All points on an equipotential surface are at the same potential. Usually it is feasible to map only the equipotential lines, and not the equipotential surfaces.

#### Natural electrical currents

**Spontaneous electric currents.** Sulphide ore bodies set up spontaneous electric currents. At the surface of the earth the current flows toward the body (Fig. 297), and, consequently, there is a drop in potential as the ore is approached. In order to produce measurable currents, the top of the ore body should be within 300 feet of the surface. The drop in potential along the surface of the earth as one approaches this *negative potential center* over the ore body may be as great as 700 millivolts. The intensity and shape of this field may be determined by preparing potential profiles, or by surveying equipotential lines.

A *potential profile* follows a straight line perpendicular to the strike of the geological structure, if its strike is known. Wooden pegs are laid out on the line of the profile every 20 to 100 feet.

The measuring instruments consist of two "porous pot" electrodes connected by wires to a potentiometer reading to 1 millivolt. One electrode is placed at peg *A*, the other at peg *B*. The difference in potential is read on the potentiometer. The first electrode is then moved to peg *B*, the other to peg *C*, and a new reading is made. The process is repeated for all the pegs

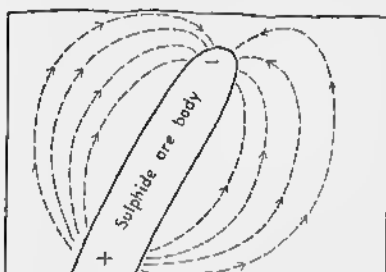


FIG. 297—Spontaneous Electric Current about a Sulphide Ore Body.  
(After S. F. Kelly.)

If there is a drop from *A* to *B* of 10 millivolts, but an increase of 7 millivolts from *B* to *C*, the total drop from *A* to *C* is only 3 millivolts. Peg *A* is arbitrarily assigned a value of zero on the vertical scale.

Ordinarily, a series of such profiles are run parallel to one another, the number depending upon the character of the investigation. Moreover, at least one profile at right angles to the others, and crossing them all, is essential in order that all the profiles may be tied to the arbitrarily-chosen starting point. An example of such a series of profiles is given in Fig. 298.<sup>16</sup> This figure is essentially a map with profiles superimposed on it. Each solid cast-west line is a line along which a potential profile was run; the solid north-south line serves a similar function. The potential profile is shown by a broken line. Each profile is numbered in order that it may be correlated with the correct line on the map; each line serves as the base of a graph. The millivolt scale for the profiles is given below the map. The point on the map represented by the intersection of lines 11 and 4 was arbitrarily assigned a value of zero. A maximum of 470 millivolts is found on profile 27.

<sup>16</sup> Kelly, S. F., Geophysical delineation of structure in mining operations; *Transactions American Geophysical Union*, pt. 3, pp. 245-269, 1939.

From such profiles, a map of equipotential lines may be deduced, just as a contour map can be constructed from a series of topographic profiles (Fig. 299).

*Equipotential lines* may be surveyed by the same instruments, although a milliammeter may be used instead of a potentiometer.

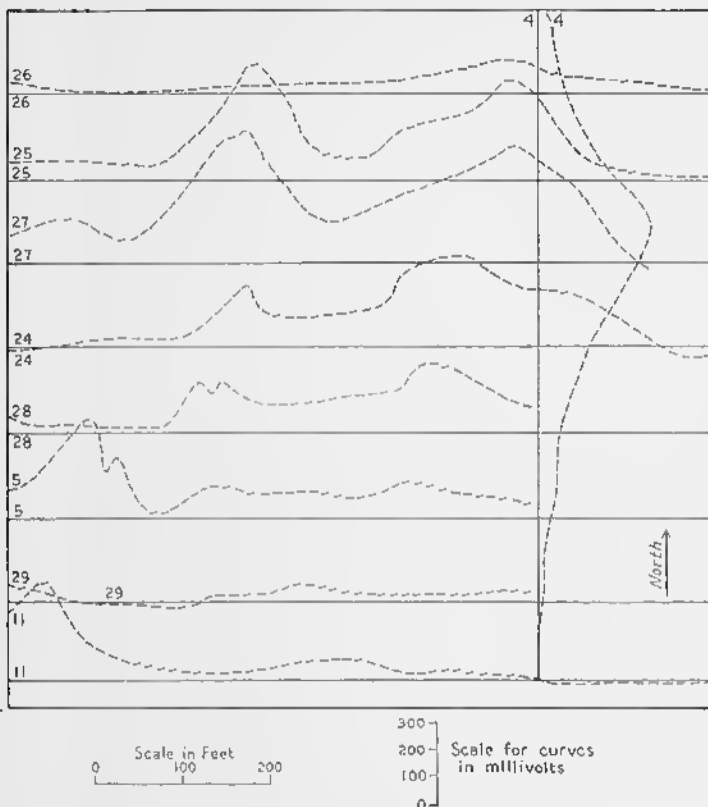


FIG. 298—Combined Map and Potential Profiles of Spontaneously Generated Electric Currents at Noranda Mines, Ltd., Quebec. (After S. F. Kelly.)

One of the "porous pot" electrodes is placed in the ground, and the other is placed in successive trial locations, until no current flows through the measuring instrument; that is, until either an ammeter or potentiometer would read zero. This means that two electrodes are on an equipotential line. One electrode is then moved to the location of the second electrode, and the

second is moved on to find a new location on the equipotential line. If possible, the equipotential line should be followed back to the starting point. Several such equipotential lines may be surveyed, although one line will ordinarily indicate rather clearly the center of the electrical disturbance. No numerical values can be assigned to these equipotential lines unless they are tied together by a potential profile.

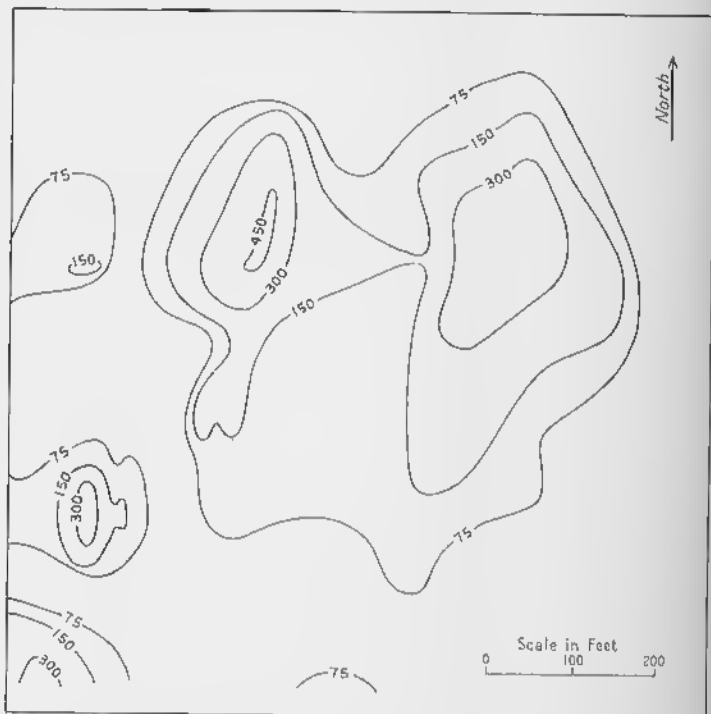


FIG. 299—Equipotential Lines for Same Area Shown in Fig. 298.

In these methods, some corrections have to be applied for polarization of the electrodes and for topography.

Although spontaneous electric currents are used most extensively in the search for ore bodies, they may be employed in other ways. A notable example is the Luushia anticline of Katanga; beds rich in graphite are brought nearer the surface by the anticline. The spontaneous currents generated by the graphite cause a negative potential over the anticline; a negative potential

thus indicates the presence of an anticline. Anthracite coal causes strong spontaneous currents, but a positive potential center occurs above anthracite beds. Some faults are characterized by spontaneous currents, apparently due to differences in the conductivity of solutions in the fractures along the fault.

**Telluric currents.** Telluric currents are natural currents of electricity flowing through the lithosphere, and are of solar origin.<sup>17</sup> The technique of studying these currents is new, and it will undoubtedly be modified in the future. Most electrical methods are not useful for depths greater than 6,000 feet, but the telluric currents give information for greater depths.

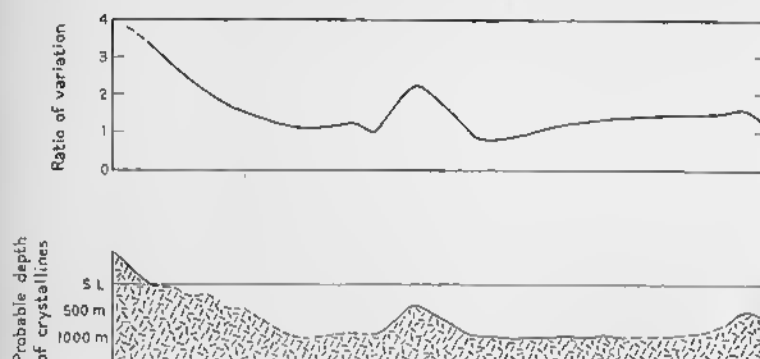


FIG. 300—Upper Diagram Is "Ratio of Variation" Obtained from Telluric Currents in Southern Sumatra. Lower diagram shows inferred depth to crystalline rocks. No horizontal scale given in original paper. (After M. Schlumberger.)

Even at a single locality, the character of the telluric currents is constantly changing because of diurnal variations and magnetic storms. It is necessary, therefore, to occupy a base station with which measurements made at a mobile station may be compared. The "preferential direction" of the currents is determined, as is the ratio of the intensity at the mobile station to the intensity at the base station. The telluric currents are influenced by inhomogeneities in the lithosphere; they avoid rocks of high resistivity, and tend to flow around them. If a circular, highly-resistant mass is at the surface of the earth, the telluric currents flow around it. If a lump of resistant mate-

<sup>17</sup> Schlumberger, M., The application of telluric currents to surface prospecting: *Transactions American Geophysical Union*, pt. 3, pp. 271-280, 1939.

rial is at the depth, the currents not only go around it, but also rise over it.

One of the few applications of this method has been in a study of Alsatian salt domes, which affect both the trend and the intensity of the telluric currents.<sup>18</sup> In southern Sumatra, the depth of the crystalline basement rocks is excellently portrayed by this method. In Fig. 300,<sup>19</sup> the curve in the upper diagram represents the intensity of the currents. The horizontal scale is distance along the profile; the vertical scale gives the ratio of the intensity of the telluric field at each station relative to the intensity at the base station. High ratios correspond to anticlines, low ratios indicate synclines. The inferred depth to the crystalline basement rocks is presented in the lower diagram.

### Artificial currents

**Principles.** In most electrical methods, the ground is artificially energized, either by direct introduction of currents or by induction. The power may be provided from available power lines or by mobile generators.

**Potential profile and equipotential line methods.** Direct current is introduced by two electrodes known as the *power pegs* or *current electrodes*, which may be iron pegs or coils of copper wire. These two electrodes should be on a line parallel to the strike of the strata, if such information is available, and should be a mile or more apart. If the field were homogeneous, the current flow lines and the equipotential lines would be symmetrically distributed about the two electrodes, as in Fig. 296. If, however, bodies of unusually low or unusually high resistivity are present, the flow lines and equipotential lines are distorted. The *potential profile* or *equipotential lines* may be surveyed in the same way as is outlined above for spontaneous currents; two electrodes, known as reading pegs, are used in the same way that they are used for spontaneous currents. If alternating current is used, it is introduced into the ground by point electrodes or by line electrodes, which are usually uninsulated copper wire 2000 to 2500 feet long, placed about 2000 to 2500 feet apart.

This method may be used to detect ore bodies, which distort

<sup>18,19</sup> Schlumberger, M., *op. cit.*

the equipotential lines. The equipotential lines form ellipses parallel to the strike of steeply dipping strata.

**Resistivity methods.** These methods are particularly suitable for horizontal or gently dipping beds. The resistivity, defined on p. 389, can be calculated if the current and potential are known. Two current electrodes introduce the energy to the ground, but the number and arrangement of the reading electrodes vary with different methods. In the Wenner-Gish-Rooney method, two additional electrodes are placed in line

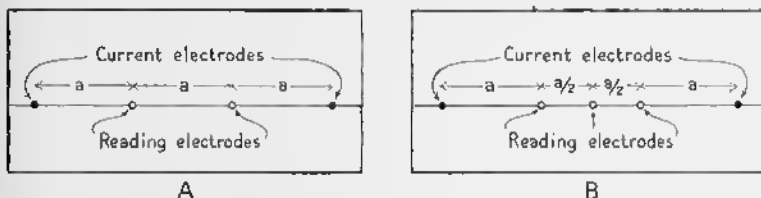


FIG. 301—Arrangement of Current Electrodes and Reading Electrodes in Two Different Resistivity Methods. A. Wenner-Gish-Rooney method. B. Lee partitioning method.

with the current electrodes, and all four electrodes are the same distance apart (Fig. 301A).

$$\rho = 2\pi a \frac{V}{I}. \quad (18)$$

In this equation  $\rho$  = resistivity in ohms per unit distance;  $a$  = distance between electrodes;  $V$  = difference in potential between two inner electrodes; and  $I$  is the current.

In the Lee partitioning method, a fifth electrode is placed half way between the middle electrodes (Fig. 301B).

$$\rho = 4\pi a \frac{Vc}{I}. \quad (19)$$

Here  $Vc$  = difference in potential between the central electrode and either adjacent electrode; other terms are as in equation 18.

There are several other methods for measuring resistivity.

The greater the interval between the power electrodes, the greater is the depth of penetration, which is essentially equal to the distance  $a$  (Fig. 301). As  $a$  is increased, a layer of contrasting resistivity may be penetrated. In such cases, the *apparent resistivity* is measured at the surface. By calculations

and graphs, it is possible to determine the depth to the lower layer, and to determine the true resistivities of the upper and lower layer. The problem can also be solved for three horizontal layers. Even if the beds are dipping, the depth to a stratum can be determined as long as the distance between the electrodes is less than one-half the depth. It is thus possible to make structure contours on subsurface horizons. If one or more drill holes are available, such a map can be related directly to the stratigraphy of the region.

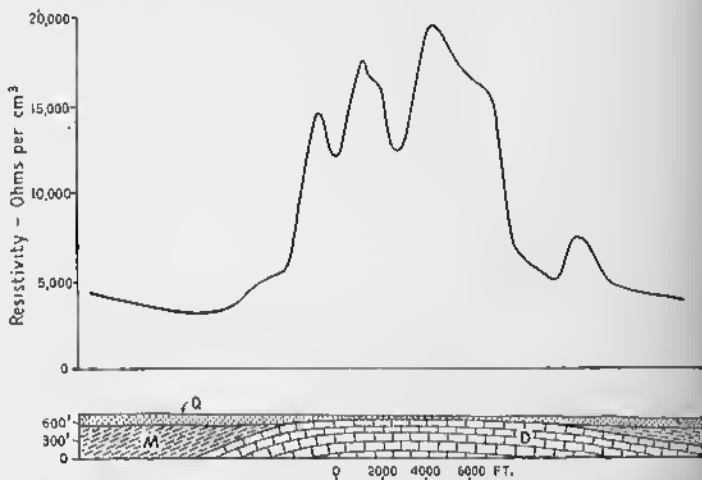


FIG. 302—Resistivity Profile Across an Anticline.  $D$  = Devonian limestone;  $M$  = Mississippian-Pennsylvanian shale and sandstone;  $G$  = glacial till. (After M. K. Hubbert, American Institute of Mining Metallurgical Engineers.)

Resistivity methods may be used either qualitatively or quantitatively in determining the geological structure. If the separation of the power electrodes is a constant value, variations in the resistivity indicate different kinds of rock at the same depth beneath the surface. Fig. 302 shows the influence of an anticline on the resistivity curve.<sup>20</sup> The resistivity of the Devonian limestone is much higher than that of the Mississippian and Pennsylvanian shale. If, however, an anticline brings up a formation of low resistivity, the curve would be the reverse

<sup>20</sup> Hubbert, M. K., Results of earth resistivity survey on various geologic structures in Illinois: *American Institute Mining Metallurgical Engineers, Transaction*, vol. 110, Geophysical Prospecting, pp. 9-39, 1934.

of that in Fig. 302. Salt has a high resistivity, and salt domes usually appear as resistivity highs; in some instances, however, the reverse is true, because strata of low resistivity lie directly above the dome. Many faults are zones of low resistivity because of electrolytes in the solutions along the fault. Formations of contrasting resistivity may be brought into contact along the fault, and this affects the resistivity curves.

Other electrical methods are the *potential-drop ratio method*, the *electromagnetic-galvanic methods*, and *electromagnetic-inductive methods*.

## LABORATORY EXERCISES

## EXERCISE 1

### Thickness and Depth of Strata

#### Introduction

It is essential in structural, stratigraphic, and economic problems to be able to calculate the thickness and depth of strata. A stratum is tabular in shape, like a sheet of paper. Strata may be horizontal, inclined, or vertical. The thickness is measured perpendicular to the plane of the bedding ( $t$  of Fig. 303). The depth is the vertical distance measured from any defined point on the surface of the earth to the top

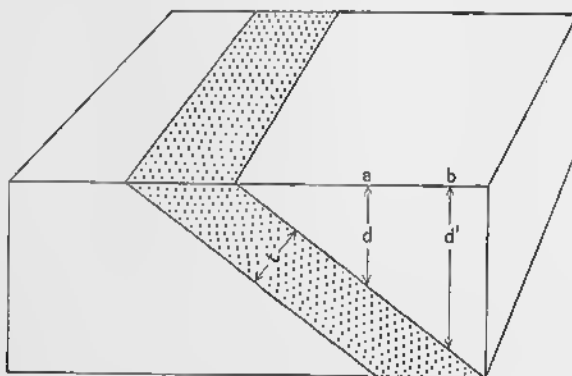


FIG. 303—Bed of Sandstone Shown by Dots; Shale above and below It Left Blank.  $t$  = Thickness of sandstone;  $d$  = depth of top of sandstone at point  $a$ ;  $d'$  = depth of top of sandstone at point  $b$ .

of the desired stratum. In Fig. 303,  $d$  is the depth at  $a$ , and  $d'$  is the depth at  $b$ .

If the whole stratum is favorably exposed in a cliff, the thickness may be measured directly by tape. Ordinarily, however, a direct measurement is impossible, and the thickness must be calculated by means of data obtained from a map, such as the top of the block in Fig. 303.

## EXERCISE 1

## Equations

The fundamental equations for calculating the thickness of beds and the depth of beds are given below. The derivation of some of the

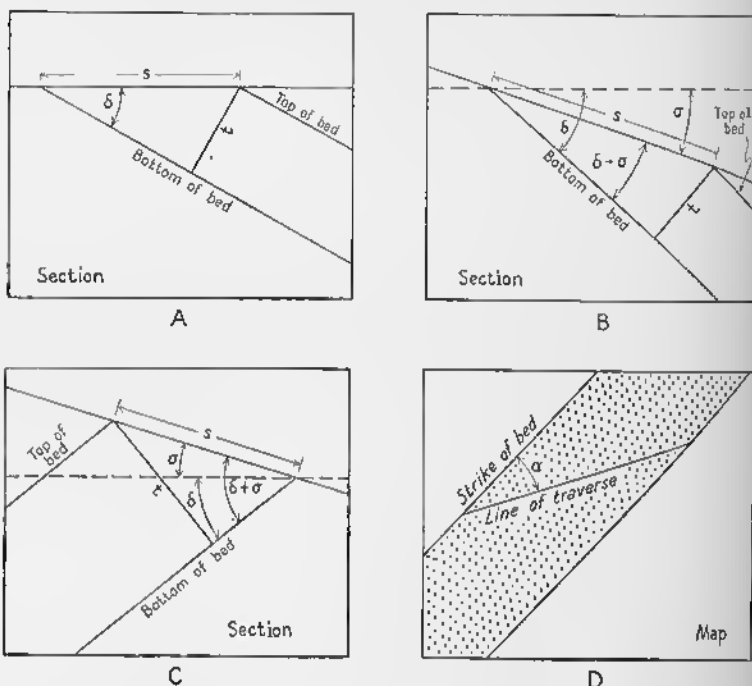


Fig. 304.—Measurement of Thickness.  $t$  = Thickness;  $\delta$  = angle of dip of bedding;  $s$  = slope distance between outcrop of top of bed and outcrop of bottom of bed;  $\sigma$  = angle of slope of ground;  $\alpha$  = angle between strike of bedding and trend of traverse. A. Ground horizontal. B. Bedding dips in same direction that ground slopes. C. Bedding dips in opposite direction to that in which ground slopes. D. Map for case in which traverse is not at right angles to strike of bedding.

simpler equations is given. For a more complete discussion the reader is referred to a series of papers by Palmer and Mertie.<sup>1</sup>

<sup>1</sup> Palmer, H. S., New graphic method for determining the depth and thickness of strata and the projection of dip, U. S. Geological Survey Professional Paper 120, pp. 122-128, 1918.

Mertie, J. B., Jr., Graphic and mechanical computation of thickness of strata and distance to a stratum, U. S. Geological Survey Professional Paper 129, pp. 39-52, 1922.

Mertie, J. B., Jr., Stratigraphic measurements in parallel folds, Bulletin Geological Society of America, Vol. 51, pp. 1107-1134, 1940.

**Case a**

Thickness, if the ground surface is horizontal, and if the breadth of outerop of the bed is measured at right angles to its strike. As shown in cross section in Fig. 304A,

$$\sin \delta = \frac{t}{s},$$

or

$$t = s \sin \delta, \quad (1)$$

where  $t$  = thickness of the bed,  $\delta$  = angle of dip of the bed, and  $s$  = breadth of the outcrop at right angles to the strike, measured along a horizontal surface.

**Case b**

Thickness, if the ground surface slopes in the same direction that the bed dips, and if the breadth of outcrop is measured at right angles to the strike of the bed. As shown in cross section in Fig. 304B,

$$\sin (\delta - \sigma) = \frac{t}{s},$$

or

$$t = s \sin (\delta - \sigma), \quad (2)$$

where  $t$  = thickness of bed,  $\delta$  = angle of dip of the bed,  $\sigma$  = angle of slope of the surface of the ground, and  $s$  = breadth of outcrop measured at right angles to the strike and along the surface of the ground, *not* the map distance.

**Case c**

Thickness, if the ground surface slopes in the opposite direction to that in which the bed dips, and if the breadth of outcrop is measured at right angles to the strike of the bed. As shown in a cross section in Fig. 304C,

$$\sin (\delta + \sigma) = \frac{t}{s},$$

or

$$t = s \sin (\delta + \sigma), \quad (3)$$

where symbols are the same as for equation (2).

**Case d**

Thickness, if the ground surface is sloping, and if the breadth of outcrop is not measured at right angles to the strike of the bed. A plan is shown in Fig. 304D.

$$t = s (\sin \delta \cos \sigma \sin \alpha + \sin \sigma \cos \delta), \quad (4)$$

and  $t = s (\sin \delta \cos \sigma \sin \alpha - \sin \sigma \cos \delta), \quad (5)$

where  $t$  = thickness,  $s$  = slope distance (*not* the map distance),  $\alpha$  = azimuth of traverse—that is, the horizontal angle between the strike of the stratum and the direction in which the slope distance is measured,  $\delta$  = dip of the bed, and  $\sigma$  = angle of slope of the surface of the ground in the direction of the traverse.

Equation (4) is used if the dip of the bed and the slope of the ground are in opposite directions. Equation (5) is used if the dip of the bed and the slope of the ground are in the same direction.

#### Case e

Depth, if the ground surface is horizontal, and if the distance is measured at right angles to the strike of the bed. As shown in a cross section in Fig. 305A, in which  $p$  is the point at which the depth is to be determined,

$$\tan \delta = \frac{d}{s}, \quad \text{or} \quad d = s \tan \delta, \quad (6)$$

where  $d$  = depth to the bed,  $\delta$  = angle of dip of the bed, and  $s$  = distance along surface of ground between the outcrop of the bed and the point at which the depth of the bed is to be calculated.

#### Case f

Depth, if the ground surface slopes in the same direction that the bed dips, and if the distance is measured at right angles to the strike of the bed. As shown by a cross section in Fig. 305B, in which  $p$  is the point at which the depth is to be determined,

$$\cos \sigma = \frac{x}{s}, \quad \text{and} \quad x = s \cos \sigma;$$

$$\sin \sigma = \frac{y}{s}, \quad \text{and} \quad y = s \sin \sigma;$$

$$\tan \delta = \frac{d + y}{x} = \frac{d + y}{s \cos \sigma}.$$

$$\begin{aligned} & d + y = s \cos \sigma \tan \delta, \\ \text{or} \quad & d + s \sin \sigma = s \cos \sigma \tan \delta, \\ \text{or} \quad & d = s \cos \sigma \tan \delta - s \sin \sigma, \\ \text{or} \quad & d = s (\cos \sigma \tan \delta - \sin \sigma), \end{aligned} \quad (7)$$

where  $d$  = depth,  $s$  = slope distance,  $\sigma$  = angle of slope, and  $\delta$  = angle of dip of bed.

## Case g

Depth, if the ground surface slopes in the opposite direction that the bed dips, and if the distance is measured at right angles to the strike

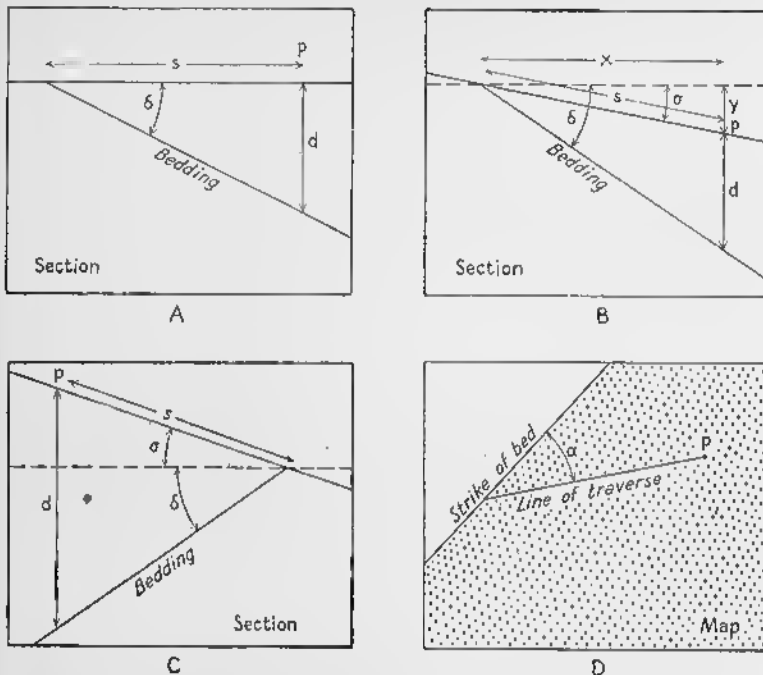


FIG. 305—Measurement of Depth to a Stratigraphic Horizon.  $d$  = Depth at point  $p$ ;  $\delta$  = angle dip of bedding;  $\sigma$  = angle of slope of ground;  $s$  = slope distance between outcrop of bed and point  $p$ ;  $\alpha$  = angle between strike of bedding and trend of traverse. A. Ground horizontal. B. Bedding dips in same direction that ground slopes. C. Bedding dips in opposite direction to that in which ground slopes. D. Map for case in which traverse is not at right angles to strike of bedding.

of the bed. From Fig. 305C, in which  $p$  is the point at which the depth is to be determined, the following equation may be derived:

$$d = s (\cos \sigma \tan \delta + \sin \sigma), \quad (8)$$

where the symbols have the same meaning as in equation (7).

## Case h

Depth, if the ground surface is sloping and the distance is not measured at right angles to the strike of the bed. A plan is shown in Fig. 305D;  $p$  is the point at which the depth is to be determined.

$$d = s (\tan \delta \cos \sigma \sin \alpha + \sin \sigma), \quad (9)$$

$$\text{and} \quad d = s (\tan \delta \cos \sigma \sin \alpha - \sin \sigma), \quad (10)$$

where  $d$  = depth,  $s$  = slope distance,  $\alpha$  = azimuth of traverse (that is, the horizontal angle between the strike of the bed and the direction of the traverse),  $\delta$  = dip of the bed, and  $\sigma$  = slope of the surface of the ground in the direction of the traverse.

Equation (9) is used if the dip of the beds and the slope of the ground are in opposite directions. Equation (10) is used if the dip of the bed and the slope of the ground are in the same direction.

### Diagrams to Scale

Solutions of the problems by the construction of diagrams to scale may be modeled after the diagrams in Figs. 304 and 305. A scale of 1 inch equals 200 feet should give sufficient accuracy for the problems at the end of this exercise.

### Alignment Diagrams

Figs. 306, 307, 308, and 309 are alignment diagrams. Figs. 306 and 307 may be used if the breadth of outcrop or distance perpendicular to the strike of the bed is known and if the ground is horizontal; Fig. 306 is for thickness, and Fig. 307 is for depth. In Fig. 306 a line drawn from the breadth of outcrop on the left-hand scale to the dip on the right-hand scale gives the thickness on the central scale. Fig. 307 is used in the same way to determine depth. These two diagrams may be used also where the ground is sloping if the breadth of outcrop perpendicular to the strike of the bedding is known. But "width of outcrop" on the diagram is the slope distance, and "dip" is the dip plus (or minus) the slope angle. If the bedding dips in the opposite direction to that in which the ground slopes, the slope angle is added to the dip; if the bedding dips in the same direction as that in which the ground slopes, the slope angle is subtracted from the dip.

Figs. 308 and 309 are more complicated diagrams and may be used for sloping ground where the breadth of outcrop is not measured perpendicular to the strike.

Using Fig. 308, the thickness diagram, we first locate a point which we may call  $a$  on the left-hand scale, on which "azimuth of traverse" means the angle between the strike of the beds and the line along which the breadth of outcrop is measured. Thus, if the breadth of outcrop is measured perpendicular to the strike of the beds, the "azimuth of traverse" is 90 degrees. If the strike of the beds is north, whereas the breadth of outcrop is measured in a northeasterly direction, the "azimuth of traverse" is 45 degrees. The upper half of the scale is used if the bed and the ground slope in opposite directions; the lower half of the scale is used if the bed and the ground slope in the same direction.

A second point, which for convenience we may call  $b$ , is located on the triangle near the center of the diagram. The intersection of the

angle of dip, given on the horizontal scale, and the angle of slope, given on the vertical scale, is located; this is point *b*.

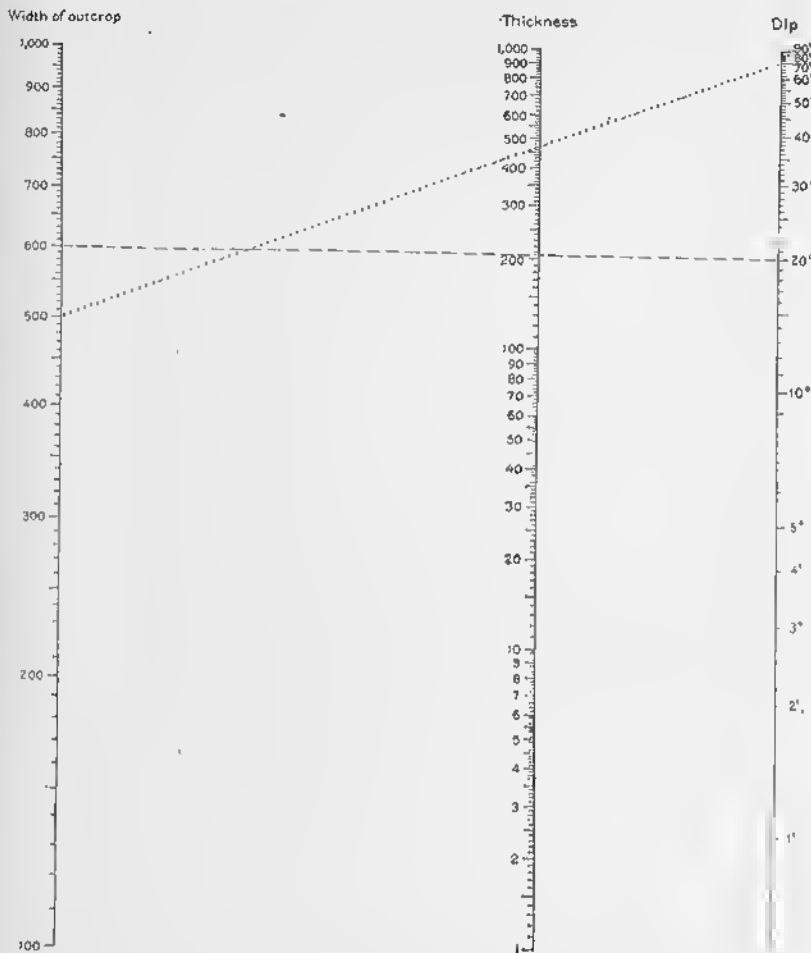


FIG. 306—Alignment Diagram for Computing Thickness. This form is to be used only where breadth (width) of outcrop is measured at right angles to strike of bed. If ground surface is horizontal, if width of outcrop is 500 feet, and if dip is 70 degrees, the thickness is 470 feet. If the ground surface is horizontal, if width of outcrop is 600 feet, and if dip is 20 degrees, the thickness is 205 feet. (After H. S. Palmer.)

A line drawn from *a* to *b* is extended to its intersection with the scale labeled *t'*. The point of intersection may be called *c*.

A new point, which we may call *d*, is located on the slope-distance scale; this point is the breadth of outcrop of the bed measured along the sloping surface of the ground. It is *not* the map distance, unless

## EXERCISE 1

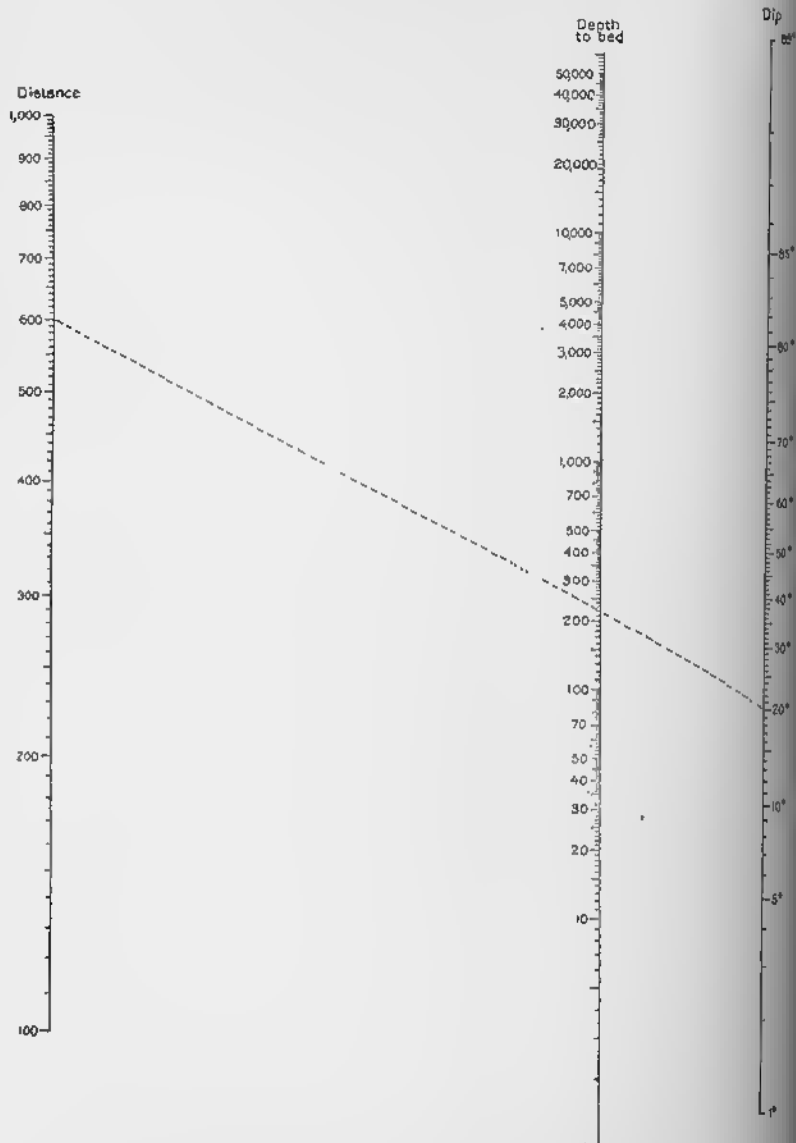


FIG. 307.—Alignment Diagram for Computing Depth to a Stratigraphic Horizon. This diagram is to be used only where distance to the outcrop of the horizon is measured at right angles to the strike of the horizon. If the ground surface is horizontal, if the distance to the outcrop is 600 feet, and if dip of bed is 20 degrees, the depth is 220 feet. (After H. S. Palmer.)

the surface of the ground is horizontal. If *c* is on the upper half of the diagram, *d* is likewise located on the upper half. If *c* is on the lower half, so is *d*.

A line connecting *c* and *d* is extended to intersect the right-hand vertical scale (*t* scale); this intersection is point *e*, which is the thickness of the bed. If points *c* and *d* are on the upper half of the diagram, read the *t* scale as though it were numbered from 0 at the top to 2000 at the bottom. If points *c* and *d* are on the lower half of the diagram, read the *t* scale as though it were numbered from 0 at the bottom to 2000 at the top.

The alignment chart for depth, Fig. 309, is used in a similar way.

### Problems

The student must submit for each problem a neat diagram showing the relations.

1. Determine the thickness of a shale that strikes N. and dips  $25^\circ$  E.; the breadth of outcrop, measured in an east-west direction, is 750 feet. The region is one of no relief. Solve this problem in the following order: (a) by construction of a diagram to scale; (b) by the alignment diagram in Fig. 306; (c) by the alignment diagram in Fig. 308; and (d) by the equation.
2. Determine the thickness of a sandstone that is exposed on the side of a mountain; the sandstone strikes N. and dips  $29^\circ$  W. The top of the sandstone is exposed at an altitude of 1625 feet, and the bottom is exposed at an altitude of 1200 feet. The distance between the top and bottom of the sandstone, measured along the slope and perpendicular to the strike, is 2830 feet. Solve in the following order: (a) by the alignment diagram in Fig. 306; (b) by the alignment diagram in Fig. 308; and (c) by the equation.
3. A stream flows in a southerly direction across a limestone that strikes N.  $90^\circ$  E. and dips  $30^\circ$  S. Determine the thickness of the limestone if the base of the limestone is exposed at an altitude of 4200 feet, and the top is exposed at an altitude of 3800 feet. The breadth of the limestone along the stream, as shown on a map, is 1500 feet. Solve in the following order: (a) by the alignment diagram in Fig. 306; (b) by the alignment diagram in Fig. 308; and (c) by the equation.
4. In a region of no relief a conglomerate strikes N.  $45^\circ$  W. and dips  $35^\circ$  NE. The top and bottom of the conglomerate are 3800 feet apart as measured along an east-west line on the surface. Calculate the thickness of the conglomerate in the following order: (a) by the alignment diagram in Fig. 306; (b) by the alignment diagram in Fig. 308; and (c) by the equation.
5. A stream flows N.  $50^\circ$  E. across a limestone that strikes N.  $10^\circ$  E. and dips  $33^\circ$  E. The base of the limestone is exposed in the stream

## EXERCISE 1

at an altitude of 2230 feet; the top of the limestone is exposed in the stream at an altitude of 1710 feet. The *map distance* between the top and bottom of the limestone, measured along the stream, is 2930 feet. Calculate the thickness of the limestone (a) by the alignment diagram in Fig. 308; and (b) by the equation.

6. The bedding in an exposure of a gold-bearing conglomerate strikes N. and dips  $25^\circ$  W. The surface of the ground is flat. At a distance of 800 feet west of the exposure, how deep a vertical shaft must be sunk to reach the conglomerate? Solve (a) by the alignment diagram in Fig. 307; (b) by the alignment diagram in Fig. 309; and (c) by the equation.

7. A bed of coal that strikes N.  $45^\circ$  E. and dips  $40^\circ$  NW., outcrops on a mountain at an altitude of 1500 feet. At an altitude of 1250 feet down the slope to the northwest a distance of 700 feet, measured perpendicular to the strike of the coal bed and along the slope, a vertical shaft is sunk to the coal bed. How deep must the shaft be? Solve (a) by the alignment diagram in Fig. 309; and (b) by the equation.

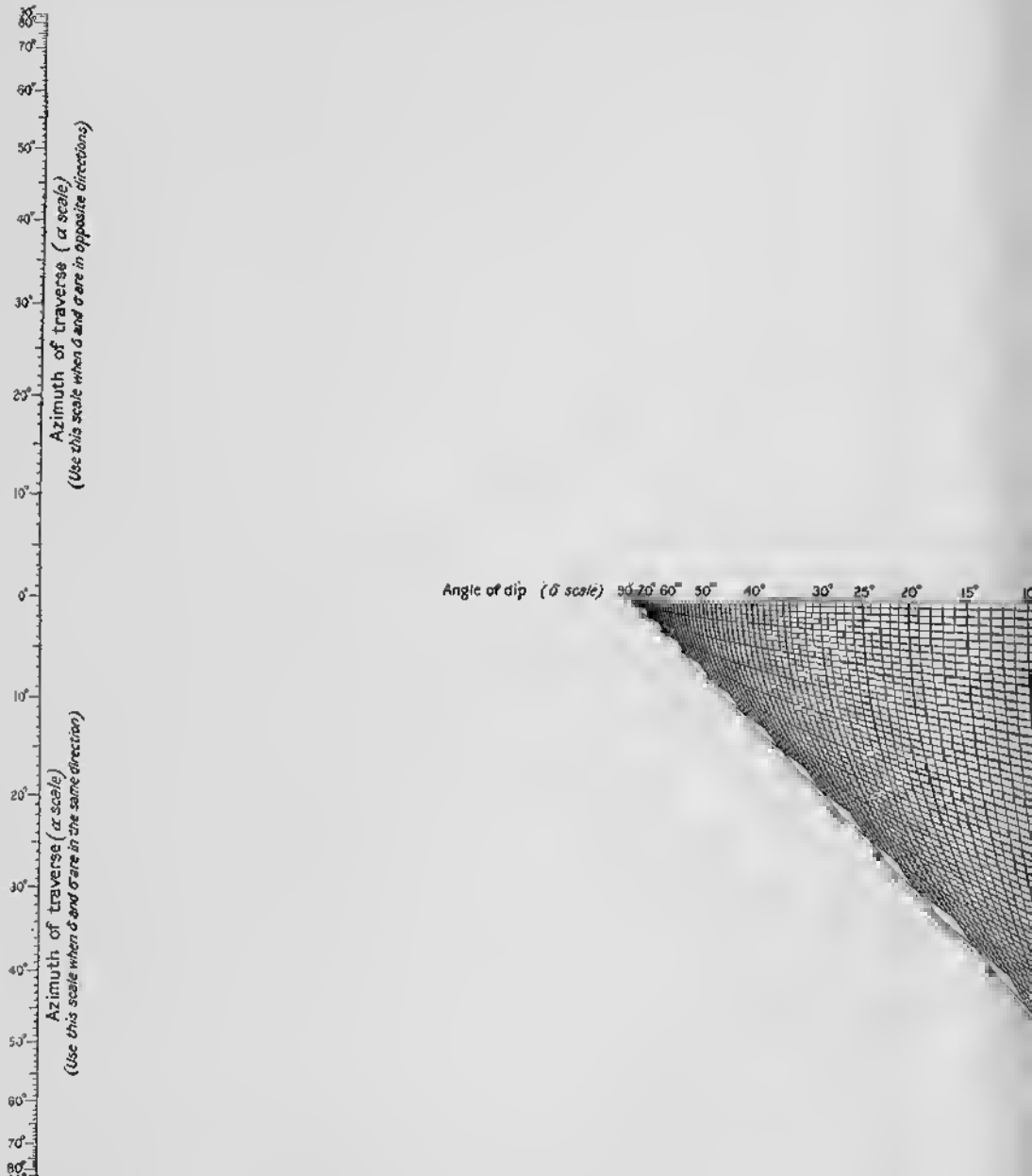
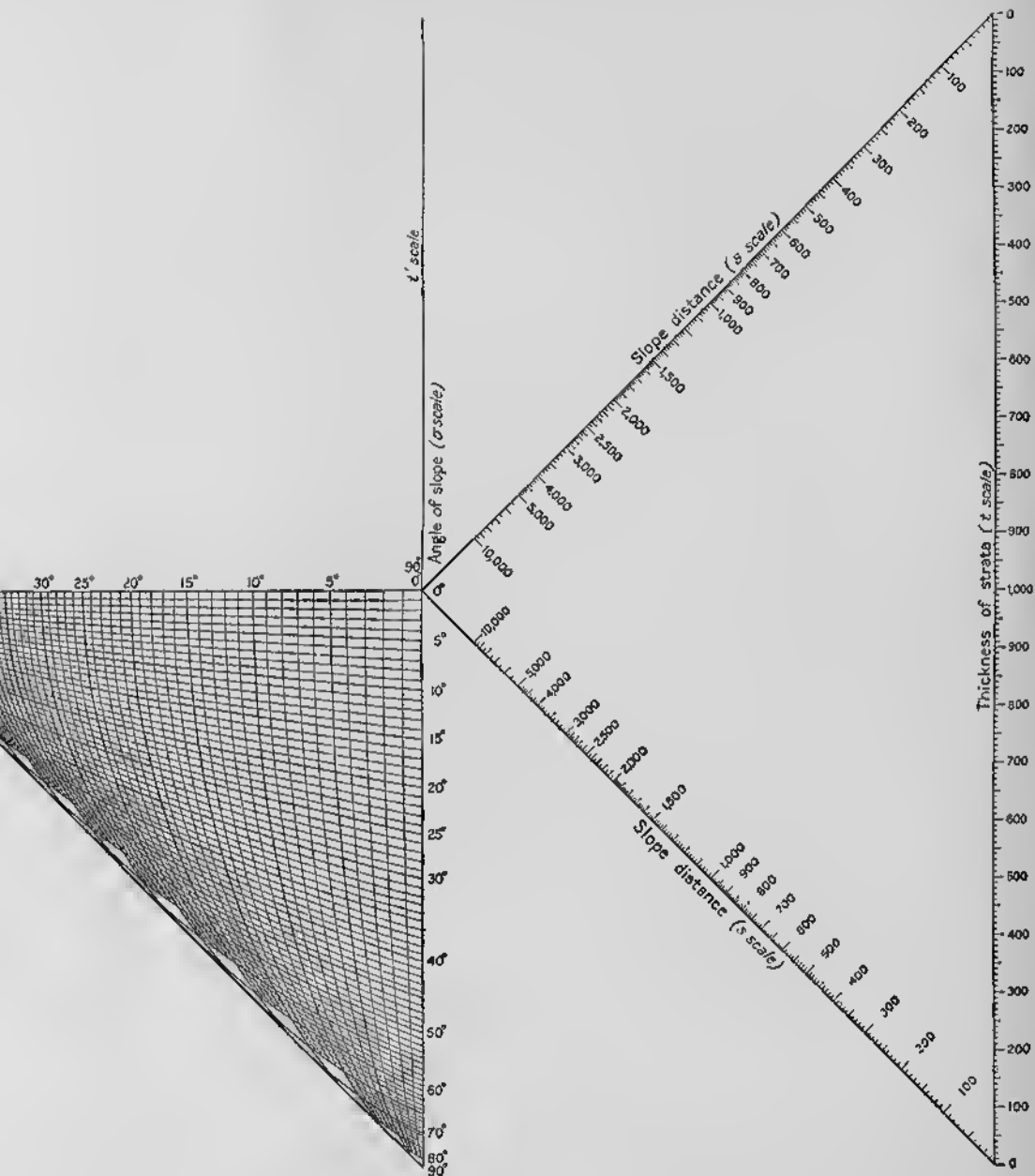


FIG. 308—Alignment Diagram for Computing Thickness. (See text for use.) In reading the right-hand scale labeled "Thickness of Strata," a special word of caution is necessary. If the scale is read from the bottom, the figures continue progressively upward beyond 1,000; that is, the 900 that is above 1,000 should be read as 1,100, the 800 that is above 1,000 should be read as 1,200, etc.; the 100 near the top of the

scale should be read from the bottom as 900 below the 1,000 mark.

Mertie, Jr.



or use.) In  
of caution is  
progressively  
is 1,100, the  
top of the

scale should be read as 1,900, and the 0 at the top should be read as 2,000. If the scale is read from the top, the figures continue progressively downward from 1,000; that is, the 900 below 1,000 is read as 1,100, etc.; 0 at the bottom is read as 2,000. (After J. B. Mertie, Jr.)

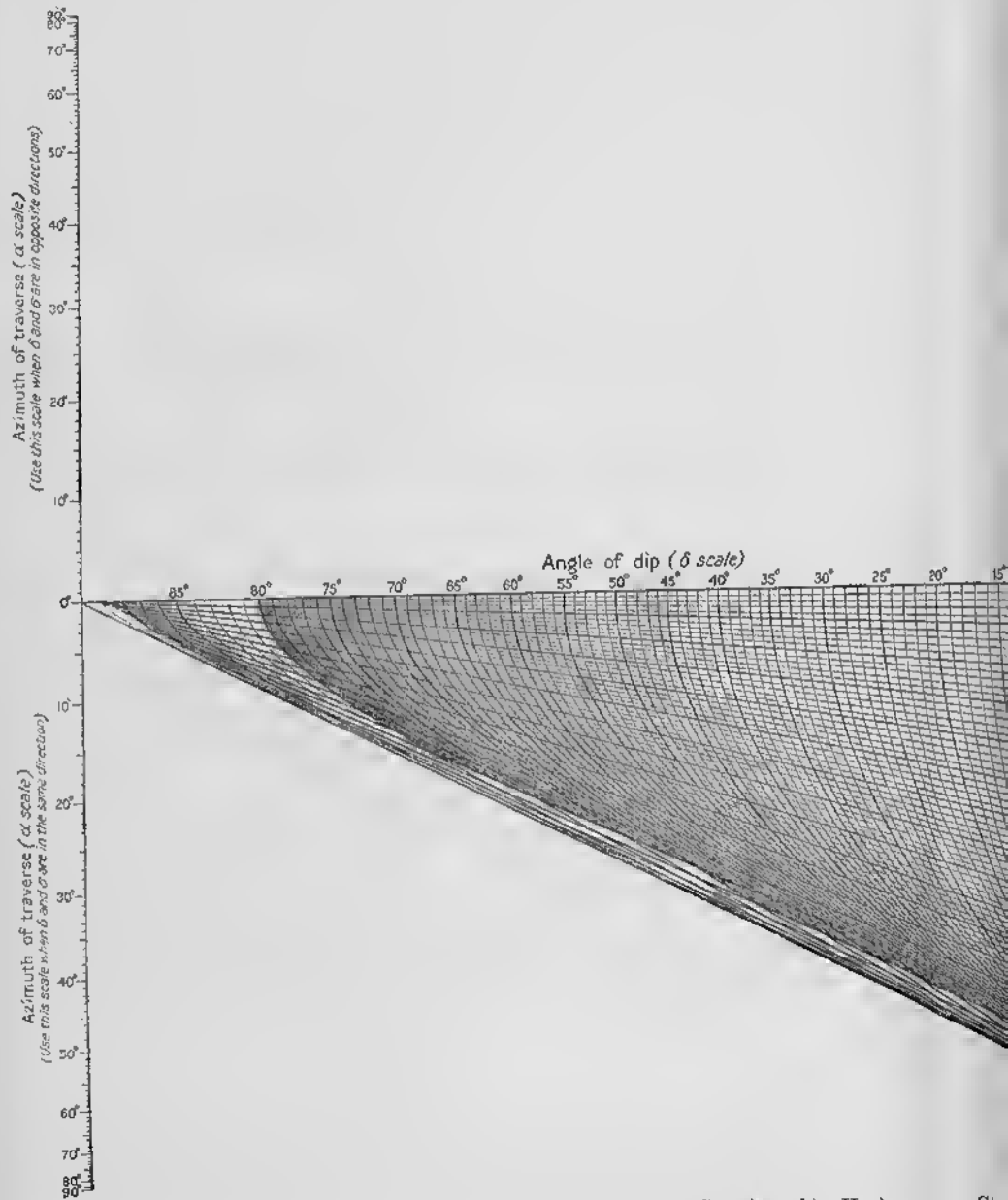
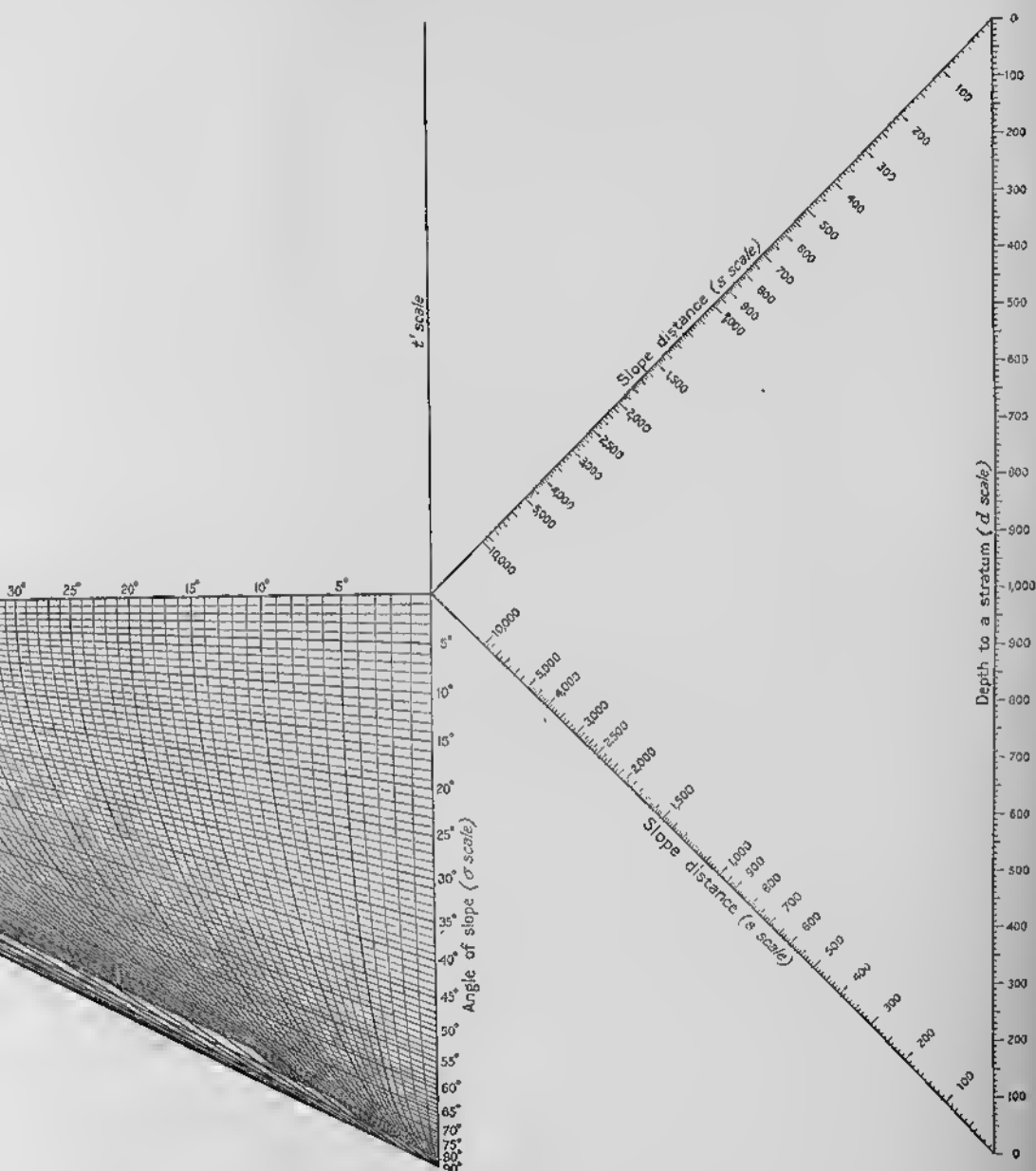


FIG. 309—Alignment Diagram for Computing Depth to a Stratigraphic Horizon (stratum). (See text for use.) For reading the right-hand scale labeled "Depth to"



"Stratum," see legend under Fig. 308. (After J. B. Mertie, Jr.)

## EXERCISE 2

### Outcrop Pattern of Horizontal and Vertical Strata

#### Patterns

If the strata in an area are horizontal, each stratigraphic horizon,<sup>1</sup> such as the top or bottom of a bed, occurs everywhere at the same altitude. Horizontal beds are shown in Fig. 53A. The outcrop of the top or bottom of a horizontal bed thus follows topographic contours. The width of outcrop of a horizontal bed depends upon the thickness of the bed and upon the topography. The width of outcrop of a bed is greatest where the slopes are gentle—that is, where the contours are far apart.

The relation between the attitude of a bed, the outcrop pattern displayed by the bed, and the topography may be remembered by the "rule of V's." This rule states in part that the outcrop of a horizontal bed forms a V as it crosses a valley and that the apex of the V points upstream (formation shown by circles in Fig. 53A). The top and bottom contacts of the bed are parallel to topographic contours.

If an horizon is exposed at one place in a region of horizontal beds, it is obviously possible to predict the location of the horizon everywhere else on the map. If the known exposure of the horizon coincides with a contour, the location and the pattern of the horizon will be identical with that of the contour. If the altitude of the exposure of the horizon falls between two contours, interpolation is necessary in order to locate the position of the horizon on the map. In regions of low relief the error of the predicted location may be considerable.

The top and bottom of a vertical bed will appear on the map as straight lines parallel to the strike of the bed. Topography has no control on the outcrop pattern of vertical beds. The outcrop pattern of a vertical bed is shown in Fig. 53B.

#### Structure Sections

Structure sections show the geological structure as it would appear on the sides of an imaginary vertical trench cut into the earth. Sometimes they portray the structure as observed on vertical cliffs, in highway cuts, or in mine openings. More commonly they are predictions based on exposures at the surface of the earth. Consequently they are only an approximation to the truth, their precision depending

<sup>1</sup> *Horizon* is used in this book to refer to a surface having no thickness.

upon the simplicity of the structure, the number of exposures, and the skill of the geologist.

In regions of low relief the surface of the earth may be represented by a straight line, but ordinarily the top of the structure section shows the topography. The first step, therefore, in preparing a structure section is to make a topographic profile. Such a profile is prepared from the topographic map in the following way. In Fig. 310A the structure section is to be made along the line AB. A strip of blank paper is laid across the topographic map, the top of the strip coinciding with the line of the section. A mark is made on this strip of paper at each place that a contour crosses the line of the section. The altitude represented by each of these marks may be written on the strip.

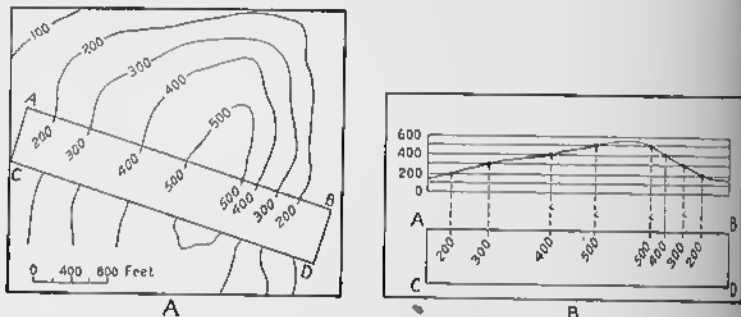


FIG. 310—Preparation of Topographic Profile. A. Line AB is line along which profile is to be made. ABCD is strip of blank paper laid over topographic map. B. Plotting profile; scale along left side of profile is same as horizontal scale of the map.

A base on which to plot the profile is then prepared, as shown in the upper part of Fig. 310B. The horizontal scale is the same as that of the map. The altitude above sea level of each horizontal line is written on this diagram; each line thus corresponds to a contour. Generally the vertical scale should be the same as the horizontal scale; otherwise the geological structure becomes distorted. If the strata are horizontal, however, it is sometimes necessary to exaggerate the vertical scale.

The strip of paper prepared from the topographic map is then placed under the diagram (Fig. 310B). Each pencil mark on the strip is then projected upward to the appropriate altitude line and a dot is made. These dots are then connected by a smooth line to make the topographic profile.

To add the geology to the profile, place a new strip of paper along the line of the section on the map and make a pencil mark wherever a geologic contact crosses the line of section. This strip is then placed beneath the topographic profile, and the contacts are projected vertically upward to the profile. If the beds are horizontal, horizontal

lines drawn through these points are the geological contacts in the profile.

#### Problems

1. In Fig. 312 assume that the top of a horizontal bed of sandstone 150 feet thick is exposed on the east side of Bear Mountain at an altitude of 1700 feet. Color in blue (inking the contacts) those parts of the area in which the sandstone constitutes the surface formation.
2. In Fig. 312 assume that the base of a series of vertical limestone beds 1302 feet thick is exposed at bench mark 1342 near the northwest corner of the map. The rocks strike N.  $70^{\circ}$  W. and are younger toward the southwest. Color in red (inking the contacts) that part of the area in which the limestone outcrops.
3. In Fig. 311 different patterns are used to show various geological formations. (a) What is the attitude of the strata? (b) Describe briefly the outcrop pattern. (c) Draw a topographic profile and geologic section along the line *AB*.

If the instructor desires, he may use one or more of the following folios of the Geological Atlas of the United States, published by the U. S. Geological Survey: 200, Galena-Elizabeth, Illinois-Iowa; 109, Cottonwood Falls, Kansas; 208, Colchester-Macomb, Illinois; 206, Leavenworth-Smithville, Missouri-Kansas; 87, Camp Clarke, Nebraska; 202, Eureka Springs-Harrison, Arkansas-Missouri; 176, Sewickley, Pennsylvania; 178, Foxburg-Clarion, Pennsylvania.

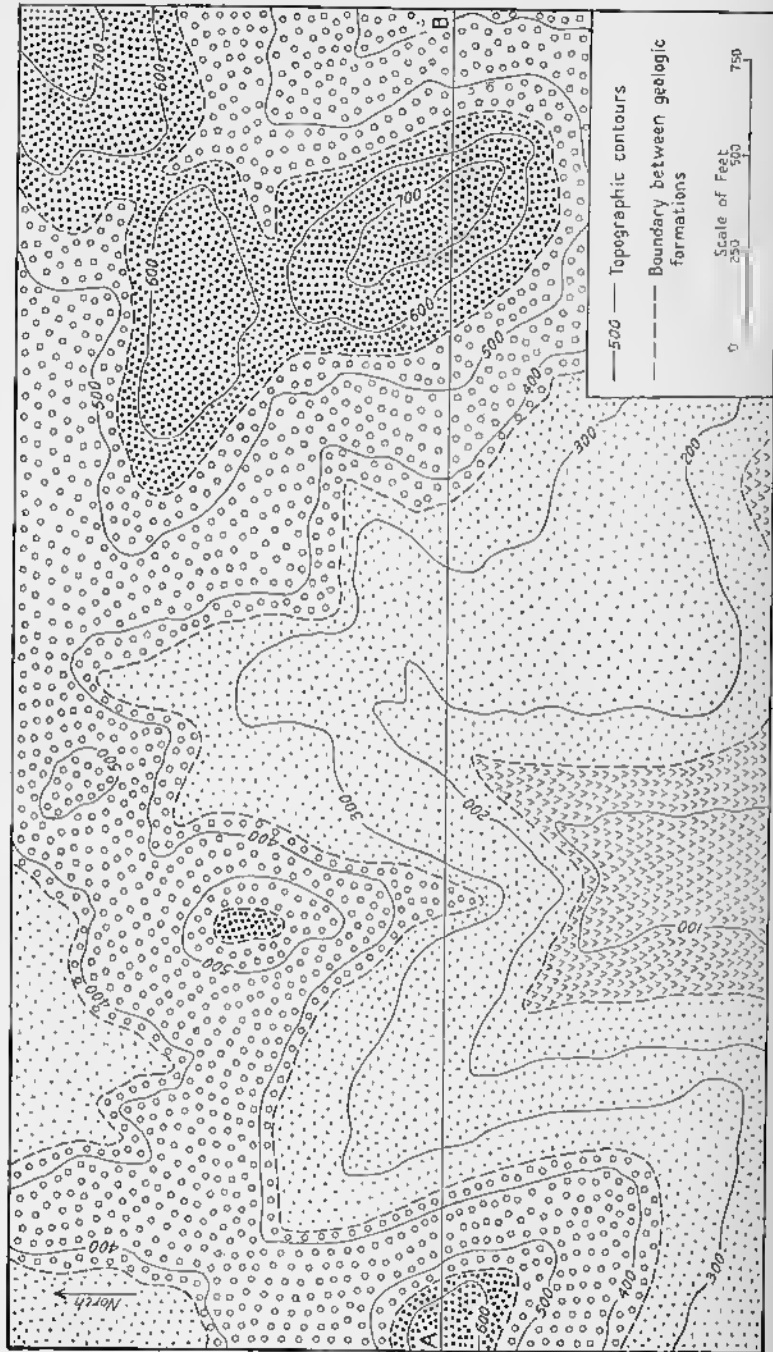


Fig. 311.—Geologic Map for Problem in Exercise 2. Checks = basalt; small dots = sandstone; circles = conchomerite; heavy dots = volcanic tuff.

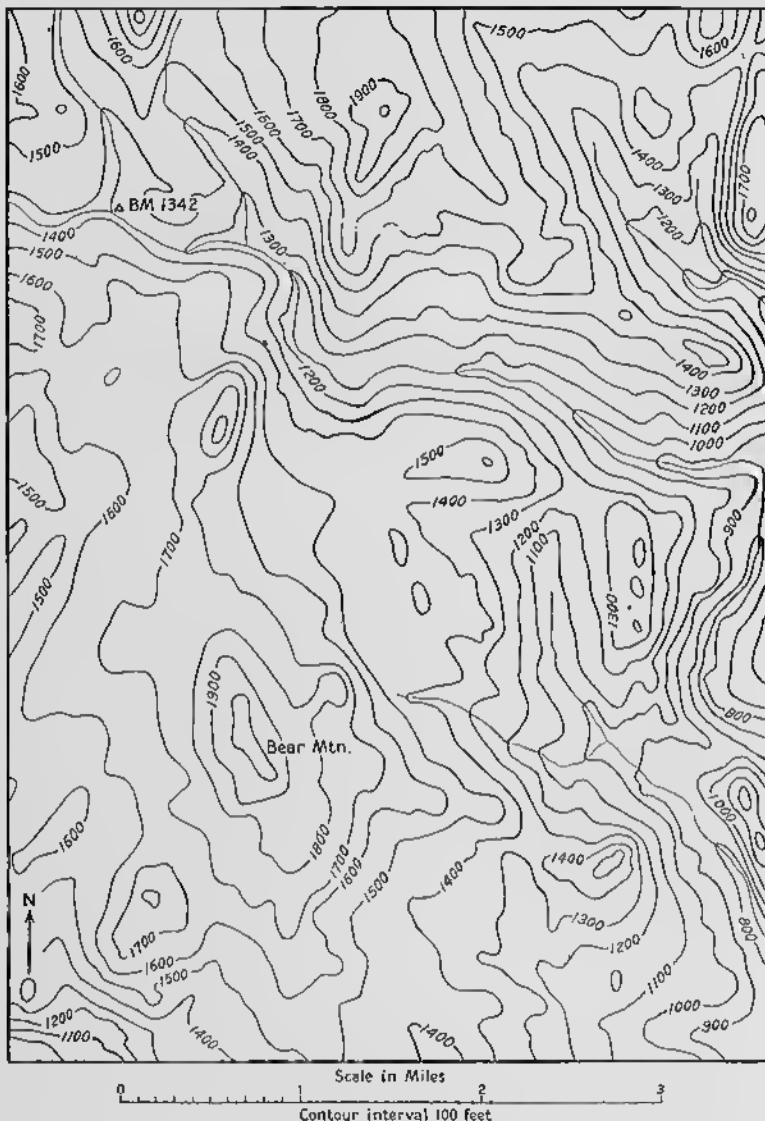


FIG. 312—Topographic Map for Problems in Exercise 2.

## EXERCISE 3

### Patterns of Dipping Strata; Three-point Problems

#### Rule of V's

It has been shown in Exercise 2 that the contacts of horizontal beds follow topographic contour lines, and that wherever such strata cross a valley their outcrop pattern forms a *V* that points upstream. It was also shown that topography has no influence on the pattern of vertical beds whose outcrop pattern forms straight lines parallel to the strike of the beds.

The outcrop pattern of beds that dip upstream forms a *V* whose apex is upstream, as shown in Fig. 54. The contacts of the bed are not parallel to topographic contours. Fig. 313A shows the same thing. The horizon, known to outcrop at *a* and *b*, strikes N. 90° E. and dips 11.3° N.; that is, it drops 20 feet vertically every 100 feet horizontally. The heavy line shows the expected outcrop pattern.

The outcrop pattern of beds that dip downstream at an angle greater than the stream gradient forms a *V* the apex of which points downstream. In Fig. 313B let us assume that an horizon strikes N. 90° E. and dips downstream at an angle of 11.3 degrees; that is, it drops 10 feet vertically every 50 feet horizontally. Moreover, the stream gradient is 10 feet vertically every 100 feet horizontally. If the horizon is known to outcrop at *c* and *d*, the heavy line shows the predicted outcrop pattern.

The outcrop pattern of beds that dip downstream at an angle less than the gradient of the stream forms a *V* the apex of which points upstream. The contacts of the beds are not parallel to topographic contours. In Fig. 313C let us assume that the horizon strikes N. 90° E. and dips south (downstream) at an angle of 5.7 degrees; that is, it drops 10 feet vertically every 100 feet horizontally. Moreover, the stream gradient is 10 feet vertically every 50 feet horizontally. If the horizon outcrops at *e* and *f*, the heavy line shows the predicted outcrop pattern.

Application of the rule of *V*'s to geological maps enables one to determine the approximate dip of beds from the outcrop patterns. By use of the three-point method, which will be described later, it is possible to determine the value of the dip with considerable precision.

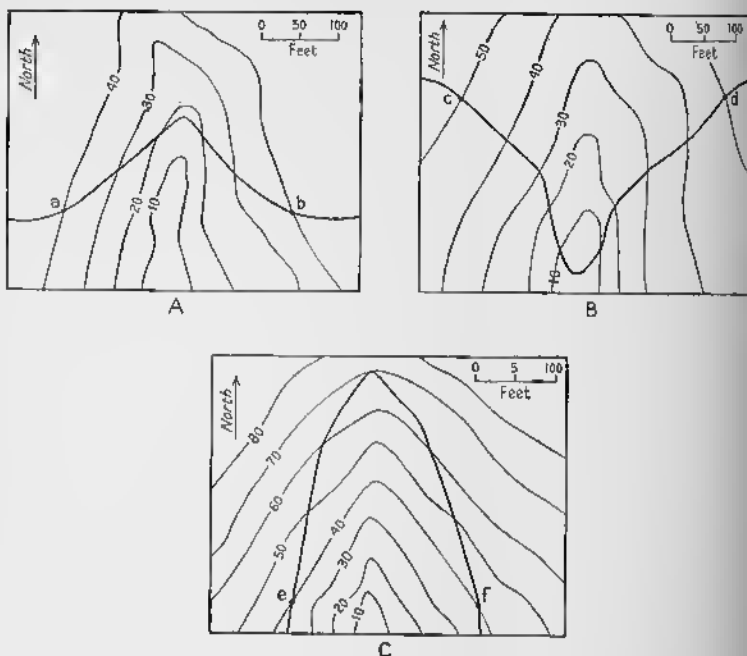


FIG. 313—Rule of V's (see text).

### Outcrop Pattern of Dipping Bed

The outcrop pattern of an horizon can be predicted if a contour map showing the topography is available, if the dip and strike of the horizon are known, and if the location of one exposure of the horizon is given. This is possible, however, only if the horizon is truly a plane surface—that is, if its dip and strike are constant.

Fig. 314 illustrates the procedure that may be followed. The horizon outcrops at  $X$ . The ground surface is represented by 100-foot contours. Inasmuch as the horizon is known to strike N.  $90^\circ$  E. and to dip  $20^\circ$  S., it is possible to predict its position at any place in the area. The position of the horizon may be represented by structure contours, which are more fully described in Exercise 6.

Draw the line  $SS'$  through the outcrop,  $X$ , parallel to the strike of the horizon (N.  $90^\circ$  E.). Inasmuch as the outcrop is at an altitude of 800 feet, at every place on this line the horizon has an altitude of 800 feet. Now make a vertical section at right angles to the strike by drawing  $AB$  perpendicular to the strike of the bed at any convenient distance from the map. The intersection of  $AB$  and  $SS'$  may be designated by  $C$ . At  $C$  lay off the angle  $BCE$  equal to the dip of the horizon, in this instance 20 degrees.  $CE$  is the trace of the horizon on the vertical section. Along  $SS'$  from point  $C$  lay off 100-foot units

(equal to the topographic contour interval), using the same scale as that of the map.

Through each 100-foot point above or below *C* draw a line parallel to *AB* to an intersection with line *CE*. The intersections are points on the bedding plane; they are 100 feet apart vertically. From each of these intersections draw lines parallel to *SS'*. These lines are 100-foot structure contours on the horizon. At each point where a structure contour intersects a topographic contour of the same altitude the horizon will outcrop. The locations of these intersections have been

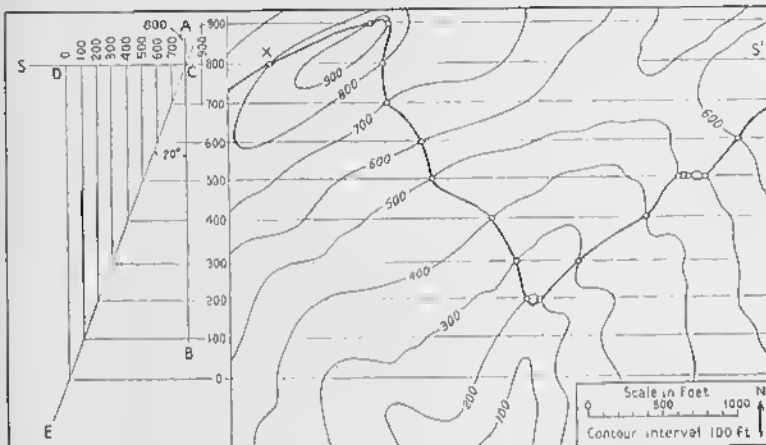


FIG. 314—Prediction of Outcrop Pattern. If a stratigraphic horizon at *X* strikes N.,  $90^\circ$ E. and dips  $20^\circ$ S., the expected outcrop pattern is shown by the heavy line passing through the open circles.

marked by small circles. Connecting these circles, as shown in Fig. 314, shows the predicted outcrop pattern.

### Three-Point Problems

The method of working a three-point problem is the opposite of constructing an outcrop pattern. It is possible to calculate the dip and strike of a horizon if the location and altitude of three points on that horizon are known and if the horizon is truly a plane and not a warped surface.

A simple illustration of a three-point problem will be given first. Fig. 315A is a map giving the location and altitude of three points on an horizon; these points are *A*, *B*, and *C*. Inasmuch as the strike of any plane is a line connecting points of equal altitude on that plane, line *AB* is the strike of the horizon under consideration, because *A* and *B* are at the same altitude. The dip is measured at right angles to the strike, and in this case it is toward the southeast. A perpendicular is dropped from *C* to *AB*, the intersection being labeled *D*. To find the

value of the dip a vertical triangle is rotated to the surface around  $DC$  as an axis.  $CF$  is erected perpendicular to  $DC$ . The difference in altitude between points  $C$  and  $D$ , 600 feet, is set off, on the same scale as the map, along the line  $CE$ . The angle  $CDE$  is the dip of the horizon.

A more general problem is illustrated by Fig. 315B. The location and altitude of three points on the horizon are shown. Some point, to be determined, between points  $B$  and  $C$ , will have the same altitude as  $A$  (1050 feet); a line connecting that point with  $A$  will be the strike of the horizon. The unknown point can be located by proportion:

$$\frac{\text{Altitude of } A \text{ minus altitude of } B}{\text{Altitude of } C \text{ minus altitude of } B} = \frac{\text{Distance } BD}{\text{Distance } BC},$$

where  $D$  is the point we wish to find. Solving the equation, we obtain  $BD = 1100$  feet. This distance is set off from point  $B$  using the same scale as the map.  $AD$  is the strike of the horizon. The dip may be found in the same way as in Fig. 315A.

### Problems

1. Fig. 316 is a topographic map on which two geologic horizons are shown, one by a broken line and the other by a dotted line. In the vicinity of point  $a$  what is the attitude of the horizon shown by the broken line?
2. In Fig. 316 what is the attitude of this same horizon in the vicinity of  $b$ ?
3. In Fig. 316 what is the attitude of the horizon shown by the dotted line in the vicinity of  $c$ ?
4. In Fig. 316 what is the attitude of this same bed along the whole line that passes through  $d$ ?
5. In Fig. 317 assume that at 3000 feet at the north end of the summit of Bald Mountain the base of a bed of limestone which strikes N.  $90^\circ$  E. and dips  $10^\circ$  N. is exposed. Draw on the map the outcrop pattern of the base of the limestone.
6. In Fig. 317 assume that the base of a bed of sandstone is exposed on top of the westernmost knob of Bickford Mountain, at the  $X$  on Gale River marked 1160, and at B. M. 990. Find the dip and strike of this bed by the three-point method, assuming that the bed is a perfect plane.
7. In Fig. 317 assume that a trap dike, with an east-west strike, is exposed on top of Scrag Hill at an elevation of 1780 feet, and that the same dike also outcrops on Gale River at the  $X$  marked 1040 feet. What is the dip of the dike?

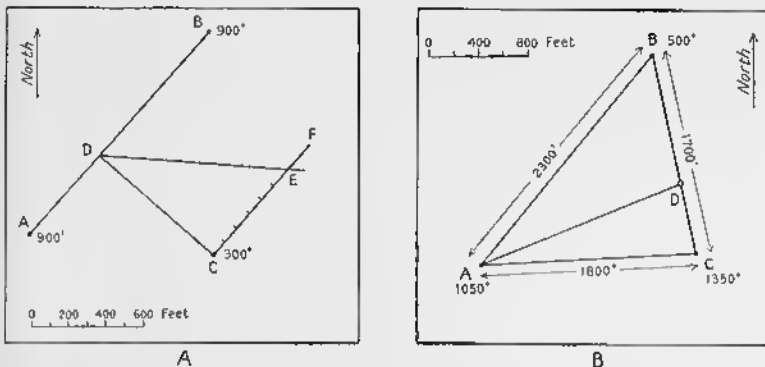


FIG. 315—Three-point Method. Location and altitude of a plane surface at *A*, *B*, and *C* are given. Dip and strike of the surface can be determined.

8. In Fig. 317 assume that a vertical quartz vein striking N.  $20^\circ$  E. is exposed on Meadow Brook at an altitude of 1400 feet. It is expected that an ore shoot will be found at the intersection of this vein with the base of the limestone that outcrops on Bald Mountain. Indicate where on the map one should look for the outcrop of the ore shoot.

9. In Fig. 317 how deep a vertical shaft, sunk from the top of Bickford Mountain, would be necessary in order to intersect the base of the limestone?

If the instructor desires, he may use one or more of the following folios of the Geological Atlas of the United States, published by the U. S. Geological Survey: 142, Cloud Peak—Fort McKinney, Wyoming; 56, Little Belt Mountains, Montana; 174, Johnstown, Pennsylvania; 175, Birmingham, Alabama; 153, Ouray, Colorado; 141, Bald Mountain—Dayton, Wyoming.

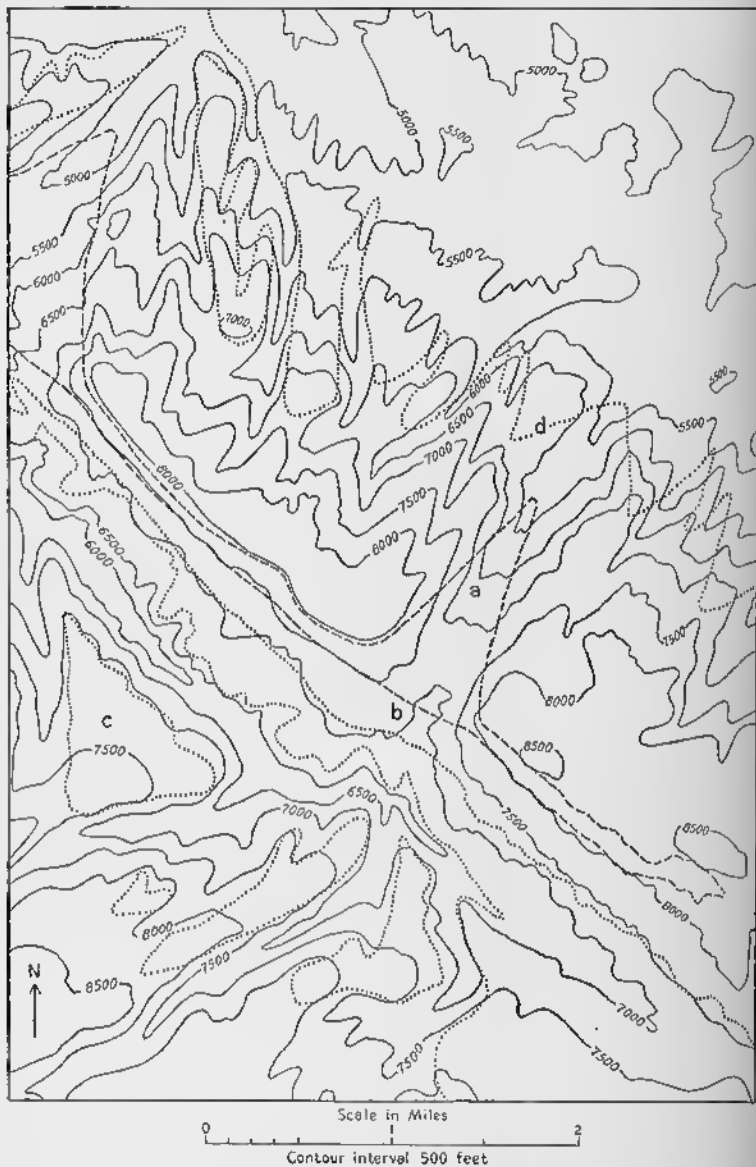


FIG. 316—Topographic Map for Use in Problems in Exercise 3. Dotted line is base of Amsden formation; broken line is base of Big Horn limestone. (Folio No. 141, U. S. Geological Survey.)

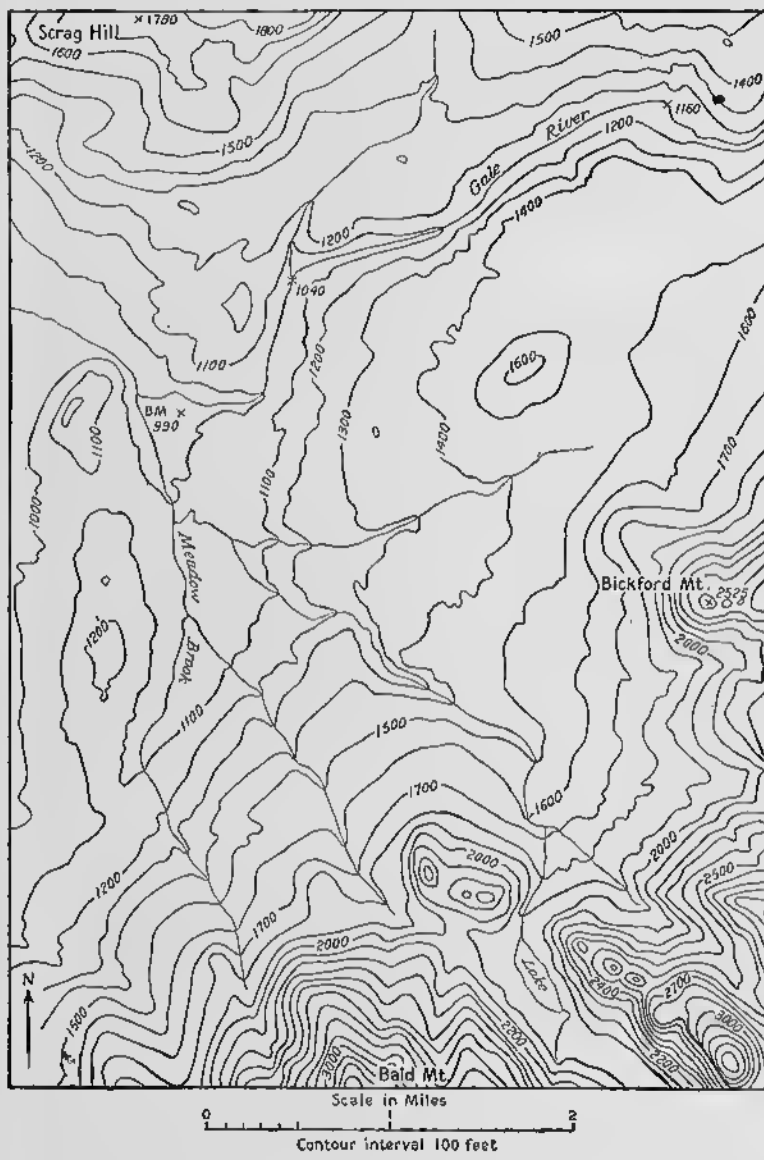


FIG. 317—Topographic Map for Use in Problems in Exercise 3. Part of Franconia quadrangle, New Hampshire.

## EXERCISE 4

### Structure Sections of Folded Strata

#### Method

In the preparation of structure sections the topographic profile is prepared as indicated in Exercise 2. The contacts between geologic formations are also transferred in the manner indicated.

If the structure section that is to be constructed is approximately at right angles to the general trend of the structure, dips can be used as they appear on the map without any correction. The strike-dip symbols on the map are seldom located right on the line of the structure section. How close a symbol must be in order to be used depends upon the complexity of the geology. In regions in which the structure is simple, symbols a mile or so away may be used. The student should use a protractor in laying off the dips on the structure section.

The depth of the section depends on many variables. In this exercise it is suggested that they go to about half a mile below sea level. The beds should be connected above the ground surface by broken lines in order to emphasize the structure. Care must be taken to connect the horizons properly. The thickness of a formation should be approximately constant throughout the section.

A title, a legend, the scale, and the orientation should appear on the structure sections.

If the strike of a bed is not at right angles to the strike of the structure section, the apparent dip in the structure section is not the same as the true dip. If the strike of the bed is within 10 or 20 degrees of perpendicular to the strike of the structure section, the discrepancy ordinarily may be neglected.

The apparent dip of a bed in any desired direction may be calculated from the true dip by the equation

$$\tan \rho = \tan \delta \sin \alpha,$$

where  $\rho$  is the apparent dip on a vertical plane,  $\delta$  is the true dip, and  $\alpha$  is the angle between the strike of the bed and the direction of the apparent dip.

Ordinarily the apparent dip can be determined with sufficient precision by using the alignment diagram of Fig. 318. The true dip is given on the left-hand scale; the angle between the strike of the bed and the strike of the vertical section upon which the apparent dip is

## EXERCISE 4

plotted is given in the right-hand scale. A line connecting the points on these two scales gives the apparent dip on the central scale.

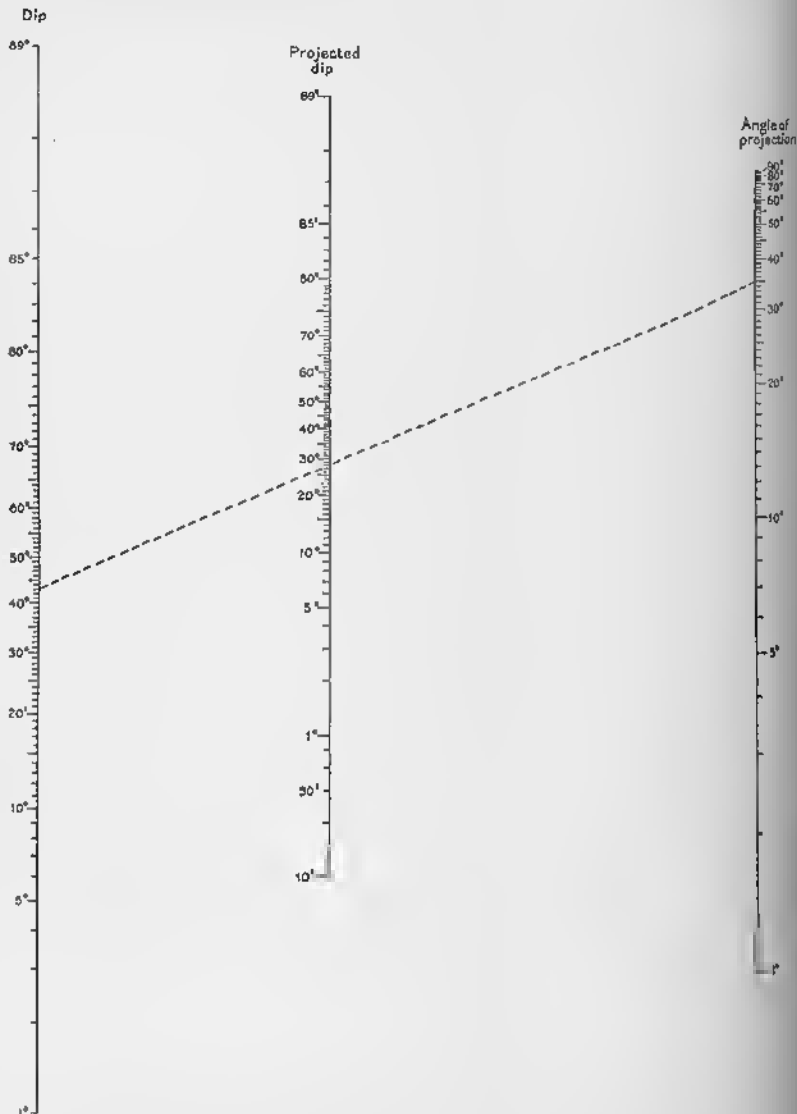


FIG. 318—Alignment Diagram for Computing Apparent Dip (Projected Dip). If true dip is  $43^\circ$ , the apparent dip on a vertical section making a  $35^\circ$  angle with the strike of the bedding would be  $28^\circ$ . (After H. S. Palmer.)

Examples of the use of the alignment diagram may be cited. If the strike of an horizon is N.  $45^\circ$  E. and the dip is  $30^\circ$  NW., what is the

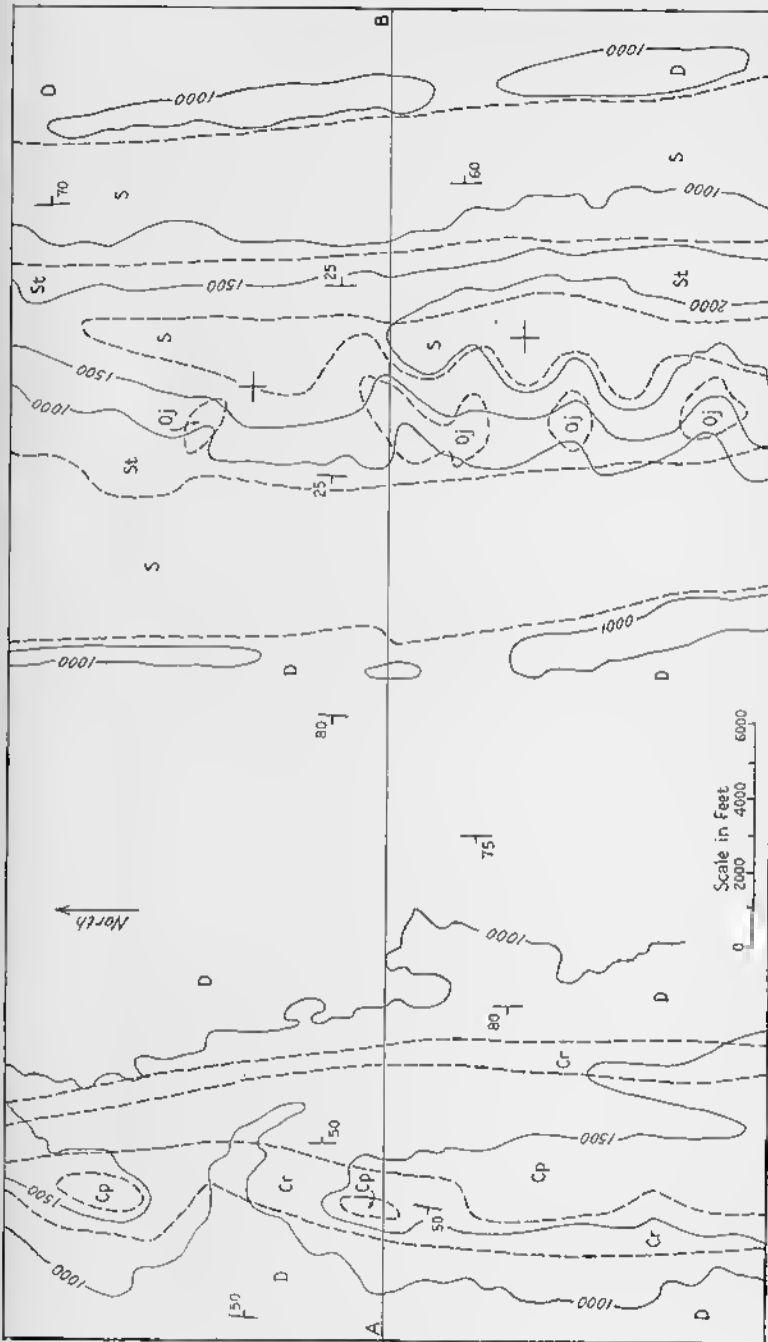


FIG. 319.—Combined Topographic and Geologic Map. Contours are solid lines; contour interval is 500 feet. Geologic boundaries are broken lines.  $O_f$  = Juniata formation (Ordovician);  $St$  = Tuscarora formation (Lower Silurian);  $S$  = Silurian above the Tuscarora formation;  $D$  = Devonian formations;  $C_r$  = Rockwell formation (Mississippian);  $C_p$  = Purdon sandstone (Mississippian). (After Folio 179, U. S. Geological Survey.)

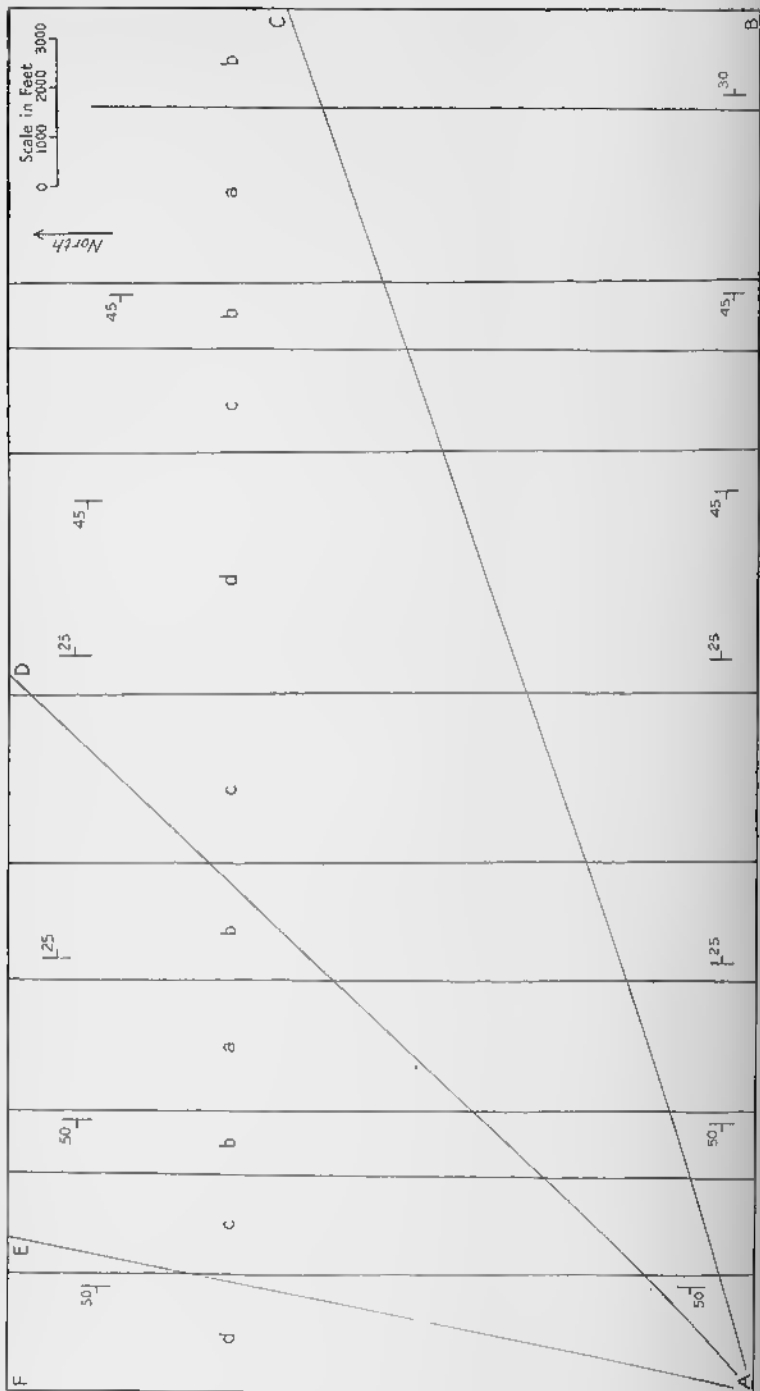


FIG. 320.—Map for Problem in Exercise 4.

apparent dip on a vertical section that trends N.  $5^{\circ}$  W.? The point on the left-hand scale is 30 degrees. The point on the right-hand scale is 50 degrees. A line connecting these two points crosses the central scale at 24 degrees. Therefore 24 degrees is the apparent dip in a N.  $5^{\circ}$  W. direction.

Tables and charts for apparent dip are given in Lahee.<sup>1</sup>

#### Problems

1. (Use Fig. 319.) (a) Make a topographic profile and geologic structure section along the line *AB*. Do not exaggerate the vertical scale. (b) The structure exemplified in this section is typical of what geologic province? (c) Describe the structure in 25 words or less.

2. (Use Fig. 320.) Draw a series of structure sections along the lines *AB*, *AC*, *AD*, *AE*, and *AF*. Connect the beds above the ground surface by broken lines in order to show the structure more clearly.

If the instructor desires, one or more of the following folios of the Geologic Atlas of the United States, issued by the U. S. Geological Survey, may be used for making structure sections: 221, Bessemer-Vandiver, Alabama; 175, Birmingham, Alabama; 151, Roan Mountain, Tennessee-North Carolina; 143, Nantahala, North Carolina-Tennessee; 215, Hot Springs, Arkansas.

---

<sup>1</sup> Lahee, F. H., *Field Geology*, 4th edition, Appendices XIII and XIV. New York: McGraw-Hill Book Company, 1941.

## EXERCISE 5

### Geometrical Reconstruction of Folds

#### Method

##### Application

Two principal geometrical relations between successive bedding planes in a fold are possible. The folds may be parallel or similar (see p. 53). This exercise gives a method of reconstructing parallel folds if the location of several exposures is given and if the attitude of the beds in those exposures is known. The method cannot be used for reconstructing similar folds nor is it suitable for reconstructing tight

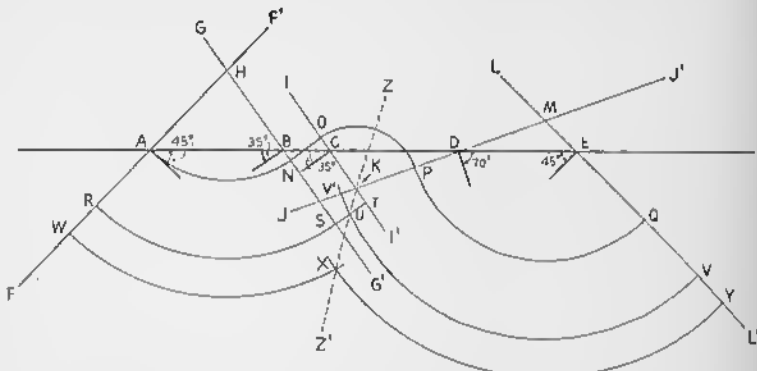


FIG. 321—Geometrical Construction of Folds. Dip of beds is known at *A*, *B*, *C*, *D*, and *E*. (After Busk.)

or complicated folds. Moreover, the distance between exposures must be less than the distance between the axes of folds.

##### Principle

Fig. 321 shows the method of reconstructing parallel folds.<sup>1</sup> The attitude of strata at points *A*, *B*, *C*, *D*, and *E* is shown. These points are on a line perpendicular to the trend of the folds. If the strike of the section is not at right angles to the strike of the bedding, the apparent dip in the direction of the section must be calculated for each

<sup>1</sup> Busk, H. G., *Earth Flexures*. Cambridge: Cambridge University Press, 1929.

outerop. Perpendiculars to the bedding at each outcrop are constructed and extended to intersect the perpendiculars to the bedding of adjacent outcrops.  $FF'$ , the perpendicular to  $A$ , intersects  $GG'$ , the perpendicular to  $B$ , at  $H$ . The dip of the bedding is the same at any point along  $FF'$  as it is at  $A$ . Similarly, the dip at any point on  $GG'$  is the same as that at  $B$ . With  $H$  as a center, and  $HA$  as the radius, an arc is swung from  $A$  to intersect  $GG'$  at  $N$ . Inasmuch as the dip at  $B$  and  $C$  is the same in this problem, the perpendiculars to the bedding at these points will not intersect. The horizon is extended from  $N$ , parallel to the dip of the beds, to intersect  $II'$  at  $O$ . With  $K$ , which is the intersection of  $II'$  and  $JJ'$ , as a center, and  $KO$  as the radius, an arc is constructed to intersect  $JJ'$  at  $P$ . With  $M$ , which is the intersection of  $JJ'$  and  $LL'$ , as a center and  $MP$  as a radius, an arc is swung from  $P$  to intersect  $LL'$  at  $Q$ .  $ANOPQ$  is the position of the horizon outcropping at  $A$ .

In reconstructing an horizon at  $R$ , we find that the horizon falls at  $T$  below the intersection  $K$ . In such a case the distance  $QV$  is set off on line  $LL'$  equal to the distance  $AR$ . From  $V$ , with  $M$  as a center and  $MV$  as the radius, an arc is swung to intersect  $JJ'$  at  $V'$ . The position of the horizon that occurs at  $R$  is  $RSUV$ .

At the depth at which horizon  $W$  occurs, the dip at  $C$  no longer has any influence.  $WXY$  shows the form assumed by the horizon at  $W$ .

$ZZ'$  is the trace of the axial plane of the central anticline on the vertical section.  $ZK$  bisects angle  $IKJ'$ ;  $KZ'$  passes through points  $U$  and  $X$ .

#### Interpolation

The accuracy of the reconstructed fold depends upon the number of dip and strike readings in the section. If outcrops are missing in a critical locality, the reconstruction may not be accurate. A key bed, for example, may be recognizable in several different localities. Its position, as predicted by the method outlined above, may not correspond to its actual position. Dips may then be interpolated to make the fold pattern fit the field facts. The method is outlined below.

In Fig. 322, points  $A$ ,  $B$ ,  $C$ , and  $D$  show the location and attitude of folded beds. When the fold is reconstructed according to the method given above, the horizon at  $A$  should reappear at  $J$ . The theoretical position of the horizon is  $AHHIJ$ . If field mapping has shown that the horizon at  $A$  is the same as that at  $D$ , then a dip must be interpolated at some point in the section to erase the apparent discrepancy. A dip should be interpolated for a point between the two outcrops that are farthest apart—that is, between  $B$  and  $C$ .

With  $G$  as a center and  $GD$  as a radius, an arc is constructed to intersect  $EE'$  at  $K$ . For arc  $HI$  two arcs that are tangent to each other and tangent to  $H$  and  $K$  will be substituted. From  $K$ ,  $KL$  is drawn perpendicular to  $EE'$ . From  $H$ ,  $HM$  is drawn perpendicular

to  $VV'$ . These two lines intersect at  $N$ .  $H$  and  $K$  are connected by a straight line,  $HK$ . A perpendicular to  $HK$ , drawn through point  $N$ , is extended to intersect  $EE'$  at  $R$  and  $VV'$  at  $S$ . With  $R$  as a center and  $RK$  as a radius, arc  $KT$  is constructed. Arc  $HT$  is drawn with  $S$  as a center and  $SH$  as a radius.  $AHTKD$  is the pattern of the fold. A perpendicular to  $OP$  at  $T$  gives the interpolated dip, which is the angle  $UTC$ .

### Problems

**1.** A traverse is made due east across a series of rocks that strike north-south. The following data are obtained on the dip of the beds. The left-hand column gives the distance in feet from the west end of the traverse; the right-hand column gives the dip.

Distance in Feet	Dip
0	40° E.
500	35° W.
1500	25° E.
2000	50° E.
3000	30° W.
3500	50° E.
4500	25° W.
5000	25° W.
6000	40° E.
7000	65° W.

(a) Reconstruct the folds, assuming parallel folding. (b) If a distinctive bed outcrops at the west end of the traverse, at what depth (or height, in which case it would be eroded) would the bed be located at the east end of the section (distance 7000)?

**2.** A traverse is made due south across a series of rocks that strike N. 90° E. The following data are obtained on the dip of the beds. The left-hand column gives the distance in feet from the north end of the traverse; the right-hand column gives the dip.

Distance in Feet	Dip
0	60° N.
600	40° S.
1000	25° N.
1500	50° S.
2000	0°
2400	60° N.

(a) Reconstruct the folds, assuming parallel folding. (b) If a distinctive bed outcrops at the north end of the traverse, at what depth (or height, in which case it would be eroded) would the bed be located at the south end of the section? (c) Actually the distinctive bed out-

crops at the south end of the traverse (distance 2400). Adjust the section to allow for the known position of the distinctive bed. Do this by interpolating a dip between the 1500-foot and 2000-foot points. What is the location and value of the interpolated dip?

3. A traverse is made in a due east direction across a series of rocks that strike N. The following data are obtained on the dip of the beds.

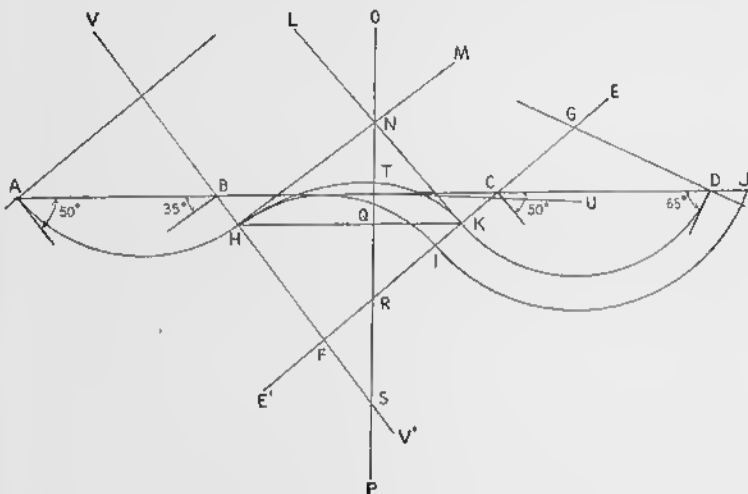


FIG. 322—Geometrical Construction of Folds. Dip of beds is known at *A*, *B*, *C*, and *D*. Same stratigraphic horizon crops out at *A* and *D*. (After Busk.)

The left-hand column gives the distance in feet from the west end of the traverse. The right-hand column gives the dip.

<i>Distance in Feet</i>	<i>Dip</i>
0	20° W.
100	20° W.
150	25° E.
200	40° E.
300	60° E.
450	20° W.
500	20° W.

(a) Reconstruct the folds, assuming parallel folding. (b) On the surface of the earth what is the horizontal distance of the crest of the anticline from the west end of the section? (c) At a depth of 100 feet what is the horizontal distance of the crest of the anticline from the west end of the section? (d) At a depth of 200 feet?

## EXERCISE 6

### Structure Contours and Isopachs

#### Structure Contours

A structure contour is an imaginary line connecting points of equal altitude on a single horizon, usually the top or bottom of a sedimentary bed. A structure contour map thus shows the form of the horizon. Structure contours are analogous to topographic contours, which show the form of the surface of the earth.

The dip of an horizon represented by structure contours can be calculated with great precision. The closer the structure contours are to each other on a map, the steeper is the dip, just as the closer topographic contours are to each other, the steeper is the slope. The method of determining the dip quantitatively is discussed on p. 85.

The method of preparing a structure contour map is illustrated by Fig. 323. First of all, some horizon must be chosen to be represented by the structure contours; it may be the top or bottom of a coal bed, the top of an oil-bearing stratum, or the top or bottom of some bed that is readily recognizable. Wherever this horizon is exposed at the surface of the earth, the altitude may be plotted on the map. The data may also come from drill holes or mines. If the thicknesses of the various stratigraphic units have been precisely determined, it is possible to predict at what depth the key horizon occurs, even though it is not exposed or penetrated by drill holes or mines.

The altitudes of numerous points on the top of a bed of limestone are given in Fig. 323. It is decided to use a structure contour interval of 100 feet. In the lower left-hand corner of Fig. 323 the altitude of the top of the limestone at one point is shown to be 800 feet. The 800-foot structure contour will pass through this point. Otherwise it is necessary to interpolate proportionally between each pair of points for which data are given. In the northeast corner of the map, two points on the horizon being contoured have the altitudes of 740 feet and 960 feet, respectively. The 800-foot and 900-foot contours will pass between these two points. The difference in altitude between these two points is 220 feet. The distance of the 800-foot contour from the 740-foot point will be  $\frac{6}{22}$  of the total distance between the two points. The distance of the 900-foot contour from the 740-foot point will be  $\frac{16}{22}$  of the total distance between the two points. The location of contours over all the map may be found in the same way.

The contours obtained in this way may be modified somewhat, so that sharp curves may be smoothed out.

If an area is entirely enclosed by one or more contours, it is known as a *closed structure*; this usage is not to be confused with the use of the term *closed fold* (p. 42). The closure of a fold is the vertical distance between the highest and the lowest contours that completely enclose the fold. The precision of the measurement of the closure of a fold, as

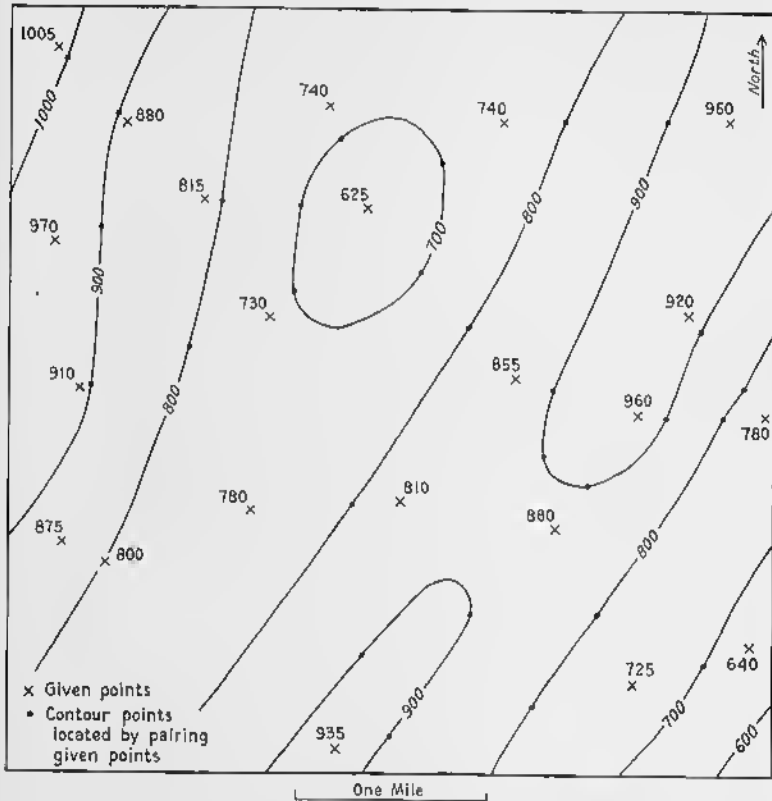


FIG. 323—Preparation of Structure Contour Map.

determined from a structure contour map, depends upon the contour interval. If a fold has a closure less than the contour interval that is used, the closure may not appear on the map.

### Isopachs

A bed or formation is not constant in thickness. If the thickness is known at many localities, it is possible to draw *isopachs*, which are lines connecting points at which the bed is of equal thickness. Suppose, for example, that a formation is known to be 100 feet thick at

three localities that are designated *a*, *b*, and *c*, but 300 feet thick at three other localities designated *e*, *f*, and *g*. The 100-foot isopach would pass through *a*, *b*, and *c*, and the 300-foot isopach would pass through *e*, *f*, and *g*. The 200-foot isopach would lie between the 100-foot and the 300-foot isopachs; if no other data were available, it would be placed halfway between them. In the preparation of isopach maps from data at numerous localities interpolation is performed in the same way as in the preparation of structure contour maps.

### Problems

1. Fig. 324 is a structure contour map on the top of a coal bed. Assume that the region is one of no relief 1800 feet above sea level. Are any folds with closure shown on the map?

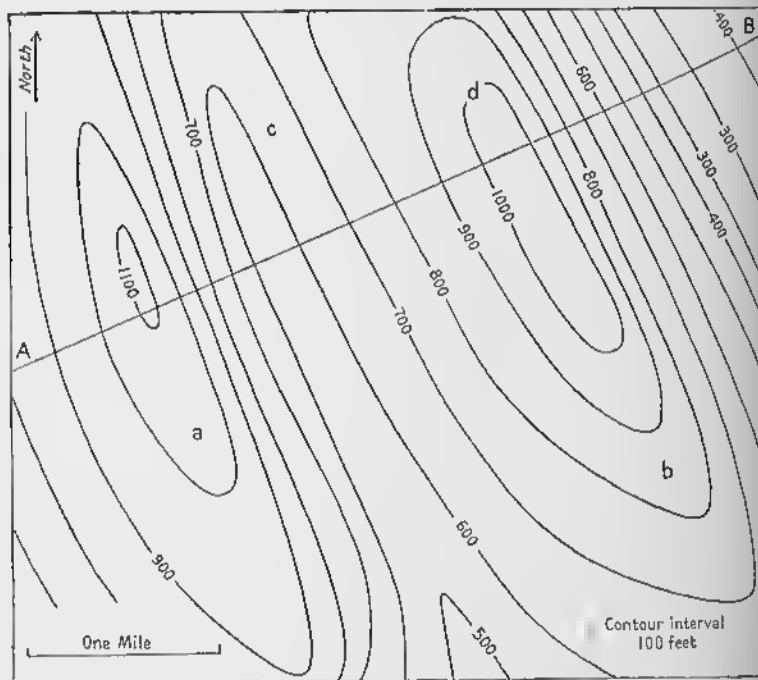
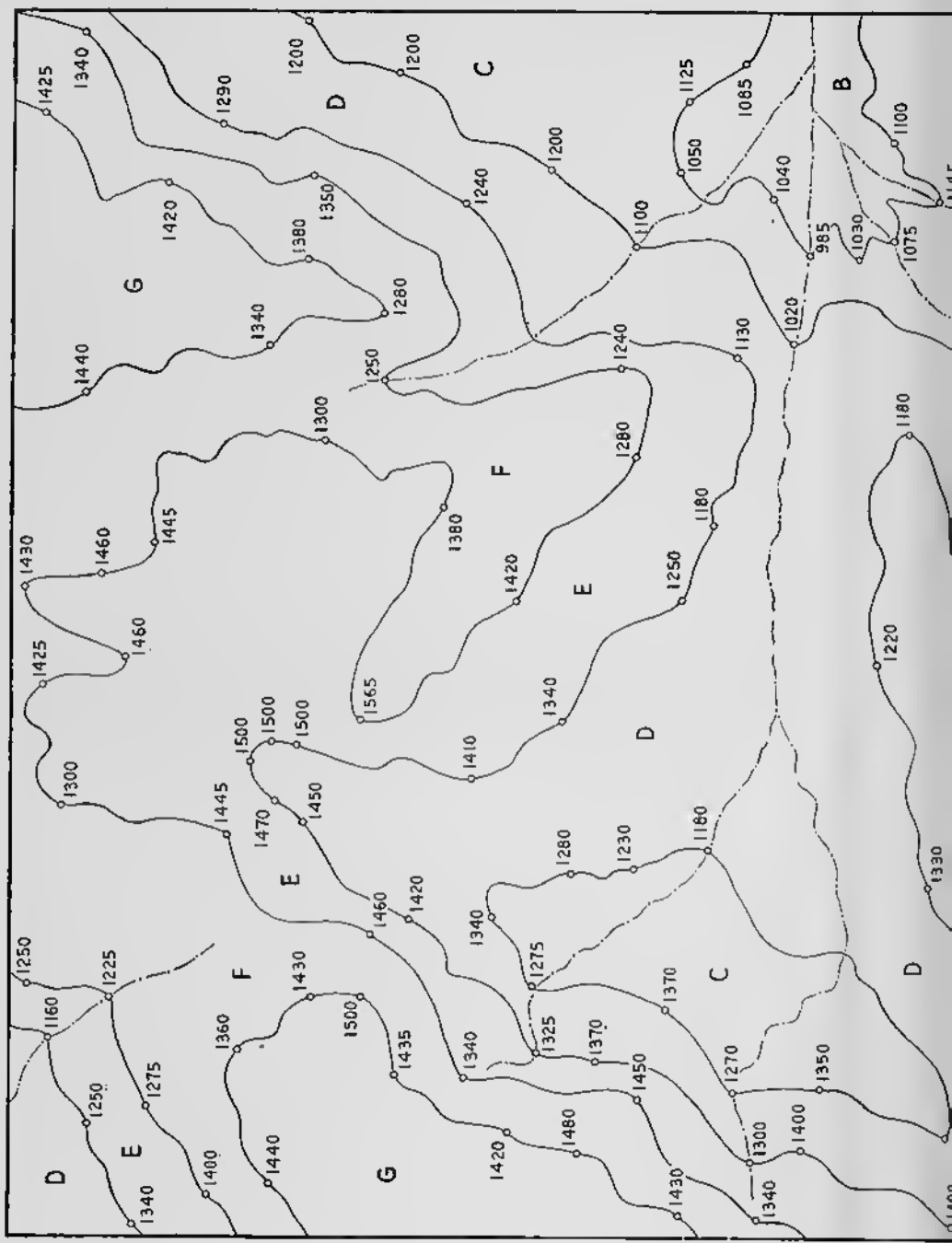


FIG. 324—Structure Contour Map for Problems in Exercise 6.

2. In what parts of the area covered by Fig. 324 does the coal dip most steeply? What is the dip at these places? Give the dip in feet per mile and in degrees.

3. What is the average dip of the coal on the nose of the fold around locality *a* in Fig. 324? Around locality *b*? Give the dips in feet per mile and in degrees.



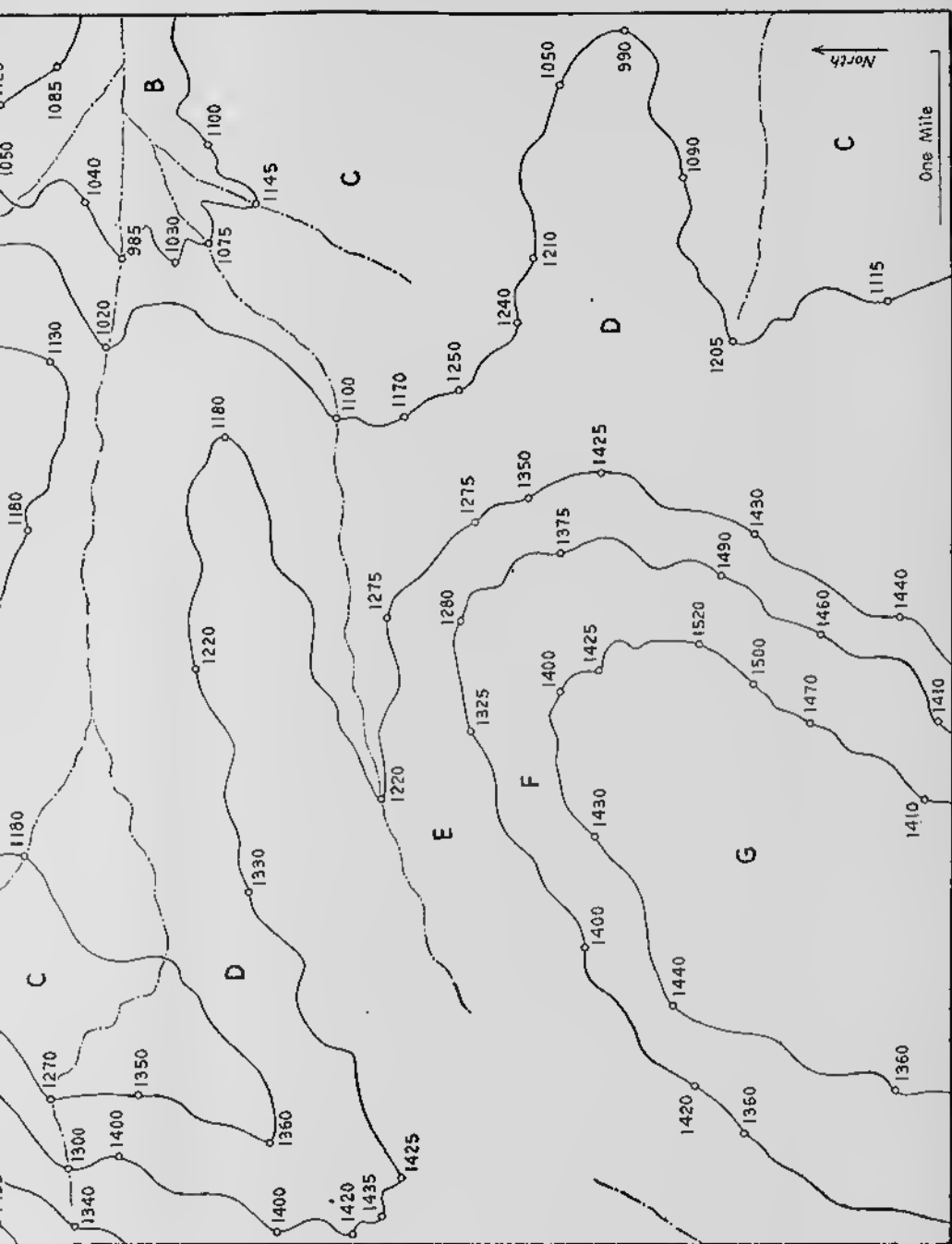


Fig. 325—Geologic map for problem in Exercise 6. B, C, formations are solid lines. Dash-dot lines are streams. Figures D, E, F, and G, are geologic formations; boundaries between them are altitude of points on contacts.

4. Describe the trend and character of the structure shown in Fig. 324.

5. Draw a structure section along the line *AB* of Fig. 324.

6. What is the depth to the coal at *c* in Fig. 324? At *d*?

7. Fig. 325 is a geological map. Formation *B* is the oldest of the exposed formations, and formation *G* is the youngest. The altitude of many points on the contacts is given. Well records show that the formations have the following thicknesses: *F* is 55 feet; *E* is 175 feet; *D* is 90 feet; *C* is 270 feet; *B* is 210 feet; and *A*, which does not outcrop, varies in thickness. Well records indicate that *A* is 100 feet thick in the northeast corner of the map; seven miles due west of here it is 500 feet thick. In the southeast corner of the map it is 150 feet thick; six miles due west it is 350 feet thick. Other drill records indicate that the variation in thickness is uniform throughout the area.

Prepare a structure contour map on the top of formation *A*, using a contour interval of 100 feet.

8. Prepare a structure contour map on the base of formation *A*, using a contour interval of 100 feet.

If the instructor desires, he may use one or more of the following folios of the Geological Atlas of the United States, published by the U. S. Geological Survey: 185, Murphysboro-Herrin, Illinois; 189, Barnesboro-Patton, Pennsylvania; 174, Johnstown, Pennsylvania; 175, Birmingham, Alabama; 133, Ebensburg, Pennsylvania; 125, Rural Valley, Pennsylvania.

## EXERCISE 7

### Trigonometric Solution of Fault Problems

#### Method

The types of faults and the definition of terms relating to the movement along faults are given on pp. 130-154.

The solution of the problems should be accompanied by a plan, as well as by one or more structure sections that show the fault and the disrupted beds.

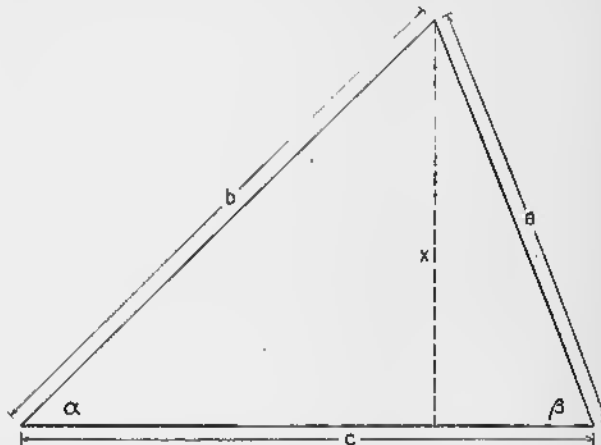


FIG. 326—Triangle to Illustrate the *Law of Sines*.

The law of sines, which can be used to solve any triangle, is useful in this exercise. This law states that the sines of angles are proportional to the sides opposite the respective angles. As shown in Fig. 326, if  $abc$  is the triangle, and  $x$  is a perpendicular to  $c$ ,

$$\sin \alpha = \frac{x}{b};$$

$$\sin \beta = \frac{x}{a};$$

$$\frac{\sin \alpha}{\sin \beta} = \frac{\frac{x}{b}}{\frac{x}{a}};$$

$$\frac{\sin \alpha}{\sin \beta} = \frac{xa}{xb};$$

and

$$\frac{\sin \alpha}{\sin \beta} = \frac{a}{b}.$$

The following problem, illustrated by a structure section given in Fig. 327A, will be solved to illustrate the method used.

A horizontal tunnel extends east-west and intersects a fault that strikes north and dips 40 degrees to the west. At a distance of 500 feet east of this intersection the tunnel cuts a bed of sandstone that strikes north and dips 30 degrees east. At a distance of 700 feet west of the fault the tunnel cuts the same sandstone, also striking north and dipping 30 degrees east. The slickensides on the footwall rise from north to south (Fig. 327B) and make an angle of 30 degrees with a horizontal line in the fault plane; that is, the pitch of the slickensides is 30 degrees north.

Calculate the net slip, dip slip, strike slip, heave, throw, stratigraphic separation, vertical separation in a plane perpendicular to the fault, and horizontal separation in the same plane.

From Fig. 327A, which is a vertical section at right angles to the strike of the fault, we obtain

$$\text{Dip slip} = DB + BE.$$

In triangle  $ABD$

$$\frac{\sin 110^\circ}{\sin 30^\circ} = \frac{AB}{DB},$$

and

$$BD = \frac{AB \sin 30^\circ}{\sin 110^\circ}.$$

In triangle  $EBC$

$$\frac{\sin 110^\circ}{\sin 30^\circ} = \frac{BC}{BE},$$

and

$$BE = \frac{BC \sin 30^\circ}{\sin 110^\circ}.$$

$$\text{Dip slip} = DB + BE = \frac{700 \sin 30^\circ}{\sin 110^\circ} + \frac{500 \sin 30^\circ}{\sin 110^\circ},$$

$$\text{Dip slip} = 638 \text{ feet.}$$

From Fig. 327B,

$$\text{Strike slip} = EH.$$

$$\tan 30^\circ = \frac{DB + BE}{EH} = \frac{638}{EH},$$

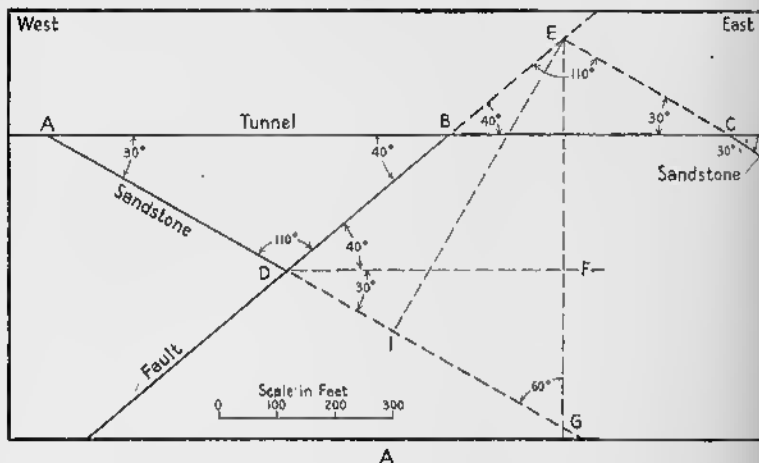
$$EH = 1105 \text{ feet.}$$

$$\text{Net slip} = DH.$$

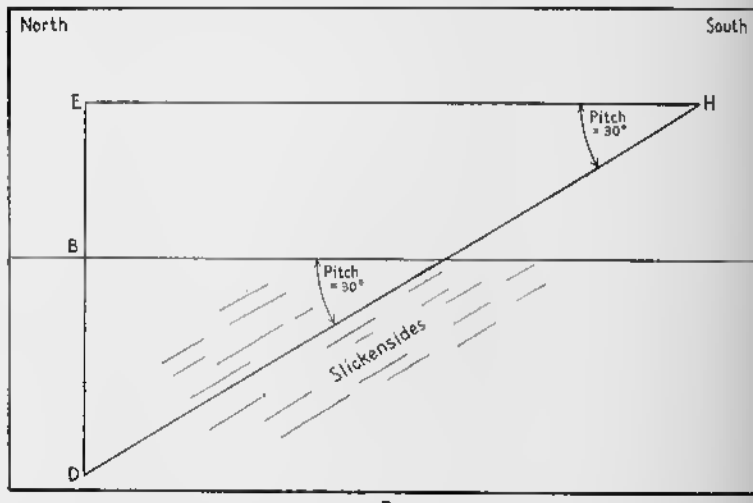
## EXERCISE 7

$$\sin 30^\circ = \frac{DB + BE}{DH} = \frac{638}{DH},$$

$$DH = 1276 \text{ feet.}$$



A



B

FIG. 327—Trigonometric Solution of Fault Problems. A. Vertical cross-section of a thin bed of sandstone that is displaced along a fault. B. Slickensides on fault pitch 30° N.

From Fig. 327A, triangle  $DEF$ ,

$$\text{Throw} = EF.$$

$$\sin 40^\circ = \frac{EF}{DB + BE},$$

$$EF = (DB + BE) \sin 40^\circ,$$

$$EF = 638 \sin 40^\circ = 410 \text{ feet.}$$

*Heave* =  $DF$ .

$$\cos 40^\circ = \frac{DF}{DB + BE}.$$

$$DF = (DB + BE) \cos 40^\circ,$$

$$DF = 638 \cos 40^\circ = 488 \text{ feet.}$$

From Fig. 327A, triangle  $DEI$ ,

*Stratigraphic separation* =  $EI$ .

$$\sin (30^\circ + 40^\circ) = \frac{EI}{DB + BE},$$

$$EI = 638 \sin 70^\circ = 599 \text{ feet.}$$

From Fig. 327A, triangle  $DEG$ ,

*Vertical separation* =  $EF + FG$ .

$$\frac{\sin (30^\circ + 40^\circ)}{\sin 60^\circ} = \frac{EF + FG}{DB + BE},$$

$$\frac{\sin 70^\circ}{\sin 60^\circ} = \frac{EF + FG}{638},$$

$$EF + FG = 692 \text{ feet.}$$

From Fig. 327A,

*Horizontal separation* =  $AB + BC$ ,

$$AB + BC = 1200 \text{ feet.}$$

### Problems

These problems are to be solved by trigonometry.

1. A bed that strikes N.  $90^\circ$  E. and dips  $45^\circ$  N. is broken by a strike fault that dips  $45^\circ$  S. The hanging wall has moved 1200 feet directly down the dip of the fault plane. Calculate (a) net slip, (b) strike slip, (c) dip slip, (d) throw, (e) heave, (f) horizontal separation in a vertical plane perpendicular to the strike of the fault, (g) vertical separation in the same plane, and (h) stratigraphic throw.

2. A sandstone that strikes N.  $45^\circ$  E. and dips  $50^\circ$  SE. is broken by a strike fault that dips  $30^\circ$  SE. The sandstone outerops 1500 feet southeast of the fault and 900 feet northwest of the fault. Assuming the movement to have been directly down the dip of the fault plane, calculate the (a) net slip, (b) dip slip, (c) strike slip, (d) throw, (e) heave, (f) horizontal separation in a vertical plane perpendicular to the strike of the fault, (g) vertical separation in the same plane, and (h) stratigraphic throw.

## EXERCISE 7

3. A north-south tunnel cuts a fault that strikes N.  $90^\circ$  E. and dips  $55^\circ$  S. The strata also strike N.  $90^\circ$  E., but dip  $40^\circ$  N. The hanging wall has gone down diagonally toward the west; the pitch of the net slip is 25 degrees; and the value is 2500 feet. Calculate the (a) dip slip, (b) strike slip, (c) throw, and (d) heave.

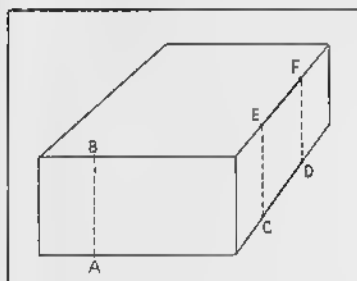
4. A fault plane strikes N.  $90^\circ$  E. and dips  $30^\circ$  N. A coal bed, striking N.  $90^\circ$  E. and dipping  $60^\circ$  S., is exposed 700 feet north of the fault and again 1000 feet south of the fault. The pitch of the slickensides on the fault is 40 degrees toward the west. Assuming that the slickensides are parallel to the net slip, calculate the (a) net slip, (b) dip slip, (c) strike slip, (d) heave, (e) throw, and (f) stratigraphic throw. (g) Is this a normal or a reversed fault?

## EXERCISE 8

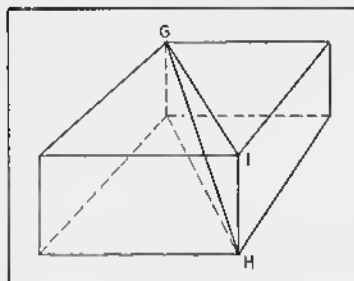
### Projections

#### Method

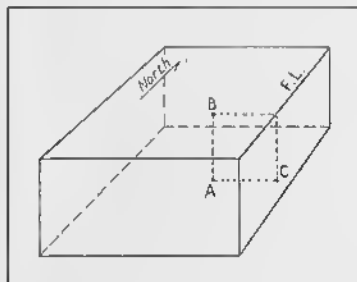
An object having three dimensions may be shown on a single plane by means of projection. The projection of a point on a plane is a point. The projection of a line on a plane is generally a line. The plane upon which points or lines are projected is the *plane of projection*. The *direction of projection* is the direction in which a point is



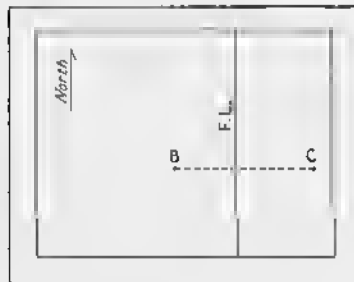
A



B



C



D

FIG. 328—Projections (see text).

projected into the plane of projection. *Normal projection*, in which the direction of projection is perpendicular to the plane of projection, is used in this exercise.

Normal projections are illustrated in Fig. 328. Points and lines have been projected into the horizontal plane represented by the upper surface of the blocks. In Fig. 328A, point *B* is the projection of point

## EXERCISE 8

*A*; line *EF* is the projection of line *CD*. In Fig. 328B, line *GI* is the projection of line *GH* into this plane.

The line of intersection of two planes is the trace of one plane upon the other. The trace of one plane of projection upon a second plane of projection is called a *folding line*. In normal projection the angle between two planes having a common folding line is always 90 degrees.

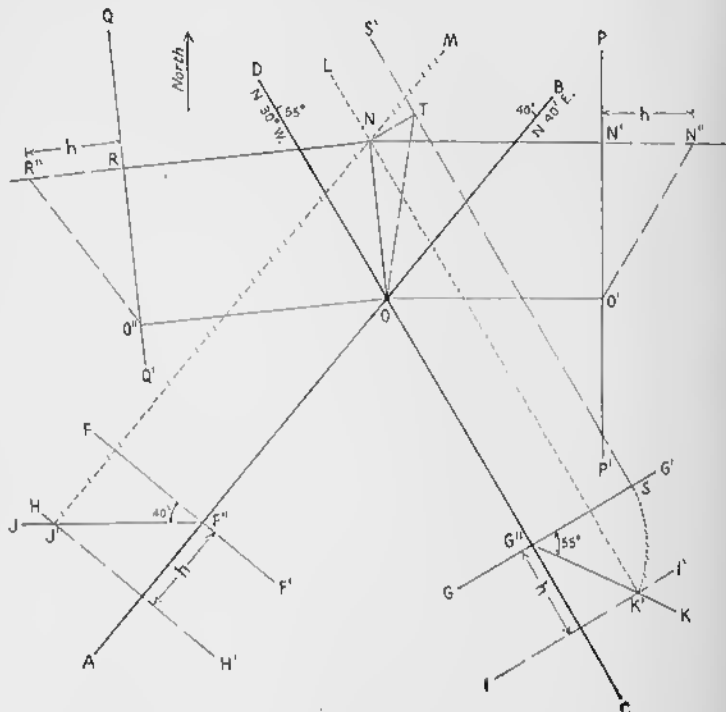


FIG. 329—Projection to Find Attitude of Intersection of Two Veins: one striking N.  $40^{\circ}$  E., dipping  $40^{\circ}$  NW.; the second striking N.  $30^{\circ}$  W., dipping  $55^{\circ}$  NE.

In most cases one plane of projection is horizontal, whereas the others are vertical. In geology the horizontal plane is a plan, corresponding more or less precisely with the map. A map portrays the relations on the surface of the earth, regardless of its topographic irregularities. A plan is made on a plane surface. In areas of low relief the geological map may be treated as a plan, and, whenever the term *map* is used in the ensuing descriptions, it is to be considered synonymous with the word *plan*. In geology the other planes of projection are structure sections. However, a plane of projection does not have to be either horizontal or vertical.

To represent a plan (map) and a section on one plane (the plane of the paper), it is necessary to rotate the section into the plane of the map around the folding line as an axis. In the following problems it is best to consider the section as lying below the folding line; the section will then be rotated upward into the horizontal plane. In Fig. 328C, point *B* is the projection of point *A* into a horizontal plane; point *C* is the projection of point *A* into the vertical plane represented by the side of the block. Fig. 328D shows the projection after the vertical plane has been rotated into the plane of the paper about the folding line (*F. L.*) as an axis.

The attitude of a line is defined by the strike of its horizontal projection and by its plunge (see p. 44).

The following problem, similar to those at the end of the exercise, illustrates the procedure to be followed.

**PROBLEM:** As shown in Fig. 329, a vein that strikes N.  $40^\circ$  E. and dips  $40^\circ$  NW, intersects a vein that strikes N.  $30^\circ$  W. and dips  $55^\circ$  NE. Draw the projections of the intersection of the two veins (a) on a horizontal plane, (b) on a vertical plane striking north-south, and (c) on a vertical plane striking parallel to the direction of plunge of the intersection. (d) Show the trace of the N.  $40^\circ$  E. vein on the N.  $30^\circ$  W. vein. (It will be necessary to rotate the N.  $30^\circ$  W. vein into the horizontal to show the projection.) (e) What is the attitude of the intersection?

**SOLUTION:** Draw *AB* and *CD* parallel to the respective strikes of the veins, as shown in Fig. 329. The veins intersect at point *O*. Construct a folding line, *FF'*, perpendicular to *AB*; construct a folding line, *GG'*, perpendicular to *CD*. These folding lines may be constructed at any convenient point along *AB* and *CD*.

Using these folding lines as the horizontal, now make cross sections. Draw *HH'* parallel to and at an arbitrary distance *h* from *FF'*; construct *II'* at the same distance from *GG'*. *HH'* and *II'* represent a level which will be called the *lower reference plane*; it is *h* distance below the level of the plan (map). Throughout any one problem the elevation of the lower reference plane remains constant. *F''* is the intersection of *FF'* with *AB*; *G''* is the intersection of *GG'* with *CD*. Draw angles *FF''J* and *G''G'K* equal to the respective dips of the two veins. *F''J* intersects *HH'* at *J'*; *G''K* intersects *II'* at *K'*. Draw *J'M* and *K'L* parallel to *AB* and *CD*, respectively. These two lines represent the horizontal projections of contours on the two veins at *h* distance below the plan; that is, these two lines are the horizontal projection of the intersection of the two veins with the lower reference plane. Point *N* is the horizontal projection of the intersection of the two veins on the lower reference plane, and point *O* is the intersection of the two veins on the plan. Therefore line *ON* is the horizontal projection of the intersection of the two veins. The strike of the intersection in this case is N.  $6^\circ$  W.

Draw line  $PP'$  in a north-south direction through some arbitrary point. This line is the trace of a north-south vertical plane on the plan. The vertical plane must be rotated into the upper reference plane (the plan) around  $PP'$  as the axis of rotation to show the projection of the intersection,  $ON$ , on the vertical plane.

Project point  $O$  to  $O'$  in the north-south plane; similarly project point  $N$  to  $N'$  in the north-south plane. Draw a line through  $NN'$  and extend it to the right of  $N'$ . Lay off point  $N''$  at a distance  $h$  from point  $N'$ . Point  $N''$  is the intersection of the two veins in the lower reference plane projected into a north-south vertical plane; line  $O'N''$  is the intersection of the two veins projected into the north-south vertical plane.

Through some arbitrary point construct line  $QQ'$  parallel to line  $ON$ . Line  $QQ'$  is the trace on the plan (map) of a vertical plane that strikes parallel to the direction of the plunge of the intersection of the two veins. This vertical plane must be rotated into the horizontal around the folding line  $QQ'$  in order to show the projection of the intersection of the two veins upon it. Project point  $O$  into this plane to  $O''$ ; similarly project point  $N$  to  $R$  in this same plane and extend line  $NR$  to the left of  $R$ . From point  $R$ , lay off  $RR''$  equal to  $h$ . Point  $R''$  is the intersection of the two veins with the lower reference plane projected into a vertical plane that strikes parallel to the intersection of the two veins. Line  $O''R''$  is the intersection of the two veins projected to this same plane. Angle  $RO''R''$ ,  $31^\circ$ , is the plunge of the intersection of the two veins.

To draw the trace of the N.  $40^\circ$  E. vein on the N.  $30^\circ$  W. vein, it is necessary to rotate the N.  $30^\circ$  W. vein into the plan (map).  $CD$ , the trace of the vein on the plan, is used as the axis of rotation. Using the line  $G''K'$  as the radius and the point  $G''$  as the center, draw an arc to intersect  $GG'$  at  $S$ . Through point  $S$  draw a line  $SS'$  parallel to the strike of the N.  $30^\circ$  W. vein. This line,  $SS'$ , is the trace of the N.  $30^\circ$  W. vein on the lower reference plane, now rotated into a horizontal position. From point  $N$ , construct  $NT'$  perpendicular to  $SS'$ .  $N$  is the horizontal projection of a point on the lower reference plane; this point on the lower reference plane falls at  $T'$  when it is rotated to the surface. Line  $OT$  is the trace of the N.  $40^\circ$  E. vein on the N.  $30^\circ$  W. vein. Angle  $DOT$ ,  $39^\circ$ , is the pitch of the trace of the N.  $40^\circ$  E. vein on the N.  $30^\circ$  W. vein.

#### Problems

1. A vertical vein that strikes N.  $45^\circ$  E. intersects a vein that strikes N.  $90^\circ$  E. and dips  $30^\circ$  N. Determine the direction and amount of plunge of the intersection.

2. The two limbs of a fold strike N.  $45^\circ$  W. and N.  $5^\circ$  E., and dip  $40^\circ$  SW. and  $70^\circ$  W., respectively. What is the direction and amount of plunge of the fold?

3. A vein that strikes N.  $25^\circ$  E. and dips  $30^\circ$  NW. intersects a vein that strikes N.  $35^\circ$  W. and dips  $50^\circ$  SW. Draw the projections of the intersection (a) on a horizontal plane, (b) on a vertical plane striking north-south, (c) on the plane of the N.  $25^\circ$  E. vein, and (d) on a vertical plane striking parallel to the direction of the plunge of the intersection. (e) In which of these projections can the plunge be measured directly? (f) What is the direction and amount of the plunge of the intersection?

4. A vein that strikes N.  $25^\circ$  E. and dips  $30^\circ$  SE. intersects a vein that strikes N.  $35^\circ$  W. and dips  $50^\circ$  SW. Perform the same operations and answer the same questions as in Problem 3.

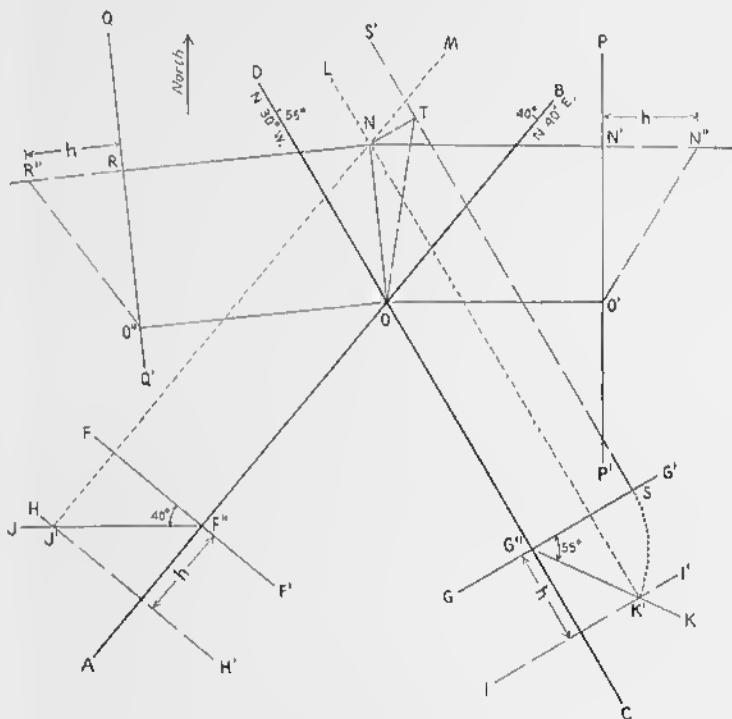


(FIG. 329—Repeated.)

## EXERCISE 9

### Solution of Three-Point Problems and Vertical Fault Problems by Descriptive Geometry

#### Three-Point Problem

The method used in this exercise for the solution of three-point problems is based on the graphic solution of similar triangles. The following problem illustrates the procedure to be followed:

**GIVEN:** Points  $A$ ,  $B$ , and  $C$ , all on top of a sandstone bed. Point  $B$  lies N.  $45^\circ$  W. of  $A$  at a *map distance* of 300 feet. Point  $C$  lies N.  $60^\circ$  E.

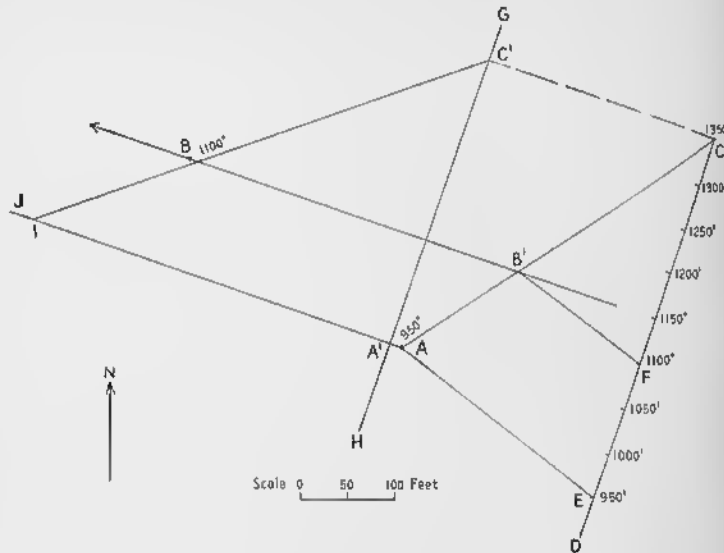


FIG. 330—Graphic Solution of Three-point Problem. Location and altitude of  $A$ ,  $B$ , and  $C$  are known.

of  $A$  at a *map distance* of 400 feet. The elevations of points  $A$ ,  $B$ , and  $C$  are 950, 1100, and 1350 feet, respectively.

**To FIND:** The strike and dip of the top of the bed of sandstone. In all such cases the top of the bed must be a plane surface.

**CONSTRUCTION** (Fig. 330): Locate the three points according to the data given, using some convenient scale. Draw line  $AC$ , connect-

ing the *highest* and the *lowest* of the three points. Some point along this line has the same altitude as the intermediate point, *B*.

Along line *CD*, drawn in some convenient direction from point *C*, lay off *CE* equal to the difference in elevation between points *A* and *C*, using any convenient scale. On the same line, using the same scale, lay off *CF* equal to the difference in elevation between points *B* and *C*.

Connect points *A* and *E* by a line. Through point *F* draw a line parallel to line *AE* to intersect line *AC*. This intersection, point *B'*, is the point having the same altitude as point *B*. The line connecting points *B* and *B'* is the strike of the top of the bed.

At any convenient place draw line *GH* perpendicular to the strike of the bed. Project points *A* and *C* into this line to points *A'* and *C'*. Line *CC'* is the strike line on the top of the bed at an altitude of 1350 feet, and line *AA'* is the strike line on the top of the bed at an altitude of 950 feet. The dip is therefore from point *C'* toward point *A'*—that is, toward the southwest.

Now make a vertical section along line *GH*. Erect the perpendicular *A'J* to *GH* at point *A'*, and on this line, using the same scale as the horizontal map scale, lay off *A'I* equal to the difference in altitude between points *A* and *C*. Connect points *I* and *C'*. Angle *A'C'I* is equal to the dip of the top of the sandstone.

### Vertical Fault

The following example illustrates the graphic method of determining the displacement of a fault where the attitude and location of two displaced horizons on both sides of the fault are known.

**GIVEN** (Fig. 331): On a surface of no relief, fault *FF'* strikes N. 90° E. and dips vertically; a vein striking N. 40° W. and dipping 30° NE. is exposed at *A* and *A'* on the south and north sides of the fault, respectively; another vein, striking N. 60° E. and dipping 65° NW., is exposed at *B* and *B'* on the south and north sides of the fault, respectively.

**FIND:** (a) the net slip, (b) the plunge of the net slip, (c) the strike of the horizontal projection of the net slip, and (d) the relative movement along the fault plane.

**CONSTRUCTION:** Draw *AC* and *A'C'* parallel to the strike of the N. 40° W. vein, and draw *BD* and *B'D'* parallel to the strike of the N. 60° E. vein (Fig. 331). Draw *EE'* and *GG'* perpendicular to the strikes of the veins at convenient places, such as points *E''* and *G''*. Using these lines as the horizontal, we shall now make structure sections.

Draw *HH'* parallel to and at some arbitrary distance *h* from *EE'*; draw *II'* parallel to and at a distance *h* from *GG'*. These lines represent a level which we will call the *lower reference plane*; it is *h* distance below the surface plan. Draw angles *G'G''J* and *EE''K* equal to the

respective dips of the N.  $40^\circ$  W. and N.  $60^\circ$  E. veins. Draw  $J'L$  and  $K'M$  parallel to  $AC$  and  $BD$ , respectively. These lines represent the horizontal projection of contours on the two veins; at all points on these contours the two veins are exactly distance  $h$  below the horizontal surface represented by the plan. Point  $L$  is the horizontal projection of the intersection of the fault, the lower reference plane, and the N.  $40^\circ$  W. vein on the south side of the fault. Point  $M$  is the horizontal projection of the intersection of the fault, the lower reference plane, and the N.  $60^\circ$  E. vein on the south side of the fault.

We will now make a vertical section along line  $FF'$ —that is, in the plane of the fault. Draw  $OO'$ ,  $h$  distance away from and parallel to  $FF'$ . This construction, in reality, amounts to rotating the vertical fault into the plane of the map (plan). Draw  $LL'$  and  $MM'$  perpendicular to  $FF'$ . Inasmuch as  $L'$  and  $M'$  are points on the section,  $h$  distance below  $L$  and  $M$  on the surface plan, they represent points on the veins in the cross section.

Draw  $AL'$  and  $BM'$ ; extend them to an intersection at  $S$ .  $AS$  and  $BS$  represent the traces of the two veins on the fault plane (in the cross section), and  $S$  represents their intersection on the south wall. Draw  $A'N$  and  $B'N$  parallel to  $AS$  and  $BS$ , respectively.  $A'N$  and  $B'N$  represent the traces of the two veins on the fault plane on the north wall, and  $N$  is their intersection.

Draw  $NS$ . This line is the total displacement in the fault plane between the two points  $N$  and  $S$ , which were together before the faulting;  $NS$  is therefore the net slip.

Extend  $NS$  to intersect  $FF'$  at  $P$ . The angle  $SPF'$  is the pitch of the net slip; in a vertical fault the pitch and plunge are equal.

The net slip must lie in the fault plane. Inasmuch as the fault plane is vertical and strikes N.  $90^\circ$  E., the strike of the horizontal projection of the net slip is also N.  $90^\circ$  E. Point  $S$  is at a lower elevation in the vertical section along the fault than point  $N$  and is to the east of a vertical line through point  $N$ ; therefore the south side of the fault has moved down toward the east relative to the north side of the fault.

#### Problems

1. The top of a coal bed crops out at an altitude of 1500 feet. A second outcrop of this horizon lies 500 feet (map distance) to the north at an altitude of 2000 feet; and a third outcrop lies 250 feet (map distance) N.  $35^\circ$  W. from the first outcrop at an altitude of 1800 feet. Determine the strike and dip of the coal bed.
2. A vertical fault strikes N.  $90^\circ$  E. across a featureless plain. Two veins, which may be called  $A$  and  $B$ , are disrupted by the fault. The data are as follows: "Distance" is measured toward the east from the point on the map at which the southern segment of vein  $A$  abuts against the fault.

Vein	Strike	Dip	Distance on South Wall	Distance on North Wall
A	N. 25° W.	55° NE.	0 feet	100 feet
B	N. 40° E.	40° NW.	550 feet	450 feet

Determine (a) the value of the net slip; (b) the plunge of the net slip; (c) the strike of the horizontal projection of the net slip; and (d) the relative movement along the fault (that is, which block has gone up relatively).

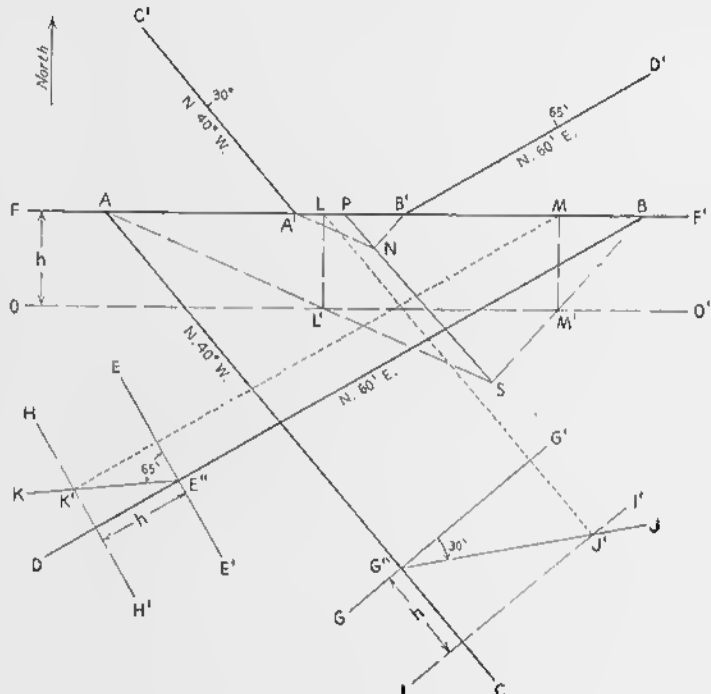


FIG. 331—Graphic Solution of a Vertical Fault Problem.

## EXERCISE 10

### Solution of Inclined Fault Problems by Descriptive Geometry

#### Method

The following example illustrates the graphic method of determining the displacement on a fault that dips at an angle other than 90 degrees, if the attitude and location of each of two displaced horizons are known on both sides of the fault.

The example also shows the method of locating a disrupted horizon on one side of a fault, if the location and attitude of the disrupted horizon on the opposite side of the fault are known; the direction and amount of movement along the fault must also be known.

**GIVEN** (Fig. 332): On a surface of no relief, fault  $FF'$  strikes N.  $90^{\circ}$  E. and dips  $40^{\circ}$  S.; a vein striking N.  $30^{\circ}$  W. and dipping  $35^{\circ}$  NE. is exposed at  $A$  and  $A'$  on the south and north sides of the fault, respectively; another vein, striking N.  $30^{\circ}$  E. and dipping  $60^{\circ}$  NW., is exposed at  $B$  and  $B'$  on the south and north sides of the fault, respectively; a third vein, striking N.  $40^{\circ}$  E. and dipping  $70^{\circ}$  SE., is exposed at  $X$  (Fig. 333) on the south side of the fault.

**To FIND:** (a) the net slip of the fault, (b) the strike of the horizontal projection of the net slip, (c) the plunge of the net slip, (d) the relative movement along the fault—that is, which block moved up—and (e) the location of the third vein on the north side of the fault.

**CONSTRUCTION:** As shown in Fig. 332, draw  $AC$  and  $A'C'$  parallel to the strike of the N.  $30^{\circ}$  W. vein, and draw  $BD$  and  $B'D'$  parallel to the strike of the N.  $30^{\circ}$  E. vein. Draw  $EE'$ ,  $FF'$ , and  $GG'$  perpendicular to  $BD$ ,  $AC$ , and  $FF'$ , respectively, at any convenient points such as  $E''$ ,  $F''$ , and  $G''$ . Using these lines as horizontals, we shall now make cross sections.

Draw  $HH'$  parallel to and at an arbitrary distance  $h$  from  $EE'$ ; construct  $II'$  and  $JJ'$  in a similar way. These lines represent a level that we shall call the *lower reference plane*; it is  $h$  distance below the surface plan. Lay off angle  $GG''K$  equal to the dip of the fault,  $G''K$

intersects  $JJ'$  at  $K'$ . Lay off angle  $EE''L$  equal to the dip of the N.  $30^\circ$  E. vein;  $E''L$  intersects  $HH'$  at  $L'$ . Lay off angle  $F'F''M$  equal to the dip of the N.  $30^\circ$  W. vein;  $F''M$  intersects  $II'$  at  $M'$ . From  $K'$ , draw  $K'O$  parallel to  $FF'$ . From  $L'$ , draw a line parallel to  $BD$  to intersect  $K'O$  at  $P$ . From  $M'$ , draw a line parallel to  $AC$  to intersect

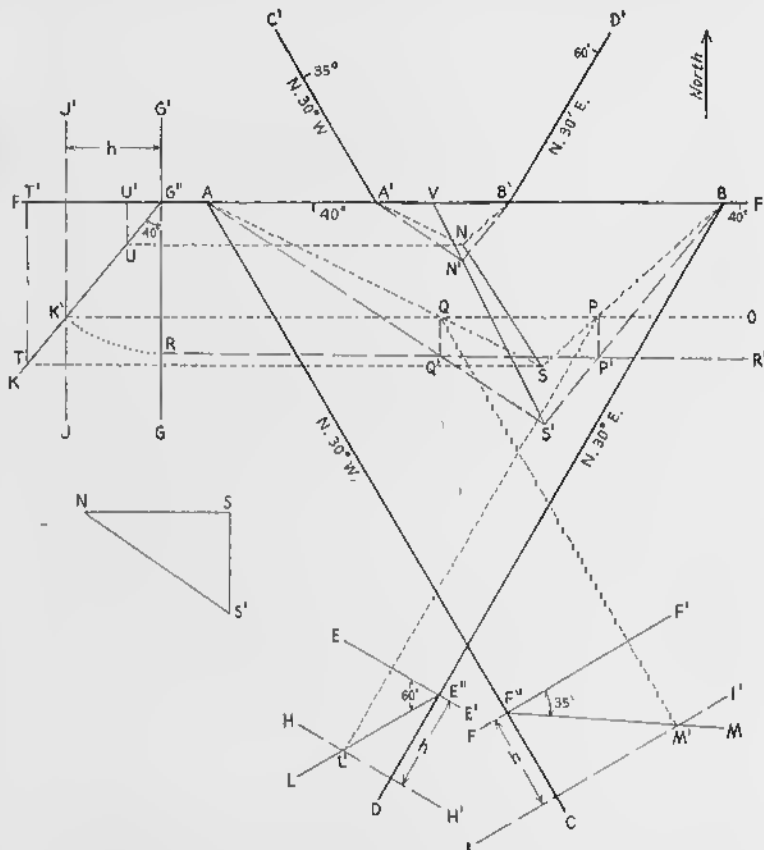


FIG. 332—Graphic Solution of an Inclined Fault Problem. Two veins, one striking N.  $30^\circ$  W. and dipping  $35^\circ$  NE., the other striking N.  $30^\circ$  E. and dipping  $60^\circ$  NW., are displaced along the fault  $FF'$ .

$K'O$  at  $Q$ .  $K'O$ ,  $L'P$ , and  $M'Q$  represent contours on the fault and the veins; at all points on these lines the respective fault or vein is exactly  $h$  distance below the surface of the plan. The intersections of the two veins with the fault on this lower reference plane are at  $P$  and  $Q$ .

We shall now make a section in the plane of the fault. It is necessary to rotate the fault plane into the plane of the map in order to show this section. Line  $FF'$  is used as the axis of rotation. Using  $G'K'$  as the radius and  $G'$  as the center, draw an arc to intersect  $GG'$  at  $R$ .  $G'R$  is the true slope distance in the fault plane between the surface plan and the lower reference plane. From  $R$ , draw  $RR'$  parallel to  $FF'$ .  $BG'RR'$  is a section in the plane of the fault.

From  $Q$ , construct a line perpendicular to  $K'O$  to intersect  $RR'$  at  $Q'$ . From  $P$ , construct a line perpendicular to  $K'O$  to intersect  $RR'$  at  $P'$ .  $Q'$  and  $P'$  represent the intersection of the veins with the lower reference plane, viewed in the fault plane.

Draw  $AQ'$  and  $BP'$  to an intersection at  $S'$ .  $AS'$  and  $BS'$  represent the trace of the two veins on the south wall of the fault plane;  $S'$  represents their intersection on the south wall. Draw  $A'N'$  and  $B'N'$  parallel to  $AS'$  and  $BS'$ , respectively.  $N'$  represents the intersection of the trace of the two veins on the north wall. Draw  $N'S'$ , which is the net slip.

Draw  $AQ$  and  $BP$  to an intersection at  $S$ .  $AS$  is the horizontal projection of the intersection of the N.  $30^\circ$  W. vein and the fault.  $BS$  is the horizontal projection of the intersection of the N.  $30^\circ$  E. vein and the fault.  $S$  is the horizontal projection of the intersection of the two veins on the south wall of the fault plane. Draw  $A'N$  and  $B'N$  parallel to  $AS$  and  $BS$ , respectively. Draw  $NS$ , which is the horizontal projection of the net slip.

To determine the plunge of the net slip, it is necessary to find the altitude of the points for which  $N$  and  $S$  are the horizontal projections. Draw a line from  $S$ , parallel to  $FF'$ , to intersect  $G''K$  at  $T$ ; and draw a line from  $N$ , parallel to  $FF'$ , to intersect  $G''K$  at  $U$ . Lines perpendicular to  $FF'$  are then erected, one from  $T$  and the other from  $U$ . These perpendiculars intersect  $FF'$  at  $T'$  and  $U'$ .  $T'U'$ , on the same scale as the map, whatever it may be, is the difference in altitude between the points of which  $N$  and  $S$  are the horizontal projections.

Lay off  $NS$  on a separate part of the paper. Drop a perpendicular from  $S$  to  $S'$  such that  $S'S = T'U'$ . Draw  $NS'$ .  $SNS'$  gives the vertical angle that the net slip makes with its horizontal projection; it is the plunge of the net slip. As a check on your work,  $NS'$  in this diagram should equal  $N'S'$  in the main construction.

The point of intersection of the two veins on the south side of the fault with the fault plane lies at a lower altitude and to the east of the corresponding intersection of the north side of the fault. The relative movement along the fault is such that the south side has moved down and to the east in relation to the north side. Extend  $N'S'$  to intersect  $FF'$  at  $V$ . Angle  $S'VB$  is the pitch of the net slip.

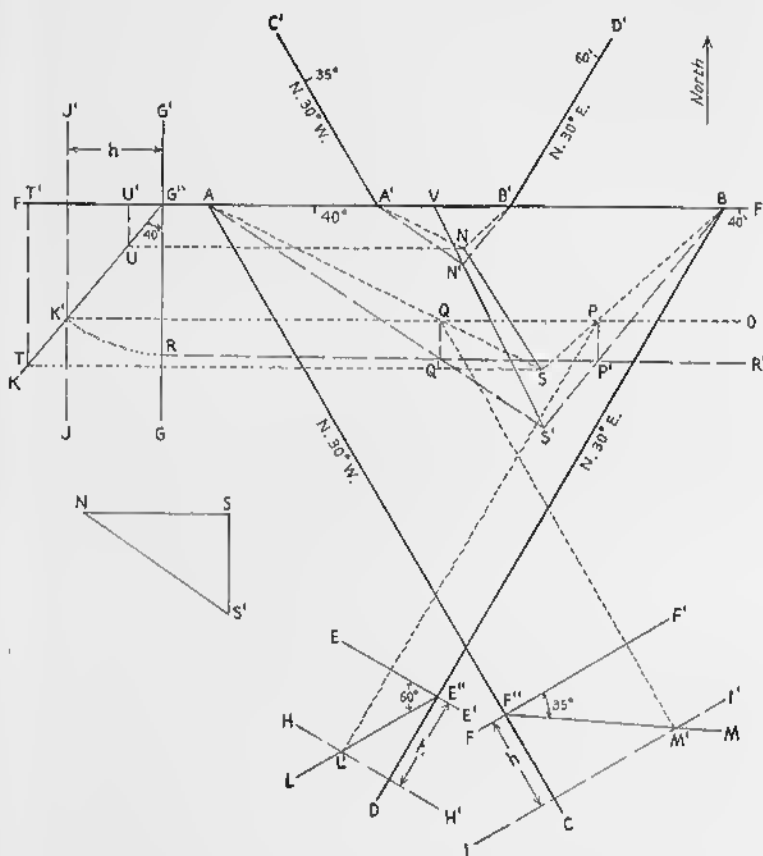


(FIG. 332—Repeated.) Graphic Solution of an Inclined Fault Problem. Two veins, one striking N. 30° W. and dipping 35° NE., the other striking N. 30° E. and dipping 60° NW., are displaced along the fault  $FF'$ .

Fig. 333, which illustrates the method used to locate the N.  $40^{\circ}$  E. vein on the north side of the fault, shows data concerning the fault identical with that in Fig. 332.  $FF'$  is the trace of the fault on the map.  $K'O$  is the horizontal projection of the intersection of the fault and the lower reference plane, and  $RR'$  is this intersection after it has been rotated into the plane of the map.

The location of the N.  $40^{\circ}$  E. vein on the south side of the fault is shown. Draw  $XY$  parallel to the strike of the vein. At some con-

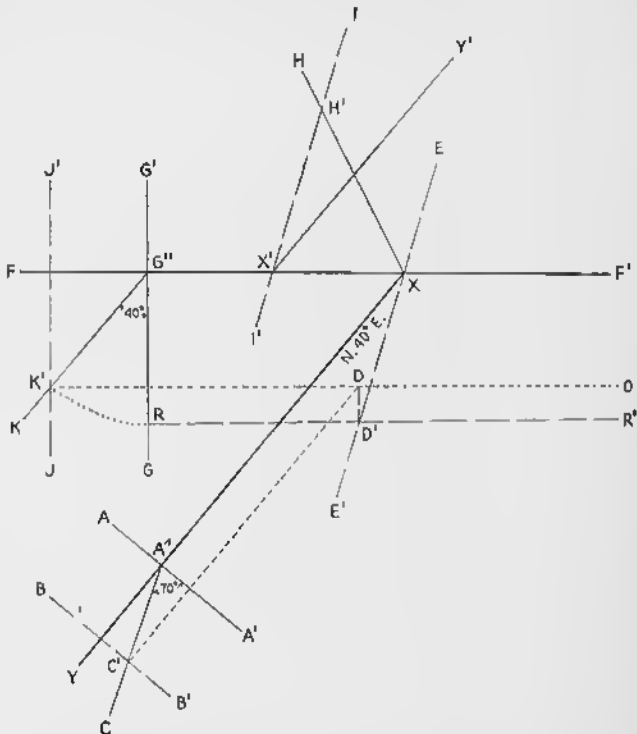


FIG. 333.—Graphic Solution of a Fault Problem. Position of N.  $40^{\circ}$  E. vein is known on south side of fault,  $FF'$ . Net slip is same as in Fig. 332. Problem is to find position of N.  $40^{\circ}$  E. vein on north side of fault. N.  $40^{\circ}$  E. vein dips  $70^{\circ}$  SE.

venient point along  $XY$ , such as  $A''$ , draw  $AA'$  perpendicular to  $XY$ . At  $h$  distance (the same distance as used in Fig. 332) from  $AA'$ , draw  $BB'$  perpendicular to  $XY$ . Lay off angle  $A'A''C$  equal to  $70^\circ$ , the dip of the N.  $40^\circ$  E. vein. From  $C'$ , the intersection of  $A''C$  with  $BB'$ , draw a line parallel to the strike of the N.  $40^\circ$  E. vein to intersect  $K'O$  at  $D$ .  $C'D$  represents a contour on the vein; at all points on this line the vein is exactly  $h$  distance below the surface of the plan. The intersection of the vein with the fault on this lower reference plane is

at  $D$ . From  $D$  draw a line perpendicular to  $K'O$  to intersect  $RR'$  at  $D'$ .  $D'$  represents the intersection of the vein with the lower reference plane, viewed in the fault plane.

Draw  $EE'$ , which passes through points  $X$  and  $D'$ .  $EE'$  is the trace of the N.  $40^\circ$  E. vein on the south wall of the fault plane. Fig. 332 shows that the north block has moved up and to the west; therefore the trace of the vein on the north wall of the fault plane will be above and to the west of  $EE'$ . At any convenient point along  $EE'$ , as at  $X$ , lay off angle  $G'XH$  equal to the pitch of the net slip, which is the angle  $S'VB$  of Fig. 332; and on  $XH$ , lay off  $XH'$  equal to the net slip, which is  $N'S$  of Fig. 332. Through  $H'$ , draw  $II'$  parallel to  $EE'$ .  $II'$  is the trace of the vein on the north side of the fault. From  $X'$ , draw  $X'Y'$  parallel to  $XY$ . Point  $X'$  represents the intersection of the vein with the fault on the north side of the fault, and  $X'Y'$  is the trace of the N.  $40^\circ$  E. vein on the plan, north of the fault.

### Problems

1. A vertical fault strikes east-west across a featureless plain. Three veins, which may be called  $A$ ,  $B$ , and  $C$ , are disrupted by the fault. The data are as follows: "Distance" is measured from west to east along the fault, the starting point being indicated by 0 distance.

<i>Vein</i>	<i>Strike</i>	<i>Dip</i>	<i>Distance on North Wall</i>	<i>Distance on South Wall</i>
$A$	N. $10^\circ$ E.	$45^\circ$ SE.	0 feet	150 feet
$B$	N. $40^\circ$ W.	$30^\circ$ SW.	550 feet	500 feet
$C$	N. $45^\circ$ E.	$60^\circ$ SE.	700 feet	?

(a) Determine the net slip, the pitch of the net slip, the strike of the horizontal projection of the net slip, and the relative movement on the fault—that is, which block moved relatively upward. (b) Locate vein  $C$  on the south side of the fault.

2. A fault plane, exposed on a featureless plain, strikes N.  $90^\circ$  E. and dips  $40^\circ$  N. Three veins, which may be called  $A$ ,  $B$ , and  $C$ , are disrupted by the fault. The data are as follows:

<i>Vein</i>	<i>Strike</i>	<i>Dip</i>	<i>Distance on North Wall</i>	<i>Distance on South Wall</i>
$A$	N. $35^\circ$ E.	$25^\circ$ SE.	0 feet	100 feet
$B$	N.	$50^\circ$ W.	600 feet	500 feet
$C$	N. $45^\circ$ W.	$55^\circ$ NE.	800 feet	?

(a) Determine the net slip, the plunge and pitch of the net slip, the strike of the horizontal projection of the net slip, and the relative movement on the fault. (b) Locate vein  $C$  on the south side of the fault.

## EXERCISE 11

### Unconformities, Faults, and Folds

#### Problems

No additional instructions are necessary for this exercise.

1. Use Fig. 334. For ease of reference each formation has been given a letter symbol. The alphabetical order of the symbols does not refer to the age relations between the formations. (a) Draw two cross sections, one along the line *AB* and the second along *CD*. Assume

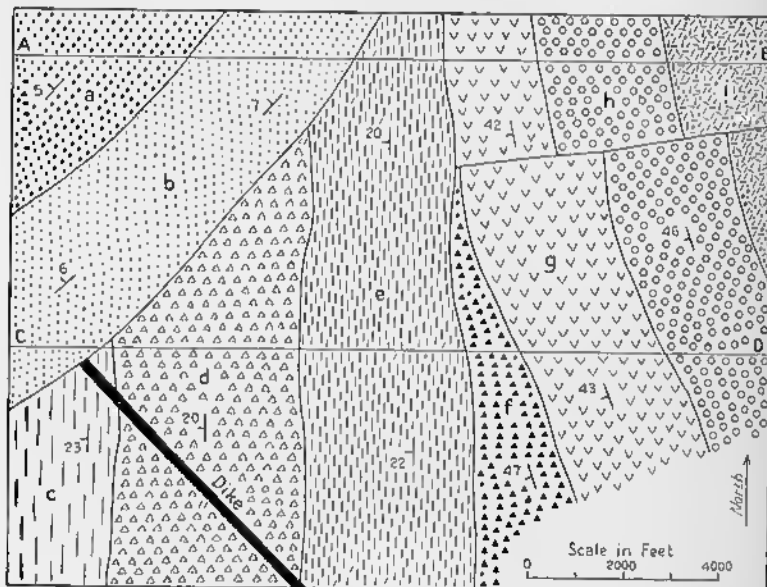


FIG. 334—Problem for Exercise 11.

that the surface is flat. (b) How many unconformities exist and between what formations? (c) Date the cross-faulting at the northeast corner of the map. (d) Date the dike in the southwest corner of the map. (e) Tabulate the geologic history.

2. Use Fig. 336, which is a map of an area that includes part of Glacier National Park, Montana. (a) Make a structure contour map of the contact between the Algonkian and Cretaceous rocks. (b)

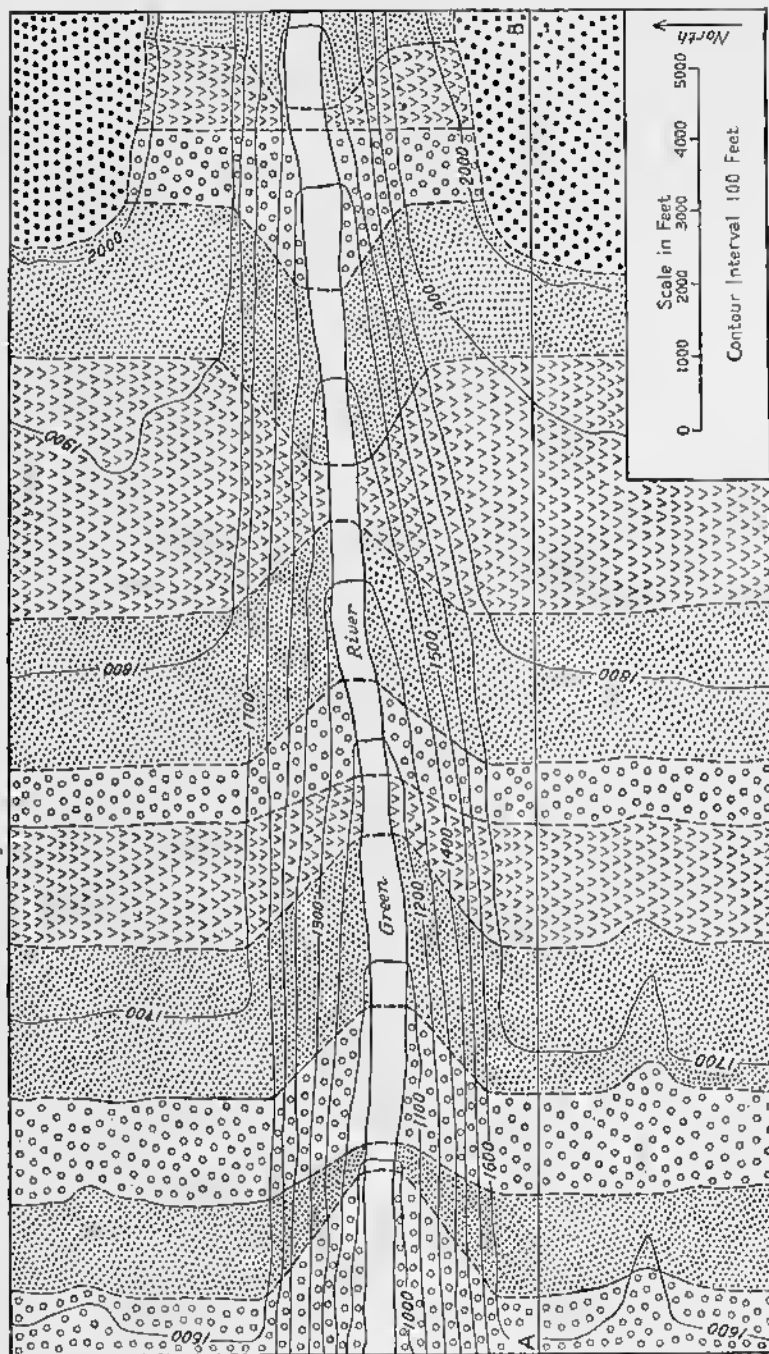


FIG. 335—Problem for Exercise 11.

Draw structure sections along the lines *AB* and *CD*. (c) What relation exists between the rocks of the Great Plains and the Rocky Mountains in this area?

3. Fig. 335 represents a plateau region cut by a deep gorge through which a fictitious Green River flows. Four formations are present: one shown by circles, a second by dots, a third by checks, and a fourth by the solid dots. Draw a structure section along the line *AB*.

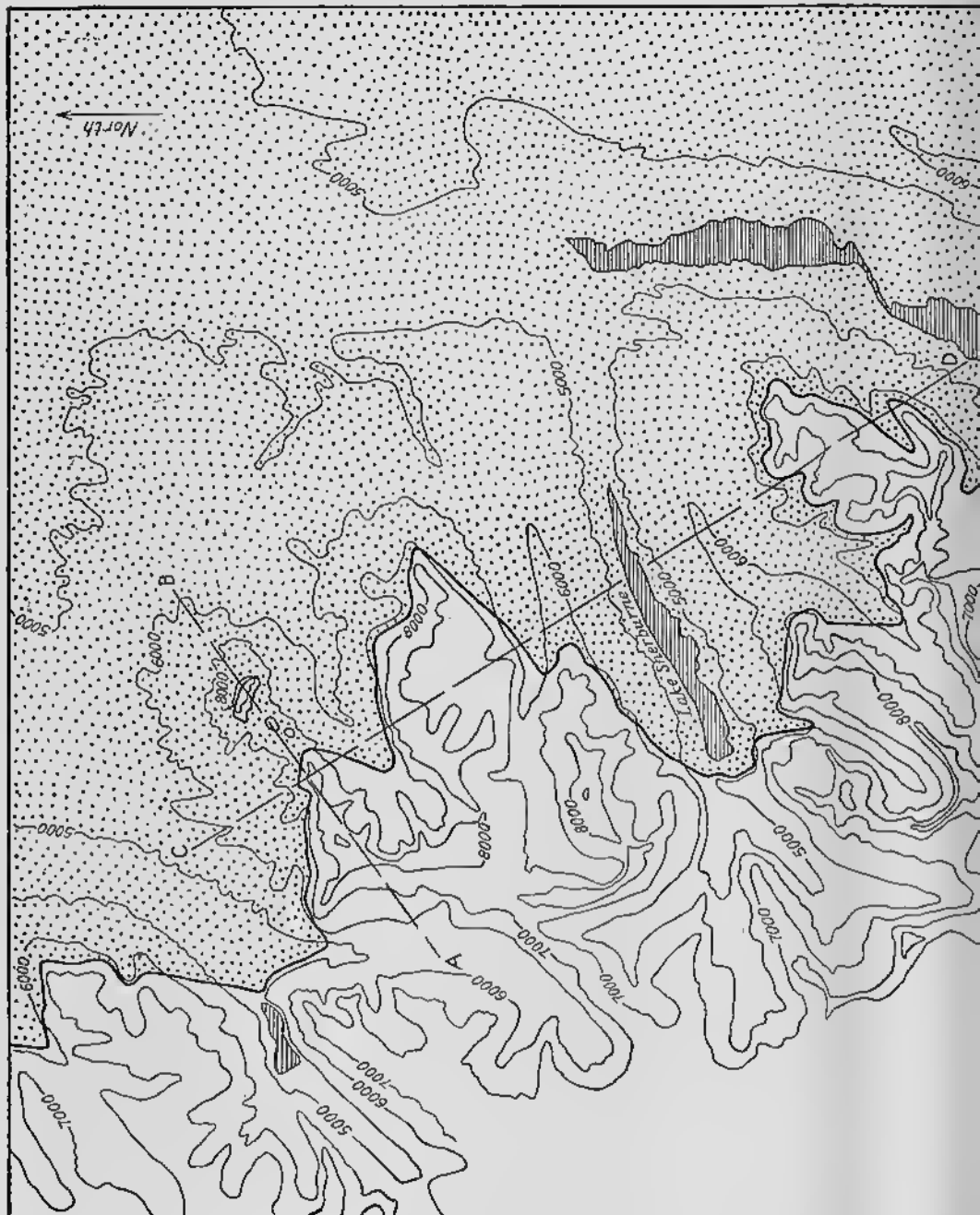




FIG. 336—Problem for Exercise 11.

# Index

## A

$\alpha$ , 336, 342, 345, 350, 351  
 Aa lava, 314  
 Abnormal anticlinorium, 50, 51  
 Abnormal synclinorium, 50, 51  
 $ab$ -plane, 337, 351  
 Absolute movements on faults, 153-154  
 Abyssinia, 325  
 Acceleration, 10, 11, 359  
     of gravity, 359  
 $ac$ -girdle, 354  
 $ac$ -plane, 337, 351, 354  
 $ac$ -crystallographic axis of muscovite, 353  
 Adirondack Mountains, 113, 114, 118,  
     119, 277, 311  
 Adjusted isogam map, 363, 365, 368  
 Adventive cones, 321  
 Aerial photographs, 2  
 Africa, 205, 209, 211, 275, 279, 318, 330,  
     374, 392  
 Agglomerate, 283, 317  
 Agglomerate, vent, 317  
 Alabaster, 24  
 Alaska, 326; *Pl. II*, *op. p.* 3; *Pl. VIII*,  
     *op. p.* 76; *Pl. XV*, *op. p.* 215  
 Alignment diagrams for thickness and  
     depth, 400-409  
 Allotrothion, 181  
 Allochthonous, 181, 183  
 Alps, 54, 58, 82, 159, 161, 183, 184, 185,  
     347  
 Alsation salt domes, 391  
 Alternating current, 394  
 Aluminum, gliding in, 27  
 American salt domes, 251-259  
 Amorphous solids, 8  
 Ampere, 387  
 Analysis:  
     petrofabric, 332-355  
     statistical, 334  
 Anderson, E. M., 288  
 Angle of incidence, 370  
 Angle of reflection, 382  
 Angle of refraction, 379  
 Angle of slope, 403-406  
 Angular unconformity, 212-247; *Pl. XVII*,  
     *op. p.* 242  
 Animal tracks, 75  
 Anomaly:  
     gravity, 363  
     magnetic, 373  
 Anthracite coal, 393  
 Anticline, 36, 38, 40, 45, 47, 48, 59, 61,  
     63, 82, 85, 88, 367, 374, 392, 396;  
     *Pl. V*, *op. p.* 38  
     plunging, 44, 45, 47, 84, 85, 176, 365,  
     368  
 Anticlinorium, 50, 51  
 Antithetic faults, 205-206

Apophysis, 283  
 Appalachia, 51  
 Appalachian geosyncline, 51  
 Appalachian Highlands (Province, Monu-  
     ments, Area), 49, 58, 82, 92, 93, 94,  
     174, 176, 369  
 Apparent dip, 421, 422, 426  
 Apparent movements on faults, 137-143  
 Apparent resistivity, 395  
 Applications of structural petrology,  
     field, 354-355  
 Aquatic ripple-marks, 69  
 Arch-bend, 40  
 Arch of flow structures in pluton, 306-  
     307, 311  
 Ardenites, *nudus*, 318, 324  
 Argentina, 327  
 Arizona, 193, 208, 241, 321; *Pl. XVIII*,  
     *op. p.* 314  
 Artificial electrical currents, 387, 394-397  
 Ash, volcanic, 317, 326  
 Assynt district, Scotland, 180, 181  
 Asymmetric anticline, 61, 63  
 Asymmetric fold, 39  
 Asymmetric Incolith, 273  
 Asymmetry, cause of, 94  
 Aetectonic plutons, 296  
 Atmosphere, 21  
 Atomic lattice, 333  
 Atomic structure, 7  
 Atoms, 26-28, 332-334  
 Attitude of axial plane, 31, 35, 59-61  
 Attitude of beds, 31, 35, 39, 61, 65, 66, 82  
 Attitude of cleavage, 214  
 Attitude of folds, 34, 35, 59-61  
 Attitude of schistosity, 214  
 Austria, 347, 354  
 Autochthon, 181  
 Autochthonous, 181, 183  
 Autolith, 262, 294  
 Average velocity, effective, 384  
 Axial plane, 34, 35, 59-61, 95  
     cleavage, 215-217  
 Axial surface, 35  
 Axial symmetry of fabric, 343  
 Axial symmetry of movement, 346, 347  
 Axial trace, 44-49  
 Axis:  
      $c$ -crystallographic, quartz, 338  
     optic, 337, 338, 339, 341  
     strain, 30, 106  
 Azimuth of traverse, 404, 406

## B

*b*, 336, 342, 344, 345, 353, 354  
*B*, 336  
 Bailey, F. B., 183  
 Bain, G. W., 81  
 Baker, A. A., Jr., 204, 205

## INDEX

Balance, torsion, 363-367  
 Balanced forces, 10  
 Balk, R., 114, 277, 298, 304  
 Balmhorn, Switzerland, 54  
 Bandai-San, Japan, 325  
 Banded intrusive rocks, 262  
 Banding:  
     cleavage, 219  
     segregation, 219  
 Bamock overthrust, 182, 183, 184, 185  
 Barrell, J., 197, 290  
 Barton, D. C., 251, 253, 257  
 Basalt, joints in, 123-124; *Pl. XII*, op. p. 122; *Pl. XIII*, op. p. 123  
 Basin, 46, 47  
 Batholiths, 261, 288-296  
*hc*-plane, 337, 351  
 Beckwith, R. H., 140  
 Bedding cleavage, 218-219, 220  
     relation to major structure, 232  
 Bedding fault, 149  
 Bedding fissility, 213, 220  
 Bedding schistosity, 218  
 Bedding thrust, 173, 175  
 Beds:  
     attitude of, 33-35, 36, 61, 65, 66, 82  
     pyroclastic, 316-318, 320, 321  
 Belknap Mountains, New Hampshire, 284, 285  
 Bell, J. P., 351  
 Beouding, 89  
 Ben More thrust, 180, 183  
 Bentz, A., 327  
 Beude, 92  
 Billings, M. L., 171, 185, 203, 242, 250  
 Biotite in structural petrology, 337, 340, 341, 349  
     showing lineation, 221, 223  
 Birrell, F., 5  
 Blackwelder, E., 168  
 Blisters, lava, 311  
 Block, 317  
     tilted fault, 195-201  
 Block diagrams, 85  
 Block lun, 314  
 Block mountains, fault, 195-201  
 Bombs, 317  
 Boston, Massachusetts, 242, 279  
 Bouguer reduction, 361  
 Boulders:  
     elongated, 221, 223  
     origin of, 234-236  
     "stretched," 221, 223  
     origin of, 234-236  
 Branches, 36  
 Breadth of overthrusts, minimum, 179, 185  
 Break in stream profile, 166  
 Break thrust, 172, 175, 200  
 Breccia:  
     fault, 158, 254  
     volcanic, 283, 317  
 Brefven dike, Sweden, 279  
 Bridgman, P. W., 103  
 British Columbia, 291  
 Brittle substances, 17, 100  
 Broad warps, 33  
 Bryce Canyon, Utah; *Pl. I*, op. p. 2  
*B*-tectonite, 353  
 Bucher, W. H., 4, 57, 210, 329, 331  
 Buckling, 89  
 Buddington, A. F., 311  
 Buffalo Mountain, Tennessee, overthrust at, 185  
 Buried ridges, 96, 367, 374  
 Bushveld igneous complex, South Africa, 275, 276  
 Busk, H. G., 426  
 Buwalda, J. P., 167  
 Buxtorf, A., 56  
 Bysmalith, 273  
  
 C  
  
 c, 335, 342, 344, 345  
 Calcite in structural petrology, 336, 337, 341, 349, 353  
 Cahlers, 319, 325-328; *Pl. XIX*, op. p. 315  
     collapse, 325, 326-328  
     erosion, 325, 328  
     explosive, 325  
     Morro, Argentina, 327  
 California, 83, 95, 164, 166, 169, 295; *Pl. IX*, op. p. 77; *Pl. XI*, op. p. 113  
 Callaghan, E., 202  
 Campbell, C. D., 159  
 Campbell, M. R., 174, 176  
 Canadian Rockies, 175, 176  
 Cap rock, 252, 253, 254, 255, 366  
     origin of, 257  
 Caspian Sea, 251, 252  
 Castle Peak stock, British Columbia, 291  
 Cast of mud-cracks, 75  
 Cast of ripple-marks, 70, 71  
 Cauldron subsidence, 285-288, 295, 313  
     surface, 285, 287, 327  
     underground, 285, 286, 294  
 c-crystallographic axis:  
     calcite, 336, 353  
     quartz, 336, 338, 349, 351, 352, 354  
 Ceiliar Mountain, Nevada, 202  
 Counter counter, 120  
 Central eruptions, 319-330  
 Cerro de Pasro, Peru; *Pl. V*, op. p. 38; *Pl. VI*, op. p. 39  
 Chalk, 100, 104  
 Chamberlin, R. T., 55, 105  
 Chamberlin, T. C., 3  
 Channeling, 72, 74  
 Chapman, C. A., 277, 291, 292  
 Chapman, R. W., 291, 292  
 Chemical composition, folds due to changes in, 92, 97  
 Chevron folds, 41  
 Chilled contact, 263  
 China, 95, 169  
 Cinder, 317  
 Cinder cone, 321; *Pl. XVIII*, op. p. 314  
 Circular sections of ellipsoid, 30, 106-108  
 Clay, C. H., 185  
 Clark, R. P., 364, 366, 372, 373, 386  
 Clark, W. O., 324  
 Classification of faults, 148-154  
 Cleavage, 32, 213-220, 223-233; *Pl. XV*, op. p. 215  
     axial plane, 215-217, 228-230  
     bedding, 218-219, 220  
         relation to major structure, 232  
     flow, 32, 215-217, 220, 224-230, 233; *Pl. XV*, op. p. 215  
         relation to major structure, 224-230

Cleavage (*cont.*):  
 fracture, 217, 220, 230-232; *Pl. XV*,  
*op. p. 215*  
 and lineation, 238  
 relation to major structure, 230-232  
 mineral, 213, 337, 340-341  
 pole of, 341  
 relation to major structure, 223-233  
 rock, 213  
 shear, 217-218, 220, 232  
 shear and lineation, 238  
 relation to major structure, 232  
 slaty, 215-217  
 symbols for, 214  
 types of, 215-220

Cleavage banding, 219

Cleveland dike, England, 279

Clinometer, 60

Gloos, E., 298, 355

Cloos, H., 92, 205, 206, 209, 211, 298

Closed fold, 42

Closed structure, 431

Closure, 431

Clough, C. T., 181, 241

Cluster, volcanic, 323

Coal, anthracite, 393

Coefficient of friction in thrusting, 186-190

Cognate xenolith, 202

Collapse calderas, 325, 326-328

Collapse depression, 315

Collective diagram, 342

Colorado, 363, 365  
 Plateaus, 163, 321

Columbia Plateau, 315, 318

Columnar jointing, 123-124; *Pl. XII*,  
*op. p. 122*; *Pl. XIII*, *op. p. 123*

Compaction of sediments, fulis due to, 94-97

Compass, Swedish mining, 371

Competency, 88

Competent, 42, 88, 89, 224, 230

Components of force, 11

Composite batholith, 290

Composite dome, 320, 321

Composite dike, 279

Composite fault scarp, 163, 168-171

Composite sill, 268, 200

Composition of forces, 10, 11

Compound volcanoes, 322

Compressibility, 17

Compression, 15, 87, 99, 172  
 fractures resulting from, 90, 101-103  
 horizontal, 92-94, 95, 101

Compressive strength, 19, 100, 106

Compressive stress, 13, 16

Concentric faults, 320

Concordant, 254, 264

Concordant plutons, 217-279

Conductivity, electrical, 389

Cone:  
 adventive, 321  
 cinder, 321; *Pl. XVIII*, *op. p. 314*  
 composite, 320, 321  
 driblet, 314  
 lava, 320  
 parasitic, 321  
 pyroclastic, 321  
 spatter, 314  
 volcanic, 319-321

Cone sheets, 280, 281, 283, 288

Confining pressure, 14, 20-22, 99, 102, 159

Conglomerate, volcanic, 317, 318

Conical fracture, 100, 103, 124, 283

Conjugate joint system, 112, 126

Connecticut Valley, 197

Constant, gravitational, 359

Contact, chilled, intrusive, 263

Contemporaneous deformation, 97-98

Contour diagram, 119-121, 340, 341

Contour, structure, 84-85, 363, 365, 386,  
 387, 430-433

Convection currents, 92, 95

Convergence of axial traces, 48

Cordillera, North American, 94

Core of recumbent fold, 40

Correction:  
 Bouguer, 361, 363, 364  
 free air, 361, 363, 364  
 isostatic, 363  
 terrain (topographic), 362, 363, 364

Corrections in gravimetric methods, 360-362

Corrections in magnetic methods, 372-373

Corrections in pendulum method, 360-362

Corrections in surveying natural electrical currents, 392

Corrugations, 221

Coulomb, 388

Counter:  
 center, 120  
 peripheral, 120, 121

Couplets, 15, 30, 31, 87, 95, 99, 105, 108,  
 124, 127, 172, 184-195, 210, 224,  
 233, 306  
 fractures resulting from, 103-104  
 horizontal, 92, 94-95

Crater, 310, 323-325  
 pit, 324

Crater Lake, Oregon, 326

Creep, 22, 23

Creep recovery, 23

Crystal plane, 36, 37

Crest of folds, 36, 37

Crevasses in glaciers, 124

Crinkled schist, 347

Crinkles, 221

Criticism of granite-tectonics, 310-311

Cross-hedging, 62, 69, 71-72, 73, 156

Cross joints, 303, 306, 307, 311

Cross-lamination, 71

Crushing strength, 88  
 of rocks in thrusting, 188

Crush-rock, flinty, 159

Cryptovolcanic caldera, 327

Cryptovolcanic structures of United States, 328-330

Crystalline solid, 8

c-section, 337

Cumulation, 49

"Cup and socket" fractures, 123-124

Cupolas, 289, 290

Current:  
 alternating, 394  
 artificial electrical, 387, 394-397  
 convection, 92, 95  
 natural electrical, 389-394  
 spontaneous electrical, 380-393  
 telluric, 393-394

Current electrodes, 394, 395

Current flow-lines, 388, 389

Current ripples, 69-71

Curvature value, Eötvös differential, 366  
 Curve, travel-time, 376-381

D

Daly, R. A., 4, 218, 260, 289, 291  
 Darton, N. H., 52, 53, 67  
 Daubrée, A., 104  
 Declination, magnetic, 371  
*Décollement*, 55, 56, 173  
 Deep domes, 255  
 Deer Creek lincolith, Wyoming, 309  
 Deformation, 16  
     contemporaneous, 92, 97-98  
     elastic, 17, 32, 99  
     mechanics of plastic, 25-29  
     plastic, 19, 25, 32, 88, 90, 216  
     repeated, and cleavage, 232-233  
     successive stages of, 348  
         three stages of, 17  
 Deformation ellipsoid, 30  
 Deformation in outer shell of earth, 31-32  
 Deformed strata; *Pl. II, op. p. 3*  
 De Golyer, L., 251  
 Depression, 49  
     collapse, 315  
 Depressions on lavas, 315  
 Depth of folding, 51-57  
 Depth of horizon:  
     refraction method, 384  
     refraction method, 381  
     resistivity methods, 395-396  
 Depth of strata (horizon), 401-409  
 Descriptive geometry, 444-453  
 Detector, 375  
 Diagonal fault, 149  
 Diagonal joint, 112, 304  
 Diagonal slip fault, 148  
 Diagrams:  
     alignment, for thickness and depth, 408-409  
     collective, 342  
     contour, 119-121, 340, 341  
     eccentric symmetry, 346  
     non-selective, 342  
     partial, 342  
     petrofabrie, 337-343, 352, 353  
     point, 118, 338, 340, 341  
     selective, 342  
     stress-strain, 18  
 Diagrams for plotting joints, 114, 115,  
     118, 119  
 Diapir folds, 64, 257  
 Diatremes, 330  
 Difference of potential, 389  
 Differential compaction of sediments, 96-97  
 Differential curvature, 366  
 Differential forces, 14-16  
 Differential vertical movements, 91-92  
 Differentiated dike, 279  
 Differentiated lopolith, 276  
 Differentiated sill, 269-270  
 Digitations, 40  
 Dike, 279-283, 318, 330; *Pl. XVII, op. p.*  
     243  
     composite, 279  
     differentiated, 279  
 Dike (cont.):  
     multiple, 279  
     radiating, 280, 281  
     replacement, 279  
     simple, 279  
 Dike set, 280  
 Dike swarm, 280  
 Dilatation, 16  
 Dip, 35; *Pl. II, op. p. 3; Pl. III, op. p. 32*  
     apparent, 421, 422, 426  
     magnetic, 371  
     projected, 422  
 Dip fault, 149  
 Dip joint, 112  
 Dip needle, 371  
 Dip of joint, 111  
 Dip shooting, 385  
 Dip slip, 134, 135, 435  
 Dip-slip fault, 148  
 Dip-strike symbols, 33, 35, 39, 214  
 Dipping strata, outerop pattern of, 65-66,  
     415-419  
 Directing force, horizontal, 366  
 Direction:  
     of projection, 430  
         "preferential," 393  
 Disconformity, 243-246  
 Discontinuity of structures at faults, 155-156  
 Discordant, 254, 284  
     plutons, 279-296  
 Disharmonic folds, 52, 53  
 Distance:  
     map, 403, 404  
     slope, 403, 404  
 Distortion, 16, 17  
     lines of no, 106  
     surfaces of no, 107, 108  
 Distributive faulting, 131  
 Diurnal variation, 372, 393  
 Divergence of axial traces, 48  
 Dome, 46, 47  
     deep, 255  
     endogenous, 320, 322  
     exogenous, 320, 321  
     intermediate-depth, 255  
     salt, 32, 95, 251-259, 295, 358, 364, 366,  
         367, 368, 372, 374, 377, 385, 394, 397  
     salt, non-piercement, 254  
     salt, piercement, 254  
     shallow, 255  
     volcanic, 321-322  
 Dossor, Russia, 368  
 Doubly-plunging anticline, 47, 84, 85, 176,  
     365, 368  
 Doubly-plunging fold, 46, 47  
 Doubly-plunging syncline, 46, 47, 171  
 Downbuilding of salt domes, 257  
 Drift along faults, 158  
 Drift folds, 42, 43, 76-81, 183, 184, 221;  
     *Pl. VIII, op. p. 76*  
 Dribblet cones, 314  
 Drill holes, 53, 67, 356, 430  
 Drilling, 67  
 Ductile material, 100, 102  
 Ductile substances, 17, 100  
 Duluth lopolith, 275, 276  
 Dust, volcanic, 317  
 Dutch East Indies, 326  
 Dyne, 10, 359, 364, 369

## E

c, 336, 353  
 Wardley, A. J., 193, 198, 199, 201  
 Earth, magnetic field of, 370  
 Earthquake, 98, 168, 169  
     Cedar Mountain, Nevada, 202  
     Owens Valley, California, 164, 165  
     Pleasant Valley, Nevada, 165  
 Earthquake waves, 32, 210  
 East Indies, Dutch, 326  
 Eby, J. B., 364, 366, 372, 373, 386, 387  
 Eccentric symmetry diagrams, 345  
 Effective average velocity, 384  
 Elastie afterworking, 23  
 Elastic deformation, 17, 32, 99  
 Elastic flow, 23  
 Elastic limit, 17, 23, 30  
     proportional, 18, 21  
 Elastie waves, 374, 376, 377-380  
 Electrical currents:  
     artificial, 387, 394-397  
     natural, 387, 389-394  
     spontaneous, 389-393  
 Electrical methods, 67, 386-397  
 Electrodes, 390, 391, 394, 395  
     current, 394, 395  
     line, 394  
     point, 394  
     rending, 395  
 Electromotive force, 388  
 Electrons, 7  
 Ellipse, strain, 30, 95, 106, 107, 109,  
     124, 224, 229  
 Ellipsoid, deformation, 30  
 Ellipsoid, strain, 29-31, 101, 106-110,  
     124, 125, 126, 127, 216-218, 220,  
     224-232  
 Elongated pebbles and boulders, 221,  
     223, 234-236  
 Enigma region, Russia, 308  
 Embryonic volcanoes, 325  
 Endogenous domes, 320, 322  
 Endurance limit, 22  
*En échelon* faults, 150, 200, 203  
*En échelon* folds, 46, 48  
*En échelon* fractures, 108  
*En échelon* gravity faults, 194-195,  
     200, 201, 202, 203  
 Englund, 279  
 Eolian ripple-marks, 69  
 Kötvös, 364  
 Kötvös curviture value, 366  
 Kötvös null, 364, 366, 367, 368  
 Epidote in structural petrology, 349  
 Equal-arc net, Schmidt, 349  
 Equal-arc projection, 117  
 Equilibrium, 11  
 Equipotential line, 389, 391, 392, 394-395  
 Equipotential surface, 389  
 Erosion calderas, 325, 328  
 Erosion thrust, 173, 175  
 Eruption:  
     central, 319-330  
     fissure, 318-319  
 Erzgebirge, 289  
 Europe, 205, 209  
 Evolution of salt domes, structural,  
     257-258  
 Exercises, laboratory, 401-457  
 Exogenous domes, 320, 321

Explosion, phreatic, 325  
 Explosion in seismic work, 374, 376  
 Explosion pits, 325  
 Explosive calderas, 325  
 Extension fractures, 103, 125, 129, 281,  
     288

Extension joints, 125  
 External forces, 13, 99  
 Extrusive igneous rocks, 260, 313-331

## F

Fabric, 333-335  
     structural, 333-335  
     symmetry of, 343-345, 346-348  
 Facets, triangular, 165-166, 198, 201, 206  
 Facies:  
     metamorphic, 248  
     sedimentary, 160  
 Failure by rupture, 99-100  
 Fairbairn, H. W., 234, 333, 337  
 False-bedding, 71  
*Fan* fold, 41  
 "Fan" of joints, 306, 307  
*Fan* scarp, 164  
*Fan* shooting, 375, 377  
*Fauillet* salt dome, Texas, 364, 366, 372,  
     373  
 Fauth, A. E., 194  
 Fatigue, 22  
 Fatigue limit, 22  
 Fault block mountains, 195-201, 206  
 Fault block, tilted, 193, 195-201  
 Faulting:  
     distributive, 131  
     intermittent, 206, 208  
 Fault-line, 131  
 Fault-line scarp, 162, 166, 168, 169  
 Fault outcrop, 131  
 Fault pattern, 149-160  
 Fault problems, solution of, 434-438, 445-  
     446, 448-453  
 Faults, 32, 98, 108, 130-213, 255, 305,  
     306, 307, 335, 367, 369, 374, 385, 386,  
     393, 397, 435, 445-446, 448-453, 454;  
     Pl. XIV, op. p. 214  
     antithetic, 205, 206  
     apparent movements, 137-142  
     classification of, 148-154  
     concentric, 329  
     criteria for distinguishing from uncon-  
         formities, 249-250  
     criterion for recognition of, 165-171  
     description of, 130-147  
     discontinuity of structures at, 155-156  
     effects on disrupted strata, 137-142  
     *en échelon*, 150, 194-195  
     flat-lying gravity, 305, 311  
     general characteristics, 130-131  
     genetic classification of, 152-154  
     geometrical classifications of, 148-151  
     gravity, 152, 166, 192-212, 305, 311  
     attitude of, 192-193  
     *en échelon*, 194-195, 200, 201, 202, 203  
     on salt domes, 255  
     origin of, 208-212  
     pattern, 193  
     size, 192-193  
     high-angle, 150  
     longitudinal, 149, 152  
     low-angle, 150  
     nature of movement along, 131-137

Faults (*cont.*):  
 normal, 150, 192-212  
 oblique, 149  
 obsequent fault-line, 163  
 parallel, 150  
 peripheral, 150, 330  
 radial, 150, 329, 330, 331  
 reverse, 150  
 step, 193  
 strike, 148  
 strike slip, 148  
 tear, 152  
 thrust, 104, 105, 152, 153, 166, 172-191  
 transverse, 149, 152  
 vertical, 95, 202, 205, 445-446

Fault scarps, 162, 165, 168, 169  
 composite, 163, 168-171

Fault trace, 131

Fault troughs, 210

Fault zone, 131  
 Haywars, California, 166

Feather joints, 124, 125

Feldspar in structural petrology, 349

Fenster, 176

Ferden Rothoro, 54

Field applications of structural petrology, 354-355

Field, magnetic, 370

Field technique in structural petrology, 335

Finland, 215, 354

Fissility, bedding, 218, 220

Fissure eruptions, 318-319

Fissure, marginal, 304, 306, 307, 311

Flanks, 36

Flat-lying gravity faults, 306, 311

Flat-lying joints, primary, 304

Flaws, 152

Flexure, 33, 92, 302, 306, 307

Flexure folding, 87-89

Flinty crush-rock, 159

Flow:  
 elastic, 23  
 lamellar, 299  
 lava, 208, 313-316; *Pl. XIX*, *op. p.* 315  
 mud, 318  
 pseudoviscous, 23  
 turbulent, 299

Flow cleavage, 32, 215-217, 220, 224-230, 233

Flow folding, 87, 89-90

Flow lines, current, 388, 389

Flow stage, structures of, 299-302

Flow structure, 300-302, 306

Flow units, 315

Flowage folds, 81

Fluid mechanics of salt domes, 256

Fluorite in structural petrology, 349

Folded overthrusts, 176, 177, 183

Foliated strata, 421-425; *Pl. II*, *op. p.* 3

Folded thrusts, 171, 177, 179, 183

Folding:  
 causes of, 92-98  
 contrast in intensity, 248-249  
 incipient of, 87-92  
 parallel, 50, 53, 426  
 shear, 87, 90-91  
 similar, 50, 53  
 slip, 90  
 supratenuous, 50, 54  
 true, 87

Folding line, 440

Folds, 33-98, 454  
 description of, 33-57  
 drag, 42, 43, 76-81, 183, 184, 221; *Pl. VIII*, *op. p.* 76  
 geometrical reconstruction of, 426-429  
 piercing, 54  
 ploughing, 45, 46, 226-228, 236-237  
 recognition of, 58-81  
 recumbent, 39, 40, 54, 58, 181; *Pl. VII*, *op. p.* 39  
 representation of, 82-86  
 symmetrical, 39  
 tight, 42

Foliation systems, 46-51

Foliation structure, 213

Foliation, 213-220, 223-233, 261, 266, 300, 307-308, 333, 334, 335, 336  
 classification of, 220  
 definition of, 213  
 primary, 261, 266, 297, 300, 307-308  
 secondary, 213-220, 223-233, 261, 308  
 secondary, description of, 213-220  
 secondary, distinguished from primary, 307-309  
 secondary, relation to major structure, 223-233

Footwall, 130, 131, 133, 135, 150, 152, 153, 154, 172, 192, 435

Force, 4-16, 99, 358, 359  
 differential, 14-16  
 electromotive, 388  
 extremal, 13, 99  
 horizontal directing, 366  
 lines of, magnetic, 370  
 magnetite, 369  
 resolution of, 10, 11, 12  
 unbalanced, 10  
 vertical, 92, 95-116, 191

Forceful injection, 295, 297

Foreland, 181

Fossils, 1, 62, 68

Powler-Billings, K., 278

Fracture cleavage, 217, 220, 230-232

Fracture cleavage and lineation, 238

Fracture cleavage, relation to major structure, 230-232

Fractures, SH, 90, 100, 103, 104, 105, 106, 108, 109, 124, 125, 128, 129, 281, 283, 288, 294, 304, 327, 328  
 conical, 100, 103, 124, 283  
 extension, 103, 125, 129, 281, 288  
 helical, 104, 105  
 release, 103  
 ring, 294, 327, 328  
 shear, 99, 100, 101, 104, 105, 106, 108, 129, 288, 304  
 tension, 99, 100, 103, 104, 105, 106, 108, 109, 124, 128, 274, 288

Franconia quadrangle, New Hampshire, after *p.* 420

Free-air correction, 361, 363, 364

French, C. A., 367, 369

French Pond pluton, New Hampshire, 278

Friction in thrusting, 185-191

Fundamental strength, 23, 25

## G

Gal, 350, 360

Garnets, 370, 372

Gardner, L. S., 208

Gas, 7

Gauss, 369, 370, 371  
 Geanticline, 51  
 Geikie, A., 283  
 Genetic classification of faults, 152-154  
 Geologic mapping, 2-4  
 Geometrical classification of joints, 112-122  
 Geometrical reconstruction of folds, 420-429  
 Geometry, descriptive, 444-453  
 Geophone, 375  
 Geophysical methods, 67, 356-397  
     technique of, 357  
 Geophysics, 2  
 German salt domes, 252, 253, 257  
 Germany, 251, 253, 256, 325, 327, 329  
 Gianella, B. P., 202  
 Gilbert, G. K., 4, 193, 212, 271  
 Gilhuly, J., 196, 198, 212  
 Girdles, 352, 353  
 Glacial ice, folds due to, 97  
 Glacier National Park, Montana, 454  
 Glaciers, crevasses in, 124  
 Glarus district, Switzerland, 183, 185  
 Glass subjected to torsion, 104, 105  
 Glass, volcanic, 316  
 Glasses, 8  
 Glide directions, 27, 349, 350  
 Glide planes, 26, 348-353  
 Gliding, 26-28, 216, 348-353  
     translation, 26  
     twist, 27  
 Gneiss, 213, 214  
 Goodspeed, G. E., 279  
 Gouge, 158, 254  
 Graben, 164, 165, 193, 201-206  
     Great, Africa, 205, 209  
     Rhine, 205, 209, 211  
     origin of, 210-212  
 Graben of Africa, 205, 209, 211  
 Graben of Europe, 205, 209  
 Graben of Wasatch Plateau, Utah, 203-205  
 Grade of metamorphism, 248  
 Graded bedding, 72, 73  
 Gradient, gravity, 364, 366, 367, 368  
 Gradient map, 364, 366, 368  
 Gravity, rotation of, 26, 216, 349  
 Grand Canyon, Arizona, 241, 243  
 Granite-filled shears, 302-303, 306, 307, 308  
 Granite tectonics, 298-312  
     bearing on mechanics of intrusion, 311-312  
     criticized, 310-311  
 Granulation, 26, 216, 221, 297, 310  
 Graphite, 392  
 Gravimeter, 360  
 Gravimeter method, corrections in, 360-362  
 Gravimeter methods, 67, 360  
 Gravitation, 358  
 Gravitational constant, 359  
 Gravitational methods, 358-369  
 Gravity, 359, 360  
     acceleration of, 359  
     horizontal gradient of, 364, 366, 367, 368  
     relation to latitude, 359  
     relation to structure, 367-369  
 Gravity anomaly, 363  
 Gravity faults, 152, 166, 192-212  
 Gravity, faults (*cont.*):  
     altitude of, 192  
     en échelon, 193, 194-195, 200, 201  
     flat-lying, 305, 306, 307, 311  
     origin of, 208-212  
     pattern of, 193  
     on salt domes, 255  
     size of, 192-193  
 Great Basin, 198  
 Great Britain, 319  
 Great Dike, Rhodesia, 279  
 Great Glen Fault, Scotland, 193  
 Great Graben, Africa, 205, 209  
 Great Plains, 456  
 Greenland, 319  
 Greely, E., 3  
 Griggs, D. T., 5, 20, 23, 24, 95, 103, 270, 351  
 Groundwater, 9  
 Grout, F. F., 274  
 Gulf Coast of the United States, 358  
 Gulf of Mexico, 51  
 Gunn, W., 181  
 Gypsum in structural petrology, 349

H

Hadek, H., 373  
 Haile, 130, 131  
 Halite, 256  
 Hall, A. L., 275  
 Hancock, E. T., 194  
 Hanging wall, 130, 131, 133, 141, 144, 145, 152, 153, 154  
 Parker, A., 248, 276  
 Harmonic folding, 62  
 Hawaii, 210, 327  
 Hawaiian Islands, 321, 324  
 Hayes, C. W., 3  
 Haywards fault zone, California, 166  
 Heave, 136, 143-145, 436  
 Heiland, C. A., 357, 361, 364, 371, 374, 376, 382, 385  
 Heim, A., 183  
 Heitancz, A., 354, 355  
 Helical fracture, 104, 105  
 Hemisphere of projection in structural petrology, 339  
 Henry Mountains, Utah, 271  
 Hewett, D. F., 246, 247  
 Hexagonal columns (joints), 123-124  
 High-angle faults, 150, 151, 166  
 Hinge, 132  
 Hinge line, 132  
 Hinman, W. W., 181, 241  
 Hobbs, W. H., 184, 185  
 Homocline, 42  
 Hooke's law, 17  
 Horizon:  
     defined, 411  
     phantom, 385  
 Horizontal compression, 92-94, 95, 191  
 Horizontal couple, 92, 94-95  
 Horizontal directing force, 366  
 Horizontal gradient of gravity, 364, 366, 367, 368  
 Horizontal magnetic intensity, 371, 373  
 Horizontal projection, 44, 222, 441, 450  
 Horizontal separation, 145, 437  
 Horizontal strata, 33, 65, 411; *Pl. I.*, *op. p. 2*

Hornblende in structural petrology, 349  
 Hornblende, showing lineation, 220, 221,  
 223, 236, 300  
 Horne, J., 181, 193, 241  
 Hornitos, 320  
 Horse, 158  
 Horsts, 193, 201-206  
 Hotchkiss superdip, 371  
 Howe, E., 274  
 Ihuasteca Canyon, Mexico; *Pl. IV, op. p.*,  
 33  
 Hubbert, M. K., 5, 396  
 Hudson Bay, 370  
 Hull-Gloucester fault, Ontario, 367, 369  
 Hurlbut, C. S., 270  
 Hurricane fault, Utah and Arizona, 208  
 Hydrogen, 7  
 Hydrostatic pressure, 14  
 Hypotheses, working multiple, 3  
 Hypothetical pluton, structures of, 306-  
 307

## I

Ice, folds due to glacial, 97  
 Ice push, 97  
 Igneous, 270, 315, 319  
 Idaho, 182, 183, 184, 211  
 Igneous rocks:  
 extrusive, 260, 313-331  
 intrusive, 260-297, 298-312  
 Illinois, 396  
 Imbricate structure, 174, 175  
 Incidence, angle of, 379  
 Inclined fault problems, 448-453  
 Inclusions, 262, 263, 298, 299, 306, 307,  
 308, 311  
 Incompetent, 43, 88, 89, 224, 225, 227,  
 228, 230  
 Index of refraction, 379, 381  
 India, 313, 318  
 Induration, contrast in, indicating unconformity, 247  
 Inertia in thrusting, 190  
 Ingerson, E., 121, 333, 337, 340  
 Initial shear thrust, 173, 175  
 Injection, forceful, 295, 297  
 Instruments, magnetic prospecting, 371  
 Intensity:  
 horizontal magnetic, 371, 373  
 magnetic, and structure, 374  
 ratio of, 393  
 vertical magnetic, 371, 372, 373  
 Interformational laccolith, 373  
 Intergranular movements, 25-26  
 Intermediate-depth domes, 255  
 Intermittent faulting, 206, 208  
 Internal structure of plutons, 261-263  
 Internal structure of volcanoes, 319-322  
 Interpolation for geometrical reconstruction of folds, 427-428  
 Interpolation for structure contours, 430  
 Interval, structure contour, 84, 85, 430  
 Intragranular movements, 26-28  
 Intrusion:  
 bearing of granite tectonics on mechanics of, 311-312  
 "permissive," 295  
 time of, 296-297  
 Intrusion of magma, folds due to, 95  
 Intrusion of rock salt, folds due to, 95

Intrusive contacts, 156, 263  
 Intrusive igneous rocks, 260-297, 298-312  
 Intrusive rocks, banded, 262  
 Intrusive rocks, layered, 262  
 Inverted limb, 39, 40  
 Inverted plunge, 46  
 Iran, 251  
 Iranian salt domes, 256, 257  
 Isanomalies, 372, 373  
 Isoclinal folds, 40-41, 218; *Pl. VI, op. p.*,  
 39  
 Isogam, 363, 365  
 Isogam map, 365, 366, 368  
 adjusted, 363, 365, 368  
 Isomomalies, 372, 373  
 Isomomaly map, 372, 373  
 Isopachs, 431-433  
 Isostatic correction, 363  
 Isostatic factors, 360  
 Isotropic, 333

## J

Jagger, T. A., Jr., 271  
 Jakovsky, J. J., 357  
 Japan, 325  
 Jefferson County, Texas, 364, 366, 372  
 Joe's Valley Graben, Utah, 203  
 Joint set, 112  
 Joint system, 112  
 Joint, 32, 111-129, 303-304, 310, 335;  
*Pl. IX, op. p.*, 77; *Pl. X, op. p.*, II0;  
*Pl. XI, op. p.*, 111  
 junctional, 123-124; *Pl. XII, op. p.*, 122;  
*Pl. XIII, op. p.*, 123  
 cross, 303, 306, 307, 311  
 diagonal, 112, 304  
 dip, 112  
 due to a couple, 127, 304  
 extension, 125  
 "fan" of, 306, 307, 311  
 feather, 124  
 geometrical classification, 112-122  
 hexagonal, 123  
 longitudinal, 303-304, 306  
 oblique, 112  
 poles of, 116  
 primary flat-lying, 304  
 Q-, 303  
 release, 125  
 S-, 303-304  
 shear, 122, 125-128  
 strike, 112  
 tension, 122, 123-125  
 Jones, J. C., 164, 166  
 Jura Mountains, 55, 57, 82, 93

## K

K, 369  
 Katanga, 392  
 Keith, A., 185  
 Kelly, S. F., 390, 391  
 Kilauau, 327  
 Kiruna, Sweden, 373, 374  
 Klippe, 176, 177, 178, 183, 184  
 Knopf, E. B., 121, 333, 337, 340  
 Krakatau, Dutch East Indies, 326  
 Krynnine, P. D., 193  
 Kyanite in structural petrology, 349

## L

Labeling thin sections in structural petrology, 335-336  
 Laboratory exercises, 401-457  
 Laboratory experiments, 5, 20-25, 92-95, 99-108, 205, 351  
 Laboratory investigations, 5  
 Laboratory technique in structural petrology, 335-343  
 Laccolith, 95, 261, 271-274, 328  
 asymmetric, 271, 273  
 Deer Creek, Wyoming, 309  
 Henry Mountains, Utah, 271  
 interlaminar, 273  
 La Croix, A., 318, 322  
 Lahce, F. H., 2, 67, 425  
 Lakes on fault lines, 168, 169  
 Lake Superior, 358  
 Lamellae, twin, 337, 341, 353  
 Lamellar flow, 299  
 Lapilli, 317  
 Lenticular folding, 200  
 Latitude, relation to gravity, 359-360  
 Lattice:  
 atomic, 333  
 space, 333, 337  
 Lattice orientation, 333  
 Lava, 75-76, 320, 324  
 aa, 314  
 block, 314  
 pahoehoe, 314  
 pillow, 75  
 lava blisters, 314  
 lava cones, 320  
 lava flows, 268, 313-316; *Pl. XIX, op. p.*, 316  
 criteria to distinguish from sills, 315-316  
 size of, 315  
 lava pits, 325  
 lava tunnels, 315  
 Law of sines, 434-435  
 Lawson, A. C., 83, 187  
 Layered intrusive rocks, 262  
 Lee, J. S., 95  
 Lee partitioning method, 395  
 Legs, 36  
 Leith, C. K., 213  
 Leitrim, Ontario, 367, 369  
 Lewis overthrust, Montana, 185; *Fig. 336, op. p.*, 456  
 Limb, 36, 39  
 inverted, 39  
 normal, 39, 40  
 reversed, 39  
 Limestone, Solenhofen, 20, 21, 23, 24  
 Limit:  
 elastic, 17, 23, 30  
 endurance, 22  
 proportional elastic, 18, 21  
 Line electroiles, 394  
 Line, folding, 440  
 Linear flow structure, 300, 302  
 Linear parallelism, 220  
 Linear structure, 220, 300-302  
 Lineation, 220-223, 223-239, 300-302, 306, 309-310, 311, 335, 336, 337, 347, 353  
 altitude of, 222  
 distinction between primary and secondary, 309-310, 311

Lineation (*cont.*):

primary, 220, 300-302, 306  
 secondary, description of, 220-223, 233-239, 347, 353  
 secondary, use and origin of, 233-239

## Lines:

current flow, 388, 389  
 equipotential, 389, 391, 392, 394

Lines of force, magnetic, 370

Lines of no distortion, 106

Liquid, 8

Liquids, supercooled, 8

Local metamorphism, 218

Local unconformities, 72-74, 243

Longitudinal fault, 149, 152

Longitudinal joints, 303-304, 306

Longwell, C. R., 173, 185, 193, 197

Loomis, F. B., Jr., 242

Lopoliths, 274-276

Louisiana, 251, 256

Löve, A. E., 11, 13

Low angle faults, 150

Lower reference plane, 441, 445, 448

Lowther, G. K., 354

Lubricant, 55

Lutgeon, M., 183, 184

Lushtia anticline, Katanga, 392

## M

m, 336, 349

Maastricht, 325

MacCurdy, G. R., 274

Magnetism:

folds due to intrusion of, 95

movement of, 299

Magnetic stoping, 293-295, 311

Magnetic anomaly, 373

Magnetic declination, 371

Magnetic dip, 371

Magnetic field, 370

Magnetic intensity and structure, 374

Magnetic intensity, horizontal, 371, 373

Magnetic intensity, vertical, 371, 372, 373

Magnetic meridian, 371

Magnetic methods, 67, 369-374

Magnetic poles, 369, 370

Magnetic prospecting, 371

Magnetic storms, 372, 393

Magnetite ore body, 373, 374

Magnetometer, 371, 372

Mansfield, G. R., 182, 183, 185, 211

Map, 440

adjusted isogam, 363, 365, 368

gradient, 364, 366, 368

isogam, 365, 366, 368

Map indicating folds, 82-83

Map pattern, indicating folds, 62, 63

Marginal fissures, 304, 306, 307, 311

Marginal thrusts, 305, 311

Marginal upthrusts, 305

Martha's Vineyard, Massachusetts, 97

Martinique, 318

Maryland, 59, 193, 355

Marysville stock, Montana, 290, 291

Mason, S. L., 3, 252

Mass, 368, 359

Massachusetts, 97, 242, 279

Massive igneous rocks, 261, 298

Materials of outer shell of earth, 7-9

Mather, K. F., 3

## INDEX

Maxima, in quartz, 351  
 Maximum (maxima), 341, 351, 353, 354  
 Maximum shearing stress, 107  
 Mend, W. J., 94, 104, 105, 213, 233  
 Measurement of stress, 10  
 Mechanical principles, 7-32  
 Mechanical properties of rocks, 9  
 Mechanics of folding, 87-92  
 Mechanics of intrusion, 293-296, 311-312  
     bearing of granite tectonics on, 311-312  
 Mechanics of mineral orientation, 348-353  
 Mechanics of plastic deformation, 25-29  
 Mechanics of salt domes, fluid, 256  
 Mechanics of thrusting, 185-191  
 Medford, Massachusetts, dike, 270  
 Mectectic Area, Wyoming, 246, 247  
 Megascopic fabric symmetry, 343-345  
 Meridian, magnetic, 371  
 Mertie, J. B., Jr., 402  
 Meta-igneous rocks, 215  
 Metallurgy, 349  
 Metamorphic facies, 248  
 Metamorphism, contrast in grade of  
     indicating unconformity, 247-248  
     grade of, 248  
     load, 218  
 Metasediments, 215  
 Metavolcanics, 215  
 Method:  
     electrical, 386-397  
     electromagnetic-galvanic, 397  
     electromagnetic-induction, 397  
     equipotential line, 394-395  
     geophysical, 350-397  
     gravimeter, 360  
     gravitational, 67, 358-369  
     Lee partitioning, 395  
     magnetic, 67, 369-374  
     pendulum, 360  
     potentiometer-drop ratio, 397  
     potential profile, 394-395  
     reflection, 382-385, 386  
     refraction, 377-381  
     resistivity, 395-397  
     seismic, 374-386  
         Wenner-Gish-Rooney, 395  
 Mexico; *Pl. IV*, op. p. 33  
 Mexico, Gulf of, 51  
 Mica, glide plane in, 353  
 Mica in structural petrology, 337, 340, 341,  
     349, 353  
 Microscopic fabric symmetry, 343-345  
 Migmatite, 215  
 Miller, A. H., 367, 369  
 Millianpore, 388  
 Milligal, 359  
 Millivolt, 388  
 Mimetic, 218  
 Mineral cleavage, 213, 337, 340-341  
 Mineral orientation, mechanics of, 348-  
     353  
 Mineralization along faults, 160  
 Minerals:  
     platy, 300, 306, 333, 336  
     prismatic, 300, 301  
 Minerals studied in structural petrology,  
     337  
 Mines, 430  
 Minimum breadth of overthrusts, 179, 185  
 Mining, 67  
 Mining compass, Swedish, 371  
 Minnesota, 275  
 Minor folds, 50, 81, 90  
 Missouri; *Pl. X*, op. p. 110  
 Model, D., 284, 285  
 Models, 86  
     scale, 5  
 Moine overthrust, 180, 182  
 Monocline, 41  
 Monoclinic symmetry of fabric, 343, 341-  
     345  
 Monoclinic symmetry of movement, 315  
 Montana, 185, 194, 270, 290, 291, 454  
 Morro caldera, Argentina, 327  
 Mountains, fault-block, 195-201, 206  
 Movement:  
     absolute, on faults, 153-154  
     relative, on faults, 132-137, 152-153,  
         450  
     rotational, on faults, 131, 132, 133  
     symmetry of, 345-346  
     translatory, on faults, 131, 133  
     vertical, 91-92, 210  
 Movement of magma, 209  
 Movement symmetry and fabric sym-  
     metry, correlated, 346-348  
 Mrazec, M. I., 54  
 Mt. Ascutney, Vermont, 289, 291, 292  
 Mt. Cardigan, New Hampshire, 278  
 Mt. Clough, New Hampshire, 340  
 Mt. Clough pluton, New Hampshire, 277  
 Mt. Etna, Sicily, 321  
 Mt. Katmai, Alaska, 326-327  
 Mt. Monadnock, New Hampshire; *Pl.*  
     *II*, op. p. 32; *Pl. VII*, op. p. 39  
 Mt. Pelée, Martinique, 318, 322  
 Mud-cracks, 74-75, 124  
 Mud Bow, 318  
 Murdy Mountain overthrust, 185  
 Mullion structure, 158  
 Multiple dike, 279  
 Multiple sill, 268  
 Muscovite in structural petrology, 337,  
     341, 349, 353  
 Musinia graben, Utah, 204, 205  
 Mylonite, 159

## N

Nappe, 181  
 Natural electrical currents, 387, 389-394  
 "Neek," 17  
 Neck, volcanic, 282, 283, 330  
 Necking, 100  
 Negative potential center, 389, 392  
 Net, Schmidt equal area, 340  
 Net slip, 134, 142, 435, 446, 450  
     of overthrusts, 177-179, 183, 185  
 Nettleton, L. L., 256, 357, 369  
 Neutrons, 7  
 Nevada, 165, 166, 173, 185, 202, 206, 207  
 New Hampshire, 277, 278, 284, 285, 295;  
     Fig. 340, after p. 420; *Pl. III*, op. p.  
         32; *Pl. VII*, op. p. 39  
 New Mexico, *Pl. XIV*, op. p. 214; *Pl.*  
     *XVII*, op. p. 243  
 New Zealand, 354  
 Nichols, R. L., 314, 315  
 Nomenclature of folds, 37-43  
 Nonconformity, 243, 244, 245  
     exposed in outcrop, 245  
     shown by areal mapping, 246-247

Noncrystalline solid, 8  
 Non-piercement domes, 254  
 Non-plunging fold, 43, 45  
 Nonrotational strain, 31  
 Non-selective diagram, 342  
 Non-tectonite, 353  
 Normal anticlinorium, 50, 51  
 Normal fault, 150, 192-212  
 Normal horizontal separation, 145  
 Normal limb, 31, 40  
 Normal projection, 439  
 Normal synclinorium, 50, 51  
 North America, eastern, Triassic rocks, 195  
 North American Cordillera, 94  
 North Atlantic volcanic field, 318-319  
 North pole, 369, 370  
 North-seeking pole, 369  
 Nose, 44, 62  
*Nubes ardentes*, 318, 324  
 Nunnerov, B., 368  
 Nyassa graben, Africa, 205

## O

Oblate spheroid, 29, 106, 343, 359  
 Oblique fault, 149  
 Oblique joint, 112  
 Obsequent fault-line scarp, 163  
 Offset, 145  
 Offset ridge, 161  
 Offset stream, 166  
 Ohm, 388  
 Oklahoma, 194  
 Omission of strata at faults, 156  
 Ontario, 275, 367, 391  
 Open fold, 42  
 Optic axis, 336, 337, 338, 339, 340, 341  
 Ouray Range, Utah, 196, 198  
 Ore body, 374, 389, 390  
     magnetite, 373, 374  
 Oregon, 326; *Pl. XIX*, *op. p.* 315  
 Orientation:  
     lattice, 333  
     mechanics of mineral, 348-353  
     preferred, 334, 341  
     random, 334  
     shape, 333  
 Orientation of calcite, 353  
 Orientation of quartz, 349-353  
 Oriented specimens, 335  
 Origin of folds, 92-98  
 Origin of graben, 210-212  
 Origin of gravity faults, 208-212  
 Origin of salt domes, 256-257  
 Original of mud-cracks, 75  
 Original of ripple-marks, 70, 71  
 Orogen, 46  
 Orogenic belts, 94, 95, 289, 309  
 Orthogneiss, 215  
 Orthorhombic symmetry of fabric, 343-344  
 Orthorhombic symmetry of movement, 346  
 Orthoschist, 215  
 Osborne, F. F., 354  
 Oscillation ripples, 69-71  
 Oslo graben, 211  
 Outerop, exposure of unconformity in, 243-245

Outerop pattern of strata, 63, 411-419  
     of dipping strata, 63, 65-66, 415-419  
     of horizontal strata, 65, 411  
     of vertical strata, 65, 66, 411  
 Outer shell of earth, deformation in, 31-32  
 Overfold, 39  
 Overhang of salt domes, 252  
 Overlap, 146  
 Overthrust, 154, 159, 172, 176-185, 191, 248  
     Banff, 182, 183, 184, 185  
     Ben More, 180, 183  
     Buffalo Mountain, Tennessee, 185  
     direction of movement, 184  
     folded, 176, 177, 183  
     Glarus district, Switzerland, 183, 185  
     Glencoul, 180  
     Lewis, 185  
     Mointain, 180, 182  
     Muddy Mountain, 185  
 Overthrust block, 176, 177  
 Overthrust sheet, 176, 181  
 Overturned fold, 39  
 Overturned limb, 39, 40, 200  
 Overturned strata, 39, 67  
 Owens Valley, California, 104, 105  
 Oxidized tops of lavas, 76  
 Ozark Mountains, Missouri; *Pl. X*, *op. p.* 110

## P

Pacific Ocean, 321  
 Pahoehoe lava, 314  
 Paige, S., 3, 273  
 Paleontological methods, studying folds, 68-69  
 Palaeontology, 1  
 Paligenesis, 295  
 Palmer, H. S., 402, 407, 408, 422  
 Paragneiss, 215  
 Parallel faults, 150  
 Parallel folding, 60, 53, 420  
 Parallelism, linear, 220  
 Paraschist, 215  
 Parasitic cones, 321  
 Parsons, W. H., 281  
 Partial diagram, 342  
 Pattern:  
     fault, 149-150  
     map, indicating folds, 62, 63  
 Pattern of dipping strata, 65-66, 415-419  
 Pattern of horizontal strata, 65, 411  
 Pattern of strata, outerop, 411-418  
 Pattern of vertical strata, 65, 411  
 Paulina Mountains, Oregon; *Pl. XIX*, *op. p.* 315  
 Peach, B. N., 181, 193, 241  
 Pebbles:  
     elongated, 221, 223  
     origin of, 234-236  
     "stretched" described, 221, 223, 334  
     origin of, 234-236  
 Pegs, power, 394  
 Pegs, reading, 394  
 Pendants, roof, 289, 290  
 Pendulum, 360  
 Pendulum method, 360-362  
 Pennsylvania, 52, 53, 59, 67, 103, 355  
 Peripheral counter, 120, 121  
 Peripheral faults, 50, 330

"Permissive" intrusion, 295  
 Perpendicular slip, 136  
 Peru; *Pl. V*, op. p. 38; *Pl. VI*, op. p. 39  
 Petrofabric analysis, 332-335  
 Petrofabric diagram, 337-343, 352, 353, 359  
 Petroleum, 9, 251, 253  
 Petroleum industry, 356  
 Petrology, 1, 261, 313  
     structural, 310, 332-335  
 Petrotectonics, 332, 334  
 Phacoliths, 276-277  
 Phantom horizon, 385  
 Phillips, F. C., 354  
 Phone, 375  
 Photographs, 82  
     aerial, 2  
 Physiographic criteria of faulting, 161-171  
 Physiography, 1, 313  
 Pickup, 375  
 Piccencal stoping, 286, 293-294, 312  
 Piedmont scarps, 164, 168, 198, 201, 206  
 Piercement domes, 254  
 Piercing folios, 54  
 Pillow lava, 75  
 Pillow structure, 75  
 Pipe, volcanic, 317, 324, 330  
 Pit:  
     explosion, 325  
     lava, 325  
 Pit craters, 324  
 Pitch, 135, 435, 442, 446, 450  
 Plan, 440  
 Planar flow structure, 299-306  
 Planar structure, 299-300, 307-309, 311  
 Plane:  
     ab-, 337, 351  
     ac-, 337, 351, 354  
     bc-, 337  
     glide, 26, 348-353  
     lower reference, 441, 445, 448  
     slip, 338-353, 354  
     upper reference, 442  
 Plane of projection, 439  
 Plane of stretching, 305  
 Plastic deformation, 19, 25-24, 32, 88, 99, 216; *Pl. VIII*, op. p. 76  
 Platy flow structure, 299-300  
 Platy minerals, 300, 306, 333, 336  
 Pleasant Valley, Nevada, 165, 166  
 Plugs, 283, 330; *Pl. X VIII*, op. p. 243  
 Plunge, 44, 135, 442, 446, 450  
 Plunge of folds, 43-49  
 Plunging folds, 45, 46, 226-228, 236-237  
 Plunging syncline, 44, 47, 85, 176  
 Pluton, 280-297  
     age relative to adjacent rocks, 263  
     atextonic, 296, 297  
     concordant, 267-279  
     defined, 261  
     determining shape and size, 267  
     discordant, 279-296  
     hypothetical, structure of, 306-307  
     internal structure, 201-203  
     post-tectonic, 296-297  
     pre-tectonic, 296-297  
     structural relations to surrounding rocks, 264-267  
     subsequent, 296-297  
     synchronous, 296-297  
     syntectonic, 296-297

Point:  
     receiving, 375  
     shot, 375, 376, 377, 378, 379, 381, 382, 383, 384  
 Point diagram, 118, 338, 340, 341  
 Point electrodes, 394  
 Pole:  
     magnetic, 369, 370  
     north, 369, 370  
     north-seeking, 369  
     south, 369  
     south-seeking, 369  
 Pole of cleavage, 341  
 Pole of joint, 118  
 Poles, in structural petrology, 351  
 Pore space, 9, 24, 29  
 Positive potential center, 393  
 Positrons, 7  
 Post-tectonic plutons, 296-297  
 Potential center:  
     negative, 389, 392  
     positive, 393  
 Potential, difference of, 389  
 Potential-drop ratio method, 397  
 Potential profile, 389-391, 394  
 Potential profile method, 394-395  
 Power pegs, 394  
 Powers, S., 251  
     "Preferential direction," 393  
 Preferred orientation, 334, 341  
 Pressure box, 92, 93  
 Pressure ridges, 314  
 Pre-tectonic plutons, 296-297  
 Primary features of sedimentary and extrusive rocks, 67-76  
 Primary flat-lying joints, 304  
 Primary foliation, 261, 266, 297, 300, 307-308  
 Primary lineation, 220, 300-302, 306  
 Primary structures of sedimentary and extrusive rocks, 49  
 Primary structures distinguished from secondary structures, 307-310  
 Primary and secondary structures confused, 310-311  
 Prism rule for orientation of quartz, 349-350, 351  
 Prismatic minerals, 300, 301  
 Profile:  
     break in stream, 166  
     potential, 389-391, 394  
     resistivity, 396  
     reversed, 381  
     topographic, method of preparing, 412  
 Profile shooting, 375, 377-385  
 Projected dip, 422  
 Projection, 439-443  
     equal area, 117  
     horizontal, 44, 221, 411  
 Prolate spheroid, 29, 106, 343  
 Proportional elastic limit, 18, 21  
 Prospecting, magnetic, 371  
 Protons, 7  
 Pseudo-tachylite, 159  
 Pseudoviscous flow, 23  
 Pyroclastic beds, 316-318, 320, 324  
 Pyroclastic cones, 321

## Q

Q-joints, 303

Quartz in structural petrology, 337, 338-341, 349-352  
 Quebec, 354

R

R, 336  
 r (rhombohedron of quartz), 336  
 R value, 366  
 Radial faults, 150, 329, 330, 331  
 Radiating dikes, 280, 281  
 Radioactivity, 7  
 Rain-imprints, 75  
 Random orientation, 334  
 Rating of intensity, 393  
 Raymond, P. E., 175, 176  
 Reading electrodes, 395  
 Reading pegs, 394  
 Recess, 49  
 Receiving point, 375  
 Recognition of folds, 58-81  
 Recognition of unconformities, 243-249  
 Reconstruction of folds, geometrical, 426, 429  
 Recovery, creep, 23  
 Recrystallization, 24, 28-29, 216, 343  
 Recumbent folds, 30, 40, 54, 58, 181; *Pl. VII, op. p. 39*  
 Reference plane:  
     lower, 441, 445, 448  
     upper, 442  
 Reflection, angle of, 382  
 Reflection methods, 382-385, 386  
 Refraction:  
     angle of, 379  
     index of, 379, 381  
 Refraction methods, 377, 381  
 Refraction profile shooting, 377-381  
 Reid, H. V., 132  
 Relative age of plutons, 263  
 Relative movements on faults, 132-137, 152-153, 450  
 Release fractures, 103  
 Release joints, 125  
 Repeated deformation and cleavage, 232-233  
 Repetition of strata on faults, 156  
 Replacement dikes, 270  
 Replacement, plutons formed by, 279, 295  
 Representation of folds, 82-86  
 Reservoir fault-line scarp, 162  
 Resistance, specific, 389  
 Resistivity, 389  
     apparent, 395  
 Resistivity methods, 395-397  
 Resistivity profile, 396  
 Resolution of forces, 10, 11, 12  
 Resources of salt domes, economic, 258-259  
 Resultant, 10  
 Reverse fault, 150  
 Reversal limb, 39  
 Reversed profile, 381  
 Reyer, E., 322  
 Rhine graben, 205, 209, 211  
 Rhodesia, 279  
 Rhombic symmetry of fabric, 343-344  
 Rhombohedron rule in orientation of quartz, 350-351  
 Richey, J. E., 281  
 Ridges:  
     buried, 96, 367, 374  
     offset, 161  
     pressure, 314  
 Riecke principle, 28  
 Ries Basin, Germany, 327, 329  
 Rifts, 152  
 Ring-dike, 282, 284-288  
 Ring-fracture, 327, 328  
 Ring-fracture stoping, 291  
 Ripple-marks, 69-71  
*Roche moutonnée*, 157  
 Rock cleavage, 213  
 Rocky Mountains, 58, 185, 456  
 Rod, under tension, 99, 100  
 Roof pendants, 289, 290  
 Root, 40  
 Root-holes, 75  
 Root zone, 40, 177  
 Rootless slices, 327  
 Rotation of grains, 26, 216, 349  
 Rotational movements on faults, 131, 132, 133  
 Rotational strain, 31  
 Rouse, J. T., 309  
 Ruby-East Humboldt Range, Nevada, 206, 207  
 Rule, prism, in orientation of quartz, 349-350, 351  
 Rule, rhombohedron, in orientation of quartz, 350-351  
 Rule of V's, 411, 415-416  
 Romanian salt domes, 254-255, 256, 257  
 Rupture, 17, 32  
     failure by, 99-110  
 Russell, R. J., 167  
 Russia, 251, 252, 257, 368  
 Russian salt domes, 251, 252, 257

S

Sagponds, 169  
 Salient, 49, 235-237  
 Salt, 8, 32, 95, 251-259, 358, 364, 366, 367, 368, 372, 374, 377, 385, 394, 397  
 Salt domes, 32, 95, 251-259, 295, 358, 364, 366, 367, 372, 374, 377, 385, 391, 397  
     American, 251-259, 364, 366, 368, 372  
     composition of, 252  
     defined, 251  
     downbuilding of, 257  
     economic resources of, 258-259  
     gravity faults associated with, 255  
     origin of, 256-257  
     Russian, 251, 252, 257, 368  
     shape of, 252, 253  
     size of, 252  
     structural evolution of, 257-258  
     upthrusting of, 257  
 Samler, B., 333  
 Samlers, C. W., 251, 255, 257  
 San Francisco, California, 83, 166  
 San Francisco Mountains, Arizona, 321  
 San Luis, Argentina, 327  
 Sawtelle, G., 251  
 Scale models, 5  
 Scapolite in structural petrology, 349  
 Scarps:  
     composite fault, 163, 168-171  
     defined, 161  
     fan, 164  
     fault, 162, 165, 168, 169  
     fault-line, 162, 166, 168, 169  
     obsequent fault-line, 103  
      piedmont, 164, 168, 198, 201, 206

Scarp (*cont.*):  
  resequent fault-line, 162

Scarples, 164

Schist, 213, 214  
  crinkled, 347

Schistosity, 213, 336, 337, 353  
  bedding, 218  
  symbols for, 214

Schlieren, 262, 295, 300, 306

Schlumberger, M., 393, 394

Schmidt, W., 333

Schmidt equal area net, 340

Schmidt magnetometer, 371, 372

Schollendau, 314

Schwarz Mönch, Switzerland, 58

Scotland, 180, 181, 192, 193, 241, 283, 288, 354; *Pl. XII*, *op. p.* 122; *Pl. XIII*, *op. p.* 123

Scottish cone sheets, 281

Secondary foliation, 213-220, 223-233, 261, 308  
  description of, 213-220  
  relation to major structure, 223-233

Secondary foliation distinguished from primary foliation, 307-309

Secondary lineation:  
  description of, 220-223, 233-239, 347, 363  
  use and origin of, 233-239

Secondary structures distinguished from primary structures, 307-310, 311

Section, *c.*, 337

Sections, structure, 83-84, 356, 421-425  
  method of constructing, 411-413

Seilerholz, J. J., 215

Sedimentary facies, 160

Segregation, 202

Segregation banding, 214

Seismic method, 67, 374-386  
  speed of elastic waves, 374

Seismogram, 376

Seismogram of reflection shooting, 381

Seismology, 1

Selective diagram, 342

Separation, 145-147, 437

Set:  
  dike, 280  
  joint, 112

Shallow domes, 255

Shanks, 36

Shape and size of plutons, determining, 267

Shape of minerals in structural petrology, 333, 337

Shape of rock bodies by geophysical methods, 357

Shape of salt domes, 252, 253

Sharp, R. P., 206, 241

Shear, 13, 15  
  Shear cleavage, 217-218, 220, 232, 238  
    and lineation, 238  
    relation to major structure, 232

Shear folding, 87, 90-91

Shear fractures, 99, 100, 101, 104, 105, 106, 108, 129, 288, 304

Shear joints, 122, 125-128

Shear thrust, 173, 175  
  initial, 173, 175  
  subsequent, 173, 175

Shearing stress, 13, 102, 107, 349  
  surface of maximum, 107

Shears, granite-filled, 302-303, 306, 307, 308

Sheet, 267  
  cone, 280, 281, 283, 288

Sheeting, 128-129; *Pl. IX*, *op. p.* 77

Shell of recumbent fold, 40

Sheppards Mott dome, Texas, 386, 387

Shield volcanoes, 320

Shift, 136, 137

Stringer-block structure, 175

Shiprock, New Mexico; *Pl. XVII*, *op. p.* 243

Shekin Sag intrusive, Montana, 270

Shooting:  
  correlation, 382-385  
  lip, 385  
  fan, 375, 377  
  profile, 375, 377-385  
  vertical, 384

Shot point, 375, 376, 377, 378, 379, 381, 382, 383, 384

Shrinkage-cracks, 74

Sicily, 321

Sierra Nevada, 95, 295  
  pluton, California, 295

Silification along faults, 160

Sill, 267-270, 276  
  composite, 268, 269  
    criteria to distinguish from lava flow, 315-316  
  differentiated, 269-270  
  simple, 268

Similar folding, 50, 53

Simple dike, 279

Simple sill, 268

Sines, law of, 434-435

Sinks, volcanic, 327

Size of lava flows, 315

Size of plutons, determining, 267

Size of salt domes, 252

S-joints, 303-304

Sketches, 82

Slaty cleavage, 215-217

Slice, 158

Slices:  
  rootless, 327  
  thrust, 327

Sleeksides, 157, 238, 435

Slip, 134-136  
  lip, 134, 135, 435  
  net, 134, 435, 446, 454  
    of overthrusts, 177-179, 183, 185  
    perpendicular, 136  
    strike, 134, 135, 434  
    trace, 136

Slip folding, 91

Slip planes, 348-353, 351

Slip, angle of, 403-406

Slope distance, 403, 404

Slopes, 37

Sole, 183

Solenhofen limestone, 20, 21, 23, 24

Solid, 8

Solid stage, structures of, 303-306

Solution of fault problems, trigonometric, 434-438

Solutions, 24-25, 307

South America, 318

South Cotton Lake area, Texas, 386

South pole, 369

South-seeking pole, 369

Space lattice, 333, 337

Spatter cones, 314  
 Specific gravity, 294, 367  
 Specific resistance, 389  
 Specimen, oriented, 335  
 Speed of elastic waves, 374  
 Sphere of projection in structural petrology, 116, 339  
 Spheroid:  
     oblate, 29, 106, 343, 359  
     prolate, 29, 106, 343  
 Spheroidal symmetry of fabric, 343  
 Spicker, E. M., 203, 204, 205  
 Spine, 322, 323  
 S-plane, 336, 337, 353  
 Spontaneous electric currents, 381-393  
 Springs, related to faults, 167  
 Squeeze-ups, 314  
 S-surface, 336, 337  
 Staffa, Scotland; *Pl. XII*, op. p. 122; *Pl. XIII*, op. p. 123  
 Stage, Universal, 337, 338  
 Stages of deformation, 17, 348  
 Statistical analysis, 334  
 Stearns, H. T., 315, 324  
 S-tectonite, 353  
 Step faults, 193  
 Stevens, E. H., 190  
 Stewart, G. W., 242  
 Still, H., 252  
 Stock, 288-296  
 Stoping:  
     magnetic, 293-295, 311  
     piecemeal, 286, 293-294, 312  
     ring fracture, 294  
 Storms, magnetic, 372, 393  
 Strain, 16-20, 31  
     nonrotational, 31  
     rotational, 31  
     surface of no, 105, 107  
 Strain axis, 30, 106  
 Strain ellipse, 30, 95, 106, 107, 109, 124, 224, 229  
 Strain ellipsoid, 29-31, 101, 106-110, 124, 125, 126, 127, 216-218, 220, 224-232  
 Strata:  
     calculation of thickness and depth, 401-409  
     dipping, outcrop pattern of, 65-66  
     folded, 421-425; *Pl. II*, op. p. 3  
     horizontal, 33, 65, 411; *Pl. I*, op. p. 2  
     omission of, at faults, 156  
     repetition of, at faults, 156  
     vertical, 33, 35, 65, 411; *Pl. IV*, op. p. 33  
 Stratigraphic separation, 146, 437  
 Stratigraphic throw, 146, 177, 185, 198  
 Stratigraphy, 1  
 Stratovolcanoes, 321  
 Stratum:  
     depth, 401-409  
     thickness, 401-409  
 Stream, offset, 166  
 Stream profile, break in, 166  
 Strength, 19, 25  
     compressive, 19, 100, 106  
     fundamental, 23, 25  
     shearing, 19  
     tensile, 19, 100, 106  
     ultimate, 20, 21, 25  
 Strength of magnets, 369  
 Strength of rocks in thrusting, 185-191  
 Stress, 12-16, 18  
     compressive, 13, 16  
     tensile, 13, 16  
     unit, 13  
 Stress-difference, 13  
 Stress-strain diagram, 18  
 Stretch thrust, 172, 175  
 "Stretchel" pebbles and boulders:  
     described, 221, 223, 334  
     origin of, 234-236  
 Stretching, planes of, 305  
 Striations, 157, 238  
 Strike, 33, 111, 130  
 Strike fault, 148  
 Strike joint, 112  
 Strike slip, 134, 135, 435  
 Strike slip fault, 148  
 Strip thrust, 173, 175  
 Structural evolution of salt domes, 257-258  
 Structural fabric, 333-335  
 Structural geology, defined, 1  
 Structural petrology, 310, 332-355  
 Structural relations of plutons to surrounding rocks, 264-267  
 Structural terrace, 41, 42  
 Structure:  
     closed, 431  
     determined by gravity methods, 367-369  
     determined by magnetic methods, 374  
     determined by seismic methods, 385-386  
     discontinuity of, at faults, 155-156  
     foliate, 213  
     imbricate, 174, 175  
     internal, of plutons, 261-263  
     linear, 220, 301-302  
     million, 148  
     planar, 299-300, 307-309, 311  
     planar flow, 299, 306  
     platy flow, 299-300  
     primary, distinguished from secondary, 307-310  
     shingle-block, 175  
     subsurface, 357  
 Structure contours, 34-35, 363, 364, 386, 387, 430-433  
 Structure sections, 83-84, 356, 421-425  
     method of constructing, 411-413  
 Structures, cryptozoic, of the United States, 328-330  
 Structures of flow stage, 290-292  
 Structures of solid stage, 303-306  
 Structures of transition stage, 302-303  
 Strut, 87  
 Subdivisions of structural geology, 2  
 Subsequent pluton, 296-297  
 Subsequent shear thrust, 173, 175  
 Subsidence:  
     cauldron, 285-288, 295, 312  
     surface cauldron, 285, 287, 327  
     underground cauldron, 285, 286, 294  
 Subsurface structure, 357  
 Sudbury, Ontario, 275  
 Suess, E., 4, 288, 289  
 Sulphur, 251, 254, 258  
 Sumatra, 393, 394  
 Sun-cracks, 74  
 Sunlight area, Wyoming, 280, 281, 283  
 Supercooled liquids, 8

Superdip, Hotchkiss, 371  
 Superior, Lake, 358  
 Supratenuous folding, 50, 54  
 Surface, equipotential, 389  
 Surface cauldron subsidence, 285, 287, 327  
 Surface of maximum shearing stress, 107  
 Surface of no distortion, 107, 108  
 Surface of no strain, 105, 107  
 Swabia, 325  
 Swarm, dike, 280  
 Sweden, 209, 270, 373, 374  
 Swellings, 92  
 Switzerland, 54, 55, 58, 176, 183, 184, 185, 354  
 Symbols:  
     altitude of folds, 34, 60  
     dip-strike, 33, 35, 39, 214  
 Symmetrical folds, 39  
 Symmetrical syncline, 61, 63  
 Symmetry:  
     axial, of fabric, 343  
     axial, of movement, 346  
     megascopic fabric, 343-345  
     microscopic fabric, 343-345  
     monoclinic, of fabric, 343, 344-345  
     monoclinic, of movement, 346  
     movement and fabric correlated, 346-348  
     orthorhombic fabric, 343  
     orthorhombic movement, 346  
     rhombic fabric, 343  
     spheroidal fabric, 343  
     triclinic fabric, 343, 345, 348  
     triclinic movement, 346  
 Symmetry of fabric, 343-345  
 Symmetry of movement, 345-346  
 Symmetry diagrams, eccentric, 345  
 Synchronous plutons, 296-297  
 Syncline, 38, 61, 63, 88; *Pl. VI, op. p.* 39  
     doubly-plunging, 46, 47, 176  
     plunging, 44, 47, 85, 176  
 Synclinorium, 50, 51  
 Syntectonic plutons, 296-297  
 System, joint, 112  
 Systems, fold, 46-51

T

Taber, S., 210  
 Teal, J. L. H., 181, 241  
 Tear faults, 152  
 Technique:  
     field, in structural petrology, 335  
     laboratory, in structural petrology, 335-343  
 Technique of geophysical methods, 357  
 Tectonic geology, 1  
 Tectonics, 1  
     granite, 298, 312  
         bearing on mechanics of intrusion, 311-312  
         criticized, 310-311  
 Tectonites, 353-354  
 Telluric currents, 393-394  
 Temperature, 21-22, 25  
 Tennessee, 174, 185, 329, 331  
 Tensile strength, 19, 100, 106  
 Tensile stress, 13, 16  
 Tension, 14, 15, 99-100, 164, 205, 210, 255, 288, 294  
 Tension fractures, 99, 100, 103, 104, 105, 106, 108, 109, 124, 128, 274, 288  
 Tension joints, 122, 123-125  
 Terminology of thrust faults, 172-176  
 Terrane, structural, 41, 42  
 Terrain correction, 362, 363  
 Texas, 251, 253, 254, 255, 256, 364, 366, 372, 386  
 Thickness by geophysical methods, 381, 384, 395  
 Thickness of strata, calculation of, 401, 409  
 Thickness of stratum, defined, 401  
 Thin sections, labeling, in structural petrology, 335-337  
 Thornburgh, H. R., 379, 380  
 Three-point problems, 417-419, 444-447  
 Throw, 136, 143-145, 435  
     stratigraphic, 146, 177, 185, 198, 437  
 Thrust block, 187-191  
 Thrust faults, 104, 105, 152, 153, 166, 172-191  
 Thrust slices, 327  
 Thrusting:  
     friction in, 185-191  
     mechanics of, 185-191  
     strength of rocks in, 185-191  
 Thrusts, 152, 172-191  
     bedding, 173, 175  
     break, 172, 175, 200  
     erosion, 173, 175  
     folded, 174, 177, 179, 183  
     initial shear, 173, 175  
     marginal, 305, 311  
     shear, 173, 175  
     stretch, 172, 175  
     strip, 173, 175  
     subsequent shear, 173, 175  
 Tidal stresses, 22, 32  
 Tight fold, 42  
 Tilted fault blocks, 193, 195-201  
 Time, 22-24  
 Time of intrusion, 296-297  
 Tongues, 283  
 Top of beds by drag folds, 70-81  
 Top of beds by primary features, 67-76  
 Topographic features related to faults, 161-171  
 Topographic profile, method of preparing, 412  
 Topography, use in determining structure, 63-66  
 Torrential cross-bedding, 71, 73  
 Torsion, 15, 16, 294  
     fractures resulting from, 104-106  
 Torsion balance, 363-367  
 Tourmaline in structural petrology, 346  
 Trace slip, 136  
 Trace slip faults, 140  
 Trucks, animal, 75  
 Transition stage, structures of, 302-303  
 Translation gliding, 26  
 Translatory movements on faults, 131, 133  
 Transverse faults, 149, 152  
 Travel-time curve, 376, 381  
 Traverse, azimuth of, 404, 406  
 Trough, 36, 37  
 Trough plane, 36, 37  
 Troubles, fault, 210  
 Triangle, 434

Triangular facets, 165-166, 198, 201, 206  
 Triclinic symmetry of fabric, 343, 345, 348  
 Triclinic symmetry of movement, 346  
 Trigonometric solution of fault problems, 434-438  
 True folding, 87  
 Truncation of internal structure at faults, 167, 198, 206  
 Tuff, 283, 317, 318  
 Tuff-breccia, 317  
 Tumulus (tumuli), 314  
 Tuning fork, 375  
 Tunnels, lava, 315  
 Turbulent flow, 299  
 Turner, P. J., 354  
 Uwehofel, W. H., 69  
 Twin gliding, 27  
 Twin lamellae, 337, 341, 353  
 Tyrell, G. W., 313

U

Ultimate strength, 20, 21, 25  
 Ultramylonite, 159  
 Unbalance force, 10  
 Unconformities, 154, 156, 174, 240-250, 257-258, 263, 297, 454  
     angular, 242-247; *Pl. XVI*, op. p. 242  
     criteria for distinguishing from faults, 249-250  
     exposed in intercrop, 243-245  
     local, 72-74, 243  
     recognition of, 243-249  
     relief on, 241-242  
 Underground railroad subsidence, 285, 287, 294  
 Underthrust, 154, 172  
 Unit, Eötvös, 364, 366, 367, 368  
 Unit stress, 13  
 United States, 252, 253, 315, 318, 328-330, 358, 371  
 Units, Hwy, 315  
 Universal Stage, 337, 338  
 Upper reference plane, 442  
 Upthrusting of salt domes, 257  
 Upthrusts, 154, 172, 192  
     marginal, 305  
 Uranium, 7  
 Utah, 166, 193, 196, 198, 203-205, 208, 250, 271; *Pl. I*, op. p. 2; *Pl. XVI*, op. p. 242

V

V's, rule of, 411, 415-416  
 Value, Eötvös curvature, 366  
 Variation, diurnal, 372, 393  
 Vector, 11  
 Velocity, effective average, 384  
 Velocity of elastic waves, 374, 376, 377-380  
 Vent agglomerate, 317  
 Vents, volcanic, 282, 283-284, 330  
 Vermont, 289, 291, 292  
 Vertical faults, 95, 202, 205  
 Vertical forces, 92, 95-96, 191  
 Vertical movements, 91-92, 210  
     folding due to, 91-92  
 Vertical separation, 145  
 Vertical shooting, 384  
 Vertical strata, 33, 35, 65, 411; *Pl. II*, op. p. 33

Vesicular top of lavas, 75, 76  
 Virginia, 193  
 Viscosity of laccoliths, 273  
 Vitreous solids, 8  
 Voistest, I. P., 252  
 Volcanic ash, 317, 326  
 Volcanic breccia, 283, 317  
 Volcanic chain, 323  
 Volcanic cluster, 323  
 Volcanic cones, 319-321  
     size of, 321  
 Volcanic conglomerate, 317, 318  
 Volcanic domes, 321-322  
 Volcanic dust, 317  
 Volcanic glass, 316  
 Volcanic pipe, 317, 324, 330  
 Volcanic sinks, 327  
 Volcanic vents, 282, 283-284, 330  
 Volcanoes, 9, 319-323  
     compound, 322  
     embryonic, 325  
     shield, 320  
     size of, 321  
 Volt, 388

W

Wagner, P. A., 330  
 Wall, hanging, 130, 131, 133, 141, 144, 145, 152, 153, 154  
 Warps, 33  
 Wasatch Plateau, Utah, 203-205, 250  
 Wasatch Range, Utah, 193, 198-200  
 Waters, A. C., 151  
 Waves, elastic, velocity of, 374  
 "Weathered zone," in seismic methods, 389  
 Wellington field, Colorado, 363, 365, 368  
 Wells Creek Basin, Tennessee, 329, 331  
 Werner-Gish-Rumney method, 395  
 Wentworth, C. K., 316  
 West Indies, 322  
 Willard, B., 175, 176  
 Williams, H., 3, 315, 316, 322, 324, 325, 326  
 Willis, B., 82, 125, 126  
 Willis, R., 92, 125, 126  
 Wilson, J. H., 363, 365  
 Wilson, J. M., 386  
 Wilson, M. E., 70, 367, 369  
 Window, 176, 177, 184  
 Witwatersrand, South Africa, 374  
 Working multiple hypotheses, 3  
 Worm burrows, 75  
 Wyoming, 246, 247, 280, 281, 309, 420

X

Xenolith, 262, 294  
     cognate, 262

Y

Yosemite National Park, California; *Pl. XI*, op. p. 111

Z

Z, rhombohedron, quartz, 336  
 Zig-zag pattern of folils, 44, 45  
 Zone, fault, 131  
 Zone, cont, 40, 177  
 "Zone, weathered," 381